Duodenal ulcer promoting gene: effects on the pathophysiology of *Helicobacter pylori* infection and the host immune response

Richard James Michael Ingram

Thesis submitted to the University of Nottingham for the degree of Doctor of Philosophy

September 2016

Abstract

Duodenal ulceration remains a significant problem. *Helicobacter pylori* infection is the major cause of duodenal ulcers (DU). Worldwide, around 1 in 2 people are chronically colonised by *H. pylori*, most of whom will not develop gastroduodenal disease, though some will develop DU whilst others will develop gastric ulcer or gastric carcinoma. The risk of disease is related to bacterial virulence factors, host and environmental factors. Disease-specific bacterial risk factors have not been established.

Duodenal ulcer promoting gene (*dupA*) was proposed as a disease-specific bacterial virulence factor for DU. This study aims to examine the influence of *dupA* on clinical outcomes and whether these are epidemiologically consistent, if the *dupA* status of clinical isolates correlates with the key pathogenic features of DU *in vivo*, and if there is a biologically plausible role in disease through effects on host immune responses.

Results showed that the influence of *dupA* status on clinical outcomes was not specific to DU, but rather that epidemiological associations link *dupA* with an increased risk of gastroduodenal diseases in general for some populations. The *dupA* status of clinical isolates did not correlate with the key pathogenic features of DU *in vivo*, though there was some evidence of increased gastric mucosal inflammation in association with *dupA*+ strains. Experimental results using a human blood immune cell model show that monocyte-derived cells mediate a more pro-inflammatory response through interaction with the *dupA* system. This might be the mechanism that explains the *in vivo* associations of *dupA* with inflammation and disease.

In this study population, *dupA* did not satisfy the criteria of a true virulence factor that promotes duodenal ulceration. The assertion of this thesis is that *dupA* is misnamed.

Lay summary

Duodenal ulcers can cause recurrent abdominal pain and significant bleeding. Infection by *Helicobacter pylori* bacteria is the most important cause of duodenal ulcer (DU). *H. pylori* is acquired in childhood and lasts life-long without treatment. Most people will not be unwell as a result but, as well as DU, the infection can lead to other diseases in some people, such as stomach ulcer or stomach cancer. The types of virulence genes found in the infecting *H. pylori* strain are important determinants of the risk of disease, alongside host factors (like the genetics of the infected person) and environmental factors (like smoking). However, although the bacterial factors seem to be important in identifying the risk and severity of illness, they do not identify which sort of disease the person develops. The bacterial virulence factor called duodenal ulcer promoting gene (*dupA*) was reported to be related specifically to DU. My thesis tests this idea.

In Results One, this study found no association between *dupA* and diseases in Nottingham. However, *dupA* was associated with an increased risk of gastrointestinal diseases overall, though not specifically DU, when looking at results from studies all over the world. This link with disease was confined to Asian countries.

In Results Two, this study found no link between *dupA* and the features seen in people who go on to develop DU. These expected features are the distribution of bacteria in the stomach, and the pattern, intensity and type of inflammation in the stomach lining. However, we did find that some important signals of inflammation (called cytokines) present in the human stomach lining did appear to differ in association with *dupA*. It might be that the immune response of the body is different between people infected by *H. pylori* strains that have or lack the *dupA* system, though this was not proven.

In Results Three, this study showed a link between *dupA* and related genes, and how the human immune system responds. This used a model based on immune cells from human blood. It might be that these differences seen experimentally could explain the findings for cytokines in the stomach lining and the association of *dupA* with disease.

The overall conclusion of this thesis is that *dupA* does not specifically promote duodenal ulceration in all populations, and that it is misnamed.

Publications

J White, RJM Ingram and JC Atherton (Jul 2016). Gastritis, peptic ulceration and related conditions. In: Cohen, Powderly and Opal, *Infectious Diseases*, fourth edition, J Cohen et al. (eds.). London: Elsevier. [book chapter]

RJM Ingram, K Ragunath and JC Atherton (Dec 2015). Peptic ulcer disease. In: *Yamada's Textbook of Gastroenterology*, sixth edition, DK Podolsky et al. (eds.). New Jersey: Wiley-Blackwell. [book chapter]

JA Winter, DP Letley, KW Cook, JL Rhead, AA Zaitoun, RJM Ingram, KR Amilon, NJ Croxall, PV Kaye, K Robinson, JC Atherton (2014). A role for the vacuolating cytotoxin, VacA, in colonisation and *Helicobacter pylori*-induced metaplasia in the stomach. *Journal of Infectious Diseases*, 210(6):954-63.

KW Cook, DP Letley, RJM Ingram, E Staples, H Skjoldmose, JC Atherton and K Robinson (2014). CCL20 and CCR6 mediated migration of regulatory T-cells in *H. pylori* infected patients. *Gut*, 63(10):1550-9.

SR Patel, K Smith, DP Letley, KW Cook, AA Memon, RJM Ingram, E Staples, S Backert, AM Zaitoun, JC Atherton and K Robinson (2013). *Helicobacter pylori* down-regulates expression of human beta-defensin 1 in the gastric mucosa in a type IV secretion dependent fashion. *Cellular Microbiology*, 15(12):2080-92.

E Staples*, RJM Ingram*, JC Atherton and K Robinson (2013). Optimising the quantification of cytokines present at low concentrations in small human mucosal tissue samples using Luminex assays. *Journal of Immunological Methods*, 394(1-2):1-9. * joint first authorship

K Robinson and RJM Ingram (2012). *Helicobacter pylori* infection in childhood. *Microbiology Today*, 39 (Feb 2012): 26-29. [commissioned, not peer-reviewed]

Acknowledgements

Undertaking a PhD and writing this thesis has been one of the most demanding experiences of my life. Through this journey I have certainly learned a lot about *Helicobacter pylori* and academic research, and the many challenges and rewards of an academic career. But of equal importance, I have learned a lot about myself, the world, other people, and what really matters particularly when things get tough. It is okay not to have all the answers or achieve perfection, as my thesis will attest, but instead I will strive to ride life's rollercoaster with curiosity and wonder, with openness and honesty, and with self-acceptance and compassion.

I must begin my acknowledging the Medical Research Council, who generously supported this work and my personal development through a Clinical Research Training Fellowship. And the Wellcome Trust, who also offered me a fellowship to undertake my PhD. Financial support was also kindly provided by Nottingham University Hospitals Charity and through the Nottingham Digestive Diseases Centre.

To my supervisors – Karen Robinson and John Atherton – I could not have started, travelled or finished this journey without you. Thank you for your unwavering support, for our many thoughtful discussions, and for your kindness and compassion.

To my friends, acquaintances and colleagues from the *Helicobacter* group, from the University of Nottingham, from the wider academic community both in the UK and further afield, from the National Health Service, and to my many good neighbours both literal and metaphorical – you are too numerous to name. Thank you for your friendship, for your wisdom, for your time, for your equipment, and for getting me through the bad times, so that we could share in the good.

And finally, to my wonderful family – thank you. I love you more than words can say. I could fill the pages of this thesis again if I were to note down all your good deeds and kindnesses. You have got me through. It is to you that I dedicate this thesis.

Step by step, and one step at a time.

List of contents

Abstract ..... **ii**

Lay summary ..... **iii**

Publications ..... **iv**

Acknowledgements ..... **v**

List of figures ..... **xi**

List of tables ..... **xiii**

List of abbreviations and acronyms ..... **xv**

1. Introduction

1.1. Duodenal ulceration **1**

1.2. *Helicobacter pylori* **6**

1.2.1. Bacterial virulence factors 10

1.3. Duodenal ulcer promoting gene **14**

1.3.1. Initial description of duodenal ulcer promoting gene (*dupA*) 14

1.3.2. Systematic review and meta-analysis of the relationship between *dupA* and clinical outcomes 16

1.3.3. *dupA* sequence variation and polymorphisms 18

1.3.4. *dupA* and a putative new type IV secretion system (*tfs4*) 21

1.3.5. Insights into the functional relevance of *dupA* 26

1.4. Summary of key background information **38**

1.5. Aims **40**

2. Materials and methods

2.1. Media **41**

2.1.1. Blood agar 41

2.1.2. Lysogeny broth (LB) medium 41

2.1.3. Lysogeny broth (LB) agar 41

2.1.4. Iso-Sensitest medium with 15% (v/v) glycerol 41

2.1.5. Sulphite-free Brucella broth (SFBB) medium 42

2.1.6. Super Optimal broth with Catabolite repression (SOC) medium 42

2.2. Bacterial culture **42**

2.2.1. *H. pylori* isolation and culture on blood agar plates 42

2.2.2. *H. pylori* liquid culture 43

2.2.3. *H. pylori* frozen stocks 43

2.2.4. *Escherichia coli* culture on LB agar plates 43

2.2.5. *Escherichia coli* liquid culture 43

2.2.6. *Escherichia coli* frozen stocks 43
2.3. Patients, biopsies and clinical isolates 44
2.3.1. Power calculations and planned sample size 45
2.4. Systematic review and meta-analysis 46
2.5. Histopathological evaluation of gastric biopsies 49
2.6. Nucleic acid isolation and analysis 49
2.6.1. Preparation of *H. pylori* genomic DNA from bacterial cultures 49
2.6.2. Preparation of plasmid DNA from bacterial cultures 50
2.6.3. Preparation of total RNA from bacterial cultures 50
2.6.4. Preparation of total RNA and DNA from gastric biopsies 51
2.6.5. Nucleic acid quantification and assessment of purity 52
2.6.6. Determination of RNA integrity 52
2.6.7. DNA sequencing and analysis 53
2.7. Nucleic acid manipulation 53
2.7.1. Transfer of plasmid DNA into *Escherichia coli* competent cells 53
2.7.2. Restriction digest 53
2.7.3. DNase treatment of total RNA 54
2.7.4. Synthesis of complementary DNA from DNase-treated total RNA from gastric biopsies 54
2.7.5. Synthesis of complementary DNA from DNase-treated total RNA from bacterial cultures 55
2.8. Polymerase chain reaction (PCR), modifications of PCR and analysis .. 56
2.8.1. PCR and sequencing to determine *dupA* status 56
2.8.2. PCR to determine *cag*PAI, *vacA* type and *tfs4* status 62
2.8.3. PCR to indicate *dupA* status using biopsy DNA 64
2.8.4. Analysis of PCR products by gel electrophoresis 66
2.8.5. Quantitative real-time PCR (qPCR) – assessment of bacterial colonisation density 66
2.8.6. Quantitative reverse transcriptase real-time PCR (RT-qPCR) – assessment of relative mucosal cytokine mRNA expression 70
2.8.7. Quantitative reverse transcriptase real-time PCR (RT-qPCR) – initial development of an *in vitro* and *in vivo* assay for relative *dupA* mRNA expression 74
2.8.8. Online resources 75
2.9. Protein analysis 76
2.9.1. Luminex assays 76
2.9.2. Meso Scale Discovery (MSD) assays 76

2.9.3. Bicinchoninic acid (BCA) assay 77
2.10. Purification of cell populations from human blood 77
2.11. Bacterial co-culture experiments with immune cells from human blood 80
2.12. Flow cytometry 85
2.13. ChipCytometry 87
2.14. Statistical analysis 89
3. Results One – Influence of *dupA* status on clinical outcomes
3.1 Nottingham study population 91
3.2 Establishing *dupA* status – genotyping and sequencing 93
3.2.1 Relationship between bacterial virulence factors 94
3.2.2 Summary 95
3.3 Clinical outcomes in Nottingham study 96
3.3.1 By *dupA* status 96
3.3.2 By *tfs4* status 98
3.3.3 By *H. pylori* infection and other virulence factors 99
3.3.4 Confounding and disease risk factors 103
3.3.5 Summary 105
3.4 Systematic review and meta-analysis 106
3.4.1 Study populations 109
3.4.2 Prevalence of *dupA*-positive strains 111
3.4.3 Clinical outcomes by *dupA* status 112
3.4.4 Statistical heterogeneity and clinical diversity 115
3.4.5 Methodological diversity and risk of bias 119
3.4.6 Results of meta-analysis 124
3.4.6.1 Association between *dupA* and DU 124
3.4.6.2 Association between *dupA* and GU 126
3.4.6.3 Association between *dupA* and GC 128
3.4.7 Confounding by age and sex 128
3.4.8 Summary 130
3.5 Discussion 131
3.5.1 *dupA* status 131
3.5.2 Clinical outcomes 132
3.5.3 Strengths, weaknesses and future work 137
3.5.4 Conclusion 142

4. Results Two – Is the *dupA* status of clinical isolates associated with the key pathogenic features of duodenal ulceration?

4.1 Gastric inflammation 144

4.2 Bacterial colonisation density 146

4.2.1 Bacterial colonisation density by quantitative PCR 146

4.3 Mucosal immune responses 148

4.3.1 Optimising the quantification of multiple cytokines present at low concentrations in human gastric mucosal biopsies 148

4.3.2 Mucosal immune responses at protein-level 148

4.3.3 Mucosal immune responses at mRNA-level 158

4.4 Summary 165

4.5 Discussion 166

4.5.1 Gastric inflammation 166

4.5.2 Bacterial colonisation density 168

4.5.3 Mucosal immune responses 169

4.5.4 Gastric acid output 174

4.5.5 Strengths, weaknesses and future work 177

4.5.6 Conclusion 179

5. Results Three – Influence of *dupA* and *tfs4* status on human immune cell responses

5.1 Blood donors and cell populations 181

5.2 Co-culture of clinical strains with PBMCs 182

5.3 Co-culture of mutant strains with PBMCs 185

5.3.1 Rationale for mutant strain selection 186

5.3.2 Relative cytokine and chemokine concentrations 187

5.3.3 IL-12/23p40 expression by flow cytometry 192

5.4 Optimisation of the human blood monocyte cell model 194

5.4.1 Performance of immunomagnetic kits 194

5.4.2 Purified cell populations 199

5.4.3 Cytokine expression phenotype of purified cell populations 204

5.5 Co-culture with $CD14^+$ monocytes 207

5.5.1 Relative cytokine and chemokine concentrations 208

5.6 Co-culture of treated bacteria and other strains 212

5.6.1 Heat-inactivation (HI) 212

5.6.2 Paraformaldehyde (PFA) treatment 214

5.6.3 Other strain backgrounds 216

5.7 ChipCytometry 219
5.7.1 Feasibility study and biomarker validation 219
5.7.2 Optimisation of sample preparation 222
5.7.2.1 Final ChipCytometry sample protocol 228
5.7.3 Results of feasibility study 229
5.7.4 Summary 231
5.8 Discussion 232
5.8.1 Choice of experimental model 233
5.8.2 Experimental approaches to studying human mucosal immune responses and ChipCytometry 247
5.8.3 Summary and discussion of results of co-culture experiments and the effect of *dupA* and *tfs4* status on immune responses 250
5.8.4 Strengths, weaknesses and future work 262
5.8.5 Conclusion 265
6. Conclusion
7. Appendices
7.2 Appendix for chapter 2 – Materials and methods 267
7.3 Appendix for chapter 3 – Results One 269
7.3.1 Alignment of *dupA* sequences for *H. pylori* isolates 269
7.3.2 Example Forest plot for initial meta-analysis 275
7.4 Appendix for chapter 4 – Results Two 276
7.4.1 Interferon-gamma protein-level expression was associated with *H. pylori* infection using a different assay 276
7.5 Appendix for chapter 5 – Results Three 277
7.5.1 Co-culture of mutant strains with PBMCs – adjusted cytokine and chemokine concentrations 277
7.5.2 Co-culture of mutant strains with $CD14^+$ monocytes – adjusted cytokine and chemokine concentrations 279
7.5.3 Co-culture of clinical strains with $CD14^+$ monocytes 279
7.5.4 Co-culture of mutant strains with $CD14^+$ monocytes – IL-12/23p40 expression by flow cytometry 282
7.5.5 Co-culture of treated bacteria with PBMCs 284
7.5.5.1 Heat-inactivation (HI) 284
7.5.5.2 Paraformaldehyde (PFA) treatment 284
8 References

List of figures

Figure 1.1 – cascade of mucosal defence and repair mechanisms 2

Figure 1.2 – key factors for clinical outcomes of *H. pylori* infection and the particular role for gastric acid production and the topographical location of inflammation in the stomach 3

Figure 1.3 – schematic representation of factors contributing to disease outcome in *H. pylori* infection 8

Figure 1.4 – mechanisms and effects of epithelial cells of the *cag* virulence system .. 11

Figure 1.5 – relationship between *dupA*, *jhp0917-0918*, and *jhp0917* and *jhp0918* 15

Figure 1.6 – type IV secretion systems (T4SS) encoded in *H. pylori* chromosomes ... 21

Figure 1.7 – schematic of the type IV secretion system (T4SS) of *Agrobacterium tumefaciens* 22

Figure 1.8 – pairwise alignment of *tfs4* regions from chromosomes of various *Helicobacter pylori* genomes 24

Figure 1.9 – schematic model for potential roles of *Helicobacter pylori* type IV secretion systems in horizontal gene transfer events 28

Figure 1.10 – schematic representation of a putative structure for the *tfs4* T4SS 29

Figure 2.1 – location of *dupA* genotyping primers evaluated in this study in relation to Shi470 *Helicobacter pylori* genome 59

Figure 2.2 – location of *dupA* sequencing primers evaluated in this study in relation to Shi470 *Helicobacter pylori* genome 60

Figure 2.3 – example flow cytometry gating strategy for IL-12/23p40 and CD14 expression by peripheral blood cell populations 86

Figure 3.1 – study participant flow diagram 92

Figure 3.2 – results of meta-analysis for the risk of DU in *dupA*+ *H. pylori* infection 124

Figure 3.3 – publication bias in the DU meta-analysis 126

Figure 3.4 – results of meta-analysis for the risk of GU in *dupA*+ *H. pylori* infection 126

Figure 3.5 – publication bias in the GU meta-analysis 127

Figure 4.1 – mucosal concentrations of IL-8 152

Figure 4.2 – mucosal concentrations of pro-inflammatory cytokines 155

Figure 4.3 – mucosal concentrations of T-helper effector cytokines 156

Figure 4.4 – mucosal concentrations of IL-12/23 family cytokines 157

Figure 4.5 – relative mucosal expression of *IL8* mRNA 162

Figure 4.6 – relative mucosal expression of T-helper effector cytokine mRNA 163

Figure 4.7 – relative mucosal expression of *IL12B* mRNA 164

Figure 5.1 – cytokine expression in PBMC co-cultures with clinical strains 184

Figure 5.2 – relative cytokine concentrations for 48 h PBMC co-culture..... 191

Figure 5.3 – IL-12/23p40 events and fluorescence intensity by flow cytometry for 16 h co-culture with PBMCs 193

Figure 5.4 – cell populations purified from human leucocytes using four kits, showing unenriched, enriched and depleted cell fractions 198

Figure 5.5 – IL-12/23p40 and CD14 expression by PBMCs purified using the (1) Miltenyi Biotec and (2) STEMCELL EasySep™ protocols 201

Figure 5.6 – comparison by flow cytometry of IL-12/23p40 and CD14 expression by different cell populations..... 203

Figure 5.7 – cytokine expression phenotype of cell populations in 48 h co-cultures 206

Figure 5.8 – relative cytokine concentrations for 48 h monocyte co-culture..... 211

Figure 5.9 – cytokine concentrations from monocytes co-cultured with heat inactivated and paraformaldehyde-treated bacteria, relative to live untreated bacteria..... 213

Figure 5.10 – relative cytokine expression in cell co-cultures with P1 strains 218

Figure 5.11 – biopsy chip microscopy for ChipCytometry donor 773..... 225

Figure 5.12 – biopsy chip microscopy for ChipCytometry donor 778..... 226

Figure 5.13 – biopsy chip microscopy for ChipCytometry donors 789, 791 and 792 227

Figure 5.14 – biopsy chip microscopy for ChipCytometry donor 798..... 230

Figure 7.1 – representative growth curves for AB21 wild-type, Δ*dupA* and Δ*virB8* isogenic mutant strains 267

Figure 7.2 – pictographic representations of histopathological appearances of the gastric mucosal according to the update Sydney system 268

Figure 7.3 – alignment of representative *dupA* sequences 270

Figure 7.4 – results of initial meta-analysis for the risk DU in *dupA*+ *H. pylori* infection, before heterogeneity was identified and addressed..... 275

Figure 7.5 – antral gastric mucosal concentrations of IFN-γ using MSD assays..... 276

Figure 7.6 – adjusted cytokine concentrations for 48 h PBMC co-culture 278

Figure 7.7 – adjusted cytokine concentrations for 48 h monocyte co-culture..... 280

Figure 7.8 – cytokine expression in monocyte co-cultures with clinical strains..... 281

Figure 7.9 – IL-12/23p40 events and fluorescence intensity by flow cytometry for 16 h co-culture with monocytes 283

Figure 7.10 – cytokine concentrations from PBMCs co-cultured with heat inactivated and paraformaldehyde-treated bacteria, relative to live untreated bacteria..... 286

List of tables

Table 1.1 – relationship between *dupA* status and clinical outcomes evaluated in a meta-analysis by Shiota et al. (2010) 17

Table 2.1 – gastric biopsies donated by patients with informed consent during routine upper GI endoscopy, purpose of biopsies and storage conditions 45

Table 2.2 – cycling conditions for *dupA* typing by Takahashi primer sets 61

Table 2.3 – cycling conditions for *dupA* typing by Schmidt and Jung primer sets 62

Table 2.4 – primers used in *dupA* typing and sequencing 62

Table 2.5 – cycling conditions for PCR with *dupA_RI* primers 66

Table 2.6 – dilution series prepared for qPCR for bacterial colonisation density 69

Table 2.7 – cycling conditions for qPCR for bacterial colonisation density 70

Table 2.8 – primers used in qPCR colonisation density experiments 70

Table 2.9 – cycling conditions for RT-qPCR for mucosal cytokine expression 73

Table 2.10 – primers used in RT-qPCR mucosal cytokine expression experiments 73

Table 2.11 – cycling conditions for RT-qPCR *dupA* expression experiments 75

Table 2.12 – primers used in RT-qPCR *dupA* expression experiments and *dupA_RI* primers used in conventional PCR 75

Table 2.13 – online resources used in primer design and analysis 75

Table 2.14 – cell purification kits 79

Table 2.15 – bacterial strain characteristics (mutant and laboratory strains) 83

Table 2.16 – bacterial strain characteristics (clinical isolates) 84

Table 3.1 – characteristics of study participant populations in flow diagram 93

Table 3.2 – relationship between *dupA*, *cag*PAI and *vacA* 94

Table 3.3 – clinical outcomes and risk factors by *dupA* status 97

Table 3.4 – description of *dupA* and *tfs4* status of clinical isolates 99

Table 3.5 – clinical outcomes and risk factors for the study population overall 101

Table 3.6 – clinical outcomes and risk factors by *cag* pathogenicity island status 102

Table 3.7 – clinical outcomes and risk factors by *vacA* type 102

Table 3.8 – summary table of *dupA* prevalence and clinical outcome associations worldwide 107

Table 3.9 – summary table of reported associations between *dupA* status and clinical outcomes expressed as odds ratios 114

Table 3.10 – planned subgroup analysis for clinical diversity by region 119

Table 3.11 – study methods and assessment of risk of bias in reporting of *dupA* status 122

Table 3.12 – planned subgroup analysis for methodological diversity by risk of bias 123

Table 3.13 – analysis of age, sex and *dupA* status with respect to clinical outcome. 129
Table 4.1 – characterised histological samples 144
Table 4.2 – gastric inflammation histological scores by *dupA* status..... 145
Table 4.3 – predominant distribution of gastric inflammation by *dupA* status 145
Table 4.4 – bacterial colonisation density histological scores by *dupA* status..... 146
Table 4.5 – characterised samples for colonisation density (qPCR)..... 147
Table 4.6 – characterised mucosal immune responses at protein-level..... 149
Table 4.7 – characterised mucosal immune responses at mRNA-level 159
Table 5.1 – blood donor demographics, genotypes and phenotypes..... 183
Table 5.2 – details of PBMCs purified from donor blood..... 183
Table 5.3 – yield, viability and purity of cellular fractions with different kits 195
Table 5.4 – details of monocytes purified from donor blood..... 207
Table 5.5 – ChipCytometry biomarker validation..... 221
Table 5.6 – optimisation of sample preparation variables for ChipCytometry: donors and steps prior to stimulation 223
Table 5.7 – optimisation of sample preparation variables for ChipCytometry: stimulation and post-stimulation steps 224
Table 5.8 – summary of steps included in final ChipCytometry sample protocol..... 229
Table 5.9 – donors and samples for ChipCytometry feasibility study 229
Table 5.10 – relative $CD4^+$ and cytokine expression for ChipCytometry peripheral blood mononuclear cell chips..... 231
Table 5.11 – summary of percentage changes in cytokine expression in co-culture experiments according to *dupA* status..... 253
Table 5.12 – comparison with other studies of percentage changes in cytokine expression in co-culture experiments with AB21 wild-type and Δ*dupA* strains..... 254
Table 5.13 – summary of percentage changes in cytokine expression in $CD14^+$ monocyte co-culture experiments according to *tfs4* and *dupA* status..... 258
Table 5.14 – summary of percentage changes in cytokine expression in co-culture experiments according to *cagE* and *dupA* status..... 262

List of abbreviations and acronyms

BCA	bicinchoninic acid
bp	base pairs
BSA	bovine serum albumin
cDNA	complementary DNA
CFU	colony forming unit
CI	confidence interval
df	degrees of freedom
DNA	deoxyribonucleic acid
DU	duodenal ulcer
FD	functional dyspepsia
GC	gastric cancer
GU	gastric ulcer
IELs	intra-epithelial lymphocytes
IQR	inter-quartile range
LPMCs	lamina propria mononuclear cells
MOI	multiplicity of infection
mRNA	messenger RNA
MSD	Meso Scale Discovery
NSAID	non-steroidal anti-inflammatory drug
ORF	open reading frame
OR	odds ratio
PCR	polymerase chain reaction
PMA	phorbol myristate acetate
PPI	proton pump inhibitor
PUD	peptic ulcer disease
qPCR	quantitative PCR
RNA	ribonucleic acid
RT-qPCR	reverse transcription quantitative PCR
SNP	single nucleotide polymorphism
T4SS	type IV secretion system
TLR	Toll-like receptor

1. Introduction

1.1. Duodenal ulceration

Peptic ulcers are mucosal defects of 0.5cm or more in diameter in the lining of the upper gastrointestinal tract that penetrate through the muscularis mucosa into the submucosal layer. Lesions smaller than this are referred to as erosions. Duodenal ulcers refer to peptic ulceration in the duodenum. Clinical presentations include epigastric pain, heartburn, gastrointestinal bleeding and perforation. Traditional thinking was that '*ulcers [were] only found in white people, usually in long thin types given to worry and irritability*' (Robinson and Bruce, 1940, in Griffiths and Walker, 1997). Research into *H. pylori* completely revolutionised the management of peptic ulcer disease, and pathophysiological models for ulcers caused by acid and stress became less relevant.

Duodenal ulcers are epidemiologically distinct from other gastroduodenal disorders (Williams et al. 2007). The incidence peaks at age 45–64 years and is twice as common in men as in women (Ingram et al. 2015). Gastric cancer has a similar male predominance but mainly affects older people with 80% of cases diagnosed in people aged between 60 and 80 years old. In the same way, gastric ulcer is more common in the elderly but the incidence is equal in men and women.

The pathogenesis of duodenal ulceration is the result of an imbalance between ulcerogenic factors, including increased exposure to gastric acid in the duodenum, and protective factors such as mucosal barrier function (Malfertheiner et al. 2009). The interplay is thought to be multifactorial – smoking, alcohol excess, psychosocial factors and stress, and drugs like non-steroidal anti-inflammatory drugs (NSAIDs). The cascade of mucosal defence and repair mechanisms is shown in Figure 1.1. If these mechanisms fail or are overwhelmed then an ulcer forms. NSAIDs are the second most common cause of ulcers and suppress gastric prostaglandin synthesis leading to reduced defenses against gastric contents (Malfertheiner et al. 2009). There are multiple specific aetiologies including systemic illnesses but *H. pylori* infection remains the most important cause (Ingram et al. 2015). Its eradication almost completely prevents ulcer recurrence. *H. pylori* is present in over 90% of patients with duodenal ulceration but only 10-15% of those infected develop ulcers (Kusters et al. 2006). Why is this? Some key factors are shown in Figure 1.2.

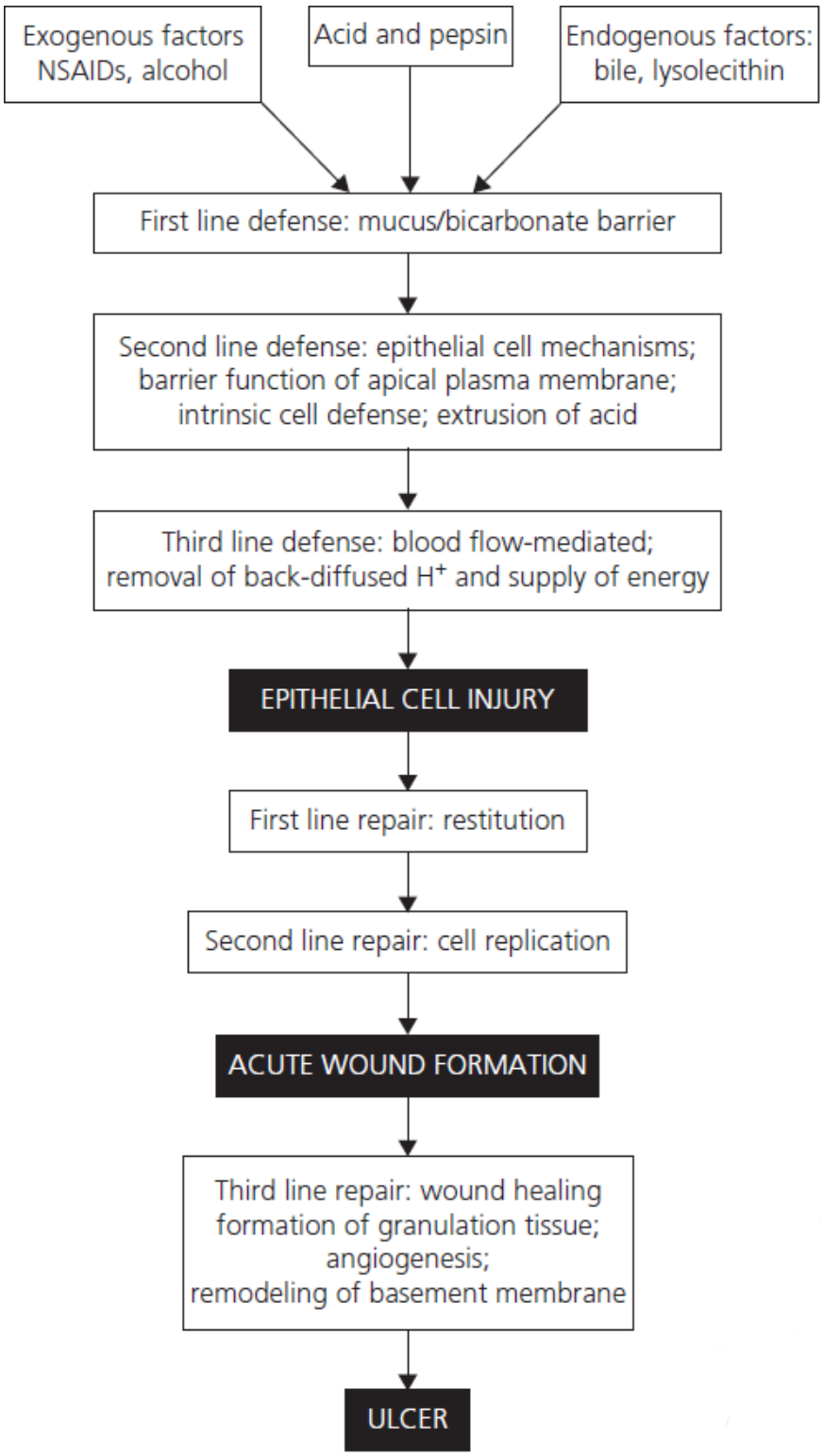

Figure 1.1 – cascade of mucosal defence and repair mechanisms

Exogenous and endogenous factors have damaging effects on gastric epithelial cells that are amplified by acid and peptic activity. If the three lines of defensive mechanisms fail, then epithelial injury occurs and an ulcer forms. Reproduced from Ingram et al. 2015 with permission from John Wiley and Sons.

NSAIDs, non-steroidal anti-inflammatory drugs.

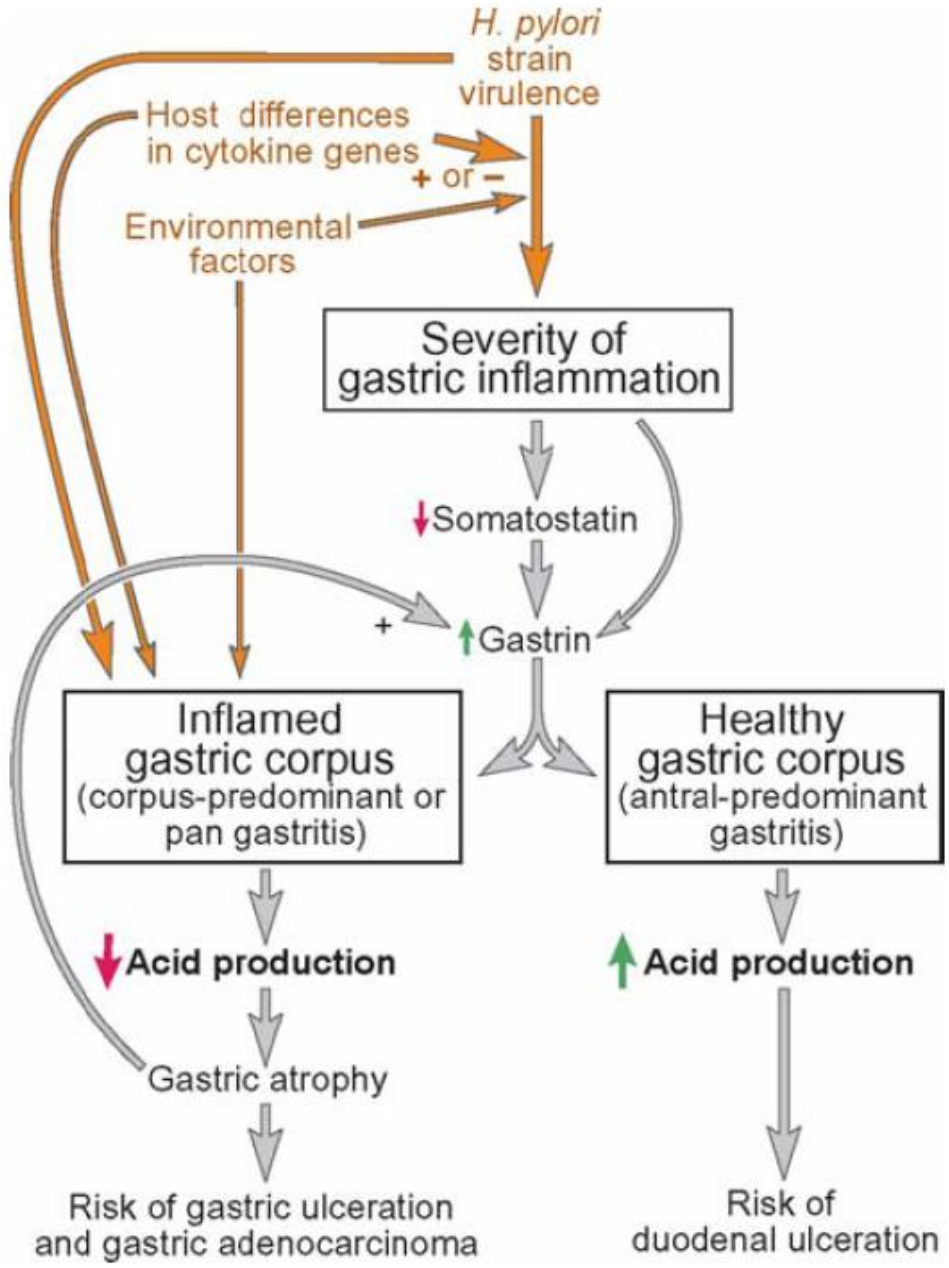

Figure 1.2 – key factors for clinical outcomes of *H. pylori* infection and the particular role for gastric acid production and the topographical location of inflammation in the stomach

Gastritis leads to hypergastrinaemia but the effects of this depend on whether the gastric corpus is inflamed. This is modulated by bacterial, host and environmental factors (shown in orange). Relatively little is known about factors that prevent corpus gastritis and impact on duodenal ulcer risk. Reproduced from Atherton (2006) with confirmation from Annual Reviews that additional permission is not required.

Duodenal ulceration is associated with density of infection and gastric inflammation in an antral-predominant pattern, with sparing of the acid-secreting body of the stomach (Schultze et al. 1998). There is a significant correlation between *H. pylori* density and the grade of acute and chronic inflammation, the severity of which underpins many gastroduodenal diseases (Varbanova and Malfertheiner 2011). The distribution of *H. pylori* changes during acid suppression with proton pump inhibitors, with reduced bacterial density in antral mucosa and increased density in the fundus (Logan et al. 1995). The degree of histological inflammation in different gastric regions changed in association with the apparent migration of *H. pylori* from the antrum to the fundus. Pre-morbid gastric acid output might be an important determinant of the topographic subtype of *H. pylori* gastritis, as anti-secretory therapy to reduce acid in patients with duodenal ulcer significantly reduces colonisation density and inflammation in the antrum leading to corpus predominant gastritis but stable bacterial counts in that region (Kuipers et al. 1995). However the bacterium itself can have significant modulating effects on acid homeostasis, such as impaired inhibitory neural control of acid production, reduced somatostatin release from D cells, consequent and direct increases in gastrin levels, with hypergastrinaemia resulting in trophic effects on specialised epithelial cells including enterochromaffin-like cells (that release histamine) and some suggest an increase in parietal cell mass (Malfertheiner et al. 2009). The hormones gastrin and histamine cause greater acid output from parietal cells in the corpus, which is unopposed due to down-regulation of negative-feedback mechanisms.

In gastritis that spares the corpus (that is, is antral-predominant), the parietal cells are unimpaired and free to respond to physiological signals to secrete acid (causing hyperchlorhydria). Furthermore, increased levels of acid reach the duodenal bulb leading to gastric metaplasia in response, and this tissue can then be colonised by *H. pylori* where it can cause local inflammation and mucosal damage (Atherton 2006). In constrast, when the body mucosa is inflamed in corpus-predominant or pan-gastritis, acid production is impaired resulting in normal or reduced levels (hypochlorhydria), with the development of atrophy leading to further reduction in acid output.

The importance of gastric acid output in the pathophysiology of duodenal ulceration has been known about for many years (Faber 1927 in Zhang et al. 2008). Acid output can be measured *in vivo* according to basal acid output (BAO) and maximal acid output (MAO). BAO is a measure of the volume of acid secreted from a fasted, unstimulated

stomach over one hour and MAO represents stimulated acid secretion defined as '*the total acid secretion for the period of 60 [minutes] after administration of a gastric stimulant that cannot be increased by higher doses of the stimulant*' (Ghosh et al. 2011). BAO is thought to represent the background tone of the vagus nerve, whereas MAO reflects the parietal cell mass. The significance of *H. pylori* infection on acid secretion was shown by El-Omar et al. (1995). This study compared infected patients with and without duodenal ulcer, followed at one month and one year after eradication therapy, against uninfected healthy controls. BAO was modestly increased in infection compared to controls but this was three times higher among patients with duodenal ulcer, which reduced by half at one month and had normalised by one year after eradication. Stimulated acid output in response to infusion of gastrin-releasing peptide was three time higher in infected patients and six times higher in patients with duodenal ulcer, with complete resolution after one month and one year respectively. Indeed only 1/25 uninfected controls had a stimulated acid response in the range of patients with duodenal ulcer. In addition MAO measured following stimulation with pentagastrin, was increased in infection but was unchanged one year after treatment. Endogenous gastrin levels were largely unchanged. Conversely in patients with gastrinoma (a gastrin-secreting tumour that causes multiple ulcers) their MAO normalised after the tumour was removed due to the loss of gastrin's trophic effects on parietal cells. The authors therefore concluded that the increased parietal cell mass in patients with duodenal ulcer could not be attributed to *H. pylori*. However overall gastric physiology is significantly altered by infection and largely recovers after eradication.

The immune response is also crucial – infiltrating inflammatory cells release factors that impair mucosal defence, a T-helper 1 (Th1)-predominant response results in more mucosal damage whilst a high regulatory T cell (Treg) response and IL-10 expression protect against duodenal ulcer (Robinson et al. 2008; Robinson et al. 2007). Other host factors have been suggested to influence duodenal ulcer development (Malfertheiner et al. 2009), including some that increase risk (*NOD1* polymorphisms and HLA-DQA 1301) and some that decrease risk (*TLR4* and *IL1β* polymorphisms). See next section.

In summary, duodenal ulcers may arise when three key criteria are met: acid output is increased, gastric inflammation is intense and the pattern of colonisation and gastritis is antral-predominant. *Helicobacter pylori* is still the major cause of DU and little is known of disease-specific bacterial factors that promote duodenal ulceration.

1.2. Helicobacter pylori

Helicobacter pylori is the major pathogen of the human stomach and it colonises approximately half the global population (Kusters et al. 2006). It causes chronic gastric inflammation – asymptomatic in the majority of carriers but a proportion (10-20%) will develop serious gastroduodenal diseases that include duodenal and gastric ulceration, non-cardia gastric adenocarcinoma and gastric lymphoma (Atherton 2006). Infection is also an important aetiological factor in the development of a number of extra-gastric diseases (Malfertheiner et al. 2007; Malfertheiner et al. 2011). Controversies remain in whether the bacterium has a role in protecting its host against conditions like reflux and reflux oesophagitis (Vicari et al. 1998; Zentilin et al. 2003; Ghoshal and Chourasia 2010), asthma (Blaser et al. 2008; Wang et al. 2012), and allergy and other diseases (Robinson 2015). Human physiology has adapted to colonisation over millennia of co-evolution and the recent absence of *H. pylori* from many individuals may contribute to the recent increases in allergic and autoimmune diseases (Atherton and Blaser 2009). Interestingly, there is growing evidence of an inverse association between *H. pylori* and inflammatory bowel disease (Papamichael et al. 2014; Shah et al. 2017) that might be explained by altered regulatory immune responses (Robinson 2015).

The causal role for *H. pylori* in peptic ulcer disease was first proposed by Robin Warren and Barry Marshall, who in 1984 isolated and cultured '*spiral bacilli*' from gastroscopy specimens (Marshall and Warren, 1994). The bacteria were Gram-negative, microaerophilic and flagellated. However bacteria had been hypothesised as a cause of peptic ulceration as early as 1875 and spiral-shaped organisms had been identified in human gastric mucosa and stomach contents from 1889 (Kidd and Modlin 1998). However, it was Warren and Marshall's discovery that launched a paradigm-shift in the management of ulcer disease and their achievements were recognised with the award of the 2005 Nobel Prize in Physiology or Medicine. Infection is usually established in childhood and without specific treatment will persist within the gastric niche lifelong, due to specific adaptations conferring acid resistance (such as urease production) and other traits, and through elegant cellular machineries that allow the bacteria to evade and perturb the host immune response (Atherton 2006; Robinson et al. 2007).

We do not fully understand why the natural history of chronic *H. pylori* infection steers some people towards antral-predominant gastritis and duodenal ulceration, and others towards corpus-predominant inflammation or pan-gastritis with an increased risk of

mucosal atrophy that leads in some to metaplasia, dysplasia and adenocarcinoma (Correa 1992; Uemura et al. 2001; Malfertheiner et al. 2009). Duodenal ulcer and gastric cancer are therefore often considered as mutually exclusive clinical outcomes where antral-predominant gastritis protects against cancer development (Kusters, van Vliet, and Kuipers 2006). Bacterial-specific factors relate to differences in the relative risk of disease outcomes rather than specificity for any particular outcome (Yamaoka and Graham 2014). However, host-specific factors and their impact on host-bacterial interactions are key determinants of pre-malignant histological changes and gastric cancer (Amieva and El-Omar 2008). Host factors are discussed further below.

Eradication therapy in infected patients who develop duodenal ulceration improves mucosal healing and prevents recurrence (Ford et al. 2011). *H. pylori* is classified as a class I human carcinogen by the World Health Organisation (IARC Working Group, 1994) although the effect of eradication therapy on the subsequent development of gastric cancer is less clear. Stomach cancer is the fourth most common cancer worldwide, affecting around one million people each year, and it is responsible for a tenth of all deaths from cancer making it the second most common cause of cancer deaths (Kusters, van Vliet, and Kuipers, 2006; Cancer Research UK, 2012 [statistics from this reference and refer to 2008]. Recent data have shown that eradication may reduce cancer risk, particularly when treatment is given before pre-malignant histological changes like atrophy are established (Wu et al. 2009; Wong et al. 2004; Fuccio et al. 2009). Although most *H. pylori*-infected individuals have no increased risk of serious disease, the fact that some will develop cancer or peptic ulceration has led to proposals for population screening to identify those at highest risk for targeted management. Such an approach was suggested to be cost-effective in a study from the United Kingdom (Roderick et al. 2003). This type of approach to primary prevention is more realistic than the alternative which would involve using eradication therapy in all infected individuals. A whole population treatment strategy has the potential to create morbidity from therapy side effects and intensify the already growing problem of antibiotic resistance (Malfertheiner et al. 2011). In addition, in some hosts the infection may have beneficial effects, such as protection against asthma, that are not yet fully explained. Therefore, important questions about the contribution of *H. pylori* to the development of (or protection from) disease in different individuals and populations, and at different time points in life, remain to be answered.

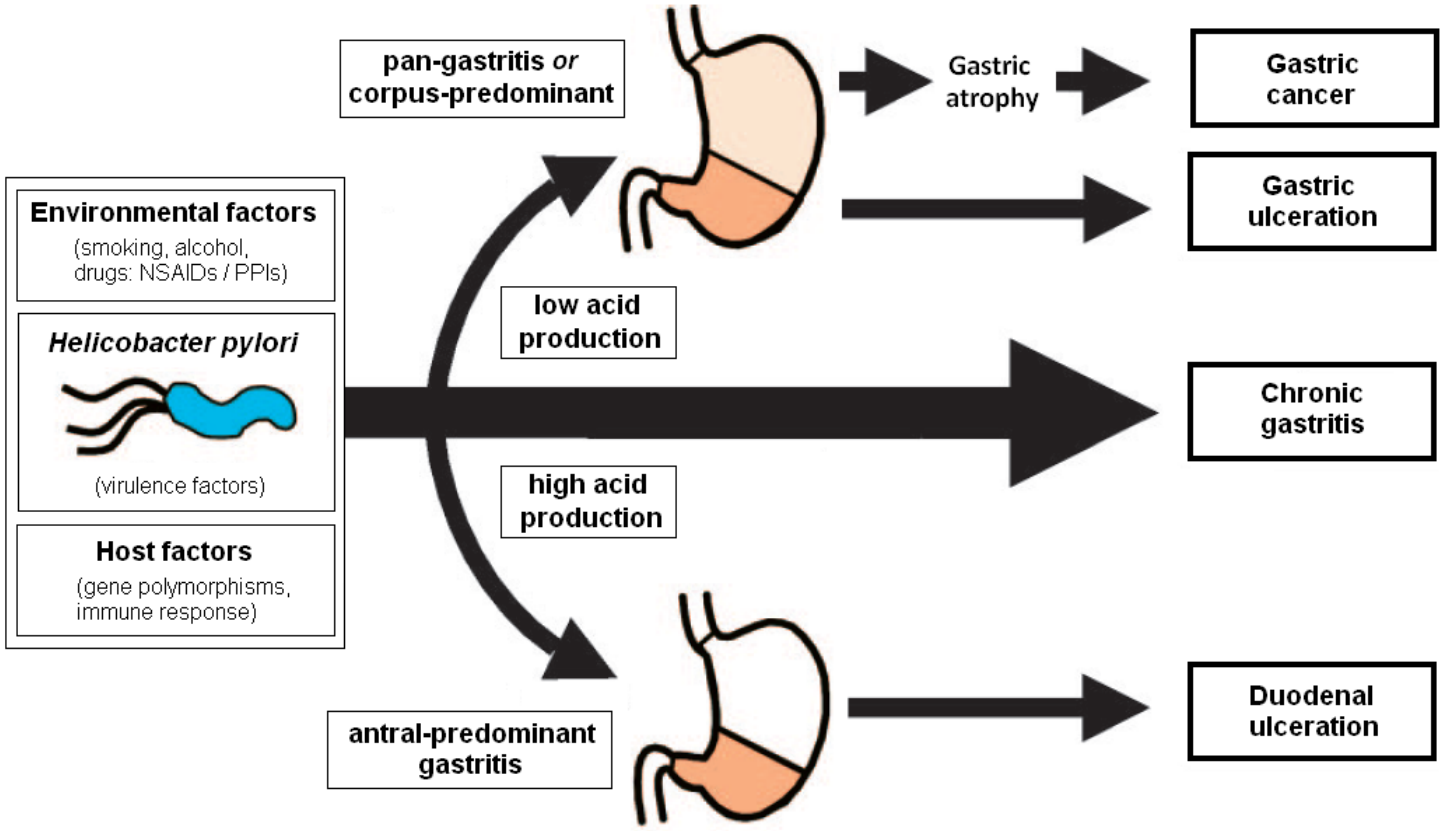

Figure 1.3 – schematic representation of factors contributing to disease outcome in *H. pylori* infection

Host factors (gene polymorphisms and the immune response), bacterial virulence factors and environmental factors interact to influence the clinical outcome of *H. pylori* infection. Adapted from Kusters et al. (2006) with confirmation from the American Society for Microbiology that additional permission is not required.

NSAID, non-steroidal anti-inflammatory drug; PPI, proton pump inhibitor.

Bacterial virulence factors, host response and environmental factors all predispose to disease (Figure 1.3). Bacterial virulence factors are discussed in Section 1.2.1.

Environmental factors

Environmental factors include smoking – smokers are at twice the risk of non-smokers and those also infected by *H. pylori* are at ten times the risk of uninfected non-smokers, diet – salt and preservatives may increase the risk whilst some dietary factors like antioxidant vitamins might be protective, and physical activity and body weight (Cancer Research UK 2014). Other factors such as concurrent helminth infection may influence the host immune response and disease risk (Fox et al. 2000; Y. Du et al. 2006). Exposure to certain drugs such as NSAIDs and PPIs can also influence disease development.

Host factors – genetic polymorphisms and the immune response

Genetic polymorphisms have been described in genes that encode immune system components, such as different *IL1B* alleles (El-Omar et al. 2000) that influence host-bacterial interactions (Amieva and El-Omar 2008). Interleukin-1β (IL-1β) is a key innate immune mediator in the host response to *H. pylori* and a potent inhibitor of gastric acid secretion (El-Omar 2001). These host factors govern and, in some individuals and in the presence of a suitable bacterial trigger, will define the intensity of the inflammatory response, the risk for pre-malignant changes in the gastric mucosa and ultimately the specific clinical outcome of gastric cancer (Hold and El-Omar 2008). Polymorphisms in various other genes have been associated with disease risk.

Helicobacter pylori elicits a stong immune response, through interaction with the gastric epithelium and secreted mucin, with various innate immune pattern recognition receptors and consequent alterations in antimicrobial peptides and pro- and anti-inflammatory cytokines, and with humoral and T cell responses due to stimulation of an adaptive immune response (White et al. 2015). The inflammation that results from this host-bacterial interaction is the main mediator of disease (Robinson et al. 2007). However, the bacteria can resist clearance and persist in its gastric niche despite these responses (Algood and Cover 2006). The balance between pro- and anti-inflammatory T-helper (Th) cell influences pathophysiology, with inadequate regulatory T cell (Treg) responses implicated in *H. pylori*-induced PUD (Robinson et al. 2008). Duodenal and peptic ulceration require a predominant Th1 response (D'Elios et al. 1997; 2005), though Th17 cells also play an important role (Serelli-Lee et al. 2012; C. Liu et al. 2016).

The complex interplay between these factors in a particular individual is thought to determine their risk of disease. The discrepancy between the numbers of people colonised and clinical outcomes, especially in some regions of the world, has been the source of considerable motivation to identify and characterise bacterial markers of virulence. Despite much research, little is yet known of disease-specific bacterial factors that might explain why gastric cancer and duodenal ulcer are at opposite ends of the spectrum of *H. pylori*-associated diseases.

1.2.1. Bacterial virulence factors

The *cag* pathogenicity island and virulence system

The main known *H. pylori* virulence determinant that increases disease risk is the 40 kb cytotoxin-associated gene pathogenicity island (*cag*PAI). Pathogenicity islands are acquired through horizontal gene transfer and have different GC-content relative to the genome (Tomb et al. 1997). The *cag*PAI contains at least 30 genes and encodes a type IV secretion system (T4SS) which the bacterium uses to interact specifically with gastric epithelial cells leading to events including interleukin-8 (IL-8) release, increased inflammation and mucosal injury. Components of the *cag*PAI share homology with *vir* genes from the *Agrobacterium tumefaciens* VirB4/VirD4 T4SS (Fronzes et al. 2009).

The effector protein of the *cag*PAI, CagA, is delivered into epithelial cells via a specialised pilus that acts like a needle-and-syringe to translocate this protein from bacterial cytoplasm into host cells (Backert and Selbach 2008). Detailed mutagenesis has identified the essential T4SS components for CagA translocation (Fischer et al. 2001). Injected CagA protein is phosphorylated on tyrosine residues by host machinery including Src family kinases and the SHP2 tyrosine phosphatase and, through phosphorylation-dependent and -independent mechanisms, activates signalling cascades resulting in multiple cellular outcomes such as disruption of apical cell-to-cell junctions, cytoskeletal rearrangements, cellular proliferation, anti-apoptotic nuclear responses and changes to motility (Atherton 2006; Backert and Selbach 2008). Bacterial peptidoglycan components also leak into eukaryotic cells as a result of the intimate interaction with the *cag* T4SS, resulting in pro-inflammatory cytokine induction following activation of the intra-cellular pattern recognition receptor Nod1 (Viala et al. 2004). CagL and other *cag*PAI components utilise host integrin $\alpha_5\beta_1$ as a cell-surface receptor, triggering the delivery of CagA (Kwok et al. 2007; Jiménez-Soto et al. 2009).

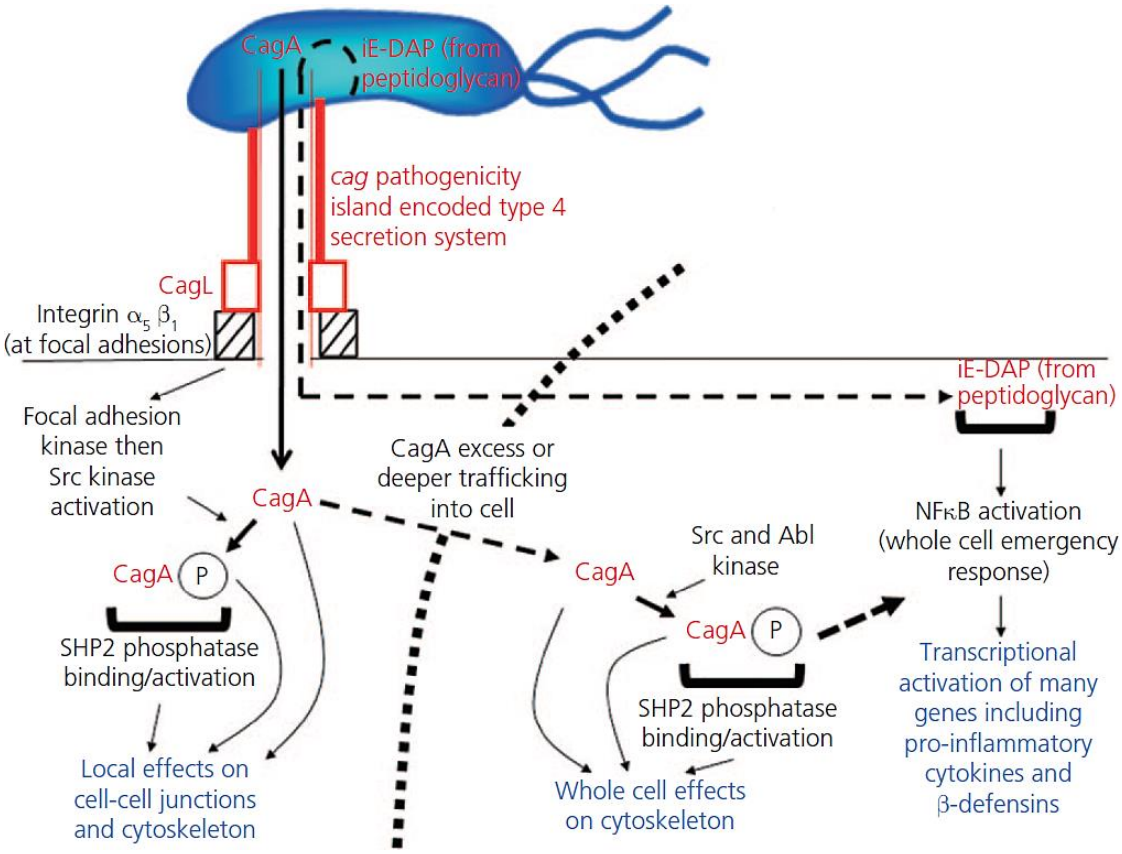

Figure 1.4 – mechanisms and effects of epithelial cells of the *cag* virulence system

The *cag* virulence system of *Helicobacter pylori* constitutes a type IV secretion system encoded by the *cag* pathogenicity island that delivers the CagA effector protein into host gastric epithelial cells. Some key bacterial factors are shown in red (CagA, CagL pilus protein, peptidoglycan components), host epithelial cell factors are in black (SHP2 phosphatase and kinases, integrin $\alpha_5\beta_1$ and kinases, NFκB activation), and effects of the cell are in blue (cytoskeletal, loosening of cell-cell junctions, transcriptional activation with induction of pro-inflammatory cytokines and β-defensins). Reproduced from Ingram et al. 2015 with permission from John Wiley and Sons.

iE-DAP, dipeptide present in peptidoglycan; P, phosphorylated.

The clinical relevance and relative importance of these effects *in vivo* are not completely clear but more virulent strains lead to a more intense inflammatory response in the human stomach as follows. A significantly greater risk of developing disease depends on regional variantion between Asian and Western strains (Kusters et al. 2006). The most striking differences in outcome relate to the number of CagA protein EPIYA motifs where SHP2 and kinases bind and phosphorylation occurs (on the side chain attached to tyrosine residues in the repeated five amino acid sequence Glu-Pro-Ile-Tyr-Ala [EPIYA]), which are classified by different flanking amino acids as EPIYA-A, -B, -C and -D motifs. CagA from Western strains consist of a combination of A, B and multiple C motifs, and the risk of gastric cancer over patients with gastritis infected by strains without *cag* is dependent on the type of CagA – odds ratio [OR] 7.4 with ≤1 EPIYA-C motifs (95% CI 1.98-27.48), OR 32.5 with ≥2 EPIYA-C motifs (95% CI 8.41-125.58) in a study of 54 clinical isolates from Italian patients (Basso et al. 2008). Similar studies from Asia (where CagA usually contains A, B and D motifs) showed that 100% of isolates from patients with gastric cancer had an EPIYA-ABD genotype, whilst this was present in 83% of patients with duodenal ulcer (P = 0.014) and 81% of patients with gastritis (P = 0.004) in 234 strains cultured from patients in South Korea (Jones et al. 2009). A role for CagA as protein with direct oncogenic potential in humans rather than as an indirect effect of increase inflammation as not been proved, although polymorphisms in EPIYA motif repeats, particularly where multiple C or D motifs are present, greatly increase CagA phosphorylation and downstream effects *in vitro* through stronger interaction with host signalling molecules (Naito et al. 2006).

Vacuolating cytotoxin A (*vacA*)

Another important *H. pylori* virulence factor that increases the risk of both peptic ulceration and gastric cancer is vacuolating cytotoxin A (*vacA*). This gene is present in all strains but it is expressed in only about 60%. Different mosaic alleles of this highly variable gene are associated with different disease risks, including the signal (s) and mid (m) regions (Atherton et al. 1995) and the intermediate (i) region (Rhead et al. 2007), with further regions of polymorphism also described. The signal sequence and autotransporter domain are cleaved from the 140 kDa pro-toxin and the mature VacA toxin is excreted into the extra-cellular space via a type V autotransport secretion system (Cover and Blanke 2005). The 88 kDa VacA protein causes pore formation in epithelial cell membranes and consequent vacuolation, it induces apoptosis through effects on

mitochondria, and also reduces T cell proliferation. The relative pathophysiological relevance of different *vacA* types is not known and may in part relate to a close association between the most virulent forms of *vacA* with a functional *cag* system (Atherton 2006; Kusters et al. 2006). The relationship of *vacA* status with clinical outcomes according to region polymorphisms varies between populations and the best overall marker(s) are not known (Yamaoka 2010), though the i region and particularly the *vacA* i1 genotype show promise as markers of gastric cancer risk (X. Liu et al. 2016). The more active s1/i1 form of VacA induced more severe inflammation and metaplasia in a mouse model (Winter, Letley, Cook et al. 2014).

Other virulence factors

Many other virulence factors have been described and can be classified as phase-variable genes (usually present in all strains and regulated by slipped strand mispairing – such as *oipA* and *babA*), genes of variable structure and genotype (such as the polymorphic *vacA*) and/or strain-specific genes (Yamaoka 2008). Nearly half of all strain-specific genes, such as the *cag* pathogenicity island, are located elsewhere in portions of the genome of lower GC content known as plasticity regions. The plasticity region of J99, a strain of *H. pylori* isolated in 1994 from an American patient with a duodenal ulcer, is a single island of 48 open reading frames from *jhp0914* to *jhp0961* (Alm et al. 1999). *jhp940* and *jhp0947* were found at increased prevalence in isolates from individuals with cancer rather than controls with gastritis in a group of 43 patients from Costa Rica (Occhialini et al. 2000). Santos et al. (2003) confirmed the association with *jhp0947* (but not *jhp0940*) in a larger study but with both duodenal ulcer and gastric cancer. A significant association between duodenal ulcer and *jhp0945*, *jhp0947* and *jhp0949* compared to gastritis was also reported in a study of 45 Dutch patients (de Jonge et al. 2004). The same study found that disruption of the *jhp0945-jhp0947-jhp0949* locus in five strains *in vitro* resulted in decreased IL-12 release from a monocytic cell line. The potential relevance of this observation is explored in more detail in Section 1.3.5.

There has been much interest in duodenal ulcer promoting gene (*dupA*), also located in the plasticity region. It was first reported to be associated with duodenal ulcer and protection from gastric cancer in some populations (Lu et al. 2005). If true, this remarkable observation would make *dupA* the first disease-specific *H. pylori* virulence factor. This study focuses around *dupA* and its role in human disease.

1.3. Duodenal ulcer promoting gene

This section considers: the initial studies on the association of duodenal ulcer promoting gene (*dupA*) with clinical outcomes in turn, subsequent disease association studies in overview, the independence of *dupA* from other bacterial virulence factors, its relationship with histological changes and patterns of inflammation in the stomach, controversial links with acid tolerance and gastric acid output, genetic aspects of *dupA* and its putative connection with a cluster of other genes in the plasticity region, and finally evidence that points towards its functional relevance, possibly in shifting the host immune response.

1.3.1. Initial description of duodenal ulcer promoting gene (*dupA*)

Lu et al. (2005) identified 14 genes with homology to *vir* genes, including 4 in the plasticity region, 7 in the *cag* pathogenicity island and 3 outside of these regions, using the then available *H. pylori* genome sequences from strains 26695 and J99. In order to examine associations with *H. pylori*-associated diseases they collected clinical isolates from 160 Japanese, 175 South Korean and 165 Colombian patients – 500 strains in total – along with clinical, histological and other data. This collection is notable not just for its large size but also because both Asian and Western types of *H. pylori* are represented and there is an approximately even contribution from each major associated disease (gastritis, duodenal ulcer, gastric ulcer and non-cardia gastric adenocarcinoma).

They used polymerase chain reaction (PCR), with confirmatory Southern blot hybridisation when negative, and showed no differential association with disease status for 12 of the 14 *vir* homologues. Two of the genes – *jhp0917* and *jhp0918* – were shown to be closely related with 98% (490/500) of strains having identical status for both. These are separate open reading frames in strain J99. An anonymous reviewer of their manuscript provided Lu et al. with the clue to ask whether *jhp0917* and *jhp0918* form one continuous gene (Figure 1.5). They referred to this gene initially as *jhp0917-0918*.

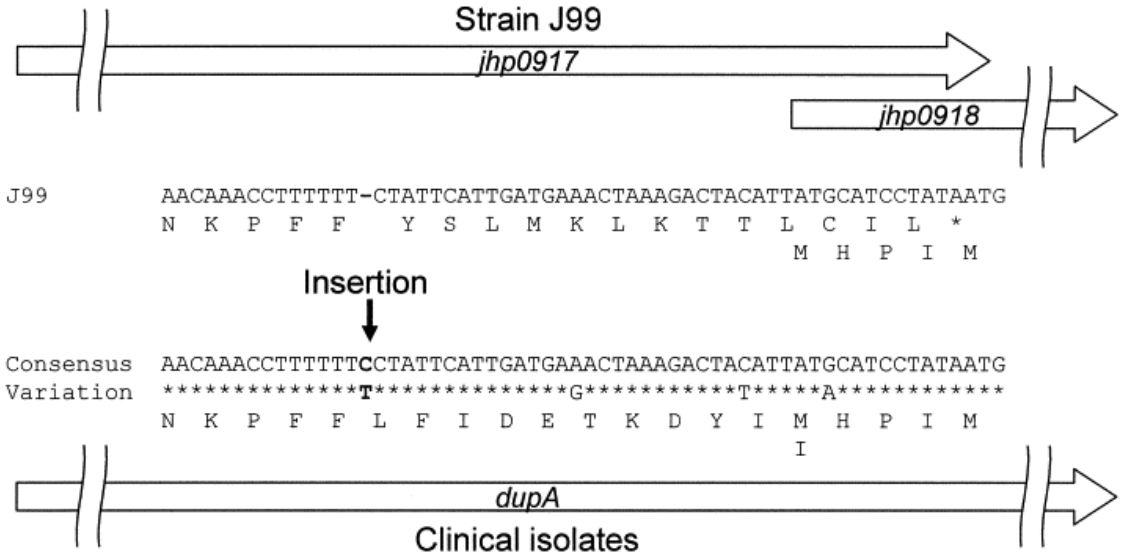

Figure 1.5 – relationship between *dupA*, *jhp0917-0918*, and *jhp0917* and *jhp0918*

Schematic structure of the *jhp0917* and *jhp0918* genes in *Helicobacter pylori* strain J99. Lu et al. (2005) identified a single nucleotide insertion (C or T) after position 1385 in 24 clinical isolates. This produced one continuous open reading frame spanning *jhp0917* and *jhp0918* (*jhp0917-0918*) that was designated as the duodenal ulcer promoting gene (*dupA*). Reproduced from Lu et al. (2005) with permission from Elsevier.

Independent univariate analysis showed differential association with disease status for *jhp0917-0918* in each region and overall. The prevalence of these genes was 42% in isolates from patients with duodenal ulcer – significantly greater than those with *H. pylori* gastritis (21%, $P < 0.01$), gastric ulcer (27%, $P < 0.05$) or gastric cancer (9%, $P < 0.01$). Multiple logistic regression, adjusting for age, sex and country of origin, confirmed that only the presence of *jhp0917-jhp0918* was an independent predictor of duodenal ulcer and was protective against gastric cancer in each region and overall (adjusted OR 8.3, 95% CI 4.0-17.4, $P < 0.001$). Similarly, *jhp0917-jhp0918* was shown to predict duodenal ulcer in East Asia against gastritis and protect against gastric cancer in Columbia against gastritis and gastric ulcer.

In support of their findings they also presented data from retrospectively *jhp0917-jhp0918* genotyped *cag*+ isolates from Japan in patients with DU and age- and sex-matched controls with gastritis (Yamaoka et al. 1999). *jhp0917-jhp0918* status was unavailable for two cases of the latter and these were excluded. Their analysis confirmed the association between *jhp0917-jhp0918* and duodenal ulceration – the genes were detected in 46% of strains from patients with duodenal ulcer compared with 15% of matched gastritis controls ($P < 0.001$). Lu et al. (2005) designated *jhp0917-jhp0918* as duodenal ulcer promoting gene (*dupA*).

1.3.2. Systematic review and meta-analysis of the relationship between *dupA* and clinical outcomes

The first such analysis was undertaken by Hussein (2010) and identified ten papers which contributed 19 study populations (marked in Table 3.8). He calculated the total patient number to be 2,358 by arithmetic combination across all studies, whereas these studies in fact included 2,396 adults and 131 children (calculation error). Formal meta-analysis was not performed. Worldwide *dupA* prevalence was calculated as 48.2%. A *dupA*+ genotype was found to be associated with a significantly increased risk of duodenal ulceration compared with gastritis (OR 1.4, 95% CI 1.1-1.7, P = 0.001). Constructing various groups by country, combination of countries or by region resulted in some that did and some that did not show associations. Of note for 561 South American patients, there were inverse associations between possession of *dupA* and both gastric ulcer (OR 0.2, 95% CI 0.1-0.4, P = 0.001) and gastric cancer (OR 0.3, 95% CI 0.2-0.6, P = 0.001). The reverse relationship was found when three Chinese populations were combined (OR 5.5, 95% CI 2.4-12.4, P = 0.001 and OR 2.0, 95% CI 1.1-3.1, P = 0.009, respectively for gastric ulcer and gastric cancer). The study concluded that '*dupA promotes duodenal ulceration in some populations and gastric cancer in others*' (Hussein 2010), which typifies observational studies of other *H. pylori* virulence factors.

Subsequently another review was published which incorporated the components expected of meta-analysis, such as assessment of study heterogeneity and for publication bias (Shiota et al. 2010). This review included one further citation that had been published later – a total of 11 articles – but excluded three different populations published in the same article where these was not case-control data. Therefore 2,466 patients from 17 populations in 13 countries (marked in Table 3.8) were evaluated. Overall, 43.0% possessed *dupA*. The prevalence was 64.1% in Western countries compared with 31.0% in Asian countries ($P < 0.0001$).

The major study findings are reported in Table 1.1 – namely the positive association between colonisation by a *dupA*+ strain and duodenal ulceration (worldwide and in Asian countries). There was no association between the presence of *dupA* gene and gastric ulcer or gastric cancer.

Overall, *dupA* was detected in around half of strains. It was confirmed as a risk factor for duodenal ulceration, particularly in Asian countries, though protective effects

against gastric cancer were not substantiated. These epidemiology data suggest that *dupA* may indeed be a disease-specific bacterial virulence factor.

These analyses informed the systematic review and meta-analysis undertaken in this study, which is reported in Section 3.4.

Table 1.1 – relationship between *dupA* status and clinical outcomes evaluated in a meta-analysis by Shiota et al. (2010)

			Clinical outcome		
			Duodenal ulcer	**Gastric ulcer**	**Gastric cancer**
Worldwide	***dupA* prevalence**	**in cases**	376/759 (50%)	93/306 (30%)	184/441 (42%)
		in controls	408/960 (43%)	191/583 (33%)	336/718 (47%)
	estimated OR (95% CI)		1.33 (1.09-1.60)	0.90 (0.66-1.20 – ns)	0.80 (0.63-1.02 – ns)
	adjusted OR (95% CI)		**1.41 (1.12-1.76)**	not necessary – no significant heterogeneity	0.88 (0.66-1.17 – ns)
	sensitivity analysis OR[1] (95% CI)		1.46 (1.15-1.85)		0.98 (0.72-1.32 – ns)
Asian countries	***dupA* prevalence**	**in cases**	183/483 (38%)	65/247 (26%)	68/252 (27%)
		in controls	180/616 (29%)	149/494 (30%)	135/423 (32%)
	adjusted OR (95% CI)		**1.57 (1.19-2.06)**	-	-
Western countries	***dupA* prevalence**	**in cases**	181/263 (69%)	28/57 (49%)	100/171 (59%)
		in controls	217/329 (66%)	42/89 (47%)	190/380 (68%)
	adjusted OR (95% CI)		**1.09 (0.73-1.62 – ns)**	-	-
	sensitivity analysis OR[2] (95% CI)		1.34 (0.85-2.13 – ns)	-	-

[1] = excluded Gomes et al. (2008) and South Korean study population from Lu et al. (2005).

[2] = excluded Gomes et al. (2008).

The South African study population from Argent et al. (2007) was not included with either Asian or Western countries.

adjusted OR, OR where the calculated proportion of total statistical heterogeneity variance was used to adjust the OR; CI, confidence interval; estimated OR, OR that includes all data; OR, summary odds ratio; ns, not significant; sensitivity analysis OR, OR where individual studies that were major sources of statistical heterogeneity are excluded to evaluate the possibility of disproportionate influences from a single study

1.3.3. *dupA* sequence variation and polymorphisms

Lu et al. (2005) presented the *dupA* gene from C142 as one open reading frame (ORF) of 1,839 bp (Figure 1.5). This was assembled using data from strain C142 and 23 other clinical isolates they sequenced, alongside the genome of the reference strain J99 (Alm et al. 1999). In J99 the *dupA* gene is not present and comprises comprises two ORFs – *jhp0917* (1,428 bp) and *jhp0918* (423 bp). The single ORF was formed by the insertion of a base T or C after position 1385 in the 3' region of *jhp0917*.

Frameshift mutations and truncated *dupA* alleles

Analysis of sequences covering the intergenic region between *jhp0917* and *jhp0918* deposited in GenBank showed that 85/89 (96%) showed the same frameshift mutation as C142 and formed a single ORF (Nguyen et al. 2010). However some clinical strains are similar to J99 with two ORFs – for example, in 3/89 isolates (Gomes et al. 2008) and in 3/34 isolates (Hussein et al. 2010). Several authors have commented on the prevalence of strains positive for *jhp0917* but which lacked the downstream *jhp0918*– for example, 11% of 166 isolates (Arachchi et al. 2007), 5% of 157 isolates (Douraghi et al. 2008) and 6% of 216 isolates (Abadi et al. 2012). Conversely *jhp0917–jhp0918+* strains were generally not detected.

In addition to the T or C insertion after position 1385, other insertions have been reported including an A inserted after position 1426 creating a premature stop codon in 16% of 86 isolates (Gomes et al. 2008). Queiroz, Rocha et al. (2008; 2011) found two adenine frameshift mutations with a deletion at position 1311 and the same insertion at position 1426. Similar findings were reported by Matteo et al. (2010) with an additional substitution at position 1633 resulting in an earlier stop codon. Another study set out to determine the stop codon position in several strains by sequencing the 3' end of *dupA* and the adjacent 5' region of *jhp0919*. In 25/34 isolates (74%) of both Western and Asian strains, sequence data showed that the stop codon was at 1884 bp, 5 bp after the start codon of *jhp0919* in J99 (Hussein et al. 2010). Given that it was the most frequently observed strain in their study they classified these types as "*dupA1*". Other shorter genes were grouped together as "*dupA2*" strains and thought likely to be degenerate forms. This "*dupA1*" form was subsequently also reported to be most common in correspondence from Brazil (Queiroz, Moura et al. 2011).

Long and short forms of *dupA*

Hussein et al. (2010) also reported as a note added in proof, following on from observations by the candidate for *dupA* in *H. pylori* genomes, that some *dupA* genes may be extended at the 5' end to form a longer ORF. Indeed, they confirmed that the *dupA* alleles in the two strains tested were extended with a total length of 2,499 bp. The presence of this "long-type" form was confirmed by sequencing in a study of 319 strains isolated from Okinawa, Japan (Takahashi et al. 2013). Matsuda et al. (2012) divided *dupA* into "Shi470-type" (2,499 bp) and "J99-type" (1,839 bp), with 58/60 *dupA*+ strains (defined by 2 dot-blots ± 2 PCRs) of the "Shi470-type" in their study of clinical isolates from Okinawa and Fukui, Japan. The "Shi470-type" strains are equivalent to "long-type" and the "J99-type" strains are equivalent to "short-type". Moura et al. (2012) also sequenced the *dupA* locus using a different method but did not identify any "long-type" forms, perhaps as the lead-in to its start codon was only 141 bases vs. 318-496 bases with the Takahashi method. They reported at least 14 further potential sites of indels and single nucleotide polymorphisms (SNPs) that rendered a truncated *dupA* form. For the "long-type" form, Takahashi et al. (2013) identified 7% of strains (6/84) with frameshift mutatations and designated the other strains as "intact long-type *dupA*". Matsuda et al. (2012) analysed a subset of "long-type" strains and found that 12/13 were intact. In another study, 50/170 Indian strains were typed as *dupA*+ by PCR with 2 primer sets and sequenced (Alam et al. 2015). They designated 17/50 strains as "*dupA2*" (frameshift mutation leading to premature stop codon and truncated form) and 33/50 as "*dupA1*", of which 21/33 were "long-type *dupA1*" (and so equivalent to "intact long-type *dupA*"; Takahashi et al. 2013) and 12/33 were "short-type *dupA1*".

Overcoming challenges of misclassification and terminology

In summary, these observations present two challenges. Firstly, not all strains classified as *dupA*+ by study authors will possess an intact long-type of *dupA* and, secondly, the use of different terminology is confusing.

The bias from misclassification of isolates as *dupA*+ when they in fact harbour a polymorphism likely to render the strain functionally DupA– is likely to be conservative. That is, the resultant underestimate of effect size may explain some of the negative disease association studies. Conversely a variant form of *dupA* that is predicted to encode a similar protein but possesses a genetic sequence with around 60% homology

to *dupA* has been detected in some genomes (Fischer et al. 2010). Therefore, some clinical isolates may have been misclassified as *dupA*–, which potentially muddies the waters even further. It is impossible to detect the various polymorphisms using a simple PCR method and sequencing is necessary to overcome this limitation. However, the *dupA* alleles that result in fully or partially functional products are not yet known. Therefore, the identification of what constitutes a functional *dupA* gene by inference from RT-PCR showing *dupA* mRNA expression, by assay for intact DupA protein, or by some other phenotypic marker is necessary.

Two reports where *dupA* mRNA expression were determined by RT-PCR pre-date the description of truncated alleles (Nguyen et al. 2010) and long and short forms (Alam et al. 2012). The former study showed that 10/10 randomly selected strains expressed *dupA* mRNA *in vitro* using non-quantitative RT-PCR, and concluded that *dupA* is a true gene and not a pseudogene. Alam et al. (2012) identified 38 strains that were *jhp0917*+ and *jhp0918*+ by PCR and dot-blot hybridisation. For 3/38 strains, they identified a single nucleotide deletion that disrupted the ORF. By RT-PCR they identified *dupA* mRNA in 28 strains of these 35, and that relative *dupA* mRNA expression *in vitro* varied up to 15-fold between strains. The impact of different *dupA* forms on transcription is unknown.

Recently, DupA protein was expressed in *E. coli* and purified (Wang, Chen et al. 2015), using the *dupA* sequence obtained from strain WH21 isolated from a Chinese patient with DU. Strain WH21 contains the intact long-type *dupA*. It is not known if other forms of *dupA* are expressed but this has not been shown, including "short-type *dupA1*" forms.

In this study, *dupA1* strains possessed an intact full-length *dupA* gene, *dupA2* strains possessed a non-intact, fragmented or less-than-full-length *dupA* gene, and *dupA*-negative strains were those not shown to possess any form of *dupA*.

Therefore, strains were classified as follows in this study:

- *dupA1* strains were defined as those with an intact full-length gene of 2,499 bp,
- *dupA2* strains were defined as those with a SNP or indel that would result in a frameshift or early termination of transcription, only fragments of the *dupA* gene, or forms shorter than 2,499 bp (including the 1,884 bp form previously designated as "*dupA1*"),
- *dupA*-negative strains were defined as those not shown to possess *dupA*.

Next, we review reports that *dupA* may only be a one component of a larger system.

1.3.4. *dupA* and a putative new type IV secretion system (*tfs4*)

In addition to the extensive evidence presented before that *dupA* exists in multiple forms, including several which are unlikely to result in functional gene products (Section 1.3.3), a growing body of work suggests that it may not function alone. *dupA* appears to be only a single component of a larger region of the plasticity region that incorporates multiple genes. It has been proposed that some of these genes together with *dupA* may form a novel and as yet uncharacterised type IV secretion system (T4SS) here referred to as *tfs4*. *Helicobacter pylori* has up to four known T4SSs encoded in its chromosome (Figure 1.6).

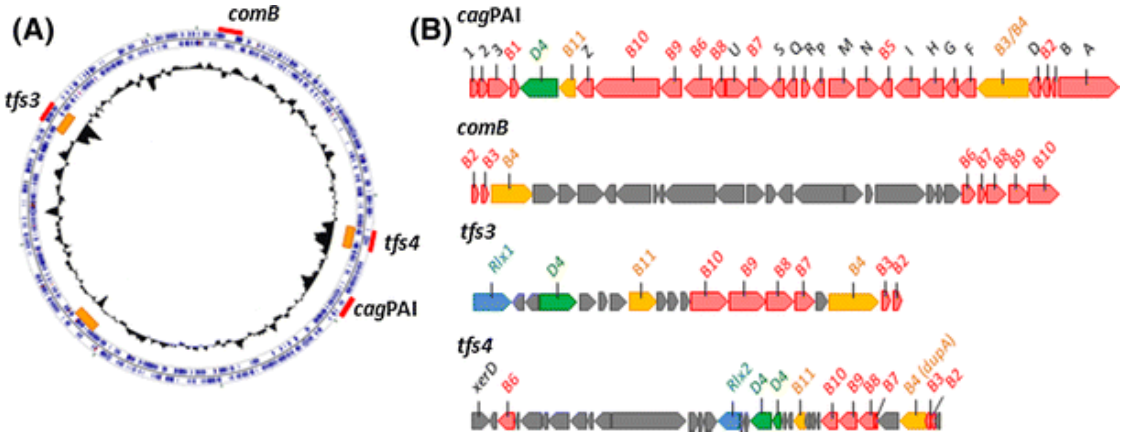

Figure 1.6 – type IV secretion systems (T4SS) encoded in *H. pylori* chromosomes

(A) Schematic representation of the chromosome of *Helicobacter pylori* strain P12. The outermost concentric blue circles denote predicted coding genes as bars on the plus strand (outer circle) and minus strand (inner circle). Guanine and cytosine (GC) content is represented by black peaks on the innermost concentric circle. The location of the four T4SSs is indicated by red bars and of the three plasticity zones by orange bars.

(B) Genetic composition of the four T4SSs (*cag*PAI, *comB*, *tfs3* and *tfs4*). Arrows in red represent genes which are described to encode structure T4SS components; in blue indicate putative conjugative relaxases; in green indicate coupling proteins; in yellow the ATPases (including *dupA*); in grey open reading frames with yet unknown functions.

Adapted from Fernandez-Gonzalez and Backert (2014) with permission from Springer.

When *dupA* was first proposed as a bacterial virulence factor only two other sequenced strains of *H. pylori* (26695 and J99) were included in bioinformatic analysis. This did not identify any neighbouring genes as candidate *vir* homologues. Lu et al. (2005) did hypothesise that '*the dupA gene in combination with other novel* vir *homologue genes ... might form a [T4SS] similar to the* cagPAI'. Indeed, like the *cag*PAI (Section 1.2.1), *tfs4* does share homology with *vir* genes from the *A. tumefaciens* T4SS (Figure 1.7).

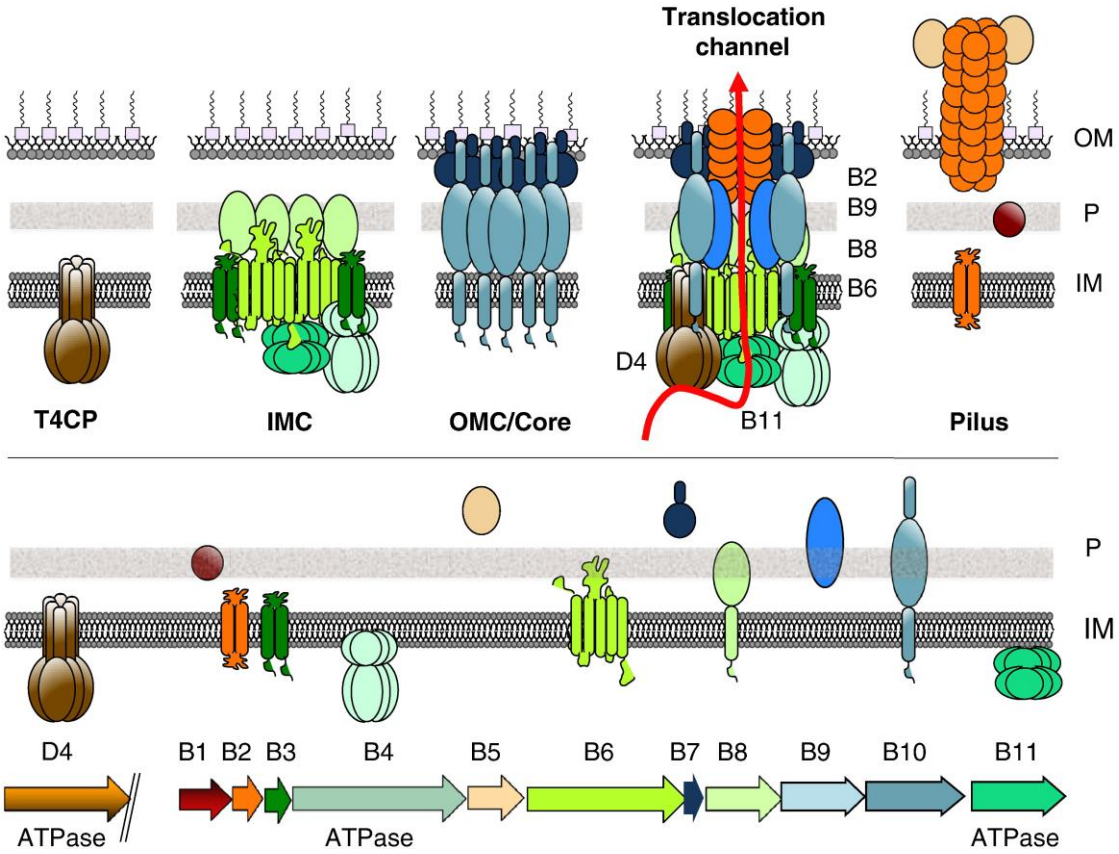

Figure 1.7 – schematic of the type IV secretion system (T4SS) of *Agrobacterium tumefaciens*

Representation of subunits and subassemblies of the *A. tumefaciens* VirB/VirD T4SS.

(Bottom) Eleven VirB subunits are synthesized from the *virB* operon and VirD4 from the separate *virD* operon.

(Middle) The VirB/VirD subunits are inserted in the inner membrane (IM) or delivered to the periplasm (P) with general topologies as indicated.

(Upper) The subunits form a network of interactions resulting in four functional subassemblies:

i) type IV coupling protein (T4CP) substrate receptor [D4],

ii) inner membrane translocase (IMC) [B3, B4, B6, B8 and B11],

iii) outer membrane complex (OMC) or core complex [B7, B9 and B10], and

iv) extra-cellular pilus [B2 and B5].

The substrate translocation channel is shown by the red arrow. Assembly of the conjugative pilus is mediated by the IMC and OMC, together with the VirB1 transglycosylase. The putative *tfs4* T4SS includes genes with identity to all components represented in this schematic, except for *virB5* and *virB6*.

Figure reproduced from Christie et al. (2014) with permission from Elsevier.

Type 4 secretion systems in *H. pylori*

The best understood and ubiquitous T4SSs of *H. pylori* are the *cag* pathogenicity island (Section 1.2.1) and the ComB system for DNA import through natural transformation (Yamaoka 2008). In 2003, the third T4SS was described in the plasticity region of a strain recovered from a Peruvian patient with gastric cancer (Kersulyte et al. 2003). This 16.3 kb cluster of 16 genes, of which seven were *vir* homologues, was named *tfs3*, and found to be present in around 20% of isolates. The authors were unable to identify any functional role for *tfs3* and no correlation between complete or partial *tfs3* and clinical outcomes was found. Other groups have similarly established that 8-33% of clinical isolates possess a complete *tfs3*, and found no relationship between *tfs3* and *dupA* or other *vir* homologues (Lu et al. 2005). The *tfs3* region contains *jhp0940* and related genes (Romo-Gonzalez et al. 2015).

The first experimental evidence that *dupA* is a gene in a cluster that form a novel T4SS was published as a conference abstract (Jung et al. 2009). Bioinformatic analyses of the additional *H. pylori* genomes from strains Shi470 and G27 revealed a 16.3 kb gene cluster of seven *vir* homologues including *dupA*, which is predicted to share homology with the ATPase-encoding gene *virB4*. PCR-based methods were used to establish the prevalence of the six additional putative cluster components in 30 *dupA*+ and 30 *dupA*– clinical isolates. Concerning *dupA*+ strains 24/30 (80%) possessed all six additional genes compared with none of the *dupA*– strains, among which 13/30 (41%) did not contain any additional genes. The candidate's own unpublished observations from this time support their findings, although half of *dupA*+ strains lacked at least one other gene. Together these suggest that the absence of *dupA* could prove to be a robust marker of an incomplete cluster. However, the presence of other hypothetical T4SS components may be required along with *dupA* for full functionality, therefore previous association studies have potentially misclassified clinical isolates leading to systematic bias.

In a follow up study, Kersulyte et al. (2009) identified genetic segments that contain *dupA* and encode equivalent though highly divergent proteins to *tfs3*. In Shi470 and G27 these regions showed highly similar sequences and were designated as *tfs3a*. In addition, in strain P12 they described a different region only half of which was closely matched in sequence to *tfs3a* though the whole segment encoded substantially similar proteins to *tfs3a*. This region was initially called *tfs3b*.

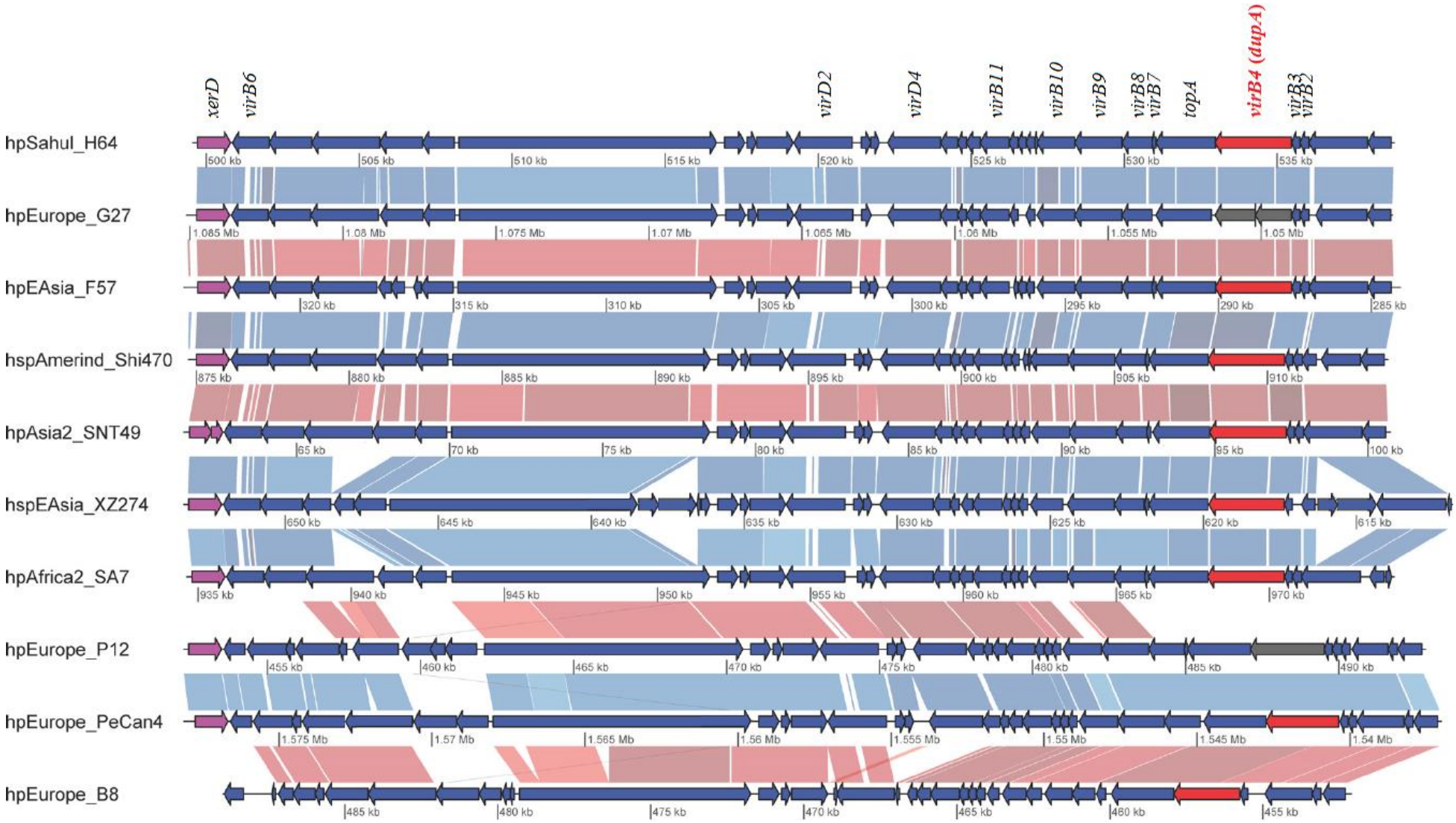

Figure 1.8 – pairwise alignment of *tfs4* regions from chromosomes of various *Helicobacter pylori* genomes

Strains (with their respective clade) are shown to the left of the figure. Putative type IV secretion system (T4SS) homologues are shown above the figure (*dupA* is highlighted in red or in grey where a frameshifted form is present). Sahul64 (H64), G27, F57, Shi470, SNT490, XZ274 and SouthAfrica7 (SA7) have the same type of *tfs4* and P12, PeCan4 and B8 have another variant form of *tfs4*. Pink arrows represent the integrase/recombinase gene (*xerD*, renamed *xerT* in *H. pylori*). Reproduced from Lu et al. (2014) with confirmation from the American Society for Microbiology that additional permission is not required.

Final designation as *tfs4*, and its relationship with *dupA* and with clinical outcomes

However, given the dissimilarity of *tfs3* and *tfs3a*/*tfs3b* found by *in silico* analysis, including multiple sequence alignments and phylogenetic trees, others have concluded that they have a different evolutionary origin and are distinct and independent T4SSs (Fischer et al. 2010). The putative secretion system containing *dupA* was therefore termed *tfs4*, which is used here instead of *tfs3b*. The authors constructed isogenic *tfs4* deletion mutants lacking the complete T4SS gene cluster and reported that the system is not involved in translocation of CagA protein to AGS cells nor in DNA uptake by natural transformation (Fischer et al. 2010). Further *in silico* analysis suggests that there may be further variants of *tfs4* and *dupA* (Fischer et al. 2014). The relationship between *dupA* and the *tfs4* gene cluster is shown for 10 *H. pylori* genomes in Figure 1.8.

Linkage analysis of microarray data from a worldwide collection of 52 strains and another 42 patients from Costa Rica has unambiguously shown that *dupA* and all other plasticity region genes with disease associations (*jhp0940*, *jhp0945*, *jhp0947* and *jhp0949*; see Section 1.2.1) are linked together and with other genes that define the *tfs4* cluster but were distinct from *tfs3* components (R. Delahay, unpublished observation).

The first study to evaluate the relationship between *dupA*/*tfs4* status and clinical outcomes was by Jung and colleagues (Jung et al. 2010; Jung et al. 2012). Firstly, 14 Asian and 14 Western strains were randomly selected from their institution's bacteria bank and used to evaluate eight PCR primer pairs. Based on their ability to detect *dupA* and degree of sequence mismatch with complete sequences for the gene, they identified one initial primer set and two further sets to be used when the initial result was negative. Other *vir* gene homologues (*virB8*, *virB9*, *virB10*, *virB11*, *virD4* and *virD2*) were also amplified with specific PCR primer sets and negative results confirmed by priming across two adjacent genes. Histology was scored as before (Lu et al. 2005; Yamaoka et al. 1999). The study recruited 245 patients from the United States of America. Almost half (47%) of isolates possessed all assayed *tfs4* genes including *dupA* (referred to by these authors as *tfs4* intact), 19% possessed no genes and 34% contained partial systems. In support of previous work, the absence of *dupA* was a good marker with an incomplete system – 68% of *dupA*+ strains showed an intact *tfs4* cluster against 0% of *dupA*– strains ($P < 0.001$). *dupA* and *tfs4* status did not correlate with *cag* status. They found no significant association between *dupA* and clinical outcome, confirming the findings of other studies of Western strains, although the prevalence of *virB9* and *virD4* were each

significantly higher in strains from patients with duodenal ulceration. Moreover, *tfs4* intact strains were more frequently found to colonise patients with duodenal ulcer than those with gastritis (61% vs. 41%, $P = 0.012$; adjusted OR 2.13, 95% CI 1.13-4.03, $P = 0.019$), whereas there was no difference in intact *tfs4* prevalence between other clinical outcomes or associations between an incomplete *tfs4* cluster and disease groups. With regard to histology, there were no significant differences observed for inflammatory scores, colonisation density or intestinal metaplasia. Interestingly there was more atrophy in the antrum and corpus of patients colonised with *dupA*+ than *dupA*– strains independent of *tfs4* status. Results of *in vitro* and *in vivo* cytokine assays are presented later (Section 1.3.5).

In summary, *dupA* is a component of *tfs4* – a novel gene cluster hypothesised to encode a T4SS of unknown function. This is in addition to the polymorphic nature of *dupA* and the possibility of functional variant forms. Consequently, assuming that the functionality of *tfs4* unpins the association of *dupA* with disease, it is highly likely that both functional and non-functional systems may have been misclassified under "*dupA*+" and "*dupA*–" categories in earlier work. Initial evidence suggests that, like *dupA*, *tfs4* can also be considered as a *H. pylori* virulence factor that may promote duodenal ulcer formation. Understanding the role of *dupA* in gastroduodenal disease requires that the function of the components of the *tfs4* cluster be established and research in this area is only beginning. Possible functions for *dupA*, and by extension *tfs4*, are considered in the next section.

1.3.5. Insights into the functional relevance of *dupA*

DupA, and any associated products of genes in the *tfs4* cluster, had not been characterised when this study was started. Indeed, other researchers have been unable to successfully utilise antibody-based methods as, although protein was expressed, the antibodies raised against them were non-specific (Dr Christian Marx, personal communication). However, this was reported during the preparation of this thesis.

The function of DupA

Regions of the expected DupA product include a CagE/TrbE/VirB and a FtsK/SpoIIIE domain (amino acid positions 3-201), with the latter domain containing a putative ATP-binding P-loop motif with predicted NTP hydrolase activity, and the adjacent region (positions 203-610) showing homologue to the TraG/TraD family (Alam et al. 2015).

These have been implicated in intercellular chromosomal DNA transfer among other functions in bacterial species (Lu et al. 2005).

DupA was recently cloned (from a *dupA1* clinical isolate from a patient with DU in China), expressed and purified (Wang, Chen et al. 2015). The DupA protein localised to the bacterial membrane (based on fractionation into periplasm, cytoplasm and membrane fractions) and showed ATPase activity (126±18 units/mg protein). An isogenic Δ*dupA* mutant was generated, which was used to show that *dupA* was not involved in adhesion to GES-1 gastric epithelial cells or in CagA protein translocation. There were cytotoxic effects on MKN45 gastric epithelial cells, with reduced cell viability and increased evidence of apoptosis with wild-type vs. mutant strains. They also reported an interaction between DupA protein and urease, though this may simply be because urease is the most abundant protein produced by *H. pylori*.

Therefore, DupA has been shown to have ATPase activity and effects on epithelial cells *in vitro*. The specific role of DupA in terms of protein-protein interactions and the function of the putative type IV secretion system (T4SS) with which it is associated have yet to be demonstrated.

dupA as a component of _tfs4_

As previously described, *dupA* and its neighbours within the *tfs4* gene cluster share homology with *vir* genes of *A. tumefaciens*. The *dupA* gene itself is homologous to *virB4*, which encodes the VirB4 ATPase. Its characterisation is reported above. VirB4 is the signature subunit of T4SS across bacterial species (Fronzes et al. 2009), with various homologues involved in secretion system assembly and energisation, or implicated in DNA update and/or DNA and protein transfer (Gomes et al. 2008).

The chromosomally-encoded plasticity zones of *H. pylori*, including *tfs4*, are reported to be integrating conjugative elements (Fischer et al. 2014). The functions of two components of *tfs4* have been reported that support a role in horizontal gene transfer. This comprises several steps: first, excision from the chromosome; second, nicking of the circular intermediate at *oriT*; third, transfer from donor to recipient by conjugation, typically mediated by a relaxosome that interacts with a T4SS coupling protein to deliver DNA or a nucleoprotein complex through the secretion channel; and fourth, chromosomal integration via site-specific or non-specific recombination. The first step utilises *XerT*, a homologue of *XerD*, which is a recombinase in *tfs4* (Fischer et al. 2010).

XerT excises the *tfs4* element at conserved motifs (5'-AAAGAATG-3') to generate a circular transfer intermediate. In the second step, this intermediate is nicked by a relaxase at *oriT*. Grove et al. (2013) demonstrated the expected nicking activity of a VirD2-like protein encoded in *tfs4*, with enhanced activity targeted towards the 5'-ATCCTG-3' that is consistent with the consensus sequence for the *oriT* nick site. The mechanisms of the third and fourth steps for *tfs4* have yet to be reported. Potential roles of T4SSs in horizontal DNA transfer are shown in Figure 1.9. The *tfs4* system has been shown not to be involved in the DNaseI-resistant conjugation of 2 natural plasmids from *H. pylori* strains P8 and P12 (Rohrer et al. 2012). Natural transformation is the major function of the *comB* system (Fernandez-Gonzalez and Backert 2014), though it is not known whether *tfs4* or its putative components could substitute for *comB* components. Or indeed, whether functional substitution between the T4SSs in *H. pylori* is possible, particularly given the presence of apparently inactive *tfs4* systems in many strains due to fragmentation and inactivating mutations.

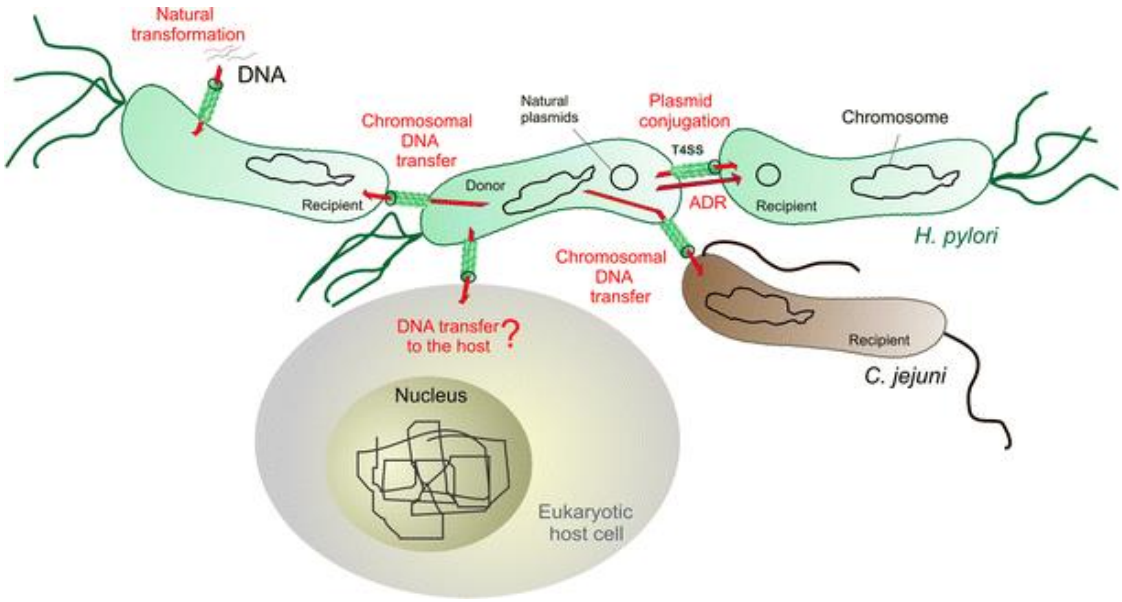

Figure 1.9 – schematic model for potential roles of *Helicobacter pylori* type IV secretion systems in horizontal gene transfer events

Potential horizontal gene transfer mechanisms and corresponding direction of DNA delivery proposed are indicated in red (natural transformation, chromosomal DNA transfer, inter-species or inter-kingdom DNA transfer, plasmid conjugation, and the alternate DNaseI-resistant mechanism [ADR, Rohrer et al. 2012]). *H. pylori* is green, *Campylobacter jejuni* is brown, and the mammalian host cell is grey. Reproduced from Fernandez-Gonzalez and Backert (2014) with permission from Springer.

Overall, the exact function of *tfs4* (and *dupA*) is yet unknown but there is increasing evidence that the role of *tfs4* is in horizontal gene transfer, most likely chromosomal DNA transfer between bacteria. Inter-kingdom transfer to host cells is conceivable, though unlike for the *cag* virulence system (Section 1.2.1), there is no clear candidate secreted effector for *tfs4*. However, just as *cag* and its components can have indirect effects on host cells, for example, through contact between the pilus and host cell surface receptors, perhaps this is important in host-bacterial interactions for *tfs4* (Figure 1.10).

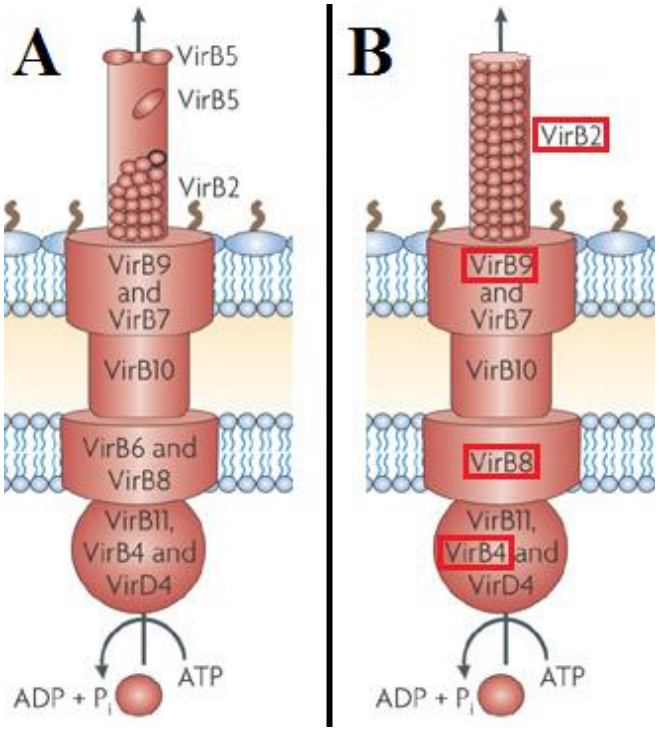

Figure 1.10 – schematic representation of a putative structure for the *tfs4* T4SS

(A) This panel shows a schematic representation of the type IV secretion system (T4SS) of *Agrobacterium tumefaciens*. See Figure 1.7 for details (VirB1 and VirB3 omitted).

(B) This panel shows a schematic representation of a putative structure for the *tfs4* T4SS of *Helicobacter pylori*. The function and topographical location for these components has not been shown, except that DupA encoded by the *virB4* homologue is located in the bacterial membrane (inner vs. outer membrane not defined) and has ATPase activity (Wang, Chen et al. 2015). This schematic is based on panel A for *A. tumefaciens*, though as there are no putative homologues for VirB5 and VirB6 these were also omitted. The pilus is shown as if constructed only from VirB2. In the *cag*PAI T4SS of *H. pylori*, CagL is the VirB5 homologue and interactions with an integrin on host cells (Kwok et al. 2007). Note that there is an uncharacterised open reading frame between the *virB4* (*dupA*) and *virB7* homologues in *tfs4* that might fulfil this role.

The *tfs4* genes selected for mutagenesis work in Chapter 5 are highlighted in red boxes. These were chosen so that one putative component was represented from the inner membrane complex [VirB8], the outer membrane (core) complex [VirB9] and the pilus [VirB10]. The components required for pilus assembly are unknown. See Section 5.3.1.

Adapted from Fronzes et al. (2009) with permission from Nature Publishing Group.

Interleukin-8 responses *in vivo* with respect to *dupA* status

We now turn to differences in host phenotype observed in association with *dupA* or in experimental models, both *in vivo* and *in vitro*.

Initial phenotypic assays with respect to *dupA* status focussed on IL-8 expression by gastric epithelial cells *in vivo* and using cell line models. Expression of the pro-inflammatory cytokine IL-8 is strongly induced *in vivo* and *in vitro* by the *cag* pathogenicity island and to some extent by other virulence factors including OipA and perhaps BabA (Robinson et al. 2007). Given that gastritis is characteristic of chronic *H. pylori* infection and the important role of IL-8 in recruiting inflammatory cells to the gastric mucosa, it is logical to examine the relationship between *dupA* and IL-8 expression. We will first consider the results of *in vivo* experiments before turning to *in vitro* approaches.

Lu et al. (2005) analysed 98 *cag*+ strains from Japanese patients – 50 with duodenal ulcer and 48 with gastritis (as explained in Section 1.3.1). Gastric mucosal IL-8 levels had previously been determined in all 98 antral biopsies and in 70 biopsies from the corpus. Biopsies were first homogenised in phosphate buffered saline, then aliquoted within ten minutes of biopsy and diluted for quantitative culture to determine *H. pylori* density, before the remaining undiluted homogenate was spun down and supernatants frozen at -80 °C. Total protein was determined by a modified Lowry method. IL-8 expression was determined in duplicate by ELISA with results expressed as mean ± standard error in pg per mg of protein, or in pg per CFU×10^3 (colony forming units) to adjust for colonisation density.

The major finding was that IL-8 expression in antral biopsies from patients with duodenal ulcer was significantly higher in those colonised by *dupA*+ strains. This was the case when expressed as IL-8 level per total protein (*dupA*+: 161±19 pg/mg protein, *dupA*-: 101±14 pg/mg protein, $P < 0.05$) and as IL-8 level per *H. pylori* (*dupA*+: 347±10 pg/CFU×10^3, *dupA*-: 258±7 pg/CFU×10^3, $P < 0.05$). They also reported a similar antral association for controls with gastritis but only when expressed as IL-8 level per *H. pylori* – 302±7 pg/CFU×10^3 for *dupA*+ strains vs. 150±19 pg/CFU×10^3 for *dupA*– strains ($P < 0.01$). No associations were found in the corpus and no comparisons between antral and corpus biopsies undertaken. Their data do hint at a more marked antral-predominant pattern of gastritis in *dupA*+ strains and corpus-predominant or antral-sparing pattern in

dupA– strains in patients with gastritis. This may be, at least in part, an effect of colonisation density. Unsurprisingly this different is not seen in patients with duodenal ulcer though the antrum to corpus inflammation ratio appears higher in those colonised by *dupA*+ strains. These observations may be confounded by the association between *dupA* and duodenal ulcer in their study population. The findings are intriguing as they suggest a biologically plausible explanation for the link with clinical outcomes at a pathophysiological level.

Queiroz, Rocha et al. (2011) collected antral mucosal specimens from 117 Brazilian patients with *H. pylori* gastritis. After addition of the protease inhibitor aprotinin, the supernatants of biopsy homogenates were used to determine *in vivo* antral IL-8 levels by ELISA in duplicate (with results expressed as mean ± standard deviation in pg per mg biopsy protein determined by Bradford's method). Their analysis was confined to 83 patients colonised by *cag*+ isolates to avoid potential bias. Among 54 strains considered to have an intact *dupA* gene, mean antral mucosal IL-8 level was 2,037±2,193 pg/mg protein. This was significantly higher than in the 29 strains without intact *dupA* where the level was 1,247±821 pg/mg protein (P = 0.04 by two-tailed Student's t test, with data first normalised by log-transformation). Although these findings agree with the observations of Lu et al. (2005), the spread of the data particularly for *dupA*+ strains was very marked. This may be because some *dupA*+ strains lack other *tfs4* components (see Section 1.3.4). The use of a protease inhibitor, the different ELISA kits, differences in biopsy size and handling, or the different protein quantification methods may explain the higher absolute IL-8 levels found in this study.

Similar research examining antral mucosal IL-8 expression according to *dupA* and *tfs4* status has been published (see Section 1.3.5; Jung et al. 2012). Twenty-seven randomly selected patients with gastritis colonised by *cag*+ strains were studied from an American population of 88 cases meeting those criteria. *In vivo* IL-8 levels were again shown to be higher in those infected with *dupA*+ rather than *dupA*– isolates. Moreover. mean IL-8 level ± standard error was 92±15 pg/mg protein for *tfs4* intact strains, significantly more than for both *tfs4* incomplete/*dupA*+ strains (60±9 pg/mg protein) and *dupA*– strains (39±11 pg/mg protein).

Finally, Wang, Shao et al. (2015) identified 94 Chinese patients infected with *cag*PAI-intact and *vacA* s1/m2 strains. Gastric mucosal IL-8 was higher for *dupA1* strains with

an intact *tfs4* (123±22 pg/mg) compared with strains with an incomplete *tfs4* (66±14, $P < 0.01$) and *dupA*– strains (59±10, $P < 0.01$).

Only one group has approached differential *in vivo* inflammatory responses by *dupA* status using RT-qPCR (quantitative, real-time reverse transcriptase PCR) with a two-stage assay and SYBR green detection chemistry to measure *IL8* mRNA expression (Hussein et al. 2010). Oligo(dT)-primed cDNA was synthesised from total RNA purified from the antral gastric biopsy specimens of 17 infected and 5 uninfected donors. Relative expression of *IL8* was normalised against the reference gene *GAPDH* and an additional uninfected comparator biopsy. Included in each assay were positive human cDNA controls, no template controls and first-stage RT minus controls to exclude DNA contamination of RNA template. *IL8* expression was five-fold higher in *dupA*+ infections – median (inter-quartile range) for relative *IL8* mRNA level was 119 (58-304) in six *dupA*+ cases and 23 (10-55) in 11 *dupA*– cases ($P = 0.02$), and was negligible in uninfected patients. The difference remained when only six *cag*+/*dupA*+ and seven *cag*+/*dupA*– samples were analysed ($P = 0.03$).

Taken together, these five studies all found significantly higher antral IL-8 (or *IL8* mRNA) expression *in vivo* among patients infected with *dupA*+ *H. pylori*. This relationship appears to be independent of *cag* status, though may of course be confounded by other unmeasured virulence factors. Two studies suggest that the *tfs4* status of the colonising strain may also be important. Unfortunately, there were limited results from corpus biopsies. Evaluation of the relative levels of IL-8 and other cytokines in different regions of the stomach is worthy of further study and may provide fascinating insights into the link between *dupA* and patterns of gastritis in humans.

Interleukin-8 responses *in vitro* with respect to *dupA* status

We next turn our attention to *in vitro* studies in this area. Lu et al. (2005) selected 54 *cag*+/*oipA* 'on' clinical isolates from their original population of 500 (with each disease group in each country contributing six strains). On two independent occasions bacteria were grown in BHI broth, co-cultured for 20 hours with cells from the MKN45 gastric epithelial cell line at a multiplicity of infection (MOI) of 100, then supernatants were assayed in duplication with IL-8 ELISA (with results expressed as mean ± standard error). Mean IL-8 level in *dupA*+ strains was 3,207±123 pg/mL compared with 2,681±118 pg/mL for *dupA*– strains ($P < 0.001$). They do not indicate that unexposed

control cells were also assayed to confirm the background level of cytokine expression from the cell line. Their findings have not been reproduced by other research groups.

Similar *in vitro* experiments were undertaken with eight *dupA*+ and ten *dupA*– strains from Japanese patients (Nguyen et al. 2010). All isolates possessed *cagA* and *cagE*, and had *oipA* 'on' status. Gastric epithelial cell lines AGS and MKN45 were grown overnight in RPMI-1640 medium supplemented with 10% foetal bovine serum under standard conditions. Bacterial cells harvested from agar cultures were washed twice, added to epithelial cells at a MOI of 100, and finally supernatant IL-8 levels were measured by ELISA after six hours of co-culture. Experiments were performed in duplicate on two occasions. There were no significant differences in IL-8 levels between strains although a trend towards higher levels from *dupA*– strains was seen (AGS: 670±419 pg/mL vs. 707±359 pg/mL, MKN45: 1093±687 pg/mL vs. 1220±420 pg/mL, respectively for *dupA*+ and *dupA*– strains). This may be the result of a shorter incubation time (six hours vs. 20 hours) or because of the greater chance of type II error from a smaller sample size. No control cells were reported to ascertain background cytokine levels.

Schmidt et al. (2010) grew overnight cultures of 22 *cagE*+ clinical isolates from Malaysian patients in supplemented Brucella broth. AGS cells were prepared in the same way as Nguyen and colleagues, although the medium was also supplemented with the buffer HEPES. Bacteria and AGS cells were combined at a MOI of 100 in at least three independent experiments, then centrifuged to synchronise infection, incubated for six hours (at 37 °C in a 10% rather than a 5% CO_2 incubator), and finally IL-8 expression was determined in duplicate by ELISA. No differences in IL-8 induction were found (*dupA*+: 1,330 pg/mL [n=8] vs. *dupA*-: 1,378 pg/mL [n=14]).

Jung et al. (2012) reported IL-8 levels after a 20-hour co-culture of 28 clinical isolates with MKN45 gastric epithelial cells as previously determined in their group (Lu et al. 2005). No difference in IL-8 production between *dupA*+ and *dupA*– strains was found. However, mean IL-8 expression ± standard error was 2,012±127 pg/mL for *tfs4* intact strains, which was around 25% higher than that of *tfs4* incomplete/*dupA*+ strains (1,616±114 pg/mL, $P = 0.01$) and *dupA*– strains (1,608±85 pg/mL, $P = 0.01$). Again, no control cells were reported.

Alam et al. 2015 co-cultured AGS cells with various Indian clinical isolates that were *cagA*+ and *vacA* s1m1 at an MOI of 100 for 8 hours. They observed higher IL-8 concentrations for *dupA1* strains than for *dupA2* and *dupA*-negative strains, though it was not clear if the *dupA1* group included both long-type and short-type (903±79 pg/mL, 536±100 pg/mL [$P = 0.008$] and 550±104 [$P = 0.009$], respectively).

Similar results were obtained by Wang, Shao et al. (2015) for 33 Chinese isolates that were *cag*PAI-intact and *vacA* s1/m2. These were co-cultured with GES-1 cells at an MOI of 100 for 24 hours. Interleukin-8 concentrations were increased for *dupA1* strains with an intact *tfs4* (1528±180 pg/mg) compared with strains with an incomplete *tfs4* (1229±75, $P < 0.01$) and *dupA*– strains (1202±92, $P < 0.01$).

On a cautionary note there is evidence that *IL8* mRNA levels and signalling pathway activity can be increased in direct response to the use of a high MOI, such as an MOI of 100 used in the preceding studies (Ritter et al. 2011). Therefore, it is possible that *dupA* and potentially other virulence factors make only a minor contribution to IL-8 expression in response to high bacterial loads. Studies have not consistently been able to reproduce the initial report showing increased IL-8 expression from gastric epithelial cells *in vitro*. Given the apparent relationship with respect to *tfs4* status, it may be that non-functional but nevertheless *dupA*+ strains have been misclassified.

Supporting experimental evidence that *dupA* has a direct role on IL-8 response *in vitro* used an isogenic *dupA* mutant, a complemented *dupA* mutant, wild-type C142 strain and appropriate controls (Lu et al. 2005). These were performed in triplicate and in the same manner as the authors' other *in vitro* experiments (including that no unexposed controls were reported). IL-8 levels were significantly higher in supernatants from co-cultures with wild-type C142 (3,421±175 pg/mL) than the Δ*dupA* mutant strain (2,480±124 pg/mL [28% reduction], $P < 0.005$), which were restored in complemented *dupA* mutant (3,354±216 pg/mL). Furthermore subsequent reports of preliminary data from the same laboratory state that IL-8 induction from gastric epithelial cells was found to be decreased in Δ*dupA* mutants of some strains compared but not in Δ*dupA* mutants prepared from other strains, compared to wild-type (Yamaoka 2008). Finally, IL-8 production from GES-1 cells co-cultured with a different wild-type *dupA1* strain and its isogenic Δ*dupA* mutant showed similar results, with an approximately 25% reduced IL-8 concentration observed after 6, 12, 24 and 48 hours (Wang, Chen et al. 2015).

In contrast, Hussein et al. (2010) rigorously re-tested these observations using four different gastric epithelial cell lines (AGS, ST16, MKN45 and MKN28 cells) and seven different isogenic *dupA* mutants (co-cultured at a MOI of 100 for 48 hours) in multiple independent experiments. The original strain (C142) was not available but they included one strain with the same form of *dupA* (J123). No significant differences were observed in any experiment for both *dupA1* and *dupA2* type strains, though levels were markedly lower for J123 and unexposed control cells. To confirm their methods, they were however able to demonstrate a marked reduction in IL-8 expression following *cagE* disruption to the level of control cells.

In summary, controversy remains over whether the mechanism of action of *dupA* involves induction of IL-8 secretion in gastric epithelial cells thereby leading directly to increased inflammation. It is possible that some of the *dupA*+ strains studied and classified as functional lacked other essential components of *tfs4* that are as yet unknown. Therefore, further evaluation is necessary, using strains lacking genes known to induce IL-8 (like *cagA* and *oipA*), to elucidate any contribution of *dupA* to IL-8 induction from epithelial cells. The findings of *in vivo* studies are more consistent. The question remaining is where the IL-8 is coming from if not from epithelial cells? It is possible that bacteria are exerting their effect through immune and inflammatory cells (Crabtree 1996; Guiney et al. 2003). Indeed, Ethuin et al. (2001) showed that IL-12 has a synergistic effect with bacterial products on IL-8 release from neutrophils at both mRNA- and protein- levels, with intermediate roles for tumour necrosis factor alpha (TNF-α) and interferon gamma (IFN-γ). Importantly *in vitro* experiments using a panel of *dupA* mutants support an alternative explanation for the increased mucosal IL-8 levels seen *in vivo*, and therefore a potential mechanism for the observed associations between *dupA*, histopathological biomarkers and clinical outcomes.

Other cytokine responses with respect to *dupA* status

These experiments were undertaken by Hussein et al. (2010) and are reported here according to the authors' *dupA1*/*dupA2* classification (Section 1.3.3). They first collected mononuclear immune cells from the peripheral blood of five healthy donors and co-cultured them for 48 hours with two *dupA1* isolates (AB21 and AB31) and their isogenic *dupA* mutant constructs. Supernatant were assayed by ELISA and the results expressed as the mean percentage increase in cytokine level for the wild-type strain using the Δ*dupA* mutant as the baseline. The most marked effect was on IL-12/23p40

expression – the mean increase was 176% for AB21 (P = 0.001) and 106% for AB31 (P = 0.002). There were also small but statistically significant differences observed for IL-8, IFN-γ (the prototypical Th1 effector cytokine) and TNF-α, with 4% to 35% mean increase over baseline. All were higher than unexposed controls. There were no differences in induction of IL-4 (Th2 cytokine) and IL-10 (Treg cytokine). Moreover, there were no significant differences in the secretion of any of these cytokines between two *dupA2* strains and their isogenic *dupA* mutants. Similarly, IL-12/23p40 release in response to *dupA1* strains was significantly higher than that induced by *dupA2* strains (P < 0.01). Disruption of *cagE* in isogenic and double Δ*dupA*/Δ*cagE* mutants showed no further differential effects on IL-12/23p40 levels.

IL-12 is a heterodimeric pro-inflammatory cytokine encoded by two separate genes that is a major contributor to the differentiation of naïve T cells and undifferentiated T-helper cells into Th1 effector cells. It is composed of IL-12/23p40 and IL-12p35 subunits that combine to form the 70 kDa protein IL-12, also called IL-12p70 (Beadling and Slifka 2006). Initial assays in this study focussed on the IL-12/23p40 protein, which can also exist as a homodimer (IL-12p80) or as a heterodimer with an IL-23p19 subunit to form the Th-17 cytokine IL-23. In Hussein et al. (2010), the authors compared IL-12/23p40, IL-12p70 and IL-23 *in vitro* expression in peripheral blood mononuclear cells (PBMCs) from a single donor for two *dupA1* strains and their respective isogenic *dupA* mutants. Their data showed significantly increased levels of all assayed IL-12 family cytokines in wild-type strains compared with isogenic Δ*dupA* strains. The absolute differences were most stark for IL-12/23p40, then IL-12p70 and then IL-23. In their final experiment, PBMCs from three individuals were incubated with the AB31 wild-type and *dupA* mutant strains at a MOI of 20 for 16 hours. Cells where then immunostained for IL-12/23p40, IL-12p70 and CD14, which is a marker for monocytes, and analysed by flow cytometry. This approach confirmed the higher IL-12/23p40 and IL-12p70 responses with the wild-type strain found by ELISA. The numerical majority of IL-12$^+$ events were CD14$^+$ – 51% of IL-12/23p40$^+$ events and 73% of IL-12p70$^+$ events – suggesting a role for monocytes in developing a Th1 response in this model.

Jung et al. (2012) were unable to confirm any difference in IL-12 expression *in vivo*. They assayed antral mucosal IL-12p70 levels by ELISA for 27 *cag*+ cases as previously described for IL-8. Interestingly, a similar trend in IL-12 levels that was seen with IL-8 when stratified by *tfs4* was observed but did not reach statistical significance. Mean IL-

12p70 expression ± standard error was 34±6 pg/mg protein for *tfs4* intact strains (possessing *virB8*, *virB9*, *virB10*, *virB11*, *virD4* and *virD2* homologues, and *dupA*), 22±6 pg/mg protein for *tfs4* incomplete/*dupA*+ strains, and 17±7 pg/mg protein for *dupA*– strains. The assay sensitivity was 10 pg/mL. This may be the result of protein degradation and loss during extraction (for example, no protease inhibitors were used), or inadequate study numbers, or inadequate assay sensitivity. These results certainly do not negate the findings of Hussein et al. (2010) though these should be revisited in further studies.

Antibiotic susceptibility with respect to *dupA* status

Interestingly, *dupA* positivity has been associated with a lower rate of success of a primary course of eradication therapy (one week course of PPI, amoxicillin and clarithromycin), which was an independent risk factor for failed eradication alongside charithromycin resistance by sensitivity testing (Shiota et al. 2012). This was confirmed using for the most common clarithromycin resistance mutation in Iraqi strains (A2147G) and *dupA1* (6/12 were *dupA1* strains vs. 4/62 non-*dupA1* strains, OR 14.5, 95% CI 3.4-52.9, $P < 0.001$), though not for another rarer clarithromycin resistance mutation A2146G nor for the levofloxacin resistance mutation D91N (Hussein et al. 2015). However, Rasheed et al. (2014) found no statistically significant relationships between the susceptibility to 5 antibiotics and *dupA* status, though most isolates with antibiotic resistance in this study were *dupA*-positive (metronidazole 24/34, clarithromycin 13/22, amoxicillin 20/25, tetracycline 2/2, ciprofloxacin 5/6). Similar trends towards higher resistance levels were also observed with *cagA* and *vacA* s1/m1 strains.

Differences in transcription factor activation with respect to *dupA* status

Finally and in brief, one study evaluated a panel of 54 transcription factors in MKN45 cells infected with a single *dupA*+ strain or its isogenic Δ*dupA* mutant (Lu et al. 2005). Some transcription factors were activated only by the wild-type strain. Differences were found for the *p53* tumour suppressor gene and in the activation of transcription factors that bind to the *IL8* promoter, such as NF-κB and AP-1.

Summary

In summary, much remains unknown about the function of *dupA* and associated genes in the *tfs4* cluster. Further approaches that ideally would phenotype strains according to function are needed to complement genotyping methods. The function of the putative

tfs4 T4SS and the role of *dupA* within this system has not been defined. Further work is needed to confirm and expand on differences in cytokine induction – critically in the setting of the human stomach, which cannot be reproduced in the laboratory, but also in this *in vitro* immune cell model and other models using immune cells present in the lamina propria. Overall, we speculate that virulent strains of *H. pylori* might interact with epithelial cells to induce inflammation through the *cag* system and other factors, and that the *dupA*/*tfs4* T4SS might interact with inflammatory cells to direct the host towards a pro-inflammatory cytokine response. This remarkable hypothesis, together with the pursuit of a deeper understanding of how this might explain differential effects on disease risk and pathogenesis, form a central part of this project.

1.4. Summary of key background information

H. pylori colonises the stomachs of around half the global population yet only a proportion develop serious disease. Bacterial, host and environmental factors are important determinants of disease risk but not bacterial virulence factors have been linked to a specific clinical outcome. Therefore, the report by Lu et al. (2005) was of considerable importance – they proposed a novel virulence factor associated with an increased risk of duodenal ulcer and protection against gastric cancer, which are already considered to be at opposite ends of the *H. pylori*-associated disease spectrum. They named this factor *dupA*. Worldwide, *dupA* is present in half of strains but this varies according to region with 31% of Asian and 64% of Western isolates found to be *dupA*+. Detailed review supports a positive association with duodenal ulcer both overall and when confining the analysis to Asian populations. The negative association with gastric cancer was supported by the minority of case-control studies and in a long-term retro-prospective follow-up study. Meta-analysis did not support this conclusion. Current evidence suggests that associations with *dupA* are independent of other bacterial virulence determinations but their link with host factors has not been explored.

Duodenal ulceration may occur when three key criteria are met: stomach acid output is increased, gastric inflammation is intense, and the topographical distribution of colonisation and gastritis is antral-predominant. As a proposed disease-specific bacterial factor that promotes duodenal ulcer formation, the relationship of *dupA* to acid output and the intensity and pattern of gastritis should be determined. The T-helper (Th) cell acquired immune response also appears to be an important factor in DU development.

Firstly, clinical isolates of *dupA*+ strains have been shown to be (slightly) better able to survive acid shock and to grow in low pH environments. Reports of mutagenesis experiments that go beyond such observational studies are currently unclear and that any effects are specific to *dupA* is far from established. Acid output *in vivo* is higher in *dupA*+ strains but causality has not been shown and data may be confounded. In addition, whether *dupA* transcription and expression are in some way regulated by pH is unknown. Secondly, in some cases *dupA*+ was shown to be associated with increased gastric inflammation and reduced pre-malignant changes. However, most studies, though probably using potentially inadequate histopathological assessment, did not show this relationship. The distribution or pattern of gastritis with respect to *dupA* has not been systematically investigated.

dupA is polymorphic and exists in variant forms. It is not fully clear which alleles are functional and consequently some strains may have been misclassified in earlier studies. There is likely to be a connection between *dupA* and a novel uncharacterised type IV secretion system referred to as the *tfs4* cluster. Initial reports suggest that an intact *tfs4*, including *dupA*, are twice as commonly found in isolates from patients with duodenal ulcer. Further clarification of the significance *dupA* alleles and *tfs4* status will be important for future disease association studies.

Functional studies rely on establishing methods to determine relevant phenotypes. Mucosal inflammatory responses have been the focus of much study. Transcription of *IL8* and expression of IL-8 in gastric mucosa is consistently and significantly higher in *dupA*+ (and *tfs4* intact) strains than *dupA*– strains. These observations have not been consistently replicated *in vitro* using various epithelial cell lines with both clinical isolates and constructed mutant strains. A different approach to investigating host-bacterial interactions examined the response of immune cells using a model based on human peripheral blood mononuclear cells. Experiments with this approach have shown higher IL-12 family cytokine levels (around two-fold) in response to co-culture with *dupA*+ strains. There were varying effects on other immune mediators. IL-12 responses *in vivo* have yet to be clearly demonstrated.

In conclusion, the *dupA* gene and *tfs4* status appear to be linked to key aspects of duodenal ulcer pathogenesis in some settings. The mechanisms are not yet established but differences in the inflammatory response were seen. These observations may explain the correlation between the presence of *dupA* and disease-specific risk.

1.5. Aims

The *H. pylori* virulence factor *dupA* is the only bacterial factor to be described as disease-specific in its promotion of duodenal ulceration (Lu et al. 2005). A true virulence factor should have an epidemiologically consistent disease association, *in vivo* correlates with disease, and biological plausibility (Lu, Yamaoka and Graham 2005).

This thesis aims to test whether *dupA* meets these criteria of a true virulence factor.

Firstly, the chapter 'Influence of *dupA* status on clinical outcomes' tests whether there is a disease association with DU and if this is epidemiologically consistent. The specific aims are:

1. to carefully characterise the *dupA* status and virulence determinants of clinical isolates from the Nottingham study population,
2. to report the first association study for the United Kingdom for the relationship with clinical outcomes according to *dupA* status, and
3. to undertake a systemic review and meta-analysis of the influence of *dupA* status on clinical outcomes.

The second results chapter asks 'Is the *dupA* status of clinical isolates associated with the key pathogenic features of duodenal ulceration?' The specific hypotheses relate to the following *in vivo* correlates of duodenal ulceration:

1. intense gastric inflammation that is corpus-sparing in distribution,
2. antral-predominant bacterial colonisation, and
3. pro-inflammatory gastric mucosal immune responses.

The role of gastric acid output is also discussed.

Finally, the third results chapter explores the 'influence of *dupA* and *tfs4* status on human immune cell responses'. The aims of this chapter are:

1. to identify the cytokines and types of immune cell that are important in the human immune response to *H. pylori* according to *dupA* status,
2. to investigate the relationship between *dupA* and *tfs4* profile and cytokine induction, and
3. to gain insight into the role of *dupA* and *tfs4* components in this context.

2. Materials and methods

2.1. Media

All media were sterilised as needed by autoclaving at 121˚C and 15 psi for 15 min.

2.1.1. Blood agar

Columbia blood agar plates were obtained commercially (Oxoid, UK) both with and without *H. pylori* selective (Dent) supplement, comprising vancomycin, trimethoprim, cefsulodin and amphotericin B.

2.1.2. Lysogeny broth (LB) medium

Lysogeny broth (LB) medium, also termed Luria-Bertani medium, was prepared using 4 g of tryptone (Oxoid, UK), 4 g of sodium chloride (Sigma-Aldrich, USA) and 2 g of yeast extract (Oxoid, UK), made up to 400 mL with distilled water and 1 M sodium hydroxide to adjust to pH 7.5.

For LB medium supplemented with ampicillin, 800 µL of 100 µg/mL ampicillin (0.22 µM sterile-filtered; 200 ng/mL final concentration in medium; working stock from 1:500 dilution of 50 mg/mL stock; Sigma-Aldrich, USA) was added to 400 mL of sterilised LB medium.

2.1.3. Lysogeny broth (LB) agar

Lysogeny broth (LB) agar was prepared by adding bacteriological agar number one (Oxoid, UK) to LB medium at a final concentration of 1.5% (w/v) and sterilising.

For LB agar supplemented with ampicillin, one sachet of FastMedia LB Ampicillin Media (Fermentas, Germany) was used for 200 mL of medium sufficient for 8-10 standard agar plates.

2.1.4. Iso-Sensitest medium with 15% (v/v) glycerol

Iso-Sensitest medium was prepared using 23.4 g of Iso-Sensitest media (Oxoid, UK) containing 15% (v/v) sterilised glycerol (Courtin and Warner, UK), made up to 1 L with distilled water.

2.1.5. Sulphite-free Brucella broth (SFBB) medium

Sulphite-free Brucella broth (SFBB) medium was prepared using 5 g of tryptone (Oxoid, UK), 5 g of protease peptone (BD Biosciences, USA), 1 g of yeast extract (Oxoid, UK), 0.5 g of glucose (Sigma-Aldrich, USA) and 0.5 g of sodium chloride (Sigma-Aldrich, USA), made up 475 mL with distilled water. After sterilisation, 25 mL of 0.22 μM filter-sterilised foetal bovine serum was added to 5% (v/v).

2.1.6. Super Optimal broth with Catabolite repression (SOC) medium

Super Optimal broth with Catabolite repression (SOC) medium was prepared using 20 g of tryptone (Oxoid, UK), 5 g of yeast extract (Oxoid, UK) and 0.5 g of sodium chloride (Sigma-Aldrich, USA), made up to 900 mL with distilled water. Before sterilising, 10 mL of 250 mM KCL and 5 mL of 2 M $MgCl_2$ were added to the solution. After sterilising, the medium was allowed to cool to below 50 °C and 20 mL of 0.22 μM filter-sterilised 1M glucose (Sigma-Aldrich, USA) was added. The medium was then adjusted to a final volume of 1 L with distilled water, aliquoted and stored at 4 °C or -20 °C.

2.2. Bacterial culture

2.2.1. *H. pylori* isolation and culture on blood agar plates

Two gastric biopsies, one each from the antrum and corpus, were immediately transferred to 200 μL of iso-sensitest media containing 15% (v/v) glycerol (Section 2.1.4). Biopsies were then swabbed over blood agar plates with *H. pylori* selective (Dent) supplement (Section 2.1.1) within 3 hours and incubated for 3 days in a microaerophilic workstation (MACS VA500, Don Whitley Scientific, UK) at 37 °C in a humidified atmosphere of 5% carbon dioxide. Resulting single colony isolates were passaged onto fresh blood agar plates and grown under the same conditions for 2 days.

Isolates of *H. pylori* were identified by morphology, Gram staining and urease testing.

Both clinical isolates and laboratory strains of *H. pylori* were cultured from frozen stocks on blood agar plates (Section 2.1.1) for 3-5 days in a microaerophilic workstation (MACS VA500, Don Whitley Scientific, UK) at 37 °C in a humidified atmosphere of 5% carbon dioxide. Sub-cultures were obtained through passage where necessary.

2.2.2. *H. pylori* liquid culture

H. pylori strains were grown on blood agar plates for 24 hours (Section 2.1.1) and colonies from two plates was harvested and resuspended in 5 mL of sterile SFBB supplemented with 5% (v/v) foetal bovine serum (Section 2.1.5). If needed, 200 µL of this suspension was added to 800 µL of sterile SFBB. The amount of suspension required to give a starting OD_{600} of 0.1 in a final volume of 30 mL of liquid culture was determined (GeneQuant Pro, Amersham Biosciences, UK; diluted within the range 0.05-0.30 as needed). The cultures were grown overnight in a 75 cm^3 tissue culture flask (Nunc, Denmark) with shaking at 100 rpm on a mini orbital shaker (Bibby Scientific, UK) in a microaerophilic workstation (MACS VA500, Don Whitley Scientific, UK) at 37 °C in a humidified atmosphere of 5% carbon dioxide. Cells were harvested in mid-logarithmic growth.

2.2.3. *H. pylori* frozen stocks

Frozen stocks of *H. pylori* strains were prepared from growth on blood agar plates (Section 2.1.1) by adding harvested cells to 800 µL of iso-sensitest medium containing 15% (v/v) glycerol (Section 2.1.4) and immediately freezing at -80 °C.

2.2.4. *Escherichia coli* culture on LB agar plates

Escherichia coli strains were grown overnight under aerobic conditions at 37 °C on LB agar plates supplemented with ampicillin (Section 2.1.3).

2.2.5. *Escherichia coli* liquid culture

Bacterial cells were harvested from overnight cultures on LB agar plates supplemented with ampicillin (Section 2.1.3) to prepare cultures with LB liquid medium with or without ampicillin (Section 2.1.2). These were grown overnight under aerobic conditions at 37 °C with shaking (250 rpm).

2.2.6. *Escherichia coli* frozen stocks

Frozen stocks of *E. coli* strains were prepared from 800 µL of overnight LB liquid cultures supplemented with ampicillin (Section 2.1.2) added to 200 µL of sterilised 75% glycerol (Courtin and Warner, UK) and immediately frozen at -80 °C.

2.3. Patients, biopsies and clinical isolates

Patients were recruited from clinics and endoscopy lists at Nottingham University Hospitals NHS Trust, UK. Consecutive adult patients attending for clinically indicated upper GI endoscopy were screened for eligibility and recruited between January 2002 and June 2012 (that corresponds to cases 22 to 725 inclusive in the Nottingham collection). Inclusion criteria: adults (18 years of age or older) attending for clinically indicated elective upper GI endoscopy. Exclusion criteria: informed consent not given, lack capacity to give informed consent, regular use of non-steroidal anti-inflammatory drugs (NSAIDs) but not regular aspirin for cardiovascular prophylaxis, on proton pump inhibitor in the preceding two weeks, on antibiotic in the preceding four weeks, on regular steroids or other immunosuppressive therapy, on anticoagulant medication such as warfarin, had previous gastric surgery, acute gastrointestinal bleed, endoscopist deems there would be appreciable risk to taking additional endoscopic biopsies. This study was approved by the Nottingham Research Ethics Committee.

Patient demographic data and endoscopic disease status were collected and anonymised. Gastric biopsies were taken for routine clinical care and additional research biopsies (Table 2.1). Venous blood samples were taken for routine clinical care and for research purposes when indicated. *H. pylori* infection was confirmed when either the bacterial culture was positive, or at least three of the four typing investigations were positive: CLO test (Kimberly-Clark, USA) and/or rapid urease test, histopathology, and anti-*H. pylori* IgG serology.

Cases and controls are infected and uninfected patients; no allocation into groups is required. Cases of DU were identified as those patients with endoscopic evidence of an ulcer, a previous ulcer (presence of an ulcer scar or a past medical history of definite duodenal ulceration), erosive duodenitis reported to be at least moderate or severe in its severity, and equivalent pre-pyloric lesions (ulcers, moderate or severe erosions). Cases of GU were similarly defined, though for lesions affecting the stomach of at least 2 cm distance from the pylorus.

Controls were patients investigated for dyspepsia with no evidence of peptic ulcer, lymphoma or cancer. This group included individuals with other endoscopic findings of hiatus hernia and oesophagitis (due principally to reflux) or minor findings in the

stomach or duodenum (such as fundic gland polyps, erythema or a single erosion). Normal gastric histology was not required. Controls were not age- or sex-matched.

Matching was subsequently performed in analysis to look for confounding (see Section 3.3.4). Cases were individually matched against controls, after first stratifying into male and female groups, in a step-wise fashion whereby participants of the same age were matched in the first round, an age difference of ± 1 year was matched in the second round, and so on out to ± 10 years. Where more than one option for matching was available, that case was matched against the control participant recruited earliest to the study. The numbers not matched were recorded, either because of a difference between the number of cases and controls, or because the age gap was over 10 years.

Table 2.1 – gastric biopsies donated by patients with informed consent during routine upper GI endoscopy, purpose of biopsies and storage conditions

	Biopsies	Purpose	Storage Conditions
Routine clinical care	1 × antrum	CLO test and/or rapid urease test	Not applicable (though may be recovered and used for research purposes)
	1 × antrum 1 × corpus	Histology	See Section 2.5
	1 × antrum 1 × corpus	*H. pylori* isolation and culture	See Sections 2.2.1 and 2.2.3
Research purposes	1 × antrum 1 × corpus	For nucleic acid preparation	See Section 2.6.4
	1 × antrum 1 × corpus	For protein purification	Snap frozen in liquid nitrogen and stored at -80 °C
	4 × biopsies	For flow cytometry or ChipCytometry	Depends on purpose

2.3.1. Power calculations and planned sample size

This study requires 140 patients infected with *H. pylori*, of whom 70 are infected with *dupA*+ strains and 70 with *dupA*– strains. This is based on detecting half of the difference that we have seen in preliminary data for IL-8 levels in gastric biopsies between *dupA*+ and *dupA*– strains – mean IL-8 for *dupA*+ was 185 pg/mL (n=11), for *dupA*– was 62 pg/mL (n=6); standard deviation was 136.7. This study will also require at least 30 uninfected patients as controls. This is based on detecting the total difference that we have seen in preliminary data between infected and uninfected samples – mean IL-8 was 105 pg/mL (n=17) and 1 pg/mL (n=5) respectively; standard deviation was 127.4. Power calculations used two-tailed 2-sample *t* test with alpha=0.05 and beta=0.85.

2.4. Systematic review and meta-analysis

This work followed the principles for systemic review and meta-analysis proposed in the PRISMA statement (Liberati et al. 2009), recommendations for reporting search strategies (Yoshii et al. 2009), and the Cochrane Handbook (Higgins and Green 2011).

One investigator (RI) searched MEDLINE, PubMed, EMBASE (via OVID) and Web of Science (all databases) for studies that investigated the association between *dupA* status and upper gastrointestinal diseases, specifically duodenal ulceration, gastric ulceration and gastric cancer. The complete search strategy was "(*dupA* OR *dupA**) AND (*pylori* OR *Helicobacter*)", and was designed to capture publications concerning *dupA* but also *dupA* status reported as isoforms such as *dupA1* or *dupA2*. Terms were included both as free text and as expanded MeSH subheadings (or equivalent for other databases, such as expanded terms). All available years were covered through to August 2016, from 1946 for MEDLINE, from 1996 for PubMed, from 1980 for EMBASE and from 1900 for Web of Science. The search was last run on 12/09/2016. Searches were performed without any restriction on language, publication status, article type including abstracts, or study population characteristics such as inclusion of children. Additional searches of the Cochrane Library and ClinicalTrials.gov yielded no relevant results. The reference lists of the retrieved articles were screened to expand the search, which also yielded no further studies. Key conference proceedings were hand searched from 2005 to 2016, for EHSG, BSG, UEGW and DDW conferences, though these references had already been identified by the electronic database searches. No further grey literature sources were searched, though the BIOSIS citation index is included in searches of Web of Science. No individuals or organisations were contacted. No funders were involved in the review.

Citations identified in more than one database were merged, with exact duplicates identified and excluded. The abstracts ± the full manuscript of all potentially relevant references were reviewed by one investigator (RI). Inclusion and exclusion criteria were applied to select references reporting original data (rather than reviews), concerning human subjects (rather than *in vitro*, *in silico* or animal data), that reported raw data on *dupA* status, as case-control studies, and that had not subsequently been reported as a full article identified in the literature search. When it appeared that the same subjects were presented in multiple references, the report(s) that provided the most thorough data were used but without including subjects on more than one occasion. Although all article

types were included in the literature search, ultimately abstracts, conference proceedings, letters and non-English full articles were excluded from the subsequent analysis.

Data were extracted from each study by one investigator (RI) and entered into a spreadsheet. Information retrieved covered author, year of publication, the age group of study participants (with children and adults entered as independent study populations), whether data reported at the level of human study participants or some other level (such as colony isolates or clinical outcomes, where more than one was reported per study participant), the country or countries where the study was performed (with each country in the same publication entered as an independent study population), the number of cases with relevant clinical outcomes (DU, GU and GC, as well as any other reported outcomes including peptic ulcer without a specified site, DU and GU combined in one subject, duodenitis and dyplasia), how these cases were defined if reported, the number of controls (gastritis, functional dyspepsia, normal gastric histology, reported as no peptic ulcer), how these controls were defined if reported, the characteristics of cases and controls if reported (age, gender, ethnicity, prior history of peptic ulceration, prior history of eradication therapy or other study exclusions, smoking status), the *dupA* status of subjects according to each type of case or control (alongside additional genotype groups where data were reported such as *dupA1*, intact *dupA* and intact transcribed *dupA*), any associations reported by the study authors (including the use of matching, adjustment for confounders, univariate or multivariate methods), how *H. pylori* status was determined and how uninfected participants were identified, the source DNA, the number and details of primers used for genotyping and the source of these primers, whether any other typing method was used (such as dot blot, sequencing of part or all of the strains in the study population, and methodological details), if the study was able to determine whether the *dupA* gene was intact or truncated, if the study was able to determine whether *dupA* was long-type or not, and any further evaluations (such as RT-PCR or typing of *tfs4* genes). Authors were not contacted to obtain extra data or clarification.

Studies were case-control so the effect sizes were expressed as odds ratios. All analyses were performed using the freely available MetaXL v5.3 add-in for Microsoft Excel v16.0 32-bit (available at http://www.epigear.com). Three meta-analyses were conducted, to examine for a relationship between *dupA* status and DU, GU and GC

respectively. Controls for each study population were only included in each meta-analysis where data for the relevant case under investigation were also reported. Where separate control groups were reported, for example gastritis and functional dyspepsia with normal gastric histology, then these were combined as a single control group. The description of *dupA* status least subject to bias was used when available (*dupA1* preferred, then intact *dupA*, then *dupA*). Summary odds ratios and confidence intervals were calculated. Results were presented graphically using Forest plots.

The Mantel-Haenszel fixed effects method was used to test for statistical heterogeneity, using both I^2 to quantify inconsistency between studies and Cochran's Q. Alongside evidence of a significant Q value ($P < 0.10$), I^2 was considered to represent moderate heterogeneity from 30 to 60%, substantial heterogeneity from 50 to 90%, and considerable heterogeneity from 75 to 100% (Higgins and Green 2011). Firstly, sensitivity analyses were performed with exclusion of each single study population to identify if the magnitude or statistical significance of the summary estimate was substantially altered. Statistical heterogeneity was similarly explored to identify potential sources of clinical and methodological diversity between studies, namely variability in the participants and outcomes studies, variability in the study designs and methods, and the risk of bias. All these analyses were pre-specified. Subgroup analysis by region (Eastern vs. Western) was also planned.

The risk of bias within studies was considered. As discussed in Section 3.5.2, there are at least 91 quality assessment tools that have been reported for observational studies. No standard validated method has been reported to appraise the quality of genotyping of bacterial isolates and the risk of bias introduced by misclassification. Therefore, rather than propose a novel unvalidated quality score, we planned to undertake subgroup analysis stratified based on a subjective judgement about the risk of bias. This judgement of the risk of bias in the reporting of *dupA* status considered: (1) if more than one primer set and/or another typing method was used, (2) if the method enabled alleles with nonsense mutations to be identified, (3) if the method enabled identification of the long-type 2,499 bp gene. Where all three tests were met for all strains, that study was classified as being at lower risk of bias. Where the first two tests were met for all strains or where all three tests were met but only for some strains, then that study was classified at medium risk of bias. Other studies were considered to be at higher risk of bias. Further subgroup analyses, quality effects meta-analysis and meta-regression were not planned.

Publication bias was assessed qualitatively by funnel plots and quantitatively by the LFK index. The LFK index is a measure of the asymmetry in a Doi plot, interpreted as no asymmetry for indices in range –1 to +1 (no publication bias), minor asymmetry in range –2 to +2 and major asymmetry outside this range. A Doi plot has a similar role to a funnel plot, though plots the summary effect size for each study population against their rank within the meta-analysis according to a measure derived from the standard error of the study size. The most precise studies should be close to mid-rank, such that a Doi plot that shows no evidence of publication bias will appear as a symmetrical isosceles triangle. The LKM index was included in preference to a separate Doi plot as its interpretation is more straightforward but it includes more information that a funnel plot alone. The Egger test is not available in MetaXL.

2.5. Histopathological evaluation of gastric biopsies

At least two gastric biopsies, one each from the antrum and corpus, were recovered at endoscopy and immediately fixed in formalin. Biopsies were then embedded in paraffin wax and 4 μm sections prepared using a microtome. Multiple sections were mounted on glass slides and stained with either haematoxylin and eosin or with toluidine blue. A large proportion of theses slides were prepared by the candidate. Scoring of graded variables was carried out using the updated Sydney system (Dixon et al. 1996) together with Dr Abed Zaitoun, consultant gastrointestinal histopathologist. See Appendix Figure 7.2.

In addition, a sample of slides from infected patients were scanned at 40 × magnification and converted into complete digital images using a NanoZoomer Digital Slide Scanner (Hamamatsu, Japan). In each case, multiple sections from the antrum and the corpus were available. This was intended to facilitate quantitative analysis of inflammatory and bacterial parameters, though these data are not reported.

2.6. Nucleic acid isolation and analysis

2.6.1. Preparation of *H. pylori* genomic DNA from bacterial cultures

Cultured or sub-cultured *H. pylori* cells were harvested from blood agar plates (Section 2.2.1) after 24-48 hours of growth and resuspended in 1 mL sterile phosphate buffered saline (PBS; Oxoid, UK). The suspension was centrifuged at 16,000 × g for 2 minutes at room temperature and the supernatant discarded. DNA was extracted from the cell

pellet using the GenElute Bacterial Genomic DNA Kit (Sigma-Aldrich, USA) according to the manufacturer's instructions. Two separate elutions of 200 µL were collected in Elution Solution (10 mM Tris-HCl, 0.5 mM EDTA, pH 9.0) after incubation at room temperature for 5 minutes to increase elution efficiency (optional steps in manufacturer protocol), then combined into a single tube. This was immediately used in further experiments or stored at -20 °C.

Alternatively, genomic DNA from cultured bacteria that had previously been prepared by other researchers in the laboratory was used. This had been prepared with various methods including dedicated commercial kits or standard guanidine thiocyanate / ammonium acetate / chloroform / isopropanol extraction with resuspension in nuclease-free water or TE buffer (10 mM Tris-HCl, 1.0 mM EDTA, pH 8.0).

2.6.2. Preparation of plasmid DNA from bacterial cultures

Transformed *E. coli* cells were grown overnight on LB agar ampicillin plates (Section 2.2.4) and harvested to prepare cultures in LB liquid medium without antibiotic supplementation (Section 2.2.5). Plasmids were extracted from liquid culture using the QIAprep Miniprep kit (Qiagen, USA) according to the manufacturer's instructions. Each miniprep was eluted in 100 µL of Buffer EB (10 mM Tris-Cl, pH 8.5), with multiple minipreps prepared and combined where necessary, and immediately used in further experiments or stored at -20 °C.

2.6.3. Preparation of total RNA from bacterial cultures

H. pylori cells were first grown on blood agar as described in Section 2.2.1 then in SFBB medium containing 5% (v/v) foetal bovine serum as described in Section 2.2.2. The OD_{600} of 1 mL of liquid culture was measured (GeneQuant Pro, Amersham Biosciences, UK; diluted within the range 0.05-0.30 as needed). This was used to determine the volume containing 2.5×10^8 bacterial cells, assuming that 1 mL of *H. pylori* culture with an OD_{600} of 1.00 contains approximately 1.0×10^9 cells. Two volumes of RNA*protect* Bacteria Reagent (Qiagen, USA) were added to one volume of 2.5×10^8 bacterial cells, and immediately mixed by vortexing for 5 seconds then incubated at room temperature for 5 minutes. The stabilised liquid culture was then centrifuged at 5,000 × g for 10 minutes and the supernatant discarded with any residual supernatant removed by gently dabbing the inverted tube once onto a paper towel. Cell pellets were immediately used in further experiments or stored at -80 °C.

Total RNA was prepared using the RNeasy Mini kit (Qiagen, USA) according to protocols four and seven of the RNA*protect* Bacteria Reagent Handbook (December 2005). To lyse the cells, 20 µL of proteinase K (1 mg/mL – 1:20 dilution of 20 mg/mL stock; Sigma-Aldrich, USA) was added to nuclease-free TE buffer (10 mM Tris-Cl, 1.0 mM EDTA, pH 8.0; Fisher Bioreagents, UK; preferable to DPEC-treated TE buffer) containing 15 mg/mL lysozyme (lyophilised from chicken egg white; Sigma-Aldrich, USA). This mixture was then added to the cell pellet, which was carefully resuspended by pipetting before being mixed by vortexing for 10 seconds and incubated at room temperature for 10 minutes on a shaker-incubator. Subsequent steps were performed according to the manufacturer's protocol. Total RNA was eluted in 30 µL of nuclease-free water and centrifuged at 8,000 × g for 1 minute. This elution step was repeated with another 30 µL of nuclease-free water and the eluates combined (where expected yield >30 µg of RNA) or with the original eluate to improve the yield of RNA as required. The resulting total RNA samples were kept on ice and immediately used in further experiments or stored at -80 °C.

2.6.4. Preparation of total RNA and DNA from gastric biopsies

Gastric biopsies recovered for nucleic acid extraction were transferred immediately following endoscopy in to 250 µL of RNA*later* stabilisation reagent (Qiagen, USA) and stored at -80 °C according to the manufacturer's instructions with RNA*later* reagent subsequently removed and biopsy samples re-frozen. DNA and total RNA were extracted together using the AllPrep DNA/RNA mini kit (Qiagen, USA) or total RNA was extracted alone using the RNeasy Plus mini kit (Qiagen, USA). Batches of samples were thawed on ice as required. To each biopsy was added 350 µL of Buffer RLT Plus to which had previously been added 10 µL β-mercaptoethanol (Sigma-Aldrich, USA) per 1 mL of Buffer RLT Plus to denature ribonucleases released during extraction and 0.5% (v/v) of Reagent DX to reduce foaming (Qiagen, USA). These were then disrupted and homogenised at room temperature in a class I or class II biosafety cabinet using a TissueRuptor (Qiagen, USA) for approximately 20 seconds at full speed with a fresh disposable probe for each biopsy (disinfected in 70% ethanol for at least 15 minutes between uses) that was briefly cleaned by activation in RNase-away solution (Invitrogen, USA or VWR International, USA) and then in nuclease-free water immediately prior to use. Nucleic acids were then extracted according to the manufacturer's instructions. Total RNA was eluted in 30 µL of nuclease-free water and

centrifuged at 8,000 × g for 1 minute. This elution step was repeated with another 30 μL of nuclease-free water and the eluates used separately or combined. DNA was eluted in 100 μL of Buffer EB (10 mM Tris-Cl, pH 8.5) after incubation at room temperature for 1 minute to improve the yield. This elution step was repeated in some circumstances with the eluates used separately or combined. The resulting total RNA and DNA samples were kept on ice and immediately used in further experiments or stored at -80 °C (for RNA) or -20 °C (for DNA).

Note that some samples, particular those with only antral biopsies available, were processed alongside other researchers in the group (E. Staples, S. Patel, C. Masters).

2.6.5. Nucleic acid quantification and assessment of purity

Nucleic acid concentration was quantified using a NanoDrop ND-1000 spectrophotometer (NanoDrop Technologies, USA). The purity (absence of contaminants) of extracted nucleic acids was assessed by the A_{260}/A_{280} ratio to determine protein contamination with a cut-off of 1.80. The A_{260}/A_{230} ratio to determine organic contamination of samples was also measured but not used. Note that A_{260}/A_{280} ratio is an indicator of nucleic acid contamination of protein rather than vice versa (for example, ratio / % protein / % nucleic acid – 2.00 / 0 / 100, 1.98 / 10 / 90, 1.94 / 30 / 70). All concentration and purity measurements were determined with an appropriate blank but without adjustment to neutral pH, which limits the utility of these readings.

2.6.6. Determination of RNA integrity

RNA integrity (absence of degradation) was determined for a proportion of samples with the Agilent 2100 Bioanalyzer microfluidics-based platform and Agilent RNA 6000 Pico chips (Agilent Technologies, USA), according to the manufacturer's instructions (03/2008 version). This approach provides a virtual electrophoresis gel showing 28S and 18S ribosomal rRNA peaks and a summary RNA Integrity Number (RIN) between 1 (degraded) and 10 (intact). A cut-off of ≥5 was used for acceptable RNA integrity in the setting of total RNA extracted from gastric biopsies, with ≥8 signifying perfect RNA integrity (Derveaux et al. 2010).

Further determination of RNA integrity by using RT-qPCR assays to assess the Cq ratio of 3' and 5' mRNA from a target gene such as *GAPDH* is not applicable because of the sample type and use of random-priming. Similarly, because of feasibility constraints,

the samples have not been tested for the presence of inhibitors, for example using serial dilutions of the samples, internal amplification controls that co-purify and co-amplify with the target nucleic acid, or SPUD reference assay of universal inhibition that records sample Cq relative to water alone (Taylor et al. 2010; Bustin et al. 2009).

2.6.7. DNA sequencing and analysis

Plasmid DNA from cloned NovaBlue cells (pGEM-T Easy::human *GAPDH*) – see Sections 2.6.2 and 2.7.1 – was sequenced commercially using M13F and SP6 initiation primers by SourceBioscience Lifesciences, UK. The retrieved sequences and chromatograms were analysed using BioEdit (version 7.0.9.0), Clone Manager 9 Professional Edition and CLC Sequence Viewer (version 7.7.1).

2.7. Nucleic acid manipulation

2.7.1. Transfer of plasmid DNA into *Escherichia coli* competent cells

DNA fragments of human *GAPDH* had previously been ligated into pGEM-T Easy Vector (Promega, USA) and cloned into NovaBlue competent cells (Novagen / EMD Chemicals, Merck, Germany) by S. Patel. Due to problems with the transformed cell stocks, plasmid minipreps from the original clones were retransformed into new NovaBlue competent cells by heat shock without further purification and without Test Plasmid according to the manufacturer's instructions for standard kits. In brief, transformed NovaBlue cells were incubated under aerobic conditions at 37 °C for 30 minutes with shaking (250 rpm), 10 µL of these cells was then added to a pool of 90 µL of SOC medium pipette onto an LB agar ampicillin plate (without IPTG or X-gal), spread gently with a disposable spreader, and incubated overnight under aerobic conditions at 37 °C.

2.7.2. Restriction digest

High-fidelity *NotI* restriction endonuclease enzyme and associated reagents (New England Biolabs, USA) were used according to the manufacturer's instructions. Reactions with 50 µL total volume were set up with 6 µL of DNA template, 5 µL of NEBuffer4 buffer, 5 µL of bovine serum albumin (100 µg/mL) and 1 µL *NotI*-HF endonuclease enzyme (equivalent to 20 U of *NotI*). These were incubated at 37 °C for

2 hours, held at 4 °C, and the products visualised by 1% (w/v) agarose gel electrophoresis (Section 2.8.4).

2.7.3. DNase treatment of total RNA

DNase treatment was undertaken with Ambion Turbo DNA-*free* kit (Applied Biosystems, USA) in accordance with the supplied protocol (4/2009 version). The concentration of total RNA prepared from gastric biopsies was determined (Section 2.6.5) before and after adjustment to 100.0 ng/μL to compensate for disparities in initial concentration. These samples were then adjusted to a final concentration of 50.0 ng/μL with nuclease-free water – 3.00 μg of RNA in a reaction volume of 60 μL for biopsies from the antrum and 1.75 μg of RNA in a reaction volume of 35 μL for biopsies from the corpus. Total RNA prepared from bacterial cultures was adjusted to a final concentration of 33.3 ng/μL with nuclease-free water – 1.00 μg of RNA in a reaction volume of 40 μL. To these reactions was added 1 μL of recombinant DNase I enzyme and 0.1 volumes of 10 × DNase Buffer, the resultant reaction mixes were incubated at 37 °C for 30 minutes. 0.1 volumes of resuspended DNase Inactivation Reagent was then added to each, mixed well and incubated at 22 °C for 5 minutes. Three times during the incubation period, tubes were flicked 2-3 times to redisperse the DNase Inactivation Reagent (after approximately 60, 150 and 240 seconds of incubation). The mixture was then centrifuged at 10,000 × g for 90 seconds to pellet the DNase Inactivation Reagent. The supernatant, containing DNase-treated total RNA, was carefully transferred into a fresh tube. These were kept on ice for subsequent reverse transcription (Sections 2.7.4 and 2.7.5) and any remaining sample stored at -80 °C.

2.7.4. Synthesis of complementary DNA from DNase-treated total RNA from gastric biopsies

DNase-treated total RNA from gastric biopsies (Section 2.7.3) was transcribed using SuperScript II reverse transcriptase and associated reagents (Invitrogen, USA). The enzyme is engineered to have reduced RNase H activity but further removal of RNA complementary to cDNA is not required unless PCR targets to be amplified are >1 kb. Each standard reaction volume of 20 μL comprised: 4 μL of DNase-treated total RNA (50 ng/μL), 6 μL of nuclease-free water, 1 μL of dNTP mix (10 nmol/μL each nucleotide, therefore 0.5 mM final concentration in reaction; Promega, USA), 1 μL of random primers (supplied mostly as hexamers at 250 ng/μL, therefore 6.4 μM final

concentration in reaction [assuming average molecular weight of 6 × 327 g/mol]; Invitrogen, USA), 4 μL of 5 × First-Strand Buffer (250 mM Tris-HCl, 375 mM KCl, 15 mM $MgCl_2$, pH 8.3; included with enzyme), 2 μL of dithiothreitol (DTT supplied at 0.1 M; included with enzyme), 1 μL of RNaseOUT (40 U; Invitrogen, USA) and 1 μL of SuperScript II Reverse Transcriptase enzyme (200 U). First-strand reverse transcription PCR (RT-PCR) to generate complementary DNA (cDNA) was performed according to the manufacturer's instructions. cDNA was immediately used in further experiments or stored at -20 °C.

As a control for DNA contamination of the template, first-strand RT-PCR samples produced with 1 μL of nuclease-free in place of reverse transcriptase were also synthesised. These are referred to as RT– controls. For each biopsy from the antrum, two parallel sets of 5 × RT+ reactions and one set of 3 × RT– controls were prepared. For each biopsy from the corpus, two parallel sets of 3 × RT+ reactions and one set of 2 × RT– controls were prepared.

2.7.5. Synthesis of complementary DNA from DNase-treated total RNA from bacterial cultures

DNase-treated total RNA from bacterial cultures (Section 2.7.3) was transcribed initially using QuantiTECT reverse transcriptase and associated reagents (Qiagen, USA). In subsequent experiments, future the Omniscript reverse transcriptase kit (Qiagen, USA) and RNaseOUT (both Invitrogen, USA) were used. The manufacturer's instructions were followed with RT+ and RT– reactions comprising 400 ng and 200 ng respectively of template in a final volume of 20 μL. Initially parallel reactions were set up to compare the supplied RT Primer Mix (a proprietary combination of oligo(dT) primers and random oligomers) and random hexamers (equivalent to 6.4 μM final concentration in reaction; Invitrogen, USA). The latter required an additional incubation step at 25 °C for 10 minutes to optimise primer annealing prior to first-strand reverse transcription PCR (RT-PCR) performed according to the manufacturer's instructions. Subsequently only random hexamers were used. RT+ reactions were then diluted 1 in 2 and immediately used in further experiments or stored at -20 °C.

As a control for DNA contamination of the template, first-strand RT-PCR samples produced with 1 μL of nuclease-free in place of reverse transcriptase were also synthesised. These are referred to as RT– controls. For each biopsy from the antrum,

two parallel sets of 5 × RT+ reactions and one set of 3 × RT– controls were prepared. For each biopsy from the corpus, two parallel sets of 3 × RT+ reactions and one set of 2 × RT– controls were prepared.

2.8. Polymerase chain reaction (PCR), modifications of PCR and analysis

2.8.1. PCR and sequencing to determine *dupA* status

Accurate and thorough determinations of *dupA* status are fundamental to this study. The literature reports a wide range of different primers and confirmatory methods, which have evolved as knowledge has increased of the different alleles of *dupA* (that includes truncated froms due to frameshifts and indels that are likely to be non-functional) and of long and short forms of *dupA* (the open reading frame of long-type is extended by approximately 600 bp at the 5' end, reported as note in proof in Hussein et al. 2010 following analysis by the candidate and in Takahashi et al. 2013). One proposed explanation for the discrepant reports of *dupA* disease associations is the technical limitations of different PCR assays (Abadi et al. 2014).

Primer selection is critical to accurate *dupA* typing.

Abadi et al. (2014) systematically tested several primer sets *in silico* against sequences available through the NCBI database on 30/06/2014 and *in vitro* for 394 clinical *H. pylori* isolates with sufficient DNA quality selected from consecutive patients in the Netherlands between 2005 and 2007. The predicted *in silico* detection rates for the *jhp0917* and *jhp0918* primers of Lu et al. (2005) were 66% (118/179) and 33% (69/206) respectively. Newly designed real-time PCR primers with hydrolysis probe detection chemistry were reported (*AR-dupA*) that predicted 99% of sequences (284/288). Amongst the Dutch clinical strains, the rates were: 38% (149/394) for *jhp0917*, 30% (118/394) for *jhp0918*, 16% for concordant *jhp0917+jhp0918+* strains (concordant for 254/394 isolates, *dupA* prevalence 41/254), and 64% (253/394) for *AR-dupA*. This latter result was in line with their observation that 67% (254/379) of *H. pylori* genomes carried a *dupA* gene. Those strains that were *dupA+* only using the *AR-dupA* primers were confirmed as true positives by sequencing.

Two reports of experimental evaluations of conventional *dupA* primers were available. Further *in silico* analysis was performed.

There is as yet no method of *dupA* typing with consensus in the literature. In this study, we first considered conventional PCR primers used in two studies that evaluated the performance of each experimentally against both Western and Eastern isolates (Schmidt et al. 2009; Jung et al. 2012). We evaluated *in silico* the final primers recommended by Schmidt et al. (*dupA1274F* and *dupA1674R*) and three sets evaluated by Jung et al. (set A [*jhp0917* primers of Lu et al. (2005)], set C [*DupAR113* and *DupAR1083* primers of Argent et al. (2005)] and set H [Jung et al. (2012), though the reverse primer is identical to *DupAR1083* of Argent et al. (2005)]). The location of these primers is shown in relation to the Shi470 *H. pylori* genome in Figure 2.1.

Each primer was compared *in silico* to the *dupA* gene of 15 genome sequences (J99, Shi470, G27, Cuz20, F57, 908, 2017, 2018, SouthAfrica7, Gambia 94/24, Puno 135, Shi112, Shi169, Shi417 and SNT49). Primer alignment was performend in CLC Sequence Viewer (version 6.5.4; CLC Bio, Denmark). Bases where the sequence varied were identified and considered a major difference if present in >20% of genomes and a minor difference if present in ≤20%. For the Schmidt and Jung primer sets, this sequence variation is shown below Figure 2.1. For the Schmidt primer set (yellow), there were 2 sites of major difference in the forward primer (plus 1 site of minor difference) and 1 site in the reverse primer (plus 2 sites). There were no sites of major difference in the Jung primer set (red, plus 2 sites of minor difference in the reverse primer). Similarly, there was no sites of major difference in the Argent primer set (blue, plus 3 sites of minor difference in the forward primer and 2 sites in the reverse primer [identical to Jung reverse primer]). For the Lu *jhp0917* primer set, there was 1 site of major difference in the forward primer (plus 4 sites of minor difference) and 2 sites in the reverse primer (plus 1 site). Indeed, the primer sequences in the reference included several mixed bases (Lu et al. 2005).

The Schmidt primer set were shown to be equivalent to an elegant 5 primer multiplex PCR for *dupA* in an evaluation of 17 Eastern and 12 Western clinical strains, isolated from patients with a variety of clinical outcomes (Schmidt et al. 2009). In Jung et al. (2012), the Jung primer set was 94% sensitive for the detection of *dupA* in an evaluation of 8 primer sets against 28 isolates (equal Eastern/Western), as were the Lu and Argent primer sets (all detected 15 of the 16/28 strains that were *dupA*+ by at least one method).

However, the Lu primer set was found to underperform in another study (Abadi et al. 2014). No other primer evaluations were available to the best of our knowledge.

Next, two approaches to sequencing were evaluated. The method of Takahashi et al. was adapted in this study to classify strains as *dupA1* or *dupA2*. Where these PCRs were negative, typing was performed using the Schmidt and Jung primer sets reported above. If all PCRs were negative, strains were considered *dupA*–.

For *dupA* typing in this study, we elected to first use long PCRs and sequencing to detect *dupA1* and *dupA2* strains and, where these PCRs were negative, to perform PCR using both the Schmidt and Jung primer sets as these encompassed both the *jhp0917* and the *jhp0918* regions of *dupA*. Initially, the sequencing method of Moura et al. (2012) was tried. This involved 6 separate PCRs, the amplicons of which (shown in orange in Figure 2.2) were then sequenced and assessembled. However, given the multiple PCRs we found that this approach had more potential for PCR failure and there were some major differences in primer alignment against the 15 genome sequences studied previously (data not shown). Next, we used the method described by Takahashi et al. (2013). This first involved two long PCRs with Takahashi A and B primer sets, the amplicons of which (shown in blue in Figure 2.2) were then sequenced. Where both PCRs were negative, a further long PCR with Takahashi C primer set was performed (shown in green in Figure 2.2). Where PCRs with Takahashi A and/or B and/or C were positive, the products were cleaned up (GenElute PCR Clean-Up Kit #NA1020, Sigma-Aldrich), spectrophotometrically quantified and adjusted to 1 ng/µL per 100 bp, then sent for sequencing at Source BioScience (Nottingham, UK). Multiple primers were used for sequencing (shown in grey in Figure 2.2 [note: F2 is shown in green]). For Takahashi A and B, six sequencing primers were used (F2, F3, F4, F5, F6 and F7). For Takahashi C, six sequencing primers were also used (F3R, F3-F7). Both forward and reverse reads were performed. The resulting contigs were evaluated against their respective chromatograms and assembled in DNASTAR (Madison, Wisconsin, USA). Therefore, a minimum of 4 contigs were available at each point for assembly. Where necessary, the sequences obtained from Takasahi A and B products were aligned with 100% identity between sequences (data not shown). Sequences were aligned against AB31 and available genome sequences to assign *dupA1* or to *dupA2* status. Where all PCRs were negative (Takahashi A/B/C, Schmidt and Jung), strains were considered to be *dupA*–. Alignments were performed by ClustalW in Clone Manager 9.2 (SciEd, Denver, USA).

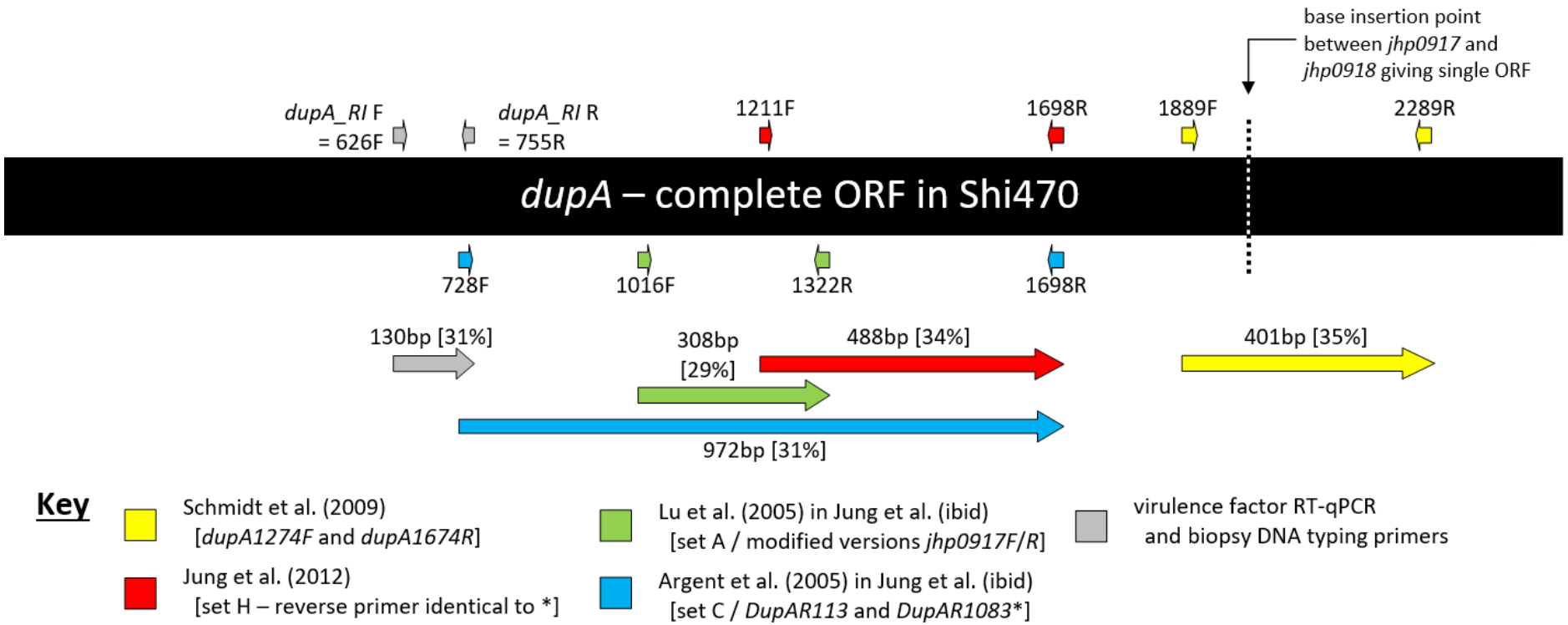

Figure 2.1 – location of *dupA* genotyping primers evaluated in this study in relation to Shi470 *Helicobacter pylori* genome

The Shi470 genome carries a *dupA* gene that is long-type (2,499 bp, encodes 832 amino acids) and not interrupted by frameshifts or indels. The relative position of various *dupA* primers is shown (see text) in relation to the 3' end of *dupA* (numbered 1 at position 908,071 in Shi470). The *dupA_RI* primers are discussed in Sections 2.8.3 and 2.8.7. The location of the frameshift present in the J99 genome is shown, which in J99 divides *dupA* into the two open reading frames (ORFs) *jhp0917* and *jhp0918*. The size and GC content of each amplicon is reported.

Primer	Sequence as given in reference	Sequence variation	Sequence in this study adjusted for variation
1889F	5'-G**C**GTGATCAATATGGATG**C**TTTTG**C**	**6T/9C**, **6C/9T**, 1T/14C	5'-G**Y**GTGATCAATATGGATG**Y**TTTTGC
2289R	5'-TTGTCT**G**GCTCTCAT**G**TC**C**GTGTTG	2A/13G, **5G/10A**, 2T/13C	5'-TTGTCTGGCTCTCAT**R**TCCGTGTTG
1211F	5'-ATTCACGCCTAAGACCTCA	all 15 identical	5'-ATTCACGCCTAAGACCTCA
1698R	5'-**C**TGAGAAGCCTTATT**A**TCTTGTTGG	1A/14C, 1G/14A	5'-CTGAGAAGCCTTATTATCTTGTTGG

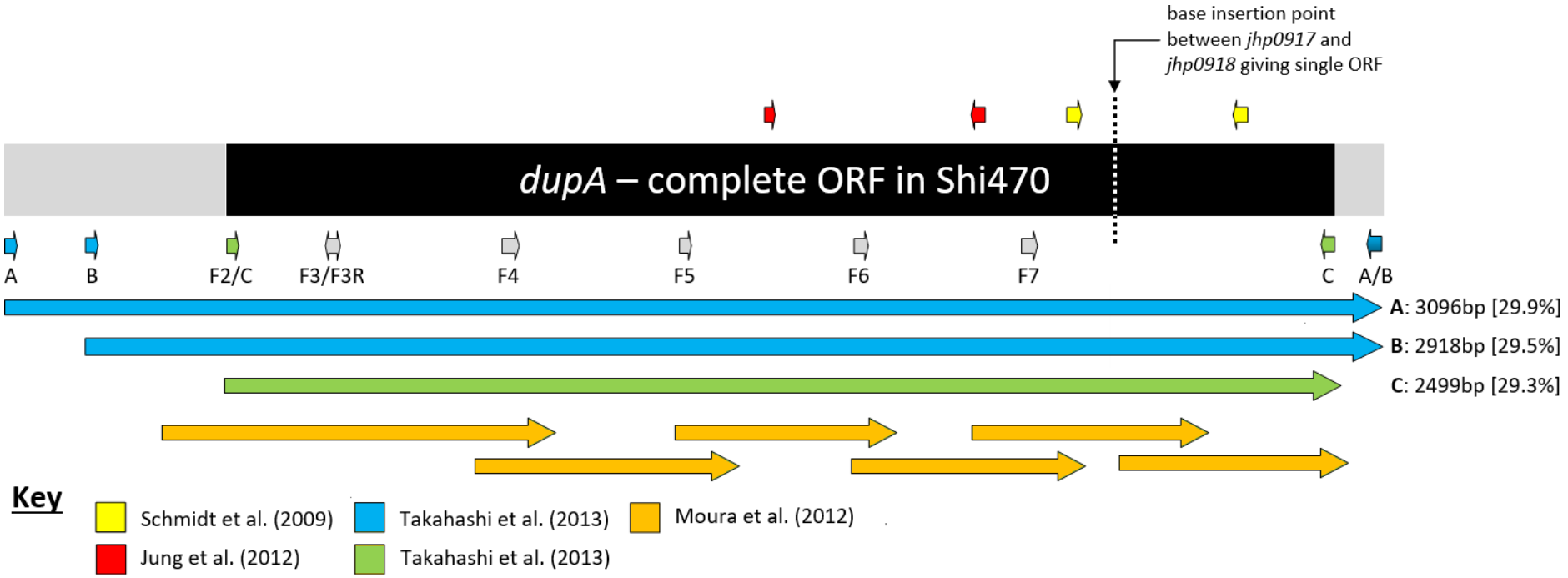

Figure 2.2 – location of *dupA* sequencing primers evaluated in this study in relation to Shi470 *Helicobacter pylori* genome

The Shi470 genome carries a *dupA* gene that is intact and long-type (2,499 bp, encodes 832 amino acids), which is shown in black. Flanking sequence is shown in grey. The relative position of various *dupA* primers is shown (see text) in relation to the 3' end of *dupA* (numbered 1 at position 908,071 in Shi470). The location of the frameshift present in the J99 genome is shown, which in J99 divides *dupA* into the two open reading frames *jhp0917* and *jhp0918*. The size and GC content of each amplicon from the long Takahashi PCRs is reported (A, B and C). The method description in Takahashi et al. (2013) includes a further primer set (D) that was used to distinguish between *dupA2* and *dupA*– strains. In this study, this function was fulfilled by the Schmidt (yellow) and Jung (red) primer sets. The amplicons of an alternative sequencing method reported by Moura et al. (2012) are indicated in orange.

Final experimental conditions for *dupA* typing and sequencing experiments

Reaction mixtures for the Takahashi PCRs were 2 μL of DNA template extracted from cultured bacterial genomic DNA (25-125 ng/μL), 10 μL of 5 × Phusion HF Buffer (with 1.5 mM $MgCl_2$ in reaction, included with enzyme), 1 μL of dNTP mix (10 nmol/μL each nucleotide, therefore 0.2 mM final concentration in reaction; Promega, Southampton, UK), 5 μL of each Takahashi primer (5 μM working stock, therefore 0.5 μM final concentration of each in reaction; see Table 2.4), 0.5 μL of Phusion High-Fidelity HS II polymerase (1 U; Finnzymes F549S/L, New England Biolabs, USA), made up to 50 μL with 26.5 μL of nuclease-free water. Cycling conditions are given in Table 2.2.

Reaction mixtures for the Schmidt and Jung PCRs were 1 μL of DNA template extracted from cultured bacterial genomic DNA, 12.5 μL of 2 × DreamTaq green PCR master mix (includes enzyme and dNTP mix, Fermentas K1081/2, Germany), 5 μL of each primer (Schmidt: 2 μM working stock, therefore 0.4 μM final concentration of each in reaction; Jung: 1 μM working stock, therefore 0.2 μM final concentration of each in reaction; see see Table 2.4), made up to 50 μL with 1.5 μL of nuclease-free water. Cycling conditions are given in Table 2.3.

Reactions were performed on a Px2 Thermal Cycler (Thermo Electron Corporation, Thermofisher Scientific, USA). Genominc DNA from AB31 and 60190 were used as positive and negative controls respectively.

Table 2.2 – cycling conditions for *dupA* typing by Takahashi primer sets

Step	Number of cycles	Time	Temperature
Initialisation	1×	30 sec	98 °C
Denaturation	35×	7 sec	98 °C
Annealing		0-20 sec	58 or 69 °C
Extension		40-60 sec	72 °C
Final Extension	1×	7 min	72 °C

Takahashi A did not include an annealing step and the extension step was for 60 sec. Takahashi B included a 20 sec annealing step at 69 °C and the extension step was for 60 sec. Takahashi C included a 20 sec annealing step at 58 °C and the extension step was for 40 sec.

Table 2.3 – cycling conditions for *dupA* typing by Schmidt and Jung primer sets

Step	Number of cycles	Time	Temperature
Initialisation	1×	3 min	95 °C
Denaturation	35×	30 sec	95 °C
Annealing		30 sec	52 or 55 °C
Extension		45 sec	72 °C
Final Extension	1×	7 min	72 °C

The annealing step was at 55 °C for Schmidt and at 52 °C for Jung primer sets.

Table 2.4 – primers used in *dupA* typing and sequencing

Primer Name	Primer Sequence	T_m (°C)	Size[1] (bp)	Ref.
Takahashi A F	5'-TGGCGTGTGGCAGTCTAATGC	70.7	3096	Takahashi et al. 2012
Takahashi A R	5'- GCTCAACAAAATGCCCACCAGTCGC	76.4		
Takahashi B F	5'-GCAAACGCTCAAACTATTGCC	65.9	2918	
Takahashi B R	same as Takahashi A R	76.4		
Takahashi C F	5'-ATGTTTCTTGGTTTAGAGGG	57.7	2499	
Takahashi C R	5'-TTATACATATTGAA**Y**ATTCTCGC	54.9		
Takahashi F2	same as Takahashi C F	57.7	n/a	
Takahashi F3	5'-CAGAACACAAGCTTTAAATGAATTG	62.8		
Takahashi F3R	5'-CAATTCATTTAAAGCTTGTGTTCTG	59.2		
Takahashi F4	5'-ATGAGTTC**C**ATACTAACAGACTTTGAGCC	63.2		
Takahashi F5	5'-GGTTTCTACTGACAGAGCAC	57.0		
Takahashi F6	5'-GATAATTGGTAGCACAGG**R**AGCGG	68.5		
Takahashi F7	5'- GGCTCTAGCGAACAAGATTTTAATGAG	66.8		
Schmidt F	5'-G**Y**GTGATCAATATGGATG**Y**TTTTGC	68.2	401	Schmidt et al. 2009
Schmidt R	5'-TTGTCTGGCTCTCAT**R**TCCGTGTTG	71.7		
Jung F	5'-ATTCACGCCTAAGACCTCA	60.4	488	Jung et al. 2012
Jung R	5'-CTGAGAAGCCTTATTATCTTGTTGG	63.2		

Primers were synthesised by Eurofins MWG Operon, Germany. Bases in the primer sequence that are highlighted in bold/underline were altered from the published reference as the modified primer shared closer identity when aligned against 15 *H. pylori* genome sequences. Each T_m was calculated using the Finnzymes Tm calculator for Phusion enzyme at http://www.thermoscientificbio.com/webtools/tmc/ (this tool is also called Fermentas REviewer).

[1] = expected product size.

2.8.2. PCR to determine *cag*PAI, *vacA* type and *tfs4* status

Other *H. pylori* bacterial virulence factors were typed by PCR from genomic DNA extracted from multiple colony sweeps after culture *in vitro*. Confirmatory sequencing was not performed.

For the *cag*PAI, the status of *cagA*, *cagE* and the empty site (*cagES*) were determined by PCR. Serological confirmation of *cag*PAI status used a CagA immunoglobulin G enzyme-linked immunosorbent assay kit (Genesis Diagnostics). The presence or absence of the *cagA* gene was carried out using the method of Argent et al. (2008) with one primer pair (A22F: 5'-TTCATGGGCGTGTTTGATG and A23R: 5'-ATAATCTTTGAGAGTGTAGCTC) alongside reference strains 60190 (*cagA*+) and Tx30a (*cagA*–). The method of Tomasini et al. (2003) was used to determine *cagE* status with the same controls using the primer pair *cagE* F (5'-TTGAAAACTTCAAGGATAGGATAGAGC) and *cagE* R (5'-GCCTAGCGTAATATCACCATTACCC). The absence of the *cag*PAI was determined using *cag* empty site primers (2: 5'-ACATTTTGGCTAAATAAACGCTG and 25: 5'-TCATGCGAGCGGCGATGTG [Akopyants et al. 1998], and Luni1: as Akopyants and R5280: 5'-CCAACGTGCGTAAAAGGGAATTAG [Mukhopadhyay et al. 2000]). Strains that were *cagA*+*cagE*+*cagES*– were designated as *cag*PAI-positives and those that were *cagA*–*cagE*–*cagES*+ as *cag*PAI-negatives. CagA serology was used to assign *cag*PAI status where there was disagreement in genotyping (for example, only *cagA* or *cagE* was present, or the strain was typed as *cagES*+ despite the presence of one or both of *cagA* and *cagE*). Data remained equivocal for 7% of genotyped strains (9/127), for which no *cag*PAI status was assigned. These experiments were performed by Dr Richard Argent, Dr Katie Cook, Dr Ameer Memon and the candidate, amongst other researchers in the group.

The *vacA* status of each strain was determined using standard methods for amplification of the *vacA* signal (s) and mid (m) region (Atherton et al. 1995), and for the intermediate (i) region (Rhead et al. 2007). These experiments were performed by Mrs Joanne Rhead and Dr Darren Letley, amongst others in the research group.

Several putative *tfs4* and related genes were typed by PCR, of which data for four were provided for analysis in this study (Dr Rob Delahay, personal communication). These were *virB8*, *virB9*, *virD4* and *virD2*. No typing was performed for *virB2*, *virB10* or *virB11*. Different combinations of primers were used for some genes. Long PCR spanning several genes was used to try to resolve any typing disagreements and to determine if the cluster was intact or fragmented/dispersed in different locations. The *tfs4* clusters with open reading frames affected by frameshifts or indels were not determined, so these data may be considered as representative of whether *tfs4* was

complete or incomplete, but cannot provide a comprehensive picture of genetic intactness or moreover of activity (see Section 3.3.2). These typing experiments were performed principally by Miss Nicola Croxall.

2.8.3. PCR to indicate *dupA* status using biopsy DNA

Genotype data used in this study were obtained using conventional PCR with genomic DNA extracted from *in vitro* bacterial cultures as a template. Where these data are unavailable, for example because of failure to culture clinical strains or contamination during subculturing, it may be possible for genotype information to be obtained from DNA extracted directly from gastric biopsies.

The two *dupA_RI* primers developed and used in this study are shown in Table 2.12 and illustrated in Figure 2.1 (shown in grey). These were developed for use both in conventional PCR on DNA extracted directly from gastric biopsies and in RT-qPCR for *dupA* mRNA expression (Section 2.8.7). This application requires a short amplicon.

With respect to the annotation of the genome of strain J99, these primers amplify a 130 bp product from position 11 to position 140 of the *jhp0917* gene at the 5' end of *dupA*. These were designed with reference to all 17 complete *H. pylori* genome sequences available in July 2011 to distinguish between *dupA* and variant *dupA* genes (Section 1.3.3), identified using alignment and phylogenetic tree functions in CLC Sequence Viewer (version 6.5.4; CLC Bio, Denmark). The primers identified the ten strains with *dupA* (J99, Shi470, G27, Cuz20, SouthAfrica7, Gambia 94/24, F57, 908, 2017 and 2018) and did not identify variant *dupA* (26695, P12, PeCan4, SouthAfrica7*, India7, B8, F30, F32, F57*, 35A and 51; note those asterisked strains appear to contain both *dupA* and variant *dupA*). NCBI BLAST and primerBLAST searches confirmed the specificity of the primers and sequence to *H. pylori*. NetPrimer (Premier Biosoft) was used to assess for secondary structures and provided a primer rating score of 100 for the forward and of 91 for the reverse primer.

There was no separate control, such as PCR for *16S rRNA*, used to confirm the presence and adequacy of bacterial DNA extracted from gastric biopsies. However, multiple gastric biopsies where genotype data were available from cultured clinical isolates to characterise the strains as *dupA*+ or *dupA*– were also tested alongside those where these data were unavailable. From these data, the number of false positives and false negatives were determined. This evaluation showed the predicted result in 17/19 strains and for

no template control (data not shown). Data from antrum and corpus biopsies agreed for all patients with paired biopsies evaluated (9/9). No bands were seen for uninfected and *dupA*– cases. However, there were two instances where bands had been expected but were not detected for strains typed *in vitro* as *dupA*+. In addition, bands were also observed for two Δ*dupA* mutant strains (constructed by ligation of a chloramphenicol cassette into the *dupA* gene but after the amplification point of the *dupA_RI* primers). Uncharacterised strains where a PCR product was detected with these primers were provisionally considered as *dupA*+ and those without a product as *dupA*–.

Frozen DNA extracted from gastric biopsies was thawed on ice and quantified spectophotometrically (mean 52 ng/μL, range 0-190 ng/μL). Samples were diluted to 100 ng/μL where necessary, aliquoted and refrozen. Reaction mixtures for PCR were prepared according to the manufacturer's instructions and comprised: 8 μL of DNA template extracted from gastric biopsies (20-100 ng/μL) or 1 μL of cultured bacterial genomic DNA, 5 μL of 10 × DreamTaq green PCR master mix (included with enzyme), 1 μL of dNTP mix (10 nmol/μL each nucleotide, therefore 0.2 mM final concentration in reaction; New England Biolabs, USA), 4 μL of each *dupA_RI* primer (1.5 μM working stock, therefore 0.12 μM final concentration of each in reaction; synthesised by Eurofins MWG Operon, Germany), 0.25 μL of DreamTaq DNA polymerase (1.25 U; Fermentas, Germany), made up to 50 μL with nuclease-free water. Reactions were performed on a PCR Express Thermal Cycler (Thermo Hybaid, UK) or Px2 Thermal Cycler (Thermo Electron Corporation, Thermofisher Scientific, USA). Cycling conditions are given in Table 2.5, with the annealing temperature having first been optimised with a ten-step temperature gradient between 46 and 55 °C using genomic DNA from strain J99. Each run included positive and no template controls.

This method has utility for classifying *dupA* status from gastric biopsies where this cannot be determined with other methods. Amplicon size was restricted because of the potential for bacterial DNA fragmentation during recovery from biopsies. The major limitations of this current method are that only one primer set was used, and the presence of truncated *dupA* alleles and long/short type *dupA* are not detected (as the amplified fragment was small and located at the 5' end). A problem with the purity or integrity of extracted DNA is the most likely explanation for the two false negative results seen during assay evaluation. The amount of DNA template available was limited, so routine further testing of all or just negative samples was not undertaken (for example, to detect

another *H. pylori* gene like *16S rRNA* or *ureB*, or for other *dupA* primers). It was reassuring that no false positive results were detected. Overall, the *dupA* status inferred from this method must be treated with caution. Ultimately, these data were not used in the classification of *dupA* status in this study.

Table 2.5 – cycling conditions for PCR with *dupA_RI* primers

Step	Number of cycles	Time	Temperature
Initialisation	1×	3 min	95 °C
Denaturation	30×	30 sec	95 °C
Annealing		30 sec	55 °C
Extension		45 sec	72 °C
Final Extension	1×	10 min	72 °C

Note that the annealing temperature was optimised with a temperature gradient between 46-55 °C using J99 genomic DNA as a template.

2.8.4. Analysis of PCR products by gel electrophoresis

PCR products were analysed in 1% or 2% (w/v) agarose gels prepared with 40 mL or 140 mL of TAE buffer (40 mM Tris-acetate, 2 mM EDTA, pH 8.0) and stained with ethidium bromide (stock 5μg/μL, final concentration in gel 0.625 μg/mL) for visualisation. First 5-10 μL of MassRule DNA Ladder Mix (80-10,000 bp; Fermentas, Canada) was loaded. Next 5-10 μL of each sample was loaded along with 6 × MassRuler DNA Loading Dye (Fermentas, Canada) where required. Gels were electrophoresed at 80 V or 120 V respectively for 40-60 minutes and visualised under UV light. Images were recorded using a GENi imaging system (Syngene, Synoptics Group, UK).

2.8.5. Quantitative real-time PCR (qPCR) – assessment of bacterial colonisation density

This is based on the method developed by Dr Sapna Patel. Her validated technique used quantitative real-time PCR (qPCR) to determine the absolute number of genome copies of *H. pylori* (bacterial *16S rRNA* gene) per human genome (human *GAPDH*; reference gene constitutively expressed, not restricted to epithelium). Each of these parameters was determined from standard curves included in each run. The primers used are given in Table 2.8. NCBI BLAST and primerBLAST searches confirmed the specificity of the human *GAPDH* primers to the gene encoded on chromosome 12p13 (accession number CCDS8549.1). The *16S_rRNA_SP* primers were designed when only 26695 and J99

genomes were available. *In silico* analysis in November 2011 identified *Helicobacter* species not restricted to *H. pylori* and only identified the *16S rRNA* gene in 52% (16/31) of fully sequenced strains. Secondary structure analyses were not performed. With respect to the *16S_rRNA_RT* primers, NCBI BLAST and primerBLAST searches in November 2011 identified *Helicobacter* species not restricted to *H. pylori* and limited homology to *Flexispira* species. The *16S rRNA* gene was identified in all 31 strains with complete genome sequences available. These primers were used in this study. The annealing temperature of all primers was optimised in 12 steps from 56 to 60 °C.

A head-to-head comparison of different qPCR reagents employing SYBR green detection chemistry was undertaken. The following 2 × master mixes were used – AB SYBR Green PCR master mix with HS AmpliTaq Gold (Applied Biosystems, USA), QuantiTect SYBR Green PCR master mix with HotStarTaq (Qiagen, USA) and Maxima SYBR Green qPCR master mix with Maxima HS Taq (Fermentas, Canada). The respective efficiencies were 1.85, 1.74 and 1.77 respectively with respect to *16S rRNA* quantification from J99 (controls and melt curves as expected, $r^2 > 0.999$ in each case, data not shown). With respect to *GAPDH* quantification from pSAP2 #2, the respective efficiencies were 2.06, 1.95 and 1.94 (controls and melt curves as expected, $r^2 \geq 0.996$ in each case, data not shown). The peak fluorescence was also higher for AmpliTaq Gold and this was more cost-effective. This reagent was used in all subsequent evaluative experiments and in the final colonisation density quantification experiments.

Before analysis and as explained in Section 2.8.3, extracted DNA was first thawed on ice, quantified spectrophotometrically, diluted to 100 ng/µL where necessary, aliquoted and refrozen. During assay validation by Dr Patel, even a single additional freeze-thaw cycle was found to affect the calculated density of infection (data not shown). In contrast, reactions that were repeated whilst DNA samples were left on ice between reactions showed similar results. In this study, all sample underwent two freeze-thaw cycles prior to analysis so that sample handling was consistent.

The human *GAPDH* standard requires a dilution series of plasmid DNA prepared from strain pSAP1 (pGEM-T Easy::human *GAPDH* transformed NovaBlue cells). Due to insufficient plasmid DNA previously prepared from pSAP1 and problems with the pSAP1 frozen stocks, samples from several original preparations of plasmid DNA were retransformed into NovaBlue cells (Section 2.7.1). Restriction digest (Section 2.7.2), DNA sequencing (Section 2.6.7) and PCR (Section 2.8) were used to confirm successful

transformation, and these new strains were named pSAP2 #1 through #5 and frozen stocks prepared (Section 2.2.6). For the human *GAPDH* and bacterial *16S rRNA* standard curves, plasmid DNA from strain pSAP2 #2 and genomic DNA from strain J99 was isolated respectively (Sections 2.6.2 and 2.6.1). These were both quantified (Section 2.6.5) and two dilution series prepared (Table 2.6).

The concentration of each step in genomes/µL is derived as follows. The average molecular weight of a molecular of DNA template that is S bp in length $= 678 \times S$ Da. Given that pmol $= \frac{\text{pg}}{\text{molecular weight}}$ and 1 mol $= 6 \times 10^{23}$ molecules, the concentration of DNA template $= C$ pg/µL $= \frac{C}{678 \times S}$ pmol/µL $= \frac{C}{678 \times S \times 10^{12}}$ mol/µL $= \frac{C \times (6 \times 10^{23})}{678 \times S \times 10^{12}}$ molecules/µL. If the template only contains one copy of the target sequence per molecule (for example, encoded in a plasmid) then the concentration in molecules/µL equates to copies/µL. Where there are n copies of the target gene per genome, concentration in genomes/µL equates to copies/µL divided by n. Therefore, concentration $= \frac{\text{template concentration (pg/µL)}}{\text{template size} \times \text{gene copies per genome}} \times \frac{1 \times 10^{11}}{113}$ genomes/µL. For human *GAPDH*, the pGEM-T Easy::*GAPDH* plasmid is 3,135 bp and there are two copies of the targeted gene on chromosome 12 per diploid human genome. For bacterial *16S rRNA*, the J99 genome is 1,643,831 bp and there are two copies of this gene per *H. pylori* genome. In the previous study by Dr Patel, *H. pylori* genome copy numbers had been calculated as if there were only one copy of *16S rRNA*, which was revised in this study. The final dilution series were extended below those used in optimisation and evaluative experiments (see legend of Table 2.6) to ensure that clinical samples would be encompassed by the linear dynamic range and limit of detection of the assay. This was likely the result of the freeze-thaw cycles in this study as reported above, which were needed due to the variety of different experiments in which biopsy samples were used. With low copy numbers, there is less precise reproducibility with Poisson modelling; therefore, clinical samples were analysed in triplicate rather than duplicate.

Reactions of 25 µL total volume were set up manually with 2.5 µL of forward and reverse primers (each at 1 pmol/µL, therefore 0.1 µM final concentration in reaction), 5 µL of template DNA from standard curve dilution series or prepared from gastric biopsies (Section 2.6.4), 2.5 µL of nuclease-free water and 12.5 µL of 2 × SYBR green master mix. Reactions were performed in triplicate in clear 100 µL strip tubes with caps

(Qiagen, USA) with the cycling conditions given in Table 2.7 on a Rotor Gene 300 system (Corbett Life Science, Qiagen, USA). No template controls (NTCs) and the final standard curves (Table 2.6) were included in each run. Specificity analysis was confirmed by single expected peaks on high resolution melt curves and where required by gel electrophoresis of PCR products (Section 2.8.4). Data were analysed with Rotor Gene software (version 6.0, Corbett Research, UK), using dynamic tube, slope correct and eliminating cycles before Cq of 5-10 if necessary. Cq numbers for each sample were used to provide an absolute quantification of *H. pylori* per human cell by matching against standard curves. In total 98 samples were processed across 13 runs, though only the data for 60 samples from paired antrum and corpus biopsies were reported. For each run, the precision for each sample (coefficient of variation [%CV] across three replicates), efficiency, r^2 and linear dynamic range were also evaluated. For *16S rRNA*, the mean efficiency was 1.71 (sd 0.02), $r^2 \geq 0.989$ in each case (mean 0.996), and mean %CV was 2.6% (>5% for 13/98, >10% for 0/98). For *GAPDH*, the mean efficiency was 1.900 (sd 0.04), $r^2 \geq 0.996$ in each case (mean 0.998), and mean %CV was 0.8% (>5% for 1/98, >10% for 0/98). All samples fell within the assay linear dynamic ranges.

Table 2.6 – dilution series prepared for qPCR for bacterial colonisation density

***GAPDH* standard curve**		**step**	***16S rRNA* standard curve**	
concentration	**genomes/µL**		**concentration**	**genomes/µL**
278 fg/µL	39205.91	**1**	200 pg/µL	53834.96
46.3 fg/µL	6534.32	**2**	25.0 pg/µL	6729.37
7.72 fg/µL	1089.05	**3**	3.13 pg/µL	841.17
1.29 fg/µL	181.51	**4**	391 fg/µL	105.15
214 ag/µL	30.25	**5**	48.8 fg/µL	13.14

The concentration in genomes/µL is provided with five significant figures. In previous optimisation and evaluative experiments, the concentration range evaluated for *GAPDH* and *16S rRNA* was 1.28-800 fg/µL and 1.28-800 pg/µL respectively. These were equivalent to genomes/µL of 180.67 and 344.56 respectively at the final steps of each dilution series. In data for 18 patients with samples processed in duplicate, 14% and 47% respectively fell below the lower limit of these standard curves for *GAPDH* and *16S rRNA*. Therefore, the dilution series in this Table were used in the final experiments.

Table 2.7 – cycling conditions for qPCR for bacterial colonisation density

Step	Number of cycles	Time	Temperature
Initialisation	1×	10-15 min[1]	95 °C
Denaturation	35×	30 sec	95 °C
Annealing		60 sec	56 °C
Extension		30 sec	72 °C
Final Extension	1×	10 min	72 °C
Melt curve (0.5 °C increments)			72-95 °C
Final Extension	1×	5 min	72 °C

[1] = 15 min for Qiagen master mix and 10 min for AB and Fermentas master mixes.

Table 2.8 – primers used in qPCR colonisation density experiments

Primer Name	Primer Sequence	T_m (ºC)	Size[1] (bp)	Reference
HuGAPDH_SP_F	5'-GGTCCGAGTCACCGCCT	66.6	118	Patel, 2010
HuGAPDH_SP_R	5'-TGGCGACGCAAAAGAAGATG	68.3		
16S_rRNA_SP_F	5'-CGATGAAGCTTCTAGCTTGC	61.8	164	Narayanan, 2005
16S_rRNA_SP_R	5'-ATAGGACATAGGCTGATCTC	54.7		
16S_rRNA_RT_F	5'-GGAGGATGAAGGTTTTAGGATTG	58.9	390	Rokbi et al. 2001, Gieseler et al. 2005
16S_rRNA_RT_R	5'-TCGTTTAGGGCGTGGACT	56.0		

Primers were synthesised by Eurofins MWG Operon, Germany. The second set of *16S rRNA* primers (labelled *RT*) were used in final colonisation density experiments.

[1] = expected product size.

2.8.6. Quantitative reverse transcriptase real-time PCR (RT-qPCR) – assessment of relative mucosal cytokine mRNA expression

Quantification of mRNA transcripts in human gastric biopsies (antrum and corpus) for the cytokines genes *IL8* (or *CXCL8*), *IFNG*, *IL12B* and *IL10*, and the reference gene *GAPDH* was undertaken using RT-qPCR. This reference gene was chosen because it is reasonably consistently expressed in human cells and a single gene was used because of limited sample availability and feasibility constraints. The primers used are given in Table 2.10. Identification of splice variant or pseudogenes, *in silico* and secondary structure analyses have not been undertaken.

Key to the analysis is a control group against which relative expression can be reported, which is referred to as the pooled negative comparator. We first randomly identified antral biopsies from 20 uninfected donors, with no evidence of *H. pylori* infection by biopsy urease test, culture, histology and serology, and with no history of past infection.

These biopsies were separately homogenised/disrupted and nucleic acids recovered. All samples show satisfactory purity (A_{260}/A_{280} 1.95-2.06 and A_{260}/A_{230} 1.95-2.37). However, the A_{260}/A_{230} was 1.21 for one sample where the RNA concentration was 26 ng/μL; this is inadequate for downstream reactions and it was excluded. Next, RNA integrity and virtual electrophoresis results were assessed as reported in Section 2.6.6. Median RNA Integrity Number (RIN) was 6.6 (range 5.0-7.8) and was therefore satisfactory for all samples except one that scored 2.0. This sample was excluded. The remaining 18 samples were used to synthesise cDNA with random hexamers from DNase-treated total RNA. Next, *GAPDH* and *IL8* were assessed by RT-qPCR to confirm that the individual samples of the negative comparator did not exhibit high levels of inflammatory cytokine expression. Most samples showed low relative *IL8* expression compared to an initial pool of these comparators – mean 1.3 arbitrary units (range 0.0 to 3.5). However, four samples showed relatively high levels (40.5, 69.5, 74.7 and 413.9 arbitrary units). The variation in these cases resulted from higher Cq values for *GAPDH* (mean Cq 25.8 vs. 19.8). These were repeated on two occasions and showed consistently higher Cq values than average for each run. In two cases, analysis of biopsy histology showed loss of glands or chronic inflammation. In one further case, the patient had a history of duodenal ulcer and was taking aspirin. These were excluded. The remaining anomalous sample was then >58 standard deviations from the new sample mean and was excluded as an outlier. Experiments with the remaining 14 samples in *IL10* and *IFNG* assays confirmed low levels of background inflammation (mean 1.1 and 3.4 arbitrary units respectively). Therefore, the negative comparator comprised 14 samples that represented uninflamed gastric tissue from uninfected patients.

Reactions comprised: 4 μL of template cDNA prepared from gastric biopsies (Section 2.7.4), 10 μL of 2 × DyNAmo SYBR Green PCR master mix with HS Modified *Tbr* DNA Polymerase (Finnzymes, Thermofisher Scientific, USA), primers each at a final concentration in the reaction of 0.15 μM and nuclease-free water to a total reaction volume of 20 μL. Reactions were set up manually in clear 100 μL strip tubes with caps (Qiagen, USA) and performed in duplicate with the cycling conditions given in Table 2.9 on a Rotor Gene 300 system (Corbett Life Science, Qiagen, USA). Included in each assay were no template controls (NTCs), positive controls with commercial human cDNA (Clontech, BD Biosciences, USA), first-stage RT minus (RT–) controls to exclude DNA contamination of RNA template, and samples of pooled negative

comparator from uninfected donors. Specificity analysis was confirmed by single expected peaks on high resolution melt curves, and where required by gel electrophoresis of PCR products (Section 2.8.4), to ensure primer specificity and absence of contamination or primer dimers.

Various serial dilutions of commercial human cDNA was used to generate standard curves, from which slope, y-intercept, r^2 were calculated and linear dynamic range could be estimated. Data were analysed with Rotor Gene software (version 6.0, Corbett Research, UK). Reaction efficiencies were calculated from standard curves with the following equation: efficiency $= 10^{-\frac{1}{slope}}$. Maximum efficiency of 100% that represents a doubling in the amplified PCR product with each cycle (efficiency = 2.00). Calculated reaction efficiencies (threshold, r^2) for each target gene were – *IL8*: 2.00 (0.0140, 0.988), *IFNG*: 1.95 (0.0822, 0.966), *IL12B*: 1.73 (0.0106, 0.941), *IL10*: 1.91 (0.0175, 0.946), *GAPDH* (with *IL8*): 1.94 (0.0160, 0.995), and *GAPDH* (with others): 1.82 (0.0536, 0.995). The standard curve for *IL12B* (that encodes IL-12/23p40) was prepared from cDNA from gastric biopsies from an infected patient, as reproducible standards for *IL12B* were not obtained from commercial cDNA.

Quantification thresholds (Cq values) were determined when sample fluorescence level crossed a threshold determined automatically from standard curves in Rotor Gene software. Samples were analysed according to the relative quantification model described by Pfaffl (2001). Here a ratio of relative mRNA expression levels is derived using calculated reaction efficiencies and the absolute difference between Cq values measured for the unknown sample and a control sample of pooled cDNA from uninfected donors. The Pfaffl method adjusts for differences in PCR reaction efficiencies and the control sample standardises each run with respect to RNA integrity, sample loading and inter-assay variations. Relative cytokine mRNA expression adjusted for the reference gene *GAPDH* is then expressed in arbitrary units for both the antrum and corpus biopsies, and an antral:corpus ratio calculated. Given the nature of the analysis with the use of exponentials and a single reference gene, results can suggest extremely high cytokine expression for a particular sample when the Cq for *GAPDH* is high (that is, there is less *GAPDH* mRNA detected). Unexpectedly high relative cytokine expression was observed for some samples, similarly to the four patients excluded from the pooled negative comparator as reported above. To identify these outliers, samples were excluded from all cytokine analyses when the Cq for *GAPDH*

measured alongside *IL8* was ≥ 21.5. A plot of *IL8*/*GAPDH* ratio against *GAPDH* Cq was used to identify the proportion of variation that was the result of variation in *GAPDH* rather than in *IL8*. The cut-off point of 21.5 above which high *GAPDH* values unduly influenced relative expression was clearly demonstrated (data not shown).

Note that some RT-qPCR experiments detected fluorescence in no template controls, principally for *IL12B* assays. Troubleshooting methods were applied, including use of reagents uncontaminated by DNA and a metitcuous workflow, uracil-N-gluocsylase pretreatment to eliminate potential dUMP-containing PCR products carried over from earlier RT-qPCR reactions, and re-synthesis of cDNA with additional DNase treatment. Affected data were excluded from the results.

Table 2.9 – cycling conditions for RT-qPCR for mucosal cytokine expression

Step	Number of cycles	Time	Temperature
Initialisation	1×	15 min	95 °C
Denaturation	45×	15 sec	95 °C
Annealing		30 sec	61 or 62 °C
Extension		30 sec	72 °C
Final Extension	1×	5 min	72 °C
Melt curve (0.5 °C increments)			72-95 °C
Final Extension	1×	5 min	72 °C

IL8 and *GAPDH* were assayed with an annealing step of 62 °C. *IFNG*, *IL12B*, *IL10* and *GAPDH* used an annealing step temperature of 61 °C.

Table 2.10 – primers used in RT-qPCR mucosal cytokine expression experiments

Target gene (accession no.)	Primer Sequence	T_m (°C)	Size (bp)	Reference
IL8† (CCDS34005.1)	F: 5'-CTCTTGGCAGCCTTCCTGA-3'	65.6	71	Robinson et al. 2008
	R: 5'-AGTTCTTTAGCACTCCTTGGCA-3'	63.9		
IFNG (CCDS8980.1)	not provided – product no. PPH00380B (but given reference point included in amplicon)	n/a	129	SABiosciences, Qiagen, USA
IL12B‡ (CCDS4346.1)	F: 5'-CTGAGGAGAGTCTGCCCATTG-3'	66.1	111	N. Hussein and K. Robinson (unpublished)
	R: 5'-TGGGTGGGTCAGGTTTGATG-3'	68.1		
IL10‡ (CCDS1467.1)	F: 5'-GCTGGAGGACTTTAAGGGTTACCT-3'	65.6	109	Robinson et al. 2008
	R: 5'-CTTGATGTCTGGGTCTTGGTTCT-3'	65.6		
GAPDH† (CCDS8549.1)	F: 5'-CCACATCGCTCAGACACCAT-3'	66.3	114	Walker et al. 2003
	R: 5'-GGCAACAATATCCACTTTACCAGAGT-3'	65.8		

Primers were synthesised commercially (Sigma-Aldrich, USA or Eurofins MWG Operon, Germany; *IFNG* primers obtained from SABiosciences, Qiagen, USA). All amplicons span at least alternate exons (not provided and cannot be determined for *IFNG*). Primers do not span (†) or at least one primer spans (‡) an intron-exon boundary.

2.8.7. Quantitative reverse transcriptase real-time PCR (RT-qPCR) – initial development of an *in vitro* and *in vivo* assay for relative *dupA* mRNA expression

This aimed to use RT-qPCR to determine *dupA* mRNA expression relative to the number of *H. pylori* organisms given by mRNA levels of the reference gene *16S rRNA*. The primers used are given in Table 2.12. The development, *in silico* analysis, optimisation and evaluation by conventional PCR of the *dupA_RI* primers are described in Section 2.8.3. The position of these primers in the *dupA* gene is illustrated in Figure 2.1. The *in silico* analysis of the *16S_rRNA_RT* primers is reported in Section 2.8.5.

Reactions of 25 μL total volume were set up manually in clear 100 μL strip tubes with caps (Qiagen, USA) with 2 μL of template cDNA prepared from gastric biopsies (Section 2.7.4) or from bacterial cultures (Section 2.7.5) and 12.5 μL of 2 × AB SYBR Green PCR master mix with HS AmpliTaq Gold (Applied Biosystems, USA). *16S_rRNA_RT* primers were used at a final concentration of 0.5 μM in the reaction (2.5 μL each of 5 pmol/μL working stock) with 5.5 μL of nuclease-free water. For *dupA_RI* primers, the final concentrations in the reaction were optimised at 0.05, 0.3 and 0.9 μM (0.25, 1.5 or 4.5 μL each of 5 pmol/μL working stock with 10, 7.5 or 1.5 μL of nuclease-free water respectively).

Reactions were performed in duplicate or triplicate with the cycling conditions given in Table 2.11 on a Rotor Gene 300 system (Corbett Life Science, Qiagen, USA) and data were analysed with Rotor Gene software (version 6.0, Corbett Research, UK). Included in each assay were no template controls (NTCs), positive controls (commercial cDNA or bacterial genomic DNA) and first-stage RT minus (RT–) controls to exclude DNA contamination of RNA template. Specificity analysis was confirmed by single expected peaks on high resolution melt curves and where required by gel electrophoresis of PCR products (Section 2.8.4). Reaction efficiencies were calculated by serially diluting (five-fold, five-step) control template cDNA to generate standard curves, from which slope, y-intercept, r^2 were calculated and linear dynamic range could be estimated. Samples were analysed according to the Pfaffl (2001) method of relative quantification with template cDNA from cultured bacteria use as the control sample in each run.

Table 2.11 – cycling conditions for RT-qPCR *dupA* expression experiments

Step	Number of cycles	Time	Temperature
Initialisation	1×	10 min	95 °C
Denaturation	45×	15 sec	95 °C
Annealing		30 sec	56 or 60 °C
Extension		30 sec	72 °C
Final Extension	1×	10 min	72 °C
Melt curve (0.5 °C increments)			72-95 °C
Final Extension	1×	5 min	72 °C

Note that the *16S_rRNA_RT* primers were initially developed with an annealing temperature of 63 °C and subsequently validated at 60 °C on a rapid thermal cycling platform. *dupA_RI* primers have been used at both 56 and 60 °C, though optimisation was performed at 56 °C.

Table 2.12 – primers used in RT-qPCR *dupA* expression experiments and *dupA_RI* primers used in conventional PCR

Primer Name	Primer Sequence	T_m (°C)	Size (bp)	Reference
dupA_RI_F	5'-TACTAACAGACTTTGAGCCTA-3'	54.0	130	This study
dupA_RI_R	5'-GATTGGATATTCCCATCGC-3'	54.5		
16S_rRNA_RT_F	5'-GGAGGATGAAGGTTTTAGGATTG-3'	58.9	390	Rokbi et al. 2001, Gieseler et al. 2005
16S_rRNA_RT_R	5'-TCGTTTAGGGCGTGGACT-3'	56.0		

Primers were synthesised by Eurofins MWG Operon, Germany.

2.8.8. Online resources

Table 2.13 shows the online resources that were used in primer design and analysis.

Table 2.13 – online resources used in primer design and analysis

Resource	URL
BLAST (Basic Local Alignment Search Tool)	http://www.ncbi.nim.nih.gov/blast/
PrimerBLAST	http://www.ncbi.nlm.nih.gov/tools/primer-blast/
Primer3	http://frodo.wi.mit.edu/primer3/
NetPrimer	http://www.premierbiosoft.com/netprimer/

2.9. Protein analysis

2.9.1. Luminex assays

Snap frozen gastric biopsies were transferred to 300 μl of ice-cold PBS (pH 7.4, Dulbecco A, Oxoid, Basingstoke, UK) supplemented with 2 mM Mg^{2+} (Sigma-Aldrich), benzonase endonuclease to reduce viscosity (Novagen, Darmstadt, Germany) and EDTA-free cOmplete mini protease inhibitors (Roche, Basel, Switzerland). These were disrupted on ice using a pellet pestle with cordless motor (Kimble Kontes, NJ, USA) for 2 min, homogenized by repeated aspiration through a 200 μl filter pipette tip, and incubated on ice for at least 5 min. Clarified supernatant was obtained by centrifugation at 10,000 × *g* for 10 min at 4 °C, then aliquoted into Protein LoBind microcentrifuge tubes (Eppendorf, Hamburg, Germany) and stored at -80 °C until analysis.

Samples were analysed using MILLIPLEX MAP Human Th17 Magnetic Bead Panels (HTH17MAG), High Sensitivity Human Cytokine Magnetic Bead Panels (HSCYTMAG) and Human Cytokine/Chemokine Magnetic Bead Panels (HCYTOMAG) (Merck Millipore, Darmstadt, Germany). Assays were run as per manufacturer's instructions with 25 μl (HTH17MAG and HCYTOMAG) or 50 μl (HSCYTMAG) of sample in duplicate, overnight incubation with shaking (18 hours, 4 °C, 750 rpm), and using a hand-held magnetic block (Merck Millipore) for wash steps. Data were acquired on a validated and calibrated Bio-Plex 200 system (Bio-Rad Laboratories, CA, USA) and analysed with Bio-Plex Manager 6.1 software (Bio-Rad Laboratories) as per manufacturer's instructions with double discriminator (DD) gates of 8000-23,000. Sample wells for individual analyte replicates with bead counts ≤20 were invalidated. Standard curves were fitted using five-parameter logistic regression with default weighting (power law variance), optimized by the software, and then reviewed. Lower and upper limits of quantification were determined as the highest and lowest fitted standards with recovery 80-120 percent and coefficient of variation <20 percent. Where the reported result for an analytes fell outside of this quantifiable range, the appropriate limit was substituted.

2.9.2. Meso Scale Discovery (MSD) assays

Samples were analysed using MSD V-PLEX Pro-Inflammatory Panel 1 assays (IL-1β, IL-6, IL-8 high sensitivity, IL-10, IL-12p70, IFN-γ, TNF-α), MSD V-PLEX Chemokine

Panel 1 assays (IL-8 high abundance) and MSD V-PLEX Cytokine Panel 1 assays (IL-23/23p40, IL-17A). Reagents, equipment and calibrator standards were prepared and the assays performed according to the manufacturer's instructions. Plates were read on a calibrated MESO QuickPlex SQ 120 (SA1LX-1) system and analysed with MSD Discovery Workbench 4.0 software. Standard curves were fitted as recommended. Lower and upper limits of quantification were determined as the highest and lowest fitted standards with recovery 80-120 percent and coefficient of variation of calculated concentration <20 percent. Where the reported result for an analytes fell outside of this quantifiable range, the appropriate limit was substituted.

2.9.3. Bicinchoninic acid (BCA) assay

Total protein was quantified using a BCA assay kit (Pierce, IL, USA) with a single set of BSA standards, and chemokine concentrations reported in pg per mg protein.

2.10. Purification of cell populations from human blood

This evaluation was planned and performed after a review of the immunology methods literature in 2012, discussion with my supervisors and University colleagues including Dr Akhmed Aslam, and personal communication with STEMCELL and Miltenyi Biotec technical support departments, and with Dr Ajay Jain and Dr Edward So (University of Maryland) (So et al. 2013). I am grateful for their time and assistance.

Given the need to process large volumes of blood to obtain sufficient cells, first different methods of preparing PBMCs were evaluated.

Peripheral blood mononuclear cells (PBMCs) were purified from buffy coats prepared from whole blood samples according to the instructions of STEMCELL. Traditional layering of cells by directly pipetting onto density gradient media was compared with STEMCELL SepMate™ tubes. The latter enables more rapid cell isolation and is recommended with RosetteSep™. Azide-free PBS-based RoboSep™ buffer (2% v/v FBS, 1 mM EDTA, STEMCELL #20124) was 0.2 μm filtered. Density gradient media used were Lymphoprep™ (density 1.077 g/mL, STEMCELL #07801) and Histopaque® (density 1.077 g/mL, Sigma-Aldrich 10771). Separate media and centrifuges were used at recommended temperatures for each step. Polypropylene disposables were used. Additional centrifugation steps to deplete platelets were included after PBMC

separation (anti-CD41 depletion was not used). Direct layering of buffy coat onto density gradient media was preferred in preparing PBMCs.

Different approaches to $CD14^+$ cell purification from human leucocytes were evaluated using four commercial kits that separate cells of interest by either positive or negative selection using immunomagnetic beads. The evaluation is reported in Section 5.4.1. Details of the different kits are shown in Table 2.14.

Donors were attending Nottingham University Hospitals NHS Trust for venesection as maintenance treatment for hereditary haemochromatosis. No donors had other medical conditions or were undergoing treatment that might affect their immune response. Ethics and regulatory approvals were in place for the Nottingham Health Science Biobank and this project, with anonymised collection of whole blood. Informed written consent was obtained from all donors, whose participation was in accordance with the principles of the Declaration of Helsinki 2008.

Ten donors each provided approximately 250 to 500 mL of whole peripheral blood (median 300 mL). Blood was drawn between 9am to 12pm with donors in a non-fasted state, collected into a blood bag system containing citrate phosphate dextrose adenine (CPDA-1) and kept at room temperature. Peripheral blood mononuclear cells (PBMCs) were extracted by density gradient centrifugation from buffy coat fractions prepared directly from whole peripheral blood. $CD14^+$ cells were then purified from PBMCs by positive immunomagnetic separation using Miltenyi Biotec CD14 MicroBeads. Total cell numbers, viability and purity were determined.

The workflow for preparing cells was time-consuming, with a single operator following the same optimised protocol. Therefore, collection and processing times across donors were carefully monitored. Donation to processing was within 1-2 h. All cells were extracted and purified on ice and aliquoted within 4-9 h. Cells were incubated in a 37 °C humidified incubator (with 5% CO_2 in RPMI-based media supplemented with foetal bovine serum) and used in downstream experiments within 3-4 h (donors G-J within 2-10 h, donor C after 20 h overnight incubation). Cells were used immediately and not frozen or thawed. Contamination was routinely screened for by phenol red pH indicator, microscopy and Gram staining.

Table 2.14 – cell purification kits

Kit	Cells	Purified from	Selection type	With antibodies against[6]	
MB[1]	$CD14^+$ cells (principally monocytes[5])	PBMCs	Positive	CD14	
ES–16dep[2] (without CD16 dep)	$CD14^+$ and $CD14^{dim}CD16^+$ monocytes	PBMCs	Negative	CD2, CD3, CD19, CD56, CD66b, CD123, GlyA	CD20, dextran, and FcR Blocker
ES+16dep[3] (with CD16 dep)	$CD14^+CD16^-$ monocytes	PBMCs	Negative		CD16, CD20, dextran, and FcR Blocker
RS[4]	$CD14^+$ and $CD14^{dim}CD16^+$ monocytes	Buffy coat	Negative		CD8

Kits used to purify cells by immunomagnetic separation evaluated during optimisation. Other purification kits are available including both positive and negative selection kits made by Miltenyi Biotec and STEMCELL.

CD, cluster of differentiation; dep, depletion; ES, EasySep™; MB, Miltenyi Biotec MACS®; PBMCs, peripheral blood mononuclear cells; RS, RosetteSep™

[1] Miltenyi Biotec MACS® human CD14 kit, #130-050-201; contains mouse anti-human IgG_{2a} antibodies against CD14 conjugated to magnetic MicroBeads

[2] STEMCELL EasySep™ human monocyte enrichment kit without CD16 depletion, #19018; contains mouse anti-human IgG_1 antibodies against CD2, CD3, CD19, CD20, CD56, CD66b, CD123, GlyA, dextran, and a mouse anti-human IgG_{2b} FcR Blocker

[3] STEMCELL EasySep™ human monocyte enrichment kit, #19019; contains identical antibodies and FcR Blocker to [2], plus mouse anti-human IgG_1 antibodies against CD16

[4] STEMCELL RosetteSep™ human monocyte enrichment kit, #15018; contains IgG_1 mouse anti-human antibodies against CD2, CD3, CD8, CD19, CD56, CD66b, CD123 and GlyA

[1-4] FcR Blocker (FcγRII, CD32a) binds to IgG aggregates and immune complexes to block non-specific labelling by Fc/FcR interactions (CD32a is present on B cells, monocytes, macrophages, granulocytes and platelets). GlyA (glycophorin A, CD235a) is present on erythrocytes. Anti-dextran antibody (raised against isomaltotetraose, binds polysaccharides) binds to dextran-coated magnetic nanoparticles to label cells.

[5] Monocytes and macrophages are $CD14^+$ and granulocytes (principally neutrophils) and some myeloid dendritic cells express low levels of CD14. However, in peripheral blood after density gradient separation and purification, $CD14^+$ cells should principally be monocytes. Note that negative selection kits did not deplete CD4, which is expressed by monocytes (17338817).

[6] Lymphoid and myeloid haematopoietic cell markers (key markers) from Human CD Marker Handbooks (BD Biosciences and eBioscience): T cells (CD2, CD3, CD8, CD16, CD20, CD56); B cells (CD2, CD19, CD20); NK cells (CD2, CD8, CD16, CD56); dendritic cells (CD16, CD19, CD123); granulocytes (CD16, CD66b, CD123).

Total cell number was determined by counting cells in a representative cell suspension after dilution and trypan blue staining using a haemocytometer (donors A-C, determined for all donors) and using acetic acid/methylene blue staining to count nucleated cells (donors D-J). There was minimal erythrocyte contamination (data not shown). Platelets were depleted by centrifugation.

Viability was determined by trypan blue exclusion and cell counting against total cell number (TB) and by propridium iodide staining of all cellular events using flow cytometry (PI). Cell purity was determined by flow cytometry gated for viable cells by PI staining (or by region gating for mononuclear cells for donors A and B).

2.11. Bacterial co-culture experiments with immune cells from human blood

Details of the *H. pylori* strains used in these experiments are reported in Table 2.15 and Table 2.16.

Controls were included in each experiment: media only negative control, lipopolysaccharide (LPS) positive control at a final concentration of 100 ng/mL (*Escherichia coli* O55:B5 LPS; Sigma-Aldrich, Gillingham, UK), and antigenic stimulation with a *H. pylori* lysate at a final concentration of 22.7 μg/mL (sonicate adjusted to 250 μg protein/mL and prepared from six clinical strains of *H. pylori* with various *cagA* and *vacA* genotypes that were isolated from patients with normal upper GI endoscopy or various gastroduodenal diseases in Nottingham, UK). Mitogenic stimulation with PMA and ionomycin was also included in some experiments but was a less effective positive control (data not shown). Cell only and bacteria only negative controls were also performed (data not shown).

Mutants were constructed principally in the AB21 strain background. This strain was selected as it has a complete and intact *dupA* gene (*dupA1*) and *tfs4* operon, and an intact *cag*PAI. Inverse PCR by high fidelity polymerase was used to amplify and engineer restriction sites into genes of interest. The chromosomal *dupA* gene was disrupted by ligation of a chloramphenicol resistance cassette to create a pGEM-T Easy plasmid (Promega, Southampton, UK), with allelic exchange mutants selected by marker rescue after natural transformation (Hussein et al. 2010, Dr Christian Marx). A similar approach using a kanamycin resistance cassette (Bebb et al. 2003) was used to disrupt *cagE* (Hussein et al. 2010, Dr Marx) and *virB8* (this study, undertaken together with Dr

Marx). Three single and two double mutants were constructed in AB21 (O, Table 2.15). Note that *cagE* disruption does not necessarily eliminate all cagPAI activity (due to *cagL* etc). All constructs were verified by sequencing. Representative growth curves for the mutants constructed as part of this study are shown in Appendix Figure 7.1. All strains exhibited similar time in the different phases of growth and reached similar bacterial numbers in liquid culture. Strains were recovered from agar for co-culture in the stationary phase (20-24 h) with colony forming unit counts and observed MOIs close to expectations.

Additional mutants were kindly provided by Dr Rob Delahay and Dr Amberley Stephens (AB21 [denoted by X], P1 and 527 backgrounds, Table 2.15). These AB21 mutants were independently derived from a separate stock of AB21 from the same parent strain. The DNA manipulation techniques used in the construction of these mutants was similar (Grove et al. 2013; Dr Rob Delahay, personal communication), though the Δ*tfs4* strain was constructed as a markerless mutant (Dailidiene et al. 2006) Co-cultures with 527 mutant strains, including the *catF* strain designed to over-express *tfs4* genes, could not be analysed due to inadequate growth.

Bacterial strains were recovered from cryo-stocks stored at -80 °C, and underwent one or two passages onto antibiotic-free horse blood agar with incubation under microaerophilic conditions. Bacteria were resuspended and diluted in two steps in order to achieve a MOI of 10, with some bacteria also heat inactivated or treated with paraformalydehyde, then washed and diluted to achieve an MOI of 10 (see below). All bacterial strains were processed, in batches if necessary, with the workflow from removal from the incubator after 20-24 h of growth, through to addition to cells for co-culture taking 30-90 min.

Bacterial viability was calculated in colony forming units (CFU) per mL using dilution plating following a similar method to Miles and Misra (1938). The CFU/mL values were used to calculate an actual MOI (both values were numerically identical owing to the volumes and concentrations used), with observed cytokine concentrations adjusted by multiplication by a correction factor calculated for each donor/strain as $\log_{10}$(expected MOI) / $\log_{10}$(observed MOI). Viability data were unavailable for co-culture experiments with cells from donors D and E due to a fault with the gas supply to the VAIN cabinet affecting only the dilution series plates, so these adjustments were based on mean MOIs for each strain across other experiments.

Plated strains were also inspected to exclude significant contamination (no contamination observed as expected), and undiluted controls, heat inactivated and paraformaldehyde-treated strains were also plated (no growth observed as expected).

Two treatments were applied to bacterial strains prior to co-culture in some cases. Bacteria were inactivated by heating to 65 °C for 30 min. Gram stain and microscopy confirmed that the bacteria were intact (data not shown). For paraformaldehyde treatment, bacterial cells were harvested and pelleted by centrifugation, resuspended in 1 mL of 4% formaldehyde (buffered pH 6.8-7.2, 0.2-0.6% methanol, azide-free), incubated at room temperature for 20 min, gently washed three times in PBS then resuspended in tissue culture media, adjusted to a concentration of 1×10^8 cells/mL using OD_{600} readings, then used in co-culture at an MOI of 10.

Cells co-cultured with bacteria and with controls were incubated at 37 °C / 5% CO_2 for 16 h (for flow cytometry) and for 48 h (for cytokine and chemokine expression). For the latter experiments, supernatants were recovered and centrifuged, then clarified supernatants were aliquoted and stored at -20 °C. These samples were analysed using MSD assays (Section 2.9.2).

Table 2.15 – bacterial strain characteristics (mutant and laboratory strains)

Strain	Type	Viability (CFU/mL)	No.	Description	Source
Expected MOI		10.0			
Overall		9.6 ± 5.1	69		
AB21 wild-type	O	9.2 ± 6.4	4	wild-type	Dr E El-Omar
	X	8.7 ± 4.5	5		
AB21 Δ*cagE*	O	12.4 ± 1.2	4	kan	Dr C Marx
	X	9.2 ± 4.8	4	kan	Dr R Delahay
AB21 Δ*dupA*	O	13.1 ± 4.6	4	chlor	Dr C Marx
	X	10.3 ± 4.8	4	chlor	Dr R Delahay
AB21 Δ*dupA*Δ*cagE*	O	12.9 ± 4.2	4	chlor/kan	Dr C Marx
	X	10.3 ± 3.4	3	chlor/kan	Dr R Delahay
AB21 Δ*virB2*	X	14.7 ± 2.9	3	chlor	Dr R Delahay
AB21 Δ*virB8*	O	12.6 ± 2.4	4	kan	this study, Dr C Marx
AB21 Δ*virB8*Δ*dupA*	O	8.0 ± 2.1	2	chlor/kan	
AB21 Δ*virB9*	X	10.8 ± 2.5	3	chlor	Dr R Delahay
AB21 Δ*tfs4*	X	15.6 ± 0.9	2	markerless	Dr A Stephens
P1	Δ	6.0	1	wild-type	Dr R Delahay, Dr A Stephens
P1 Δ*dupA*	Δ	7.8	1	chlor	
P1 Δ*tfs4*	Δ	8.8	1	markerless	
527 Δ*dupA*	-	0.7	1	chlor	Dr R Delahay, Dr A Stephens
527 Δ*tfs4*	-	1.1	1	markerless	
527 *catF*	-	3.6	1	over-express *tfs4*	

Viability expressed as mean ± standard deviation.

CFU, colony forming units; chlor, chloramphenicol resistance cassette; kan, kanamycin resistance cassette; MOI, multiplicity of infection; No., number of times strains were cultured from cryo-stocks for use in independent experiments; Site, gastric region from which strain cultured, either antrum (A) or corpus (C); Type, symbol used in figures (O, X, Δ, - denotes where data not shown).

Table 2.16 – bacterial strain characteristics (clinical isolates)

Strain	Type	Site	Viability (CFU/mL)	No.	*dupA* status	Source
242	-	A	7.5	1	unknown	Nottingham, UK
249	-	C	2.8	1	unknown	Nottingham, UK
255	-	A	10.8	1	unknown	Nottingham, UK
286	-	A	6.3	1	*dupA1* but missing 7 amino acids starting position 173 (*dupAx*)	Nottingham, UK
613	-	A	27.8	1	unknown	Nottingham, UK
dupA1 strains			4.8 ± 2.3	6		
454	X	C	4.3	1	*dupA1*	Nottingham, UK
521	X	A	1.3	1	*dupA1*	Nottingham, UK
527	X	A	6.3	1	*dupA1*	Nottingham, UK
597	X	A	7.5	1	*dupA1*	Nottingham, UK
606	X	C	6.3	1	*dupA1*	Nottingham, UK
619	X	A	3.3	1	*dupA1*	Nottingham, UK
non-*dupA1* strains			5.9 ± 3.5	6		
461	X	A	12.0	1	*dupA* negative	Nottingham, UK
529	X	A	4.5	1	*dupA* negative	Nottingham, UK
536	X	C	3.7	1	*dupA* negative	Nottingham, UK
547	X	A	3.8	1	*dupA* negative	Nottingham, UK
563	X	A	8.3	1	*dupA* negative	Nottingham, UK
565	X	A	3.1	1	*dupA* negative	Nottingham, UK

Viability expressed as mean ± standard deviation.

CFU, colony forming units; MOI, multiplicity of infection; No., number of times strains were cultured from cryo-stocks for use in independent experiments; Site, gastric region from which strain cultured, either antrum (A) or corpus (C); Type, symbol used in figures (O, X, Δ, - denotes where data not shown).

2.12. Flow cytometry

Both PBMCs and CD14 enriched cells were co-cultured (1 mL, 5×10^5 cells/mL) with media only, lipopolysaccharide (LPS, 100 ng/mL), sonicated *H. pylori* (lysate) or with sets of wild-type and isogenic mutants of *H. pylori* strain AB21 (MOI 20) that had been constructed and stored separately (denoted by O and X). Cells were incubated at 37 °C / 5% CO_2 for 16 h, and 10 µL of brefeldin A was added after 1 h. Additional control cells were stored at 4 °C in parallel to assess purity and viability. For model optimisation experiments, cells were co-cultured at 1.0×10^6 cells/mL with 2 µL of brefeldin A.

Cells were stained with mouse IgG2a anti-human CD14–FITC (AbD serotec® #MCA1568F, clone TÜK4, 2 µL), mouse IgG2a anti-human CD14–RPE-Cy5 (AbD serotec® #MCA1568C, clone TÜK4, 7.5 µL, used only for mononuclear cell model optimisation experiments), mouse IgG1 anti-human CD80–PE (Beckman Coulter® #IM1976U, clone MAB104, 5 µL, data not shown) or mouse IgG2b anti-human CD86–PE (Beckman Coulter® #IM2729U, clone HA5.2B7, 5 µL, data not shown) before fixation. After fixation/permabilisation, cells were then stained with mouse IgG1κ anti-human IL-12/23p40–PE (eBioscience #12-7235-73, clone eBioHP40, 20 µL), rat IgG1κ anti-human IL-12p70–PE (BD Pharmingen™ #557020, clone 20C2, 2 µL, data not shown), PE mouse IgG1κ isotype control (eBioscience #12-4714-42, clone P3, 5 µL) or PE rat IgG1κ isotype control (BioLegend® #400408, clone RTK2071, 2 µL, data not shown). Note that the addition of extra-cellular and intra-cellular stains was performed in separate steps for donor F, with parallel optimisation where CD14–FITC extra-cellular stain was added together with intra-cellular stains after fixation/permeabilisation (data not shown). The latter approach alone was followed for all subsequent donors (G-J). Unstained, fluorescence minus one (FMO) and isotype controls were included. Buffers and wash steps are reported in Robinson et al. (2008).

Data from 50,000 events were acquired with a Beckman Coulter FC500 flow cytometer for each donor/cell/strain combination (unless otherwise stated). For the mononuclear cell model optimisation experiments, events were acquired over 240 sec. Compensation beads were used for initial setup (data not shown). An example gating strategy is shown in Figure 2.3.

Figure 2.3 – example flow cytometry gating strategy for IL-12/23p40 and CD14 expression by peripheral blood cell populations

Peripheral blood mononuclear cells (PBMCs) were purified from 1 donor (F) using the optimised protocol. Here cells expressing CD14 were enriched from these PBMCs by positive (+) selection. Cells were co-cultured with media only and incubated for 16 h with brefeldin A added after 1 h. Control cells were stored at 4 °C in parallel. Cells were stained with mouse IgG2a anti-human CD14–FITC before fixation and with mouse IgG1κ anti-human IL-12/23p40–PE, after fixation/permeabilisation. Unstained, fluorescence minus one (FMO) and isotype controls were included. Events were acquired with a Beckman Coulter FC500 flow cytometer (maximum of 50,000 are shown in each plot) and gated for relevant cells on a forward-scatter (FS) / side-scatter (SS) plot (region coordinates for donor F: 20-150, 8-90, and for donors G-J: 20-90, 8-86). Then $CD14^+$ and IL-12/$23p40^+$ events were gated on a FL1–CD14–FITC / FL2– IL-12–PE plot ($CD14^+$ range for donor F: 86-256 and for donors G-J: 100-256; $IL\text{-}12^+$ ranges 148-256 and 140-256 respectively).

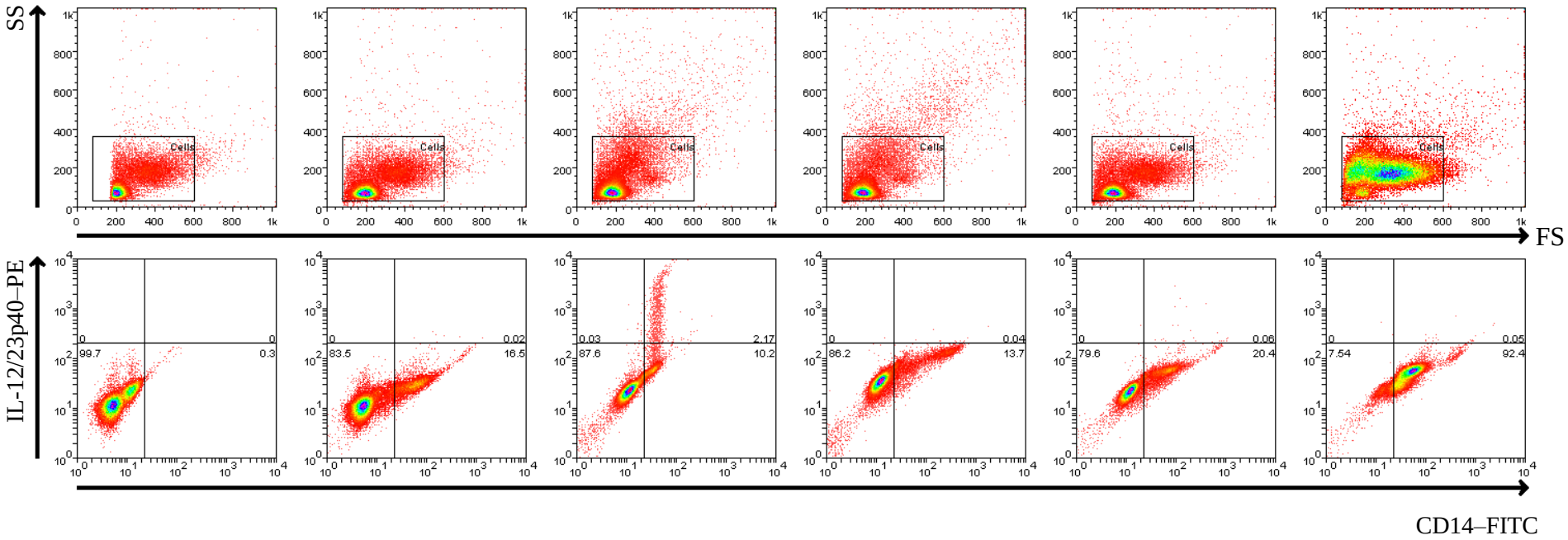

type	unstained control	FMO control	FMO control	isotype/FMO control	co-culture media	co-culture media
cells	PBMC	PBMC	PBMC	PBMC	PBMC	CD14 enriched (+)
events	36,351	52,660	151,156	86,040	50,000	50,000
gated	98.5%	98.6%	96.6%	96.2%	98.3%	96.9%
CD14	–	+	–	+	+	+
IL-12	–	–	+	–	+	+
isotype	–	–	–	+	–	–
% CD14$^+$					20.4%	92.5%

Figure 2.3 – example flow cytometry gating strategy for IL-12/23p40 and CD14 expression by peripheral blood cell populations

2.13. ChipCytometry

For this project, we collaborated with Dr Christian Hennig and Dr Jan Detmers and their team at Zellkraftwerk (Hannover, Germany) and Nottingham University Hospitals Charity kindly supported my work through pump-priming funding. I am grateful for their time and assistance. I am also grateful to United European Gastroenterology and the MacDonald group (Queen Mary, University of London) for helpful discussions about their experiences with intestinal biopsies and tissue resections.

Biomarker assays were validated (based on Cunliffe et al. 2009) to determine method protocol and dilution, precision, detection range and lower limit of detection. Protocols were developed using mitogen stimulated human PBMCs as reference material, based on our stimulation method. Non-stimulated PBMCs were used to validate protocols for surface markers. All antibody dilutions and wash steps were carried out using Permeabilization Buffer (eBioscience) and, for intra-cellular stains, cells were treated for 30 min with Fix/Perm Buffer (eBioscience). Blood samples were taken from human volunteers and PBMCs were extracted using Ficoll-Paque. The cells were suspended in 1 mL of PBS, collected by centrifugation (320 *g*, 10 min, room temperature), suspended in 1 mL of RPMI-1640 cell culture medium and adjusted to 1.00×10^6 cells/mL. In cell culture plates, 1×10^6 cells per well were stimulated with PMA (20-50 ng/mL) and ionomycin (1 μmol/mL) for 15 h, with brefeldin A (10 μg/mL, BD GolgiPlug™) added 3 h prior to cell collection. Total recovered cells were 3.7×10^5 cells/mL (37%) with viability of 65% by typan blue exclusion (images acquired with Roche Innovatis Cedex HiRes). Other stimulants were tested on including LPS (100 ng/mL) and IFN/LPS (100 ng/mL IFN-γ, 1 μg/mL LPS).

For the gastric biopsy evaluation, samples were recovered at endoscopy and kept on ice in biopsy media (RPMI-1640, 1% v/v L-glutamine, 2% v/v heat-inactivated foetal calf serum, penicillin [100 U/mL], streptomycin [100 μg/mL]). In the laboratory, biopsies were transferred within a category 2 cabinet to a Petri dish and washed in wash media to remove mucus (Hanks' balanced salt solution without $CaCl_2$/$MgSO_4$, penicillin [100 U/mL], streptomycin [100 μg/mL], amphotericin B [250 ng/mL]). Preparation 1 media was then used to begin to dissociate the biopsy and strip the epithelium (wash media, EDTA [1 mM], DTT [1 mM]) with incubation at 37 °C with shaking at 210 rpm for 10 min [15-30 min during optimisation]. The DTT is used to dissolve residual mucus and

release debris. The EDTA is used to disrupt the basement membrane and so begin to release epithelial cells, and hence IELs, from the underlying mucosa (LPMCs and stromal cells). For some samples, biopsies were next fragmented using sterile scalpels then subjected to enzymatic digestion with collagenase Ia (0.5 mg/mL) and DNase I (5 U/mL) treatment was performed at 37 °C with shaking at 210 rpm for either 30 or 35 minutes. Samples were mechanically disrupted by gently rubbing the biopsies through one or more cell strainers (40 µm or 100 µm) using the flat end of a 1mL sterile syringe plunger, with cells then washed through strainer with culture media.

Cells recovered from disrupted mucosal tissue were stimulated *ex vivo*. Stimulation used antigen in the form of bacterial lysate (25 µg protein/mL, sonicated *H. pylori* prepared from six clinical strains of *H. pylori* with various genotypes isolated from patients with or without gastroduodenal disease in Nottingham, UK) or using mitogen with PMA (20 ng/mL) and ionomycin (0.7 µg/mL). Stimulated cells were incubated at 37 °C / 5% CO_2 for the times indicated, then held at 4 °C. For both antigen and mitogen stimulation, brefeldin A (10 µg/mL) was added after 1 h of incubation to block cytokine secretion. This is based on the standard method for flow cytometry optimised by our group.

After stimulation, cells were resuspended in sterile PBS with cell number and viability were quantified by TB exclusion. The cell suspension was then centrifuged at 1000 × *g* for 10 min with the supernatant discarded (note used 400 × *g* in final protocol). The cell pellet was resuspended in 1 mL of relaxation buffer (PBS, 0.5% v/v BSA, 2 mM EDTA) and incubated at room temperature for 15 min. To remove larger debris, the cell suspension was passed through a pre-wetted cell strainer under gravity then washed through. Alternatively, cells were overlaid onto 2 mL Biocoll density gradient media, centrifuged at 500 × *g* for 10 min, then recovered and resuspended. To remove smaller debris, the cell suspension was centrifuged at 100 × *g* for 10 min with the supernatant discarded, then resuspended in PBS.

Once stimulated cells had been recovered, resuspended and debris removed, these were then immobilised as a cell monolayer onto the self-adherent surface of microfluidic CellSafe™ chips and fixed according to the manufacturer instructions. Chips were then transported to Zellkraftwerk in Germany, with the necessary ethical and regulatory agreements in place. They employ a standardised workflow, with pre-analytical, analytical and post-analytical phases including quality control and validation. First, background auto-fluorescence was determined and cells were stained with various sets

of fluorescent conjugated antibodies. High dynamic range images were acquired using their proprietary ZellScanner instrument. These images were used to recognise and track cells and to sensitively quantify fluorescence for each cell (potentially at the cell compartment level). After each round of 'stain and scan' for each set of biomarkers, remaining fluorescence was erased by photobleaching and the bioanalysis process was then repeated. The resulting cytometric data were annotated and provided to us in the form of Flow Cytometry Standard data files for analysis.

2.14. Statistical analysis

The statistics package GraphPad PRISM (version 7.01) was used. SPSS version 23 was used for linear regression analyses. Some figures were prepared using Microsoft Excel 2010. Fisher's exact test was used for categorical and 2×2 data, along with the φ (phi) correlation coefficient for this type of data. Standard non-parametric and, where it was appropriate to treat those particular data as normally distributed, parametric methods were used. The statistical test used is reported with each result, including correction for multiple comparisons. For some analyses, more than one method of analysis was used; concordant, statistically significant results were required for strong evidence to be inferred. Significance tests were two-tailed with a significance level sufficient to reject the null hypothesis of $P < 0.05$, unless otherwise specified.

3. Results One – Influence of *dupA* status on clinical outcomes

Helicobacter pylori colonisation does not lead to clinically significant gastroduodenal disease in the majority of individuals. In around 1 in 5, however, it is an important aetiological factor in the clinical outcomes of duodenal ulcer (DU), gastric ulcer (GU) or gastric cancer (GC). Disease risk is determined by bacterial virulence factors, host factors including genetic polymorphisms, and environmental factors.

The duodenal ulcer promoting gene of *H. pylori* – *dupA* – was proposed as the first disease-specific bacterial virulence factor, as it was associated in epidemiological studies with an increased risk of DU specifically and, in some populations, relative protection against cancer. There are challenges in identifying the *dupA* status of a particular strain, as the gene is polymorphic and some alleles are predicted to be non-functional. The true function(s) of the *dupA* system, the conditions under which it is employed by the bacterium, and the relationship to interactions with its human host have yet to be fully elucidated.

Here, *dupA1* strains are defined as those with an intact full-length *dupA* gene. That is, those without SNPs or non-sense mutations that would result in a frameshift or early termination of transcription, and those long-type forms of 2,499 bp in length rather than shorter forms. All non-*dupA1* strains were considered to be non-functional.

The aims of this chapter were:

1. to carefully characterise the *dupA* status and virulence determinants of clinical isolates from the Nottingham study population,
2. to report the first association study for the United Kingdom for the relationship with clinical outcomes according to *dupA* status, and
3. to undertake a systemic review and meta-analysis of the influence of *dupA* status on clinical outcomes.

3.1 Nottingham study population

This study recruited adult patients attending for upper GI endoscopy between January 2002 and June 2012 at Nottingham University Hospitals. Seven hundred and four patients were assessed for eligibility against the exclusion criteria reported in the study participant flow diagram shown in Figure 3.1. As shown in the figure, 8 patients were excluded as being unsuitable. Of the remaining 696 patients with their eligibility assessed as suitable, 72 were excluded as they did not meet study criteria.

Four investigations were then used to determine *H. pylori* status (urease test, culture, histology and serology). Strict criteria were applied, with agreement between all four tests needed for inclusion as a *H. pylori* negative participant, and either positive culture or at least 3 positive tests required for *H. pylori* positive participants. Therefore, a further 349 patients were excluded (Figure 3.1), yielding a study population of 275 participants.

The study population comprised 155 women and 120 men, with mean ages (± sd) of 54 ± 14.5 and 53 ± 15.1 years respectively (overall 54 ± 14.8 and range 18-86 years). Ethnicities were: 69% Caucasian, 5% African/Caribbean, 4% Indian or Pakistani, 3% Asian, 2% Middle Eastern and 18% unknown. The prevalence of *H. pylori* infection in the study population was 53.8%. The characteristics of the study population and of other participant populations in the flow diagram are reported in Table 3.1.

Note that the population that "did not meet study criteria" (n=72) was significantly different to some other populations. It comprised significantly more men than "*H. pylori* positive unable to culture" ($P = 0.044$), its mean age was 5.7 years greater than the population assessed for eligibility without unsuitable cases (95% CI 2.0-9.4, $P = 0.003$), and it was significantly younger on average than all other populations (mean age differences ranged between 5.2 to 8.2 years lower, $P < 0.05$). However, there were no statistically significant differences when comparing all excluded patients (n=421) against other populations after correction for multiple comparisons.

In order to test the hypothesis that *dupA* status is positively associated with duodenal ulceration, clinical *H. pylori* isolates from our study population were characterised for bacterial virulence factors.

Figure 3.1 – study participant flow diagram

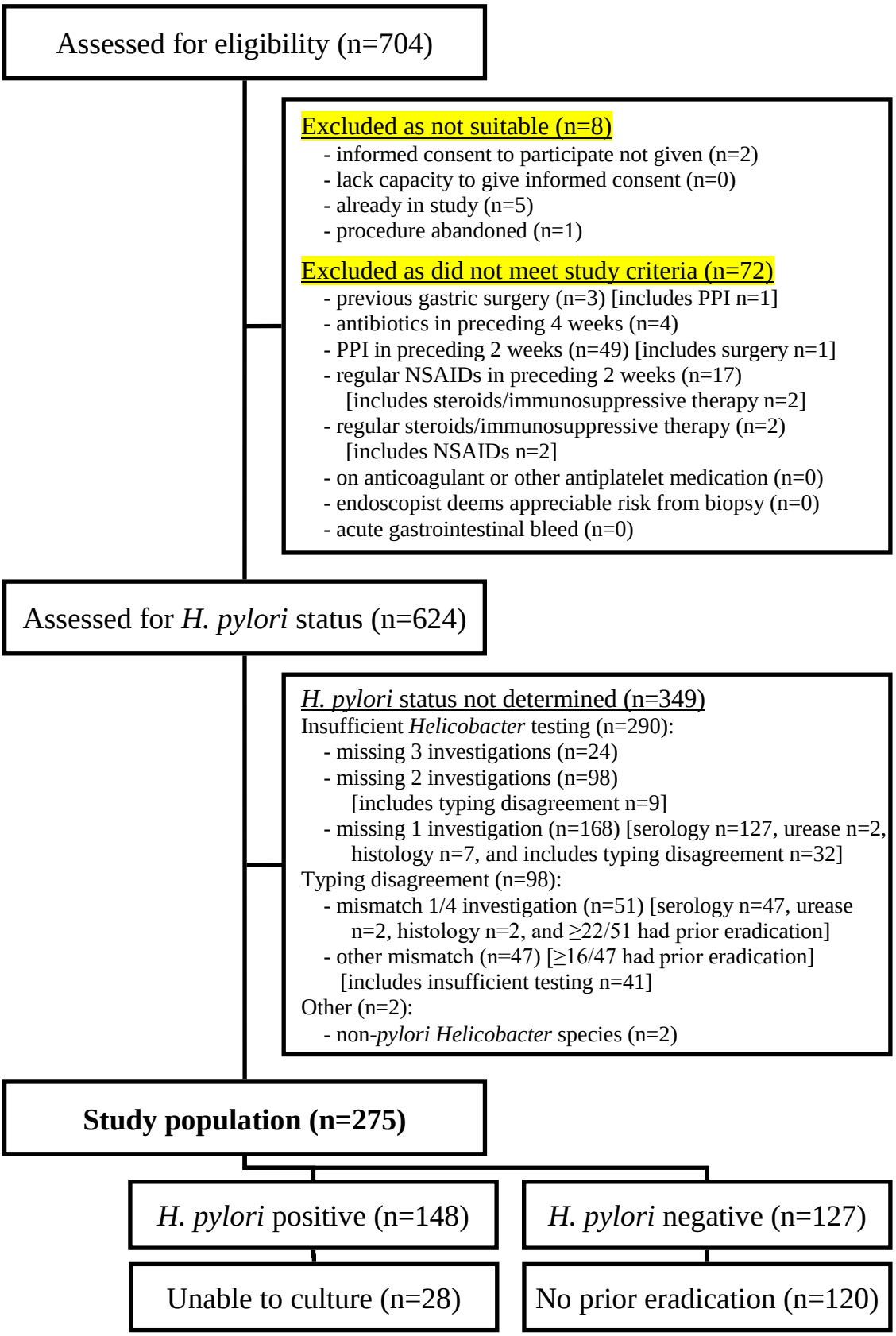

NSAID, non-steroidal anti-inflammatory drug (excludes regular aspirin for cardiovascular prophylaxis); PPI, proton pump inhibitor.

Table 3.1 – characteristics of study participant populations in flow diagram

Population	n	Male			Female		
		%	mean age ± sd (years)	age range (years)	%	mean age ± sd (years)	age range (years)
Eligibility assessed as suitable	696	44.8	54 ± 15.5	18-90	55.2	55 ± 15.2	18-85
Did not meet study criteria	72	52.8	58 ± 12.4	31-79	47.2	63 ± 14.1	27-84
H. pylori status not known	349	44.1	53 ± 16.3	19-90	55.9	55 ± 15.7	18-84
Study population	**275**	**43.6**	**53 ± 15.1**	**18-86**	**56.4**	**54 ± 14.5**	**20-85**
H. pylori positive	148	41.9	56 ± 17.1	18-85	58.1	54 ± 12.5	29-78
Unable to culture	28	28.6	55 ± 15.8	29-84	71.4	52 ± 12.1	30-78
Culture available	120	45.0	56 ± 17.4	18-85	55.0	55 ± 12.7	29-78
H. pylori negative	127	45.7	50 ± 12.3	22-86	54.3	54 ± 16.8	20-85
No prior eradication	120	46.7	50 ± 12.4	22-86	53.3	54 ± 17.2	20-85
Prior eradication	7	28.6	50 ± 12.7	41-59	71.4	53 ± 11.5	41-69

3.2 Establishing *dupA* status – genotyping and sequencing

The Nottingham study population comprised 148 *H. pylori* positive participants, though culture was unsuccessful for 19% (28/148). Strains were comprehensively characterised after culture *in vitro* to establish *dupA* status, as reported in Section 2.8.1. This was incomplete for 57% of participants (68/120) for several reasons, including template quality, problematic strain characterisation by PCR or sequencing, and time and resource constraints. This is discussed further in Section 3.5.3. Those isolates with a fully characterised *dupA* status were available for further study.

The *dupA* status of clinical isolates from 52 patients was identified. Colonising strains were identical between the gastric antrum and corpus in all cases.

Sixty-six isolates from 52 participants were grown *in vitro* and typed, with 31 isolates from the gastric antrum, 7 from the gastric corpus and 14 from both sites. Sequences for strains isolated from both sites were identical in all cases (Appendix Section 7.3.1).

Strains were *dupA1* in approximately half of these isolates.

There were 24 participants colonised by strains with an intact full-length *dupA* gene of 2,499 bp and without frameshift mutations (*dupA1*, 46%), 9 patients colonised by strains with a full-length *dupA* gene disrupted by frameshift mutations and no strains that had a truncated *dupA* gene (*dupA2*, 17%), and 18 patients colonised by strains lacking a *dupA* gene when genotyped in this study (*dupA* negative, 35%). Though 3 strains in the

latter group were positive by alternative PCR primers (Dr Rob Delahay, personal communication), suggesting a heavily fragmented or partial *dupA* gene.

In addition, the antral isolate #286 contained a *dupA* gene that was missing 21 bp from position 517 to 537 inclusive, though was otherwise full-length and without any frameshift mutations (*dupAx*). Its putative protein would be missing amino acids 173 to 179 inclusive, and was grouped together with the *dupA2* and *dupA* negative strains. This observation was confirmed by repeat sequencing and additional primers.

Therefore, 24 *dupA1* and 28 non-*dupA1* strains were available for analysis. This represents 35% of the *H. pylori*-infected study population. Of these 148 *H. pylori*-infected, it was not possible to isolate and culture the colonising strain *in vitro* in 28 cases (19%). A further 68 participants were without typing data for *dupA* status. Efforts were made to identify the status of *dupA* and other virulence factors from nucleic acids purified directly from biopsy samples, particularly to determine *dupA* transcription in clinical samples by RT-qPCR, though were unsuccessful (not shown).

3.2.1 Relationship between bacterial virulence factors

Several virulence factors have been reported for *H. pylori*. The best characterised are the *cag* pathogenicity island and the polymorphic *vacA* gene. The presence or absence of *cag*PAI and the *vacA* type were determined and compared with *dupA* (Table 3.2).

In our strain collection, there was a weak association between *dupA1* and *vacA* s1m1i1 type ($\varphi = 0.341$ [phi correlation coefficient for 2×2 contingency table], $P = 0.014$, $\chi^2 = 6.031$, n=52). No association was found between *dupA* status and the *cag*PAI ($\varphi = 0.135$, $P = 0.340$, $\chi^2 = 0.948$, n=52). As expected there was a stronger association between *cag*PAI and *vacA* (21/23 [91%] with *cag*PAI+/s1m1i1 vs.14/29 [48%] with *cag*PAI–/non-s1m1i1, $P = 0.003$; $\varphi = 0.426$, $P = 0.002$, $\chi^2 = 9.433$, n=52).

Table 3.2 – relationship between *dupA*, *cag*PAI and *vacA*

***dupA* status**	**n**	***cag*PAI**		***vacA***					
		+	**–**	**s1m1i1**	s1m1/2i1	s1m2i1	s1m2i2	s2m2i2	**non-s1m1i1**
dupA1	24	15	9	15		2	4	3	9
dupA2	9	6	3	3		1	3	2	6
dupAx	1	0	1				1		1
dupA negative	18	15	3	5	1	6	4	2	13
non-*dupA1*	28	21	7	8	1	7	8	4	20
overall	52	36	16	23	1	9	12	7	29

3.2.2 Summary

The *dupA* status of clinical isolates from 52 patients were identified. Strains were *dupA1* in 46% of cases (24/52). Colonising strains were identical between the gastric antrum and corpus in all cases where paired samples were available (14/14). Data on the expression of *dupA* transcript were not available. There was a weak association between *dupA1* and *vacA* s1m1i1 type but no association between *dupA1* and *cag*PAI.

Next, we report gastrointestinal disease outcomes, principally peptic ulceration and functional dyspepsia, in our study population according to *dupA* status.

Note that the candidate joined the Nottingham research group full-time in January 2011, towards the end of the timeframe during which patients were recruited to this study (participants were recruited between 2002 and June 2012). Therefore, colleagues had previously completed much of the patient recruitment, collection and processing of endoscopic and blood samples, analysis of urease tests, culture of clinical isolates and research serology assays. However, the candidate contributed to this during the final 18 months of the study period, with extensive involvement in the careful phenotypic characterisation of the population for demographics and disease outcome, and thorough determination of *H. pylori* status including most of the histological analysis with Dr Abed Zaitoun. He identified the study population eligible for this project. The work to culture and prepare genomic DNA from the relevant clinical isolates was shared together with two colleagues, Miss Nicki Croxall and Mrs Jo Rhead. Comparison and selection of *dupA* genotypic methods, and all the resulting PCRs were completed by the candidate. He undertook bioinformatic analyses of published gene and genome sequences, including identifying the existance of long-type *dupA*, and designing and assessing the quality of templates, primers and optimising PCRs. Typing of *tfs4*, *cag*PAI and *vacA* was mainly undertaken by others in the research group (see Section 2.8.2). The candidate prepared all samples for *dupA* sequencing, assembled these and made alignments, and determined *dupA* status. All the analysis, the systematic review and the meta-analysis were conceived, planned and carried out by the candidate.

3.3 Clinical outcomes in Nottingham study

3.3.1 By *dupA* status

Study participants infected by *H. pylori* strains for which *dupA* typing were data available were categorised according to their endoscopic diagnosis (n=52). Clinical outcomes were duodenal ulcer disease in 20 (DU, 38%), gastric ulcer disease in 4 (GU, 8%) and functional dyspepsia in 28 (FD, 54%). These are reported in Table 3.3. Clinical outcomes were also recorded for *H. pylori*-negative participants with no known history of prior eradication therapy (n=120).

There were no significant associations between *dupA* status and clinical outcome.

No statistically significant associations were found. For our strain collection, *dupA1* strains were actually less frequently associated with DU than with FD (7/20 [35%] vs. 15/28 [54%], $P = 0.249$), with OR 0.47 (95% CI 0.14-1.58). The proportion of *dupA1* strains was similar between GU and FD (2/4 [50%] vs. 15/28 [54%], $P = 1.000$), with OR 0.87 (95% CI 0.12-6.19).

We have previously described the link between *dupA* and an associated cluster of genes in *tfs4*. The functional relationship between *dupA* types and *tfs4* has not been established, though an association between clinical outcomes according to the completeness of *dupA* and the *tfs4* cluster have been demonstrated by Jung et al. (2012), though not by Alam et al (2015). Therefore, this was investigated next.

Table 3.3 – clinical outcomes and risk factors by *dupA* status

***dupA* status**	**Clinical outcome**	**%**	**n**	**female (%)**	**mean age ± sd (years)**	**smoker (%)**			
						?	**yes**	**ex**	**no**
Overall	**DU**	21	36	42	53 ± 13.4	17	28	11	44
	GU	4	7	100	63 ± 12.4	29	29		43
	FD	75	129	55	52 ± 15.4	12	17	13	58
	Total		172	54	53 ± 15.0	13.4	20	12	54.7
***Hp* positive with *dupA* status data**	**DU**	38	20	40	53 ± 15.2	15	35	10	40
	GU	8	4	100	67 ± 2.2	25	25		50
	FD	54	28	61	52 ± 15.0	7	25	14	54
	Total		52	56	53 ± 14.9	12	29	12	48
dupA1	**DU**	29	7	43	58 ± 9.8			29	71
	GU	8	2	0	67 ± 3.5		50		50
	FD	63	15	33	52 ± 16.0	13	13	20	53
	Total		24	33	55 ± 14.3	8	13	21	58
non-*dupA1*	**DU**	46	13	69	50 ± 17.0	23	54		23
	GU	7	2	0	68 ± 0.7	50			50
	FD	46	13	46	53 ± 14.2		38	8	54
	Total		28	54	52 ± 15.5	14	43	4	39
dupA2	**DU**	56	5	60	50 ± 22.2	60	40		
	GU	11	1	0	68				100
	FD	33	3	33	46 ± 3.2		33		67
	Total		9	44	51 ± 17.2	33	33		33
dupAx	**FD**	100	1	100	46		100		
dup negative	**DU**	44	8	75	50 ± 14.7		63		38
	GU	6	1	0	67	100			
	FD	50	9	44	56 ± 16.5		33	11	56
	Total		18	56	54 ± 15.4	6	44	6	44
***Hp* negative no prior eradication**	**DU**	13	16	44	53 ± 11.3	19	19	13	50
	GU	3	3	100	58 ± 19.7	33	33		33
	FD	84	101	53	52 ± 15.6	13	15	13	59
	Total		120	53	52 ± 15.1	14	16	12.5	57.5

DU, duodenal ulcer; ex, ex-smoker; FD, functional dyspepsia; GU, gastric ulcer; *Hp*, *H. pylori*; ?, unknown; grey box, 0%; to one decimal place only if needed for clarity.

3.3.2 By *tfs4* status

Genotyping data by PCR were available for *virB8*, *virB9*, *virD4* and *virD2* (see Section 1.3.4). Other authors have described these genes together with *virB10* and *virB11* as the *dupA* cluster, with the presence of all 6 genes required to label this cluster as intact (Jung et al. 2012; Alam et al. 2015; Wang, Shao et al. 2015). Data were not available for *virB10* or *virB11*, so an equivalent analysis to these studies was not possible, nor for *virB2* (see Section 1.3.5 for a description and illustration of predicted functions of putative *tfs4* components).

No biological function has yet been reported for 5/6 genes previously used to define an intact *dupA* cluster, with only VirD2 shown to have the characteristics of a relaxase (Grove et al. 2013). Moreover, the essential components of *tfs4* have yet to be defined, functional redudency by elements of other *H. pylori* secretion systems may or may not be possible, and it is not yet establihsed if any of these genes are subject to the same allelic variation as *dupA* (with putative functional and non-functional isoforms). So any attempt to classify *tfs4* as complete or incomplete (or the *dupA* cluster as intact) must be considered to be arbitrary. Strains were classified as *dupA1*/*tfs4* complete if they possessed *dupA1* and all 4 of these putative *virB* and *virD* genes. Results are shown in Table 3.4.

There was evidence that the *tfs4* cluster was genetically complete in a quarter of *dupA1* strains. Overall 10% of strains were *dupA1*/*tfs4* complete in this cohort. These were not shown to be associated with disease outcome.

Twenty-four percent of *dupA1* strains possessed all 4 *tfs4* genes (5/21 with complete data). Overall, 10% of strains were *dupA1*/*tfs4* complete (5/49). Three *dupA1* strains were missing complete *tfs4* typing data. Other results were variable, though most non-*dupA1* strains were missing at least one *tfs4* gene (70%, 14/20 with complete data).

Two of the *dupA1*/*tfs4* complete strains were *cag*PAI-positive (*vacA* s1m1i1 and s1m2i1) and three were *cag*PAI-negative (two *vacA* s1m2i2 and one s2m2i2).

Duodenal ulceration was not significantly associated with infection by *dupA1*/*tfs4* complete strains in this cohort (2/20 [10%] vs. 3/25 [12%] with FD, OR 0.82 [95% CI 0.13-4.36], note was 0/4 [0%] with GU). There was no relationship found with *cag*PAI or *vacA* status, though numbers were limited.

Table 3.4 – description of *dupA* and *tfs4* status of clinical isolates

***tfs4* status**	***dupA***	**n**	***virB8***	***virB9***	***virD4***	***virD2***	**n**		
complete	*dupA1*	21 (*dupA1*)	+	+	+	+	5		
incomplete	*dupA1*		+	+	–	+	1	16	44
			–	–	+	+	4		
			+	–	–	–	1		
			–	+	–	–	1		
			–	–	–	+	1		
			–	–	–	–	1		
			incomplete but at least one negative				7		
	dupAx	28 (non-*dupA1*)	incomplete but at least one negative				1	1	
	dupA2		+	+	+	+	5	9	
			+	–	+	+	1		
			–	–	+	+	1		
			incomplete data				2		
	dupA negative		+	+	+	+	1	18	
			+	–	+	+	1		
			–	+	+	+	1		
			+	+	–	–	1		
			+	–	–	+	1		
			–	–	+	+	2		
			–	–	–	+	4		
			–	–	–	–	2		
			incomplete data				5		

Strains were arbitrarily classified as *dupA1*/*tfs4* complete if they possessed *dupA1* and the 4 putative *virB* and *virD* genes with genotyping data available for this study (*virB8*, *virB9*, *virD4* and *virD2*). These data were kindly provided by Dr Rob Delahay.

There were also 3 *dupA1* strains with incomplete *tfs4* data that could not be classified.

3.3.3 By *H. pylori* infection and other virulence factors

Having found no associations for either *dupA* or *tfs4*, we next assessed whether there were any associations with disease for our study participants overall.

Though other groups had also been unable to establish a link between *dupA* (and *tfs4*) and disease in certain populations, we next wanted to establish that infection with *H. pylori* was associated with clinical outcomes in our study population overall (n=275). The role of *cag*PAI and *vacA* in this population were also studied.

Participants in the study population were categorised according to endoscopic findings into clinical outcome groups – duodenal ulcer disease (DU, n=75 [27%]), gastric ulcer disease (GU, n=12 [4%]), gastric cancer (GC, n=2 both intestinal-type distal gastric adenocarcinoma [1%]) or functional dyspepsia (FD, n=186 [68%]). Results are shown in Table 3.5. Participants negative for *H. pylori* infection but with a prior history of

eradication therapy were excluded (7/127 [6%]); they mostly had duodenal ulceration (4/7 [57%]). We did not exclude *H. pylori*-positive participants with a history of failed eradication therapy (41/148 [28%]).

Infection with *H. pylori* was strongly associated with duodenal ulceration in our study population vs. functional dyspepsia. Other outcomes were less frequent.

As expected, *H. pylori* infection was strongly associated with DU (55/71 [77%] vs. 82/183 [45%] with FD, $P < 0.001$), with odds ratio 4.23 (95% CI 2.30-8.05). The association with GU fell short of statistical significance (9/12 [75%] vs. FD, $P = 0.070$), with odds ratio 3.70 (95% CI 0.96-12.94). There was no difference in *H. pylori* prevalence between participants with DU and GU. There were too few cases of gastric cancer in this cohort for meaningful inferences.

Next, the impact of other virulence factors on clinical outcomes in our study population was evaluated. The results for the *cag* pathogenicity island are shown in Table 3.6 and the results for *vacA* type are shown in Table 3.7.

All *cag*PAI and *vacA* types were represented in our study population. No associations with clinical outcomes were identified.

Strains were classified as *cag*PAI-positive in 64% of cases. No association with disease was shown (DU 32/48 [67%], GU 6/7 [86%], GC 1/2 [50%], FD 37/61 [61%], total 118 strains as there were no data for 21 strains and equivocal data for 9 strains).

Typing data for the *vacA* s, m and i regions were available for 127/148 participants. Ten further cases were excluded – 2 with incomplete typing data, 2 with mixed i type, 1 with mixed m type, and 5 participants where strains of different *vacA* types were isolated from the gastric antrum and corpus (2 cases with s1m1i1 and s1m1i2, 2 cases with s1m2i1 and s1m2i2, and 1 case with s1m1i1 and s1m2i1). For the remaining 117 strains, 48% were s1m1i1, 20% were s1m2i1, 19% were s1m2i2 and 10% were s2m2i2. There was one case of each of the other 4 *vacA* types. Overall, 87% of strains were s1 vs. s2, 50% were m1 vs. m2 and 69% were i1 vs. i2. There were no disease associations found for *vacA* type, though there was a trend towards an association for the i region type for gastrointestinal disease (peptic ulceration or carcinoma) against FD (45/59 [76%] vs. 36/58 [62%] with i1, $P = 0.112$, OR 1.96 [95% CI 0.87-4.36]).

Table 3.5 – clinical outcomes and risk factors for the study population overall

Participant group	Clinical outcome	%	n	female (%)	mean age ± sd (years)	smoker (%)			
						?	yes	ex	no
Overall	DU	27	75	47	54 ± 13.9	37	23	8	32
	GU	4	12	92	63 ± 11.2	42	17	17	25
	GC	1	2	0	57 ± 19.1	50	50		
	FD	68	186	58.6	53 ± 15.2	22	14	13	51
	Total		275	56.4	54 ± 14.8	27.3	16.7	11.6	44.4
***Hp* positive (all patients)**	DU	37	55	45	54 ± 14.9	44	22	5	29
	GU	6	9	89	64 ± 7.9	44	11	22	22
	GC	1	2	0	57 ± 19.1	50	50		
	FD	55	82	65	54 ± 14.8	33	12	13	41
	Total		148	58	55 ± 14.6	38	16	11	35
Hp positive with culture available	DU	41	49	45	55 ± 15.2	43	18	6	33
	GU	6	7	86	64 ± 8.8	57	14		29
	GC	2	2	0	57 ± 19.1	50	50		
	FD	52	62	61	54 ± 15.2	40	13	11	35
	Total		120	55	55 ± 15.0	42.5	16	8	33
Hp positive with *dupA* status data	DU	38	20	40	53 ± 15.2	15	35	10	40
	GU	8	4	100	67 ± 2.2	25	25		50
	FD	54	28	61	52 ± 15.0	7	25	14	54
	Total		52	56	53 ± 14.9	12	29	12	48
Hp negative (all patients)	DU	16	20	50	55 ± 10.9	20	25	15	40
	GU	2	3	100	58 ± 19.7	33	33		33
	FD	82	104	54	52 ± 15.5	13	15	12.5	59
	Total		127	54	52 ± 14.9	15	17	12.6	55
***Hp* negative no prior eradication**	DU	13	16	44	53 ± 11.3	19	19	13	50
	GU	3	3	100	58 ± 19.7	33	33		33
	FD	84	101	53	52 ± 15.6	13	15	13	59
	Total		120	53	52 ± 15.1	14	16	12.5	57.5
Hp negative with prior eradication	DU	57	4	75	60 ± 8.6	25	50	25	
	FD	43	3	67	42 ± 2.3	33	33		33
	Total		7	71	52 ± 11.1	29	43	14	14

DU, duodenal ulcer; ex, ex-smoker; FD, functional dyspepsia; GC, gastric cancer; GU, gastric ulcer; *Hp*, *H. pylori*; ?, unknown status; grey box, 0%; to one decimal place only if needed for clarity.

Table 3.6 – clinical outcomes and risk factors by *cag* pathogenicity island status

*cag*PAI status	Clinical outcome	%	n	female (%)	mean age ± sd (years)	smoker (%)			
						?	yes	ex	no
present and intact	DU	42	32	41	56 ± 15.2	44	19	6	31
	GU	8	6	83	68 ± 1.9	33	17	17	33
	GC	1	1	0	43		100		
	FD	49	37	51	56 ± 15.0	35	14	14	38
	Total		76	49	57 ± 14.7	38	17	11	34
absent or truncated	DU	38	16	44	52 ± 14.1	38	25	6	31
	GU	2	1	100	70	100			
	GC	2	1	0	70	100			
	FD	57	24	71	53 ± 15.1	50	13	8	29
	Total		42	60	54 ± 14.7	48	17	7	29

DU, duodenal ulcer; ex, ex-smoker; FD, functional dyspepsia; GC, gastric cancer; GU, gastric ulcer; ?, unknown status; grey box, 0%.

Table 3.7 – clinical outcomes and risk factors by *vacA* type

vacA type			Clinical outcome	%	n	female (%)	mean age ± sd (years)	smoker (%)			
s	m	i						?	yes	ex	no
1	1	1	DU	39	22	45	55 ± 16.1	55	9	9	27
			GU	11	6	100	68 ± 2.1	33	17	17	33
			GC	2	1	0	43		100		
			FD	48	27	48	54 ± 17.4	41	15	15	30
			Total		56	52	56 ± 16.2	45	14	13	29
		2	FD	100	1	0	67	100			
	2	1	DU	61	14	57	53 ± 15.2	50	29		21
			GC	4	1	0	70	100			
			FD	35	8	63	59 ± 11.4			13	88
			Total		23	57	56 ± 14.0	35	17	4	43
		2	DU	36	8	75	55 ± 9.3	25	13		63
			GU	5	1	0	68	100			
			FD	59	13	69	55 ± 11.3	31	8	15	46
			Total		22	68	56 ± 10.4	32	9	9	50
2	1	1	FD	100	1	0	63	100			
		2	DU	100	1	0	51		100		
	2	1	DU	100	1	0	56			100	
		2	DU	33	4	0	55 ± 27.0		75		25
			FD	67	8	75	50 ± 16.7	50	25		25
			Total		12	50	51 ± 19.5	33	42		25

DU, duodenal ulcer; ex, ex-smoker; FD, functional dyspepsia; GC, gastric cancer; GU, gastric ulcer; ?, unknown status; grey box, 0%.

3.3.4 Confounding and disease risk factors

In addition to *H. pylori* infection, the most important risk factors for PUD are patient age, smoking and a past history of peptic ulceration (Ingram et al. 2015).

We had planned to adjust for *a priori* and potential confounders using multiple logistic regression, but this was unnecessary given the non-significant univariate findings. So, an alternative approach was adopted *ad hoc* to investigate any impact of potential confounders, accepting that there is potential bias in this analysis approach.

Firstly, although no relationship between other virulence factors and clinical outcomes had been shown in this study, there was a weak association between *dupA* and *vacA* type (Section 3.2.1). Therefore, to offset any confounding effect of other bacterial virulence factors, analysis was confined to *cag*PAI-positive *vacA* s1m1i1 strains.

There was again no significant association between *dupA* status and disease, after controlling for potential confounding by other bacterial virulence factors.

There were 13 such strains with *dupA1* (46% female, mean age 56 ± 13.5 years, 7/12 current or ex-smokers) and 8 strains without *dupA1* (38% female, 55 ± 19.7 years, 3/5 current or ex-smokers). For the former group, 4 of the infected participants had DU (31%), 2 had GU (15%) and 7 had FD (54%). For the latter group, these were 3 cases of DU (38%), 2 of GU (25%) and 3 of FD (38%). There was no association between *dupA1* and DU (4/11 [36%] vs. 3/6 [50%] with FD, OR 0.57 [95% CI 0.10-3.52]).

Next, the potential for confounding by disease risk factors in the host was assessed. We evaluated the impact in our study population of a previous diagnosis of peptic ulcer, sex and age, and smoking status. Data were not available to evaluate any role for other host factors, such as genetic polymorphisms, on the clinical outcome of PUD (Miftahussurur and Yamaoka 2015), although the role of host genetic factors is best described in GI malignancy (Macarthur et al. 2004; Hold and El-Omar 2008).

Past history of peptic ulcer disease was not relevant for our patient cohort.

In terms of past history, those participants known to have previously been diagnosed with a peptic ulcer were identified and in most cases had endoscopic findings at enrolment in keeping with duodenal or gastric ulcer disease. However, disease classification was based solely on the endoscopic diagnosis at recruitment. There were 3 cases with a suspected previous history of PUD who had an entirely normal

endoscopy. The first patient was a 52-year-old ex-smoker, negative for *H. pylori* by all tests at recruitment and had a peptic ulcer 3 years previously with no prior eradication therapy. The other two patients were undergoing endoscopy for failure of prior eradication therapy and were still infected based on successful *H. pylori* culture (and other tests), though one strain had no *cag*PAI or *vacA* data available and the *dupA* status was not known for either strain. Overall, a previous ulcer history was unlikely to play a significant role in our cohort and, therefore, was not considered in any analysis.

There was again no significant association between *dupA* status and disease, after controlling for potential confounding by sex and age by individual matching.

H. pylori-infected cases and controls were individually matched for sex and age (DU vs. FD). Matching was possible for 38/48 participants with typing data for *dupA* (8 females and 11 males for both cases and controls). The mean age was 55 ± 13.3 years for cases and 53 ± 15.5 years for controls, although these groups shared similar characteristics before matching (Table 3.5). No significant association between *dupA1* strains and DU was found (7/19 [37%] vs. 10/19 [53%], $P = 0.519$, OR 0.53 [95% CI 0.16-1.88]). Findings were similar after matching DU cases and controls across the whole *H. pylori*-positive cohort, with 102/137 matched (25 females and 26 males), though only 36 of the matched participants then had *dupA* type available (7/19 [37%] vs. 9/17 [53%], $P = 0.503$, OR 0.52 [95% CI 0.16-2.01]).

Smoking was more frequent in study participants with peptic ulceration but no significant association was shown.

Smoking is an important risk factor for PUD and continued smoking delays ulcer healing. In this study, smoking was classified as an ordinal variable from non-smoker, to ex-smoker, to current smoker. These data were reported as proportions in Table 3.5. Smoking status was unknown for 56/148 participants (38%), which were excluded for this analysis together with the one remaining individual with GC.

Therefore, the impact of smoking status on PUD vs. FD was determined using simple logistic regression (n=36 and n=55 respectively). Participants with PUD were 50% non-smokers, 14% ex-smokers and 36% current smokers. Among those with FD, 62% were non-smokers, 20% were ex-smokers and 18% were current smokers. Smoking status was not significantly related to disease ($P = 0.161$) and could not accurately predicted PUD (Nagelkerke $R^2 = 0.054$, sensitivity 82%, specificity 36%).

3.3.5 Summary

Overall, no relationships were found between *dupA* status (or that of *tfs4* and other virulence factors) and clinical outcomes. This was disappointing but not surprising, as various disease associations, or in most cases a lack thereof, have been reported for different populations from around the world.

Therefore, we sought to put our work on the influence of *dupA* status on clinical outcomes into context against the reports from other groups through systematic review and meta-analysis. This is presented in the next section.

3.4 Systematic review and meta-analysis

Following on from the initial description of *dupA* by Lu et al. (2005), other groups have studied associations between *dupA* status and disease in different populations. Two systemic reviews were reported (Hussein 2010; Shiota et al. 2010), the latter with meta-analysis, that between them included 11 studies through to August 2010.

To place the primary Nottingham study in the context of other work, an up-to-date systematic review and meta-analysis was performed. The rationale was to identify the latest evidence from a broader range of sources, and to extend previous work by assessing the risk of bias introduced by different approaches to *dupA* genotyping and by examining the extent to which confounders have been accounted for in analyses. Full details of the methods used are reported in Section 2.4. MEDLINE, PubMed, EMBASE and Web of Science databases were searched through to August 2016. The search strategy was "(*dupA* OR *dupA**) AND (*pylori* OR *Helicobacter*)". The searches were performed without any restriction on language, publication status or article type including abstracts. Additional searches of the Cochrane Library and ClinicalTrials.gov yielded no relevant results. The reference lists of the retrieved articles were screened to expand the search, which also yielded no further studies. Key conference proceedings were hand searched from 2005 to 2016, though these references had already been identified by the electronic database searches.

This systematic review identified 124 unique references. Seventy-one were excluded as follows: 27 were reviews rather than original data (including 3 non-English language), 12 reported only *in vitro* or *in silico* data rather than human data, 2 concerned animals (Mongolian gerbils and Bengal tiger), 5 did not report data on *dupA* status (including 1 non-English language), 9 were not designed as case-control studies, and 16 were abstracts that had subsequently been reported as a full article. Of the remaining 53 references, there were 15 reported as an abstract in conference proceedings, abstract only or in letter form, and 2 references where the abstract was available in English but the full article was written in Polish or in Chilean Spanish. There was marked variation in the level of detail in these abstracts and several instances where it was unclear if reported data had subsequently been included in full articles. Therefore, the decision was taken to exclude all these references from subsequent analysis.

Table 3.8 – summary table of *dupA* prevalence and clinical outcome associations worldwide

All study populations are for adults (age ≥18 years) except where specified. *dupA* status was defined by different criteria in different studies (see Table 3.11). *dupA1*, *intact dupA* and *intact transcribed dupA* are explained in the text (Section 3.4.2).

Statistically significant comparisons reported are highlighted in grey. Key to statistically significant associations of *dupA* with clinical outcomes, where $P < 0.05$ vs.:

[a] = DU, [b] = GU, [c] = GC, [d] = G, [e] = FD, [f] = no PUD, [g] = dysplasia, [h] = duodenitis, [j] = normal.

Key to study-specific notes:

[k] = *tfs4* with 4/4 genes (*virB8*, *virB9*, *virD4* and *virD2*), 3 isolates were *dupA1* with incomplete *tfs4* data.

[m] = reported for adjacent non-neoplastic tissue obtained from patients with GC, paired biopsies from the neoplastic tissue were also collected and 15/21 (71%) were *dupA*+.

[n] = *tfs4* with 6/6 genes (*virB8*, *virB9*, *virB10*, *virB11*, *virD4* and *virD2*).

[p] = reported 21/170 *dupA1*, 12/170 short-type intact *dupA* (1,884 bp) and 17/170 with frameshifts.

[q] = reported 180 clinical outcomes for 123 patients, with *dupA* prevalence for former 59/180 (32.8%).

[r] = reported *dupA* status data for the whole cohort (square brackets) but only histological outcomes were reported and the 2 adult patients with DU were excluded.

[s] = reported 354 colony isolates (plus 47 isolates missing *dupA* status data) for 240 patients.

[t] = included only *H. pylori*-infected patients with *jhp0917*$^{+}$/*jhp0918*$^{+}$ strains, then reported strains with some evidence of an intact *dupA* from partial sequencing in all strains.

[u] = recruited 232 patients but excluded 16 with negative culture and 14 with non-concordant genotyping.

[v] = recruited 244 patients but excluded 5 *cag* negative and 6 *jhp0917*$^{+}$/*jhp0918*$^{-}$ strains. Shiota et al. 2012 reports a subset of 142 patients (excludes 102 with prior eradication therapy) from Nguyen et al. 2010.

[w] = patients recruited and *dupA* genotyping performed at time of diagnosis of PUD, with follow-up for primary end-point of GC development showed *dupA*+ strains were associated with a lower risk of GC.

[x] = recruited 79 patients but excluded 14 with evidence of mixed infection and did not report *dupA* status for 5 patients (those with GU or GC).

[y] = additional data reported in Schmidt et al. (2010) for control groups of Malay and Indian ethnicity that extend the original dataset (Schmidt et al. 2009). The originally reported data for the Chinese ethnicity group were used, though the latter study reported *dupA* prevalence as 10/22 for DU, 13/22 for GC (+1), and 17/52 for FD (+2).

[z] = data for study collected as referenced but re-analysed with *dupA* genotyping data and reported in Lu et al. (2005), all isolates were *cag*+ and gastritis control group were age- and sex-matched.

DU, duodenal ulcer; DU and GU, patients found to have both types of peptic ulcer disease at endoscopy; FD, functional dyspepsia with unknown histology; G, gastritis; GC, gastric cancer; GU, gastric ulcer; *Hp*, *H. pylori*; no PUD, patients without peptic ulcer disease but gastric histology not reported; normal, functional dyspepsia without gastritis; USA, United States of American; ?, data collected but not reported; -, data not reported; † = included in previous systematic review (Hussein 2010), ‡ = included in previous meta-analysis (Shiota et al. 2010), * = included in this meta-analysis (for Rasheed et al. 2014 only GC and control were included).

Table 3.8 – summary table of *dupA* prevalence and clinical outcome associations worldwide

Country (Reference)		**Number of *Hp*+ patients**	**% with *dupA***	***dupA* prevalence by clinical outcome**					
				DU	**GU**	**GC**	**G**	**FD**	**Other**
United Kingdom[k]* (this study)		52	*dupA1* 46.2%	7/20 (35%)	2/4 (50%)	-	-	15/28 (54%)	-
		49	*tfs4*/*dupA1* 10.2%	2/20 (10%)	0/4 (0%)	-	-	3/25 (12%)	-
Brazil[m]* (Ferraz et al. 2016)		73	65.8%	-	-	22/23 (96%)[d,j]	25/47 (53%)[c]	Normal: 1/3 (33%)[c]	-
Iran (Ghalehnoei et al. 2016)		30	63.3%	Ulcer (DU or GU): 9/12 (75%)		-	10/18 (56%)	-	-
India[n,p]* (Alam et al. 2015)		170	29.4%	38/98 (39%)[e]	-	-	-	12/72 (17%)[a]	-
			dupA1 12.3%	15/98 (15%)	-	-	-	6/72 (8%)	-
			tfs4/intact *dupA* 9.4%	10/98 (10%)	-	-	-	6/72 (8%)	
Indonesia* (Miftahussurur et al. 2015)		44	6.8%	0/1 (0%)	0/5 (0%)	-	3/38 (8%)	-	-
			dupA1 0.0%	0/1 (0%)	0/5 (0%)	-	0/38 (0%)	-	-
Iran* (Haddadi et al. 2015)		128	35.9%	18/31 (58%)[e]	11/33 (33%)	5/14 (36%)	-	12/50 (24%)[a]	-
Iran[q]* (Souod et al. 2015)		123	33.3% [41/123]	13/33 (39%)	7/18 (39%)	0/3 (0%)	37/120 (31%)	-	Duodenitis: 2/6 (33%)
Iraq* (Hussein et al. 2015)		74	23.0%	?/19	?/10	-	-	?/45	-
			dupA1 16.2%	7/19 (37%)[e]	1/10 (10%)	-	-	4/45 (9%)[a]	-
Malaysia* (Osman et al. 2015)		Chinese[k] 26	23.1%	2/5 (40%)	1/9 (11%)	-	18/78 (23%)	Normal: 3/13 (23%)	note:22.9% with *dupA* overall
		Malay[k] 42	21.4%						
		Indian[k] 37	24.3%						
Turkey (Oktem-Okullu et al. 2015)		80	6.3%	Ulcer (DU or GU): 0/18 (0%)		-	5/62 (8%)	-	-
Brazil[r] (Pereira et al. 2014)	children	69 [100]	40.6% [37.0%]	-	-	-	26/58 (45%)	Normal: 2/11 (18%)	*note*: 44.0% [41.5%] with *dupA* overall
	adults	97 [105]	46.4% [45.7%]	-	-	-	44/95 (46%)	Normal: 1/2 (50%)	
Pakistan* (Rasheed et al. 2014)		46	71.7%	Ulcer (DU or GU): 7/8 (88%)		3/4 (75%)	23/34 (68%)	-	-

Table 3.8 – summary table of *dupA* prevalence and clinical outcome associations worldwide (cont.)

Country (Reference)	Number of *Hp+* patients	% with *dupA*	*dupA* prevalence by clinical outcome					
			DU	GU	GC	G	FD	Other
South Korea[s]* (Kim et al. 2014)	240 [354]	? [48.0%]	74/99 (75%)[c,e,g]	52/64 (81%)[c.e.g]	22/95 (23%)[a,b]	-	12/72 (17%)[a,b,g]	Dysplasia: 10/24 (42%)[a,b,e]
China* (Wang et al. 2013)	116	31.0%	11/26 (42%)	10/25 (25%)	4/11 (36%)	11/54 (20%)	-	-
Iraq* (Salih et al. 2013)	154	18.8%	11/45 (24%)	4/23 (17%)	-	-	-	No PUD: 14/86 (16%)
Japan* (Takahashi et al. 2013)	319	32.9%	32/114 (28%)[b]	45/95 (47%)[a,d]	9/22 (41%)	19/88 (22%)[b]	-	-
		dupA1 24.5%	25/114 (22%)[b]	33/95 (35%)[a,d]	8/22 (36%)[d]	12/88 (14%)[b,c]	-	-
Brazil[t]* (Moura et al. 2012)	75	100.0%[t]	29/29 (100%)	-	20/20 (100%)	26/26 (100%)	-	-
		intact *dupA* 54.7%	19/29 (66%)	-	10/20 (50%)	12/26 (46%)	-	-
India* (Alam et al. 2012)	140	27.1%	31/83 (37%)[e]	-	-	-	7/57 (12%)[a]	-
		transcribed intact *dupA* 20.0%	23/83 (28%)[e]	-	-	-	5/57 (9%)[a]	-
Iran[u]* (Abadi et al. 2012)	202[u]	41.6%	56/65 (86%)[b,c,d]	12/59 (20%)[a]	4/32 (13%)[a]	12/46 (26%)[a]	-	-
Japan* (Matsuda et al. 2012)	248	*dupA1* 23.0%	12/46 (26%)	7/38 (18%)	20/65 (31%)	18/99 (18%)	-	-
USA[n]* (Jung et al. 2012)	245	69.4%	45/61 (74%)	23/33 (70%)	19/27 (70%)	83/124 (67%)		-
		tfs4/*dupA* 47.3%	37/61 (61%)[d]	15/33 (45%)	13/27 (48%)	51/124 (41%)[a]	-	-
Brazil[t]* (Queiroz, Rocha et al. 2011)	252	100.0%[t]	77/77 (100%)	-	58/58 (100%)	117/117 (100%)	-	-
		intact *dupA* 69.8%	62/77 (83%)[c]	-	28/58 (49%)[a,d]	86/117 (75%)[c]	-	-
Japan[v]†‡* (Nguyen et al. 2010; Shiota et al. 2012)	233	28.8%	17/62 (27%)	17/59 (29%)	10/34 (29%)	23/78 (30%)	-	-
Japan[w] (Imagawa et al. 2010)	56	32.1%	9/20 (45%)	9/36 (25%)	-	-	-	-
Taiwan‡* (Yeh et al. 2010)	181	23.8%	13/57 (23%)	6/30 (20%)	-	24/94 (26%)	-	-
Turkey[x]* (Tuncel et al. 2010)	60[x]	25.0%	7/23 (30%)	?/3	?/2	8/37 (21%)	-	-
Australia† (Schmidt et al. 2009)	45	37.8%	-	-	-	-	17/45	-

Table 3.8 – summary table of *dupA* prevalence and clinical outcome associations worldwide (cont.)

Country (Reference)		Number of *Hp*+ patients	% with *dupA*	*dupA* prevalence by clinical outcome					
				DU	GU	GC	G	FD	Other
Malaysia/Singapore[y]†‡* (Schmidt et al. 2009; Schmidt et al. 2010)		Chinese 90	41.1%	10/16 (63%)[e]	-	12/22 (55%)[e]	-	15/52 (29%)[a]	note: 31.4% with *dupA* overall, and control 28/121 (23%)[a,c]
		Malay 20	30.0%	-	-	-	-	6/20[y]	
		Indian 49	14.3%	-	-	-	-	7/49[y]	
Sweden†‡* (Schmidt et al. 2009)		52	63.5%	7/11 (64%)	-	13/21 (62%)	-	13/20 (65%)	-
Brazil (Gomes et al. 2008)	children*	131	100.0%	34/34 (100%)	-	-	97/97 (100%)	-	*note*: 92.3% with *dupA* overall
	adults†‡*	351	89.5%	110/126 (87%)	-	71/81 (88%)	133/144 (92%)	-	
Brazil†‡* (Pacheco et al. 2008)		79	62.0%	13/20 (65%)	14/24 (58%)	-	18/29 (62%)	Normal: 4/6 (67%)	-
China†‡* (Zhang et al. 2008)		360	35.3%	46/101 (46%)[b,c]	11/47 (23%)[a]	19/79 (24%)[a,d]	51/133 (38%)	-	-
Iran†‡* (Douraghi et al. 2008)		157	49.7%	15/30 (50%)	9/23 (39%)	20/36 (56%)	34/68 (50%)	-	-
Iran (Hussein et al. 2008)		59	39.0%	Ulcer (DU or GU): 6/17 (35%)		-	-	-	No PUD: 17/42 (40%)
Iraq†‡* (Hussein et al. 2008)		49	12.2%	9/15 (60%)[f]	2/5 (40%)	-	-	-	No PUD: 5/29 (17%)[a]
Belgium†‡* (Argent et al. 2007)		135	43.7%	20/40 (50%)	-	10/19 (53%)	29/76 (38%)	-	-
China†‡* (Argent et al. 2007)		31	32.3%	2/11 (18%)	2/5 (40%)	1/1 (100%)	3/12 (25%)	-	DU and GU: 2/2 (100%)
India†‡* (Arachchi et al. 2007)		166	44.8%	36/96 (38%)[e]	-	-	-	16/70 (23%)[a]	-
South Africa†‡* (Argent et al. 2007)		46	84.8%	12/13 (92%)	-	16/18 (89%)	11/15 (73%)	-	-
USA†‡* (Argent et al. 2007)		46	43.5%	9/21 (43%)	2/3 (67%)	-	9/20 (45%)	-	DU and GU: 0/2 (0%)
Columbia†‡* (Lu et al. 2005)		165	35.2%	22/45 (49%)[c]	12/30 (40%)[c]	6/50 (12%)[a,b,d]	15/40 (38%)[c]	-	-
South Korea†‡* (Lu et al. 2005)		175	19.4%	24/65 (37%)[c,d]	5/30 (17%)	3/50 (6%)[a]	2/30 (7%)[a]	-	-
Japan†‡* (Lu et al. 2005)		160	21.3%	11/30 (37%)[c,d]	13/50 (26%)	3/30 (10%)[a]	7/50 (14%)[a]	-	-
Japan[z]†‡* (Yamaoka et al. 1999)		98	30.6%	23/50 (46%)[d]	-	-	7/48 (15%)[a]	-	-

3.4.1 Study populations

Thirty-six studies were included in the systematic review with 45 independent study populations reported. Together these studies included 6,106 patients/isolates. Some authors did not report independent case-control data for all study populations.

In total 36 studies were reviewed, covering 45 populations from around the world. Data are summarised in Table 3.8, which details the proportion of isolates reported to possess the *dupA* gene and clinical outcomes by *dupA* status.

Overall, 4,125 patients/isolates were recruited from 11 countries with East Asian strains of *H. pylori* (China, India, Indonesia, Iran, Iraq, Japan, Malaysia, Pakistan, Singapore, South Korea and Taiwan), and 1,981 patients/isolates from 8 countries where Western strains are typically more prevalent (Australia, Belgium, Brazil, Columbia, South Africa, Sweden, Turkey and the United States of America). Only patients/isolates associated with DU, GU, GC or control were included. Six patients with duodenitis (Souod et al. 2015), 24 patients with gastric dysplasia (Kim et al. 2014) and 4 patients with both DU and GU (Argent et al. 2007) were excluded from the analysis.

For one pair of studies, the original data set was extended by 13 control patients in the later publication (Schmidt et al. 2009; Schmidt et al. 2010). They were considered to be a single study and the extended dataset was used. Similarly, Shiota et al. (2012) reported antibiotic resistance data for a subset of Japanese patients for whom clinical outcomes by *dupA* status had previously been reported (Nguyen et al. 2010). They were also considered to be a single study and the data from the original study were used.

Four studies reported combined results for peptic ulcer disease (Iranian population in Hussein et al. 2008; Rasheed et al. 2014; Oktem-Okullu et al. 2015; Ghalehnoei et al. 2016), so only the GC and control data from Rasheed et al. could be used for meta-analysis. Therefore, no patients could be included from two of these studies (Oktem-Okullu et al. 2015; Ghalehnoei et al. 206). Similarly, Imagawa et al. (2010) did not report control data, so could not be included. Pereira et al. (2014) only reported control groups with gastritis and normal gastric histology, so the study could not be included for 2 study populations of adults and children. Although Schmidt et al (2009) also reported *dupA* results for Australia, data were only case-control from the Swedish and

Malaysian/Singaporean study populations (Schmidt et al. 2009; Schmidt et al. 2010). Therefore, these Australian study population data could not be used for meta-analysis.

Therefore, we excluded 6 studies and 7 study populations from subsequent analysis by in effect excluding one each from 2 paired studies, excluding 4 studies without case-control data (5 study populations), and excluding 2 study populations (Hussein et al. 2008; Schmidt et al. 2009).

Data for 5,769 patients/isolates from 19 countries were used for subsequent analysis. These represent data from 31 studies including this study, comprising 39 independent study populations including our study population from Nottingham.

This study from Nottingham was the first to include patients from the United Kingdom. Overall, 4,009 patients/isolates were recruited from 11 Asian and Middle Eastern countries and 1,760 patients/isolates from 8 Western and South American countries.

Note that two studies did not report one clinical outcome per patient. Kim et al. (2014) included 240 patients for each of whom 1 or 2 single colony isolates were obtained (mean 1.67 and total 401 isolates, *dupA* status data were missing for 47 isolates). Up to 8 colonies were isolated per patient, from which one was selected for the antrum and/or one for the corpus. Fifty-seven patients (24%) were identified as being colonised by non-identical strains (*cagA*, *vacA* genotypes, *dupA*, *iceA* genotypes and *oipA* virulence factors were studied). Clinical outcome data are presented for 354 colony isolates and patient-level data were not reported. Souod et al. (2015) included 41/123 patients colonised by *dupA*+ strains, however, they reported that '*63% of patients had several diseases together*' so that 180 clinical outcomes were reported. Both studies were included in the meta-analysis.

One study from Brazil recruited children as well as adults (Gomes et al. 2008). All age groups were included in subsequent analysis, though with data for children and for adults entered as two study populations.

Several studies included results for multiple ethnicities or different ethnic groups within the same country or region (for example, Schmidt et al. 2009; Miftahussurur et al. 2015; Osman et al. 2015), but in all but one study clinical outcomes were only reported overall at country level. Schmidt et al. (2010) reported data for the same study cohort from 2009, though this later article included an additional 7 patients of Indian ethnicity and an additional 6 patients of Malay ethnicity (only control group data were reported for

these ethnicities, with the same case-control data reported for the Chinese ethnic group in both studies). In subsequent analysis, data for the three ethnic groups reported from Malaysia/Singapore combined in the studies by Schmidt et al. were combined and entered as one independent study populations.

Four studies included more than one study population as data were reported for more than one country (four in Lu et al. 2015 including a second Japanese population from Yamaoka et al. 1999, four in Argent et al. 2007, two in Hussein et al. 2008 though one was excluded as above, and three in Schmidt et al. 2009 and 2010 though one was excluded as above). Data for each country were entered as independent study populations for meta-analysis, which contributed an additional 7 study populations relative to the number of studies.

3.4.2 Prevalence of *dupA*-positive strains

The reported prevalence of *dupA* varied from 6.8% in Indonesia to 100.0% in Brazilian children (and 92.3% across both adults and children). However, there was marked variation between studies in the genotyping methods used to determine *dupA* status. This is discussed further in Section 3.4.5.

Some studies did account for frameshift nonsense mutations in *dupA* and these results are reported as intact *dupA* in Table 1.1Table 3.8. Indeed, two studies included only patients colonised by *H. pylori* strains that were positive by PCR for *jhp0917* and *jhp0918* (Queiroz, Rocha et al. 2011; Moura et al. 2012). Many studies would have classified all of these strains as *dupA*+. However, in 110/327 (33%) the gene was disrupted by indels such that it would not be transcribed. Alam et al. (2012) studied *dupA* transcription by RT-PCR and reported clinical outcomes accordingly (transcribed intact *dupA* in Table 3.8). They identified 38 strains as *jhp0917*+/*jhp0918*+ by PCR and dot-blot, 3 of which were found to contain nonsense mutations by partial sequencing, with evidence of *dupA* transcription in 28/35 strains. Four studies determined which strains possessed the long-type *dupA* gene of 2,499 bp vs. truncated alleles (Alam et al. 2015; Miftahussurur et al. 2015; Hussein et al. 2015; Takahashi et al. 2013). The clinical outcomes and *dupA* prevalence reported as *dupA1* in Table 3.8 refer to strains with an intact long-type *dupA* gene

Where findings were reported according to different potential classifications of *dupA* status (for example, intact *dupA* or *dupA1*), the clinical outcomes based on the most

comprehensive determination of *dupA* status, and so that least likely to be biased, are reported below and were used in further analysis.

Around 41% of clinical isolates were reported to possess the *dupA* gene. The prevalence was higher in strains isolated from Western and South American countries, where two-thirds of strains were *dupA*+, than in Eastern and Middle Eastern countries, where the prevalence of *dupA* was 30%.

Overall, the prevalence was 41.1% (2371/5769). The prevalence was 29.9% (1197/4009) in Eastern and Middle Eastern countries and 66.7% (1174/1760) in Western and South American countries. However, 2 studies from Brazil excluded patients not colonised by *jhp0917*+/*jhp0918*+ strains and, as described above, reported the proportion of these strains with an intact *dupA* gene as 217/327 (Queiroz, Rocha et al. 2011; Moura et al. 2012). Excluding these studies had no relevant impact on overall or regional prevalence.

Clinical isolates were *dupA1* in around 21% of cases, which were identified as strains with an intact long-type *dupA* gene.

For 10 studies that reported data for intact *dupA*, transcribed intact *dupA* or *dupA1*, the prevalence was 31.7% (473/1490). Excluding the 2 Brazilian studies, this was 22.0% (256/1163). For 5 studies that reported data for *dupA1* (intact long-type *dupA*), the prevalence was 20.5% (135/659).

3.4.3 Clinical outcomes by *dupA* status

Data from the 39 independent study populations were used. The control groups were taken as reported in Table 3.8, as patients/isolates with functional dyspepsia, with non-ulcer dyspepsia, without peptic ulcer disease, with gastritis or without histological gastric inflammation. For 3 studies, the controls were patients with gastritis and with normal gastric histology (Pacheco et al. 2008; Osman et al. 2015; Ferraz et al. 2016).

Based on simple combined data, there was a significant positive association between *dupA* status and duodenal ulceration.

Overall, the prevalence of *dupA* for patients/isolates with DU was 48.9% (840/1718), for GU was 41.1% (319/776), for GC was 35.0% (266/761) and in controls was 37.6% (946/2514). Analyses of these data show that *dupA* is significantly associated with DU vs. control (OR 1.6, 95% CI 1.4-1.8, $P < 0.001$), with DU vs. GC (OR 1.8, 95% CI 1.5-

2.1, $P < 0.001$), and with DU vs. GU (OR 1.4, 95% CI 1.2-1.6, $P < 0.001$). However, GU vs. control fell short of significance (OR 1.2, 95% CI 1.0-1.4, $P = 0.084$) and no significant protection against malignancy was observed (OR 0.9 for GC vs. control, 95% CI 0.8-1.1, $P = 0.184$), though *dupA*+ strains were less frequent in GC vs. GU (OR 0.8, 95% CI 0.6-1.0, $P = 0.014$).

However, every study population did not include cases of DU, GU and GC. Thirty-seven study populations were reported with case-control data for DU (1718 cases, 2430 controls, total of 4148), 25 study populations for GU (776 cases, 1674 controls, total of 2450), and 23 study populations for GC (761 cases, 1523 controls, total of 2284). These populations were used in subsequent meta-analysis.

Given that all studies were case-control in their design, with dichotomous outcomes, findings for each study population are summarised using odds ratios (OR) as the outcome measure, rather than risk ratios or absolute measures such as risk differences.

Associations between *dupA* status and clinical outcomes were reported for 14/31 studies and 17/39 study populations.

Fourteen studies reported at least one association for 17 study populations, as shown in Table 3.9. Seventeen studies, comprising 22 study populations, do not report an association. Four further studies reported no association between ulcer (DU or GU) vs. control (Iranian population in Hussein et al. 2008; Rasheed et al. 2014; Oktem-Okullu et al. 2015; Ghalehnoei et al. 2016). Imagawa et al. (2010) did not report any control group, though did show that *dupA*+ strains were associated with a lower risk of developing GC during follow up.

Table 3.9 – summary table of reported associations between *dupA* status and clinical outcomes expressed as odds ratios

There was a positive association between DU vs. control and between DU vs. GC in every case where an association was found (n=12 and n=7 respectively, though see note 2). There were 1 negative and 2 positive associations reported between DU vs. GU. There were 2 negative and 3 positive associations reported between GC vs. control, and 2 negative associations reported between GC vs. GU.

Odds ratios were calculated using GraphPad Prism v7.01 with the Baptista-Pike method to compute 95% confidence intervals. Grey boxes denote disease groups included in a particular study (white boxes indicate where that clinical outcome was not studied). The control group used in individual studies is provided. Black boxes indicate where the comparison was not possible because the study included no patients in that disease group. *dupA1*, *intact dupA1* and *transcribed intact dupA1* are explained in Section 3.4.2.

[1] Kim et al. (2014) reports outcomes for 354 colony isolates, not for the 240 study patients.

[2] This result strictly fell just short of statistical significance as the full confidence interval was 0.99-3.99 ($P = 0.062$ by Fisher's exact test, $P = 0.045$ by Chi-square test)

DU, duodenal ulcer; FD, functional dyspepsia; GU, gastric ulcer; GC, gastric cancer; G, gastritis; no PUD, patients without peptic ulcer disease; ns, the comparison was made but was not statistically significant.

Country / Population Reference	**Odds ratios**					**Disease groups**			
	DU vs. control	DU vs. GU	DU vs. GC	GC vs. control	GC vs. GU	DU	GU	GC	control
Brazil Ferraz et al. 2016				19.4 (3.2-209)					G
India Alam et al. 2015	3.2 (1.5-6.6)								
Iran Haddadi et al. 2015	4.4 (1.7-10.7)	ns	ns	ns	ns				FD
Iraq – *dupA1* Hussein et al. 2015	6.0 (1.4-20.0)	ns							FD
South Korea Kim et al. 2014[1]	14.8 (6.9-32.6)	ns	9.8 (5.0-19.1)	ns	0.1 (0.0-0.2)				FD
Japan Takahashi et al. 2013	ns	0.4 (0.2-0.8)	ns	ns	ns				G
dupA1	ns	0.5 (0.3-1.0)	ns	3.6 (1.2-10.0)	ns				
India Alam et al. 2012	4.3 (1.7-10.8)								FD
transcribed intact *dupA*	4.0 (1.4-10.1)								
Iran Abadi et al. 2012	17.6 (6.7-46.0)	24.4 (9.7-61.8)	43.6 (11.8-128)	ns	ns				G
Brazil – intact *dupA* Queiroz, Rocha et al. 2011	ns		4.4 (2.0-9.2)	0.3 (0.2-0.7)					G
Malaysia/Singapore Schmidt et al. 2009/10	5.5 (1.9-17.0)		ns	4.0 (1.6-9.9)					FD
China Zhang et al. 2008	ns	2.7 (1.2-5.8)	2.6 (1.4-5.0)	0.5 (0.3-0.9)	ns				G
Iraq Hussein et al. 2008	7.2 (1.7-33.1)	ns			ns				no PUD
India Arachchi et al. 2007	2.0[2] (1.0-4.0)								FD
Columbia Lu et al. 2005	ns	ns	7.0 (2.4-19.7)	0.2 (0.1-0.7)	0.2 (0.1-0.6)				G
South Korea Lu et al. 2005	8.2 (2.1-36.8)	ns	9.2 (2.7-30.1)	ns	ns				G
Japan Lu et al. 2005	3.6 (1.3-9.9)	ns	5.2 (1.4-18.8)	ns	ns				G
Japan Yamaoka et al. 1999	5.0 (1.9-12.4)								G
Summary: type of association where observed	Positive	Varies	Positive	Varies	Negative				

Table 3.9 – summary table of reported associations between *dupA* status and clinical outcomes expressed as odds ratios

Where associations were reported, *dupA* was consistently linked to an increased risk of DU vs. control and DU vs. GC. These were inconsistent for GC vs. control.

Reported associations were consistent in their direction for DU vs. control (12/12 positive), for DU vs. GC (7/7 positive) and for GC vs. GU (2/2 negative). However, there was evidence that colonisation by a *dupA*+ strain was protective against GC vs. control for 3 study populations whilst increasing the risk of GC in 3 other study populations. Results were also variable for DU vs. GU (2 positive, 1 negative).

3.4.4 Statistical heterogeneity and clinical diversity

The Mantel-Haenszel fixed effects model was used to test for heterogeneity between study populations when determining the association between *dupA* status and cases of DU (n=37 study populations), GU (n=25) and GC (n=23) compared with control. Both I^2 as a method of quantifying inconsistency across studies and Cochran's Q were used to test for heterogeneity. Alongside evidence of a significant Q value ($P < 0.10$), I^2 was considered to represent moderate heterogeneity from 30 to 60%, substantial heterogeneity from 50 to 90%, and considerable heterogeneity from 75 to 100% (Higgins and Green 2011).

Substantial heterogeneity between study populations was identified for all three meta-analyses, suggesting the existence of either clinical or methodological diversity.

There was strong evidence of substantial heterogeneity between study populations for DU ($I^2 = 66.3\%$, 95% CI of $I^2 = 52.4\text{-}76.1\%$, $Q = 106.7$ and $P < 0.001$ [36 df]). Similarly, there was substantial heterogeneity for GU ($I^2 = 65.7\%$, 95% CI of $I^2 = 47.6\text{-}77.5\%$, $Q = 69.9$ and $P < 0.001$ [24 df]) and for GC ($I^2 = 61.1\%$, 95% CI of $I^2 = 38.7\text{-}75.3\%$, $Q = 56.5$ and $P < 0.001$ [22 df]). An example Forest plot for this meta-analysis for DU is shown in Appendix Figure 7.4. Next, we proceeded to explore this statistical heterogeneity to identify the sources of clinical and methodological diversity between studies, and in order to determine strategies to address heterogeneity.

Sensitivity analysis results for the study populations of Kim et al. (2014) and Queiroz, Rocha et al. (2011) suggest they introduced significant heterogeneity. Minor contributions to heterogeneity were identified for 7 other study populations. These sources typically contributed larger study populations and/or had amongst the largest differentials in *dupA* prevalence between cases and controls.

First, sensitivity analyses where each single study population was excluded were performed for each meta-analysis to assess any influence of a single study.

For the DU meta-analysis, heterogeneity by I^2 was within ±1.0% except when excluding the adult study population from Gomes 2008 – Brazil (I^2 = 64.1, 95% CI of I^2 = 48.8-74.8), Abadi 2012 – Iran (I^2 = 59.3, 95% CI of I^2 = 41.3-71.8), and Kim 2014 – South Korea (I^2 = 55.5, 95% CI of I^2 = 35.2-69.4). In all cases, *P* for Cochran's Q remained less than 0.001 and there was no relevant alteration in the magnitude or statistical result of the summary estimate. This approach suggested that no significant heterogeneity was introduced by the only paediatric study population in any of the meta-analyses (Gomes et al. 2008).

The largest study population was Gomes 2008 – Brazil (adults), which also reported the second highest overall prevalence of *dupA*+ strains (90.0% vs. median 31.8%). The other studies had the largest differential in *dupA* prevalence between DU cases and control of 60.1% (Abadi et al. 2012) and 58.1% (Kim et al. 2014) vs. median 8.8%.

For the GU meta-analysis, heterogeneity by I^2 was within ±1.5% except when excluding Takahasi 2013 – Japan (I^2 = 63.8, 95% CI of I^2 = 44.0-76.6), Zhang 2008 – China (I^2 = 63.2, 95% CI of I^2 = 42.9-76.2), and Kim 2014 – South Korea (I^2 = 21.5, 95% CI of I^2 = 0.0-52.4). Other tests of heterogeneity were no longer statistically significant on exclusion of the latter study by Kim et al. (Q = 29.3, P = 0.171 so $P > 0.10$) and the statistical significance of the summary estimate was lost, though otherwise there was no relevant difference in the summary estimate.

These included the second and third largest study populations respectively (Takahashi et al. 2013; Zhang et al. 2008), and the study with the largest differential in *dupA* status between GU cases and control (64.6% vs. median 9.3%).

For the GC meta-analysis, heterogeneity by I^2 was within ±1.0% for exclusion of 3/23 study populations, within ±1.5% for 10/23, and within ±2.0% for 17/23. The other 6 study populations were: Takahashi 2013 – Japan (I^2 = 59.0, 95% CI of I^2 = 34.5-74.4),

Zhang 2008 – China (I^2 = 58.2, 95% CI of I^2 = 33.1-74.0), Ferraz 2016 – Brazil (I^2 = 56.9, 95% CI of I^2 = 30.7-73.2), Schmidt 2009/2010 – Malaysia/ Singapore (I^2 = 56.8, 95% CI of I^2 = 30.5-73.2), Lu 2005 – Columbia (I^2 = 56.3, 95% CI of I^2 = 29.6-72.9), and Queiroz 2011 – Brazil (I^2 = 51.4, 95% CI of I^2 = 20.7-70.2). On exclusion of the latter study by Queiroz, Rocha et al., the summary estimate then just reaches statistical significance but Cochran's Q remains significant (Q = 43.2, P = 0.003 so P < 0.10). However, P < 0.001 for Cochran's Q in all other cases. Note that in this meta-analysis, exclusion of the South Korean study population of Kim et al. (2014) has no relevant impact on heterogeneity (I^2 = 62.3, 95% CI of I^2 = 40.3-76.2, Q = 55.7, P < 0.001).

Zhang et al. (2008) was the largest study populations. Queiroz, Rocha et al. (2011) contributed the second largest study population, had the highest *dupA* prevalence in controls (73.5% vs. median 30.8%) and ranked 6/23 for the size of the differential in *dupA* prevalence between cases and controls. The other studies ranked 2nd, 3rd, 5th and 7th, which were within the top tercile.

Next, potential sources of heterogeneity from clinical diversity were considered. For observational studies, this refers to variability in the participants and outcomes studied.

Two studies did not use individual patients as their unit-of-analysis and reported clinical outcomes for isolates of *H. pylori* or multiple clinical outcomes per patient. There was still moderate to substantial heterogeneity in DU and GC meta-analyses after exclusion of these studies.

The study by Kim et al. (2014) reported clinical outcomes for 354 colony isolates rather than 240 patients (see Section 3.4.1), which is a potential explanation for the significant heterogeneity identified. The study design used by Souod et al. (2015), which reported 180 clinical outcomes for 123 patients, has similar potential to introduce heterogeneity although no major impact was identified in the preceding sensitivity analysis. These studies were considered to be sources of potential clinical diversity as "participants" were different. Both were excluded from all subsequent analyses. A *post hoc* subgroup analysis for these 2 study populations was not performed given their different study designs.

For the DU meta-analysis, at least moderate heterogeneity remained (I^2 = 56.6, 95% CI of I^2 = 36.7-70.3, Q = 78.4, P < 0.001 [34 df]) and statistical significance was lost for the summary estimate. There was substantial residual heterogeneity for the GC meta-

analysis though no change in the significance of the summary estimate (I^2 = 63.7, 95% CI of I^2 = 42.1-77.3, Q = 55.1, P < 0.001 [20 df]).

However, for the GU meta-analysis, there was potentially no important heterogeneity after these 2 studies were excluded and the summary estimate was now non-significant (I^2 = 24.4, 95% CI of I^2 = 0.0-54.7, Q = 29.1, P = 0.142 [22 df]).

Planned subgroup analyses by region indicated that heterogeneity was still important. Clinical diversity was unlikely to be the only source of statistical heterogeneity.

In addition to this source of clinical diversity, there could be variability between the participants of each study population, as they are from different countries and regions, ethnicities and, where reported, there were differences between and within study populations in sex and age (see Section 3.4.7). Other known disease risk factors, such as smoking status and host genetic polymorphisms, were not reported. There could also be variability in the outcomes studied, as different countries may also have different standards for disease definition or diagnosis. However, these are unlikely to explain the apparent significant heterogeneity from Queiroz, Rocha et al. (2011) in sensitivity analysis, for example, as there were several South American study populations. Finally, variability in other *H. pylori* bacterial virulence factors was reported, typically between East Asian-type and Western-type strains according to these regions.

Planned subgroup analysis was performed by Eastern and Western regions, respectively comprising Asian and Middle Eastern countries, and the USA, European countries (including Turkey) and South American countries. The South African study population was not included in either region. The results are summarised in Table 3.10. The summary OR for DU meta-analysis by Eastern region subgroup was significant, though should be interpreted with caution given that there was substantial heterogeneity. At least moderate heterogeneity was found in 4 of 6 analyses. No further *post hoc* subgroup analyses were performed for clinical diversity. We did not undertake *post hoc* meta-regression.

Therefore, potential sources of statistical heterogeneity from methodological diversity were considered next. This refers to variability in study design and methods, and the risk of bias.

Table 3.10 – planned subgroup analysis for clinical diversity by region

Meta-analysis	Region	n	Summary OR (95% CI)	I^2 (95% CI)	Cochran's Q (*P*)	Heterogeneity
DU	**Eastern**	22	2.2 (1.8-2.7)	63.2 (41.8-76.7)	57.0 (<0.001)	Substantial
	Western	12	1.2 (0.9-1.6, ns)	0.0 (0.0-51.1)	9.4 (0.587)	None shown
GU	**Eastern**	17	1.2 (0.9-1.5, ns)	38.9 (0.0-65.7)	26.2 (0.051)	Moderate
	Western	6	0.9 (0.6-1.5, ns)	0.0 (0.0-35.7)	2.0 (0.853)	None shown
GC	**Eastern**	13	1.2 (0.9-1.6, ns)	49.7 (4.7-73.4)	23.8 (0.021)	Moderate
	Western	6	0.8 (0.6-1.2, ns)	76.2 (50.0-88.7)	25.2 (<0.001)	Substantial

CI, confidence interval; DU, duodenal ulcer; GC, gastric cancer; GU, gastric ulcer; n, number of study populations in meta-analysis subgroup; ns, not significant; OR, odds ratio.

3.4.5 Methodological diversity and risk of bias

Conclusions about the association between *dupA* and clinical outcomes drawn from these varied observations may be correctly reflected in each study population. However, study design and methods were highly variable, as summarised in Table 3.11, such that most study populations were at risk of bias from misclassification of *dupA* status. There was marked methodological diversity in several areas.

Firstly, bacterial DNA was extracted with a variety of methods – some directly from biopsy, others from cultures or sub-cultures expanded from singles colonies (Zhang et al. 2008; Schmidt et al. 2009), homogenates of multiple biopsies (Douraghi et al. 2008), or harvested as sweeps or as a pool of bacterial colonies (Hussein et al. 2008; Pacheco et al. 2008). Matteo et al. (2010) reported inter- and intra-niche diversity in *dupA* status (and other genes) with multiple biopsies from the same patients at different time points. It is not certain if the isolated strain used for culture was the dominant strain, or whether other colonising organisms with different virulence profiles might be the major bacterial contributors to pathogenesis. The resulting classification error could lead to false-negative or false-positive results in the sample population.

Secondly, there were fundamental differences in genotyping methods between studies. Most studies used more than one primer pair or a confirmatory method such as DNA dot-blot and/or Southern blotting. Admittedly the use of both multiplex PCR and up to eight PCR primer sets did not significantly improve the accuracy of genotyping over

one or two simple primer pairs (Schmidt et al. 2009). Some studies where DNA was prepared directly from biopsies including an additional PCR to confirm template adequacy and lack of inhibitors. Some authors designed primers using sequencing data for local strains and in some cases these were validated (Gomes et al. 2008; Schmidt et al. 2009; Jung et al. 2012; Takahashi et al. 2013; Alam et al 2015). Choice of *dupA* primers has been shown to be very important (Abadi et al. 2014). These methodological inadequacies are more likely to result in misclassification of a *dupA*+ isolate as *dupA*-, and so will cause a conservative bias that increases the risk of type II error (false negative result, where null hypothesis is rejected in error).

Thirdly, some classification methods relied on detecting PCR products from limited regions of the *dupA* gene and would not identify point mutations that are a frequent cause of frameshifts in relevant studies or mutations that may theoretically affect promotor activity. Only a limited number of studies identified non-sense mutations by sequencing. Moreover, in only a minority was sequencing extended to distinguish between long-type (2,499 bp) and short-type (truncated) alleles of *dupA*. No studies to date have investigated quantitative expression of *dupA* mRNA, DupA protein or anti-DupA antibodies in serum, in relation to clinical outcomes. Equally, differences in culture conditions, type of media and length of incubation may or may not lead to alterations in relevant genetic sequences such as primer annealing sites, or in *dupA* mRNA expression by RT-PCR. So currently the least biased method available to determine *dupA* status, is detailed genotyping to identify intact long-type *dupA* (*dupA1*). Study populations that were classified as intact by partial sequencing or for a subset of strains only, or that did not distinguish between long-type and short-type *dupA*, were considered still to have some risk of bias. Twenty-four of the 34 independent studies identified for this systematic review (after accounting for the two pairs of studies) undertook no sequencing of *dupA*. Therefore, there was a risk of bias for the majority of studies that were not designed to distinguish and stratify by intact and non-functional polymorphic alleles.

Finally, *dupA* is present within a cluster of other genes. Components of this so-named *dupA* cluster (here termed *tfs4*) might be important in determining the genetic potential for virulence of a particular strain. The two studies that reported clinical outcomes for *tfs4*, as well as *dupA* or intact *dupA*, reported conflicting results in its utility in their

patient populations as a marker for increased risk of DU compared with control (Jung et al. 2012; Alam et al. 2015).

It is not yet known which form(s) of *dupA* and related *tfs4* genes are functional, and which *tfs4* genes are essential. This analysis focussed on *dupA* alone and, where the methods and reported data allowed, reported clinical outcomes for *dupA1* strains. These are classified as those strains that possess an intact full-length *dupA* allele.

Table 3.11 – study methods and assessment of risk of bias in reporting of *dupA* status

Study	Risk of bias	Source DNA	No. primers sets (exc. sequencing)	Source	Another typing method(s) used	Checked intact?	Checked long type?	Further checks?
this study[1]	lower	cultured *in vitro* (antrum and corpus)	Methods Section 2.8.1		sequencing	yes	yes	*tfs4* (4 genes)
Ghalehnoei 2016	higher	cultured *in vitro* (antrum and corpus)	1 (in multiplex)	this study	-	-	-	-
Ferraz 2016	higher	biopsy DNA (site not stated)	2	Gomes 2008	-	-	-	-
Miftahussurur 2015[1]	lower	cultured *in vitro* (antrum)	2	Takahashi 2013	sequencing	yes	yes	-
Oktem-Okullu 2015	higher	biopsy DNA (antrum and corpus)	1 (in multiplex)	this study	-	-	-	-
Souod 2015	higher	biopsy DNA (antrum)	2 (including *jhp0917*/*jhp0918*)	Lu 2005	-	-	-	-
Haddadi 2015	higher	cultured *in vitro* (antrum)	1	Argent 2007	partial sequencing 20/46	some	-	-
Hussain 2015[1]	lower	biopsy DNA (site not stated)	3	Hussain 2010 and Takahashi 2013	sequencing	yes	yes	-
Alam 2015[1]	lower	cultured *in vitro* (antrum and corpus)	4 (including *jhp0917*/*jhp0918*)	Lu 2005 and this study	sequencing	yes	yes	*tfs4* (6 genes)
Osman 2015	higher	biopsy DNA (antrum)	1	Gomes 2008	-	-	-	-
Rasheed 2014	higher	cultured *in vitro* (antrum)	2 (including *jhp0917*/*jhp0918*)	Lu 2005	-	-	-	-
Pereira 2014	higher	biopsy DNA (antrum)	1	Gomes 2008	-	-	-	-
Kim 2014	higher	cultured *in vitro* (antrum and corpus)	3 (including *jhp0917*/*jhp0918*)	Lu 2005 and Nguyen 2010	-	-	-	-
Salih 2013	higher	biopsy DNA (antrum and corpus)	1	Argent 2007	-	-	-	-

Table 3.11 – study methods and assessment of risk of bias in reporting of *dupA* status (continued)

Study	Risk of bias	Source DNA	No. primers sets (exc. sequencing)	Source	Another typing method(s) used	Checked intact?	Checked long type?	Further checks?
Wang 2013	medium	cultured *in vitro* (antrum, corpus and margin of lesion)	3 (including *jhp0917*/*jhp0918*)	Lu 2005 and this study (R primer from Hussain 2010)	partial sequencing 8/36	some	some	-
Takahashi 2013[1]	lower	cultured *in vitro* (antrum)	4	this study (F5 primer from Lu 2005)	sequencing	yes	yes	-
Alam 2012[2]	medium	cultured *in vitro* (antrum and corpus)	2 (including *jhp0917*/*jhp0918*)	Lu 2005	dot-blot, sequencing	yes	-	*dupA* RT-PCR
Moura 2012[2]	medium	cultured *in vitro* (site not stated)	2 (including *jhp0917*/*jhp0918*)	Lu 2005	sequencing	yes	-	-
Matsuda 2012[1]	medium	cultured *in vitro* (antrum and corpus)	5	Argent 2007 and this study	dot-blot, partial sequencing 15/60	some	some	-
Jung 2012	higher	cultured *in vitro* (antrum)	3	this study, Lu 2005 and Argent 2007	-	-	-	*tfs4* (6 genes)
Abadi 2012	higher	cultured *in vitro* (antrum)	3 (including *jhp0917*/*jhp0918*)	Lu 2005 and Nguyen 2010	-	-	-	-
Queiroz 2011[2]	medium	biopsy DNA (antrum and corpus)	3 (including *jhp0917*/*jhp0918*)	Lu 2005 and Gomes 2008	sequencing	yes	-	-
all studies 2005-2010	higher					-	-	

DNA, deoxyribonucleic acid; exc., excluding; RT-PCR, real time polymerase chain reaction; -, not reported.

[1] Reported clinical outcomes for *dupA1* strains, which were considered to possess the intact long-type *dupA* gene.

[2] Reported clinical outcomes for intact *dupA* strains. Note that Alam 2012 reported for transcribed intact *dupA* strains.

Risk of bias in reporting of *dupA* status considers: (1) if more than one primer set and/or another typing method was used, (2) if method enabled alleles with nonsense mutations to be identified, (3) if method enable the long-type 2,499 bp gene to be identified. Where all three tests were met for all strains then that study was classified as being at lower risk of bias. Where the first two tests were met for all strains, or where all three tests were met for some strains, then that study was classified at medium risk of bias. Other studies were considered to be at higher risk of bias.

Planned subgroup analyses by methodology and risk of bias identified those judged to be at higher risk of bias in classification of *dupA* as the main source of statistical heterogeneity. There was substantial residual heterogeneity for GC.

To measure the contribution of methodological diversity to heterogeneity, subgroup analysis stratified by risk of bias was planned. This was performed for study populations where the risk of bias in their parent studies were judged to be higher, medium or lower (Table 3.12). Moderate or substantial heterogeneity was found for all subgroups a higher risk of bias. The lower and medium risk subgroups were not shown to have heterogeneity for DU and GU meta-analyses. There was substantial residual heterogeneity across all subgroups for GC, therefore, meta-analysis even using a random effects model may be misleading and was not performed. No further *post hoc* subgroup analyses were performed for methodological diversity. We did not undertake *post hoc* meta-regression nor meta-analysis using the quality effects model.

Table 3.12 – planned subgroup analysis for methodological diversity by risk of bias

Meta-analysis	Risk of bias	n	Summary OR (95% CI)	I^2 (95% CI)	Cochran's Q (*P*)	Heterogeneity
DU	**Higher**	27	2.0 (1.7-2.4)	72.3 (59.4-81.1)	93.9 (<0.001)	Substantial
	Medium	5	2.1 (1.4-3.1)	0.0 (0.0-73.9)	3.2 (0.527)	None shown
	Lower	5	1.7 (1.0-2.7)	57.6 (0.0-84.3)	9.4 (0.051)	Moderate
	Medium & Lower	10	1.9 (1.4-2.6)	29.9 (0.0-66.5)	12.8 (0.170)	None shown
GU	**Higher**	19	1.3 (1.0-1.6)	70.3 (52.6-81.4)	60.6 (<0.001)	Substantial
	Medium	2	1.6 (0.8-3.1, ns)	41.0 (n/a)	1.7 (0.193)	None shown
	Lower	4	2.7 (1.4-5.2)	0.0 (0.0-79.3)	2.2 (0.527)	None shown
	Medium & Lower	6	2.1 (1.3-3.4)	3.8 (0.0-75.6)	5.2 (0.392)	None shown
GC	**Higher**	18	1.1 (0.9-1.4, ns)	52.5 (18.6-72.2)	35.8 (0.005)	Moderate
	Medium	4	0.9 (0.6-1.3, ns)	79.9 (46.8-92.4)	14.9 (0.002)	Substantial
	Lower	1	n/a	n/a	n/a	n/a
	Medium & Lower	5	1.0 (0.7-1.5, ns)	80.8 (55.1-91.8)	20.8 (<0.001)	Substantial

CI, confidence interval; DU, duodenal ulcer; GC, gastric cancer; GU, gastric ulcer; n, number of study populations in meta-analysis subgroup; n/a, not applicable; ns, not significant; OR, odds ratio.

3.4.6 Results of meta-analysis

3.4.6.1 Association between *dupA* and DU

The prevalence of the *dupA* gene in patients with DU was examined in 10 study populations from the 10 studies with lower and medium risks of bias. The Forest plot using fixed effects model is shown in Figure 3.2. All of these studies were published after the previous systematic review and meta-analysis (Hussein 2010; Shiota et al. 2010). These reviews did not include any studies where *dupA* status was determined with identification of alleles with nonsense mutations or the long-type of *dupA*, as these methods for classifying *dupA* status were not reported prior to 2011.

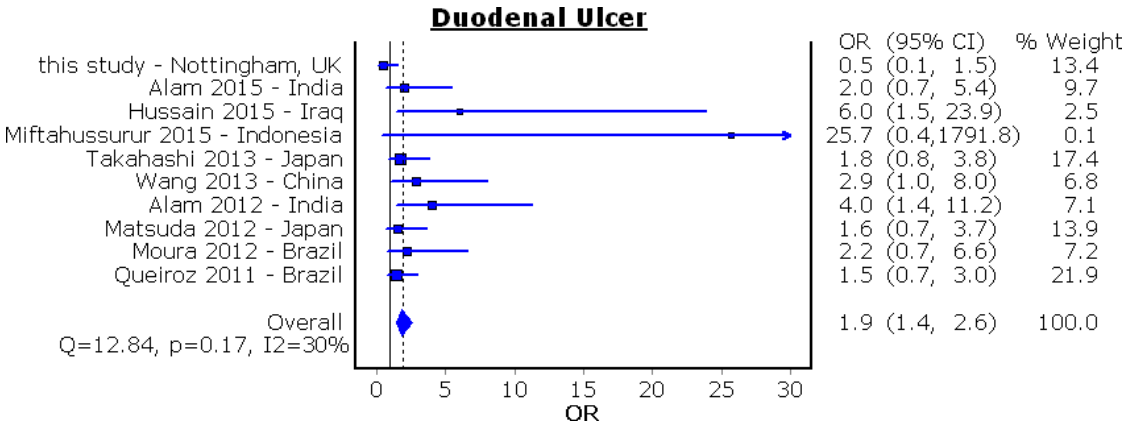

Figure 3.2 – results of meta-analysis for the risk of DU in *dupA*+ *H. pylori* infection

There was strong evidence of a positive association between *dupA* and DU, with a summary OR of 1.9.

Summary odds ratio was 1.9 (95% CI 1.4-2.6), indicating a higher risk of DU in individuals infected by *H. pylori* strains that possess the *dupA* gene. This was consistent, in both effect size and significance, with the previously reported summary ORs for all study populations (OR 2.0, 95% CI 1.7-2.3, substantial heterogeneity) and risk of bias subgroups (Table 3.12). When the analysis was confined to the studies that also reported *tfs4* status (this study; Jung et al. 2012; Alam et al. 2015), the summary OR was 1.8 (95% CI 1.1-3.0) for the risk of DU with *dupA* / *tfs4* complete strains (I^2 = 0.0, 95% CI of I^2 = 0.0-86.4, Q = 1.5, *P* = 0.465 [2 df]).

The evidence that *dupA*+ strains are associated with an increased the risk of DU was significant only in Asian countries.

This result was driven by Eastern region studies, with summary OR 2.4 (95% CI 1.6-3.5) for the 7 Asian study populations (I^2 = 0.0, 95% CI of I^2 = 0.0-68.6, Q = 5.6, *P* = 0.471 [6 df]). Whereas for the 3 study populations from the Western region (UK and Brazil), there was no significant association (summary OR 1.3, 95% CI of OR 0.8-2.2, I^2 = 49.5, 95% CI of I^2 = 0.0-85.4, Q = 4.0, *P* = 0.138 [2 df]). This was consistent with regional subgroups analysis for all study populations reported above.

The equivalent risk of DU was approximately 50% higher for *dupA*+ vs. *dupA*– strains. However, two-thirds of the cases of DU occurred with *dupA*– infections.

Odds ratios are the standard measure of effect in case-control studies. The interpretation of ORs can be problematic (Persoskie and Ferrer 2017), with a common misunderstanding that they denote probabilities or have the same meaning as risk ratios. Zhang and Yu (1998) reported a method to derive an estimate of relative risk, that may enable clearer interpretion of the magnitude of an association. This method uses the incidence of the outcome of interest in the non-exposed group, which in this case is the proportion of study participants with DU in the *dupA*– group.

For 1490 participants in these study populations, 38% (181/473) of *dupA*+ strains were isolated from patients with DU and 33% (332/1017) of *dupA*– strains were isolated from patients with DU. The summary OR of 1.9 is approximately equivalent to a relative risk of 1.47 (equivalent 95% CI 1.24-1.71). Therefore, patients infected with *dupA*+ strains of *H. pylori* were at approximately 50% higher risk of DU. However, note that 65% of cases of DU were in association with *dupA*– strains, so *dupA* cannot be essential, either directly or indirectly, to the development of duodenal ulceration.

There was evidence of publication bias, with fewer negative studies reported.

There was evidence of publication bias in favour of positive association in those studies at lower or medium risk of bias (blue circles in funnel plot shown in Figure 3.3, with LFK index 2.23 indicating major asymmetry) and to a lesser extent across all 37 study populations (red circles in addition, LFK index 1.47, indicating minor asymmetry).

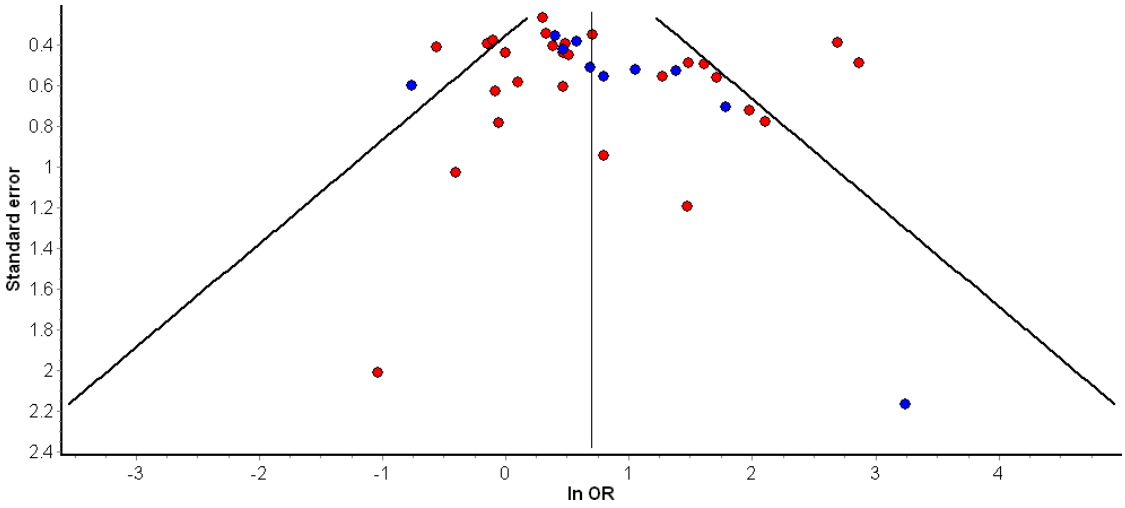

Figure 3.3 – publication bias in the DU meta-analysis

Funnel plot of standard error (measure of study size, with smaller values indicating more precise estimates of effect size due to larger study populations) against the natural logarithm of OR (odds ratio, measure of study effect size). The vertical line marks the summary OR. Blue circles denote studies judged to be at lower or medium risk of bias in reporting *dupA* status (n=10). Red circles denote other study populations (n=27).

3.4.6.2 Association between *dupA* and GU

Next, the prevalence of the *dupA* gene in patients with GU was examined in 6 study populations from the 10 studies with lower and medium risks of bias. The Forest plot using fixed effects model is shown in Figure 3.4.

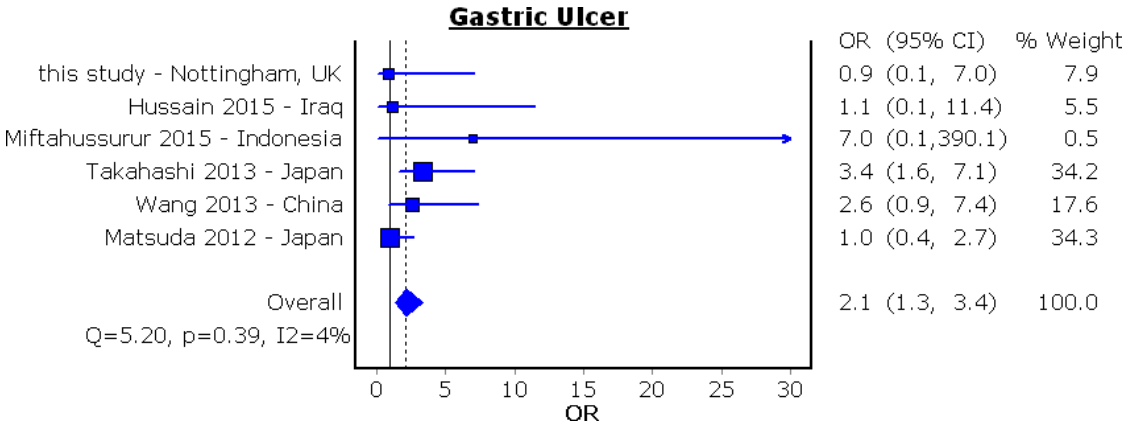

Figure 3.4 – results of meta-analysis for the risk of GU in *dupA*+ *H. pylori* infection

There was also evidence of a positive association between *dupA* and GU.

Summary odds ratio was 2.1 (95% CI 1.3-3.4), indicating a higher risk of GU in individuals infected by *H. pylori* strains that possess the *dupA* gene. This was consistent

with the summary ORs for all study populations (OR 1.4, 95% CI 1.1-2.7, substantial heterogeneity as previously reported) and the majority of the risk of bias subgroups (Table 3.12). All study populations were from the Eastern region, except for this study which did not show an association with GU.

The equivalent risk of GU was approximately 75% higher for *dupA*+ vs. *dupA*– strains. However, 70% of GU cases occurred with *dupA*– infections.

To aid interpretation note that, for 853 participants in these study populations, 26% (53/207) of *dupA*+ strains were isolated from patients with GU and 19% (124/646) of *dupA*– strains were isolated from patients with GU. Based on the prevalence of GU in this non-exposed group, the summary OR of 2.1 is approximately equivalent to a relative risk of 1.73 (equivalent 95% CI 1.23-2.33) (Zhang and Yu 1998). Therefore, patients infected with *dupA*+ strains of *H. pylori* were at approximately 75% higher risk of GU. Note that 70% of cases of GU were in association with *dupA*– strains.

There was no strong evidence of publication bias in the GU meta-analysis.

There was no strong evidence of publication (blue circles in funnel plot shown in Figure 3.5, with LFK index -1.52 indicating minor asymmetry) and across all 25 study populations (red circles in addition, LFK index 0.85 indicating no asymmetry).

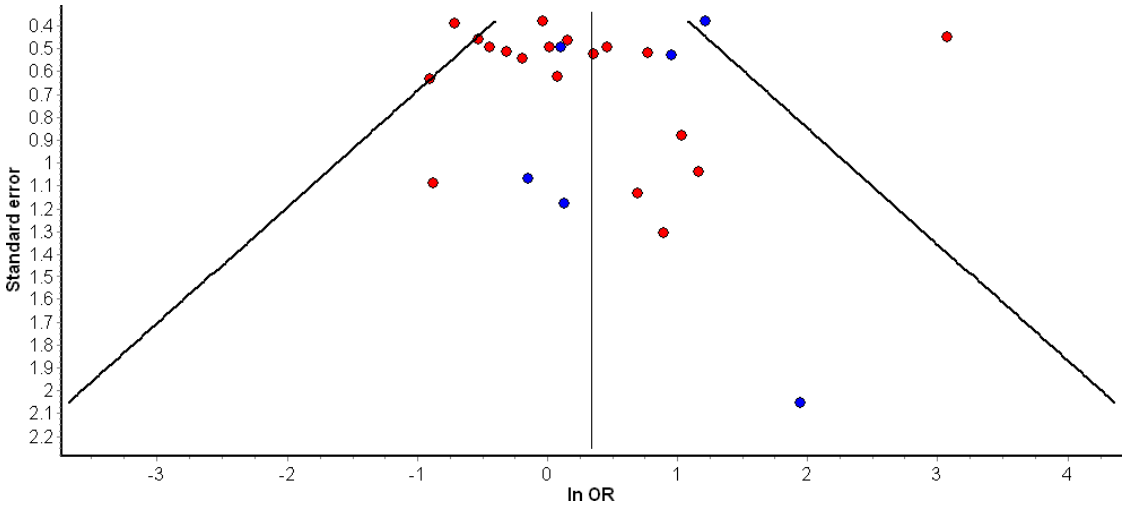

Figure 3.5 – publication bias in the GU meta-analysis

Funnel plot of standard error (measure of study size, with smaller values indicating more precise estimates of effect size due to larger study populations) against the natural logarithm of OR (odds ratio, measure of study effect size). The vertical line marks the summary OR. Blue circles denote studies judged to be at lower or medium risk of bias in reporting *dupA* status (n=6). Red circles denote other study populations (n=19).

3.4.6.3 Association between *dupA* and GC

As discussed in the previous section, there was considerable heterogeneity between study populations in this meta-analysis that could not be fully addressed. Therefore, meta-analysis was not performed. There was no consistent evidence of an association between *dupA* status and the risk of malignancy, either positive or protective.

3.4.7 Confounding by age and sex

There were considerable differences between groups beyond disease or *dupA* status in individual studies. The differences related to sex, for example, 89% of patients with duodenal ulcer were male against 60% of those with dyspepsia (Arachchi et al. 2007), and in another study 67% of cancer patients were male that was a third more than any other disease group (Gomes et al. 2008). Similar discrepancies are seen with age, for example, in one study the mean age of patients with duodenal ulcer was 41 years whilst that for patients with gastritis was 59 years (Zhang et al. 2008).

More patients with DU were male and they were younger on average than controls. Matching and/or analysis to account for age, sex and other potential confounders was very infrequent. The majority of association studies did not account for confounding.

To assess this further, all studies that reported data on population demographics by clinical outcome were identified and summarised in Table 3.13.

Males were over-represented in cases vs. controls (52.4% vs. 47.8%, $P = 0.015$). Patients with DU were significantly younger than controls and when compared against individuals with GU and GC, and both the GU and GC groups were significantly older than controls and for GC vs. GU ($P < 0.001$ adjusted for 6 multiple comparisons).

There were no age- and sex-matched case-control studies in this systematic review, except for the Yamaoka 1999 study population reported by Lu et al. (2005). Some studies did undertake logistic regression to adjust for age, sex and other confounders such as bacterial virulence factors (Lu et al. 2005; Gomes et al. 2008; Pacheco et al. 2008; Takahashi et al. 2013; Kim et al. 2014; Hussein et al. 2015).

Table 3.13 – analysis of age, sex and *dupA* status with respect to clinical outcome.

Clinical outcome	Number of *Hp*+ patients	% with *dupA* [no. with data]	% male [no. with data]	mean age ± estimated sd (years)
DU	962	52.2% [854]	61.8% [895]	46.6 ± 12.9
GU	374	40.7% [284]	74.1% [305]	53.8 ± 11.8
GC	386	49.2% [386]	66.6% [386]	61.5 ± 11.0
Cases (DU, GU, GC)	1629	46.1% [1458]	52.4% [1629]	52.1 ± 13.7
Controls (G or FD)	1218	45.1% [1047]	47.8% [1218]	49.1 ± 13.4
Overall	2965	47.5% [2596]	57.7% [2829]	50.6 ± 13.6

These data were extracted from 13 adult study populations where the authors provided population demographics (including mean age) grouped by clinical outcome category.

Study populations were: India – Arachchi 2007, Brazil – Gomes 2008 (adults), China – Zhang 2008, Malaysia/ Singapore – Schmidt 2009/2010, Japan – Imagawa 2010, Taiwan – Yeh 2010, United States of America – Jung 2010, Brazil – Queiroz 2011, Brazil – Moura 2012, India – Alam 2012, Japan – Takahashi 2013, South Korea – Kim 2014, United Kingdom – this study.

Mean age and sd for individual and combined clinical outcome groups was calculated using algebraic combination of each study population using the formulae for mean and sd when reported (https://www.statstodo.com/commeans_pgm.php).

Two studies examined *dupA* status in a subgroup of patients with each clinical outcome (Imagawa et al. 2010; Yeh et al. 2010). One study reported *dupA* status by clinical isolates having recovered a mean of 1.67 isolates per patient (Kim et al. 2014), the prevalence of which was assumed to be representative of the patient population. This study also reported details for 25 patients with dysplasia (41.6% *dupA*+ for 32 isolates, 60.0% male, age 61.4 ± 8.0 years). One study did not report the number of males and females (Imagawa et al. 2010). Two studies did not report sd with mean age (Zhang et al. 2008; Schmidt et al. 2009 and 2010). One study reported mean age and sd separately for males and females (Alam et al. 2012), which were combined.

DU, duodenal ulcer; FD, functional dyspepsia; G, gastritis; GC, gastric cancer; GU, gastric ulcer; *Hp*, *H. pylori*.

3.4.8 Summary

Systematic review identified 36 studies. Data for 5,769 patients/isolates from 19 countries were used for subsequent analysis. These represent data from 31 studies including this study, comprising 39 independent study populations.

Around 41% of clinical isolates were reported to possess the *dupA* gene. Where it was reported, clinical isolates were *dupA1* in around 21% of cases.

Associations between *dupA* status and clinical outcomes were reported for 14/31 studies and 17/39 study populations. *dupA* was consistently associated with DU.

Substantial heterogeneity between study populations was identified for meta-analyses of DU, GU and GC vs. control, and investigated using sensitivity and subgroup analyses. Studies judged to be at higher risk of bias in classification of *dupA* were identified as the main source of statistical heterogeneity.

There was strong evidence of a positive association between *dupA* and DU, with a summary OR of 1.9 and an approximately 50% higher relative risk. This was significant only in Asian countries (OR 2.4). There was evidence of publication bias, with fewer negative studies reported for DU. There was also evidence of a positive association between *dupA* and GU, with a summary OR of 2.1 and an approximately 75% increase in relative risk. Residual heterogeneity precluded meta-analysis for GC. The majority of cases of DU and of GU in *H. pylori*-infected individuals occurred with *dupA*– strains (65% and 75% respectively).

More patients with DU were male and they were younger on average than controls. The majority of reported associations were from studies that did not adequately account for confounding.

3.5 Discussion

Duodenal ulcer promoting gene (*dupA*) was proposed as the first disease-specific virulence factor of *H. pylori*, based on epidemiological data and other evidence (Lu et al. 2005).

In this section, we discuss the results of work:

1. to carefully characterise the *dupA* status and virulence determinants of clinical isolates from the Nottingham study population,
2. to report the first association study for the United Kingdom for the relationship with clinical outcomes according to *dupA* status, and
3. to undertake a systemic review and meta-analysis of the influence of *dupA* status on clinical outcomes.

The hypothesis was that *dupA1* strains would be positively associated with DU but not with other clinical outcomes.

3.5.1 *dupA* status

This study characterised the colonising clinical isolates of *H. pylori* from 52 patients in Nottingham. It is the first study of the influence of *dupA* status on clinical outcomes in the United Kingdom. Strain genotype was comprehensively determined using multiple PCR primer pairs and sequencing to cover the entire *dupA* gene with a minimum of 4 contigs at each point for assembly (see Section 2.8.1). Colonising strains were identical in their *dupA* sequence between the gastric antrum and corpus in all cases.

Strains were *dupA1* in approximately half of these isolates. In systematic review, around 41% of clinical isolates were reported to possess the *dupA* gene. The prevalence was higher in strains isolated from Western and South American countries, where two-thirds of strains were *dupA*+, than in Eastern and Middle Eastern countries, with a 30% prevalence of *dupA*. Clinical isolates reported in other studies were *dupA1* in around 21% of cases (Takahashi et al. 2013; Alam et al. 2015; Hussein et al. 2015; Miftahussurur et al. 2015), in studies from India, Indonesia, Iraq and Japan.

There was evidence that the *tfs4* cluster was genetically complete in a quarter of *dupA1* strains. Ten percent of strains were *dupA1*/*tfs4* complete in this cohort, though based on a more restrictive definition of *dupA* and a less restrictive definition of *tfs4*.

There was a weak association between *dupA1* and *vacA* s1m1i1 type (φ = 0.341, *P* = 0.014). Pereira et al. (2014) reported an association between *dupA* and *vacA* s1m1 type (reported as relative risk of 1.7, 95% CI 1.3-2.2). One other study has reported an association (Arachchi et al. 2007). There is no established complementarity or redundancy between *dupA* and *vacA*. It is not clear if there a genuine relationship between *dupA* and *vacA*, and its significance bacteriologically or clinically.

We found no association between *dupA1* and *cag*PAI (φ = 0.135, *P* = 0.340). Others have reported associations with *cagA* or with *cag*PAI typed according to various criteria (Matsuda et al. 2012; Takahashi et al. 2013; Pereira et al. 2014; Romo-Gonzalez et al. 2015). Where appropriately reported, such correlations were typically very weak. For example, the correlation reported in Takahashi et al. between *dupA1* and *cagA* (ρ = 0.12 [Spearman's rank correlation coefficient], *P* = 0.02) and the correlation between *dupA1* and East Asian-type *cagA* (vs. the Western-type and *cagA*– combined) in Okinawan strains that can be calculated as φ = 0.261 from the contingency data reported by Matsuda et al. (*P* = 0.002, χ^2 = 9.269, n=136). Where this has been studied in most detail by Jung et al. (2012), no important correlations have been demonstrated between *cag*PAI-positive status (7/7 loci positive by PCR) and *dupA*, putative *tfs4* components (for 5/6 genes, as *virD4* was very weakly correlated with φ = 0.12, *P* = 0.04), or the complete *dupA* cluster.

3.5.2 Clinical outcomes

No association between *dupA1* status and clinical outcomes was shown.

There were no significant associations between *dupA1* status and disease in the Nottingham study population. This is in keeping with the literature, as the majority of studies did not report associations with clinical outcomes (17/31 studies and 22/39 study populations, Section 3.4.3).

Researchers in many countries have an interest in *dupA* research, with the majority of data reported for populations in the Eastern region (4,125 patients/isolates from 11 countries). Most research interest in now in the East, probably because the majority of positive association studies concerned patients from this region (14/17 "positive" studies) and because of the greater burdern of *Helicobacter*-associated disease (Hunt et al. 2011; Ingram et al. 2015). However, *dupA* status and clinical outcome have also been

assessed in 8 countries where Western strains of *H. pylori* are more prevalent, including reports from Australia, Europe, North and South America, and South Africa.

To place the primary Nottingham study in the context of other work, an up-to-date systematic review and meta-analysis was performed. The rationale was to identify the latest evidence from a broader range of sources, and to extend previous work by assessing the risk of bias introduced by different approaches to *dupA* genotyping and by examining the extent to which confounders have been accounted for in analyses. Data for 5,769 patients/isolates overall were included in meta-analyses of the association between *dupA* and duodenal ulceration, gastric ulceration and gastric cancer. These representation data from 31 studies, comprising 39 independent study populations from 19 countries. Sixty-nine percent of participants were recruited in Asian and Middle Eastern countries.

Through meta-analysis to account for variability in study methods and address statistical heterogeneity, infection by strains that possess a *dupA* gene was shown overall to be associated with DU. This was driven by data from Asian countries and no association was found for the Western region.

Where associations were reported, *dupA* was consistently linked to an increased risk of DU vs. control and DU vs. GC. All 12 study populations that reported an increased risk of DU vs. control with *dupA*+ strains were conducted in Asian and Middle Eastern countries (Table 3.9). Systematic review and meta-analysis was performed for the clinical outcomes of DU, GU and GC vs. control, which alongside this study identified a further 38 independent study populations comprising over 5000 patients from 19 countries. There was evidence to suggest publication bias in the DU meta-analysis, with fewer negative studies reported. Moreover, substantial heterogeneity between study populations was identified, which was driven by:

- clinical diversity – from the use of units-of-analysis other than individual patients, from certain sources that contributed larger study populations and/or had amongst the largest differentials between cases and controls in *dupA* prevalence, and from differences between Eastern and Western studies; and
- methodological diversity – particularly from the genotyping method(s) used in each study, whereby those judged to be at higher risk of bias in classification of *dupA* status were the main source of statistical heterogeneity.

Subgroup analysis of study populations judged to be at lower or medium risk of bias was able to overcome this heterogeneity in DU and GU meta-analyses.

The approach to identify, measure, investigate and address heterogeneity was informed by the Cochrane Handbook (Higgins and Green 2011).

The subgroup analysis by Eastern and Western regions was included in previous meta-analysis (Shiota et al. 2010). Phylogenetic analysis of *dupA* has identified two distinct strain clusters, with Japanese, Chinese and Indian strains in one cluster, and Brazilian and Colombian strains in the second cluster (termed the Western cluster) (Alam et al. 2015). Turkish clinical isolates are typical of Western countries (Saribasak et al. 2004). Regional variations in association with clinical outcome are typical of other bacterial virulence determinants (Hussein 2010).

Consensus standards and quality assessment tools are well described for meta-analysis: there are the QUOROM and PRISMA statements for randomised-controlled trials that evaluate healthcare interventions (Liberati et al. 2009), for which the Jadad scale is the best known quality assessment tool; the STARD statement for studies of diagnostic accuracy (Bossuyt et al. 2003), for which the QUADAS and QUADAS-2 quality assessment tools (Whiting et al. 2003; Whiting et al. 2011); MOOSE and STROBE statements for reporting and meta-analysis of observational studies (Stroup et al. 2000; von Elm et al. 2008); and STREGA statements for genetic association studies (Little et al. 2009; Minelli et al. 2009). However, at least 91 quality assessment tools have been reported for observational studies that have been subject to limited systematic evaluation (Whiting et al. 2005; Shamliyan et al. 2010; Shamliyan et al. 2011; Shamliyan et al. 2012). In the field of *H. pylori* research, meta-analyses that take differences in quality into account as a potential source of heterogeneity are confined to association studies of host genetic polymorphisms and gastric cancer risk (Camargo et al. 2006; Persson et al. 2011; Zhang et al. 2012). The Newcastle-Ottawa Scale has emerged as a valuable tool to assess the quality of observational studies (Wells et al. 2011) and there is growing emphasis on critical evaluation in evidence-based laboratory medicine (Christenson 2007). However, no standard validated method was available to appraise the quality of genotyping of clinical bacterial isolates and the risk of bias introduced by misclassification. Therefore, rather than propose a novel quality score and incorporate this into a quality effects meta-analysis, we used the approach of subgroup analysis based on a subjective judgement about the risk of bias. There is evidence that those

studies at higher risk of bias (Table 3.11), of which many used the *jhp0917* and *jhp0918* primers originally described by Lu et al. (2005), may misclassify the majority of isolates. Concordant *in vitro* PCRs for *jhp0917* and *jhp0918* identified only 16% of *dupA*+ Dutch clinical isolates and respectively predicted *in silico* 66% and 34% of *dupA* genes listed in NCBI as PCR positive (Abadi et al. 2014). The method we used gives the best currently available assessment of the association of DU with true *dupA*+ status (mostly those with intact *dupA* or *dupA1*).

The summary OR was 1.9 for DU meta-analysis in the subgroup without studies at higher risk of bias, which represents an approximately 50% higher risk of DU for strains with the *dupA* gene.

There was strong evidence of a positive association between *dupA* and DU, with a summary OR of 1.9 (95% CI 1.4-2.6). This was consistent across analyses. Meta-analysis confirmed that the increased risk of DU seen with *dupA*+ strains was significant only in Asian countries (OR 2.4, 95% CI 1.6-3.5). The equivalent relative risk of DU overall was approximately 50% higher for *dupA*+ vs. *dupA2*/*dupA*– strains.

The conclusions of this study on the positive association between *dupA* and DU are in keeping with the earlier meta-analysis by Shiota et al. (2010), which included data that in this study were judged to be at higher risk of bias. There was significant heterogeneity in their meta-analysis, though the sources were identified in sensitivity analysis and the summary results were consistent. In keeping with Shiota et al. and this study, a contemporaneous systematic review shared similar findings (Hussein 2010).

However, duodenal ulceration most frequently occurred in strains lacking *dupA* or with a disrupted gene.

Despite this association, two-thirds of the cases of DU occurred in individuals with *dupA2*/*dupA*– infections. This is not unexpected as there were are other important risk factors for peptic ulceration, including younger age, smoking and a prior history of DU or GU (Ingram et al. 2015), which were not accounted for in this meta-analysis.

Past history of peptic ulcer disease was not shown to be relevant for our patient cohort. Some studies specified that patients with ulcer scars were included in the ulcer group (Lu et al. 2005; Zhang et al. 2008), as in this study, though in the majority this was not specified. There was no significant association between *dupA* status and disease, after controlling for potential confounding by sex and age by individual matching. Only one

other study population included an age- and sex-matched control group, though multiple logistic regression was reported in several studies (Section 3.4.7). For example, Gomes et al. (2008) reported independent associations of increasing age, male gender and possession of *cagA* with both DU and GC in multivariate analysis. Smoking was more frequent in study participants with peptic ulceration but no significant association was shown. Smoking status was only reported by one study (Souod et al. 2015). They reported correlations between *dupA* and patient age, smoking and individuals who suffer flatulence. Whether these associations extend to other researchers in this field is not known.

Helicobacter pylori infection was confirmed as a statistically significant risk factor for DU in this study, though no associations between *cag*PAI or *vacA* types and clinical outcomes were identified. These may be expected but associations are not universally observed (Atherton et al. 1995; Rhead et al. 2007; Basso et al. 2008). There was no significant association between *dupA* status and disease, after controlling for potential confounding by other bacterial virulence factors. Heterogeneity in bacterial virulence factors is insufficient to explain observed disease phenotypes and host genetic polymorphisms, particularly in IL-1β and TNF-α, are important factors for clinical outcome (Datta De and Roychoudhury 2015; Miftahussurur and Yamaoka 2015), though are best described for their role in gastric cancer pathophysiology (El-Omar et al. 2000; Macarthur et al. 2004; Snaith and El-Omar 2008). Only one study examined the relationship between IL-1β polymorphisms and *dupA* (for IL-1β-31 and IL-1β-511) and found no association (Zhang et al. 2008).

In addition to the association between *dupA* and DU, there was evidence from meta-analysis of a positive association between *dupA* and GU. There was no clear overall relationship for GC, with substantial heterogeneity precluding formal meta-analysis. The initial report that *dupA* is a protective factor against cancer has not been substantiated.

The risk of GU was higher in individuals colonised by *dupA*+ strains, with summary OR of 2.1 (95% CI 1.3-3.4). This was consistent across the majority of analyses. Again, the association with disease was driven by studies from the Eastern region. The equivalent risk of GU was approximately 75% higher for *dupA*+ vs. *dupA2*/*dupA*– strains. However, 70% of GU cases occurred with *dupA2*/*dupA*– infections. There was no strong evidence of publication bias. The previous meta-analysis found no association

for GU (Shiota et al. 2010), though these populations were excluded in this study. Hussein (2010) reported an association for South America but not for East Asia.

There were no GC cases in this study. Meta-analysis was not performed in light of the substantial residual heterogeneity. Shiota et al. (2010) did perform a meta-analysis, and summary ORs were consistently non-significant in all analyses. They were able to overcome the significant heterogeneity in their analysis by excluding one South American study. Negative associations between GC vs. control and *dupA* were reported only for Brazilian and Columbian study populations (Hussein et al. 2010). Reported associations were also inconsistent for GC vs. control, with 2 negative and 3 positive associations reported (Table 3.9). One study enrolled Japanese patients with PUD and during follow-up found that there was a reduced risk of developing gastric cancer for *dupA*+ compared with *dupA*– isolates (Imagawa et al. 2010). In terms of pre-malignant pathology, conflicting associations have been reported between *dupA* and dysplastic changes in non-malignant tissues, with 17% of Iranian patients with dysplasia colonised by *dupA*+ strains vs. 70% without dysplasia (Douraghi et al. 2008) and 42% vs. 17% respectively in South Korea (Kim et al. 2014).

3.5.3 Strengths, weaknesses and future work

The main strength of this study is the comprehensive genotyping used to determine *dupA* status, including both antral and corporal biopsies. Our study included matching of controls to cases by sex and age. Confounders were recorded and reported, though multivariate analysis had been planned this was not necessary.

The main weakness of this study was its smaller size such that it may be relatively underpowered. Reported study populations ranged from 30 to 360 individuals (median 120), so this study lies between the first and second quintiles.

Some studies increased power by reporting outcomes per isolate with more than one isolate per patient (Kim et al. 2014) or by assigning more than one clinical outcome per patient (Souod et al. 2015). In this study, results for 14 paired isolates were available so could have also been analysed. However, this approach undermines the basis of case-control studies as data are not independent and was a significant contributor to the heterogeneity seen in meta-analysis.

Culture was not available in the Nottingham study population for 19% of participants colonised with *H. pylori* (28/148). This is in line with expectations, with reported

sensitivity between 80 and 95% under optimal conditions (Mégraud and Lehours 2007). Several authors undertook genotyping directly on templates prepared from gastric biopsies (Table 3.11), including one study that reported using these templates to fully classify *dupA* as intact and long-type (Hussein et al. 2015), though most studies at lower risk of bias prepared genomic DNA from confluent plate cultures as in this study. Further work to fully genotype the remaining 68 cultured strains should be considered, potentially alongside further work to optimise biopsy-based typing compared to the culture-based results, such that 28 more strains may potentially also be genotyped. Use of the ChargeSwitch® bacterial genomic DNA kit (Invitrogen) was planned initially for 34 strains, as magnetic purification methods have been shown to be preferable in the minimisation of PCR inhibitors co-purified with *H. pylori* DNA from more challenging samples (Enroth and Engstrand 1995; Monteiro et al. 2001; Horemans et al. 2011). Nested PCR directly on biopsy specimens, intended to address false negative results from low bacterial counts and PCR inhibitors, has been proposed as the gold standard to identify and classify *H. pylori* infection (Patel et al. 2014).

The disadvantage with these methods is that they are time-consuming and may not permit full and unambiguous classification of the virulence genotypes of each strain. Primer design can have a marked impact on sensitivity to detect *dupA* (Abadi et al. 2014). There is some evidence from *H. pylori* genomes of a variant form of *dupA* that shares approximately 60% identity and may encode a homologous protein (Fischer et al. 2010). It is necessary to characterise other virulence factors and, for example, some authors examined 7 or 8 loci by PCR in characterising the *cag*PAI (Jung et al. 2012; Wang et al. 2013). One alternative approach is whole genome sequencing using novel methodologies, then proceeding to assembly and annotation. However, this is still costly for multiple strains, time-consuming and approaches to assembly are potentially open to bias. Rapid, alignment-free genome comparison is possible using feature frequency profiles (Sims et al. 2009). This can be used as a basis for *in silico* PCR using bioinformatics tools (Kruczkiewicz et al. 2013) and for virtual genotyping and sequencing of *H. pylori* and other pathogenic bacteria (Dr Arnoud van Vliet, personal communication). A pilot study was planned to sequence a representative set of *H. pylori* clinical isolates by next generation sequencing, targeted workflow and analysis to provide data on virulence determinants, and validate this against PCR and conventional sequencing to identify SNPs. Unfortunately, the cost was prohibitive.

Some used RT-PCR to further classify *dupA* status (Nguyen et al. 2010; Alam et al. 2012). The primers developed by Nguyen et al. amplify a region closer to the 3' of *dupA* than the *dupA_RI* primers reported in Section 2.8.7. With respect to J99 annotation, the 349 bp amplicon encompasses 1271-1619 of *jhp0917-jhp0918*. Recently, it was reported that a DupA antibody has been successfully developed (Wang, Chen et al. 2015), though this is yet to be utilised in case-control studies of clinical outcomes.

The overarching limitation with these approaches is that they are observational and causality cannot be inferred. For example, there was evidence from our systemic review that the apparent association of *dupA* and duodenal ulcer may be confounded by patient age (Section 3.4.7). Gomes et al. (2008) reported that 100.0% of isolates from a paediatric population were *dupA*+, using 4 primer pairs and partial sequencing in 18% of strains. The prevalence of *dupA* was significantly higher in these than in strains from adults (89.5%, $P < 0.001$). That 25% of children infected with *H. pylori* had duodenal ulceration is unusual – the figure is usually less than 10% (Sýkora and Rowland 2011), though the children recruited are older on average. However, the only other paediatric study population, also from Brazil, had a lower prevalence of *dupA* than the adult population (37.0% vs. 45.7%, $P = 0.257$). Larger age- and sex-matched case-control studies are required; a conclusion shared by Shiota et al. (2010).

However, studies without longitudinal follow up cannot account for micro-evolution or infection by multiple strains. Matteo et al. (2010) separately cultured single colonises of *H. pylori* from 6 different gastric niches (3 antral and 3 corporal) in 40 Argentinian patients and, in 2 of the participants, obtained further samples after one year following eradication therapy failure. They used 4 primer sets and partial sequencing of some PCR products. In around one quarter of patients (9/40), there were inter-niche differences in whether *dupA* was present or absent. In 5 cases, the 3 niches in the antrum and corpus showed opposite *dupA* status, although randomly amplified polymorphic DNA PCR suggested that the strains were otherwise identical. In 8 cases, inter-niche genetic differences seemed to represent the diversification of a single strain. Data from the 2 participants with follow up biopsies suggested microevolution of *dupA*, with both loss and acquisition of mutations in *dupA* observed, resulting in a truncated gene. In one case following eradication therapy, loss of *dupA* was shown despite the strains being otherwise identical. Kim et al. (2014) reported 354 clinical isolates obtained from 240 patients. Fifty-seven patients (24%) were identified as being colonised by non-identical

strains (*cagA*, *vacA* genotypes, *dupA*, *iceA* genotypes and *oipA* virulence factors were studied), though the variation in *dupA* specifically was not reported. For all 14 cases in our study where *dupA* status was available for antrum and corpus, the full sequences were identical. Therefore, where *dupA* status was available for only the antrum or the corpus, this was taken to be representative of the dominant infection in that host. In addition, even in mono-colonised hosts, genes may be lost *in vivo* (Israel et al. 2001) or phase-regulated (Yamaoka 2008). There are no other comparative reports of inter- and intra-niche diversity of *dupA* available. Virulence gene microevolution has been shown to be common in other settings, such as differences in *cagA* and *vacA* status between individual members of the same families who share a common parent strain of *H. pylori* (Argent et al. 2008). It is not certain if the isolated strain used for culture was the dominant strain, or whether other colonising organisms with different virulence profiles might be the major bacterial contributors to pathogenesis.

Another important hypothesis to consider is that *dupA* and *tfs4* function are only required at certain points during the potentially life-long interaction between *H. pylori* and its human host. This is suggested by *tfs4* fragmentation (Delahay, unpublished observation), polymorphism between *dupA* alleles and evidence for microevolution of strains within the gastric niche. It is possible that *dupA* might be important for initial colonisation and then be lost or modified during long-term infections, in which age-dependent changes in the pattern of gastric adherence molecule expression occur, or atrophic gastritis and pre-malignant changes develop. This would occur prior to sexual maturity and peak reproductive age of the host, so *H. pylori* strains that still possess *dupA* could be passed on and would still persist in the population. Therefore, if *dupA* is lost over time then the positive association with DU (and the inverse association with GC observed by some) could simply be the result of confounding by age at the time of diagnosis and strain isolation for genotyping.

Except for Imagawa et al. 2010, in all these studies *dupA* status was determined at the point that endoscopy was performed, which was after the development of symptoms that necessitated the endoscopy. Thus, it is not possible to comment on a putative role for *dupA* in the future development of DU. As in Imagawa, it may be possible to retrospectively undertake *dupA* typing in a cohort of *H. pylori*-infected individuals that has already been prospectively followed for the development of gastrointestinal disease. Alternatively, a large longitudinal cohort study would be necessary, most probably in

Asian centres. It was not possible to address this prospectively with children or adults in Nottingham during the time-frame of this work. Insufficient data were reported for meta-regression by sex and age, where the demographics of case groups and controls are entered as separate study populations, to be a viable option. A further strategy would be to perform an individual patient data meta-analysis by contacting the study authors to request patient-level data available for any potential confounders and these demographic details in particular.

Other study designs could be considered to test the hypothesis that a functionally intact *dupA* system has a specific aetiological role in the pathogenesis. Animal models provide powerful tools to investigate disease pathophysiology and mechanisms in *H. pylori*-associated gastric carcinogenesis and other gastrointestinal conditions such as inflammatory bowel disease, however, variables such as animal breed and housing conditions can have a major impact on results (Oertli and Müller 2012; Rogers 2012; Schoeb and Bullard 2012; Yu et al. 2014). The generalisability of their findings to humans is questionable and open to challenge. The microbiological and functional characterisation of *dupA*, *tfs4* and their products are currently at too early a stage to ethically undertake hypothesis testing using animal models.

3.5.4 Conclusion

Overall, a universal relationship has not been identified between *dupA* and specific clinical outcomes. In Asian countries, the original finding of increased risk of DU in those with *dupA*+ strains is confirmed. But the risk of GU is also increased. Reports of negative associations with GC are relatively few and inconsistent, and the relationship if any between *dupA* and cancer risk remains uncertain. Studies have been observational and open to confounding by other parameters, so no conclusions on a causal role for *dupA* in human gastroduodenal diseases can be inferred. The majority of cases of peptic ulceration occur in the absence of *dupA*.

Whether *dupA* is legitimately the first disease-specific bacterial marker for an increased risk of duodenal ulceration and protection from gastric malignancy has not been confirmed. Indeed, the currently available evidence overall suggests that this is not the case, though it might be in some cases. Much like other *H. pylori* virulence factors, *dupA* is best considered as a modifier of disease risk in certain populations.

The next chapter examines potential mechanisms that might underlie a relationship between *dupA* and gastroduodenal diseases, and its role in mucosal inflammation.

4. Results Two – Is the *dupA* status of clinical isolates associated with the key pathogenic features of duodenal ulceration?

Helicobacter pylori infection is characterised predominantly by two diverging clinical sequelae – a proportion of colonised patients will develop duodenal ulcer disease (with duodenal and pre-pyloric erosions and ulceration), whilst others will progress down a pathway linked to gastric ulceration, pre-malignant histological changes and adenocarcinoma. Duodenal ulcers may arise when:

1. gastric inflammation is intense and corpus-sparing in distribution,
2. bacterial colonisation density is antral-predominant, and
3. the gastric mucosal immune responses are pro-inflammatory.

The *H. pylori* virulence factor *dupA* is the only bacterial factor that has been described as disease-specific in promoting duodenal ulceration. These pre-clinical endpoints might be expected, despite the lack of association with disease outcome overall, if *dupA* has a role in DU pathogenesis. Increased gastric acid output is another key criterion for duodenal ulceration, though was not evaluated in this study.

Therefore, we hypothesised that *dupA* status would be associated with these pathogenic features of duodenal ulceration. The overall aim of this chapter was to test this hypothesis. The aims of this chapter were:

1. to ascertain the intestity and distribution of gastric inflammation with respect to *dupA* status,
2. to identify any association of bacterial colonisation density with *dupA*, and
3. to undertake a detailed characterisation of the gastric mucosal immune responses at protein-level and mRNA-level according to *dupA* status.

The results of this work, and the comprehensive multi-modal characterisation of study participant phenotypes, are presented in this chapter.

4.1 Gastric inflammation

Gastric mucosal biopsies were prepared and then examined alongside an expert gastro-intestinal histopathologist, blinded to other factors, to provide scores of gastritis severity according to the updated Sydney system (Dixon et al. 1996). Biopsies from *H. pylori*-infected study participants were characterised (Table 4.1). Histological data were available for 72% (106/148) of the *H. pylori*-positive participants in the Nottingham study population. Of those with *dupA* status data, results for paired gastric biopsies from the antrum and corpus were available in 96% of cases (50/52, antrum only for 1 participant, no histological data for 1 participant).

Table 4.1 – characterised histological samples

Participant group	Total (n) [%]	female (%)	mean age ± sd (years)	Antrum only (n)	Corpus only (n)	Paired antrum and corpus (n)
All processed samples	127	56	53 ± 15.0	5	0	122
Hp positive (all patients)	106 [72%]	57	53 ± 14.9	4	0	102
Hp positive with culture available	82 [68%]	52	54 ± 15.3	2	0	80
***Hp* positive with *dupA* status data**	51 [98%]	55	54 ± 14.7	1	0	50

Hp, H. pylori.

No clear differences were found in the intensity or distribution of gastritis by *dupA* status, though antral active inflammation was more marked for non-*dupA1* strains.

The results are shown in Table 4.2. Active inflammation in antral biopsies was actually more marked for non-*dupA1* strains using the chi-square test for trend, which has higher power, but not using Fisher's exact test to compare the lowest two and the highest two graded inflammation scores. No other statistically significant differences were found. The distribution of gastric inflammation was not shown to be corpus-sparing for *dupA1* strains (Table 4.3).

Table 4.2 – gastric inflammation histological scores by *dupA* status

		antrum				corpus			
***dupA* status**	**score**	**chronic inflammation**		**active inflammation**		**chronic inflammation**		**active inflammation**	
		n	**%**	**n**	**%**	**n**	**%**	**n**	**%**
dupA1	**0**	0	0	5	22	0	0	11	48
	1	1	4	3	13	11	48	3	13
	2	19	83	15	65	10	43	9	39
	3	3	13	0	0	2	9	0	0
non-*dupA1*	**0**	0	0	1	4	0	0	8	30
	1	5	18	3	11	16	59	6	22
	2	21	75	22	79	10	37	13	48
	3	2	7	2	7	1	4	0	0
0/1 vs. 2/3		*P* = 0.204		*P* = 0.107		*P* = 0.570		*P* = 0.577	
Trend		*P* = 0.459		***P* = 0.025**		*P* = 0.341		*P* = 0.289	

dupA1 vs. non-*dupA1* was analysed using two-tailed Fisher's exact tests (2×2 contingency tables for scores 0/1 vs. 2/3) and overall using chi-square test for trend.

chronic inflammation, mononuclear cell infiltration; active inflammation, neutrophil infiltration (activity); 0, absent; 1, mild; 2, moderate; 3, marked or severe.

Table 4.3 – predominant distribution of gastric inflammation by *dupA* status

***dupA* status**	**predominant distribution of gastric inflammation**	**n**	**%**
dupA1	**antral**	15	65
	pan-gastritis	6	26
	corporal	2	9
non-*dupA1*	**antral**	20	74
	pan-gastritis	5	19
	corporal	2	7
corpus-sparing (antral) vs. others		*P* = 0.548	

dupA1 vs. non-*dupA1* was analysed using a two-tailed Fisher's exact test.

4.2 Bacterial colonisation density

Bacterial colonisation density scores for the gastric antrum and corpus are included in the updated Sydney system using a four-point ordinal scale (Dixon et al. 1996). No statistically significant differences were found (Table 4.4). Therefore, a quantitative method was employed.

Table 4.4 – bacterial colonisation density histological scores by *dupA* status

		antrum		corpus	
***dupA* status**	**score**	***H. pylori***		***H. pylori***	
		n	**%**	**n**	**%**
dupA1	**0**	1	22	0	0
	1	5	13	10	44
	2	6	65	7	30
	3	11	0	6	26
non-*dupA1*	**0**	1	4	0	0
	1	8	11	18	67
	2	5	79	3	11
	3	14	7	6	22
0/1 vs. 2/3		*P* = 0.761		*P* = 0.153	
Trend		*P* = 0.906		*P* = 0.254	

dupA1 vs. non-*dupA1* was analysed using two-tailed Fisher's exact tests (2×2 contingency tables for scores 0/1 vs. 2/3) and overall using chi-square test for trend.

chronic inflammation, mononuclear cell infiltration; active inflammation, neutrophil infiltration (activity); 0, absent; 1, mild; 2, moderate; 3, marked or severe.

4.2.1 Bacterial colonisation density by quantitative PCR

Quantitative PCR (qPCR) was used to assess bacterial colonisation density. Templates containing combined bacterial and human DNA were prepared from gastric biopsies. This is expressed as absolute copy numbers of *H. pylori* genomes per human cell, respectively determined against standard curves of *16S rRNA* and human *GAPDH*. This method was developed and validated by Dr Sapna Patel, though was revised and re-established for this study (Methods Section 2.8.5).

Paired antrum and corpus biopsies were characterised (Table 4.5). The number of *H. pylori* genomes per human cell was correlated with *H. pylori* density scores from histology (data not shown).

Table 4.5 – characterised samples for colonisation density (qPCR)

Participant group	Total (n) [%]	female (%)	mean age ± sd (years)	Paired antrum and corpus (n)
All processed samples	30	53	53 ± 15.5	30
Hp positive (all patients)	27 [18%]	48	52 ± 15.8	27
Hp positive with culture available	26 [22%]	46	53 ± 16.1	26
***Hp* positive with *dupA* status data**	23 [44%]	43	54 ± 16.9	23

Hp, *H. pylori*.

Bacterial colonisation density was not shown to be antral-predominant for *dupA1* strains. No difference in the pattern of bacterial colonisation was found.

The number of *H. pylori* genome copies per human cell was expressed as a ratio by dividing the antral result by the corporal result. Values over one indicate antral-predominant colonisation. There was no significant difference between the median antrum:corpus ratio for *dupA1* clinical isolates of 0.73 (IQR 0.44-11.40, >1: n=4/10) vs. that for non-*dupA1* clinical isolates of 1.44 (0.56-14.80, >1: n=8/13, $P = 0.637$).

4.3 Mucosal immune responses

Gastric mucosal immune responses were characterised at protein-level and at mRNA-level. Cytokine responses represent a complex network of signalling and interaction between multiple cell types. The expression of multiple cytokines was determined.

4.3.1 Optimising the quantification of multiple cytokines present at low concentrations in human gastric mucosal biopsies

The quantification of multiple cytokines in small tissue biopsies presents a significant challenge, particularly when some are present at low concentration. Substantial work was first undertaken to optimise the sample preparation protocol (comparing different tissue processing methods and extraction buffers) and to evaluate the performance of three commercial Luminex kits (technical performance, sensitivity, linear dynamic range, accuracy and precision). This work was published under co-first authorship and with open access in the Journal of Immunological Methods (Staples and Ingram et al. 2013), available at http://doi.org/10.1016/j.jim.2013.04.009 or via PMID 23644159.

4.3.2 Mucosal immune responses at protein-level

One hundred and seventy-six gastric mucosal biopsies were processed and assayed using the optimised method. Characterised antrum only, corpus only and paired biopsies from the study population were identified (Table 4.6). One hundred and one biopsies from 84 participants were included in the analysis of mucosal immune responses at protein-level between *H. pylori*-infected and uninfected participants and with respect to *dupA* status.

This analysis was focussed on the chemokine IL-8, the pro-inflammatory cytokines IL-1β, IL-6 and TNF-α, the principle T-helper cell subset effector cytokines (IFN-γ, IL-17A, IL-4 and IL-10) and the pro-inflammatory mediators of the IL-12/23 family.

Table 4.6 – characterised mucosal immune responses at protein-level

Participant group	Total (n) [%]	female (%)	mean age ± sd (years)	Antrum only (n)	Corpus only (n)	Paired antrum and corpus (n)
All processed samples	147	52	53 ± 15.1	115	3	29
Study population	117 [43%]	52	52 ± 15.2	89	3	25
Hp positive (all patients)	64 [43%]	52	52 ± 15.7	50	2	12
Hp positive with culture available	49 [41%]	47	53 ± 16.4	39	1	9
***Hp* positive with *dupA* status data**	35 [67%]	46	54 ± 15.2	27	1	7
Hp negative (all patients)	53 [42%]	53	52 ± 14.6	39	1	13
***Hp* negative no prior eradication**	49 [41%]	53	52 ± 14.8	38	1	10

Hp, H. pylori.

No difference in mucosal IL-8 levels was found for *dupA1* vs. non-*dupA1* strains.

First, mucosal IL-8 concentrations were determined (Figure 4.1). There was no evidence of increased IL-8 induction in participants colonised by *dupA1* strains, nor were levels higher in *dupA1*/*tfs4* complete strains (shown in red).

The highest two antral *dupA1* data points are for strains lacking at least two of the putative *tfs4* genes tested. The highest four antral non-*dupA1* data points are for *dupA* negative strains lacking between one and four *tfs4* genes. The variation does not appear to be explained by genotypic data for other bacterial virulence factors.

The number of corpus biopsies with valid data was not sufficient for analysis, with exclusions for technical reasons during quality control (inadequate bead counts, Section 2.9.1). See Section 4.3.3 for these data at mRNA-level.

Marked antral induction of IL-8 expression was observed in participants infected with *H. pylori*. IL-8 was correlated with both *cag*PAI and *vacA* status.

This finding was unexpected so we studied other participant and strain characteristics.

Mucosal IL-8 concentrations were markedly higher in patients with *H. pylori* infection compared with uninfected participants (26.8-fold higher median conc., $P < 0.001$).

In antral mucosal biopsies, IL-8 production was significantly increased for *cag*PAI-positive vs. *cag*PAI-negative isolates (median [IQR], 38.9 pg/mg protein [19.0-122.1] vs. 16.6 pg/mg protein [7.7-41.4], n= 27 vs. 23, $P = 0.018$).

There was also a correlation for *vacA* status. Firstly, s1m1i1 vs. s2m2i2 showed signficiantly increased mucosal IL-8 (46.6 pg/mg protein [16.3-98.5] vs. 3.1 pg/mg protein [2.9-6.3], n=17 vs. 4, *cag*PAI-positive in 82% vs. 25%, $P < 0.001$). This was driven mainly by *vacA* s type, though there were differences for the m and i regions that did not reach significance (s1 vs. s2: 36.2 vs. 3.1 pg/mg protein, n=35 vs. 5, $P < 0.001$; m1 vs. m2: 46.6 vs. 27.4 pg/mg protein, n=17 vs. 22, $P = 0.255$; i1 vs. i2: 36.2 vs. 19.4 pg/mg protein, n=25 vs. 14, $P = 0.133$).

The finding of no association between *dupA* status and IL-8 was reproducible.

The IL-8 results for *H. pylori* status and other virulence factors were in line with expectations. Therefore, we sought to confirm the observation that there was no association between mucosal IL-8 and *dupA* status at protein-level. This observation used Luminex assays to analyse IL-8 concentrations (MILLIPLEX High Sensitivity Human Cytokine Panel) with valid data for 28 samples [12 *dupA1*, 16 non-*dupA1*] of 34 antral *H. pylori*-positive biopsies with *dupA* status data. IL-8 data were not available for some samples due to exclusions for technical reasons during quality control (inadequate bead counts, Section 2.9.1). Of the 176 samples assayed in total, 28 (16%) were affected by lower bead counts, perhaps related to bead aggregiation due to the use of relatively viscous tissue homogenates as samples (Staples and Ingram et al. 2013) or a limitation of this particular assay panel.

To confirm the performance of the Luminex assays, some samples were independently re-tested using a separate assay panel (MILLIPLEX Human Cytokine/Chemokine Panel [CP1]). In contrast to the other assay panel, none of the samples tested were affected by lower bead counts (0/71). Note that the samples tested were separate aliquots, so there were no differences in storage conditions or freeze-thaw cycles. There was a strong correlation between panels for IL-8 ($R^2 = 0.839$, $P < 0.001$), though the second panel reported higher IL-8 concentrations. This panel confirmed the finding that IL-8 and *dupA* status were not associated (*dupA1* vs. non-*dupA1*: 156.6 pg/mg protein [102.5-330.2] vs. 235.6 pg/mg protein [65.6-289.9], n=13 vs. 15, $P = 0.928$).

Finally, we used a different multiplex technology (MSD V-PLEX assays) to confirm these observations. Luminex assays use multiple sets of paramagnetic beads, pre-coated with capture antibody and each fluorescently colour-coded to be identifiable on a dedicated flow cytometry platform. Sandwich immunoassays are built around these beads, with analyte quantification via a biotinylated detection antibody-streptavidin-phycoerythrin cascade. In contrast, MSD assays use multi-spot microplates with multiple high binding carbon electrodes in the bottom of each well, each pre-coated with a capture antibody. Detection antibodies are conjugated to electrochemiluminescent labels, which generate light when electrically stimulated by an MSD instrument in the presence of an appropriate chemical environment. Potential advantages include high sensitivity, broad dynamic range, low background, and rigorous validation of performance and reference standards. All the IL-8 observations for the Luminex panels had been within the quantifiable range of the assay and above the lowest point in the standard curve, though were towards the lower end of the dynamic range.

Sixty antral samples were re-tested for IL-8 using (MSD V-PLEX assays), with n=13 for *dupA1* strains, n=15 for non-*dupA1* strains, n=19 from *H. pylori*-negative participants and n=13 not characterised. Results from this method were correlated with those for the original Luminex assays (R^2 = 0.787, P < 0.001). The findings were identical, with no association between IL-8 and *dupA* status (*dupA1* vs. non-*dupA1*: 251.5 pg/mg protein [171.9-251.5] vs. 284.1 pg/mg protein [112.0-382.5], n=13 vs. 15, P = 0.821) and with a 24.0-fold higher median concentration for infected vs. uninfected participants (263.0 vs. 11.0 pg/mg protein, n=28 vs. 19, P < 0.001). This was similar to the 26.8-fold increase seen using the MILLIPLEX panel (Figure 4.1).

Therefore, the lack of association between mucosal IL-8 concentrations and *dupA* status in our study population was independently reproduced in two other protein-level assays. These observations were confirmed at mRNA-level (reported in Section 4.3.3).

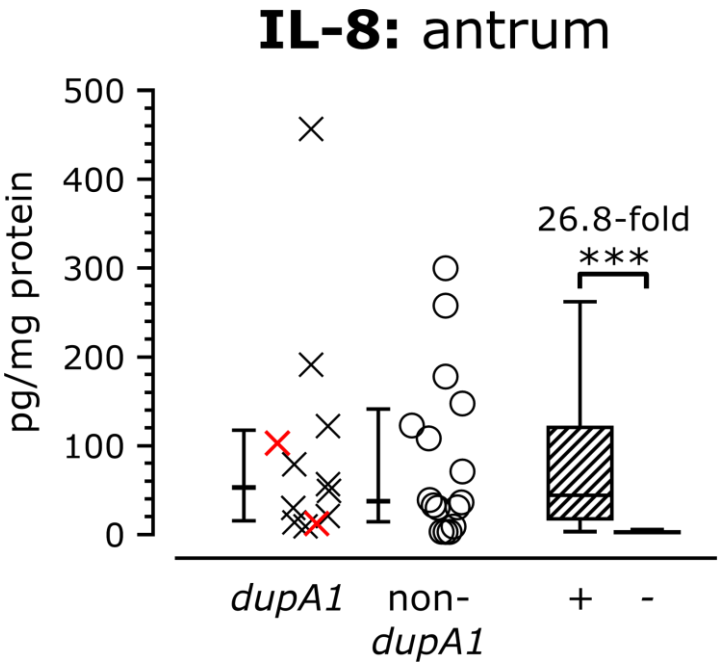

Figure 4.1 – mucosal concentrations of IL-8

IL-8 mucosal concentrations were determined in homogenised snap frozen human gastric biopsies in duplicate using MILLIPLEX multiplex assays (HS kit) and adjusted for total protein concentration.

Clinical isolates typed as *dupA1* are shown by X symbol (includes *dupA1*/*tfs4* complete strains highlighted in red; n=12) and those typed as non-*dupA1* are shown by O symbol (includes *dupA2*, *dupAx* and *dupA* negative strains; n=16). *H. pylori*-infected participants (+, n=28) are shown by a hatched box and uninfected participants (–, n=45) by a white box. The horizontal and error bars show median values and inter-quartile ranges (IQRs) respectively. The box-and-whisker plots show median values, IQRs and 10-90th centiles. Data for the corpus are not shown as these were limited (n=1 *dupA1*, n=2 non-*dupA1*, n=10 uninfected).

Data for *H. pylori*-infected vs. uninfected participants and for *dupA1* vs. non-*dupA1* strains from typing of these clinical isolates were separately compared by Mann-Whitney U tests. Statistically significant differences are shown above the plotted data with the fold-difference in group medians (* $P < 0.05$, ** $P < 0.01$, *** $P < 0.001$).

There was some evidence that IL-1β expression was slightly higher in association with *dupA1* strains.

Next, the concentrations of a panel of pro-inflammatory cytokines implicated in the innate immune response were determined (Figure 4.2).

There was evidence for significantly higher IL-1β expression in the antral mucosa of those infected with *dupA1* strains vs. non-*dupA1* strains (median [IQR], 0.18 pg/mg protein [0.08-0.31] vs. 0.09 pg/mg protein [0.05-0.13], n=14 vs. 18, P = 0.039). However, this did not reach statistical significance with MSD assays (23.80 pg/mg protein [10.30-28.60] vs. 10.80 pg/mg protein [6.35-19.90], n=13 vs. 15, P = 0.316, note that the reference standards are different between these methods). The *dupA1*/*tfs4* complete strains were clustered together with the other *dupA1* strains.

Although a statistically signficant difference was shown for IL-1β, this may or may not be biologically or clinically significant. The fold increase in median expression was 2.0-fold higher, so there may be residual confounding. This cytokine was also quantified as being at very low concentration, though the numerical abudance differed between methods. Moreover, the statistically significant finding at protein-level was not confirmed by MSD assays and *IL1B* expression data at mRNA-level were not available.

***H. pylori*-infected participants had significantly higher IL-6 and TNF-α concentrations detectable in their gastric antral mucosa.**

No significant differences in IL-6 or TNF-α concentrations were found relative to *dupA* status, which was confirmed using MSD kits (data not shown). Conversely, *H. pylori* infection was associated with higher levels of IL-6 (2.7-fold) and TNF-α (11.1-fold) as shown in Figure 4.2. These observations were replicated using MSD assays (respectively 2.4-fold higher [P = 0.001] and 6.4-fold higher [P < 0.001]).

Infection with *H. pylori* was associated with significantly higher expression of the Th17 cytokine IL-17A and of the Treg cytokine IL-10. There was some evidence for IFN-γ (Th1) and IL-4 (Th2) in addition, though this was less strong.

In this analysis, the expression in gastric mucosa of the principle effector cytokines of human T-helper subsets is reported (Figure 4.3); firstly, for comparisons between *H. pylori*-infected and uninfected participants, secondly, according to *dupA* status.

We found significantly increased concentrations of IL-17A and IL-10 (in both antrum and corpus) and of IL-4 (in the corpus only) in association with *H. pylori* infection. We did not demonstrate any association for IFN-γ at protein-level (though see Section 4.3.3 for the results at mRNA-level). The sensitivity of this assay was 0.06-0.62 pg/mL across 5 runs (median 0.14 pg/mL) and overall 56% (87/155) of sample concentrations fell below the lower limit of quantification. This analysis was repeated using MSD assays for a proportion of these samples, as these assays have a greater resolution at the limits of detection. In this case, 49% (35/71) below the limit of detection for this assay of 0.28 pg/mL. However, a small but statistically significant difference between *H. pylori*-infected and uninfected participants was then identified (1.7-fold, $P = 0.008$, Appendix Figure 7.5).

There was some evidence that *dupA1* clinical isolates were associated with higher concentrations of IFN-γ in antral gastric mucosa.

There was evidence for significantly higher IFN-γ expression in the antral mucosa of those infected with *dupA1* strains vs. non-*dupA1* strains (median [IQR], 0.33 pg/mg protein [0.13-0.51] vs. 0.12 pg/mg protein [0.04-0.21], n=12 vs. 16, $P = 0.008$). However, this did not reach statistical significance with MSD assays (1.22 pg/mg protein [0.45-2.13] vs. 0.67 pg/mg protein [0.46-1.46], n=13 vs. 15, $P = 0.446$). The *dupA1*/*tfs4* complete strains were clustered together with the other *dupA1* strains.

IL-12/23p40 family cytokines were not shown to differ in association with *dupA* status. Participants infected with *H. pylori* were found to have higher antral levels of IL-12p70 and lower antral levels of IL-23.

Finally, given these observations the concentrations of IL-12/23p40, IL-12p70 and IL-23 were analysed (Figure 4.4). No significant differences were observed when comparing *dupA1* with non-*dupA1* strains. IL-12p70 concentrations were slightly increased for *H. pylori*-positive individuals (1.3-fold higher vs. uninfected, $P = 0.050$). Conversely, lower antral mucosal expression of IL-23 was associated with infection (2.1-fold lower vs. uninfected, $P = 0.008$).

Figure 4.2 – mucosal concentration of pro-inflammatory cytokines

IL-1β, IL-6 and TNF-α mucosal concentrations were determined in homogenised snap frozen human gastric biopsies in duplicate using MILLIPLEX multiplex assays and adjusted for total protein concentration.

Clinical isolates typed as *dupA1* are shown by X symbol (includes *dupA1*/*tfs4* complete strains highlighted in red; IL-1β and TNF-α: n=14/4, IL-6: n=13/4 [antrum/corpus]) and those typed as non-*dupA1* are shown by O symbol (includes *dupA2*, *dupAx* and *dupA* negative strains; IL-1β: n=18/2, IL-6: n=17/2, TNF-α: n=18/3). *H. pylori*-infected participants (+, IL-1β: n=32/6, IL-6: n=30/6, TNF-α: n=32/7) are shown by a hatched box and uninfected participants (–, IL-1β and TNF-α: n=46/11, IL-6: n=46/10) by a white box. The horizontal and error bars show median values and inter-quartile ranges (IQRs) respectively. The box-and-whisker plots show median values, IQRs and 10-90th centiles.

Data for *H. pylori*-infected vs. uninfected participants and for *dupA1* vs. non-*dupA1* strains from typing of these clinical isolates were separately compared by Mann-Whitney U tests. Statistically significant differences are shown above the plotted data with the fold-difference in group medians (* $P < 0.05$, ** $P < 0.01$, *** $P < 0.001$).

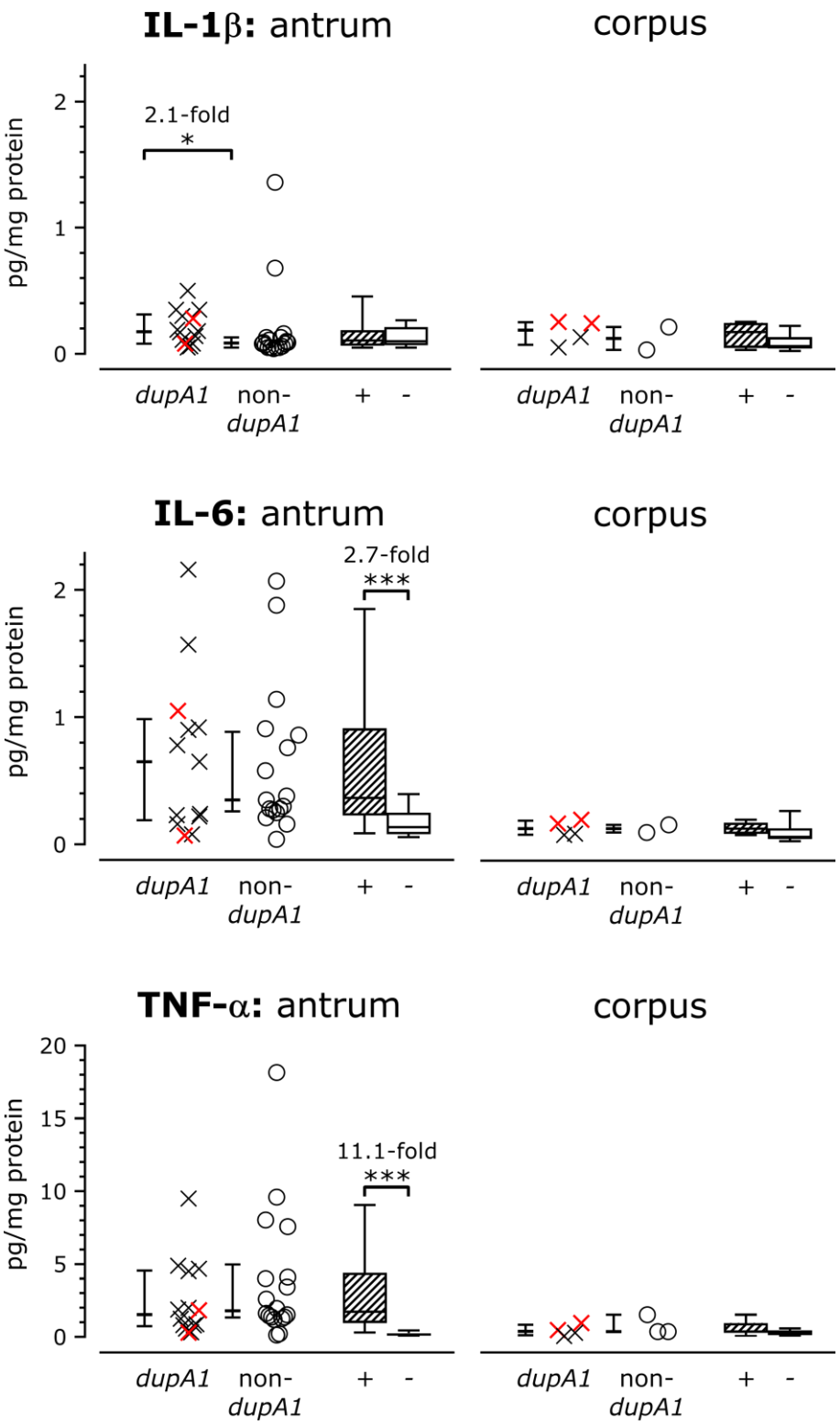

Figure 4.2 – mucosal concentrations of pro-inflammatory cytokines

Figure 4.3 – mucosal concentration of T-helper effector cytokines

IFN-γ (Th1), IL-17A (Th17), IL-4 (Th2) and IL-10 (Treg) mucosal concentrations were determined in homogenised snap frozen human gastric biopsies in duplicate using MILLIPLEX multiplex assays and adjusted for total protein concentration.

Clinical isolates typed as *dupA1* are shown by X symbol (includes *dupA1*/*tfs4* complete strains highlighted in red; IFN-γ: n=12/3, IL-17A and IL-4: n=15/5, IL-10: n=15/4 [antrum/corpus]) and those typed as non-*dupA1* are shown by O symbol (includes *dupA2*, *dupAx* and *dupA* negative strains; IFN-γ: n=16/2, IL-17A and IL-4: n=19/3, IL-10: n=18/3). *H. pylori*-infected participants (+, IFN-γ: n=28/5, IL-17A and IL-4: n=34/8, IL-10: n=33/7) are shown by a hatched box and uninfected participants (–, IFN-γ: n=43/10, IL-17A: n=36/4, IL-4 and IL-10: n=46/11) by a white box. The horizontal and error bars show median values and inter-quartile ranges (IQRs) respectively. The box-and-whisker plots show median values, IQRs and 10-90th centiles.

Data for *H. pylori*-infected vs. uninfected participants and for *dupA1* vs. non-*dupA1* strains from typing of these clinical isolates were separately compared by Mann-Whitney U tests. Statistically significant differences are shown above the plotted data with the fold-difference in group medians (* $P < 0.05$, ** $P < 0.01$, *** $P < 0.001$).

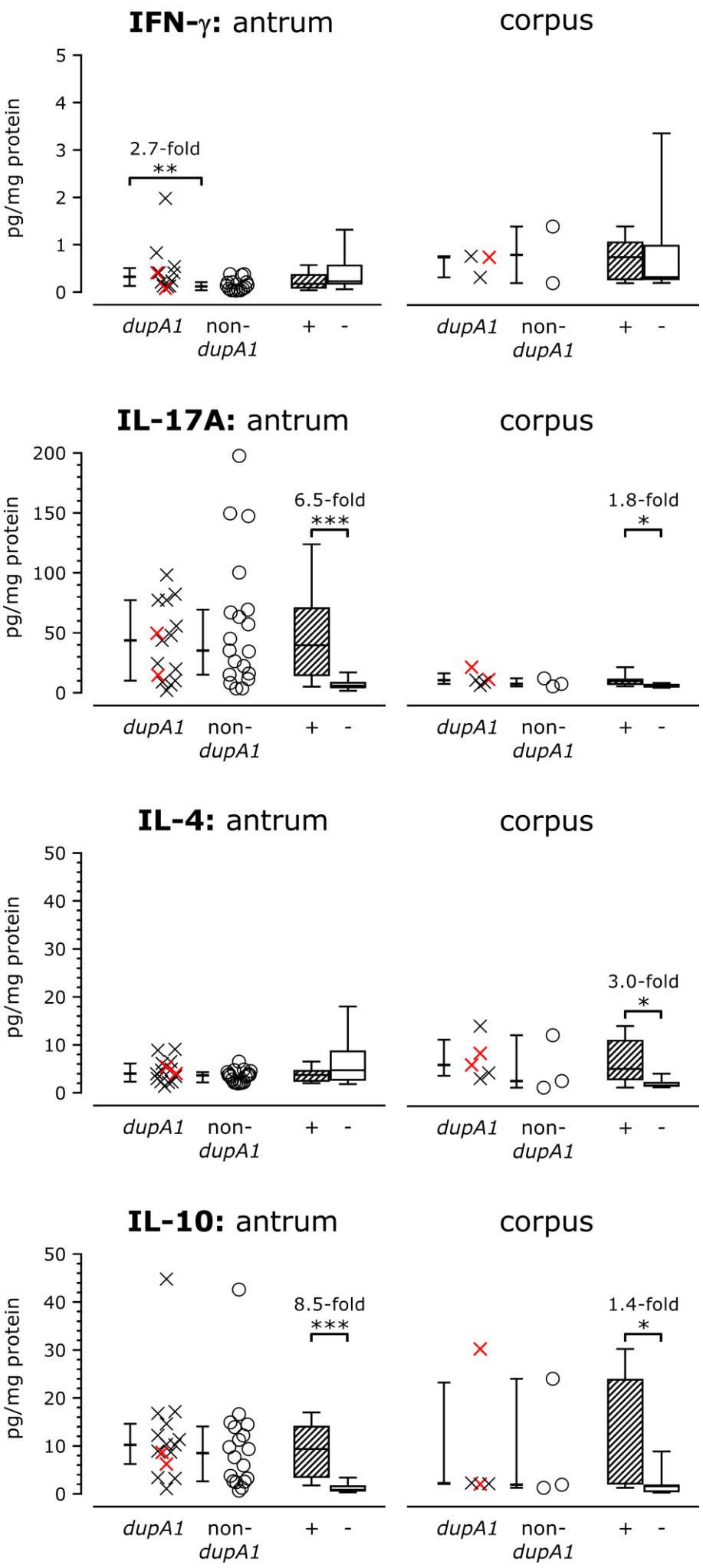

Figure 4.3 – mucosal concentrations of T-helper effector cytokines

Figure 4.4 – mucosal concentration of IL-12/23 family cytokines

IL-12/23p40, IL-12p70 and IL-23 mucosal concentrations were determined in homogenised snap frozen human gastric biopsies in duplicate using MILLIPLEX multiplex assays and adjusted for total protein concentration.

Clinical isolates typed as *dupA1* are shown by X symbol (includes *dupA1*/*tfs4* complete strains highlighted in red; p40: n=13/3, p70: n=12/3, IL-23: n=15/5 [antrum/corpus]) and those typed as non-*dupA1* are shown by O symbol (includes *dupA2*, *dupAx* and *dupA* negative strains; p40: n=15/2, p70: n=17/1, IL-23: n=18/3). *H. pylori*-infected participants (+, p40: n=28/5, p70: n=29/4, IL-23: n=33/8) are shown by a hatched box and uninfected participants (–, p40: n=19/3, p70: n=44/9, IL-23: n=36/4) by a white box. The horizontal and error bars show median values and inter-quartile ranges (IQRs) respectively. The box-and-whisker plots show median values, IQRs and 10-90th centiles.

Data for *H. pylori*-infected vs. uninfected participants and for *dupA1* vs. non-*dupA1* strains from typing of these clinical isolates were separately compared by Mann-Whitney U tests. Statistically significant differences are shown above the plotted data with the fold-difference in group medians (* $P < 0.05$, ** $P < 0.01$, *** $P < 0.001$).

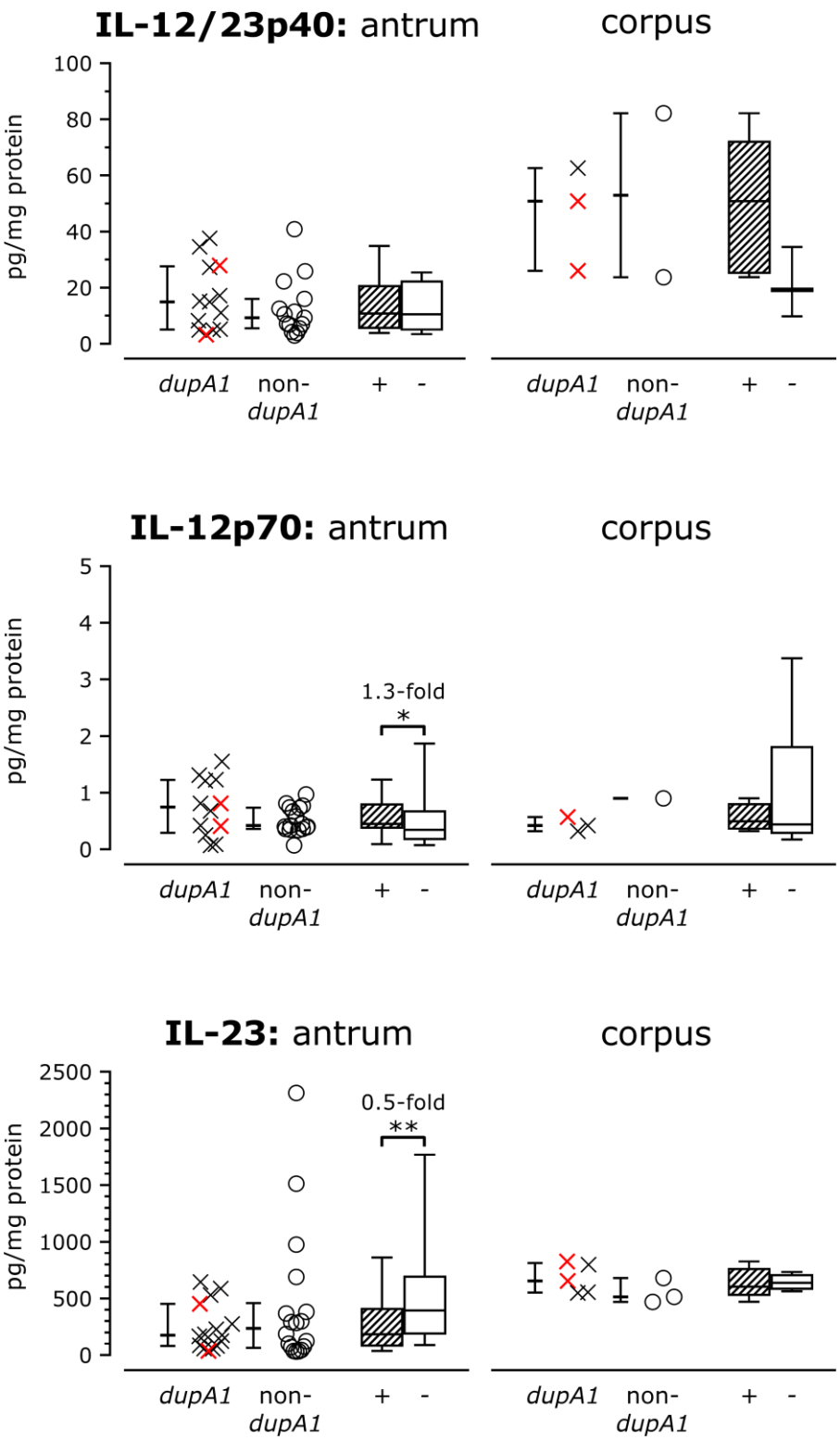

Figure 4.4 – mucosal concentrations of IL-12/23 family cytokines

4.3.3 Mucosal immune responses at mRNA-level

Immune responses at mRNA-level were investigated next, in order to confirm findings at protein-level. Fractions of RNA and DNA of sufficient quality were obtained from 195 gastric mucosal biopsies. Complementary DNA was transcribed and used in RT-qPCR. Characterised antrum only, corpus only and paired biopsies from the study population were identified (Table 4.7). Ninety-nine biopsies from 68 participants were included in the analysis of mucosal immune responses at mRNA-level between *H. pylori*-infected and uninfected participants and with respect to *dupA* status.

This analysis focussed on a subset of those markers investigated at protein-level. We assayed the chemokine *IL8*, the T-helper effector cytokines *IFNG*, *IL17A* and *IL10*, and the pro-inflammatory mediator *IL12B* (that encodes IL-12/23p40). Expression of mRNA was determined relative to a pooled comparator of cDNA prepared from 14 uninfected donors, and expressed as fold difference relative to the reference gene *GAPDH*.

The pooled comparator was used as the RT-qPCR experiments required that a large number of assays be performed, due to numerous samples, the need for multiple technical replicates and controls per 96-well run, and different PCR conditions for different analytes. Therefore, a large pool of comparator was prepared and split into aliquots. In addition, a comparator derived from 14 donors should reduce the potential for biological variability to impact on the results.

The *GAPDH* reference gene was chosen because it is reasonably consistently expressed in human cells for this experimental approach (Robinson et al. 2008) and a single gene was used because of limited sample and feasibility constraints. The MIQE guidelines were used to inform this work (Bustin et al. 2009; Taylor et al. 2010).

Note that samples for 7/68 participants (and 11/99 biopsies) were prepared by Dr Sapna Patel. Data for *IL17A* were provided by Dr Emily Staples (only antral data were available for *IL17A*). The negative comparator was planned, quality controlled by nucleic acid quantification and bioanalyzer, and prepared together with Dr Staples.

Table 4.7 – characterised mucosal immune responses at mRNA-level

Participant group	Total (n) [%]	female (%)	mean age ± sd (years)	Antrum only (n)	Corpus only (n)	Paired antrum and corpus (n)
All processed samples	127	63	54 ± 14.6	56	3	68
Study population	105 [38%]	63	54 ± 14.4	47	3	55
Hp positive (all patients)	73 [49%]	64	53 ± 13.4	24	3	46
Hp positive with culture available	58 [48%]	60	54 ± 13.5	17	3	38
***Hp* positive with *dupA* status data**	38 [73%]	55	55 ± 14.0	14	0	24
Hp negative (all patients)	32 [25%]	61	55 ± 16.4	23	0	9
***Hp* negative no prior eradication**	30 [25%]	59	55 ± 16.6	23	0	7

Hp, *H. pylori*.

In confirmation of data at protein-level, no difference in relative mucosal *IL8* expression was found between *dupA1* and non-*dupA1* strains. Marked increases in relative *IL8* expression were observed in both the antrum and corpus of participants infected with *H. pylori*.

Relative expression of *IL8* mRNA in tissue was determined (Figure 4.5). In support of the findings for cytokine protein induction, there was no evidence that relative mucosal *IL8* expression was increased in the antrum of participants colonised by *dupA1* strains, nor were levels higher in *dupA1*/*tfs4* complete strains (shown in red). The data points with highest relative expression at mRNA-level corresponded to those with highest expression at protein-level. The lack of association between *IL8* and *dupA* status observed for antral biopsies was also replicated in samples from the gastric corpus at mRNA-level. Sufficient protein-level data were not available for this biopsy site.

IL8 expression was markedly increased in both the antrum and corpus for participants infected with *H. pylori* (33.5-fold and 25.6-fold higher relative expression respectively, P <0.001).

Infection with *H. pylori* was associated with significantly higher relative mRNA expression for the Th1 cytokine *IFNG*, the Th17 cytokine *IL17A* and the Treg cytokine *IL10*.

Results are shown in Figure 4.6.

IFNG relative expression was increased in *H. pylori*-infected vs. uninfected antral biopsies (median [IQR], fold difference of 2.4 [1.6-4.3] vs. fold difference of 0.8 [0.5-1.3], n=22 vs. 8, 3.1-fold higher relative expression, P = 0.007). This was similar for the corpus but fell short of statistical significance (median [IQR], fold difference of 2.4 [1.2-3.1] vs. fold difference of 0.9 [0.7-3.0], n=15 vs. 6, 2.7-fold higher relative expression, P = 0.158). No association for IFN-γ was found at protein-level using the Luminex assay. However, a statistically significant difference was identified using a more sensitive assay (see Section 4.3.2 and Appendix Figure 7.5).

We also found significantly increased relative expression of *IL17A* in antral biopsies obtained from participants infected with *H. pylori* vs. uninfected (median [IQR], fold difference of 13.6 [5.7-62.0] vs. fold difference of 0.7 [0.2-2.0], 19.4-fold higher relative expression, P < 0.001). This supports the protein-level IL-17A observation.

Finally, the relative expression of *IL10* mRNA was also increased in infected vs. uninfected participants. This reached significance for corporal biopsies (median [IQR], fold difference of 11.4 [6.1-22.9] vs. fold difference of 1.5 [0.7-2.6], n=21 vs. 6, 7.6-fold higher relative expression, $P < 0.001$). Statistical significance was not shown for antral biopsies (median [IQR], fold difference of 13.9 [4.1-19.5] vs. fold difference of 3.1 [2.0-21.2], n=27 vs. 8, 4.5-fold higher relative expression, $P = 0.195$). Together, these support the observations for IL-10 at protein-level, for which significance was shown for both the antrum and the corpus.

No evidence was found that *dupA1* clinical isolates were associated with different relative expression of *IFNG*. Therefore, taking protein-level and mRNA-level data together, there was no strong evidence that *dupA* status had an impact.

No significant differences in relative mRNA expression were found with respect to *dupA* status of the isolated clinical strain (Figure 4.6). The *dupA1*/*tfs4* complete strains were clustered together with the other *dupA1* strains.

No significant differences in *IL12B* relative expression were found.

In confirmation of the result at protein-level for IL-12/23p40, *IL12B* relative expression did not differ in association with *dupA* status or for *H. pylori*-infected vs. uninfected participants (Figure 4.7). For the latter comparison, this fell short of statistical significance for the antrum (median [IQR], fold difference of 2.7 [0.3-5.3] vs. fold difference of 0.7 [0.5-1.5], n=19 vs. 8, 3.9-fold higher relative expression, $P = 0.087$) and for the corpus (median [IQR], fold difference of 3.1 [0.9-7.0] vs. fold difference of 1.2 [0.7-1.7], n=13 vs. 6, 2.6-fold higher relative expression, $P = 0.122$).

Assays were not performed for *IL12A* (which encodes IL-12p35 that, along with the product of *IL12B*, forms IL-12p70) or for *IL23A* (which encodes IL-23p19 and forms IL-23 along with the product of *IL12B*).

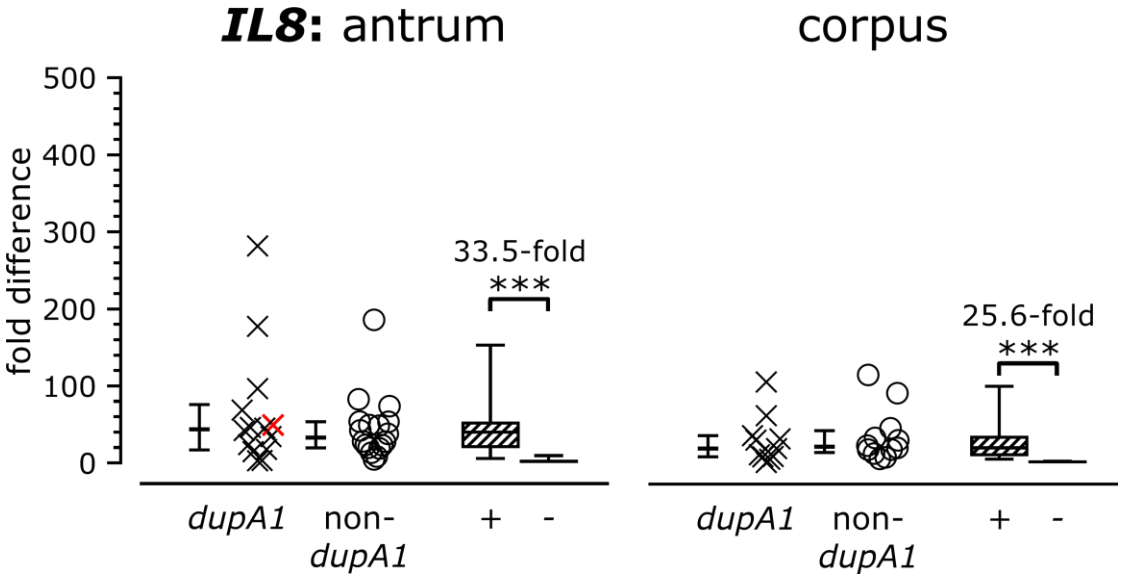

Figure 4.5 – relative mucosal expression of *IL8* mRNA

IL8 expression in human gastric mucosal biopsies was determined in duplicate, using RT-qPCR and expressed relative to a negative comparator of pooled cDNA prepared from 14 uninfected donors and the reference gene *GAPDH*. Each run included non-template control, positive control of commercial human cDNA and first-stage control prepared without reverse transcriptase.

Clinical isolates typed as *dupA1* are shown by X symbol (includes *dupA1*/*tfs4* complete strains highlighted in red; n=14/11 [antrum/corpus]) and those typed as non-*dupA1* are shown by O symbol (includes *dupA2*, *dupAx* and *dupA* negative strains; n=18/12). *H. pylori*-infected participants (+, n=32/23) are shown by a hatched box and uninfected participants (–, n=24/7) by a white box. The horizontal and error bars show median values and inter-quartile ranges (IQRs) respectively. The box-and-whisker plots show median values, IQRs and 10-90th centiles.

Data for *H. pylori*-infected vs. uninfected participants and for *dupA1* vs. non-*dupA1* strains from typing of these clinical isolates were separately compared by Mann-Whitney U tests. Statistically significant differences are shown above the plotted data with the fold-difference in group medians (* $P < 0.05$, ** $P < 0.01$, *** $P < 0.001$).

Figure 4.6 – relative mucosal expression of T-helper effector cytokine mRNA

IFNG (Th1), *IL17A* (Th17) and *IL10* (Treg) expression in human gastric mucosal biopsies was determined in duplicate, using RT-qPCR and expressed cDNA prepared from 14 uninfected donors and the reference gene *GAPDH*. Each run included non-template control, positive control of commercial human cDNA and first-stage control prepared without reverse transcriptase.

Clinical isolates typed as *dupA1* are shown by X symbol (includes *dupA1*/*tfs4* complete strains highlighted in red; *IFNG*: n=7/5, *IL17A*: n=10/0, *IL10*: n=10/8 [antrum/corpus]) and those typed as non-*dupA1* are shown by O symbol (includes *dupA2*, *dupAx* and *dupA* negative strains; *IFNG*: n=14/10, *IL17A*: n=18/0, *IL10*: n=17/13). *H. pylori*-infected participants (+, *IFNG*: n=22/15, *IL17A*: n=29/0, *IL10*: n=27/21) are shown by a hatched box and uninfected participants (–, *IFNG* and *IL10*: n=8/6, *IL17A*: n=29/0) by a white box. The horizontal and error bars show median values and inter-quartile ranges (IQRs) respectively. The box-and-whisker plots show median values, IQRs and 10-90th centiles.

Data for *H. pylori*-infected vs. uninfected participants and for *dupA1* vs. non-*dupA1* strains from typing of these clinical isolates were separately compared by Mann-Whitney U tests. Statistically significant differences are shown above the plotted data with the fold-difference in group medians (* $P < 0.05$, ** $P < 0.01$, *** $P < 0.001$).

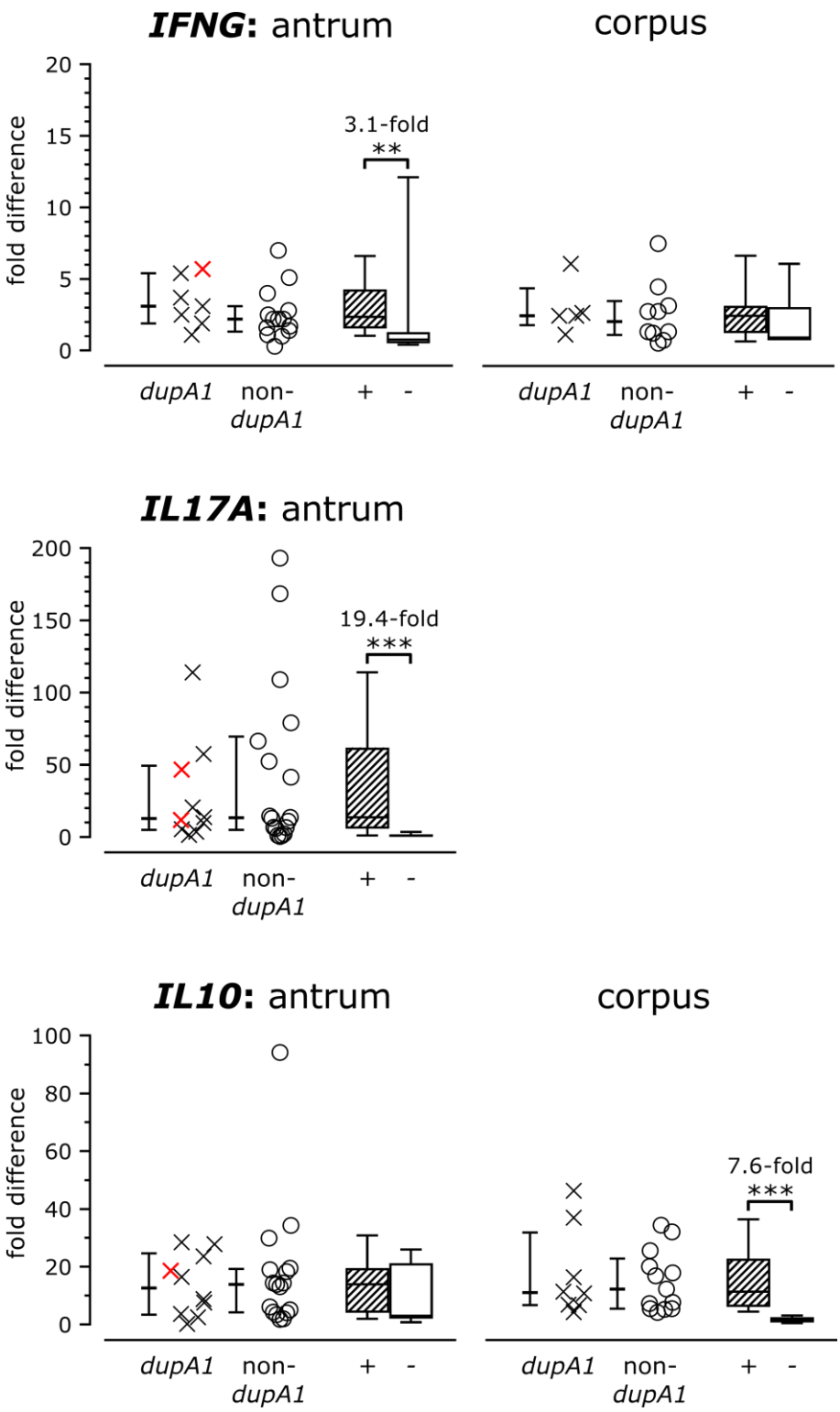

Figure 4.6 – relative mucosal expression of T-helper effector cytokine mRNA

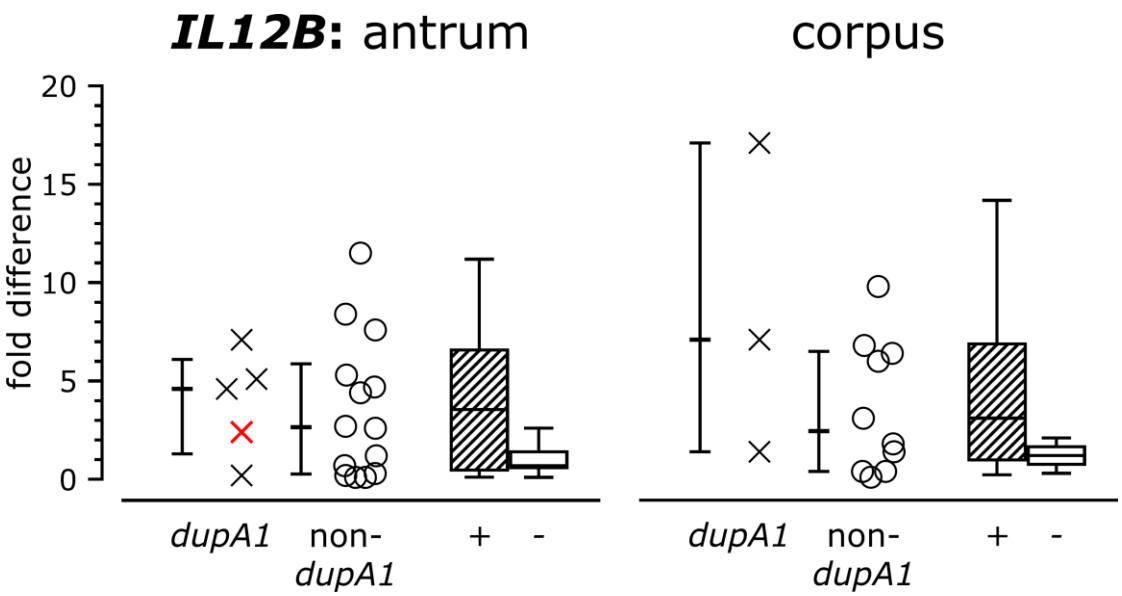

Figure 4.7 – relative mucosal expression of *IL12B* mRNA

IL12B encodes IL-12/23p40. *IL12B* expression in human gastric mucosal biopsies was determined in duplicate, using RT-qPCR and expressed relative to a negative comparator of pooled cDNA prepared from 14 uninfected donors and the reference gene *GAPDH*. Each run included non-template control, positive control of commercial human cDNA and first-stage control prepared without reverse transcriptase.

Clinical isolates typed as *dupA1* are shown by X symbol (includes *dupA1*/*tfs4* complete strains highlighted in red; n=5/3 [antrum/corpus]) and those typed as non-*dupA1* are shown by O symbol (includes *dupA2*, *dupAx* and *dupA* negative strains; n=14/10). *H. pylori*-infected participants (+, n=20/13) are shown by a hatched box and uninfected participants (–, n=19/6) by a white box. The horizontal and error bars show median values and inter-quartile ranges (IQRs) respectively. The box-and-whisker plots show median values, IQRs and 10-90th centiles.

Data for *H. pylori*-infected vs. uninfected participants and for *dupA1* vs. non-*dupA1* strains from typing of these clinical isolates were separately compared by Mann-Whitney U tests. Statistically significant differences are shown above the plotted data with the fold-difference in group medians (* $P < 0.05$, ** $P < 0.01$, *** $P < 0.001$).

4.4 Summary

In this section, we set out to test the hypotheses that the *dupA* status of the isolated clinical strain would be associated with the pathogenic features of DU, namely that:

1. gastric inflammation would be intense and corpus-sparing in distribution,
2. bacterial colonisation density would be antral-predominant, and
3. the gastric mucosal immune responses would be pro-inflammatory.

In relation to hypothesis one, no difference was found in the intensity or distribution of gastritis by *dupA* status, although there was some evidence that active inflammation was actually more marked in antral mucosa for non-*dupA1* strains.

In relation to hypothesis two, bacterial colonisation density was not shown to be antral-predominant for *dupA1* strains.

In relation to hypothesis three, there was evidence of higher expression of IL-1β and of IFN-γ in gastric antral biopsies obtained from participants infected with *dupA1* strains, when compared with participants infected with non-*dupA1* strains. These observations were not confirmed with confirmatory assays at protein-level or, for *IFNG*, at mRNA-level. Moreover, no associations were demonstrated for other pro-inflammatory cytokines and, in particular, no difference was found for IL-8 and *IL8* between *dupA1* and non-*dupA1* strains. Data points for *dupA1*/*tfs4* complete strains were clustered amongst the other data points.

Overall, *dupA* status was not found to be related to duodenal ulcer pathogenesis. There was some evidence for an association with increased mucosal inflammation.

4.5 Discussion

A true virulence factor should have an epidemiologically consistent disease association, correlates with disease present *in vivo* (such as increased severity of mucosal inflammation), and biological plausibility (Lu, Yamaoka and Graham 2005). The discussion of the previous chapter concludes that *dupA* has not consistently been associated with disease risk across different regions and populations, nor with a specific clinical outcome. In testing the hypothesis that *dupA* does indeed promote duodenal ulceration in its putative role as a bacterial virulence factor, we here discuss the correlation with expected pre-clinical endpoints *in vivo* if there were a biologically plausible role in DU pathogenesis.

The overall aim of this chapter was to determine if the *dupA* status of clinical isolates is associated with the key pathogenic features of duodenal ulceration. The associations between *dupA* and these key pathogenic features are discussed in turn, namely whether:

1. gastric inflammation is intense and corpus-sparing in distribution,
2. bacterial colonisation density is antral-predominant,
3. the gastric mucosal immune responses are pro-inflammatory, and
4. gastric acid output is increased.

4.5.1 Gastric inflammation

Duodenal ulceration may arise when gastric inflammation is intense and corpus-sparing in distribution. Therefore, we hypothesised that *dupA1* strains would be associated with higher grades of histological inflammation and with antral-predominant inflammation (vs. pan-gastritis and corpus-predominant). No clear differences were found in the intensity of gastritis, although there was evidence from one analysis that active inflammation was actually more marked in antral mucosa for non-*dupA1* strains. The was no evidence that the distribution of gastric inflammation was corpus-sparing for *dupA1* strains.

These findings are in keeping with the majority of studies (Douraghi et al. 2008; Zhang et al. 2008; Nguyen et al 2010; Abadi et al. 2012; Shiota et al. 2012; Pereira et al. 2014; Rasheed et al. 2014; Miftahussurur et al. 2015; Ghalehnoei et al. 2016). Populations were from Brazil, China, Indonesia, Iran, Japan and Pakistan. These studies also used the Sydney system.

International consensus favours the use of the updated Sydney system for describing and classifying gastritis, in clinical but also in research settings (Dixon et al. 1996). Other approaches have been developed that are particularly focussed on predicting subsequent cancer risk, including the Operative Link on Gastritis Assessment (OLGA; Rugge et al. 2008) and the Operative Link on Gastric Intestinal Metaplasia Assessment (OLGIM; Capelle et al. 2010). Numerous stains can be used including haematoxylin and eosin and specific stains for *H. pylori* such as modified Giemsa or toluidine blue.

The Sydney system includes five graded variables to be scored using a four-point ordinal system of 0 (absent/normal), 1 (mild), 2 (moderate) and 3 (marked). Five biopsies are recommended with two from the antrum, two from the corpus and one from the incisura angularis. The graded variables are: chronic inflammation (density of lymphocytes and plasma cells in the lamina propria), acute inflammation (neutrophils polymorph cell infiltration of the lamina propria, pits or surface epithelium), atrophy (loss of specialised glands from gastric mucosa), intestinal metaplasia and *H. pylori* (density of organisms). In research studies the graded parameters are frequently presented as mean values, or even summated, though it is not appropriate to treat these discrete ordinal variables as if they were continuous.

Using the Sydney system, only Queiroz, Rocha et al. (2011) reported associations between histopathology and *dupA*. They found a positive association with chronic inflammation in antral mucosa and a negative association with atrophy in the corpus.

Other investigators have used a broader 6-point visual analogue scale from 0 (absent/normal) to 5 (maximal intensity) for graded variables (Lu et al. 2005; Wang, Shao et al. 2015). Japanese and Columbian patients with *dupA*+ strains (*jhp0917*$^{+}$/*jhp0918*$^{+}$), though not South Korean patients, were reported in univariate and multivariate analyses to be associated with increased neutrophil infiltration in both the antrum and corpus (Lu et al. 2005). An inverse association was also shown in both stomach regions with intestinal metaplasia and atrophy, which are precursors of gastric cancer development. Wang, Shao et al. (2015) reported that individuals infected with *dupA1* strains show higher inflammatory cell infiltration than *dupA*– strains. This was the case for *dupA1* strains both with and without a complete *tfs4* cluster, with the former having the highest scores of gastric inflammation. However, they have reported parametric summary statistics for ordinal variables and do not state which statistical test was used. No association was found for atrophy.

The expected pathogenic features of inflammation for DU development have not been conclusively shown for *dupA* strains. To the best of our knowledge, this study reports the first systematic comparison of relative antrum and corpus scores.

4.5.2 Bacterial colonisation density

These experiments were designed to test the hypothesis that bacterial colonisation density is antral-predominant for *dupA*+ strains. Using a four-point ordinal scale, no statistically significant differences in *H. pylori* density were found between *dupA1* and non-*dupA1* strains.

This is in keeping with other reports that used both four- and six-point scales, for *dupA* strains and for *dupA1* strains with and without an intact *tfs4* cluster (Lu et al. 2005; Jung et al. 2012; Miftahussurur et al. 2015; Wang, Shao et al. 2015).

There was a significant relationship between *dupA* positive genotype and antral bacterial colonisation density by histological scores in Pakistan (score 0: *dupA*+ 0.0%, score 1: 35.7%, score 2: 85.7%, score 3: 90.9%, $P = 0.002$), although this study only evaluated antral biopsies and did not determine whether infecting strains were long-type (*dupA1*), or truncated or short-type (Rasheed et al. 2014).

Given the potential limitations of using Sydney scores as a research measure of bacterial colonisation density, a validated qPCR was revised and used in this study. This is the most comprehensive analysis to date, based on 23 paired biopsies that had been fully genotyped. There was no difference in the pattern of bacterial colonisation for *dupA1* strains. Our group previously reported a significant increase in the antrum:corpus ratio for *dupA*+ vs. *dupA*– strains (median 2.8 vs. 0.5 units, $P = 0.025$, n=20) suggesting that *dupA*+ strains have a tendency towards antral-predominant colonisation (Patel et al. 2009). However, this work was limited by *dupA* typing that was performed before polymorphisms and different allelic forms of *dupA* had been described. To the best of our knowledge, no other studies have been reported using other methods than histology to assess colonisation density.

Overall, the evidence suggests that bacterial density is relatively consistent between the antrum and the corpus for *H. pylori* infection with respect to *dupA* status. The level of inflammation associated with *cagA*+ strains of *H. pylori* has been suggested in part to be the result of an increase in bacterial density (Yamaoka et al. 1999). Rather than being related to denser bacterial colonisation, the differences in mucosal immune responses

according to *dupA* status discussed in the next section may be the result of different interactions between *dupA*+ and *dupA*– bacteria and their human host.

4.5.3 Mucosal immune responses

Interleukin-8 is the hallmark chemokine in *H. pylori*-associated gastroduodenal disease (Robinson et al. 2007) and is implicated in the pro-inflammatory contributors to pathogenesis for the major bacterial virulence factors (White et al. 2015). Expression of IL-8 is strongly induced *in vivo* and *in vitro* by the *cag*PAI, VacA, and to some extent by other virulence factors including OipA and BabA. Gastritis is characteristic of chronic *H. pylori* infection and IL-8 has an important role in recruiting inflammatory cells to the gastric mucosa. Duodenal ulcers, along with GU and GC, may arise when the gastric mucosal immune responses are pro-inflammatory. Therefore, we tested the hypothesis that *dupA* status is associated with induction of pro-inflammatory cytokines at protein-level and at mRNA-level.

This study found no association between *dupA* status and IL-8 or *IL8* expression in gastric antral or corporal mucosa. The majority of studies reported higher expression of this pro-inflammatory cytokine for *dupA*+ strains in antral biopsies.

No differences in mucosal IL-8 levels or in relative mucosal *IL8* expression were found between *dupA1* and non-*dupA1* strains in the antrum or corpus. This was surprising, though one other study has reported no significant differences in antral gastric concentrations of IL-8 between *dupA1*, *dupA2* and *dupA*-negative isolates from Iraq (Hussein et al. 2015). These findings were confirmed by multiple protein-level assays.

The initial report by Lu et al. (2005) found that IL-8 expression in antral biopsies from Japanese patients with DU was significantly higher in those colonised by *dupA*+ strains, both when adjusted for total protein and per CFU of *H. pylori*. A similar antral association for controls with gastritis was reported but only when expressed as IL-8 level per CFU. No associations were found in the corpus. Similar findings for the antrum were reported for intact *dupA* strains from Brazilian patients although with marked spread in these data (Queiroz, Rocha et al. 2011), for *dupA*+/*tfs4* complete strains among *cag*PAI+ clinical isolates from an American population (Jung et al. 2012), for *dupA1* and for *dupA1*/*tfs4* complete strains from Iraqi patients (Hussein et al. 2012; Hussein and Tuncel 2015), and for *dupA1*/*tfs4* complete strains among *cag*PAI+ and *vacA* s1/m2 type isolates from Chinese patients with gastritis (Wang, Shao et al. 2015). Hussein et

al. (2010) reported that *IL8* expression in antral biopsies was 5-fold higher for *dupA*+ vs. *dupA*– infections, and neglible in uninfected patients.

The lack of association in this study may be because some *dupA1* strains actually cannot express DupA or are non-functional, or because the study population analysed included individuals with different clinical outcomes and colonised by strains with a variety of other bacterial virulence determinants. The genetic makeup of different populations may play a role in the differences observed in IL-8. Smoking has also been shown to be an important determinant of gastric mucosal IL-8 levels (Hussein and Tuncel 2015), such that bacterial, environmental and host factors should be taken into account wherever possible (Nagashima and Yamaoka 2015). In these analyses, age and sex were not related to mucosal IL-8 expression. However, the optimised sample preparation method and consistent results across a range of sensitive methods support and strengthen our observations. Moreover, marked antral induction of IL-8 expression and marked increases in relative *IL8* expression were observed in both the antrum and corpus of *H. pylori*-infected participants.

A positive association was identified between *dupA1* and the pro-inflammatory cytokine IL-1β. The biological significance of this observation is not clear, but it may be relevant given the importance of this cytokine.

In this study, infection with a *dupA1* strain was associated with a 2-fold increase in IL-1β expression in the gastric antrum. mRNA-level data were not available for *IL1B* and, although IL-1β expression was still higher for *dupA1* strains, statistical significance was not shown with a confirmatory protein-level assay. There are currently no other reports of IL-1β expression according to *dupA* status.

Interleukin-1β is one of the most important cytokines in the gastrointestinal tract. It is a key innate immune mediator in host-environmental interactions for microbial and non-microbial agents with potent pro-inflammatory effects, yet it also promotes healing and repair; it induces gene expression by immune and epithelial cells; and, it is a potent inhibitor of gastric acid so infleunces gastric physiology (El-Omar 2001). Although we found that IL-1β was present at low concentrations in the gastric mucosa, it is a very potent molecule (Wolfe and Nompleggi 1992), so may not need to be abundant or markedly increased in association with *dupA1* to have a biologically significant impact. The importance of IL-1β in *Helicobacter*-associated disease is best demonstrated

through the impact of host genetic polymorphisms of *IL1B* on pre-malignant histological changes and gastric cancer risk (El-Omar et al. 2000; Macarthur et al. 2004; Snaith and El-Omar 2008).

Therefore, the association between *dupA* and IL-1β may be important, and we sought potential explanations. The cellular sources of this IL-1β was unknown. Human monocytic cells are the major source of IL-1β (Semper et al. 2014), though there are other sources in the mucosa such as epithelial and stromal cells. Note that the monocyte immune cell model is the core experimental method of the next results chapter.

No definite regulation by IL-1 receptor antagonist (IL-1RA) was shown.

We speculated that the increased IL-1β may be clearly counteracted by regulatory signals. There are other IL-1β family cytokines, including IL-1α and IL-1RA (Dinarello 2009). The latter binds tightly to IL-1β and blocks its activity. Therefore, the ratio between them can be an important marker in inflammation, such as in inflammatory skin conditions (Janssens et al. 2009). No data for IL-1α were available. We speculated *post hoc* that there may be an association with IL-1RA to counterbalance the small difference observed for IL-1β, therefore, further analysis of Luminex data was undertaken and is reported here in brief. There was no difference in antral IL-1RA expression for *dupA1* vs. non-*dupA1* (median [IQR], 6432 pg/mg protein [4359-9957] vs. 5488 pg/mg protein [4543-7056], n=13 vs. 15, $P = 0.440$) or for *H. pylori*-infected and uninfected participants (data not shown). However, although significance was lost after correction, there was still a trend towards an association between *dupA* status and the IL-1β / IL-1RA ratio (27.0 arbitrary units [18.8-38.3] vs. 13.1 arbitrary units [9.3-19.4], n=13 vs. 15, $P = 0.065$). A trend was also observed according to infection status (19.3 arbitrary units [11.7-33.7] vs. 14.0 arbitrary units [8.6-21.7], n=28 vs. 19, $P = 0.086$). It is not clear if this ratio is a valid marker of inflammation in the gastric mucosa or whether other IL-1 family cytokines must also be considered.

Evidence for inflammasome activation was sought, and there were no associations with *dupA* status for IL-6 or TNF-α, but also no difference for IL-18.

A key contributor to IL-1β induction is the inflammasome, which is a multiprotein oligomer that promotes the maturation of IL-1β from pro-IL-1β in response to innate immune signals (Guo et al. 2015). The secretion by mononuclear cells of IL-1β induced by *H. pylori* results from the cleavage of pro- IL-1β by caspase-1 following

inflammasome activation (NLRP3), which is adhesion-mediated and partly dependent on *cagE* (and to a lesser extent on *vacA*) but independent of *cagA* (Semper et al. 2014).

The putative *tfs4* bacterial secretion system, and *dupA* as the homologous component to *cagE*, could be important in inflammasome activation. This is supported by the similar levels of IL-6 and TNF-α in the gastric mucosa between strains with differing *dupA* status, as these innate cytokines are mainly induced by separate non-inflammasome pathways. No data for pro-IL-1β were available. However, it was possible to ascertain mucosal IL-18 responses and this further analysis is briefly reported here. There was no significant difference in IL-18 levels according to *dupA* or infection status (MSD assay, n=13 *dupA1*, n=15 non-*dupA1*, n=19 uninfected). As maturation of IL-18 also results from inflammasome activation, this observation goes against the hypothesis that the inflammasome contributes to increased IL-1β levels in association with *dupA1* strains. This could be studied directly in future work.

An association was also shown between *dupA1* and the pro-inflammatory cytokine IFN-γ. Stastical significance was not shown at mRNA-level. Again, the biological relevance of this observation is not clear. There were no associations for other T-helper cell subset effector cytokines, so Th1 cells and the adaptive immune response may be influenced by *dupA* status.

Interferon-gamma concentrations were approximately 3-fold higher in antral gastric mucosa for *dupA1* clinical isolates. The trends for *IFNG* expression and the confirmatory protein-level assay were the same, though fell short of significance. Therefore, taking protein-level and mRNA-level data together, there was only some evidence that *dupA* status may have an impact. Oktem-Okullu et al. (2015) reported a positive association between *dupA* status and *IFNG* expression by RT-PCR in combined antrum and corpus biopsies from patients with gastritis (Pearson's $r = 0.31$, $P < 0.05$). However, these *dupA* genotyping data were at higher risk of bias (Table 3.11), and there was no correction for 88 comparisons from which 2 statistically significant results were reported. No other reports are currently available.

Interferon-gamma is the principle Th1 effector cytokine and is essential for the induction of gastric inflammation in a mouse model of *H. pylori* infection (Sawai et al. 1999). There is precedent for it to be associated with more virulent strains. For example, more IFN-γ-producing cells were identified by immunohistochemistry in patients with

chronic gastritis who were infected by strains with non-*vacA* s2m2 forms (82.0-86.5% vs. 69% with *vacA* s2m2), with no major impact from *cagA* status (Martínez-Carrillo et al. 2014). Interestingly, *in vitro* IFN-γ can bind to the surface of *H. pylori* and downregulate the expression of CagA (Zhao et al. 2011). Inflammasome activation is also important for the subsequent adaptive Th1 and Th17 response in a mouse model (Semper et al. 2014).

No differences were observed in the expression of IL-17A, IL-4 or IL-10 with respect to *dupA* status. It might be that Th1 cells are more central if the adaptive immune response were affected by *dupA* status. We hoped to investigate this in Section 5.7.

No differences were shown for IL-12/23p40, IL-12p70 or IL-23.

Interleukin-12/23 family cytokines were not shown to differ in association with *dupA* status and no significant differences in *IL12B* relative expression were found. This observation has been confirmed for IL-12p70 in antral mucosa (Jung et al. 2012). Both studies do not replicate *in vivo* the marked reductions in IL-12/23 family cytokine induction by human monocytic cells for Δ*dupA* mutants and *dupA2*/*dupA*– strains reported by our group (Hussein et al. 2010). Increased IL-12p70 concentrations would have been expected if the adaptive immune response were skewed toward a Th1 phenotype through interaction with *dupA1* strains.

Interleukin-1β is a potent stimulator of IFN-γ production – though principally when present in conjunction with IL-12p70 – by T cells (Tominaga et al. 2000) and also by NK cells (Cooper et al. 2001). Non-inflammasome cytokines including IFN-γ can influence the transcription of inflammasome components and so promote the activation of caspase-1 and the secretion of active IL-1β (Barker et al. 2011).

There were widespread differences in the mucosal immune response to infection.

Patients infected with *H. pylori* had significantly higher IL-6 and TNF-α concentrations detectable in their gastric antral mucosa. Infection with *H. pylori* was associated with significantly higher expression of IFN-γ and *IFNG* (Th1), of IL-17A and *IL17A* (Th17), and of IL-10 and *IL10* (Treg). The cytokine concentrations and relative expression of Th17 and Treg effectors were much more markedly increased than IFN-γ/*IFNG*. Expression of the Th2 cytokine IL-4 was increased in association with bacterial infection only in corpus mucosa. *Helicobacter pylori*-infected participants were found

to have higher antral levels of IL-12p70 and lower antral levels of IL-23. No significant differences in IL-12/23p40 or in *IL12B* relative expression were found.

In summary, increased mucosal inflammation was observed for IL-1β and IFN-γ with respect to *dupA* status. The biological and clinical relevance of these associations is not clear. However, it is possible that *dupA1* strains are influencing the host immune response and further study is required.

Overall, there was evidence of that *dupA* status was associated with a stronger pro-inflammatory cytokine response for IL-1β and IFN-γ, though not for IL-8. This suggests that *dupA* may have a role in stimulating a stronger host immune response in some colonised individuals. The role may be direct or indirect, for example if *dupA* is acting only as a biomarker. Potentially, *dupA* and/or other putative components of *tfs4* are detected by the host and so directly influencing the innate and adaptive immune responses. This could explain the observed associations with disease, though this would not predispose to or protect from particular clinical outcomes. No studies have undertaken such a comprehensive analysis of mucosal immune responses according to *dupA* status. Further study is required to elucidate any true effects of *dupA*.

4.5.4 Gastric acid output

Pan-gastritis and corpus-predominant gastritis result in destruction of oxyntic mucosa from the corpus, thereby reducing the stomach's ability to produce gastric acid (and resulting in hypochlorhydria). Conversely, antral-predominant or corpus-sparing gastritis increases gastrin levels, along with other hormones, act on the preserved parietal and other cells of the corpus (Atherton 2006). This results in increased gastric acid or hyperchlorhydria. This is another important pathogenic mechanism that underpins the development of duodenal ulceration (Sobala et al. 1991; Kuipers et al. 1995; Kusters et al. 2006). Ulcer development requires gastric acid as well as pro-inflammatory cytokines (Watanabe et al. 2001). This study did not seek to examine the hypothesis that *dupA*+ strains are better adapted to a more acidic environment *in vivo* and associated with greater gastric acid output by its host. Published data from 5 studies provide some insights into a possible link between *dupA* and gastric acid.

There is *in vitro* evidence that *dupA*+ strains are better able to survive acid shock and to grow during prolonged exposure to low pH. The relevance and potential survival advantage for bacterial growth *in vivo* is not clear.

The presence of *dupA* was linked to an increased resistance to acid shock *in vitro* in the first description of *dupA* (Lu et al. 2005). Bacteria were pre-exposed and adapted to pH 6 in broth for 24 h, then resuspended for 20 min at pH 3, 4 or 5, then plated for viable counts before and after acid shock. A greater proportion of bacteria from *dupA*– strains were killed (6.4 ± 0.9 $\log_{10}$ kill, mean ± standard error) than their counterparts from *dupA*+ strains (6.0 ± 0.9 $\log_{10}$ kill). Although this difference was statistically significant, it means that only around 6 more bacteria survived per 10,000,000 killed for *dupA*+ strains, which may or may not confer an actual survival advantage *in vivo*. Abadi et al. (2012) observed higher acid resistance for *dupA*+ strains isolated from patients with gastritis. Bacteria on pH-adjusted agar plates were better adapted to grow at pH 4 (*dupA*+ 12/12 strains produced visible colonies vs. *dupA*– 8/20, $P = 0.020$) and at pH 3 (4/12 vs. 2/20, $P = 0.015$).

Lu et al. (2005) also reported results for an isogenic Δ*dupA* mutant, a complemented and the wild-type strains. The Δ*dupA* mutant strain was more susceptible to 20 minutes of exposure to pH 3 than the wild-type strain – equivalent to 13 more bacteria surviving per 10,000,000 killed (wild-type: 6.6 ± 0.1 $\log_{10}$ kill vs. mutant: 5.8 ± 0.1 $\log_{10}$ kill, $P < 0.001$, complemented: 6.8 ± 0.1 $\log_{10}$ kill), though there is some ambiguity in their report when comparing the text and the figure. Results were similar though proportionately lower for exposure to pH 4. Most strains survived exposure to pH 5 regardless of whether the strain was wild-type or mutant.

In separate experiments an isogenic *dupA* mutant (shown not to express DupA protein or have polar effects on the sequences or expression of neighbouring genes) had stronger exponential growth after 72 hours at pH 3-6 (Wang, Chen et al. 2015). Reduced urease levels were found in supernatants for the Δ*dupA* mutant. Ghalehnoei et al. (2016) reported no link between urease activity and *dupA* status.

Further analysis of publicly available microarray data from one study investigating the transcriptome of G27 (Merrell et al. 2003) shows no consistent changes in expression of *jhp0917* or *jhp0918* at different time points of pH 5.0 acid exposure. It is not known if *dupA* transcription (or indeed translation or other modification) are regulated by pH.

The true pH of the mucosal niche *in vivo* remains controversial – some methods suggest a relatively neutral pH layer whilst others suggest a much more acidic habitat for *H. pylori* with a pH of less than 4.5 (Krulwich et al. 2011).

Human studies show a non-significant increase in gastrin levels and a significant association between higher gastric acid output and *dupA* status

Serum gastrin levels were numerically higher in patients with gastritis colonised by *dupA*+ strains (257.2 ± 289.7 pg/mL, n=14) vs. *dupA*– strains (142.8 ± 77.9 pg/mL, n=31), though statistical significance was not shown (Shiota et al. 2012).

Imagawa et al. (2010) enrolled 136 patients with DU or GU and followed them for the development of GC for a median of 14.4 years (range 1-30 years). Data on *dupA* status were available for a subgroup from formalin-fixed, paraffin-embedded sections of gastric biopsies using a single set of primers to amplify an 82 bp fragment. Measurements of maximal acid output (MAO), reflecting parietal cell mass, and basal acid output (BAO) had been made at enrolment for another subgroup. Individuals with evidence of colonised by *dupA*+ strains were associated with significantly higher MAO (20.3 ± 2.6 mmol/h, n=10) vs. *dupA*– strains (12.4 ± 1.9 mmol/h, n=19) and BAO.

This study was observational so it is not possible to comment on whether *dupA* has some direct or indirect influence on gastric pH, though preferential colonisation and inflammation in particular areas of the stomach has not been observed, or if *dupA*+ strains are better adapted to survive at lower pH *in vivo*. During follow-up, 1/18 *dupA*+ cases developed GC vs. 13/38 *dupA*– cases (log rank test $P = 0.04$). This is perhaps not surprising given the relationship found between *dupA* and acid output, since gastric acid level is itself intimately associated with disease development as discussed earlier, which may have confounded the association with *dupA* status. Given the longitudinal design, we can at least be confident that any influence *dupA* status may have had predates the development of gastric cancer.

However, this study does not help us to know if *dupA*+ strains are important in altering the conditions that lead to gastroduodenal disease or might merely serve as a biomarker by conferring a survival advantage when the gastric environment changes for other reasons. It was also not setup to test the hypothesis that the virulence determinants of the colonising strain are associated with different gastric acid output. The typing method for *dupA* is at extremely high risk of bias and potential confounders were not considered.

Overall, there is poor quality *in vivo* evidence that gastric acid output is increased with *dupA*+ infection. There is now good *in vitro* evidence that such strains are better able to survive under acidic conditions, though this may or may not be relevant *in vivo* and there is a classic "the chicken or the egg" causality dilemma. Given that *dupA* is positively associated with both DU and GU in Eastern populations, and has been both positively and negatively associated with GC in some populations but not others, no specific relationship with gastric pH would be expected.

4.5.5 Strengths, weaknesses and future work

This study provides by far the most comprehensive analysis of human mucosal immune responses to *H. pylori* according to *dupA* status of the infecting strain. The process of preparing mucosal biopsies for multiplex protein-level analysis was carefully optimised. Both protein and mRNA expression were quantified, and two assays were used at protein-level. In addition, paired antrum and corpus samples were used, so that regional differences in the gastric immune response might be identified.

Histological gastric inflammation was systemically evaluated between the antrum and corpus, which provided the first report of relative antral and corporal scores. In assessing bacterial colonisation density, a quantitative assay was also used.

The histopathological scoring systems available are a potential limitation as they lack resolution, and should only be analysed using non-parametric methods. This research question might be better addressed with quantitative histological methods that provide continuous variables for inflammatory and bacterial parameters for analysis. For example, slide scanning using a NanoZoomer Digital Slide Scanner (Hamamatsu, Japan) to generate photomicrographs that could be automatically analysed for particular cells by particle counting in freeware such as ImageJ. An alternative would be so-called "non-invasive" biopsy using serum pepsinogen levels (Kiyohira et al. 2003).

This limitation also applies to histological quantification of bacterial density based on toluidine blue staining. Alternative methods include immunohistochemical staining to identify and quantify organisms. The quantitative analysis of bacterial colonisation density was based on a final sample size of 23, so could be extended where biopsies and strain virulence data are available. This method lacks precision and is based on the bacterial density in two small biopsies, which may be patchy and so not necessarily

representative. Urease breath tests and endoscopic pH testing are alternative approaches to quantify *H. pylori* load (Perri et al. 1998; Cho et al. 2008).

No experiments were conducted to test the hypothesis that *dupA*+ strains are associated with greater gastric acid output by its host. A human study using pentagastrin-stimulated peak acid output is an option (Ghosh et al. 2011), though ethical considerations mean this would be observational and there would be numerous regulatory considerations. It may be possible to retrospectively analyse patient cohorts where acid output data are already available, ideally using more robust typing for *dupA* and accounting for confounding factors. Animal models could also be used, ideally where it is possible to block or switch DupA expression on and off. The *in vitro* work could be extended by examining bacterial survival with and without attachment to a polarised gastric cell line. The relationship of pH to the expression of the *dupA* system could be assessed in relation to DupA or if a quantitative assay for *dupA* mRNA were successfully developed.

Finally, the analysis of mucosal pro-inflammatory cytokine expression was undertaken according to *dupA1* status. Similar strains have been shown to express DupA (Wang, Chen et al. 2015). However, it is not known if the strains in this study express DupA or are non-functional in some other way. The comprehensive analysis in this study by its nature is time-consuming and expensive. If further *dupA* typing data were available, as discussed in Section 3.5.3, then potentially cytokine expression data for a further 29 study participants could also be analysed. Subgroup analysis of individuals with particular clinical outcomes or gastritis only, or according to other bacterial, environmental and host factors, may then be possible. This study was conducted in a Western population. Epidemiological data suggest assocations between *dupA* and human diseases are confined to Asian and Middle Eastern countries. Therefore, a similar study in a different population could be considered.

4.5.6 Conclusion

The expected pathogenic features, *in vivo* correlates and biological plausibility for DU development have not been shown for *dupA*. This suggests that it is not a true virulence factor that promotes duodenal ulceration, at least in this study population, and so may be misnamed.

However, there was evidence of increased mucosal inflammation in association with *dupA1* strains. No association was established with the severity of gastric inflammation by histology, though this approach lacks resolution and sensitivity. Chronic gastric inflammation underpins the pathophysiology of *Helicobacter*-associated gastroduodenal disease, though is not specific to DU development. Interleukin-8 upregulation is typically seen, though was not associated with *dupA* status in this study. The observations for IL-1β and IFN-γ might be a subtler indicator of an interaction between the host immune response and *dupA1* strains, though the biochemical and clinical relevance of these associations has not been established.

The main focus of the next results chapter is to refine an *in vitro* model using circulating human immune cells, then to use this model to further study host cellular immune responses with respect to *dupA* status and other bacterial factors. The evaluation of a novel approach to investigate the response of primary human gastric mucosal immune cells recovered from biopsies is also reported.

5. Results Three – Influence of *dupA* and *tfs4* status on human immune cell responses

There was evidence from *in vivo* studies of a more pro-inflammatory host response to *H. pylori* strains that possess *dupA*. The associations for different disease outcomes observed in some populations may be the result of alterations in host-bacteria interaction between *dupA*+ and *dupA*– strains, which could explain the evidence that *dupA* does not specifically increase the risk of DU nor was it linked with DU pathogenesis.

Our group has previously suggested that, in contrast to the pro-inflammatory effects of *cag*PAI that are mediated mainly through gastric epithelial cells, the *dupA* system may interact with host immune cells (Hussein et al. 2008). An *in vitro* system based on human peripheral blood mononuclear cells (PBMCs) was developed to use as a tool to investigate the influence of immune cell responses according to *dupA* status.

This system was refined and extended in this study. Putative functions have been ascribed to *dupA* and *tfs4* genes based on homology, *in silico* and the study of Wang, Chen et al. (2015) that reports the *in vitro* characterisation of DupA (Section 1.3.5). However, it is not known when or why the *dupA* system is employed by *H. pylori*.

The aims of this chapter were:

1. to identify the cytokines and types of immune cell that are important in the human immune response to *H. pylori* according to *dupA* status,
2. to investigate the relationship between *dupA* and *tfs4* profile and cytokine induction, and
3. to gain insight into the role of *dupA* and *tfs4* components in this context.

5.1 Blood donors and cell populations

In order to purify an adequate number of cells for planned experiments, a large volume of blood was required (>250 mL). Individuals with hereditary haemochromatosis (HH) attending for planned venesection were donors in this study. Most cases of HH result from the inheritance of a mutated *HFE* gene (type 1 HH), leading to increased gastrointestinal iron absorption and, without treatment, the accumulation of iron causing end-organ damage. This donor cohort and the potential impact on this *in vitro* model used to investigate immune responses are discussed in Section 5.8.1. In brief, there are potential advantages, including a common ancestry resulting in a more homogenous study population (note that all donors in our study were of white British descent) and that large blood volumes could be obtained ethically, quickly and without additional costs. There are also potential disadvantages, though there are no established immunological defects in this cohort that would preclude their selection in this study as an *in vitro* model of immune responses.

Blood donor characteristics are shown in Table 5.1. Characteristics such as gender and age can have a profound impact on immune responses in experimental models (see Section 5.8.1). We also report the serum ferritin and haemoglobin immediately prior to donation (all of which were within the laboratory normal reference range), the *HFE* genotype, the time from diagnosis to indicate the phase of treatment (all donors were in the maintenance phase with their iron stores having been normalised through venesection, except for donor G) and *H. pylori* status (where available).

Total cell numbers, viability and purity of extracted cell populations are reported in Table 5.2. The median total number of PBMCs recovered was 1.62×10^8 cells (IQR 0.70-2.42×10^8 cells). Overall viability was 98-99%. Some data were missing (Table 5.2, donors A-C), though for donors A and B the trypan blue exclusion method alone was used to determine total viable cell counts (non-viable cells were not counted).

Given the potential impact of *HFE* mutations, as well as other characteristics such as gender and age, on the cellular and molecular host immune system, these experiments were carefully designed. Purified cells were co-cultured with positive and negative controls, with various clinical *H. pylori* isolates, and with sets of wild-type, isogenic and double mutant strains in different backgrounds, including some that were treated prior to co-culture. This work is presented below in Sections 5.2 to 5.6.

At least 2 technical replicates were included for each experimental condition included in each co-culture experiment (donor/control or donor/strain pair). Both 16 h and 48 h co-cultures were performed, analysed by flow cytometry and sandwich immunoassays respectively. For the latter, the supernatant for each technical replicate was clarified by centrifugation after co-culture, which were combined for each experimental condition and these samples aliquoted and stored for use in subsequent analysis experiments. Again, at least 2 technical replicates for each sample were analysed, and these observations were averaged to derive a single biological replicate for each analyte. Finally, these unadjusted observations for each biological replicate were adjusted (see Section 2.11). In brief, bacterial strains were carefully adjusted to a multiplicity of infection (MOI) of 10 prior to co-culture, which was the expected MOI. However, given the potential for differences in viability between strains and between experiments, an observed MOI was determined for every biological replicate based on bacterial viability calculated using dilution plating. The concentrations of each analyte was multiplied by a correction factor to adjust for any difference between the observed and expected MOI. Controls were not adjusted for MOI. Therefore, every plotted data point represents an independent biological replicate that has been appropriately adjusted for MOI for each donor/strain experimental condition.

5.2 Co-culture of clinical strains with PBMCs

Adjusted cytokine concentrations are shown in Figure 5.1.

Peripheral blood mononuclear cells were purified from 4 donors (G-J) and co-cultured 48 h. Experimental controls were included: media only (negative control), lipopolysaccharide and sonicated *H. pylori* lysate (positive controls). Controls performed as expected, with no cytokine induction for negative controls and higher concentrations observed for positive controls (see Appendix Figure 7.6).

Clinical strains isolated from patients in Nottingham, UK were selected according to their characterised *dupA* status. The results for six isolates with a complete full-length *dupA* gene (*dupA1* strains) and six strains without a complete *dupA* gene (non-*dupA1* strains) are reported (see Table 2.16 on page 84 for strain characteristics).

Concentrations of various pro-inflammatory cytokines (IL-1β, IL-6 and TNF-α, IL-12/23p40 and IL-12p70, IFN-γ and IL-17A), the pro-inflammatory chemokine IL-8 and the anti-inflammatory cytokine IL-10 were determined in co-culture supernatants.

Table 5.1 – blood donor demographics, genotypes and phenotypes

Donor	Gender	Age (years)	Hb (g/L)	Ferritin (μg/L)	*HFE* genotype	Diagnosed (years ago)	*H. pylori* status
Overall	80% male	61.3 ± 9.1	140 ± 14	146 ± 39		3.6 ± 3.7	
A	Female	51	131	99	$C282Y^{+/+}$	4	unknown
B	Male	72	114	144	$C282Y^{+/+}$	11	previous positive
C	Male	55	165	136	$C282Y^{+/+}$	1	negative
D	Male	74	138	119	unknown	9	unknown
E	Male	70	135	150	$C282Y^{+/+}$	1	unknown
F	Male	53	154	117	$C282Y^{+/+}$	5	unknown
G	Male	55	147	226	$C282Y^{+}$/ $H63D^{+}$	4 months (induction)	unknown
H	Female	53	128	123	$C282Y^{+/+}$	2	unknown
I	Male	60	145	201	$C282Y^{+/+}$	2	unknown
J	Male	70	147	140	$C282Y^{+/+}$	1	unknown

Overall data expressed as mean ± standard deviation.

Hb, haemoglobin; *HFE*, gene responsible for type 1 hereditary haemochromatosis with common mutant alleles C282Y and H63D.

Table 5.2 – details of PBMCs purified from donor blood

Donor	Volume of blood (mL)	Total cell number ($\times 10^8$)	Viability by TB (%)	Viability by PI (%)
Overall	345 ± 96	1.69 ± 1.14	98 ± 1.4	98.5 ± 0.9
A	250	0.24 *	-	-
B	250	0.50 *	-	-
C	500	2.68	99	-
D	250	0.39	96	98.5
E	300	1.31	99	99.7
F	300	3.80	97	99.2
G	300	2.23	99	98.7
H	400	2.48	99	98.6
I	450	1.43	99	98.1
J	450	1.80	96	96.9

Overall data expressed as mean ± standard deviation, excluding donors A and B.

PBMC, peripheral blood mononuclear cell; PI, propidium iodide staining; TB, trypan blue staining; *, only viable cells counted (see text); -, missing data point (see text).

Figure 5.1 – cytokine expression in PBMC co-culture with clinical strains

Peripheral blood mononuclear cells (PBMCs) were purified from 4 donors (G-J). Cells were co-cultured with clinical isolates of *H. pylori* characterised by sequencing as *dupA1* (n=6) or non-*dupA1* (n=6). Cytokine/chemokine concentrations in 48 h co-culture supernatants were measured for 9 analytes in at least duplicate using Meso Scale Discovery V-PLEX assays (panels A to I).

The *dupA1* strains were 454, 521, 527, 597, 606 and 619, and the non-*dupA1* strains, which lack a complete full-length *dupA1* gene, were 461, 529, 536, 547, 563 and 565. The non-*dupA1* strains were all typed as *dupA* negative.

Data points represent the measured concentration adjusted for observed multiplicity of infection after determination of colony forming units and cell counts for each donor/strain combination. The overlaid red horizontal bars show overall mean values. The separate black horizontal and error bars show overall median values and inter-quartile ranges (IQRs) respectively.

Data from *dupA1* and non-*dupA1* groups for each analyte were compared by Mann-Whitney tests. Statistically significant differences are shown (* $P < 0.05$, ** $P < 0.01$, *** $P < 0.001$).

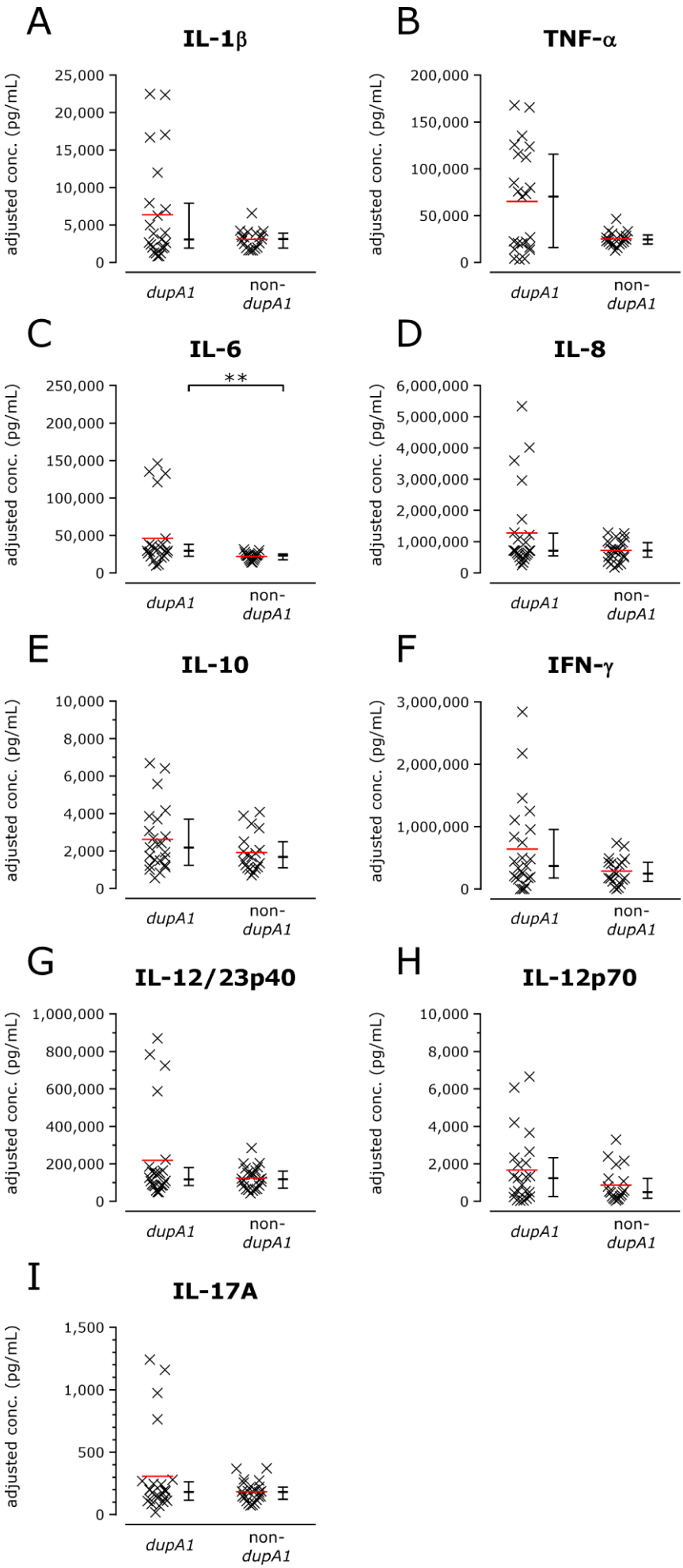

Figure 5.1 – cytokine expression in PBMC co-cultures with clinical strains

IL-6 expression by PBMCs was significantly higher for *dupA1* isolates. No other significant differences were observed for clinical strains.

The median adjusted concentration of IL-6 was significantly higher for *dupA1* isolates co-cultured both with PBMCs (29.5 vs. 23.1 ng/mL, $P = 0.003$) and with $CD14^+$ monocytes (26.2 vs. 16.0 ng/mL, $P = 0.008$). No other statistically significant differences were observed between *dupA1* and non-*dupA1* clinical isolates.

The 4 highest data points represent antral clinical isolate 521 in co-culture with PBMCs from donors G-J (Figure 5.1, panels A, C, D, G and I). This may be partly explained as this strain showed the lowest viability so would have higher adjusted concentrations (1.3 CFU/mL vs. expected MOI equivalent to 10 CFU/mL, see Table 2.16), though the difference were more marked for some analytes. No other correlation between measurements or potential explanation (in relation to *dupA* or other virulence determinants) for the wider spread of data for *dupA1* strains was established. This was more notable for TNF-α and IFN-γ, for more strains than 521.

However, these data reflect concentrations for non-isogenic strains, so may represent other important factors than *dupA* status. Results for co-culture of PBMCs with wild-type and mutant strains constructed in the AB21 background are reported next.

5.3 Co-culture of mutant strains with PBMCs

First, we planned to test the previous observation that *dupA1* strains of *H. pylori* stimulate human mononuclear immune cells and that this is attenuated for Δ*dupA* mutant strains (Hussein et al. 2008, who also reported attenuated responses for *dupA2* strains). Strain AB21 was selected as the background for these mutatagenesis experiments, as it is a *dupA1* strain with a complete *tfs4* operon.

We used two sets of wild-type, isogenic mutant and double mutant strains, denoted by O and X, which had been independently constructed in the AB21 background and stored separately (Section 2.11). Two sets of strains were used to provided additional independent data points, particularly as strain complementation was not planned at this stage. Two strains were available for the isogenic Δ*dupA* mutant, the isogenic Δ*cagE* mutant, and the double Δ*dupA*Δ*cagE* mutant (and each was compared against its own parent wild-type strain). These were made by Dr Rob Delahay and Dr Christian Marx.

The previous co-culture experiments were extended to assess isogenic mutants of the putative *tfs4* components *virB2*, *virB8* and *virB9*, as well as a double Δ*virB8*Δ*dupA* mutant that was available, so that any role in cytokine induction in this model could be tested experimentally against wild-type. Only one of each of these mutants was constructed. See Section 2.11 and note that the candidate prepared isogenic and double mutants lacking *virB8* together with Dr Marx, assisted in the genotypic characterisation and confirmation, and conducted growth curve experiments (Appendix Figure 7.1).

The suitability for these experiments of a markerless Δ*tfs4* mutant lacking the whole *tfs4* operon was also assessed. This was constructed by Dr Amberley Stevens.

Therefore, 11 mutant strains and the 2 wild-type comparator strains were included in these 48 h co-culture experiments. The rationale for strain mutant strain selection is explained in the next section. The experimental design, for example, in terms of technical and biological replicates, controls, adjustment to account for differences in expected and observed MOI between strains and across experiments, was as already described (Section 5.1). Multiple donors were included to increase precision.

These initial experiments evaluated the response of PBMCs in terms of cytokine profile and its relationship with *dupA* and *tfs4*. Subsequent experiments were performed to identify the type(s) of immune cell most important to this *in vitro* model.

5.3.1 Rationale for mutant strain selection

Mutants used are reported in Table 2.15.

The *cag*PAI is the best described virulence system of *H. pylori*. Disruption of *cagE* will eliminate most *cag*PAI activity, though some activity is related to other components such as *cagL*. Therefore, Δ*cagE* mutants were used. It was not feasible or relevant to include mutants for multiple other *cag*PAI genes.

Alongside the *dupA* (*virB4*) mutant, isogenic mutants lacking *virB2*, *virB8* and *virB9* were selected. As shown in Figure 1.10, these were predicted to disrupt putative components of the pilus, inner membrane complex, and outer membrane complex respectively (Figure 1.10). These are predicted to comprise an operon encompasing *virB2* to *virD4* inclusive as well as several ORFs (Figure 1.8). *virD4* encodes the putative type IV coupling protein (T4CP) substrate receptor (Figure 1.7). The other putative T4CP component *virD2* is encoded by a separate operon (VirD2 has relaxase

activity, see Section 1.3.5). The isogenic mutants used in this study are not expected to have polar effects on other downstream genes in the *virB*/*D4* operon.

The Δ*dupA* strain should not affect *virB2* (or *virB3*). The extra-cellular pilus is predicted to consist of VirB2. This is more likely to be able to interact with other cells, such as the human mononuclear immune cells in this model. Therefore, any interaction would be expected to be reduced for the *virB2* mutant. However, the pilus is expected to be elaborated across the periplasm and outer membrane through the substrate translocation channel, formed by the interaction of VirD1, the inner membrane complex and the outer membrane or core complex (Figure 1.7). So, normal pilus construction and VirB2 expression on the bacterial cell surface may also be dependent on some of these other components. But a complete *tfs4* cluster, predicted to encode a functional T4SS, may not be needed for a full or partial immune response in this model provided any genes encoding potentially immunogenic component proteins are still present and intact. It might still be possible, for example, to get expression of VirB2 on the bacterial surface or in the extra-cellular environment independent of an underlying T4SS structure.

VirB8 is hypothesised as a key component of the inner membrane complex, along with the ATPase VirB4 (encoded by *dupA*) with its putative role of providing energy for translocation and secretion system assembly.

VirB9 is predicted to contribute to the outer member complex. It may or may not be expressed on the bacterial surface (or indirectly affect potential antigens present these).

The Δ*tfs4* strain has a markerless deletion of the entire *tsf4* operon (Dailidiene et al. 2006). One would predict the Δ*tfs4* mutant to attenuate any host response that is dependent on one or a combination of *tfs4* components.

5.3.2 Relative cytokine and chemokine concentrations

Relative cytokine concentrations for co-culture of mutrant strains with PBMCs are shown in Figure 5.2. These experiments evaluated the cytokine profiles of PBMCs in relation to *dupA* and *tfs4*.

Peripheral blood mononuclear cells (PBMCs) were purified from 10 donors and co-cultured for 48 h, with media only, with lipopolysaccharide (LPS) or sonicated *H. pylori* (lysate), or with sets of wild-type and isogenic/double mutants of strain AB21.

Unadjusted data for controls and absolute concentrations for each strain adjusted for MOI are shown in Appendix Figure 7.6.

To enable comparison between strains and between donors, each adjusted cytokine concentration was expressed as a percentage of the corresponding wild-type strain for each donor/strain combination. This was done to correct for any biological variation between individuals, such that all comparisons between the different mutants or experimental conditions (for example, Δ*dupA* and wild-type) were made within the same donor. Therefore, the data are presented as relative cytokine concentrations (where the adjusted cytokine concentrations after co-culture and correction for MOI are expressed as a percentage of the corresponding wild-type strain).

Two complementary steps to inferential statistical analysis were used, which had been planned *a priori*. First, an analysis was performed to identify any differences for each analyte in a particular strain or strains. This used Kruskal-Wallis tests with post-test adjustment for planned comparisons. Although this approach is robust in attributing statistical significance, the additional planned comparisons mean that it may lack power to detect a difference between each mutant and its corresponding wild-type. Therefore, an additional second analysis was planned and performed, which exploits the fact that data were presented as relative concentrations against wild-type (and that relative concentrations were expressed as a percentage that for wild-type was always 100%). This analysis used Wilcoxon signed-rank tests to compare the median of the biological replicates for each mutant strain against 100. The second analysis approach is valid but does not account for multiple comparisons so has greater risk of falsely identifying an observation as statistically significant (type I error) compared with the first analysis approach. These two approaches are complementary. The results for each are clearly identifiable both in the Figures and in the text. When only one approach demonstrated statistical significance, typically the second Wilcoxon analysis, this was taken as weak evidence of an effect. Significance was required for both analysis methods for the statistical evidence of an effect to be considered strong.

For relative cytokine concentrations for co-culture of mutrant strains with PBMCs (Figure 5.2), first Kruskal-Wallis tests were used across all 9 strain types per analyte, to test the null hypothesis (for each analyte) that strain groups were sampled from populations with identical distributions. These tests provided evidence to reject the null hypothesis for all analytes except for IL-17A ($P \leq 0.007$ for all, except IL-17A where P

= 0.240; Chi-square values, mean ranks and individual *P* values are not shown). Post-test Dunn's correction was then used for 8 planned comparisons (each isogenic mutant vs. wild-type, Δ*cagE* vs. Δ*dupA*Δ*cagE*, Δ*virB8* vs. Δ*virB8*Δ*dupA*) for each analyte reaching statistical significance.

Peripheral blood mononuclear cells co-cultured with isogenic Δ*dupA* mutants expressed lower relative levels of pro-inflammatory cytokines and chemokines than cells co-cultured with wild-type strains.

Wilcoxon signed-rank tests showed that there were statistically significant differences in the median percentage cytokine/chemokine expression after co-culture with isogenic Δ*dupA* mutants compared against wild-type strains for IL-1β (*P* = 0.021, 13.7% lower), TNF-α (*P* = 0.016, 28.4% lower), IL-6 (*P* = 0.003, 24.2% lower), IL-8 (*P* = 0.001, 23.3% lower), IFN-γ (*P* = 0.025, 30.9% lower) and IL-12/23p40 (*P* = 0.002, 30.6% lower). These are indicated by asterisks below the plotted data. There were no differences in the median relative expression of IL-10, IL-12p70 or IL-17A.

After correction for multiple comparisons, PBMCs co-cultured with isogenic *dupA* mutants expressed significantly lower relative levels of TNF-α, IL-6, IL-8 and IL-12/23p40 (all $P < 0.01$) when compared with wild-type strains (Figure 5.2, shown above the plotted data). The largest reduction was observed in relative expression of IL-12/23p40. Significance was not established for IL-1β or IFN-γ.

Overall, there was strong evidence for lower TNF-α, IL-6, IL-8 and IL-12/23p40 expression by PBMCs co-cultured with strains that lack *dupA* compared with wild-type. There was some evidence for lower IL-1β and IFN-γ expression.

Note that statistical significance was not established for any analyte when comparing double mutants that also lack *dupA* against their isogenic counterparts (Δ*cagE* and Δ*virB8*), though there were fewer experimental comparisons made than for isogenic Δ*dupA* vs. wild-type. However, there was a consistent trend for lower median relative expression of all analytes after co-culture with Δ*virB8*Δ*dupA* strains (n=3) than with Δ*virB8* strains (n=8).

Cells co-cultured with isogenic Δ*cagE* mutants also expressed lower relative levels of IL-6 and IL-8.

Wilcoxon signed-rank tests showed statistically different median percentage expression of IL-6 ($P < 0.001$, 17.9% lower), IL-8 (*P* = 0.003, 21.8% lower) and IL-10 (*P* = 0.044,

12.7% lower) by PBMCs co-cultured with Δ*cagE* isogenic mutants. Significance remained after correction for multiple comparisons for IL-6 and IL-8 (both $P < 0.05$), so there was strong evidence from both analyses for these analytes.

IL-12 family cytokine expression by PBMCs co-cultured with isogenic Δ*virB2* was significantly lower than for cells co-cultured with wild-type.

Wilcoxon signed-rank tests showed statistically lower median percentage expression of IL-12/23p40 ($P = 0.031$, 38.2% lower) and of IL-12p70 ($P = 0.031$, 27.8% lower) by cells co-cultured with Δ*virB2*. Statistical significance was only shown after correction for multiple comparisons for IL-12/23p40 expression in PBMC/Δ*virB2* co-culture (Figure 5.2 panel G, $P < 0.01$).

There was some evidence of differences in relative expression by PBMCs of IL-12 family cytokines for mutants lacking other putative *tfs4* components.

Wilcoxon signed-rank tests showed statistically lower median percentage expression of IL-12/23p40 by cells co-cultured Δ*virB8* ($P = 0.016$, 15.7% lower) and Δ*virB9* ($P = 0.031$, 16.1% lower). These were lost after correction for multiple comparisons.

Surprisingly, cells co-cultured with the markerless Δ*tfs4* mutant strain expressed significantly higher median TNF-α levels relative to wild-type strains ($P = 0.031$, 22.7% higher), though no difference was shown after correction for multiple comparisons.

For other analytes, relative cellular expression following co-culture with bacteria lacking other *tfs4* genes was often highly variable. In most instances the inter-quartile ranges crossed 100% (dotted red line, signifies no difference from wild-type). There was no statistical evidence that medians were significantly different, though power was lower as fewer of these donor/strain combinations were assayed (see Figure 5.2 legend).

Overall, there was strong evidence for lower IL-12/23p40 expression by PBMCs for isogenic Δ*virB2* mutants compared with wild-type. There was some evidence for Δ*virB8* and Δ*virB9* strains, and for lower IL-12p70 expression by Δ*virB2*.

Lower IL-12/23p40 expression was also observed for Δ*dupA* mutants, along with strong evidence for lower TNF-α, IL-6 and IL-8. Taken together, these data suggest that *dupA* and *virB2* were more important determinants of cytokine expression in this model than *virB8*, *virB9* and *tfs4*.

We next planned to determine the cellular sources of IL-12/23p40 by flow cytometry.

Figure 5.2 – relative cytokine concentrations for 48 h PBMC co-culture

Peripheral blood mononuclear cells (PBMCs) were purified from 10 donors and co-cultured with sets of wild-type and isogenic/double mutants of strain AB21 that had been constructed and stored separately (denoted by O and X). Cytokine/chemokine concentrations in 48 h co-culture supernatants were measured for 9 analytes in at least duplicate using Meso Scale Discovery V-PLEX assays (panels A to I).

Data points represent the percentage difference from wild-type in the mean concentration for each donor/strain combination adjusted for multiplicity of infection (wild-type n=19, Δ*dupA* n=16, Δ*tfs4* n=7, Δ*cagE* n=16, Δ*dupA*Δ*cagE* n=14, Δ*virB2* n=6, Δ*virB8* n=8, Δ*virB9* n=6, Δ*virB8*Δ*dupA* n=3; not every data point is plotted – see note). The horizontal and error bars show overall median values and inter-quartile ranges (IQRs) respectively.

Analysis followed two steps (see Section 5.3.2):

First, data across all groups for each analyte were compared by Kruskal-Wallis tests with Dunn's correction for multiple comparisons with 8 planned data pairs (each isogenic mutant vs. wild-type, Δ*cagE* vs. Δ*dupA*Δ*cagE*, Δ*virB8* vs. Δ*virB8*Δ*dupA*). Statistically significant differences after these corrections are shown above the plotted data (* $P < 0.05$, ** $P < 0.01$, *** $P < 0.001$).

Second, data for each mutant were separately compared against a median of 100% (dotted red line) by Wilcoxon signed-rank tests. Statistically significant differences are shown below the plotted data (*/*P* value combinations as before).

Where both analytical approaches were significant, there was strong evidence for a statistically important difference compared to wild-type and the strain name is highlighted in bold.

Note that for clarity some data points are not shown but were included in summary statistics and analysis – donor A Δ*dupA* O for panel B: TNF-α (275%); donor A Δ*virB8* O for panels B: TNF-α (770%) and F: IFN-γ (334%); donor D Δ*tfs4* X for panels A: IL-1β (275%), B: TNF-α (321%) and H: IL-12p70 (353%); donor E Δ*tfs4* X for panel E: IL-10 (283%); donor G Δ*cagE* O and donor H Δ*dupA*Δ*cagE* O for panel I: IL-17A (267% and 225% respectively).

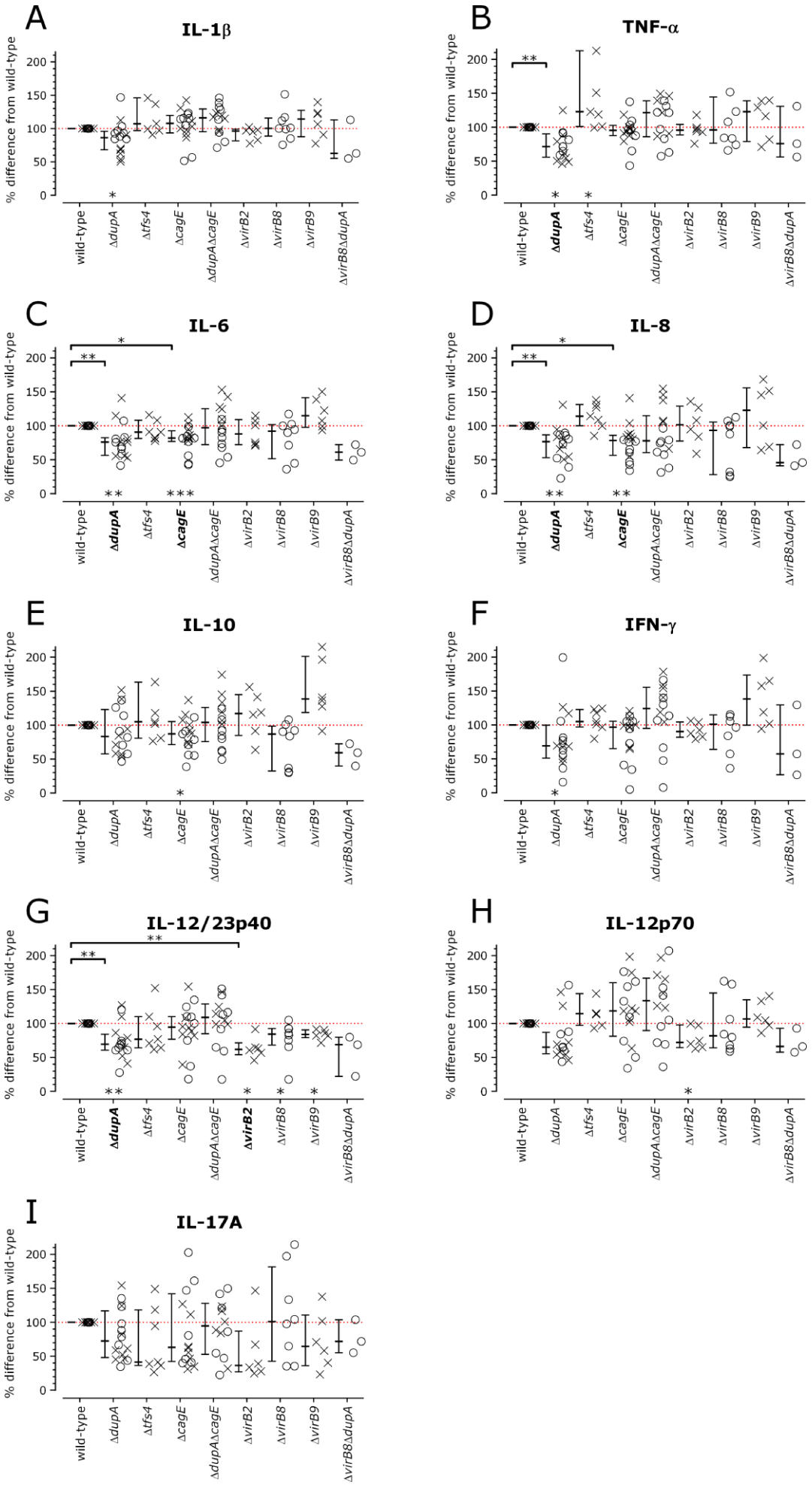

Figure 5.2 – relative cytokine concentrations for 48 h PBMC co-culture

5.3.3 IL-12/23p40 expression by flow cytometry

Results are shown in Figure 5.3.

Peripheral blood mononuclear cells (PBMCs) were purified from 5 donors (F-J) and co-cultured for 16 h, with media only, with lipopolysaccharide (LPS) or sonicated *H. pylori* (lysate), or with sets of wild-type and isogenic mutants of strain AB21.

The percentage of IL-12/23p40^{+} events (panels A and B) and the fluorescence intensity of IL-12/23p40 (panels C and D) were determined by flow cytometry. We also gated for CD14^{+} and CD14^{-} events. Panels A and C show all events gated for relevant cells, and panels B and D show CD14^{+} events. Data points on the right side of each panel represent the percentage difference from wild-type for each donor/strain combination for Δ*dupA* and Δ*tfs4* mutants.

Flow cytometric analysis of PBMCs co-cultures showed no important differences in IL-12/23p40 expression, both for all gated events and for CD14^{+} events only.

Statistically significant differences after adjustment for multiple comparisons were found only between controls and samples where PBMCs were co-cultured with various strains of live bacteria (Figure 5.3).

Overall there were no differences between strains for PBMC co-culture. In particular, no statistically significant differences were observed between wild-type and Δ*dupA* or Δ*tfs4* strains in the percentage of IL-12/23p40^{+} events or in IL-12/23p40 fluorescence intensity. Similar observations were made when comparing double and isogenic mutants (Δ*dupA*Δ*cagE* vs. Δ*cagE*, Δ*virB8*Δ*dupA* vs. Δ*virB8*) and Δ*cagE* vs. wild-type strains (data not shown). There was a large spread in these data due to variation between donors and between the separately constructed sets of isogenic mutant strains.

CD14^{+} events were confirmed as the source of the majority of IL-12/23p40^{+} events for PBMCs for all 5 donors. Very few CD14^{-} events were IL-12/23p40^{+}.

Approximately 90% of IL-12/23p40^{+} events across all controls and samples were CD14^{+} (median [IQR, n], 89.3% [86.0-99.1, 48]). As expected IL-12/23p40 mean fluorescence for CD14^{-} events was broadly similar across all samples (mean ± standard deviation [n], 30.4 ± 5.3 arbitrary units [48]). Overall less than 1% of CD14^{-} events were IL-12/23p40^{+} (median [IQR, n], 0.05% [0.01-0.15, 48]).

Therefore, we next refined our mononuclear cell model to focus on CD14^{+} monocytes.

Figure 5.3 – IL-12/23p40 events and fluorescence intensity by flow cytometry for 16 h co-culture with PBMCs

Peripheral blood mononuclear cells (PBMCs) were purified from 5 donors (F-J) using the optimised protocol. Cells were co-cultured with sets of wild-type and isogenic mutants of strain AB21 that had been constructed and stored separately (denoted by O and X) and incubated for 16 h with brefeldin A added after 1 h. There were 10 biological replicates for wild-type and Δ*dupA* strains (O and X) and 5 biological replicates for Δ*tfs4* strains (X only). Control cells (denoted by Δ) were co-cultured with media only, lipopolysaccharide (LPS) or sonicated *H. pylori* (lysate). Cells were stained with mouse IgG2a anti-human CD14–FITC and mouse IgG1κ anti-human IL-12/23p40–PE. Unstained, fluorescence minus one and isotype controls were included (data not shown). Fifty-thousand events were acquired with a Beckman Coulter FC500 flow cytometer. Events were gated for relevant cells on forward-scatter/side-scatter plots, and as $CD14^+$ and IL-12/23p40$^+$ on FL1–FITC/FL2–PE plots.

Data points in the upper panels represent the percentage of IL-12/23p40$^+$ events for all gated (panel A) and for $CD14^+$ events (panel B). The horizontal and error bars show overall median values and inter-quartile ranges (IQRs) respectively. Data across all groups were compared by Kruskal-Wallis tests with Dunn's correction for multiple comparisons (* $P < 0.05$, ** $P < 0.01$, *** $P < 0.001$).

Data points in the lower panels represent the mean fluorescence intensity of IL-12/23p40 (arbitrary units) for all gated (panel C) and $CD14^+$ events (panel D). The horizontal and error bars show overall mean values and 95% confidence intervals of the mean respectively. Data for all groups were compared by one-way ANOVAs with Tukey's correction for multiple comparisons (no significant differences).

Data points on the right side of each panel represent the percentage difference from wild-type for each donor/strain combination. The horizontal and error bars show overall median values and inter-quartile ranges (IQRs) respectively. Data for each group were separately compared against a median of 100% (dotted red line) by Wilcoxon signed-rank tests (no significant differences).

Note that for clarity some data points are not shown but are included in summary statistics and analysis – donor H for panels A, B and D: percentage difference of Δ*dupA* X from wild-type (336%, 268% and 261% respectively).

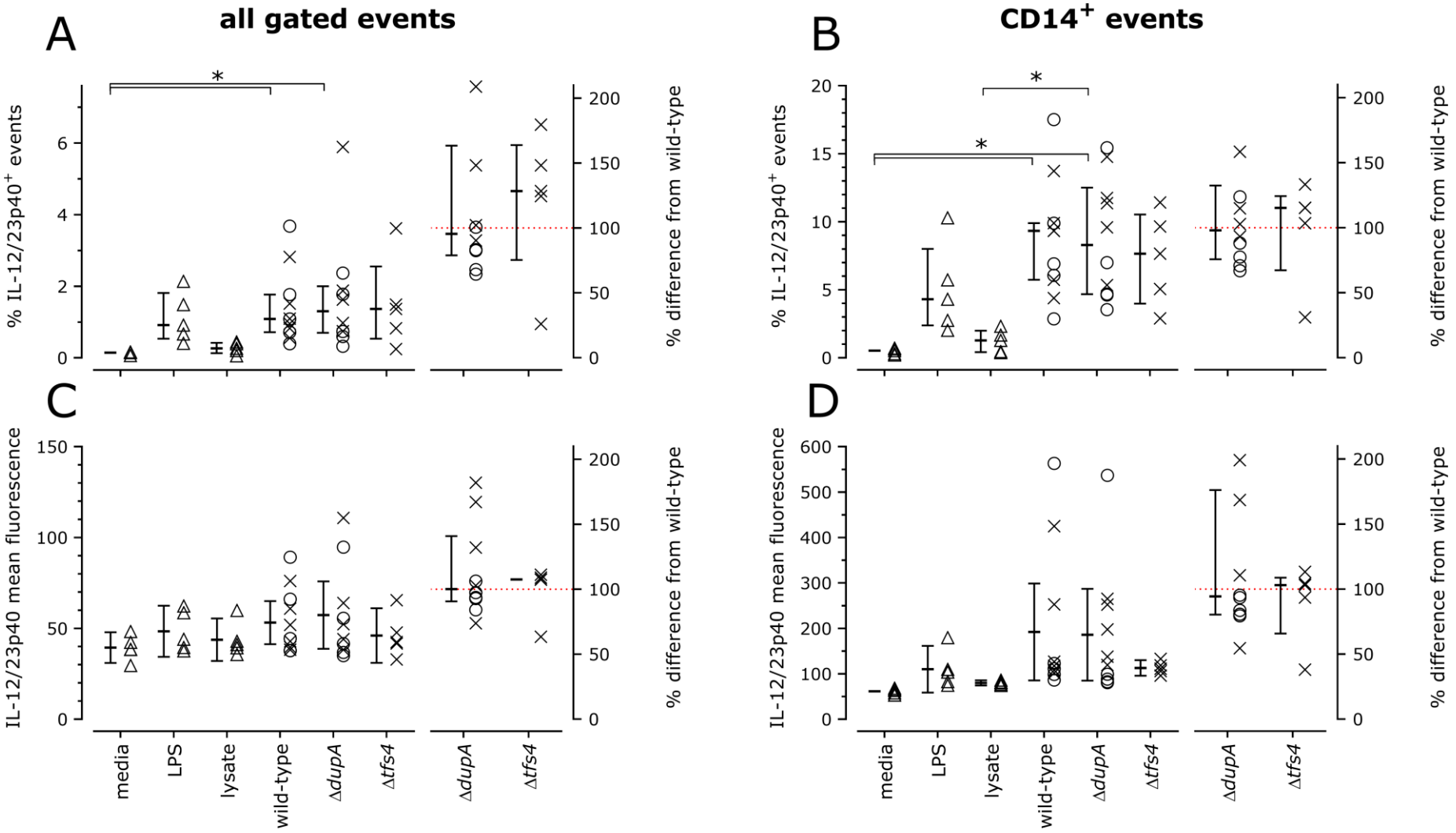

Figure 5.3 – IL-12/23p40 events and fluorescence intensity by flow cytometry for 16 h co-culture with PBMCs

5.4 Optimisation of the human blood monocyte cell model

We aimed to use an experimental model to assess interactions between human inflammatory cells and *H. pylori* strains according to their *dupA* and *tfs4* status. From previous work, we know that the *dupA* virulence system may not stimulate an inflammatory response from gastric epithelial cells (Hussein et al. 2010). We have shown that pro-inflammatory cytokine expression *in vivo* was significantly higher for *dupA1* isolates. In an experimental model using PBMCs, we have shown that isogenic Δ*dupA* mutants are less pro-inflammatory than wild-type strains and that other putative *tfs4* components are required for maximal expression of IL-12 family cytokines in particular. Human peripheral blood mononuclear cells contain different populations of cells. $CD14^+$ cells were confirmed as the most important source of IL-12/23p40. Therefore, we assessed monocytes as our experimental model.

First, we needed to optimise the purification of human monocytic cells. There are various methods and we chose to use immunomagnetic kits. We determined the performance of different immunomagnetic kits – in terms of yield, viability and purity – according to selection type (positive or negative), manufacturer and methodology. Lastly, we reported the obtained cell populations' characteristics by flow cytometry and cytokine expression phenotype in co-culture.

5.4.1 Performance of immunomagnetic kits

We evaluated different approaches to $CD14^+$ cell purification from human leucocytes using four commercial kits (described in Methods Table 2.14). These used magnetic beads to separate cells of interest using either positive or negative selection. The MB kit uses positive selection and will purify $CD14^+$ cells (principally $CD14^+$ monocytes, though some myeloid dendritic cells and residual granulocytes may also be selected, and $CD14^{dim}CD16^+$ monocytes will not be as strongly selected). The other three kits use negative selection. The ES–16dep and RS kits do not deplete $CD16^+$ cells, so will select for $CD14^+$ and $CD14^{dim}CD16^+$ monocytes. The ES+16dep kit does deplete CD16+ cells, so will select for $CD14^+CD16^-$ monocytes.

Peripheral blood mononuclear cells were purified from buffy coats prepared from whole blood from two donors with hereditary haemochromatosis (donors 1 and 2). We evaluated the cell purification kits with PBMCs for the viability, purity and yield of $CD14^+$ enriched and depleted cellular fractions. These results are shown in Table 5.3.

Table 5.3 – yield, viability and purity of cellular fractions with different kits

	Purified from (volume)	Kit and cell fraction		Total cell number ($\times 10^6$)	Number as % of cells used	Viability by TB (%)	Viability by PI (%)	$CD14^+$ purity (%)
Overall		MB en		28 ± 22.6	35 ± 0.7	99 ± 1.4	99.7	98.4 ± 1.0
		ES–16dep en		4 ± 4.2	19 ± 3.5	100	97.6 ± 3.3	78.7 ± 5.7
		ES+16dep en		3 ± 3.5	13 ± 4.2	96 ± 6.4	98.3 ± 2.1	93.3 ± 6.6
		RS en		1.5 ± 0.6	1.5 ± 0.1	97 ± 2.8	99.6 ± 0.5	86.0 ± 3.2
1	PBMC[1] (3.5 mL)			39		96	98.5	90.7
		MB	en	12	35	98	99.7	99.1
			dep	33		97	97.9	62.7
	PBMC[2] (0.5 mL for each kit)			13		94	96.8	62.6
		ES –16dep	en	0.7	16	100	95.3	74.6
			dep	1.0		*	92.5	30.2
		ES +16dep	en	0.4	10	91	96.8	88.6
			dep	1.1		*	91.2	25.6
	Buffy coat[2] (5 mL)	RS	en	1.0	1.5	95	99.2	88.2
2	PBMC[1] (4.5 mL)			140		99	99.7	73.3
		MB	en	44	34	100	99.7	97.7
			dep	100		99	99.6	41.4
	PBMC[2] (2 mL for each kit)			140		99	99.8	62.7
		ES –16dep	en	6.7	21	100	99.9	82.7
			dep	17		*	98.2	48.6
		ES +16dep	en	5.3	16	100	99.8	97.9
			dep	18		*	97.8	51.3
	Buffy coat[2] (5 mL)	RS	en	1.9	1.4	99	99.9	83.7

Evaluation of cell fractions obtained using different commercial purification kits. Overall data expressed as mean ± standard deviation. For kit details refer to methods Table 2.14. All kits were used according to the manufacturers' instructions.

Donor 1 – 74-year-old male, 40 mL buffy coat was prepared from whole blood, 1.3×10^7 leucocytes/mL, 2.0×10^9 erythrocytes/mL (154 per leucocyte)

Donor 2 – 70-year-old male, 35 mL buffy coat was prepared from whole blood, 2.8×10^7 leucocytes/mL, 4.1×10^9 erythrocytes/mL (137 per leucocyte)

dep, depleted; en, enriched; PBMCs, peripheral blood mononuclear cells; PI, propidium iodide staining; TB, trypan blue staining; *, debris and clumping affected reliability of cell counting.

[1] Prepared by layering of cells by directly pipetting buffy coat onto density gradient media (see methods).

[2] Prepared using STEMCELL SepMate™ tubes (see methods). For the ES kits, 2 × 2mL at 0.9×10^7 cells/mL and 2 × 2 mL at 2.8×10^7 cells/mL were used for donor 1 and 2 respectively. Note that the manufacturer recommends 0.5-2mL at 5×10^7 cells/mL.

Direct layering of buffy coat over density gradient media resulted in improved recovery of PBMCs with less erythrocyte contamination.

The use of STEMCELL SepMate™ tubes to isolate target cells directly from buffy coat is recommended with both the ES kits and with the RS kit, rather than direct layering of buffy coat onto density gradient media (see methods Section 2.10). These or similar tubes can be used to enable more rapid cell isolation from large volumes.

Initially in a limited comparison, PBMC recovery from identical volumes of buffy coat was 18-32% of total leucocytes with layering and 6-20% with SepMate™. Overall, erythrocyte contamination was up to 8% and 42% respectively and PBMC concentrations were 1.0-2.8×10^7 and 0.9-2.8×10^7 cells/mL respectively. Cell viability with both methods was over 97% by propidium iodide exclusion. We selected layering in preference to SepMate™ tubes unless these were specifically recommended by the manufacturer. We followed STEMCELL recommendations throughout on buffy coat preparation, quality control steps and media/buffers (see methods Section 2.10).

Cell viability was excellent.

In this comparison, the viability was generally excellent for all kits, exceeding 95% for all enriched cellular fractions and in most cases over 99%.

Positive selection of $CD14^+$ monocytes delivered the best purity of enriched cells.

Purity of $CD14^+$ monocytes was more variable. As expected, the highest proportion of $CD14^+$ cells was isolated using positive selection (MB kit, mean 98.4%). The proportion of $CD14^+$ cells was lower for negative selection, though in all instances these were still within or exceeded the expected typical ranges for the enriched fraction with each kit as reported in the manufacturer product information (ES–16dep 73-81% [lower for samples with many $CD16^+$ cells], ES+16dep 83-95%, RS 72-85%).

Positive selection resulted in improved yield of $CD14^+$ monocytes.

Cell yield was also variable. Overall, a greater number of cells were recovered using positive selection compared with negative selection. The proportion recovered as a percentage of cells used was superior with the MB kit but was more closely matched against ES kits. However, it is important to note that the number of PBMCs recovered from donor 1 for purification with ES kits was around 4- to 5-fold less than expected. This was using SepMate™ as described above and was at the lower end for our expected

recovery. This had a significant impact of the subsequent yield of enriched $CD14^+$ cells (see legend of Table 5.3).

We hypothesised that some of the observed differences in yield may have been the result of different methods of PBMC extraction or because only half the number of cells were available, as two ES kits were being evaluated. To clarify the relative contribution to lower yield from SepMate™ and from the selection process, the number of $CD14^+$ cells enriched by positive selection (MB) and negative selection (ES+16dep) were compared for a third donor (22-year-old male) by directly layering PBMCs extracted from buffy coat onto density gradient media. Recovery of $CD14^+$ cells was approximately 2-fold higher using positive selection.

One separation step was sufficient.

There was no additional benefit in purity from a second separation step for the MB kit (where the first eluted fraction was then enriched over a second column). The proportion of $CD14^+$ events gated was 95.9% with one enrichment, 96.7% with two enrichments, with 2.6% in the depleted fraction after one enrichment and 19.6% after two enrichments. Yield was lower if two enrichments were used (data not shown).

Positive selection was the preferred approach for the planned experiments.

Overall, the planned co-culture experiments required a large number of viable and pure monocytes. Sufficient numbers of PBMCs also need to be retained and not enriched for $CD14^+$ cells to enable their comparison against monocytes, so the RS kit was unsuitable as only the latter fraction would have been available. The yield, purity and viability of $CD14^+$ cells enriched by positive selection using the MB kit were most suited to our requirements. Therefore, the final method used positive selection.

However, we first wanted to confirm that this approach would yield the expected cell populations and that these would perform as expected in co-culture experiments.

Figure 5.4 – cell populations purified from human leucocytes using four kits, showing unenriched, enriched and depleted cell fractions

Forward-scatter (FS) / $\log_{10}$ side-scatter (SS) plots each with 10,000 ungated events are shown for various representative cell populations (obtained from donor 2). Data were acquired with a Beckman Coulter FC500 flow cytometer from unstained and unfixed cells. Panels A and B respectively show peripheral blood mononuclear cells (PBMCs) that were purified by layering over density-gradient media or using STEMCELL SepMate™. Panel C shows a schematic representation of different types of leucocyte according to size and density (G = granulocytes, Mo = monocytes including non-classical monocytes marked *, L = lymphocytes). Panel D shows buffy coat prepared from whole blood (100,000 events shown). The other panels show the enriched fraction (middle row) and, where available, the depleted fraction (bottom row) for cell populations after selecting for monocytes using different kits (MB, ES–16dep, ES+16dep and RS; for details see Table 2.14).

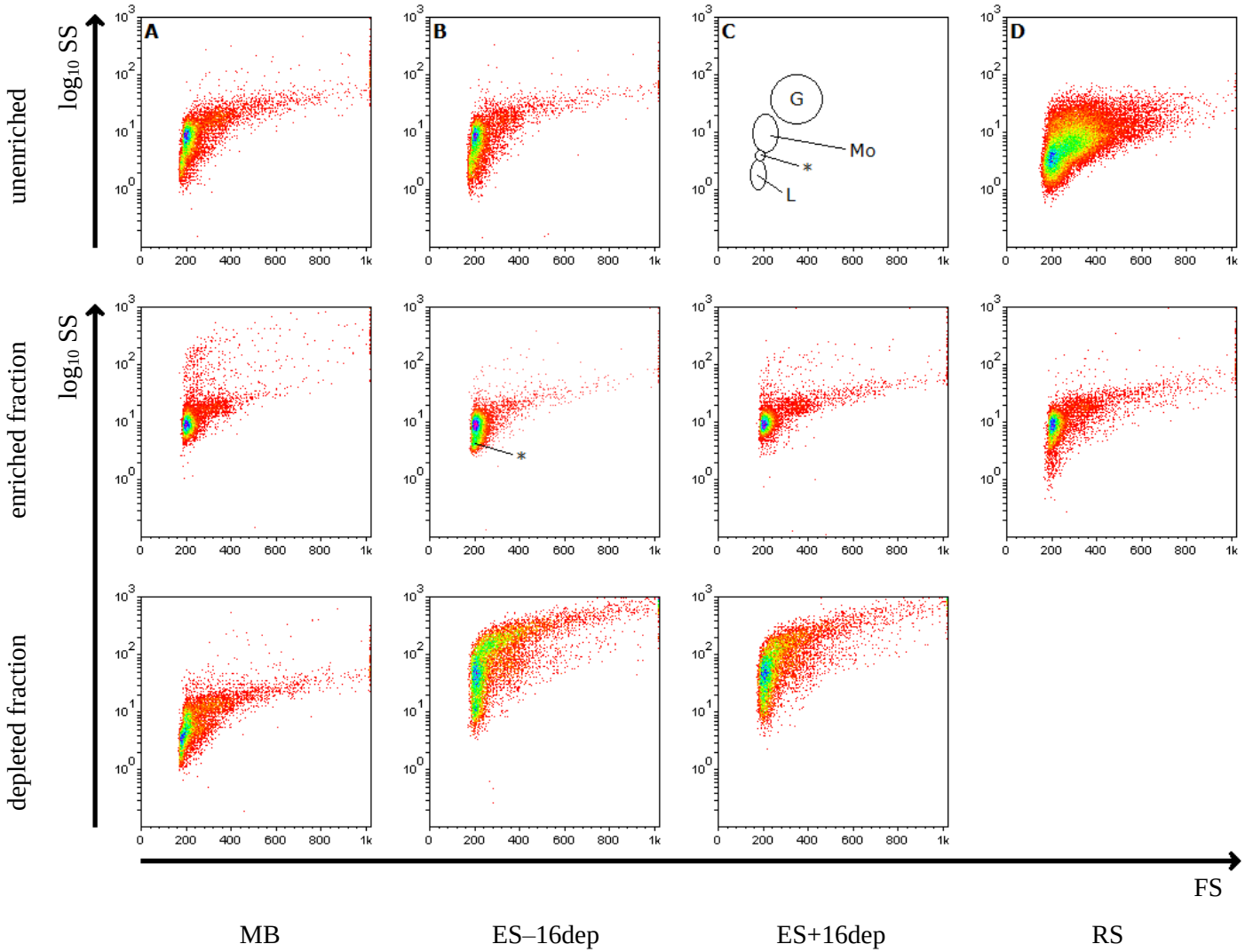

Figure 5.4 – cell populations purified from human leucocytes using four kits, showing unenriched, enriched and depleted cell fractions

5.4.2 Purified cell populations

Next, the cell populations obtained using the various evaluated methods were compared. Representative flow cytometry plots for each of the cell populations isolated from donor 2 are shown in Figure 5.4. The plots showing PBMCs (panels A and B) appeared similar, with mostly lymphocytes and monocytes (panel C) compared with the buffy coat (panel D) from which the PBMCs had been purified.

Monocytes were purified as expected using different kits, including different monocyte subsets. There was evidence for contamination of enriched fractions with other cell types.

Cell fractions enriched for $CD14^+$ monocytes, both by positive (MB) and by negative selection (others), comprised mostly monocytes (Figure 5.4). All purified populations appeared to some extent to be contaminated with granulocytes (likely neutrophils), though these should be relatively depleted by CD66b in the kits using negative selection. Neutrophil contamination appears to be of minor consequence in this model (see next section). Cells purified directly from buffy coat by RS kit negative selection appeared to have more lymphocyte and granulocyte contamination.

Non-classical $CD14^{dim}CD16^+$ monocytes could not be investigated if $CD14^+$ positive selection or certain types of negative selection were used.

The non-classical monocyte population can be identified for the ES–16dep enriched fraction (marked * on Figure 5.4), cells from which would include $CD14^{dim}CD16^+$ monocytes. These are less dense and slightly smaller (Grage-Griebenow et al. 2001) and, therefore, have lower side-scatter and forward-scatter. As expected, only classical $CD14^+$ monocytes were identified after positive selection and negative selection with the ES+16dep kit.

The depleted cell fraction was only suitable for use in subsequent experiments after positive selection.

Depleted fractions after positive selection (MB) contained mostly lymphocytes with some granulocytes (Figure 5.4). Negative selection resulted in depleted fractions which, as expected, were distorted by clumping and debris. Therefore, it was possible that these two depleted fractions would be unsuitable for use in subsequent experiments. This is

supported by minimal cytokine expression observed in response to various stimuli for depleted cell fractions after negative selection reported in the next section (Figure 5.7).

Peripheral blood mononuclear cells separated from buffy coat and co-cultured with bacteria showed upregulation of IL-12/23p40 and CD14 expression when compared with cells co-cultured with media only, regardless of the protocol used.

Figure 5.5 shows IL-12/23p40 and CD14 expression of PBMCs co-cultured for 16 h with media only or *H. pylori* AB21 wild-type. The Miltenyi Biotec (MB) and STEMCELL EasySep™ protocols (ES) both performed adequately and as expected.

The proportion of $CD14^+$ events was significantly greater with the MB protocol (73.4 vs. 65.4%, $P < 0.001$ using Fisher's exact test). The lower proportion of IL-12/23p40$^+$ events within the $CD14^+$ group seen with the MB protocol was also significant (34.9 vs. 42.8%, $P < 0.001$). However, the mean fluorescence intensity for IL-12/23p40 was numerically higher for MB than ES (45.8 vs. 29.5 units) with similar results for the Luminex analysis reported in the next section (Figure 5.7).

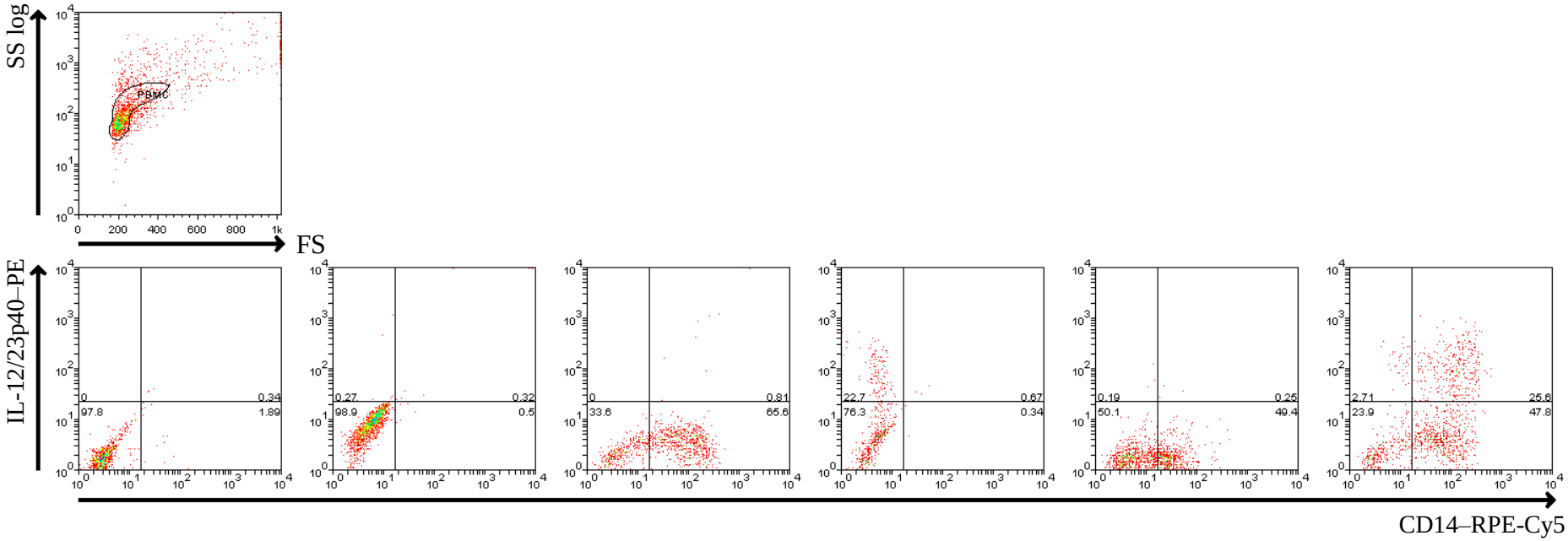

type	unstained control	isotype control	isotype/FMO control	FMO control	sample	sample
bacteria	media only	AB21	AB21	AB21	media only	AB21
events	1165	2216	1118	596	1580	1363
CD14	–	–	+	–	+	+
IL-12	–	–	–	+	+	+
isotype	–	+	+	–	–	–
% CD14$^+$					49.7	73.4
% IL-12/23p40$^+$ of CD14$^+$					0.5	34.9
IL-12/23p40 gated mean fluorescence intensity					2.0	45.8

Figure 5.5 – IL-12/23p40 and CD14 expression by PBMCs purified using the (1) Miltenyi Biotec protocol

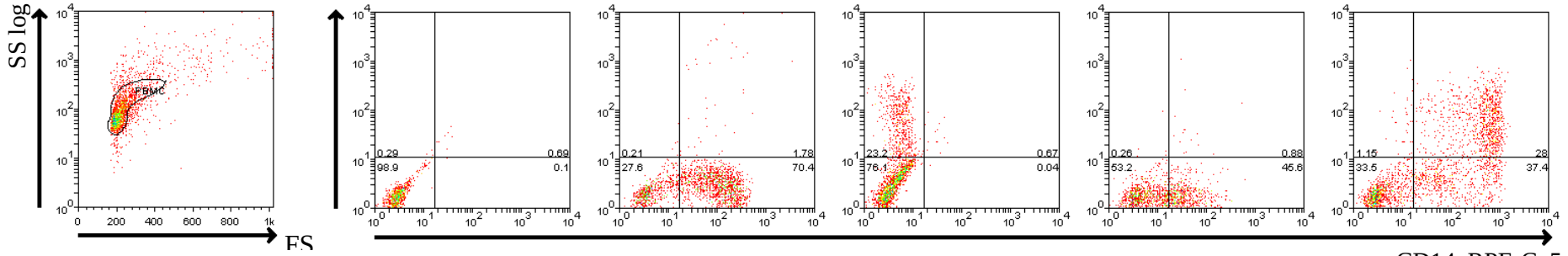

type	unstained control	isotype/FMO control	FMO control	sample	sample
bacteria	media only	AB21	AB21	media only	AB21
events	1020	2365	2399	1931	3383
CD14	–	+	–	+	+
IL-12	–	–	+	+	+
isotype	–	+	–	–	–
% CD14$^+$				46.5	65.4
% IL-12/23p40$^+$ of CD14$^+$				1.9	42.8
IL-12/23p40 gated mean fluorescence intensity				2.8	29.5

Figure 5.5 – IL-12/23p40 and CD14 expression by PBMCs purified using the (2) STEMCELL EasySep™ protocol

Figure 5.5 – IL-12/23p40 and CD14 expression by PBMCs purified using the (1) Miltenyi Biotec and (2) STEMCELL EasySep™ protocols

Peripheral blood mononuclear cells (PBMCs) were prepared from the donor 2 buffy coat using (1) the Miltenyi Biotec and (2) the STEMCELL EasySep™ protocols. Cells were co-cultured with media only or *H. pylori* AB21 strains, and incubated for 16 h with brefeldin A added after 1 h. Cells were stained with mouse IgG2a anti-human CD14–RPE-Cy5, mouse IgG1κ anti-human IL-12/23p40–PE and PE rat IgG1κ isotype control. Unstained, fluorescence minus one (FMO) and isotype controls were included. Events were acquired over 240 seconds with a Beckman Coulter FC500 flow cytometer and gated for PBMCs on a forward-scatter (FS) / side-scatter (SS) plot.

$CD14^+$ events were the source of the majority of IL-12/23p40. CD14 expression was upregulated by antigen stimulation, particularly in co-culture with live bacteria where most IL-12/23p40 expression was from $CD14^{hi}$ events.

Figure 5.6 again shows that the vast majority of IL-12/23p40 expression during PBMC co-culture was by $CD14^+$ cells. This relative expression was increased for co-culture with cells enriched for CD14 (mean fluorescence intensity of IL-12/23p40 for $CD14^+$ events was 139.8 units for PBMC co-culture [1.0% events], and 331.4 and 459.2 units for $CD14^+$ co-culture enriched by positive and negative selection respectively [15.9% and 22.4% of events respectively]).

CD14 expression was up-regulated by LPS and AB21 wild-type, and partially up-regulated by sonicated bacterial lysate. For cells cultured with lysate and particularly with live bacteria, most IL-12/23p40 expression was by cells that expressed the highest CD14 levels ($CD14^{hi}$). Expression of IL-12/23p40 by cells cultured with LPS was more equal between $CD14^+$ and $CD14^{hi}$ cells.

An additional $CD14^+$ cell population that can express IL-12/23p40 was observed. This likely represents neutrophils and accounts for the minority of events overall.

Another discrete cell population was observed above the gated region marked on the FS/SS plot for CD14 enriched by positive selection (Figure 5.6, centre panel on far right). Based on location this likely represents an enriched/expanded population of granulocytes (neutrophils). This should be partially depleted by CD66b antibodies in negative selection (compare with lower panel on far right, discussed in Section 2.10).

This cell population was expanded by co-culture with live bacteria when compared against co-culture with media only (number of events [% of total], PBMC 114 [0.2%] vs. 647 [1.3%], CD14 positive enrichment 367 [0.7%] vs. 5043 [10.1%], CD14 negative enrichment 1009 [2.0%] vs. 2529 [5.1%]). This cell population also expressed IL-12/23p40 when co-cultured with a positive control and particularly with live bacteria (mean fluorescence intensity of IL-12/23p40 for $CD14^+$ events for AB21 wild-type vs. media only [% events $CD14^+$IL-12/23p40$^+$], PBMC 440.8 vs. 133.2 units [32.6% vs. 20.2%], CD14 positive enrichment 888.5 vs. 127.3 units [56.9% vs. 7.4%], CD14 negative enrichment 908.2 vs. 118.2 units [57.7% vs. 16.5%]). These cells account for the minority of events overall.

Figure 5.6 – comparison by flow cytometry of IL-12/23p40 and CD14 expression by different cell populations

Peripheral blood mononuclear cells (PBMCs) were purified from 1 donor (F) using the optimised protocol. Cells expressing CD14 were enriched from these PBMCs by positive (+) selection (MB kit) and negative (–) selection (ES+16dep kit, with CD16 depletion). Cells were co-cultured with media only, lipopolysaccharide (LPS), sonicated *H. pylori* (lysate) or *H. pylori* AB21 wild-type strain (X) and incubated 16 h with brefeldin A added after 1 h. Cells were stained separately with mouse IgG2a anti-human CD14–FITC before fixation and with mouse IgG1κ anti-human IL-12/23p40–PE after fixation/permeabilisation. Unstained, fluorescence minus one and isotype controls were included (data not shown). Fifty-thousand events were acquired with a Beckman Coulter FC500 flow cytometer and gated for relevant cells on a forward-scatter (FS) / side-scatter (SS) plot, which encompassed the majority of events (number of events [% of total], PBMC 48,507 [97.1%], CD14 positive enrichment 40,893 [81.8%], CD14 negative enrichment 43,268 [86.5%]).

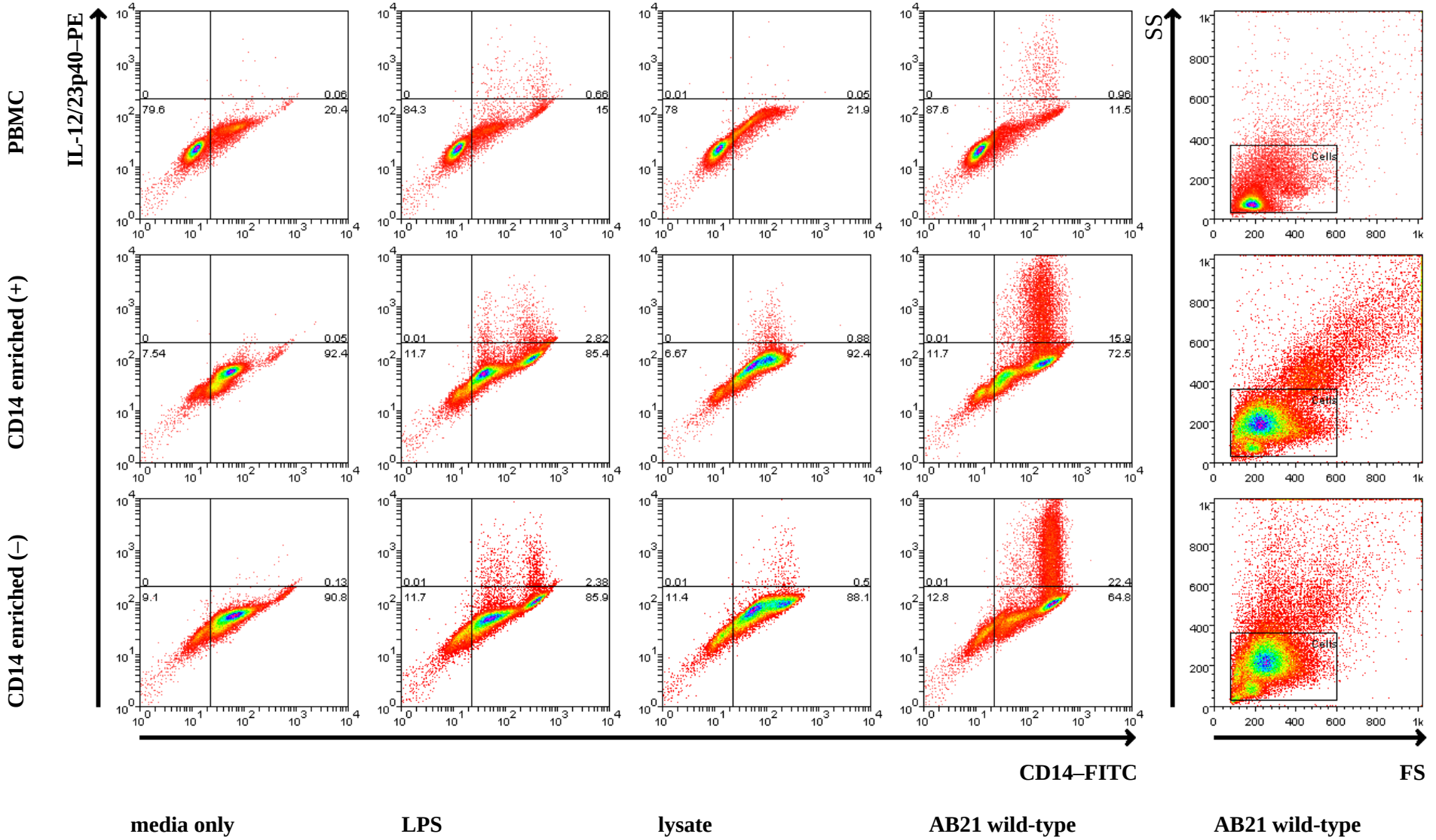

Figure 5.6 – comparison by flow cytometry of IL-12/23p40 and CD14 expression by different cell populations

5.4.3 Cytokine expression phenotype of purified cell populations

Finally, we wanted to establish if cells enriched using the various methods evaluated performed in a similar way and as expected in subsequent co-culture experiments. Peripheral blood mononuclear cells, $CD14^+$ enriched and $CD14^+$ depleted cellular fractions from donors 1 and 2 were evaluated. Cytokine expression in 48h co-culture supernatants was measured by Luminex assays. This is reported in Figure 5.7.

Various cell populations were co-cultured for 48 h with media, lipopolysaccharide (LPS) and *H. pylori* AB21 wild-type (strain O, see Table 2.15). Media only negative controls were included for all cell populations and were all below the lower limit of quantification of the assay (16 pg/mL), which suggests that engagement of CD14 during positive selection does not in itself activate monocytes to express cytokines.

One-way ANOVAs were used across all 9 cell populations (PBMC, $CD14^+$ enriched and $CD14^+$ depleted) for media only, LPS and *H. pylori* AB21 wild-type (all $P < 0.001$, Chi square values, mean ranks and individual *P* values are not shown). Post-test Tukey's correction was then used to compare all groups (36 comparisons).

Monocytes purified by positive selection expressed cytokines in response to antigenic stimulation and co-culture with live bacteria as expected. Cells purified by negative selection expressed more IL-12/23p40 than expected in response to antigen stimulation, suggesting potential contamination by other cell types.

For AB21 wild-type, this analysis showed no statistically significant difference between IL-12/23p40 expression by $CD14^+$ monocytes enriched using MB, ES–16dep and ES+16dep kits ($P > 0.05$). Cytokine expression by each of these three enriched cell populations was significantly higher than ES PBMCs and both ES CD14 depleted populations ($P < 0.05$ for each vs. MB CD14 enriched population, $P < 0.01$ for each vs. ES CD14 enriched populations). In addition, IL-12/23p40 concentrations for both ES CD14 enriched populations were significantly higher than MB CD14 depleted cells (both $P < 0.01$) and concentrations for ES+16dep monocytes were also significantly higher than MB PBMCs and RS CD14 enriched cells (both $P < 0.05$).

For cells co-cultured with LPS, cytokine expression was not significantly different except for both ES–16dep and ES+16dep enriched monocytes, which were each significantly higher than every other cell population except for each other (all $P < 0.01$). Mean ± standard deviation for IL-12/23p40 expression by ES–16dep enriched

monocytes, ES+16dep enriched monocytes and all remaining cell populations were 2,194 ± 12, 2,007 ± 36 and 447 ± 301 pg/mL respectively. Therefore, cytokine concentrations were 4- to 5-fold higher for LPS-stimulated monocytes purified using ES kits than for other cell types. This may be because of contamination of negatively selected monocytes (both with and without $CD16^+$ forms) by other cell types such as platelets or DCs (Section 2.11), as negative separation resulted in less pure isolation.

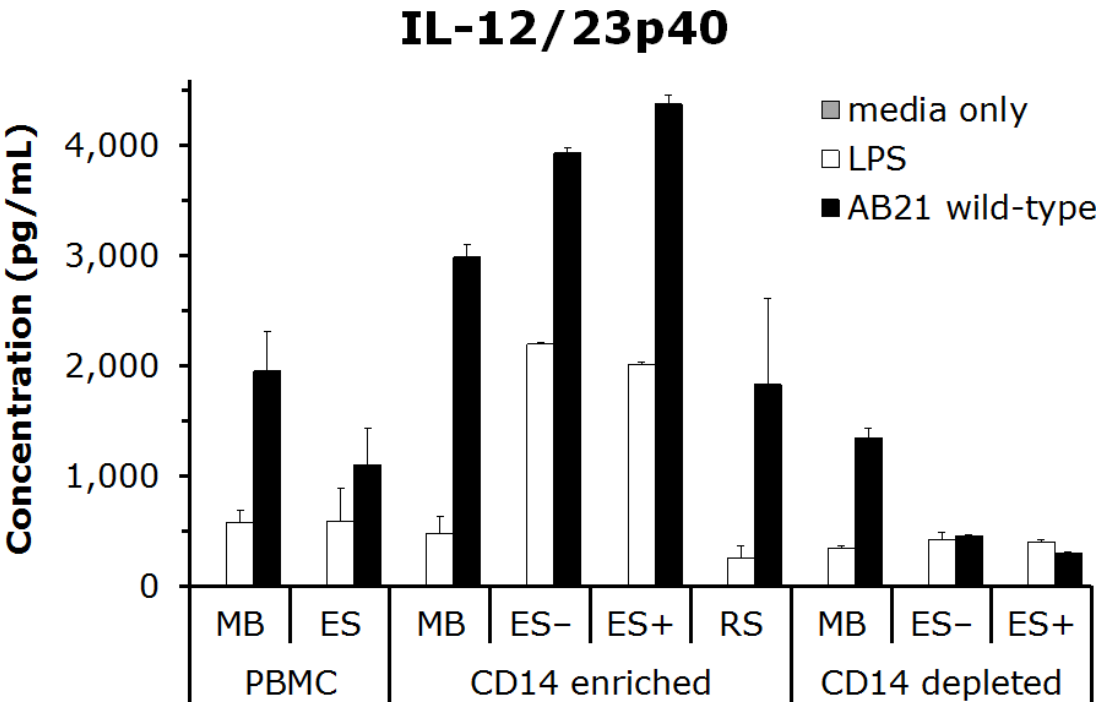

Figure 5.7 – cytokine expression phenotype of cell populations in 48 h co-cultures

Peripheral blood mononuclear cells (PBMCs) were purified from donors 1 and 2. Cells both enriched for CD14 (principally monocytes) and depleted of $CD14^+$ cells were obtained from these PBMCs using different kits (MB, ES–16dep, ES+16dep and RS; for details see Table 2.14). Cells were co-cultured with media only (all <16 pg/mL), lipopolysaccharide (LPS) or live *H. pylori* AB21 wild-type strain. IL-12/23p40 concentrations in 48 h co-culture supernatants were measured in duplicate using Luminex assays (milliPLEX Cytokine Panel 1). Luminex data for IL-8 and IL-12p70, ELISA data for IL-12/23p40 and MSD V-PLEX assay 9-plex data are not shown.

Data bars represent the mean cytokine concentration (PBMC MB, PBMC ES, CD14 enriched and depleted MB, and CD 14 enriched RS n=4, CD14 enriched and depleted ES–16S and ES+16S n=2). The error bars show standard error of the mean across technical and biological replicates.

Data for each mutant were separately compared against a median of 100% (dotted red line) by Wilcoxon signed-rank tests. Statistically significant differences are shown below the plotted data (* $P < 0.05$, ** $P < 0.01$, *** $P < 0.001$). Data across all groups were compared by one-way ANOVA with Tukey's correction for multiple comparisons with 36 planned comparisons (each group vs. every other). Statistically significant differences after these corrections are reported in the text.

5.5 Co-culture with CD14$^+$ monocytes

We therefore used CD14 positive immunomagnetic selection from PBMCs based on these observations. These purified monocytes were our principal experimental model. Cells were extracted from ten donors (see Table 5.1 in Section 5.2).

Total cell numbers, viability and purity of extracted cell populations are reported in Table 5.4. The median total number of CD14$^+$ cells recovered after immunomagnetic cell separation was 0.31×10^8 cells (IQR $0.17\text{-}0.54\times10^8$ cells). Viability was 98-99% Overall, CD14 enriched cells exceeded 90% purity by CD14–FITC staining (mean 93.8%, median 95.9%, IQR 92.5-97.7%). Data were missing for donor C.

Table 5.4 – details of monocytes purified from donor blood

Donor	Total cell number ($\times10^8$)	Viability by TB (%)	Viability by PI (%)	CD14$^+$ purity (%)
Overall	0.38 ± 0.32	99 ± 1.6	97.7 ± 2.2	93.8 ± 5.4
A	0.16 *	-	-	85.7
B	0.04 *	-	-	84.5
C	0.21	95	-	-
D	0.12	98	99.7	99.1
E	0.44	100	99.7	97.7
F	0.19	99	99.1	92.5
G	0.57	99	95.2	95.9
H	0.60	98	98.2	96.9
I	1.10	100	94.1	94.0
J	0.41	99	97.6	98.3

Overall data expressed as mean ± standard deviation.

The percentage of CD14$^+$ cells in peripheral blood mononuclear cells purified from these 10 donors varied from 12.4 to 90.7 percent (mean 38.1%, median 25.1%, IQR 20.4-55.9%).

PI, propidium iodide staining; TB, trypan blue staining; *, only viable cells counted (see text); -, missing data point (see text).

CD14$^+$ monocytes were co-cultured for 48 h, with media only, with lipopolysaccharide (LPS) or sonicated *H. pylori* (lysate), or with sets of wild-type and isogenic/double mutants of strain AB21.

Concentrations of various pro-inflammatory cytokines (IL-1β, IL-6 and TNF-α, IL-12/23p40 and IL-12p70 and IFN-γ), the pro-inflammatory chemokine IL-8 and the anti-inflammatory cytokine IL-10 were determined in co-culture supernatants. IL-17A was not analysed as it is not known to be an effector cytokine of monocytes.

5.5.1 Relative cytokine and chemokine concentrations

Relative cytokine concentrations are shown in Figure 5.8.

Controls and adjusted concentrations for each strain are shown in Appendix Figure 7.7. Adjusted concentrations for *dupA1* and non-*dupA1* clinical isolates co-cultured with $CD14^+$ monocytes are reported in Appendix Figure 7.8.

The same analysis approach as for PBMCs was used (described in Section 5.3.2). To enable comparison between strains and between donors, each adjusted cytokine concentration was expressed as a percentage of the corresponding wild-type strain for each donor/strain combination.

First, Kruskal-Wallis tests were used across all 9 strain types for each analyte. These provided evidence for all analytes to reject the null hypotheses that strain groups were sampled from populations with identical distributions ($P \leq 0.004$ for all, except $P \leq 0.025$ for IL-1β and IL-10; Chi-square values, mean ranks and individual *P* values are not shown). Post-test Dunn's correction was then used for 8 planned comparisons (each isogenic mutant vs. wild-type, Δ*cagE* vs. Δ*dupA*Δ*cagE*, Δ*virB8* vs. Δ*virB8*Δ*dupA*) for each analyte. Additional *ad hoc* multiple comparison correction was undertaken only for analysis of IL-12p70 expression to correct for 8 unplanned comparisons (all mutant strains vs. wild-type). This is explained below.

Monocytes co-cultured with isogenic *dupA* mutants expressed lower relative levels of pro-inflammatory cytokines and chemokines than cells co-cultured with wild-type strains.

Wilcoxon signed-rank tests showed that there were statistically significant differences in the median percentage cytokine/chemokine expression after co-culture of $CD14^+$ cells with Δ*dupA* isogenic mutants for IL-1β ($P = 0.022$, 34.0% lower), IL-6 ($P = 0.008$, 21.3% lower), IL-8 ($P = 0.010$, 23.0% lower), IFN-γ ($P = 0.010$, 34.0% lower) and IL-12/23p40 ($P = 0.002$, 31.0% lower). These are indicated by asterisks below the plotted data in Figure 5.8 (see legend). There was no evidence of differences in the median relative expression of TNF-α, IL-10 or IL-12p70.

Compared against wild-type strains, and after correction for multiple comparisons, monocytes co-cultured with isogenic *dupA* mutants expressed significantly lower relative levels of IL-6 ($P < 0.05$), IL-8 and IL-12/23p40 (both $P < 0.01$) compared with wild-type strains (Figure 5.8, shown above the plotted data). This was previously

observed for PBMCs (Section 5.3.2). In addition, for $CD14^+$ cells, IFN-γ expression was lower in strains lacking *dupA* ($P < 0.05$). This had not been demonstrated for PBMCs. Statistical significance was not established in these analyses for IL-1β or TNF-α.

Overall, there was strong evidence for lower expression of IL-6, IL-8, IFN-γ and IL-12/23p40 by monocytes co-cultured with isogenic Δ*dupA* mutants than with wild-type. There was some evidence for lower IL-1β expression.

Significance had previously been shown in TNF-α expression by PBMCs. For $CD14^+$ cells, median expression for isogenic Δ*dupA* mutants was 61.7% of wild-type but the inter-quartile range was 49.6-121.0% so non-significant. Neither was significance established for comparisons of double mutants against their isogenic counterparts with and without *dupA*, though again there were fewer experimental comparisons.

Monocytes co-cultured with Δ*cagE* mutants expressed relatively less IL-8.

Wilcoxon signed-rank tests showed statistically different median percentage expression of IL-6 ($P = 0.007$, 13.8% lower) and IL-8 ($P < 0.001$, 24.7% lower) by $CD14^+$ cells co-cultured with Δ*cagE* isogenic mutants. Significance remained after correction for multiple comparisons for IL-8 ($P < 0.001$). Median IL-8 expression was also lower for Δ*dupA*Δ*cagE* double mutant strains ($P = 0.017$, 8.9% lower), though this was lost after correction for multiple comparisons.

Higher levels of IL-12p70 expression were observed for cells co-cultured with both Δ*cagE* ($P = 0.041$, 21.1% higher) and Δ*dupA*Δ*cagE* strains ($P = 0.008$, 63.2% higher). No differences were shown after correction for planned comparisons, nor after additional analysis to correct for 8 comparisons of all mutant strains vs. wild-type. Therefore, these observations have only some evidence and are likely less important.

There was evidence for different cytokine expression by monocytes co-cultured with mutants lacking other putative *tfs4* components. In particular, Δ*virB2* strains induced lower relative expression of several pro-inflammatory cytokines.

An isogenic Δ*virB2* mutant strain was co-cultured with $CD14^+$ cells purified from 6 donors (C, D, G-J) and compared against wild-type strains. Supernatants showed significantly lower median expression of TNF-α (46.8% lower), IL-6 (25.5% lower), IL-8 (24.1% lower), IFN-γ (31.9% lower), IL-12/23p40 (57.2% lower) and IL-12p70 (45.4% lower) by Wilcoxon-signed rank tests (all $P = 0.031$, n=6 donor/strain pairs).

Statistical significance was confirmed after correction for multiple comparisons for IL-6 and IL-8 (both $P < 0.01$), IFN-γ ($P < 0.05$), IL-12/23p40 ($P < 0.001$) and IL-12p70 ($P < 0.05$). It was not established for TNF-α. IL-12p70 expression remained statistically significant at the same level after correction for 8 unplanned comparisons as before. This additional analysis was undertaken so as not to introduce bias by requiring fewer sources of evidence than for the isogenic and double Δ*cagE* mutants. Significance was not established in any analysis for IL-1β or IL-10.

As for PBMC co-culture with the Δ*virB9* isogenic mutant, for $CD14^+$ cells the median IL-12/23p40 expression was significantly reduced compared to wild-type ($P = 0.031$, 38.0%), though not after correction for planned comparisons. Also, median TNF-α expression for the Δ*virB8* isogenic mutant was statistically increased ($P = 0.031$, 49.4% higher), though significance was lost after correction for multiple comparisons.

Cells co-cultured with the markerless Δ*tfs4* mutant strain were not observed to express significantly different cytokine levels, though again this is based on fewer independent experiments than for some other comparisons (see legend of Figure 5.8).

Overall, there was strong evidence that monocytes co-cultured with isogenic Δ*virB2* mutants express less IL-6, IL-8, IFN-γ, IL-12/23p40 and IL-12p70 than wild-type strains. Evidence was less strong and less consistent for other cytokines and for strains lacking other putative *tfs4* components.

Similar strong evidence was found for Δ*dupA* mutants for lower expression of these pro-inflammatory cytokines, though not for IL-12p70, by $CD14^+$ monocytes. We again have shown that *dupA* and *virB2* are more important determinants of cytokine expression than *virB8*, *virB9* and *tfs4*.

Across these results, IL-12/23p40 has emerged as the most consistently affected and among the most strongly altered cytokines. Therefore, this analyte was the focus of flow cytometric analysis of $CD14^+$ monocytes from 5 donors (F-J) in 16 h co-culture (Appendix Section 7.5.4 and Figure 7.9). We did not confirm the observation of lower IL-12/23p40 expression in co-culture with Δ*dupA* strains by flow cytometry.

Next, we examine the effects of heat-inactivation and paraformaldehyde treatment, to explore whether the cellular cytokine response requires an active or passive process and if it can be potentiated by cross-linking of surface protein structures. Finally, we report data for Δ*dupA* and other mutants in different strain backgrounds.

Figure 5.8 – relative cytokine concentrations for 48 h monocyte co-culture

$CD14^+$ monocytes were purified from 10 donors and co-cultured with sets of wild-type and isogenic/double mutants of strain AB21 that had been constructed and stored separately (denoted by O and X). Cytokine/chemokine concentrations in 48 h co-culture supernatants were measured for 8 analytes using Meso Scale Discovery V-PLEX assays in at least duplicate (panels A to H).

Data points represent the percentage difference from wild-type in the mean concentration for each donor/strain combination (wild-type n=19, Δ*dupA* n=15, Δ*tfs4* n=7, Δ*cagE* n=15, Δ*dupA*Δ*cagE* n=13, Δ*virB2* n=6, Δ*virB8* n=7, Δ*virB9* n=6, Δ*virB8*Δ*dupA* n=2; every data point is not plotted – see note). The horizontal and error bars show overall median values and inter-quartile ranges (IQRs) respectively.

Analysis followed two steps (see Section 5.3.2):

First, data across all groups for each analyte were compared by Kruskal-Wallis tests with Dunn's correction for multiple comparisons with 8 planned data pairs (each isogenic mutant vs. wild-type, Δ*cagE* vs. Δ*dupA*Δ*cagE*, Δ*virB8* vs. Δ*virB8*Δ*dupA*). Further unplanned multiple comparisons were also undertaken for IL-12p70 (data not shown, see text in Section 5.5.1). Statistically significant differences after these corrections are shown above the plotted data (* $P < 0.05$, ** $P < 0.01$, *** $P < 0.001$).

Second, data for each mutant were separately compared against a median of 100% (dotted red line) by Wilcoxon signed-rank tests. Statistically significant differences are shown below the plotted data (*/*P* value combinations as before).

Where both analytical approaches were significant, there was strong evidence for a statistically important difference compared to wild-type and the strain name is highlighted in bold.

Note that for clarity some data points are not shown but were included in summary statistics and analysis – donor D Δ*tfs4* X for panels A: IL-1β (265%), B: TNF-α (873%), C: IL-6 (459%), D: IL-8 (500%), E: IL-10 (556%), G: IL-12/23p40 (594%) and H: IL-12p70 (346%); donor I Δ*dupA*Δ*cagE* O and X for panel H: IL-12p70 (242% and 228% respectively).

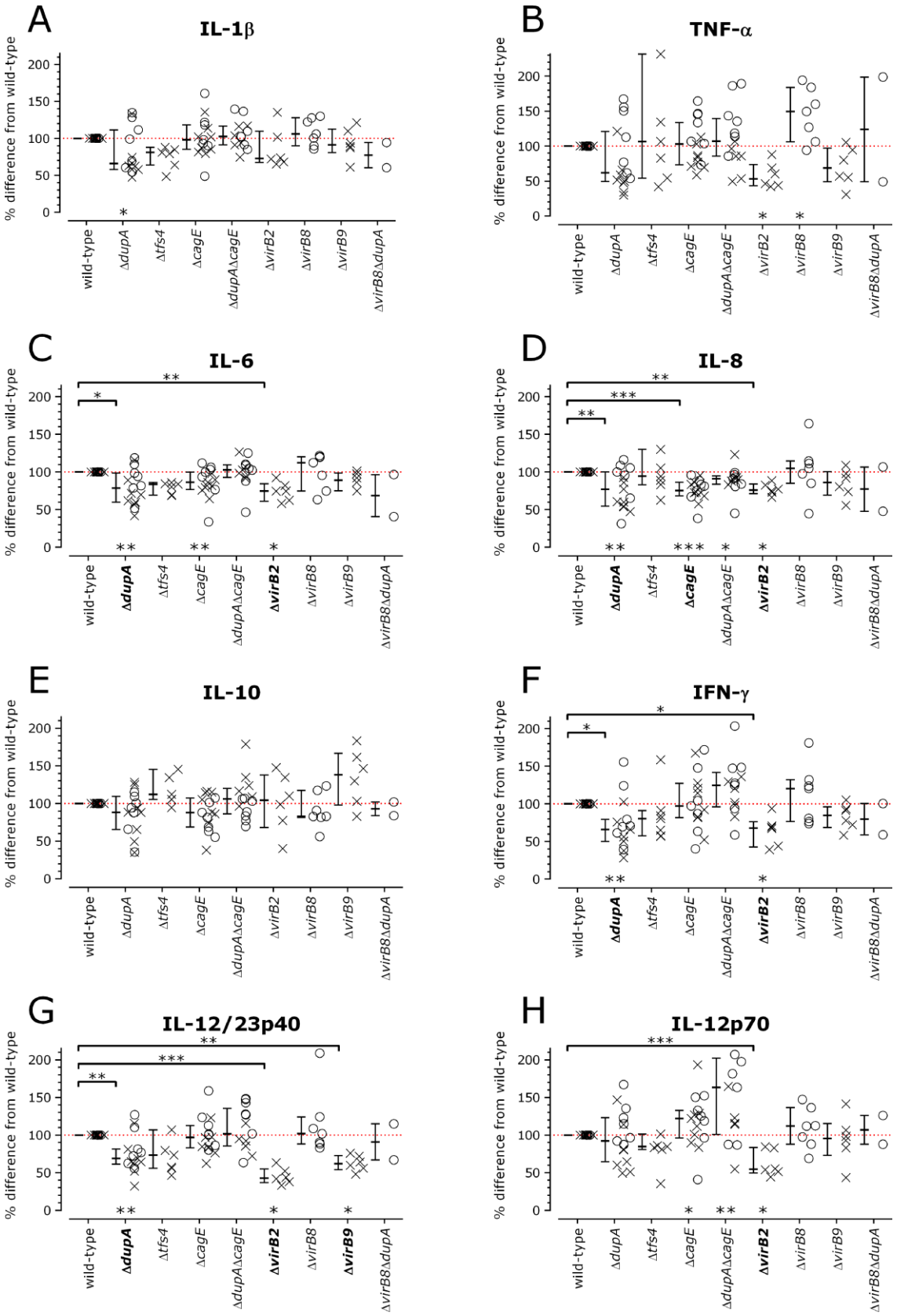

Figure 5.8 – relative cytokine concentrations for 48 h monocyte co-culture

5.6 Co-culture of treated bacteria and other strains

5.6.1 Heat-inactivation (HI)

Sonicated *H. pylori* (lysate) and purified *E. coli* LPS do not stimulate as strong a cytokine response from PBMCs or monocytes as live bacteria after 48 h co-culture (Appendix Figure 7.6 and Figure 7.7). We wanted to test in our monocyte cell model whether the differential responses seen for Δ*dupA* and other mutant strains were dependent on live bacteria and an active process, hypothesising that these are required.

Bacteria were inactivated by heating to 65 °C for 30 min. Cytokine concentrations for each HI strain were expressed as a percentage of the corresponding untreated strain.

Results are shown in Figure 5.9 and for PBMCs are reported in Appendix Figure 7.10.

Cytokine expression was dependent on live bacteria. Heat inactivation of each strain markedly reduced cytokine production relative to the corresponding untreated strain, though was relatively preserved for IL-6.

Heat inactivation markedly attenuated cytokine production by both PBMCs (Appendix Section 7.5.5) and $CD14^+$ cells across all strains. Median relative concentrations were 6.1 percent overall of those for untreated live bacteria (IQR, 2.1-21.4%). Concentrations were similar to cells stimulated with LPS (data not shown).

Relative expression for HI strains vs. untreated strains for IL-12p70 was 17.0% (10.3-30.0%), IL-10 was 10.2% (4.2-15.0%), IL-12/23p40 was 8.0% (3.5-15.6%), IFN-γ was 7.1% (4.2-14.1%) and was less than 4 percent for the remaining analytes (IL-1β, TNF-α and IL-8). For IL-6, median cytokine expression was less markedly reduced by heat inactivation (35.8% [18.5-55.1%]).

The unequivocal impact of heat inactivation can also be considered to have attained statistical significance in all cases (see legend of Figure 5.9, control of the false discovery rate was used to account for multiple comparisons for each analyte).

Overall, heat-inactivation markedly reduced the cellular cytokine responses, with no differences observed between mutants.

These data provide some support for the hypothesis that the mononuclear cell cytokine expression previously observed, including the different responses between Δ*dupA*, Δ*virB2* and wild-type strains, are dependent on live bacteria and an active process.

Figure 5.9 – cytokine concentrations from monocytes co-cultured with heat inactivated and paraformaldehyde-treated bacteria, relative to live untreated bacteria

$CD14^+$ monocytes were purified from up to 6 donors (E-J). Cells were co-cultured with wild-type and isogenic mutants of strain AB21 (denoted by X). Strains were untreated, heat inactivated (HI) or treated with paraformaldehyde (PFA). Cytokine/chemokine concentrations in 48 h co-culture supernatants were measured for 8 analytes using Meso Scale Discovery V-PLEX assays in at least duplicate (panels A to H).

Data points show each treated strain as a percentage of the equivalent untreated strain for each donor/treatment/strain combination (HI wild-type and Δ*tfs4* n=6, PFA treated wild-type and Δ*tfs4* n=5, all others n=4; every data point is plotted but note different Y-axis scales for panels D: IL-8, G: IL-12/23p40 and H: IL-12p70). The horizontal and error bars show overall median values and inter-quartile ranges respectively.

Inferential statistical analysis for HI strains was not originally planned, as non-standard analysis would be required (n=4 data points is too few to be able to show significance using Wilcoxon signed-rank tests) and the data speak for themselves. A method with sufficient power despite the small sample size was needed. The approach taken here was to use Kruskal-Wallis tests for each analyte (24 data points [6 each for wild-type and Δ*tfs4*, 4 each for other mutants] together with 4 or 6 comparator datapoints of 100 [equivalent to the corresponding untreated strains on this scale]). The false discovery rate (FDR) was used to correct for multiple comparisons, with Q = 0.05 and using the recommended two-stage method of Benjamini/Krieger/Yekutieli. This approach provided statistical evidence that, for every analyte and each strain, there was a marked decrease caused by heat inactivation relative to no treatment that was sufficient to be called a "discovery" in all cases (discovery is the equivalent term to statistically signficiant used in FDR approaches).

Analysis of PFA-treated strains followed two separate approaches, rather than the previous two step approach. Note that Wilcoxon signed-rank tests were not used.

First, in order to assess for differences between treated strains, data across all PFA-treated groups for each analyte were compared by Kruskal-Wallis tests with Dunn's correction for multiple comparisons with 6 planned data pairs (each PFA-treated mutant vs. PFA-treated wild-type, PFA-treated Δ*dupA* vs. PFA-treated Δ*virB2*, PFA-treated Δ*virB9* vs. PFA-treated Δ*dupA*). Statistically significant differences after these corrections are shown above the plotted data (*$P < 0.05$, ** $P < 0.01$, *** $P < 0.001$).

Second, to assess the impact of PFA treatment on the expression of different cytokines for each mutant strain, it was necessary to compare treated and untreated mutant strains referenced against the equivalent treated and untreated wild-types. Across these 8 datasets per analyte/cell type, Kruskal-Wallis tests and Dunn's correction for multiple comparisons were used with 4 planned data pairs (PFA-treated mutant strain as percentage of PFA-treated wild-type vs. untreated mutant strain as percentage of untreated wild-type). Statistically significant differences after these corrections are shown below the plotted data (*/*P* value combinations as before).

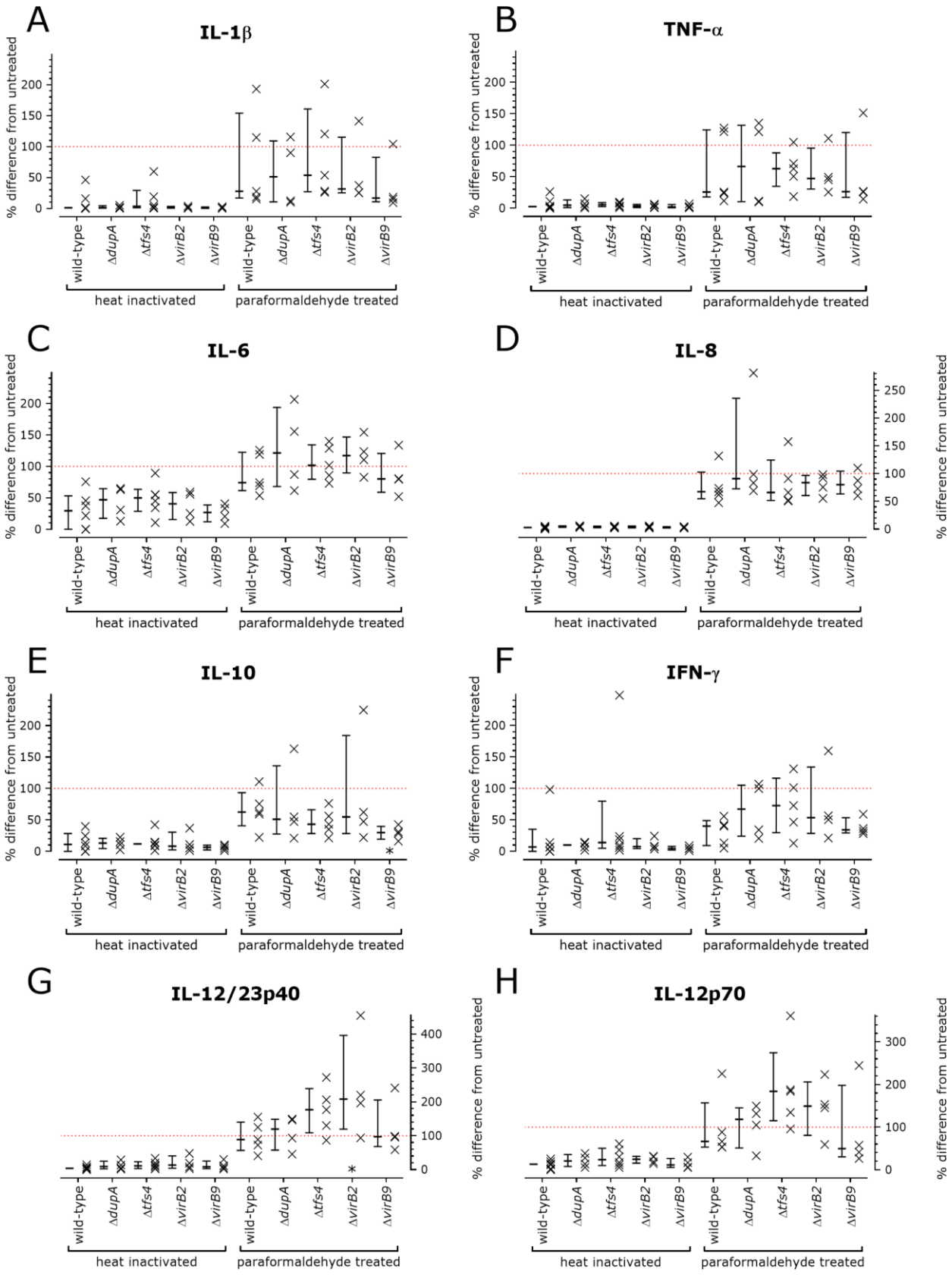

Figure 5.9 – cytokine concentrations from monocytes co-cultured with heat inactivated and paraformaldehyde-treated bacteria, relative to live untreated bacteria

5.6.2 Paraformaldehyde (PFA) treatment

As discussed in Section 5.3.1, components of the putative *tfs4* pilus (such as VirB2) may need to be present on the bacterial cell surface, and so may still be presented to inflammatory cells, despite knocking out certain *tfs4* genes. Paraformaldehyde treatment was used to fix cells with the intention of cross-linking any surface proteins that might then still stimulate or even potentiate any immune response. Therefore, the hypothesis for these experiments was that:

- there would be no difference for PFA-treated Δ*virB2* and Δ*tfs4* strains vs. wild-type (as no pili can be formed),
- no difference or possibly a potentiation for PFA-treated Δ*dupA* strains vs. wild-type or vs. Δ*virB2* (that could still express *virB2* but may lack any ATPase function to assemble extra-cellular pili), and
- no difference or a more marked potentiation for PFA-treated Δ*virB9* strains vs. wild-type or vs. *ΔdupA* (that could still express *virB2* and *dupA*).

To enable comparison between PFA-treated and untreated strains, each adjusted PFA-treated strain cytokine concentration was expressed as a percentage of the corresponding untreated strain.

Results are shown in Figure 5.9. Results for PBMCs are in Appendix Figure 7.10.

Analysis of PFA-treated strains followed two separate approaches. The first looked for differences between treated strains and the second for the impact of PFA treatment.

First, in order to assess for differences between treated strains, Kruskal-Wallis tests were used across all 5 PFA-treated strain types for each analyte. These did not provide evidence to reject the null hypothesis that strain groups were sampled from populations with identical distributions ($P > 0.05$), so no post-test analysis for planned comparisons was done. There were no statistically significant differences between treated strains.

Second, to assess the impact of PFA treatment on the expression of different cytokines for each mutant strain, treated and untreated mutant strains were compared referenced respectively against the equivalent treated and untreated wild-types. Kruskal-Wallis tests were used across 4 PFA-treated mutant and 4 untreated mutant datasets for each analyte. These provided evidence to reject the null hypothesis that strain groups were sampled from populations with identical distributions for IL-8, IL-10, IFN-γ, IL-

12/23p40 and IL-12p70 (P = 0.023, P = 0.015, P = 0.016, P < 0.001 and P = 0.023 respectively; Chi-square values and mean ranks are not shown) but not for IL-1β, TNF-α and IL-6 (P = 0.354, P = 0.155 and P = 0.112 respectively). Post-test Dunn's correction was then used for 4 planned data pairs (PFA-treated mutant strain as percentage of PFA-treated wild-type vs. untreated mutant strain as percentage of untreated wild-type). Significant results are indicated by asterisks below the plotted data.

Relative expression of IL-12/23p40 was increased for PFA-treated Δ*virB2* mutants. This was limited to one analysis relative to untreated AB21Δ*virB2*.

Median IL-12/23p40 expression was significantly increased for PFA-treated AB21Δ*virB2* relative to untreated AB21Δ*virB2* (P < 0.01, 98.6% [93.9-111.2%] vs. 42.8% [36.8-54.9%] respectively). This increase was also seen in PBMC co-culture (Appendix Section 7.5.5, P < 0.001, 171.97% [108.2-237.0%] vs. 61.9% [IQR, 54.0-71.4%] respectively). The hypothesis was that there would be no difference.

Cytokine expression was not significantly different for PFA-treated Δ*tfs4* mutant.

Paraformaldehyde treatment of AB21Δ*tfs4* had no statistically significant effects on cytokine expression relative to PFA-treated wild-type. The hypothesis was that would be no difference.

Paraformaldehyde treatment of isogenic mutant bacteria lacking *dupA* did not have any impact on cytokine expression.

Paraformaldehyde treatment of AB21Δ*dupA* had no statistically significant effects on cytokine expression relative to PFA-treated wild-type or to untreated AB21Δ*dupA*. The hypothesis was that would be no difference or possibly a potentiation.

There was evidence from several analyses that relative expression of IL-10 was decreased for PFA-treated AB21Δ*virB9*, relative both to wild-type and to Δ*dupA*.

Expression of IL-10 was significantly reduced for PFA-treated AB21Δ*virB9* relative to untreated AB21Δ*virB9* (P < 0.05, 72.9% [62.9-77.0%] vs. 138.2% [97.9-166.8%]). This increase was also seen in PBMC co-culture (Appendix Section 7.5.5, P < 0.05, 78.0% [67.8-82.1%] vs. 138.4% [118.6-201.1%]). However, as before, the reduction in IL-10 expression by $CD14^+$ cells for Δ*virB9* strains was only seen for the second analysis method and not the first.

In contrast, PBMC expression of IL-10 was significantly reduced for PFA-treated AB21Δ*virB9* relative to PFA-treated wild-type ($P < 0.05$, 33.7% [27.3-47.3%] vs. 89.6% [52.4-113.0%] respectively) and for PFA-treated AB21Δ*virB9* relative to PFA-treated AB21Δ*dupA* ($P < 0.05$, 33.7% [27.3-47.3%] vs. 95.0% [66.6-101.4%] respectively) (Appendix Figure 7.10 panel E). These were the only statistically significant findings demonstrated by the analysis approach to assess for differences between treated strains, as there were no such differences in $CD14^+$ cell co-culture.

Overall, these observations represent a relative decreased abundance of the anti-inflammatory cytokine IL-10, rather than the hypothesised potentiation of pro-inflammatory cytokines. No effects on other cytokines were seen.

5.6.3 Other strain backgrounds

We planned to test the observations made with the sets of AB21 strains and mutants with an extended panel of characterised strains and isogenic mutants (Table 2.15). As with AB21, the 432 strain has no known frameshifts in *dupA* or other putative *tfs4* components. The P1 and 527 strains do have some frameshifts of uncertain significance, though the main *tfs4* operon can be considered to be intact. In addition, our group has engineered several *catF* strains in these backgrounds to over-express *dupA* and other *virB/virD* homologues under the control of the *CATF* promoter.

Unfortunately, there were technical difficulties in growing and preparing these strains for the subset of planned experiments. Both PBMCs and $CD14^+$ monocytes were purified from 4 donors and co-cultured for 48 h with P1 wild-type, P1Δ*dupA* and P1Δ*tfs4*. Cytokines and chemokines were determined as before. Co-culture with mutants in other strain backgrounds and with *catF* strains was not possible owing to poor growth and viability (Section 2.11). This was unfortunate as the *catF* strain was designed to over-express *tfs4* genes.

The available data are presented as the percentage difference from wild-type (Figure 5.10). It was only valid to use the first analysis step, with Kruskal-Wallis tests and correction planned comparisons (only 2 for these experiments, each mutant vs. wild-type). Given that these were preliminary data with n=4 per group, the second step using Wilcoxon signed-rank tests has insufficient power to achieve statistical significance, so was not performed.

Limited data were available on cytokine expression by other laboratory strains of *H. pylori* in 48 h co-culture. Trends suggested possible lower expression of some pro-inflammatory cytokines for P1Δ*dupA* and P1Δ*tfs4* strains relative to wild-type.

There were no statistically significant differences in median cytokine expression.

However, some additional analysis was carried out. Trends were hypothesised where the full inter-quartile range was above or below the 100% line (highlighted in red, indicates no difference from wild-type). The affected strains identified by this exploratory analysis are highlighted in Figure 5.10, with the corresponding strain name highlighted in bold. These strain P1 data were then contrasted with corresponding data for AB21 strains (Figure 5.2 and Figure 5.8).

Median IL-8 expression was lower than wild-type for P1Δ*dupA* strains co-cultured with $CD14^+$ monocytes ($P > 0.05$, 16.6% lower) and PBMCs ($P > 0.05$, 33.7% lower). Similar differences were observed for AB21Δ*dupA* strains. However, there were no apparent trends for IL-1β, TNF-α, IL-6, IFN-γ or IL-12/23p40, in contrast to the significant differences observed for AB21Δ*dupA* strains. In addition, median IL-17A expression by PBMCs co-cultured with P1Δ*dupA* strains was 13.0% less than wild-type ($P > 0.05$), whereas no such differences were observed for AB21 strains.

There were no consistent statistically significant differences in cytokine expression for AB21Δ*tfs4* strains. However, a variety of trends were observed for P1Δ*tfs4* strains.

In monocyte co-culture, there was lower expression of IL-8, IL-12/23p40 and IL-12p70 (all $P > 0.05$, 27.5%, 53.3% and 66.1% lower respectively). These trends were replicated in PBMC co-culture for IL-8, IL-12/23p40 and IL-12p70 (all $P > 0.05$, 26.9%, 51.8% and 74.5% lower respectively) and extended to TNF-α and IFN-γ (both $P > 0.05$, 18.3% and 64.4% lower respectively).

Figure 5.10 – relative cytokine expression in cell co-cultures with P1 strains

Peripheral blood mononuclear cells (PBMCs) and $CD14^+$ monocytes were purified from 4 donors (G-J) and co-cultured with wild-type and isogenic mutants of strain P1 (denoted by Δ). Cytokine/chemokine concentrations in 48 h co-culture supernatants were measured for 8 or 9 analytes in at least duplicate using Meso Scale Discovery V-PLEX assays (panels A to I, no data for IL-17A for $CD14^+$).

Data points represent the percentage difference from wild-type in the mean concentration for each donor/strain combination (all n=4; every data point is plotted). The horizontal and error bars show overall median values and inter-quartile ranges respectively.

Analysis followed only the first of the two steps previously used (see Section 5.3.2), as Wilcoxon signed-rank tests were not valid. Therefore, data across all groups for each cell type and analyte were compared by Kruskal-Wallis tests and Dunn's correction for multiple comparisons with 2 planned data pairs (each mutant vs. wild-type). There were no statistically significant differences in any analysis. Finally, some additional exploratory analysis was conducted. Trends were hypothesised where the full inter-quartile range was above or below the 100% line, with the corresponding strain name highlighted in bold. The bold strain names in this Figure do not indicate strong evidence of statistical significance, unlike in some previous figures.

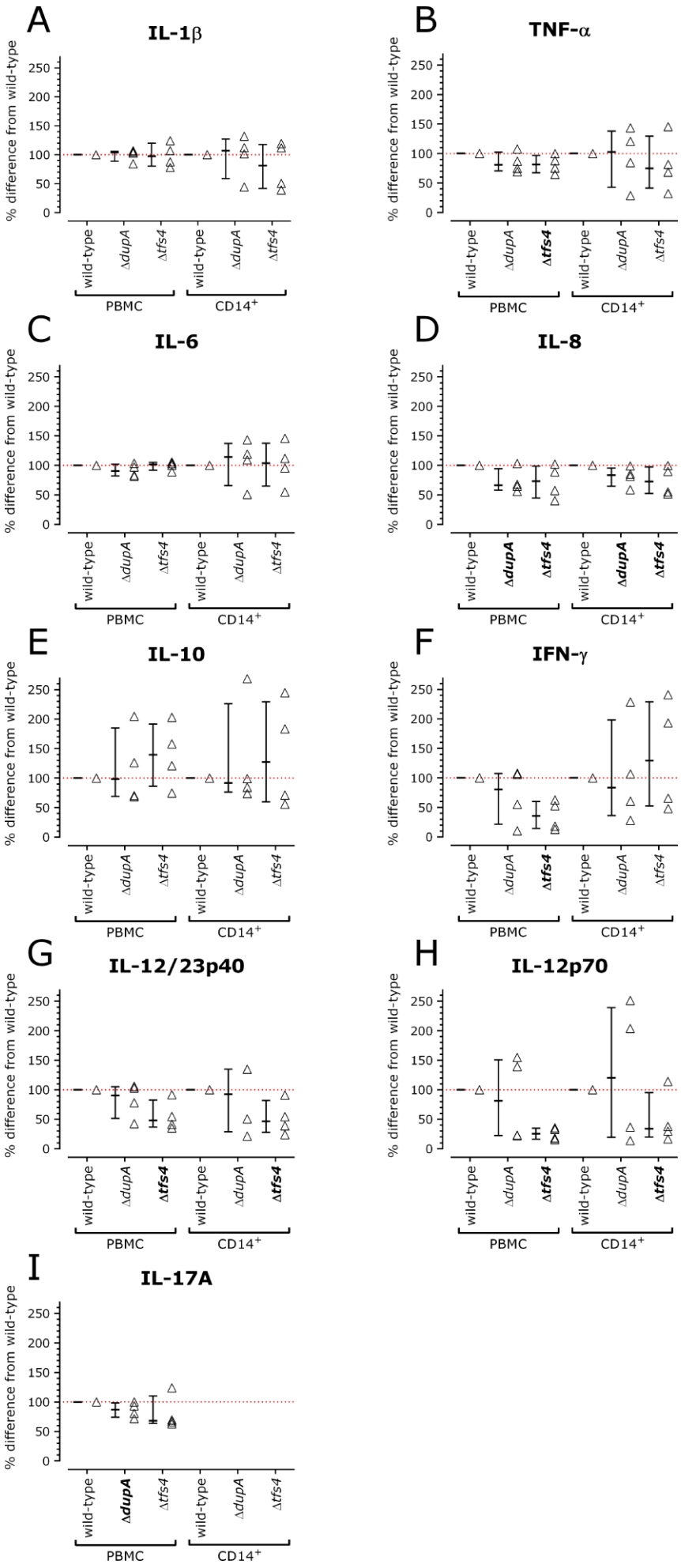

Figure 5.10 – relative cytokine expression in cell co-cultures with P1 strains

5.7 ChipCytometry

Having used our *in vitro* model, we wanted to examine the response of human gastric mucosal immune cells to *H. pylori* strains with regard to their *dupA* and *tfs4* status. This work was included so that immune and inflammatory cells within the gastric mucosa could be studied in addition to those derived from peripheral blood. Our group have conventionally used flow cytometry for such studies. However, we did not have access to an extended multicolour analysis platform during this project, which would have limited the number of markers studied. Therefore, a different approach was sought.

ChipCytometry is a novel imaging cytometric method with multiple applications that can provide detailed information on cell immunophenotypes (Hennig et al. 2009). The potential advantages for us were that the method can be used to study *ex vivo* samples of human tissue and, in particular, small sample sizes with no minimum cell number in contrast to flow cytometry. Cells can first be stimulated *ex vivo* with mitogen or antigen, or potentially with live bacteria to include isogenic mutants. These are then immobilised inside a microfluidic channel and fixed only after stimulation. Fluorescence staining of cells provides sensitive quantitative data on multiple immune parameters, which can be combined with histological stains. ChipCytometry differentiates itself from flow cytometry as the markersets are not limited by the number of available lasers/detectors and need not all be planned *a priori* such that subsequent explorative analysis is possible; multiplex staining is stepwise and iterative, rather than 'one shot', and samples can be preserved and re-analysed.

The aim was to evaluate this technology for investigating the response of *ex vivo* human gastric cells, which would complement experimental work using $CD14^+$ monocytes and mononuclear cell populations purified from peripheral blood. We first needed to optimise and validate the use of gastric samples and the biomarker panel.

5.7.1 Feasibility study and biomarker validation

We planned to study six samples in this feasibility study. Multiple mucosal biopsies (5-7) were obtained from patients attending for upper GI endoscopy. Informed written consent was obtained from all participants. We included patients with and without *H. pylori* infection. Cells were isolated as detailed in Section 5.7.2.1, following the optimisation of the method, which is reported next. Unfixed cells were stimulated with antigen or mitogen.

Antigen stimulation used *H. pylori* lysate, prepared by sonication from six clinical strains of *H. pylori* with various genotypes, previously isolated from patients with or without gastroduodenal disease in Nottingham, UK.

Mitogen stimulation used PMA and ionomycin. Ionomycin is a calcium ionophore that synergises with PMA to activate Protein Kinase C, ultimately resulting in the expression of key cytokines and immune genes. Mitogen stimulation bypasses cell-surface delivery of signals 1 and 2, so is non-physiological, but results in the intra-cellular production of cytokines such as IFN-γ (Robinson et al. 2008) to serve as a positive control. Mitogens were required to stimulate an observable production of IL-17A by T cells during flow cytometry (Dr Emily Staples, personal communication).

Unstimulated cells from each participant were included as a comparator and negative control. Human PBMCs were also included as cellular reference and positive control.

Following stimulation, each cell suspension was mounted on a chip and fixed.

We planned initially to study mucosal $CD3^+CD4^+$ T-helper cells. If successful, other immune cells could then be studied in iterations. For each chip, we planned to analyse two sets of biomarkers (21 total, Table 5.5). These were the cytokines and chemokines IL-1β, TNF-α, IL-8, IL-10, IFN-γ, IL-12 and IL-17A, and in addition IL-17F, IL-22, IL-23p19 and IL-27, the cell surface markers CD3, CD4, CD25 and CD127, CTLA-4 (CD152), the chemokine receptor CCR6, and the transcription factors T-bet (Th1), RORc2 (Th17) and FoxP3 and Helios (Treg).

Of these biomarkers, IL-23p19, IL-27 and CCR6 did not pass validation (Table 5.5). IL-12 staining performed unreliably as no positive cells were detected in the majority of samples. The IL-12 antibody used cross-reacts with IL-12/23p40 and IL-12p70, and potentially with IL-23 (see note 2 in legend of Table 5.5). We planned to re-evaluate alternative staining for IL-12/23 family cytokines in the future, with alternative clones and/or buffers, given that these were of interest.

Therefore, 17 validated biomarkers were investigated in this feasibility study (highlighted in bold in Table 5.5).

Table 5.5 – ChipCytometry biomarker validation

Biomarker	Clone	Dilution	Isotype	Control[1]	Notes
IL-1β	CRM56	1:100	mouse IgG_1	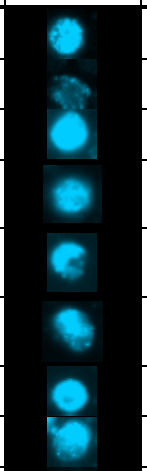	
TNF-α	MAb11	1:200	mouse IgG_1 κ		
IL-8	E8N1	1:200	mouse IgG_1 κ		
IL-10	JES3-9D7	1:200	rat IgG_1 κ		Weak but valid
IFN-γ	B27 (or 25723.11)	1:100 (1:100)	mouse IgG_1 κ		Weak but valid
IL-12[2]	C11.5	1:10	mouse IgG_1		Excluded as unreliable[2]
IL-17A	eBio64CAP17	1:30	mouse IgG_1 κ		
IL-17F	SHLR-17	1:50	rat IgG_1 κ		
IL-22	142928	1:50	mouse IgG_1		
IL-23p19	727753	1:50	mouse IgG_{2b}		Excluded as staining artefacts
IL-27	307426	1:200	mouse IgG_{2a}	neg	Excluded as no signal
CD3[3]	UCHT1	1:70	mouse IgG_1 κ	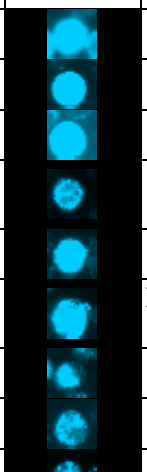	
CD4[3]	RPA-T4	1:100	mouse IgG_1 κ		
CD25[3]	M-A251	1:50	mouse IgG_1 κ		
CD127[3]	A019D5 (or HIL-7RM21)	1:200 (1:30)	mouse IgG_1 κ		Weak but valid
CTLA-4	ANC152.2/8H5	1:200	mouse IgG_1 κ		
CCR6[3,4]	53103	1:100	mouse IgG_{2b}		Excluded as live cells needed[4]
T-bet	eBio4B10	1:100	mouse IgG_1 κ		
RORc2[5]	AFKJS-9	1:100	rat IgG_{2a}		
FoxP3	236A/E7	1:30	mouse IgG_1 κ		
Helios	22F6	1:30	Armenian hamster IgG		

Details of biomarker validation, with antibody parameters and result of control studies. Stimulated and non-stimulated peripheral blood mononuclear cells were used in assay validation (see text). Four were excluded from analysis after validation (non-bold).

CD, cluster of differentiation; dep, depletion; ES, EasySep™; MB, Miltenyi Biotec MACS®; PBMCs, peripheral blood mononuclear cells; RS, RosetteSep™

[1] Internal control validation, showing single exemplary cell. Negative (neg) indicates where no significant fluorescence signal was obtained from reference cells.

[2] Clone C11.5 was developed with recombinant human IL-12p70 as the immunogen, but this antibody specifically binds with both the IL-12/23p40 monomer and IL-12p70 heterodimer and hence may cross-react with IL-23. Results were unreliable (see text).

[3] These biomarkers are extra-cellular. Others were identified by intra-cellular staining.

[4] Chemokine receptors required live cells for data capture during 15 min at 37 °C, so our paraformaldehyde-fixed samples were not suitable because of biological reasons or because the clone does not bind fixed epitopes.

[5] Clone AFKJS-9 binds mouse RORγ and RORγt but cross-reacts with human RORc2.

5.7.2 Optimisation of sample preparation

Zellkraftwerk had developed standard operating procedures for human PBMCs, human bronchoalveolar lavage fluid, cell culture of primary cells including those recovered from dissociated lung tissue, and tissue cryosections. The technology had not yet been developed for use with gastric or intestinal tissue or with lamina propria cells. One option for human gastric tissue was to use cryosections, which are reported to result in superior biomarker stability such that these are closely comparable to expression *in vivo* (Hennig et al. 2009). This involves preparing 2-4 µm cryostat sections of tissue snap frozen to -20 °C in specimen matrix, mounting between a 24×50 mm coverslip and the appropriate CellSafe™ chip, and then fixing and washing. However, this approach was not suitable as endoscopic biopsies are typically only 1-3 mm in diameter. Therefore, cells remain densely packed, which can prevent quantification of biomarker expression. We wanted to study all biopsy immune cells not just those within a thin section, and we wished to undertake *ex vivo* stimulation of samples. Therefore, for this feasibility project, it was necessary to prepare a single cell suspension of cells from gastric biopsies. This should enable sample stimulation and good quantification of biomarker expression. Our preparation technique would need careful optimisation, given that gastrointestinal tissues had not previously been studied, and consideration of the pros and cons of possible methodologies, for example, given that density gradient solutions may degrade chemokine receptor expression (Nieto et al. 2012) and that enzymatic tissue digestion may damage cell surface molecules (Mulder et al. 1994; Abuzakouk et al. 1996; Ford et al. 1996; van Damme et al. 2000; Autengruber et al. 2012).

The main challenges were, firstly, to recover an adequate number of viable cells from gastric mucosal biopsies for use in different experimental conditions, and secondly, to prepare an adequate single cell suspension whilst minimising cell clumping and non-cellular debris. Samples were obtained from 10 patients and used to optimise various preparation variables both before (Table 5.6), and during/after stimulation (Table 5.7).

This section describes the process of sample preparation, which comprised 4 optimisation phases. We were looking to achieve an adequate single cell suspension immobilised on each chip. The control or reference cells were human PBMCs (for example, see Figure 5.12 panel D and Figure 5.14(2) panel A and panels B-H).

Table 5.6 – optimisation of sample preparation variables for ChipCytometry: donors and steps prior to stimulation

Donor	Gender	Age (years)	*H. pylori* status	Number of biopsies	Strip epithelium (min)[2]		Fragment biopsies[3]	Digest (min)[4]	Disrupt (µm)[5]	Total cell number ($\times 10^6$)	Viability by TB (%)	Viable cells ($\times 10^6$)
Overall	70% male	52.0 ± 10.1		6 ± 1								
773	Female	43	negative	7	30	all			100	2.24	-	2.24
774	Male	54	unknown[1]	7	30	all			40	2.32	-	2.32
775	Male	53	unknown[1]	6	30	all			40	1.00	-	1.00
776	Male	56	negative	7	30	all			100	2.32	-	2.32
777	Female	61	negative	5	20	all			40 ×2	0.47	32	0.15
778	Male	70	negative	5	20	all			40 ×2	0.49	49	0.24
779	Male	36	positive[1]	5	20	all			40 ×2	0.43	65	0.28
789	Female	58	positive	6	20	all			40	1.50	20	0.30
791	Male	47	positive	7	15	part	yes	30	40	2.30	77	1.77
792	Male	42	positive	7	20	part	yes	35	40	3.34	70	2.34

The column order indicates the sequence of treatment steps (see text). Overall data expressed as mean ± standard deviation.

DTT, dithiothreitol; EDTA, ethylenediaminetetraacetic acid; IEL, intra-epithelial lymphocyte; LPMC, lamina propria mononuclear cell; RUT, rapid urease test; TB, trypan blue staining; -, missing data point (see text).

[1] Donors 774 and 775 were positive by RUT and negative by histology (no serology or culture results). Donor 779 previously failed eradication.

[2] Length of treatment with preparation 1 media (wash media, EDTA [1 mM], DTT [1 mM]) to separate the epithelium and IELs from the LPMCs and stromal cells; *all* or *part* indicate whether all cells suspended in the media were transferred to the next stage (epithelial, IELs, LPMCs and stromal) or if only cells that remained in the biopsy tissue were retained after treatment to strip away the epithelial cells (LPMCs and stromal).

[3] Biopsies were fragmented using sterile scalpels.

[4] Length of enzymatic digestion in minutes, with collagenase Ia (0.5 mg/mL) and DNase I (5 U/mL) treatment at 37 °C with shaking at 210 rpm.

[5] Mechanical disruption by rubbing the biopsies through a cell strainer using the flat end of a 1mL sterile syringe plunger, with cells then washed through strainer with culture media.

Table 5.7 – optimisation of sample preparation variables for ChipCytometry: stimulation and post-stimulation steps

Donor	Stimulation		Total cell number ($\times 10^6$)[2]		Relative to pre-stim. total (%)[2]		Viability by TB (%)[2]	Viable cells ($\times 10^6$)[2]		Filter (μm)[3]	Overlaid on density gradient media[4]	Spin ($\times g$, min)[5]
	type[1]	time (h)										
773	antigen	14.5	1.05		47		-	1.05				
774	antigen	14.5	0.55		24		-	0.55				
775	mitogen	14.5	0.06		6		-	0.06				
776	mitogen	14.5	0.15		6		-	0.15				
777	mitogen	10.0	0.01		2		0	0.00				
778	mitogen	10.0	0.09		18		62	0.06				
779	antigen	10.0	0.11		26		72	0.08				
789	mitogen	13.5	0.74		49		14	0.10		30		100, 10
791	antigen	13.5	2.00		87		56	1.12		30		100, 10
792	mitogen	10.0	1.06	0.59	32	35	45	0.46	0.27		yes	100, 10
	antigen	15.0		0.47		28	41		0.19		yes	100, 10

The column order indicates the sequence of treatment steps (see text). Cells were then applied to a CellSafe™ C chip, washed and fixed.

BSA, bovine serum albumin; EDTA, ethylenediaminetetraacetic acid; LPMC, lamina propria mononuclear cell; PBS, phosphate-buffered saline (Dulbecco A); PMA, phorbol myristate acetate; TB, trypan blue staining; -, missing data point (see text).

[1] Stimulation of recovered gastric mucosal cells (LPMCs and stromal cells) using antigen in the form of bacterial lysate (25 μg protein/mL, sonicated *H. pylori* prepared from six clinical strains of *H. pylori* with various genotypes isolated from patients with or without gastroduodenal disease in Nottingham, UK) or using mitogen with PMA (20 ng/mL) and ionomycin (0.7 μg/mL). Stimulated cells were incubated at 37 °C / 5% CO_2 for the time indicated, then held at 4 °C. For both antigen and mitogen stimulation, brefeldin A (10 μg/mL) was added after 1 h of incubation to block cytokine secretion. This is based on the standard method for flow cytometry developed and optimised by our group.

[2] After stimulation, cells were resuspended in sterile PBS with cell number and viability were quantified by TB exclusion. The cell suspension was then centrifuged at 1000 × *g* for 10 min with the supernatant discarded (note used 400 × *g* in final protocol). The cell pellet was resuspended in 1 mL of relaxation buffer (PBS, 0.5% v/v BSA, 2 mM EDTA) and incubated at room temperature for 15 min.

[3] To remove larger debris, the cell suspension was passed through a pre-wetted cell strainer under gravity then washed through.

[4] Alternatively, cells were overlaid onto 2 mL Biocoll density gradient media, centrifuged at 500 × *g* for 10 min, then recovered and resuspended.

[5] To remove smaller debris, the cell suspension was centrifuged at 100 × *g* for 10 min with the supernatant discarded, then resuspended in PBS.

In the initial optimisation phases (donors 773-776 and 777-779), we focused on three variables prior to stimulation – the length of treatment to strip the epithelium (20 or 30 min) and the approach to mechanical disruption using cell strainers (both size and number). In brief, endoscopic biopsies were washed, mucus and debris removed, and the basement membrane disrupted to begin to dissociate the epithelium. This released epithelial cells, and hence IELs, from the underlying mucosa comprising LPMCs and stromal cells. Initially, we hoped to be able to retain any released IELs along with the LPMCs. Therefore, after this treatment all suspended cells were transferred to the next stage in which biopsies were mechanically disrupted through a cell strainer.

Unfortunately, although there appeared to be an adequate number of viable cells (1.00-2.32×10^6), there was a significant amount of non-cellular debris that meant the prepared chips were of poor quality (Figure 5.11). We subsequently collected cell viability data by trypan blue exclusion (only total viable cell counts had been determined for donors 776-779 rather than dead cell counts). Finally, prolonged mitogen treatment (14.5 h) resulted in fewer cells surviving stimulation than antigen treatment (6 vs. 24-47%, Table 5.7). Note that brefeldin A was added early into the stimulation (after 1 h) as we had previously found that less than 6 h of blocked cytokine secretion was inadequate to observe responses from gastric biopsies for some cytokines, such as IL-17A, with flow cytometry (data not shown).

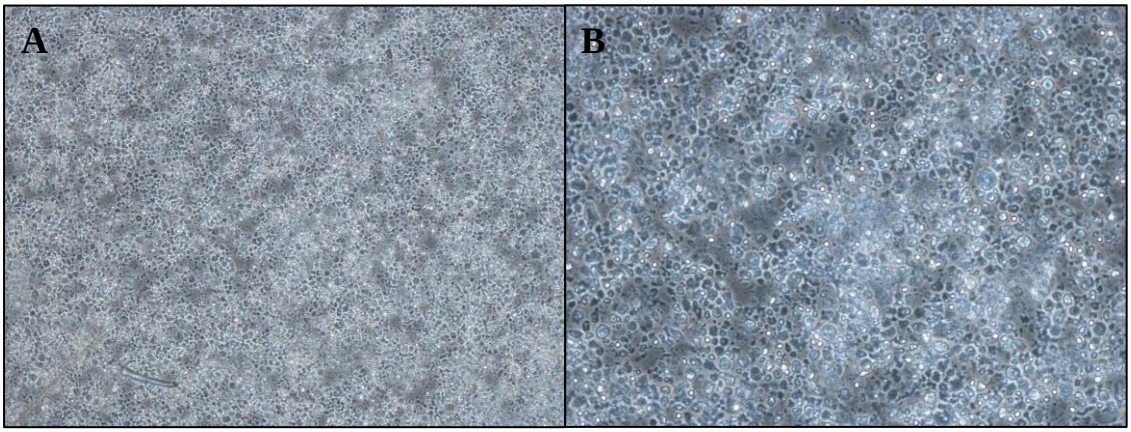

Figure 5.11 – biopsy chip microscopy for ChipCytometry donor 773
(A) unstained cells with debris, 100×, (B) unstained cells with debris, 200×.

For the second optimisation phase (donors 777-779), the sample was disrupted through two separate 40 µm cell strainers following a 20 min treatment to strip the epithelium. Incubation times during stimulation were shortened to avoid cell death, as well as

redoubling efforts to strictly maintain cells on ice, use shorter and stricter centrifuge and incubation times. Fewer cells were recovered ($0.43\text{-}0.49\times10^6$) with viability 32-65%. Following stimulation (10 h for both conditions), only 2-26% of cells were recovered with 0-72% viability.

In addition, the chips were still of poor quality. For example, for donor 778 there was a large amount of DNA-containing debris and cell fragments covering the slide surface, with only very few stressed-looking leucocytes (Figure 5.12).

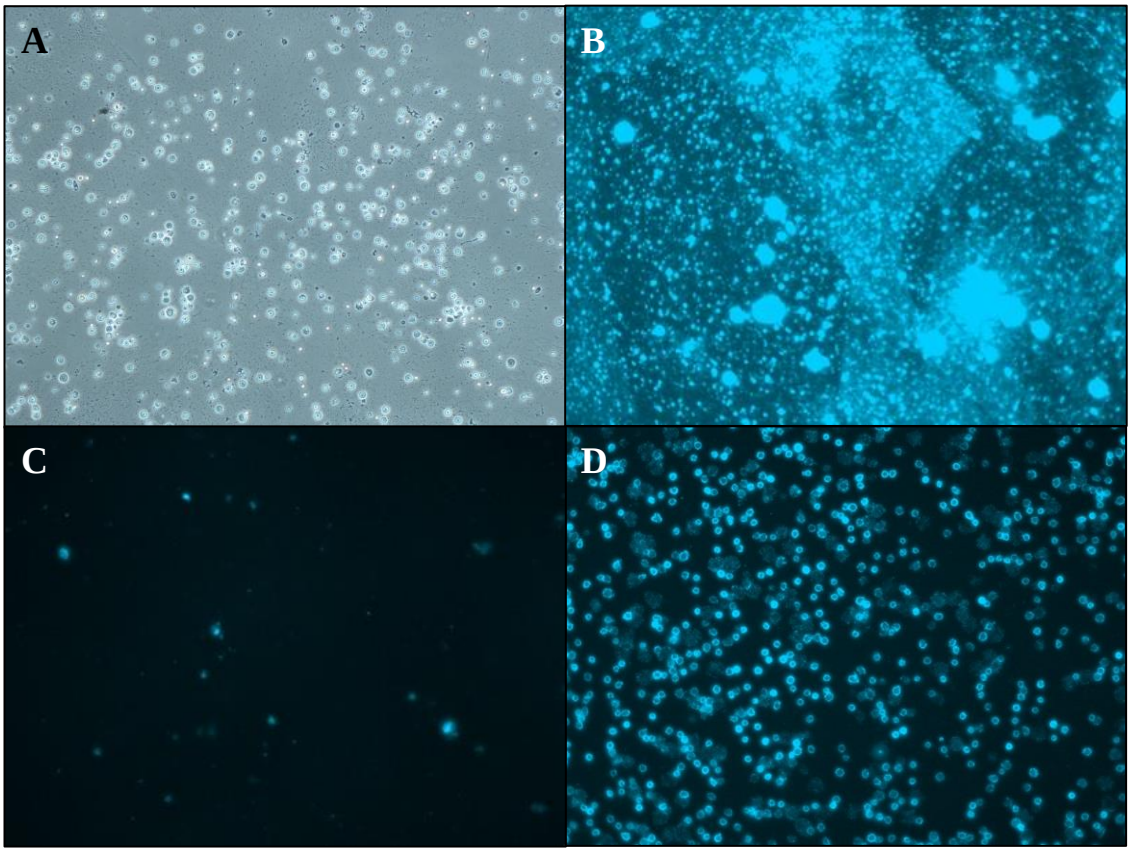

Figure 5.12 – biopsy chip microscopy for ChipCytometry donor 778

(A) unstained cells with debris, 100×, (B) DAPI staining showing nucleic acids, 40×, (C) CD45 staining showing leucocytes, 100×, (D) CD45 stained control or reference cells (human PBMCs), 100×.

DAPI, diamidinophenylindole; PBMCs, peripheral blood mononuclear cells.

For the third optimisation step (donor 789), only one cell strainer was used to mechanically disrupt the biopsies, which resulted in a higher cell recovery (1.50×10^6) though viability of 20%. Despite 13.5 h mitogen stimulation, 49% of cells were recovered but with 14% viability.

The focus of this step was to try to improve the single cell suspension produced after stimulation before applying this to a CellSafe™ chip. It is important to maximise the removal of debris and cell clumps for ChipCytometry, which are more straightforward to exclude in flow cytometry. Therefore, post-stimulation we used a 30 µM filter to remove clumps and larger debris, and a 100 × *g* centrifugation step (with careful and complete aspiration of all supernatant) to remove non-cellular debris below 5 µm (Table 5.7). The resulting cellular suspension was superior at microscopy, though few viable cells and much debris remained after stimulation (Figure 5.13 panel A).

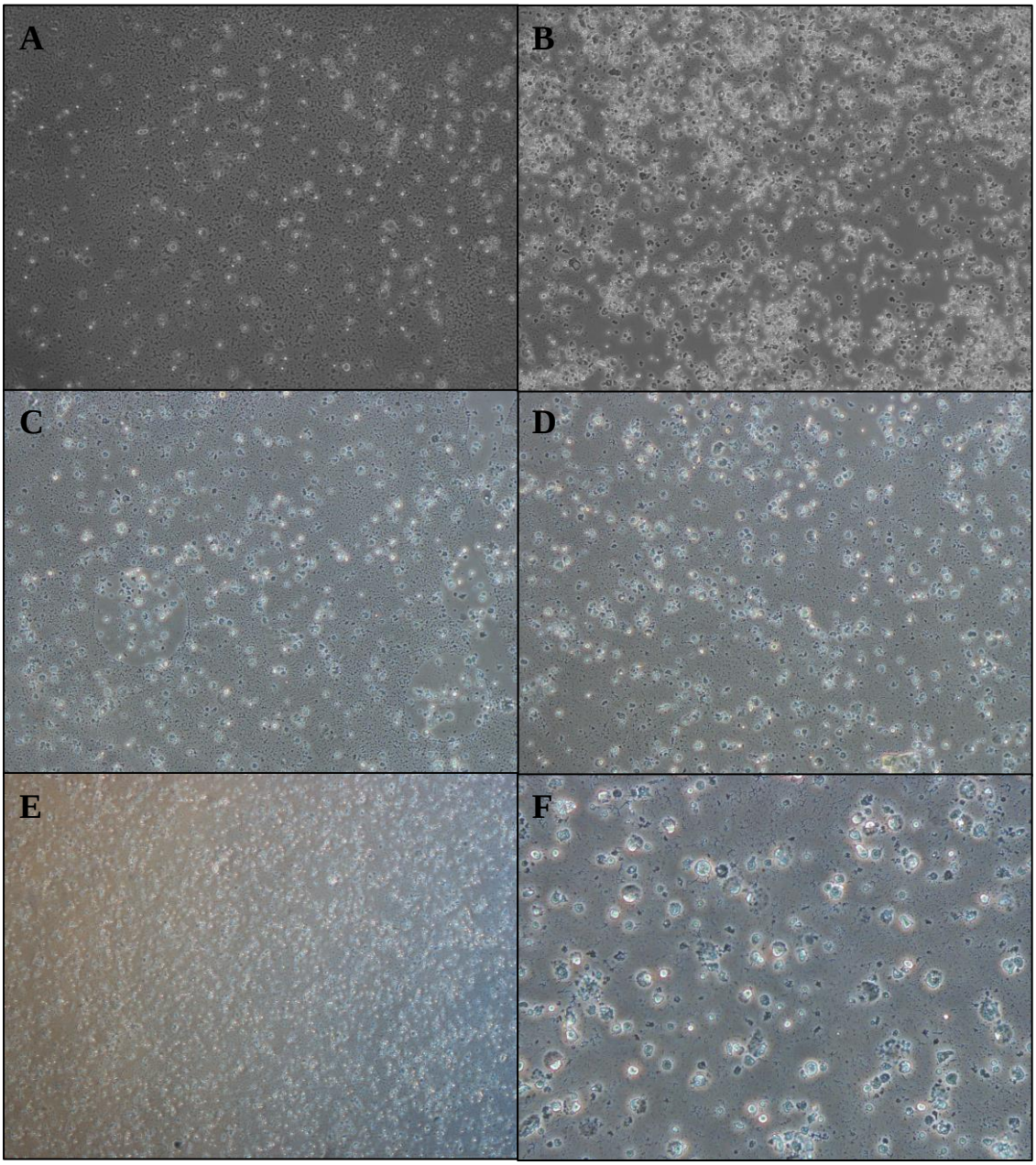

Figure 5.13 – biopsy chip microscopy for ChipCytometry donors 789, 791 and 792

Unstained cells with debris, 100× for (A) donor 789, (B) donor 791, (C) donor 792 mitogen stimulated, (D) donor 792 antigen stimulated. Panels (E) and (F) show panel (D) at 40× and 200× magnification respectively.

In the final optimisation phase (791-792), we attempted to separate cells and larger debris using density gradient media. The interphase layer was difficult to identify and, although the number of cells recovered only appeared to be slightly reduced (by approximately 20%, data not shown) compared with using a filter, overlaying was more time consuming and debris was still present. We also tried using sedimentation but this was inadequate alone to separate debris and cell counts remained similar in both upper and lower portions of the sample (data not shown).

Moreover, the major difference for this phase was the addition of fragmentation and enzymatic digestion to biopsy preparation prior to stimulation (Table 5.6). In addition, after initial treatment to dissociate the biopsy and strip the epithelium, only the remaining biopsy tissue was retained. The preparation 1 media, which contained epithelial cells including IELs, was discarded. So any recovered gastric mucosal mononuclear cells are likely to consist mostly of LPMCs.

This increased the number and viability of cells recovered (2.30-3.34×10^6 and 70-77% respectively). After stimulation, 32-87% were recovered, with more than 1×10^6 total cells (0.3×10^6 per biopsy), and viability of 41-56%. The resulting chips were now of higher quality with a greater cell density (Figure 5.13 panel E, panels B/C/D vs. panel A), though non-cellular debris remained (Figure 5.13 panel F).

There were potentially many further parameters that could be varied, such as alternative enzymatic and/or chemical treatment alongside automated mechanical disruption. It was not feasible to further extend this optimisation.

5.7.2.1 Final ChipCytometry sample protocol

We had overcome the major barrier of low cell counts and recovery, meaning that there should be sufficient cells per donor to split these in order to test different experimental conditions. This necessitated the addition of fragmentation and digestion with enzymes (Table 5.8), which as previously discussed can affect surface marker expression. We retained steps to dissociate and strip the epithelium, including discarding epithelial cells and IELs, and to mechanically disrupt the biopsies.

The second challenge, in working with mucosal biopsies and due to cell death during *ex vivo* stimulation, was to minimise cell clumping and non-cellular debris. These were

improved by including post-stimulation cell strainer filtration and a low speed centrifugation step. This may not be completely avoidable with this sample source.

For the final protocol, two additional steps were included (Table 5.8, and see Section 2.13). Firstly, DNase I was added during stimulation to reduce any sticky nuclear debris. Secondly, the low speed centrifugation step was repeated.

Table 5.8 – summary of steps included in final ChipCytometry sample protocol

Dissociate epithelium	Frag-ment	Digest	Disrupt	Stimulate	Time	DNase treat	Filter	Spin
10 min discard IELs keep LPMCs	yes	30 min	40 µm	mitogen	10 h	yes	30 µm	120 × *g* 10 min, twice
				antigen				

IEL, intra-epithelial lymphocyte; LPMC, lamina propria mononuclear cell.

5.7.3 Results of feasibility study

We studied antigen and mitogen-stimulated biopsy samples from 3 donors (796-798, Table 5.9). Alongside the gastric biopsy samples, PBMCs were also prepared from a paired peripheral blood sample from each donor. These were stimulated using the same approach and post-stimulation steps as for the biopsies, along with the inclusion of an unstimulated control.

Unfortunately, despite efforts to optimise the protocol, the biopsy chips still did not pass quality control analysis. There were few cells and no adequate single cell suspension, with clumps or debris comprising the majority of the sample (Figure 5.14(1)). In contrast, the PBMC chips passed quality control analysis, with very good cell density (Figure 5.14(2) panel A).

Table 5.9 – donors and samples for ChipCytometry feasibility study

Donor	Gender	Age (years)	*H. pylori* status	Sample	Total cell number ($\times 10^6$)	Viability by TB (%)	Viable cells ($\times 10^6$)
796	Male	29	positive	biopsy	1.8	74	1.3
				blood	1.0[2]	97	1.0
797	Female	31	positive[1]	biopsy	2.6	73	1.9
				blood	55	97	53
798	Male	28	negative	biopsy	1.2	76	0.9
				blood	32	98	31

[1] Donor 797 previously failed eradication.

[2] Technical error with layering over density gradient media.

Therefore, PBMC chips were stained for the full ChipCytometry biomarker panel (Table 5.5) instead of biopsy chips. Representative cell staining for 7 biomarkers is shown in Figure 5.14(2).

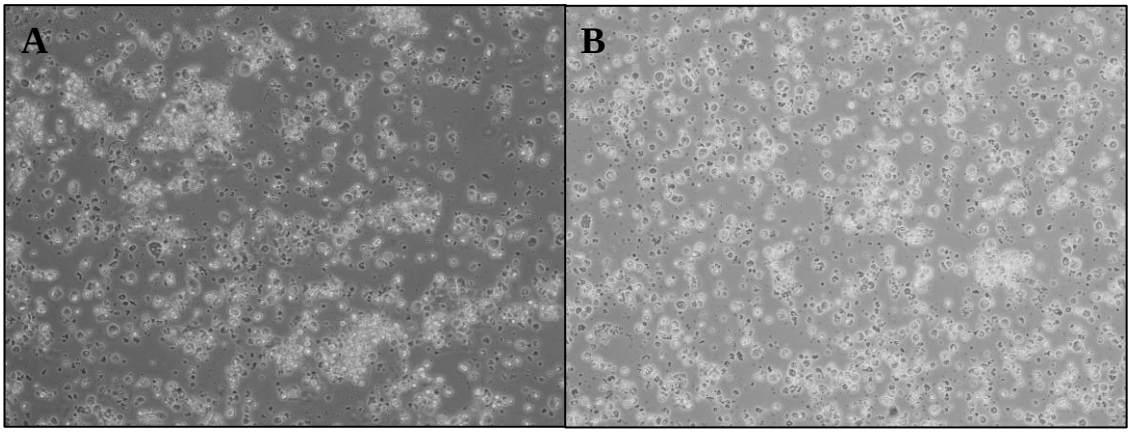

Figure 5.14(1) – biopsy chip microscopy for ChipCytometry donor 798

Unstained cells with debris, 100× for (A) antigen stimulated, (B) mitogen stimulated.

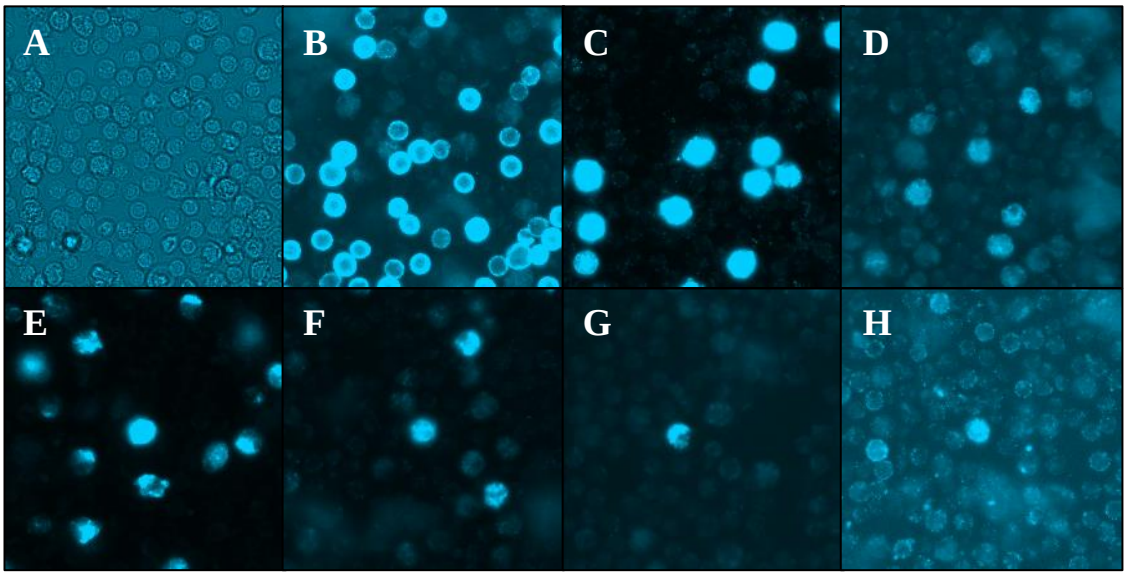

Figure 5.14(2) – peripheral blood mononuclear cell chip microscopy for ChipCytometry donor 797 antigen stimulated

(A) unstained cells showing very good single cell suspension without clumping or debris (focussing beads present in bottom left corner), representative cell staining for (B) CD4, (C) IL-1β, (D) TNF-α, (E) IL-8, (F) IL-10, (G) IFN-γ, (H) IL-17A, all 400×.

We prepared unstimulated, antigen and mitogen stimulated chips for all 3 ChipCytometry donors. However, insufficient cells were available for all conditions for donor 796. Data were not available for donor 797 mitogen stimulated or donor 798 unstimulated. Overall, quantitative data were available for 5 chips (Table 5.10).

Total events, the proportion of events that were $CD4^+$, and the proportion of these events positive for various cytokines are reported in Table 5.10. Data were not available for IL-6 or for IL-12 family cytokines.

Table 5.10 – relative $CD4^+$ and cytokine expression for ChipCytometry peripheral blood mononuclear cell chips

Donor	**797**	**796**	**797**	**798**	**798**
***H. pylori* status**	**positive**[1]			**negative**	
Stimulation	**unstimulated**	**antigen**			**mitogen**
Total events	39,290	11,655	21,529	23,262	42,661
$CD4^+$ events (%)	3545 (9.0)	3351 (28.8)	2231 (10.4)	4869 (20.9)	4843 (11.4)
% of $CD4^+$:					
IL-1β$^+$	0.00	67.50	20.84	55.00	0.00
TNF-α$^+$	0.06	63.32	7.71	6.57	0.06
IL-8$^+$	2.71	97.64	61.86	0.00	10.55
IL-10$^+$	1.18	3.55	10.98	1.66	0.74
IFN-γ$^+$	0.34	0.15	1.12	0.99	0.08
IL-17A	6.66	2.51	2.82	12.73	9.75

[1] Donor 797 previously failed eradication.

Donor 797 showed increased IL-1β, TNF-α, IL-8, IL-10 and IFN-γ following antigen stimulation compared with unstimulated cells, and event percentages could be detected (columns 1 and 3 of Table 5.10). However, there was marked variability between donors for antigen stimulation (columns 2-4 of Table 5.10). For mitogen stimulation, a high proportion of IFN-γ+ cells would be expected but this was observed to be very low (0.08%, column 5 of Table 5.10). The number of $CD4^+$ events (2231-4869 events) was lower than would be expected with flow cytometry (Robinson et al. 2008).

5.7.4 Summary

The aim of this work was to assess ChipCytometry for the purpose of studying the immune profiles of *ex vivo* human gastric cells. This evaluation found that this technology was not fit for this purpose. Other tools are now more widely available for this purpose, such as new multicolour flow cytometers.

5.8 Discussion

Helicobacter pylori interacts with its human host across a variety of different cell types. These include gastric epithelial cells, the host-bacterial interactions for which are best described for the *cag* system (Section 1.2.1), and a multitude of effects on and interactions with other cells of the human immune system and their responses both *in vivo* and *in vitro* including those shown for many bacterial virulence factors (White et al. 2015). There is evidence for pro-inflammatory cytokine secretion, differentially induced with respect to *dupA* status, by both epithelial cells (Section 1.3.5) and by mononuclear immune cells (Hussein et al. 2008); this is such that those strains believed to be functionally DupA-positive induce a stronger pro-inflammatory response.

In this chapter, human mononuclear immune cells derived from peripheral blood were used as a model to study host-bacterial interactions. The aims of this work were:

1. to identify the cytokines and types of immune cell that are important in the human immune response to *H. pylori* according to *dupA* status,
2. to investigate the relationship between *dupA* and *tfs4* profile and cytokine induction, and
3. and to gain insight into the role of *dupA* and *tfs4* components in this context.

Our group previously developed and reported an *in vitro* system based on PBMCs as a tool to investigate host-bacterial interaction via immune cell responses according to *dupA* status (Hussein et al. 2008). This system was refined and extended in this study, with further work using clinical isolates in co-culture, the inclusion of more biological replicates, work that identified monocytes as the principal source of pro-inflammatory responses, and the inclusion of mutants for *dupA* and putative *tfs4* components as well as their treatment by heat-inactivation or with paraformaldehyde prior to co-culture.

In the first part of this discussion (Sections 5.8.1 to 5.8.2), we start by considering the experimental model, including donor selection and the haemochromatosis cohort, and the rationale for and optimisation of the *in vitro* human blood monocyte model. Next, this is discussed in the context of different monocyte subsets and the relationship with other cell types of the gastric mucosal immune system with the potential to interact *in vivo* with *H. pylori*. The ChipCytometry feasibility study is also reviewed.

In the second part (Sections 5.8.3 and 5.8.4), the co-culture results are examined in the context of other findings, and strengths, weaknesses and future directions are explored.

5.8.1 Choice of experimental model

Peripheral blood mononuclear cells (PBMCs) were used as a model to study host-bacterial interaction. This model was selected as its utility in the field of study had already been demonstrated (Hussein et al. 2008). The cell populations represented in peripheral blood differ in type, distribution and function from tissue immune cells in the gastrointenstinal mucosa (Smith et al. 2013). Buffy coats prepared from peripheral blood were fractionated to relatively deplete donor samples of erythrocytes and polymorphonuclear cells (neutrophils, eosinophils and basophils). The other PBMCs comprise lymphocytes ($CD3^+$ T, B and NK cells), monocytes and dendritic cells.

The median total number of PBMCs recovered was 1.62×10^8 cells (IQR 0.70-2.42×10^8 cells). This is equivalent to approximately 0.2-0.7×10^6 cells/mL of whole blood (3.2-4.0×10^6 cells/mL of buffy coat). These cell types are expected to comprise 0.8-6.1×10^6 cells/mL, as these cell types comprise 20-55% of the normal total leucocyte count in peripheral blood of 4.0-11.0×10^6 cells/mL (Stevens and Lowe 1997). Nilsson et al. observed PBMC yields of 0.1-2.8×10^6 cells/mL in Swedish and Tanzanian healthy donors, though this was recovered from 10 mL of blood so much smaller handling volumes than in this study (Nilsson et al. 2008). In other reports, the mean yield from small blood volumes was up to 3×10^6 cells/mL (Malone et al. 1990). Recovery from buffy coats prepared from whole blood volumes up to 550 mL, with buffy coats up to 60 mL (25-40% larger), was 0.8-3.2×10^6 cells/mL (CPTP INSERM UMR 1043 France, 2015). Cell numbers in this study were in keeping with expected recovery. Mean viability was excellent, exceeding 98% and over 95% in all cases.

Large volumes of blood were required so that an adequate number of cells could be purified for study. Individuals with hereditary haemochromatosis attending for planned venesection were donors in this study, as blood could be obtained ethically, quickly and without additional costs. Potential advantages and disadvantages are considered next.

Choice of haemochromatosis donor cohort and impact on experimental model

Hereditary haemochromatosis (HH) is the most common autosomal recessive condition affecting Caucasian populations (Bokhoven et al. 2011; Pietrangelo 2015). It usually results from a mutation in the *HFE* gene (type 1 primary haemochromatosis), the protein product of which (Hfe) is involved in iron regulation, and is characterised by excessive absorption and storage of iron in the body. There are two major *HFE* mutations

recognised, C282Y and H63D, accounting for 85-90% of cases and whereby individuals can be heterozygous carriers ($^{+}$), homozygotes ($^{+/+}$) or compound heterozygotes. Treatment of haemochromatosis usually involves regular venesection, with an initial intensive treatment or induction phase (with phlebotomy every 1 to 2 weeks for up to a year in order to normalise serum ferritin), which is followed by a lifelong maintenance phase (with phlebotomy approximately 2-6 times per year when serum ferritin exceeds approximately 100 μg/L in order to maintain its concentration around this level). The penetrance is highly variable both for iron overload (up to 90% of C282Y$^{+/+}$ males, up to 50% of C282Y$^{+/+}$ females, up to 2% with other allelic forms) and for clinically important end points (such as cirrhosis, diabetes mellitus, cardiomyopathy, arthritis etc.); the reasons for these differences in natural history between individuals are still incompletely understood. Early treatment confers a normal life expectancy.

The experiments reported in this Chapter required large volumes of blood to extract sufficient numbers of immune cells. Patients with HH attending for venesection have approximately a pint of blood removed at each visit, in a similar way to blood donation. Although iron overload (and iron deficiency) may affect host immune functions and pathogen virulence (Walker and Walker 2000; Khan et al. 2007; Porto and De Sousa 2007; Johnson and Wessling-Resnick 2012), once normal iron levels have been achieved or patients are in the maintenance phase of treatment, there are no reports of increased host susceptibility to infections or an abnormal immune response (Khan et al. 2007). All donors in this study except one (donor G) were in the maintenance phase of treatment and all donors had serum ferritin measurements in the normal laboratory reference range prior to venesection (Table 1).

Notwithstanding the immunological impact of cellular iron metabolism, there are limited data for a direct role for *HFE* in human immune system function and molecular mechanisms. De Almeida et al reported *ex vivo* data that PBMCs from HH patients with the *HFE* C282Y$^{+/+}$ mutation have reduced cell surface expression of MHC class I molecules (in the subset of CD14^{+} cells) which enable recognition of intra-cellular pathogens, with altered assembly, peptide loading and stability, and maturation (de Almeida et al. 2005). However, controls were not fully matched and demographic data were not reported (WT n=19, *HFE* n=45), patients were in different treatment stages (53% in maintenance phase, of n=28 with C282Y$^{+/+}$), there were no differences in MHC class II molecules, there was no correlation with allelic frequency and no effect for the

HFE H63D mutation. The *HFE* gene itself encodes an MHC class I like (or class Ib) molecule (Feder et al. 1996), which may explain observed differences in the mean fluorescence intensity cumulative distribution function between PBMCs after staining for MHC class I molecules with FITC-conjugated anti-HLA-A, -B and –C.

Therefore, the significance of these observations on our selection of HH patients as blood donors is not fully clear. Hepcidin expression may also be reduced in *HFE*-associated haemochromatosis (Bridle et al. 2003; Ioannou and Kowdley 2004), which itself is the key regulator of iron and may be important in host defence (Ashrafian 2003; Pietrangelo 2015). There may also be differences in HH in the unfolded protein response to endoplasmic reticulum stress (de Almeida and de Sousa 2008). Macrophage pro-inflammatory cytokine expression is also attenuated in *HFE* knockout mice due to reduced mRNA translation in macrophages with lower intra-cellular iron levels from upregulation of the ferroportin iron exporter (Wang et al. 2008), though experiment-to-experiment variability was notable, host recovery from infection was actually enhanced and their observations could not adjust for abnormal metabolism due to iron overload. Transgenic mouse αβ T cell receptors can recognise Hfe independently of bound ligands resulting in cell activation (Rohrlich et al. 2005; Yewdell and Hickman-Miller 2005). Human cytomegalovirus protein US2 interferes with the expression of *HFE in vitro* as it does with other MHC class I molecules (Ben-Arieh et al. 2001), though whether this is relevant in viral replication or pathogenesis is not known. Finally, there is emerging evidence that *HFE* polymorphisms may increase the risk of certain cancers (Osborne et al. 2010; Weston and Connor 2014), though clinical data are inconsistent (including possible relative protection from cervical cancer) and confounded by linkage effects when nearby genes segregate, interactions with viral infection, and by host ethnicity, diet, menstrual status and behaviours. Basic and animal model research is ongoing.

Overall, there are no established immunological defects in patients with treated HH that would preclude their participation in this study of immune responses to *H. pylori*. Larger volumes of blood were needed than could safely and ethically be obtained from healthy volunteers. Blood donors and the NHS Blood and Transplant authority were another potential source of samples, but there would be delays and additional costs associated with non-clinical issue of donated blood products. As investigators, we would be left with unknowns over the medical history and phenotype of donors, and the population would likely be genetically more diverse with potentially greater background variation.

Patients with haemochromatosis are themselves eligible to be NHS blood donors, so could still be represented in samples from other sources.

However, given the potential impact of *HFE* mutations on the cellular and molecular host immune system, these experiments were carefully designed. Therefore, all comparisons between different conditions were made within the same donor to correct for any biological variation between individuals and then statistically analysed across all donors (for example, adjusted cytokine concentrations in bacterial co-culture were expressed as a percentage of the corresponding wild-type strain for each donor). Just as gender and age can have profound impacts on the human immune response for both clinical endpoints and cellular/molecular immunological parameters (Hulstaert et al. 1994; Oertelt-Prigione 2012; Giefing-Kröll et al. 2015), diurnal variation can also markedly impact on measured differential white cell counts (Jones et al. 1996), so variation between individuals should be minimised and accounted for in experimental design. This variation was also seen in our own data, for example, despite using the same method and polypropylene disposables rather than polystyrene, the percentage of $CD14^+$ cells in PBMCs purified from different donors varied from 12.4 to 90.7 percent (mean 38.1%, median 25.1%, IQR 20.4-55.9%).

Therefore, the choice of patients with haemochromatosis as the donor cohort was justified. Steps were taken to mitigate any potential imact on the experimental model.

IL-12/23p40 expression was most consistently and most markedly affected by the disruption of *dupA* and *tfs4* genes in the PBMC co-culture model.

Next, we discuss the rationale for focusing on monocytes in this experimental model. This decision was based on data for IL-12 family cytokine concentrations observed for PBMCs. Hussein et al. (2008) found that disruption of *dupA1* markedly reduced IL-12 cytokine responses. Conversely *in vivo*, this study found no differences between *dupA1* and non-*dupA1* clinical isolates in the expression of IL-12/23p40, IL-12p70 or *IL12B* in gastric mucosal biopsies. The only other *in vivo* study of IL-12 expression looked at IL-12p70 and showed a trend towards higher levels in association with *dupA*+/*tfs4* intact strains but no statistically significant differences (Jung et al. 2012).

In vitro using PBMC co-culture, this study also found that the effect on cytokine expression was most consistent and of greatest magnitude for IL-12/23p40. Indeed, there was strong evidence that IL-12/23p40 expression was 30.6% lower with disruption

of *dupA1* and 38.2% lower with disruption of *virB2*. However, there was no strong evidence for differences in IL-12p70 expression and IL-23 was not assayed in this study. Hussein et al. (2008) also reported differences *in vitro* in IL-12 family cytokine expression from an experiment that reported the mean of 5 technical replicates from parallel co-cultures using PBMCs from a single healthy volunteer donor. Based on Figure 6 from their paper, disruption of *dupA1* in the AB21 strain background resulted in approximately 53% lower expression of IL-12/23p40, 85% lower expression of IL-12p70 and 58% lower expression of IL-23. Results were similar in the AB31 strain background (66%, 84% and 79% respectively). Their observations for IL-12/23p40 were also demonstrated using PBMCs from 5 healthy volunteers, with a mean reduction in concentration for Δ*dupA1* vs. wild-type of 63.8% for AB21 and 51.5% for AB31 backgrounds. These differences were much more marked than for the other cytokines assayed (for example, for AB21 the equivalent reductions were 7.4% for TNF-α, 5.7% for IL-8 and 8.3% for IFN-γ, with no differences shown for IL-4 and IL-10).

Therefore, using the PBMC model, the cytokine IL-12/23p40 shown the most reproducible and marked differences.

The most important cellular sources of IL-12/23p40 were $CD14^+$, which is characteristic of monocytes.

Next, Hussein et al. (2008) looked at the cellular origin of IL-12/23p40 and IL-12p70 using flow cytometry, and found that 51% of IL-12/23$p40^+$ and 73% of IL-12$p70^+$ were from $CD14^+$ cells in wild-type co-culture (their experiments used the AB31 strain background and PBMCs from 3 healthy volunteers uninfected by *H. pylori*, though only data from one representative experiment are reported). The proportions were lower for the Δ*dupA* mutant and untreated cells. Similar experiments in this study with PBMCs from 5 donors and the AB21 strain background showed that the median percentage of IL-12/23$p40^+$ events that were $CD14^+$ was 89.3% (IQR 86.0-99.1%) across all controls and samples. Only 0.1% of $CD14^-$ events were IL-12/23$p40^+$ with an MFI of 30.4 arbitrary units. For $CD14^+$ events, 9.3% were IL-12/23$p40^+$ for wild-type with a median MFI of 192.2 arbitrary units and 8.3% were IL-12/23$p40^+$ for Δ*dupA* with a median MFI of 186.0 arbitrary units. Whereas fewer $CD14^+$ events were IL-12/23$p40^+$ for controls with media only (0.5%, median MFI of 61.7 arbitrary units), LPS (4.3%, median MFI of 110.1 arbitrary units) and lysate (1.3%, median MFI of 80.0 arbitrary units). Overall, most IL-12/23$p40^+$ events – and almost all in our hands – were from $CD14^+$ cells, and

co-culture with *H. pylori* markedly increased both the proportion of positive events and the intensity of fluorescence of IL-12/23p40. Others have shown that IL-12/23p40 is expressed at protein-level and mRNA-level by circulating human monocytes in response to *H. pylori* (Amedei et al. 2006; Fehlings et al. 2012).

Therefore, the PBMC-based system described by Hussein et al. (2008) and used to study the effects of *dupA* on cytokine induction was refined and optimised to a human blood monocyte cell model, specifically $CD14^+$ cells.

Positive immunomagnetic selection was chosen to purify $CD14^+$ monocytes.

The availability of immunomagnetic kits that separate monocytes by positive or negative selection has overtaken many more traditional approaches to monocyte purification. However, monocytes can be isolated from PBMCs by various methods (Wahl et al. 2006). These include adherence to glass (Rabinowitz 1964), adherence to plastics including polystyrene (Stanciu et al. 1996) or coated flasks (Freundlich and Avdalovic 1983); size sedimentation using density gradients (Loos et al. 1976) such as Percoll (Gmelig-Meyling and Waldmann 1980) or colloidal silica media (Nathanson et al. 1977; Vissers et al. 1988); flow sorting using a flow cytometer; and counterflow centrifugal elutriation (Figdor et al. 1982). These alternatives were not included in this evaluation: adherence and size sedimentation can result in cell activation and/or fail to separate monocytes from other lymphocyte subpopulations such as dendritic cells (de Almeida et al. 2000), cell sorting by flow cytometry is technically challenging, expensive and can have relatively low yields (Beliakova-Bethell et al. 2014), and elutriation was not available.

The performance of four immunomagnetic kits was determined, in terms of cell yield, purity and viability, cell population characteristics by flow cytometry, and cytokine expression phenotype in co-culture. Positive selection resulted in an improved yield of $CD14^+$ cells. Positive selection also delivered the best purity of enriched cells. Others have observed consistently increased cell purity using positive selection over negative selection ($95.2 \pm 2.5\%$ vs. $67.3 \pm 7.0\%$ for $CD14^+$ cells, Lyons et al. 2007). STEMCELL do report more difficulty in purifying monocytes by negative selective than say NK cells or T cells (personal communication, STEMCELL technical support). Platelet contamination has also been reported for monocytes purified by negative selection using

the kits evaluated (X. Du et al. 2006; Beliakova-Bethell et al. 2014). Cell viability was excellent, exceeding 95% for all enriched cellular fractions.

Monocyte cell populations were enriched as expected both by positive and negative selection kits. There was evidence of some contamination by other cell types but this was more so for one of the negative selection kits. Neutrophils express CD14 but at approximately one log less than monocytes (Jersmann 2005). Indeed, the TLR4 response of neutrophils to LPS can be inhibited by blocking CD14 (Sanui et al. 2017). Based on relative size and granularity, the $CD14^+$ contaminating cells observed are likely to be neutrophils. However, further staining for other markers would be required for confirmation. This cell population was expanded by bacterial co-culture and expressed IL-12/23p40 in response to bacteria, though still accounted for the minority of events overall. The implications of selection method for the isolation of different monocyte subpopulations is discussed below.

Lastly, enriched cells were evaluated in co-culture experiments. Monocytes purified by positive selection expressed IL-12/23p40 and other cytokines in response to live bacteria as expected. No important differences between the selection methods were identified in co-culture, or in the upregulation of IL-12/23p40 and CD14 expression by flow cytometry in response to live bacteria. However, cells purified by negative selection expressed much more IL-12/23p40 in response to antigenic stimulation in co-culture with LPS than expected, 4- to 5-fold more when compared against cells enriched by positive selection and other cell populations. This was similar both with and without CD16 depletion. As negative separation resulted in less pure isolation, this may be due to contamination by other cell types such as platelets or DCs.

Therefore, $CD14^+$ cells (principally monocytes) enriched by positive immunomagnetic selection from PBMCs were used as the principal experimental model in this study. The median total number of $CD14^+$ cells recovered after immunomagnetic cell separation was 0.31×10^8 cells (IQR $0.17\text{-}0.54\times10^8$ cells). This is equivalent to approximately $0.1\text{-}0.2\times10^6$ cells/mL of whole blood or approximately 20% of PBMCs. Monocytes comprise 3-7% of leucocytes in peripheral blood from healthy human adults and the absolute monocyte count is $0.15\text{-}0.70\times10^6$ cells/mL (Zhou et al. 2012). In a comparative study where cells were purified by positive selection directly from 100 mL of whole blood, monocyte yield was $0.13 \pm0.03\times10^6$ monocytes/mL (Lyons et al. 2007). Viable monocyte recovery from volumes up to 275 mL was $0.1\text{-}0.5\times10^6$ cells/mL using two

gradient-density media, with monocytes comprising 14-32% of PBMCs (de Almeida et al. 2000). Yield in this study was in line with these observations. The median viability was 99% and the median purity ($CD14^+$ proportion) of enriched cells exceeded 95%.

Monocytes and the study of *Helicobacter pylori*

Monocytes classically are identified as being $CD14^+$ cells (Ziegler-Heitbrock et al. 2010). Monocytes are the circulating prescursor cells of tissue macrophages and dendritic cells (Randolph et al. 2008). Most studies of *H. pylori* immune responses have focussed on the role of lymphocytes, and also dendritic cells, macrophages and neutrophils (Robinson et al. 2007). The inflammatory phenotype of circulating monocytes varies in association with *H. pylori* infection status in children (Helmin-Basa et al. 2012). *Helicobacter pylori* interacts with monocytes and monocytic cells to stimulate their activation and potential for endothelial adherence (Hansen et al. 1999), and to phagocytose and kill *H. pylori* strains *in vitro* (Borlace et al. 2008). Monocytes isolated from human PBMCs and stimulated with bacteria and recombinant *H. pylori* protein (HP-NAP) secrete TNF-α, IL-6, IL-8 and IL-12p70 and induce *IL12B*, *IL12A* and *IL23A* expression (Amedei et al. 2006). Other *H. pylori* peptides have been shown to activate monocytes and alter monocyte-directed interactions with both T cells and NK cells (Betten et al. 2001). Fehlings et al. (2012) showed substantial secretion by monocytes upon *H. pylori* infection of IL-6 and also of IL-1β and IL-12/23p40. They reported smaller increases in IL-10 and IL-23 secretion, but found no difference for IL-12p70. Interferon-gamma is produced by monocytes in response to LPS stimulation (Kraaij et al. 2014) and, although the impact of *H. pylori* on monocyte-derived IFN-γ has not been reported, there is disagreement over its effect on PBMC-derived IFN-γ (Fan et al. 1993; Duchmann et al. 1997).

In terms of the study of bacterial virulence factors, disruption of a genetic locus in the *tfs3* plasticity zone is associated with altered IL-12/23p40 production by THP-1 monocytic cells (de Jonge et al. 2004). Others have shown no differential effect on the ability of primary circulating human monocytes to kill *H. pylori* according to the virulence factors *cag*PAI, VacA, urease and catalase (Borlace et al. 2008). Interaction between *H. pylori* bacterial antigens and host cells can be mediated through pattern recognition receptors, particularly via Toll-like receptors (TLRs), in epithelial cells (Smith et al. 2003; Schmaußer et al. 2004; Robinson et al. 2007; Rad et al. 2009; Müller et al. 2011; Pimentel-Nunes et al. 2011) but also in monocytic cells (Zhao et al. 2007).

In summary, monocytes are a valid tool for the study host-bacterial interaction with *H. pylori*. Primary cultures obtained from human donors were preferred in this study. Cell lines are typically derived from immortalised cancer cells so may have important differences in host-antigen interactions or downstream signalling, and their use in biomedical research is frequently problematic (Geraghty et al. 2014).

CD14 is not simply a surface marker molecule (Ziegler-Heitbrock and Ulevitch 1993). It is an accessory molecule of various receptor-ligand interactions for several TLRs (Akashi-Takamura and Miyake 2008) and in particular as a co-receptor for the detection of LPS by TLR4 (Kitchens 2000). Binding to CD14 allows transfer of LPS to the extra-cellular accessory molecule MD2 that is associated with TLR4. Downregulation of CD14 in gastrointestinal tract resident mucosal macrophages to maintain tolerance has previously been reported (Smith et al. 2011) but more recently CD14 expression was shown to be maintained for newly extravasated monocytes and actually increased and $CD14^{hi}$ for mature recruited macrophages (Bain and Mowat 2014).

For a human blood monocyte experimental model, it is important to note that there are at least 3 different types of monocyte in peripheral blood. This is discussed next.

Monocyte subsets and the limitations of positive selection for CD14

The nomenclature and classification of monocytes, and the related mononuclear phagocyte lineage cells namely dendritic cells and macrophages, has evolved over recent years (Ziegler-Heitbrock et al. 2010; Kadowaki et al. 2012; Guilliams et al. 2014; Haniffa et al. 2015) and several uncertainties are known about (Durand and Segura 2015; Ziegler-Heitbrock 2015). This myeloid lineage, of which monocytes are the bone marrow-derived form that circulate in blood, are characterised by the ability to present antigen, produce cytokines and to phagocytose (Ziegler-Heitbrock 2015).

There are at least 3 human and 2 mouse monocytes subsets:

- classical monocytes ($CD14^{+}CD16^{-}$, equivalent murine cells are $Ly6C^{hi}$),
- intermediate monocytes ($CD14^{+}CD16^{lo}$, that also resemble $Ly6C^{hi}$ cells), and
- non-classical monocyes ($CD14^{lo}CD16^{+}$, equivalent murine cells are $Ly6C^{lo}$).

As already described, CD14 is part of the LPS receptor. It is found on monocytes, macrophages and granulocytes, but is also expressed by non-myeloid lineage cells (Jersmann 2005). CD16 is also called FcγRIII (Lanier et al. 1991). It is a low-affinity receptor for IgG and is expressed by a variety of cells including monocytes,

macrophages, granulocytes, NK and T cells (BD Biosciences CD Marker Handbook). It has been argued that CD14 is the more important monocyte marker (Cros et al. 2010; Hilgendorf and Swirski 2012).

In the present study, CD14 expression was upregulated by antigen stimulation, particularly in co-culture with live bacteria where most IL-12/23p40 expression was from $CD14^{hi}$ events, by also by LPS and to a lesser extent by sonicated bacterial lysate. Expression of IL-12/23p40 by cells cultured with LPS was more equal between $CD14^{+}$ and $CD14^{hi}$ cells. CD14 is known to be upregulated by LPS (Landmann et al. 1996). *Helicobacter pylori* LPS stimulates monocytes to release chemokines, though with lower potency than LPS from other bacterial species (Bliss et al. 1998). CD14 is required for *H. pylori* to activate THP-1 monocytic cells (Maeda et al. 2001). Moreover, $CD14^{hi}$ monocytes are highly phagocytic and Th1-promoting (Metharom et al. 2006; Chakrabarty et al. 2011).

Positive selection was used in our study but we found no evidence of upregulation in response to the binding of CD14 vs. negative selection. Despite potential concerns, there is actually only limited evidence of cell activation by positive immunomagnetic selection (Stanciu et al. 1996). The theoretical benefits of negative selection are probably overstated (Lyons et al. 2007), though will be a more important consideration for some applications. Beliakova-Bethell et al. (2014) reported for cell isolation from frozen samples that positive selection results in improved yield and minimises the cellular stress response that was enhanced by negative selection. They concluded that these observations were at least partly due to the timing of incubation steps and the 10× higher platelet contamination in negative selection. CD14 expression was not affected. We determined that positive selection was preferable in this study. Others have proposed this as the method of choice for monocyte enrichment (Zhou et al. 2012).

One potential disadvantage or limitation of positive selection is that non-classical $CD14^{dim}CD16^{+}$ monocytes are excluded by this method. We putatively identified the non-classical monocyte population using the negative selection kit without CD16 depletion (marked * on Figure 5.4). These are less dense and slightly smaller (Grage-Griebenow et al. 2001) and, therefore, have lower side-scatter and forward-scatter. This population was not observed after positive selection or negative selection with CD16 depletion. Further staining would be required for definitive conclusions.

It is recognised that infections can increase the number of intermediate and non-classical monocytes (Ziegler-Heitbrock 2015). So it is possible that we could miss some interesting aspect of host-bacterial interaction by excluding non-classical monocytes from our experimental model. Cros et al. showed that in response to LPS, classical monocytes produce IL-6, IL-8 and IL-10 (and also CCL2, reactive oxygen species and myeloperoxidase) and intermediate monocytes secrete TNF-α, IL-1β and IL-6. Non-classical monocytes produced IL-1β, TNF-α and CCL3 in response to viral or immune complex nucleic acids via TLR7/8-MyD88-MEK pathway (Cros et al. 2010).

Our overall intention was to select an experimental model to study host-bacterial interactions and any impacts of *dupA* or *tfs4* status on immune responses. It was not selected to represent the human gastrointestinal mucosal immune system. As we discuss next, it would be naïve to think that any *in vitro* model can truly match its complexity.

The gastrointestinal mucosal immune system

The human immune system is an organ formed by diverse tissues and cell types that are distributed throughout the body and comprise a series of anatomical compartments (Janeway et al. 2001). The largest of these compartments embraces the mucosa-associated lymphoid tissue (MALT) and the major component of human MALT is gut-associated lymphoid tissue (GALT), consisting of Peyer's patches in the small intestine, the appendix and isolated lymphoid follicles throughout the gastrointestinal tract (Smith et al. 2013). The GALT is classified as the inductive compartment of the gastrointestinal mucosal immune system and, although this distinction is neither anatomical or absolute, the two key effector compartments of this system are the surface epithelial barrier and the underlying lamina propria, with juxtaposed lymphatics, that drain to lymph nodes, along with blood vessels and nerves (Brandtzaeg et al. 2008). It is remarkable!

Our mucosal immune systems interact with the microbial ecosystem of the human gastrointestinal tract, named that microbiome, that consists of trillions of microbial cells (Lynch and Pedersen 2016). *Helicobacter pylori* is the best studied but not the only species in the gastric human microbiome (Ianiro et al. 2015). Interactions between *H. pylori* and its human host, and its ability to persist inspite of host responses, has evolved over tens of thousands of years (Atherton and Blaser 2009). Central to this interaction is the ability of the host to sense *H. pylori*, which is mediated through a wide array of pattern recognition receptors (Hold et al. 2011). Most of the antigenic mass of *H. pylori*

is found in the lumen and so epithelial-bacterial interactions have been the focus for studies of the initiation of the host response (Ernst and Gold 2000). However, we were interested in studying the interaction between *H. pylori* and host immune cells; furthermore, blood monocytes were studied. Is this rational?

Gastric inflammation in response to established *H. pylori* is characterised by infiltration of a mixture of acute and chronic inflammatory cells, with lymphocytes, macrophages and plasma cells permeating the lamina propria, and neutrophils, mast cells, eosinophils and dendritic cells infiltrating as far as the mucus-secreting cells of the epithelial surface (Ieni et al. 2016). Traditionally considered to be a non-invasive pathogen, *H. pylori* has been shown to penetrate into the gastric lamina propria *in vivo* and to invade epithelial and immune cells (Dubois and Borén 2007). It is postulated that protein components and secreted products of *H. pylori* may cross the epithelial barrier and so act on leucocytes leading to their activation or migration into the mucosa (Hansen et al. 1999). The *cag*PAI virulence system and other soluble factors including urease and VacA cause tight junctions between epithelial cells to loosen (Atherton 2006). Integrins are expressed on the basolateral surface of the polarised epithelium and so could only be encountered and contacted by bacteria (or bacterial proteins such as CagL) that have traversed the epithelial barrier (Posselt et al. 2013). Loosening of intercellular junctions may also explain how *H. pylori* encounters phagocytic cells in human gastric tissue. Interactions with intraepithelial T cells may be a common occurrence even without epithelial disruption (Algood and Cover 2006). Epithelial cells were shown *in vitro* to secrete cytokines in a polarised manner, predominantly from the basolateral surface (Fiorentino et al. 2013).

Overall, it is possible for human immune cells to directly encounter *H. pylori*. There are other potential mechanisms of host-bacterial interaction. Dendritic cells can penetrate gut epithelium to sample bacteria and have been identified in humans infected with *H. pylori* (Rescigno et al. 2001; Necchi et al. 2009). *Helicobacter pylori* produces membrane vesicles, which may cross the gastric epithelium, and mean it is possible for high concentrations of bacterial antigens (such as VacA) to be delivered to epithelial or perhaps immune cells (Winter, Letley, Rhead et al. 2014). Lastly, it is possible that *H. pylori*, either dead or alive, interacts with its host via Peyer's patches in the small intestine; these were shown to be essential for the induction of gastritis in a mouse model of *H. pylori* infection (Nagai et al. 2007).

Therefore, there are multiple lines of evidence that immune cells have a direct role in host-*H. pylori* interactions, rather than an indirect role following epithelial-bacterial ineractions. The relative importance of these interactions is not known.

So, which cell type(s) should be studied? Hussein et al. (2008) showed an experimental model using PBMCs to have utility in this field. They chose to use this model as they had observed an association between *dupA* status and mucosal cytokine concentrations, that was not explained by epithelial cell responses as these were shown to be unchanged by *dupA1* disruption and for *dupA2* strains in detailed *in vitro* analysis. The rationale for the study of monocytes has already been explained. Monocytes are the circulating form of the mononuclear phagocyte lineage (Ziegler-Heitbrock 2015). One could argue that a study of other cells of the mononuclear phagocyte lineage, such as macrophages or dendritic cells, would have more face validity as these cells are found in gastric mucosa.

Many laboratories will focus their efforts on particular cell types. For example, Fehlings et al. (2012) studied and compared the interaction of *H. pylori* with PBMCs, monocytes purified by positive selection for CD14, IL-4/GM-CSF monocyte-derived dendritic cells, GM-CSF monocyte-derived M1 macrophages and M-CSF monocyte-derived M2 macrophages. There were various differences between these cell types on surface marker expression, cytokine secretion and phagocytic ability. The candidate undertook some initial experiments using M-CSF monocyte-derived macrophages (kindly provided by Dr Sonali Singh) and another colleague investigated IL-4/GM-CSF monocyte-derived and primary $CD1c^{+}$ myeloid dendritic cell responses (Dr Emily Staples). It is not clear if such monocyte-derived dendritic cells have a true counterpart *in vivo* (Tacke and Randolph 2006). Cell lines such as THP-1 monocytic cells were also considered (Chanput et al. 2014) but these differ from monocytes, PBMCs and whole blood with respect to cytokine release after LPS stimulation (Schildberger et al. 2013).

There is no good reason to consider any *in vitro* experimental system that uses mononuclear phagocytic cells to be any more representative of the situation *in vivo*. Deriving other cell types from monocytes in the laboratory introduces more complexity, cost and potential for uncontrolled variability into experimental design. The truth is that none of these models can begin to approximate the mucosal immune system. However, as discussed in the rest of Section 5.8.1, although monocytes are by definition only found in the circulation, there is clear evidence that they have an important role in the human gastrointestinal mucosal immune system and its responses to *H. pylori*.

Macrophages in the gastrointestinal mucosa are derived from blood monocytes

The traditional view is that monocytes are derived from bone-marrow precursors, circulate in blood in their a mature form for 3-4 days, and then migrate into tissues whereupon they undergo local differentiation to generate mature macrophages (Smith et al. 2013). $CD14^{hi}$ cells derived from circulating monocytes accumulate in inflammed intestinal tissue in inflammatory bowel disease (Grimm et al. 1995). These cells have an enhanced ability to produce several cytokines, principally IL-1β, TNF-α and IL-6, and also behaviours specific to the disease condition, such as IL-23 in Crohn's disease but not in ulcerative colitis (Bain and Mowat 2014).

A distinct form of tissue-resident macrophages has been described that originate from yolk sac progenitor cells, migrate to various organs, and undergo maintenance by local self-renewal (Gomez Perdiguero et al. 2014). This form is thought to be less important in the gastrointestinal tract, particularly in adults, as macrophages that reside in the lamina propria are derived principally from blood monocytes (Cipriani et al. 2016).

As well as differentiating into macrophages or dendritic cells following migrating into inflamed tissues, monocytes themselves are early modulator of the immune response in *H. pylori* infection (Randolph et al. 2008). Similar to observations for the colonic mucosa in inflammatory bowel disease, the gastric mucosal concentration of monocyte chemoattractants such as CCL2 are increased in *H. pylori* infection (Cook et al. 2014, experiment providing this evidence were performed by the candidate).

Monocytes are key determinants and co-ordinators of host-bacterial interaction

Indeed, macrophages in the gastrointestinal tract are typically quiescent, with down-regulated CD14 expression and attenuated responses to TLR agonists mediated by stromal TGF-β, and moreover it is monocytes recently recruited to the mucosa that assist the response to invading microbial organisms (Smith et al. 2011). The required pathogenic response will differentially mobilise circulating monocyte and determine the composition and nature of the local mononuclear phagocyte response (Yona and Jung 2010). Macrophages are believed to exist in two main types: pro-inflammatory M1 macrophages and anti-inflammatory M2 macrophages, which can interact with other cells types and so also initiate and direct adaptive immunity (Mills 2015).

Peripheral blood also contains circulating dendritic cells and dendritic cell precursors (Satpathy et al. 2012), though unravelling the roles of these heterogeneous cells is a key

challenge for immunologists (Geissmann et al. 2010). Some dendritic cell subtypes are also derived from monocytes (Ziegler-Heitbrock et al. 2010) and are important determinants of the outcome of *H. pylori* infection in mouse models (Müller et al. 2011).

It would be possible to use monocyte-derived macrophages or dendritic cells to study immune responses with respect to *dupA* status. As already discussed, there are no compelling biological reasons to consider these to be better models, though idifferent responses between mononuclear phagocyte lineage cells could provide some insight into how *dupA* or *tfs4* interacts with *in vitro* immune cells. It was not feasible to conduct the experiments in this study with multiple cell types. Therefore, monocytes were used.

In conclusion, the choice of experimental model and the use of monocytes was justified as a means to study human immune cell responses and host-bacterial interaction *in vitro* and the influence of *dupA* and *tfs4*

This section has argued that the selection of patients with haemochromatosis as donors was justified and discussed the evidence to focus on monocytes as the key source of the differences in interaction observed with PBMCs *in vitro* with respect to *dupA* status. Positive selection had the best utility to purify monocytes. The major potential limitation of this approach was depletion of non-classical monocytes, but this may or may not be important. We have addressed the challenges against the face validity of a blood monocyte based model and maintain that this is relevant to the study of interactions between *H. pylori* and its human host. Such interactions are certainly not confined to the epithelium, though clearly this also has an essential role. There is evidence that many of the immune cells of the gastrointestinal mucosal are derived from or closely related to monocytes. However, making bold inferences about *in vivo* responses and disease process would be extravagant and not justified. Next, experimental approaches to complement and extend the human blood monocyte experimental model are discussed.

5.8.2 Experimental approaches to studying human mucosal immune responses and ChipCytometry

It is not wise to simply generalise findings from our monocyte model to host-bacterial interactions *in vivo*, so further evidence would be desirable and additional experimental models were considered. This is a study of human pathophysiology so we wished to look at the response of relevant human cells and tissues, rather than use animal models or arbitrarily selected cancer cell lines. Mice and men differ, and the widespread mouse

immune models currently reported are useful experimentally but the relevance to human disease is open to question and challenge (Steinman and Banchereau 2007). Moreover, the use of animal models fell outside of the fellowship funding awarded to the candidate. Ideally, the model should have face validity, by utilising cells and tissues present *in vivo*, though also be possible to manipulate experimentally rather than being observational.

Bimczok et al. (2010) used 10 cm^2 sections of gastric tissue from resection specimens recovered from patients undergoing bariatric surgery in Alabama, USA. Their method recovered $108.1 \pm 6.3 \times 10^6$ total cells per g gastric tissue, of which 15±5% were $CD45^+$ leucocytes. Non-surgical sources such as organ donors were considered but not available. Resections of gastric tissue could be obtained through a collaboration with surgical colleagues at Nottingham University Hospitals, UK. However, most specimens were from patients with malignancy who had often received chemo- or radiotherapy. Specimens from non-cancer patients, such as those undergoing elective surgery for peptic ulceration, could not be obtained sufficiently frequency for this study.

It was more straightforward to obtain endoscopic pinch biopsies from the human gastrointestinal mucosa. There are established methods to isolate lamina propria mononuclear cells (LPMCs) from colonic biopsies (Rogler et al. 1998; Hart et al. 2004; Bowcutt et al. 2015). There are similar approaches to recover mucosal cells from gastric biopsies (Mattsson et al. 1998; Robinson et al. 2008; Bimczok et al. 2010; Booth et al. 2014). Similarly, other groups have reported tissue culture of whole mucosal biopsy tissues (Bowcutt et al. 2015), including culture of gastric tissues for the *ex vivo* study of *H. pylori* infection (Pellicanò et al. 2007). Potential concerns with using tissue culture approaches were that: cytokines are often secreted at low concentration so may be difficult to detect (Staples and Ingram et al. 2013), cellular source(s) of cytokines cannot be identified, experimental design would be more restricted as more than one parallel condition or cross-over is not possible with a single small biopsy and it is hard to control for differences in cell composition and density between biopsies from same host.

Immunohistochemistry would be observational rather than experimental. Our group have conventionally used flow cytometry and cell sorting for studies of the immune and inflammatory cells within the gastric mucosa. However, we did not have access to a multicolour analysis platform with a sufficient number of lasers and detectors, which would limit the immune biomarkers studied. Therefore, a different approach was sought.

ChipCytometry was evaluated in a feasibility study and was found not to be a viable method to study the responses of *ex vivo* gastric immune cells

ChipCytometry is described in Sections 2.13 and 5.7. This method had been used with human PBMCs, human bronchoalveolar lavage fluid, cell culture of primary cells including from dissociated lung tissue, and tissue cryosections, but had not be optimised with gastric or intestinal tissue or with lamina propria cells (Hennig et al. 2009; Dr Christian Hennig, personal communication). The main challenges were:

- to recover an adequate number of viable cells from gastric mucosal biopsies for use in different experimental conditions, and
- to prepare an adequate single cell suspension whilst minimising cell clumping and non-cellular debris.

The first challenge was address by fragmentation and enzyme digestion stages in the protocol. One impact of this was that only LPMCs and stromal cells would remain, as the epithelium and intra-epithelial lymphocytes would be stripped away. Enzymatic tissue digestion may damage cell surface molecules (Mulder et al. 1994; Abuzakouk et al. 1996; Ford et al. 1996; van Damme et al. 2000; Autengruber et al. 2012), and others have reported no impact on the proportion of surface marker expression by T cells recovered from gastric LPMCs but significantly higher mean fluorescence intensity of CD4 and CD8 following collagenase vs. dispase treatment (Booth et al. 2014).

The second challenge was not overcome as, despite testing additional stages and treatments in the protocol, it was not possible to adequately prevent cell clumping and remove debris. Therefore, the chips prepared from gastric biopsies samples were of poor quality. In contrast, the control PBMC chips passed quality control analysis, with good single cell suspensions following *ex vivo* stimulations that translated into good cell density on the chip. The observations for gastric biopsy chips were supported by staining results, with no consistent results for cytokine staining and an inadequate number of cells for analysis (for example, there were fewer than 0.05×10^5 $CD4^+$ events).

Typical recovery from 4 gastric biopsies by mechanical disruption was $5\text{-}30\times10^5$ cells, allowing 1-6 aliquots for parallel analysis by flow cytometry per patient (Robinson et al. 2008). Therefore, we had predicted to recover $10\text{-}50\times10^5$ cells from 5-6 biopsies and $10\text{-}20\times10^5$ LPMCs. Gastric biopsy chips provided approximately $1\text{-}4\times10^5$ events, though it appeared that only the minority represented analysable LPMCs. Others have

used a combination of epithelial stripping and various enzymatic treatments to isolate 0.7-9.8×10^5 LPMCs from 10 gastric biopsies (Mattsson et al. 1998), 46±3.3×10^5 total cells from 10 gastric biopsies that were then sorted by flow cytometry to over 95% purity and viability (Bimczok et al. 2010), and 2.3-22.9×10^5 viable LPMCs from 5 gastric biopsies obtained from adults (Booth et al. 2014). Booth et al. showed that total LPMC recovery from biopsies from adults >65 years and from children, though when adjusted for biopsy weight the range of cells per mg tissue were broadly equivalent, though with a negative correlation with increasing age (ρ = -0.3, P = 0.021). Booth et al. had also optimised their protocol for gastric LPMC recovery with the inclusion of automated mechanical disruption by a bead-basher system under standard and modified conditions, which showed that mild disruption using the bead system resulted in at least a doubling of the LPMC yield without detrimental effects on viability. Unfortunately, this was published after our ChipCytometry feasibility project had been concluded.

If the ChipCytometry method were to be revisited in future for studying cells recovered from disrupted mucosal biospies, then the bead-basher approach to disruption should be used. However, other tools such as next generation multicolour flow cytometers are now more widely available and could be used to study the immune response of *ex vivo* human gastric cells to *H. pylori*.

5.8.3 Summary and discussion of results of co-culture experiments and the effect of *dupA* and *tfs4* status on immune responses

In the first part of this discussion, the *in vitro* human blood monocyte and mononuclear cell experimental models were reviewed. The ChipCytometry feasibility study found this technology to be unsuitable for the study of *ex vivo* host immune cells responses under the conditions evaluated. Here, the results of co-culture experiments using the *in vitro* models are summarised, and discussed in the context of other studies and the earlier observations in this study of mucosal immune responses in association with *dupA*.

Monocytes and PBMCs expressed lower levels of pro-inflammatory cytokines in response to co-culture with *H. pylori* strains with a disrupted *dupA* gene

This study found that monocytes co-cultured with isogenic *dupA* mutants expressed lower relative levels of pro-inflammatory cytokines and chemokines than cells co-cultured with wild-type strains. Overall, there was strong evidence for lower expression of IL-6, IL-8, IFN-γ and IL-12/23p40 by monocytes co-cultured with isogenic Δ*dupA*

mutants than with wild-type (Table 5.11). Monocytes have been shown to express these cytokines in response to *H. pylori* (Fan et al. 1993; Duchmann et al. 1997; Betten et al. 2001; Fehlings et al. 2012). This is the first evaluation of monocyte responses according to *dupA* status. Although LPS is an important determinant, other soluble *H. pylori* surface proteins can indepently activate monocytes (Mai et al. 1991) Other virulence factors have been shown to influence cytokine production by mononuclear phagocyte lineage cells, as well as epithelial, innate and adaptive immune cells (White et al. 2015), such as urease (Harris et al. 1996) and HP-NAP (Amedei et al. 2006).

This was not replicated by flow cytometry for IL-12/23p40, perhaps owing to the shorter co-culture time (16 h vs. 48 h). Expression at mRNA-level of IL-12 family genes by monocytes in response to *H. pylori* antigen shows different kinetics over multiple time points up to 24 hours (Amedei et al. 2006). Maximum cytokine concentrations in co-culture supernatants are typically seen at or after 48 h (Ruschen et al. 1992). Similar differences to the monocyte experiments were observed in PBMC co-culture, although in this experimental model there was also significantly reduced TNF-α expression following disruption of *dupA*, and significance was lost after correction for multiple comparisons for IFN-γ. This presumably reflects the mixed population of cells present in PBMCs, and in different proportions between donors. However, there was some evidence for lower IL-1β expression by both monocytes and PBMCs co-cultured with Δ*dupA* strains vs. wild-type, though statistical significance was lost once adjusted for multiple comparisons. Tumour necrosis factor alpha, IL-1β, IL-6, IL-8 and IL-12/23p40 (and IL-23) are the dominant cytokines produced by monocytes in response to *H. pylori* antigen, as seen in our data, with IFN-γ, IL-10 and IL-12p70 produced to a lesser extent (Harris et al. 1996; Amedei et al. 2006; Fehlings et al. 2012).

Only Hussein et al. (2010) have reported mononuclear cell responses to *H. pylori* with respect to *dupA* status, using wild-type *dupA1* strains, *dupA2* strains and isogenic Δ*dupA* mutants. These findings are summarised in Table 5.12. They also found IL-12/23p40 expression by PBMCs co-cultured with the *dupA2* strains 93-67 and A101 was similar to the disrupted *dupA1* strains AB21Δ*dupA* and AB31Δ*dupA*, and no further reduction with 93-67Δ*dupA* or A101Δ*dupA*. Our findings were similar for TNF-α, IL-8, IL-10 and IL-12/23p40, though with a different magnitude of difference. This may be due to differences between donors and the differences in both the reporting (see legend of Table 5.12) and analysis methods, with paired parametric methods without adjustment

for multiple comparisons used by Hussein and colleagues. Allowing for this, the findings were also similar for IFN-γ, which lost significance in this study in PBMC but not monocyte co-culture only after adjustment. Other analytes were not included in both studies (IL-1β, IL-4, IL-6, IL-17A and IL-23).

Therefore, the only apparent discrepancy between the results of this study and Hussein and colleagues was for IL-12p70. No statistical evidence of reduced IL-12p70 expression for Δ*dupA* strain was found in this study, however, the direction of the difference was the same (panel H of Figure 5.2). Indeed, this was the case for 13 of the 16 donor/strain combinations (approximate range 10-60% lower vs. wild-type) but overall significance was not demonstrated. Hussein et al. (2010) used a single donor and set of mutants for IL-12p70. In this study, much lower concentrations of IL-12p70 were detected (typically <200 pg/mL, around 10× lower than with wild-type in the study by Hussein and colleagues), though different assays and reference standards were used. The standards in this study are externally validated and rigorously quality controlled.

It is important to emphasise that there was no difference for IL-12p70 in pure monocyte co-cultures in this study (panel H of Figure 5.8, vs. panel G for IL-12/23p40). Hussein et al. (2010) found that 16% of IL-12p70^{+} events were CD14^{+} for untreated PBMCs, 17% for AB31Δ*dupA* co-culture and 73% for AB31 wild-type co-culture, so potentially the majority of IL-12p70 was not produced by monocytes. Inconsistent IL-12p70 responses of monocytes in response to *H. pylori* are reported. Some authors have found no expression (Fehlings et al. 2012), with co-culture at MOI of 10 for 1 h, then the bacteria were washed out, then cells were incubated for 24 h. Whereas HP-NAP was critical for the induction of a substantial proportion of IL-12p70 secretion by monocytes (Amedei et al. 2006). With regard to other mononuclear phagocytic lineage cells, IL-12p70 is produced by M1 but not by M2 macrophages (Fehlings et al. 2012), and Bimczok et al. (2010) showed that *H. pylori* does not induce the secretion of IL-12 family cytokines by primary gastric mucosal dendritic cells, though this was observed for monocyte-derived DCs.

Overall, CD14^{+} monocytes expressed mainly IL-1β, TNF-α, IL-6, IL-8 and IL-12/23p40 in response to *H. pylori*, and the production of IL-6, IL-8, IFN-γ and IL-12/23p40 was reduced by up to one-third by disruption of the *dupA* gene.

	Co-culture (Δ*dupA1* vs. wild-type)		**Flow cytometry** (Δ*dupA1* vs. wild-type)		**Clinical isolates** (non-*dupA1* vs. *dupA1*)		**Mucosal biopsies** (non-*dupA1* vs. *dupA1*)		
Cytokine	**CD14$^+$**	**PBMC**	**CD14$^+$**	**PBMC**	**CD14$^+$**	**PBMC**	**Protein-level** (Luminex)	**Protein-level** (MSD)	**mRNA-level**
IL-1β	*(34.0% ↓)*	*(13.7% ↓)*	-	-	ns	ns	**50.0% ↓**	ns	-
TNF-α	ns	**28.4% ↓**	-	-	ns	ns	ns	-	-
IL-6	**21.3% ↓**	**24.2% ↓**	-	-	**38.9% ↓**	**21.7% ↓**	ns	-	-
IL-8	**23.0% ↓**	**23.3% ↓**	-	-	ns	ns	ns (×2)[1]	ns	ns
IFN-γ	**34.0% ↓**	*(30.9% ↓)*	-	-	ns	ns	**63.6% ↓**	ns	ns
IL-4	-	-	-	-	-	-	ns	-	-
IL-10	ns	ns	-	-	ns	ns	ns	-	ns
IL-17A	-	ns	-	-	-	-	ns	-	ns
IL-12/23p40	**31.0% ↓**	**30.6% ↓**	ns[2]	ns[2]	ns	ns	ns	-	ns
IL-12p70	ns	ns	-	-	ns	ns	ns	-	-
IL-23	-	-	-	-	-	-	ns	-	-

Table 5.11 – summary of percentage changes in cytokine expression in co-culture experiments according to *dupA* status

Summary of the principal findings of this study for the relationship between *dupA* status and cytokine expression, for co-culture (Sections 5.5.1 and 5.3.2), for flow cytometry (Appendix Section 7.5.4 and Section 5.3.3), for clinical isolates (Appendix Section 7.5.3 and Section 5.2), and for mucosal biospies at protein-level (Section 4.3.2) and mRNA-level (Section 4.3.3). Arrows show the direction of difference for Δ*dupA* mutant or non-*dupA1* strains against the corresponding wild-type or *dupA1* strains. Italicised data in brackets indicate weak evidence (see Section 5.3.2).

ns, no statistically significant difference; -, not assessed; CD14$^+$, human blood monocyte experimental model; PBMC, peripheral blood mononuclear cell experimental model.

[1] = two different Luminex assay kits were used to analyse IL-8 expression at protein-level

[2] = ns by IL-12/23p40 flow cytometry [median (inter-quartile range)] – CD14$^+$ 95.5% (82.7-136.7%), PBMC 126.7% (85.0-153.6%)

	Co-culture with AB21 strains (Δ*dupA1* vs. wild-type)			
	This study		Hussein et al. (2010)	
Cytokine	**CD14$^+$** (10 donors)	**PBMC** (10 donors)	**PBMC** (5 donors)	**PBMC** (1 donor)
IL-1β	ns[1]	ns[1]	-	-
TNF-α	ns	**28.4% ↓**	**7.4% ↓**	-
IL-6	**21.3% ↓**	**24.2% ↓**	-	-
IL-8	**23.0% ↓**	**23.3% ↓**	**5.7% ↓**	-
IFN-γ	**34.0% ↓**	ns[1]	**8.3% ↓**	-
IL-4	-	-	ns	-
IL-10	ns	ns	ns	-
IL-17A	-	ns	-	-
IL-12/23p40	**31.0% ↓**	**30.6% ↓**	**63.8% ↓**	**53% ↓**[2]
IL-12p70	ns	ns	-	**85% ↓**[2]
IL-23	-	-	-	**58% ↓**[2]

Table 5.12 – comparison with other studies of percentage changes in cytokine expression in co-culture experiments with AB21 wild-type and Δ*dupA* strains

Hussein et al. (2010) reported data as the mean increase in wild-type vs. mutant. To compare with this study, where data are reported as the percentage reduction in median cytokine expression for mutant relative to wild-type (wild-type = 100%), the following formula was used to convert the data reported by Hussein at al. Percentage change in cytokine expression vs. wild-type = $\frac{((1 + \%\text{ mean increase expressed as decimal}) \times 100) - 100}{((1 + \%\text{ mean increase expressed as decimal}) \times 100)}$.

The findings of Hussein et al. for AB31 were broadly similar (that is, %CV was <25%), except for IFN-γ (25.9% ↓ for AB31 vs. 8.3% ↓ for AB21, %CV 73%) and TNF-α (3.8% ↓ for AB31 vs. 7.4% ↓ for AB21, %CV 45%).

ns, no statistically significant difference; -, not assessed; CD14$^+$, human blood monocyte experimental model; PBMC, peripheral blood mononuclear cell experimental model; %CV, coefficient of variation.

[1] = ns overall but there was weak evidence for a difference (statistical significant was lost after adjustment for multiple comparison)

[2] = calculations are based in Figure 6 from Hussein et al., as the mean increases reported in the text of their manuscript do not correspond to this figure. The manuscript states that PBMCs from one additional donor were used to study IL-12 family cytokine responses, with 5 replicate wells per culture condition (which are, therefore, technical replicates). However, 3 donors were used for their flow cytometry experiments for IL-12/23p40 and IL-12p70, though Table 1 states that only data for one respresentative experiment are displayed (and these results correspond with the text). Therefore, it is possible that the mean increases reported in the text for IL-12 family co-culture are also for 3 donors (and so biological replicates). If not, then it is likely that either the text or Figure 6 is incorrect. The equivalent percentage reductions in Table 5.12 calculated from the figures given in the text are 46.8% ↓ for IL-12/23p40, 61.5% ↓ for IL-12p70 and 40.8% ↓ for IL-23.

Host-bacterial interactions: the potential role of pattern recognition receptors

The monocyte model was used as an *in vitro* experimental model to investigate the impact of *dupA* on cytokine induction by human immune cells. Findings cannot be generalised to interactions *in vivo* for reasons already discussed. Indeed, for mucosal biopsies *ex vivo* it was IL-1β and IFN-γ that were reduced at the protein-level in some assays in association with non-*dupA1* vs. *dupA1* strains (Table 5.11, Sections 4.3 and 4.5.3). It was IL-6, IL-8, IFN-γ and IL-12/23p40 expression that was reduced for the *in vitro* monocyte model. Only IL-6 expression was reduced in association with non-*dupA1* vs. *dupA1* strains in co-culture of clinical isolates with this model and with the PBMC model. These clinical isolates were not isogenic for *dupA*. What might these observations tell us about host-bacterial interaction?

The *tfs4* type IV secretion system, of which *dupA* is the putative ATPase (Wang, Chen et al. 2015), is likely to have a role in horizontal gene transfer and bacterial conjugation (see Section 1.3.5). It is possible that this system can translocate protein, DNA or other bacterial components into the extra-cellular milieu or even into host cells. However, an indirect effect through host detection of surface-expressed components of *tfs4* is also possible. Such pathogen-associated molecular patterns are detected by pattern recognition receptors, including the cell surface-associated Toll-like receptors (TLRs) and the intra-cellular nucleotide-binding oligomerisation domain (NOD)-like receptors (Mogensen 2009). Regarding some of the key TLRs in host-bacterial interactions: TLR2 recognises lipoproteins, porins and other lipid-containing microbial components, TLR4 is activated by LPS, TLR5 recognises flagellin from flagellated bacteria, and TLR9 detects unmethylated CpG DNA (Smith et al. 2013). The intra-cellular NOD1 and NOD2 receptors recognise diaminopimelic acid (specifically iE-DAP) and muramyl dipeptide respectively, which are bacterial molecules derived from the synthesis and degredation of peptidoglycan (Philpott et al. 2014).

Innate immune receptors are central in host recognition of *H. pylori* (Müller et al. 2011) and triggering responses, though these are attenuated relative to many other bacteria (Robinson et al. 2007; White et al. 2015). Several factors contribute to the type, timing and intensity of responses following host-bacterial interaction.

Interactions are influenced by the type of cell, the cellular compartment, host polymorphisms, and the signalling cascades activated

Firstly, different cells express different receptors, both constitutively and following activation. The gastric epithelium expresses TLR2, -4, -5 and -9 (Smith et al. 2003; Schmaußer et al. 2004; Pimentel-Nunes et al. 2011) and NOD-like receptors (Viala et al. 2004; Castaño-Rodríguez et al. 2014). In terms of TLRs, monocytes express TLR1, -2, -4, -5, -6 (at low levels) and -8, whereas $CD11c^{+}$ dendritic cells express predominantly TLR1, -2 and 3, and plasmacytoid dendritic cells express TLR7 and -9 (Kadowaki et al. 2001). Monocytes subsets have different TLR profiles, such as TLR7 and -8 receptors on human non-classical $CD14^{lo}$ monocytes (Cros et al. 2010). Monocyte-derived macrophages show increased TLR4 and similar TLR2 and -5 expression compared to monocytes (O'Mahony et al. 2008). In addition, the pathways of cytokine secretion and export differ between cell types (Stanley and Lacy 2010).

Our group has found that immature monocyte-derived dendritic cells produce IL-1β, IL-6, IL-8, IL-10, IL-12/23p40, IL-12p70 and IL-23 following co-culture with *H. pylori* for 24 h, with reduced expression of IL-6 (*c*. 10% ↓), IL-10 (*c*. 20% ↓), IL-12/23p40 (*c*. ⅓ ↓), IL-12p70 (*c*. ½ ↓) and IL-23 (*c*. 20% ↓) observed for some donors for an isogenic *dupA* mutant strain (Staples 2013, University of Nottingham PhD thesis). These differences were most consistent for IL-12p70 and IL-23. $CD1c^{+}$ myeloid dendritic cells produced less IL-23 and no detectable IL-12p70 compared with monocyte-derived dendritic cells from the same donors, and no difference was seen for Δ*dupA* mutants. When these two types of *H. pylori*-stimulated dendritic cells were incubated with naïve T cells, there were variable effects on IFN-γ and IL-17A production by T cells and no consistent impact of *dupA* disruption. No systematic evaluation of monocyte-derived macrophages in relation to *dupA* status has been reported.

Secondly, induction of certain cytokines may be dependent on phagocytosis and degradation of bacteria, as was proprosed for IL-6 production by macrophages in response to *H. pylori* (Odenbreit et al. 2006). Gastric dendritic cells also internalise *H. pylori* (Bimczok et al. 2010) and may interact with intra-cellular receptors. For example, TLR9 binding by *H. pylori* DNA results in a pro-inflammatory IL-6 and IL-12/23p40 response, in cooperation with detection by extra-cellular receptors (Rad et al. 2009).

Thirdly, polymorphisms in TLR genes and other pattern recognition signalling pathway genes can modulate host-bacterial interaction and disease risk (Castaño-Rodríguez et al. 2014). These might contribute to inter-donor differences in cytokine response. TLR4 polymorphisms affect the risk of gastric cancer and its precursors (Hold et al. 2007).

Fourthly, there is a complex interplay between different receptors, signalling pathways and cytokines. MyD88-dependent and -independent signalling is triggered by all TLRs except TLR3, to drive inflammatory gene expression via different pathways involving NF-κB and mitogen-activated protein kinase (MAPK) cascades (Mogensen 2009). The MyD88 intra-cellular adaptor protein is central in cell activation and cytokine secretion in models using $MyD88^{-/-}$ mice (Rad et al. 2007). There is cross-talk between activated receptors and cooperation between multiple signalling pathways to regulate cytokine expression (Liu and Ding 2016). This results in the co-ordinated expression of pro- and anti-inflammatory genes including IL-1β, TNF-α, IL-6, IL-8, IL-10 and IL-12/23p40 (Mogensen 2009), and of type I interferons by TLR7 and -9 MyD88-dependent signalling. Inflammasome activation induces IL-1β and IL-18 secretion (Barker et al. 2011; Semper et al. 2014; Guo et al. 2015). There is complex cell signalling, involving temporal regulation and multiple cell type *in vivo* (Turner et al. 2014), for example, IFN-γ has differing functions depending on the timing and intensity of exposure (Schroder et al. 2004; Kerkar et al. 2014).

Pro-inflammatory cytokine responses following disruption of *tfs4* genes

We hypothesised that different putative components of *tfs4* may differ in their ability to elicit an immune response and tested this using different isogenic mutants. Figure 1.10 shows the putative structure of *tfs4* and the isogenic mutants selected, which lacked *virB2*, *dupA* (*virB4*), *virB8* and *virB9*. These are respectively predicted to disrupt putative components of the pilus, the inner membrane/cytosolic ATPase believed to provide energy for translocation and secretion system assembly, the inner membrane complex, and the outer membrane complex. Results from co-culture experiments using the human blood monocyte model are summarised in Table 5.13.

There was evidence for different cytokine expression by monocytes co-cultured with mutants lacking other putative *tfs4* components. In particular, Δ*virB2* strains induced lower relative expression of several pro-inflammatory cytokines. Overall, there was strong evidence that monocytes co-cultured with isogenic Δ*virB2* mutants express less

IL-6, IL-8, IFN-γ, IL-12/23p40 and IL-12p70 than wild-type strains. This was similar to the Δ*dupA* mutant, for which significant differences in IL-12p70 were not shown.

Evidence was less strong and less consistent for other cytokines and for strains lacking other putative *tfs4* components. Interleukin-12 family cytokine expression by PBMCs co-cultured with isogenic Δ*virB2* was significantly lower than for cells co-cultured with wild-type, with strong evidence only found for IL-12/23p40 expression. Why there were differences between monocyte and PBMC responses for disruption of *virB2* but not of *tfs4* is not clear, but may relate to reduced power from the smaller number of biological replicates (n=6 vs. n=16) given that monocytes present within PBMCs are likely to be an important sources of these cytokines. Flow cytometric analysis of $CD14^+$ monocytes and PBMCs co-cultured with wild-type and mutant bacteria showed no consistent differences in IL-12/23p40 expression between strains, again perhaps because of the shorter co-culture time.

Overall, both *dupA* and *virB2* were shown experimentally to be important determinants of cytokine expression by monocytes in this *in vitro* model of host-bacterial interactions. Whereas, essentially no important impacts of *virB8* or *virB9* were shown.

	$CD14^+$ co-culture with AB21 strains (predicted location/function of *tfs4* component)			
Cytokine	Δ*virB2* vs. wild-type (pilus)	Δ*dupA1* vs. wild-type (ATPase)	Δ*virB8* vs. wild-type (inner membrane complex)	Δ*virB9* vs. wild-type (outer membrane complex)
IL-1β	ns	*(34.0% ↓)*	ns	ns
TNF-α	*(46.8% ↓)*	ns	*(49.4% ↑)*	ns
IL-6	**25.5% ↓**	**21.3% ↓**	ns	ns
IL-8	**24.1% ↓**	**23.0% ↓**	ns	ns
IFN-γ	**31.9% ↓**	**34.0% ↓**	ns	ns
IL-4	-	-	-	-
IL-10	ns	ns	ns	ns
IL-17A	-	-	-	-
IL-12/23p40	**57.2% ↓**	**31.0% ↓**	ns	*(38.0% ↓)*
IL-12p70	**45.4% ↓**	ns	ns	ns
IL-23	-	-	-	-

Table 5.13 – summary of percentage changes in cytokine expression in $CD14^+$ monocyte co-culture experiments according to *tfs4* and *dupA* status

Comparison of the findings of this study for the relationship between *cagE* and *dupA* status and cytokine expression in co-culture (Section 5.5.1). Arrows show the direction of difference for mutant strains against the corresponding wild-type strains. Italicised data in brackets indicate weak evidence (see Section 5.3.2).

ns, no statistically significant difference; -, not assessed.

The extra-cellular pilus is predicted to consist of VirB2, which as it is surface expressed. is more likely to be able to interact with host cells. There is precent for this for CagL and host cell integrins (Kwok et al. 2007). Moreover, the pilus is expected to be elaborated across the periplasm and outer membrane through the substrate translocation channel, so normal pilus assembly may also be dependent on other putative *tfs4* components, as seen for the *cag*PAI (Shaffer et al. 2011) and other secretion systems (Christie et al. 2014). This might be the mechanism by which the Δ*dupA* mutant attenuates host-bacterial interaction and cytokine reponses. It might still be possible to get expression of VirB2 on the bacterial surface or in the extra-cellular environment independent of an underlying T4SS structure, which could explain why there were essentially no differences from wild-type for the Δ*virB8* and Δ*virB9* mutants. Surprisingly, the *tfs4* mutant did not have any important impact on cytokine expression, as one would expect the Δ*tfs4* mutant to attenuate any host response that is dependent on one or a combination of *tfs4* components (such as *virB2* and/or *dupA*). Perhaps there was a problem with the AB21Δ*tfs4* mutant, as its mRNA- and protein-level characteristics were not available (Dr Amberley Stevens, personal communication). However, trends seen in preliminary data from another set of mutants in the P1 background suggested lower expression of pro-inflammatory cytokines for both P1Δ*dupA* and P1Δ*tfs4* strains relative to wild-type. If effects could be strain-specific, then it would be important to evaluate additional mutants in other backgrounds that have been fully characterised for *dupA*, *tfs4* and other bacterial virulence determinants.

Cytokine expression was dependent on live bacteria, as heat inactivation of any strain markedly reduced cytokine production relative to the corresponding untreated strain, but with no differences observed between mutants. Paraformaldehyde treatment was used to fix cells with the intention of cross-linking any surface proteins, such as a putative *tfs4* pilus, that might then still stimulate or even potentiate any immune response. This approach has been used to cross-link DNA and protein in studies of type IV secretion system function (Cascales 2004) but hypothesised effects on pilus structure are speculative and could be more elegantly studied by electron microscopy (Shaffer et al. 2011). Relative expression of IL-12/23p40 was actually increased for PFA-treated AB21Δ*virB2* in one analysis relative to untreated AB21Δ*virB2*. This mutant should be unable to form pili and so a reduction was hypothesised, however, it might be that there is then relevative over-expression of another putative component that cannot interact as

normal with the product of *virB2*, which is still exported and detected by monocytes. Paraformaldehyde treatment of isogenic mutant bacteria lacking *dupA* did not have any impact on cytokine expression, which might be expected as this mutant should lack any ATPase function to assemble extra-cellular pili. We observed a consistent relative decreased abundance of the anti-inflammatory cytokine IL-10 principally in PBMC co-culture, rather than a potentiation of pro-inflammatory cytokines, for PFA-treated Δ*virB9* strains. VirB9 is speculated to be a component of the core complex associated with the outer membrane, so might have the potential to interact with or to alter interactions with inflammatory cells. Note that there were no significant effects for PFA-treated wild-type vs. untreated wild-type. This could suggest that this form of PFA treatment does not affect surface structures, that no relevant immunogenic surface structures are present in AB21 wild-type under these conditions (from *tfs4* or other systems), or a type 2 error. Therefore, the PFA data should be interpreted with caution.

Finally, it is not yet clear what factors regulate the expression of *tfs4* components, but adherence and pH may be important determinants. Silva et al. (2015) assessed the *in vitro* expression of *virB2*, *dupA*, *virB8* and *virB10* by qPCR during co-infection of human gastric epithelial cells (NCI-N87) for adherent and non-adherent fractions at different pHs. They reported in abstract form that the region spanning *virB2* to *virB10* constituted an operon, and that expression was increased in the adherent fraction and in both fractions under acidic conditions. There is precedent for pH-regulated expression for a type III secretion system in *Salmonella enterica* within the acidic environment of macrophage phagosomes (Rappl et al. 2003).

Overall, the production of IL-6, IL-8, IFN-γ and IL-12 family cytokines by $CD14^+$ monocytes was reduced by disruption of *virB2* and *dupA* genes, but not of *virB8* or *virB9*. Further work is required to confirm these differences. The similar cytokine profiles suggest that these effects may be mediated in similar ways in the host cell. This is in contrast to responses seen with disruption of the *cag*PAI.

Monocyte responses are different for Δ*dupA* and Δ*cagE* mutants

Interesting differences were observed in cytokine responses for the Δ*cagE* mutant compared with the Δ*dupA* mutant. Table 5.14 summarises this comparison. Of the main cytokines found to be expressed by $CD14^+$ monocytes in response to *H. pylori* (IL-1β, TNF-α, IL-6, IL-8 and IL-12/23p40), we found that disruption of *cagE* reduced the

expression of IL-8 by approximately one-quarter. Observations were similar for PBMC co-culture, although statistical significance remained after correction for multiple comparisons for IL-8 and also for IL-6.

Disruption of *cagE* will eliminate most *cag*PAI activity, including CagA-dependent effects on host epithelial cells and up-regulation of many of the immune response genes (Guillemin et al. 2002). Some effects are *cagE*-independent. CagL and related *cag*PAI components interact with the host integrin $\alpha_5\beta_1$ cell-surface receptor (Kwok et al. 2007; Jiménez-Soto et al. 2009), though the bacterial surface pili is not detectable by scanning electron microscopy for the Δ*cagE* mutant (Shaffer et al. 2011).

Hussein et al. (2010) found no differences for Δ*cagE* mutants in the IL-12/23p40 response of PBMCs, though did not report experimental results for IL-6, IL-8 or other cytokines. Interleukin-8 secretion is the protypical immunological impact of the *cag*PAI system on gastric epithelial cells (Crabtree 1996), through mechanisms explained in Section 1.2.1. *Helicobacter pylori* is a potent inducer of monocyte secretion of IL-8, in particular through an LPS-CD14-dependent pathway (Bliss et al. 1998). However, LPS prepared from different *H. pylori* strains does not differ in its ability to induce IL-8, though is much less potent than LPS from *Escherichia coli* (Innocenti et al. 2001) Production of IL-8 by monocytic THP-1 cells did not correlate with *cag*PAI or *vacA* status (de Jonge et al. 2001). However, other bacterial factors have been shown to be important determinants of IL-8 expression by monocytic cells, such as heat-shock protein 60 (Lin et al. 2005), via a TLR2, extra-cellular signal-regulated kinase (ERK), p38 MAPK, NF-κB pathway (Zhao et al. 2007). The NF-κB pathway was essential for *cag*PAI-mediated responses by MKN45 epithelial cells, but was still activated by a Δ*cagE* mutant in THP-1 monocytic cells and this activation involves CD14 and TLR4 (Maeda et al. 2001). Release of IL-8 by monocytes and macrophage-like cells (derived from THP-1 cells through PMA treatment) follows a similar pathway through ERK and MAPK cascades stimulated in part through LPS and CD14 (Bhattacharyya et al. 2002). Enhanced effects on the IL-8 promotor were driven by activation of NF-κB and to a lesser extent through activator protein-1 (AP-1).

Therefore, given that disruption of *dupA* impacts not only IL-8 production by monocytes but also IL-6, IFN-γ and IL-12/23p40, any host-bacterial interactions that depend on *dupA* may involve additional or different pathways to those affected for Δ*cagE* mutants.

	Co-culture with AB21 strains			
	Δ*dupA1* vs. wild-type	Δ*cagE* vs. wild-type	Δ*dupA1* vs. wild-type	Δ*cagE* vs. wild-type
Cytokine	**CD14$^+$**		**PBMC**	
IL-1β	*(34.0% ↓)*	ns	*(13.7% ↓)*	ns
TNF-α	ns	ns	**28.4% ↓**	ns
IL-6	**21.3% ↓**	*(13.8% ↓)*	**24.2% ↓**	**17.9% ↓**
IL-8	**23.0% ↓**	**24.7% ↓**	**23.3% ↓**	**21.8% ↓**
IFN-γ	**34.0% ↓**	ns	*(30.9% ↓)*	ns
IL-4	-	-	-	-
IL-10	ns	ns	ns	*(12.7% ↓)*
IL-17A	-	-	ns	ns
IL-12/23p40	**31.0% ↓**	ns	**30.6% ↓**	ns
IL-12p70	ns	*(21.1% ↑)*	ns	ns
IL-23	-	-	-	-

Table 5.14 – summary of percentage changes in cytokine expression in co-culture experiments according to *cagE* and *dupA* status

Comparison of the findings of this study for the relationship between *cagE* and *dupA* status and cytokine expression in co-culture (Sections 5.5.1 and 5.3.2). Arrows show the direction of difference for Δ*dupA* mutant strains against the corresponding wild-type strains. Italicised data in brackets indicate weak evidence (see Section 5.3.2).

ns, no statistically significant difference; -, not assessed; CD14$^+$, human blood monocyte experimental model; PBMC, peripheral blood mononuclear cell experimental model.

5.8.4 Strengths, weaknesses and future work

The main strength of this study was the inclusion of a greater number of biological replicates than in previous work. Ten donors and two sets of bacterial mutants were used, and all data were analysed and reported. Even then, it may be that the study was insufficiently powered to show strong statistical evidence for some differences that were found in only the first step of inferential analysis but not after correction for multiple comparisons. The inclusion of additional replicates, mutants and experimental conditions can impact on the feasibility of experiments designed using our model.

Ideally, isogenic mutants in other strain backgrounds and complemented mutants would be included in future work. Additional mutants in other putative *tfs4* components could be studied, alongside experiments to determine mutant expression profiles at the mRNA-level (including any polar effects) and ideally at the protein-level. Further potential approaches include incubation with purified *tfs4* bacterial proteins, pre-treatment with azide to inhibit ATP synthesis, pre-treatment ± co-culture with antimicrobials to inhibit protein synthesis, and bacterial inactivation using other

methods. For the latter, it was desirable to inactivate surface proteins through changes in tertiary structure but not to completely denature them or lyse the bacterial cells. Time- and temperature-limited heat treatment was used, but other methods such as irradiation may better preserve surface structure. Other approaches to determine conditions for *dupA*/*tfs4* expression were discussed above.

The current design of these co-culture experiments means that it is not practical to include a greatly expanded number of bacterial strains and mutants, multiple parallel controls or to undertake complex pre-treatment. Immortalised transformed cells such as THP-1 monocytic cells are an alternative option, and experimental design using cell lines is likely to be more straightforward, but any such approach is intrinsically artificial as cell responses differ from primary human cells (Schildberger et al. 2013). Primary culture of gastric lamina propria mononuclear cells is feasible (Bimczok et al. 2010), provided there is access to sufficient tissue for research purposes. These data could then be used to support the selection of appropriate *in vitro* cell culture(s) for phenotypic and mechanistic assays. In support of any findings, immunohistochemical staining of gastric biopsies could be performed and then scanned images analysed to identify cellular responses and any apparent co-localisation or interaction. Another approach would be to convert and mature $CD14^{+}$ cells in the presence of biopsy supernatants from infected and uninfected patients, although differences would not be monogenic or confined to bacterial factors. Comparative studies of different mononuclear phagocytic lineage cells may provide insights into differences in host-bacterial interactions (Fehlings et al. 2012). It would be interesting to extend this study and other work in our group using dendritic cells (Dr Emily Staples) to look at the effect of *dupA* status on monocyte-derived macrophages, ideally using stromal-conditioned and standard media to assess any impact of the gastric environment (Bimczok et al. 2011). However, these alternative *in vitro* models probably do not better reflect any potential *in vivo* interactions. Gastric organoids are an emerging approach in *H. pylori* research that enable biologists to study the impact of infection in a long-lived three-dimensional primary culture system comprising organised epithelial structures (Schlaermann et al. 2016). There is also interest in engineering complex multi-cellular models based on organoids, for example that incorporate immune cells and perhaps even microbiota (for example, National Institute of Health project grant 1U19AI116482).

These are still reductionist systems, but simple *in vitro* models are the logical approach to characterise the signalling pathways that underlie different cytokine responses. For example, by profiling the TLR and transcription factor responses to different bacterial mutants and conditions. These experiments could be extended using specific inhibitors of surface receptors and signalling cascade molecules alongside other methods like RNA knockdown (Patel et al. 2013), and perhaps using inhibitors of inflammasome activity or $NOD^{-/-}$ and $TLR^{-/-}$ cells. It may prove relevant to determine why there may be a difference in response between different cell types, for example by indentifying receptors specific to certain immune cells but missing from epithelial cells.

Different experimental models are also available, such as mouse and Mongolian gerbil animal models. However, all the *H. pylori* strains currently available for these models have disrupted *dupA* genes, including the more virulent PMSS1 strain that has been employed alongside *H. felis* strains in elegant studies using knockout mice (Hitzler et al. 2012). Phase I human infection trials of *H. pylori* in human volunteers have also been reported to be safe (Graham et al. 2004), and even proposed as a system of antigen delivery in vaccine development (Marshall and Schoep 2007). Ultimately, it is prudent and ethical to defer complex interventional experiments until the microbiological and molecular characterisation of *dupA* and *tfs4* is more advanced. Generalisable and confident conclusions about the potential *in vivo* interactions between *H. pylori* and its human host with regard to a *dupA* virulence system – whether these be via immune cells, epithelial cells or a combination of these and other cell types – are premature. Research using *in vitro* models, as in this study, can complement work to extend our knowledge of the assembly and expression of *tfs4* components, and its potential to contribute to host-bacterial interactions.

5.8.5 Conclusion

In this chapter, human mononuclear immune cells derived from peripheral blood were used as a model to study host-bacterial interactions. Monocytes and PBMCs were found to have different cytokine responses to *H. pylori* according to *dupA* and *tfs4* status, that were distinct from those mediated through *cagE* and the *cag*PAI. Both the putative *virB2* homologue and *dupA* itself had the most marked impact on cytokine induction. This was dependent on live bacteria. We hypothesise that host immune cells interact with surface-expressed components of *tfs4*, the full expression of which may rely on *virB2* and *dupA*.

There is much work that remains to be done in order to understand the function of *dupA* and the putative *tfs4* system, whether this is involved in horizontal gene transfer between bacteria or interacts directly with host cells, the conditions in which such a system is expressed and utilised by the bacteria, and whether it constitutes a novel means of host-bacterial interaction. It remains to be shown whether *H. pylori* interacts with human immune cells *in vivo* through the *dupA*/*tfs4* system, and whether the *in vitro* observations of this study are duplicated *in vivo*. However, we have shown that *dupA* is able to mediate a more pro-inflammatory host response, which may be the mechanism that explains the association of *dupA* with gastroduodenal diseases.

6. Conclusion

Helicobacter pylori infection is common. Host genetic, environmental and bacterial virulence factors contribute to the risk of a person colonised by *H. pylori* developing disease. The unfulfilled promise of bacterial virulence factors (Graham and Yamaoka 2000) is their failure to accurately distinguish between the two divergent clinical outcomes of duodenal ulceration and gastric cancer.

The *H. pylori* virulence factor *dupA* is the only bacterial factor to be described as disease-specific in its promotion of duodenal ulceration (Lu et al. 2005). The criteria of a true virulence factor are: an epidemiologically consistent disease association, *in vivo* disease correlates, and biological plausibility (Lu, Yamaoka and Graham 2005).

This thesis aimed to test whether *dupA* meets the criteria of a true virulence factor.

The key findings of this study are that:

1. the influence of *dupA* status on clinical outcomes is not specific to duodenal ulceration, but rather epidemiological associations link *dupA* with an increased the risk of gastroduodenal diseases in general in some populations,
2. the *dupA* status of clinical isolates is not associated with the key pathogenic features of duodenal ulceration, though there is evidence of increased gastric mucosal inflammation *in vivo* with *dupA*+ strains, and
3. the influence of *dupA* and *tfs4* status on human immune cells responses using an *in vitro* model suggests that monocyte-derived cells may mediate a more pro-inflammatory response through interaction with the *dupA* system. This may be the mechanism that explains the association of *dupA* with disease.

In relation to the specific *H. pylori*-associated clinical outcome of duodenal ulceration, *dupA* does not have an epidemiologically consistent disease association, and *dupA* status does not correlate with key pathogenic features *in vivo*.

The evidence of increased mucosal inflammation with *dupA*+ strains and the relationship between the *dupA* system and pro-inflammatory responses by human cells, lend biological plausibility to a role for *dupA* as a true virulence factor for *H. pylori*-associated gastroduodenal diseases in general.

The assertion of this thesis is that duodenal ulcer promoting gene is misnamed.

7. Appendices

7.2 Appendix for chapter 2 – Materials and methods

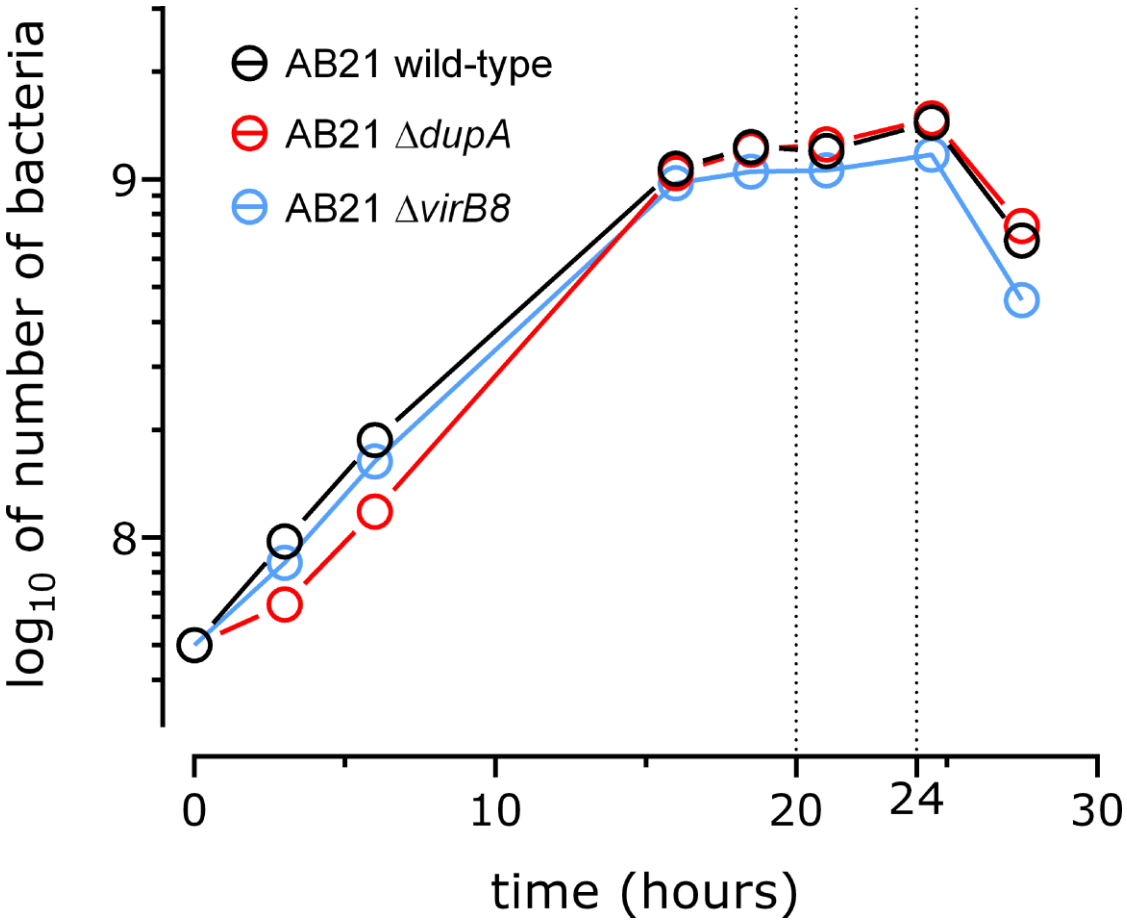

Figure 7.1 – representative growth curves for AB21 wild-type, Δ*dupA* and Δ*virB8* isogenic mutant strains

H. pylori were grown from cryo-stocks then passaged once on blood agar plates. Brain-heart infusion (BHI) broth was prepared and freshly supplemented 10% (v/v) with sterile-filtered heat inactivated foetal bovine serum (FBS). In duplicate for each strain, bacteria were harvested after 24 h growth from three agar plates and transferred with a wetted sterile swab to 5 mL of BHI/FBS solution under sterile conditions. Liquid bacterial cultures were grown overnight with shaking at 400 rpm in a microaerophilic workstation at 37 °C in a humidified atmosphere of 5% carbon dioxide. The following day the OD_{600} was determined initially by 1 in 25 dilution with 40 µL of bacterial culture into 1 mL of BHI/FBS, then by dilution with calculated volume of bacterial culture to give an OD_{600} of 0.05. The OD_{600} was determined and the volume necessary to give an OD_{600} of 0.05 re-calculated, scaled up, inoculated in duplicate into 20 mL of pre-warmed BHI/FBS solution in vented 75 cm^3 tissue culture flasks and incubated as before. The average OD_{600} was determined for each replicate at 0 h, 3 h, 6 h, 16 h, 18.5 h, 21 h, 24.5 h and 27.5 h. The mean OD_{600} was calculated, expressed as equivalent number of bacteria (OD_{600} of 1.00 indicates approximately 1.0×10^9 cells) and plotted. The coefficients of variation were all less than 10.0% for the first seven time points (mean 2.6%), though for the last time point were 28.3% for wild-type, 7.6% for Δ*dupA* and 18.4% for Δ*virB8*. Contamination was excluded by Gram stain. For the co-culture experiments, bacteria were harvested after 20 to 24 h of growth on agar.

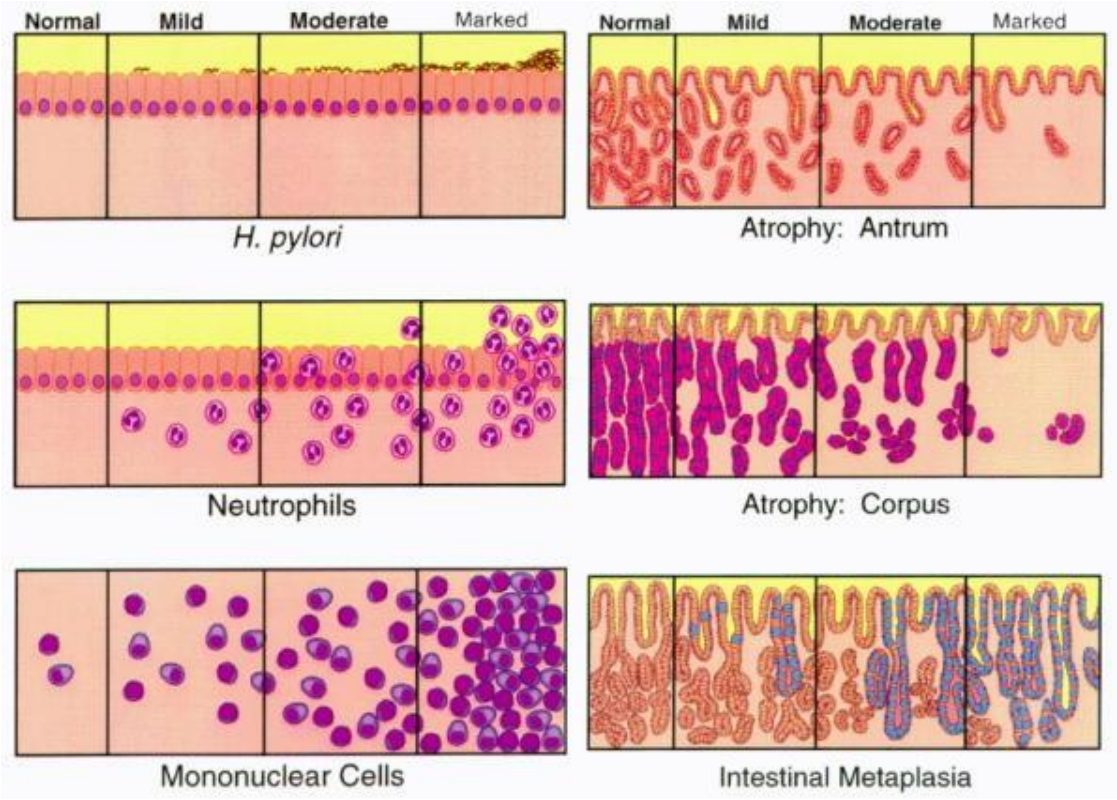

Figure 7.2 – pictographic representations of histopathological appearances of the gastric mucosal according to the update Sydney system

These visual analogue scales for graded variables in the updated Sydney system as intended to aid recognition of the magnitude of each ordinal variable, scored from 0 (normal) to 3 (marked or severe). Neutrophil grading was based on the depth of neutrophil infiltration. Reproduced from Dixon et al. (1996) with permission from Wolters Kluwer Health Inc.

7.3 Appendix for chapter 3 – Results One

7.3.1 Alignment of *dupA* sequences for *H. pylori* isolates

Figure 7.3 shows an alignment of representative *dupA* sequences in this study. The figure legend reports the indels and resulting frameshifts for *dupA2* strains. The single nucleotide polymorphisms in *dupA1* strains included conservative and non-conservative mutations, though the open reading frames remained intact at 2499 bp in length.

All the sequences for isolates obtained from paired antrum and corpus biopsies are shown, which were identical between gastric sites in all 10 cases. These paired sequences were available for 7 patients for *dupA1* strains (322, 495, 511, 597, 619, 652 and 654) and for 3 patients for *dupA2* strains (194, 444 and 639). The other 4 patients with matching *dupA* typing between gastric sites were colonised by *dupA*– strains (461, 462, 529 and 565). Therefore, in total from the 52 participants in this study, paired isolates were available in 14 cases (as reported in Section 3.2).

The figure also shows representative *dupA* sequences for other participants where only one isolate from either the gastric antrum or corpus was available – for *dupA1* strains for 3/11 antral isolates (295A, 521A and 527A, sequences not shown for 448, 451, 473, 476, 568, 579, 638 or 653) and 3/6 corporal isolates (233C, 454C and 606C, sequences not shown for 274, 320 or 335), for the *dupAx* strain for 286A (*dupAx* is missing 21 bp but is otherwise in frame), and for *dupA2* strains for 2/5 antral isolates (404A and 506A, sequences not shown for 247, 308 or 339) and the only corporal isolate 253C. Some sequences were omitted for reasons of space but those for all *dupA1* strains from co-culture experiments are reported (454, 521, 527, 597, 606 and 619). Note that the other *dupA*– strains in this study without paired biopsies were 192A, 443A, 447A, 465A, 518A, 519A, 535A, 536C, 537A, 547A, 549A, 563A, 644A and 645A (18 in total).

In addition to these 20 clinical isolates, the figure shows *dupA* sequences from Shi470, J99 and G27 *H. pylori* chromosomal genomes (NCBI RefSeq NC010698.2, NC000921.1 and NC011333.1 respectively) and for strain AB21. See Figure 1.8 for a representation of the *tfs4* regions of G27 and Shi470, with the frameshifted *dupA* of G27 shown in grey. Putative variant form *dupA* genes such as for the P12 chromosomal genome are not shown in this alignment.

Figure 7.3 – alignment of representative *dupA* sequences

Sequences are shown aligned against the Shi470 *dupA* sequence (NC010698.2, gene designated *HPSH04615*) and positions are reported relative to the start of this open reading frame (ORF). Matching residues are shown as dots. Gaps due to insertions or deletions are coloured in pink.

dupAx (clinical isolate shown in figure, considered with *dupA2* strains)

286 – missing 21 bp from 517 to 537 inclusive but otherwise is in frame – single ORF from 1 to 2499 inclusive (2478 bp)

dupA2 (reported chromosomal genomes and clinical isolates shown in figure)

J99 – missing first 615 bp (this encompasses the 3' end of *jhp0916* and the next 211 bp, the alignment is generally poor except for the 67 bp before the 5' end of *jhp0917* [Shi470 position 616] where 63/67 residues are identical to the equivalent residues in Shi470) and two deletions (missing a cytosine at 2001, missing an adenine at 2349) – *jhp0917* from 616 to 2044 (1428 bp), overlapping *jhp0918* from 2032 to 2455 inclusive (423 bp)

G27 – insertion (extra thymine after 1183) – ORF1 (5' end of *HPG27_963*) from 1 to 1196 inclusive (1197 bp), ORF2 (3' end of *HPG27_963*) from 1258 to 2499 inclusive (1242 bp)

194A/194C – deletion (missing a guanine at 576) – ORF1 from 1 to 597 inclusive (597 bp), ORF2 from 616 to 2499 inclusive (1884 bp)

253C – deletion (missing a guanine at 1303) – ORF1 from 1 to 1399 inclusive (1399 bp), ORF2 from 1408 to 2499 inclusive (1092 bp)

404A – insertion (extra guanine after 2042) – ORF1 from 1 to 2063 inclusive (2064 bp), overlapping ORF2 from 2044 to 2448 inclusive (405 bp)

444A/444C – deletion (missing a guanine at 1087) – ORF1 from 1 to 1093 inclusive (1093 bp), ORF2 from 1165 to 2499 inclusive (1335 bp)

506A – insertion (extra adenine after 249) and missing 21 bp from 517 to 537 inclusive – ORF1 from 1 to 275 inclusive (276 bp), ORF 2 from 451 to 1371 inclusive (900 bp), ORF 3 from 1408 to 2499 inclusive (1092 bp)

639A/639C – insertion (extra adenine after 340) – ORF1 from 1 to 347 inclusive (348 bp), ORF2 from 616 to 2499 inclusive (1884 bp)

dupA2 (clinical isolates not shown in figure)

247A – same as 253C (note that *dupA* sequences for these strains are 100% identical)

308A – two substitutions (codon TGA [stop] instead of GGG [glycine] at 1426 to 1428) – ORF1 from 1 to 1428 inclusive (1428 bp), ORF2 from 1486 to 2499 inclusive (1014 bp)

339A – deletion (missing an adenine at 2303) – single truncated ORF from 1 to 2344 inclusive (2343 bp)

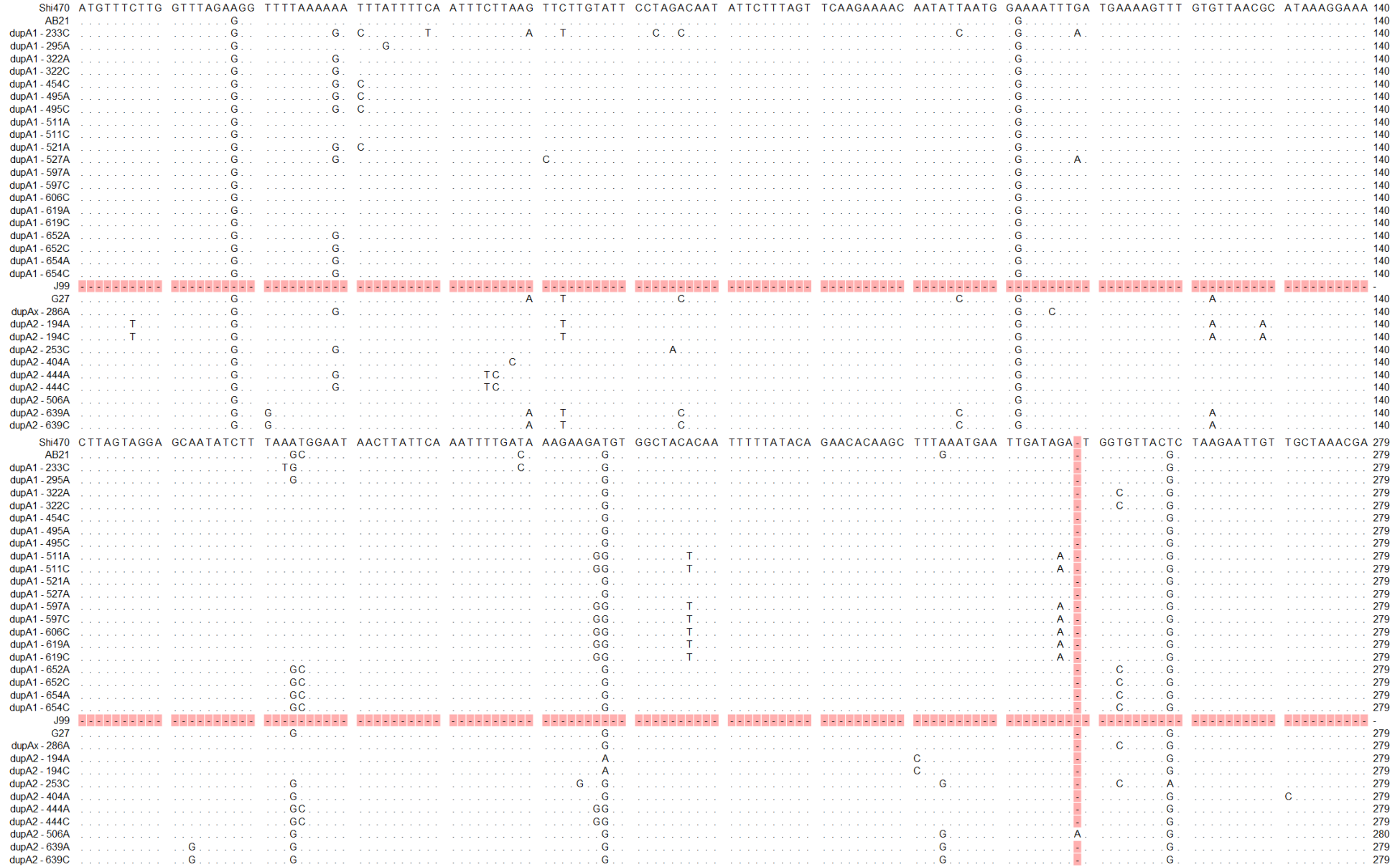

Figure 7.3 – alignment of representative *dupA* sequences

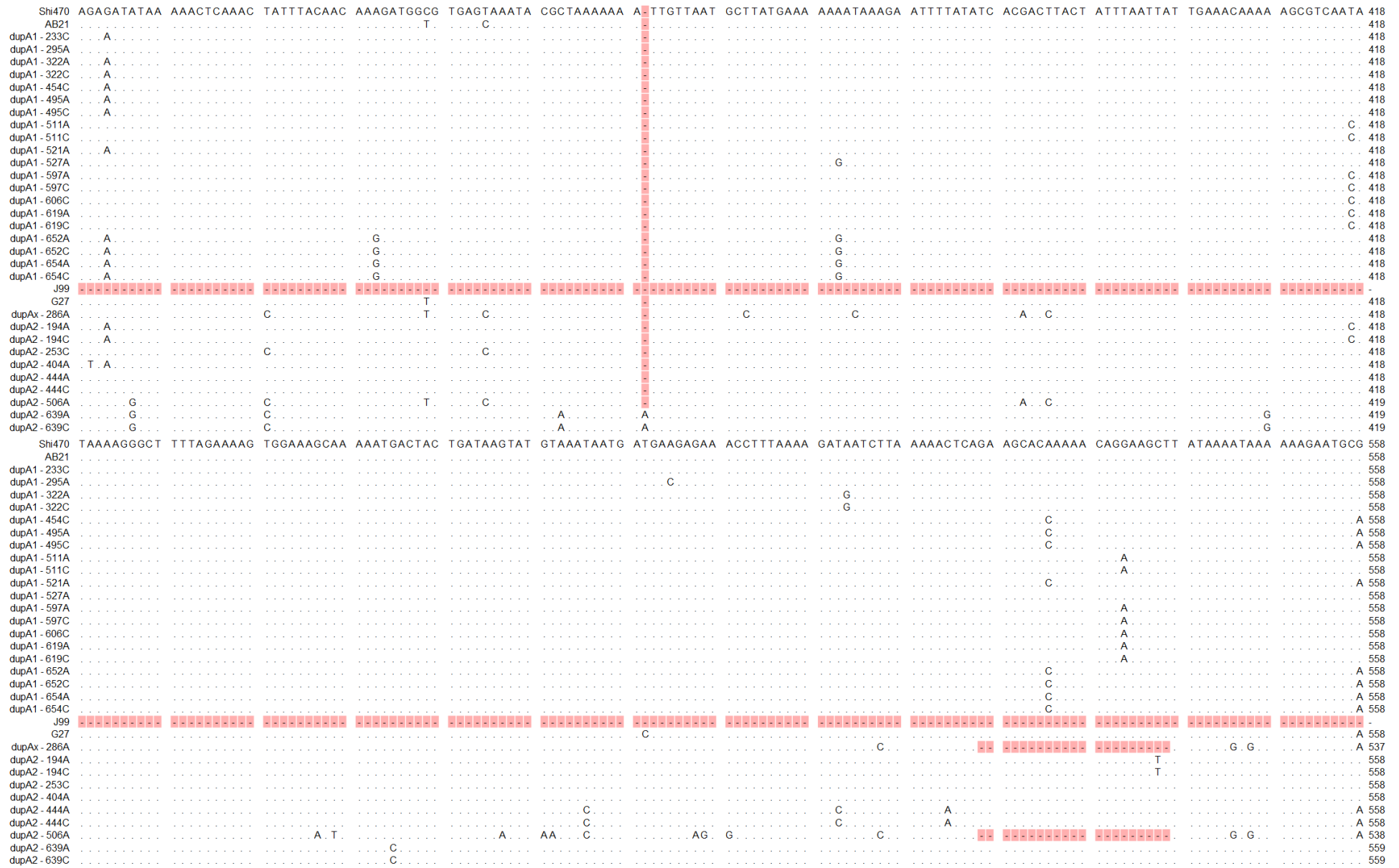

Figure 7.3 – alignment of representative *dupA* sequences (cont.)



Figure 7.3 – alignment of representative *dupA* sequences (cont.)

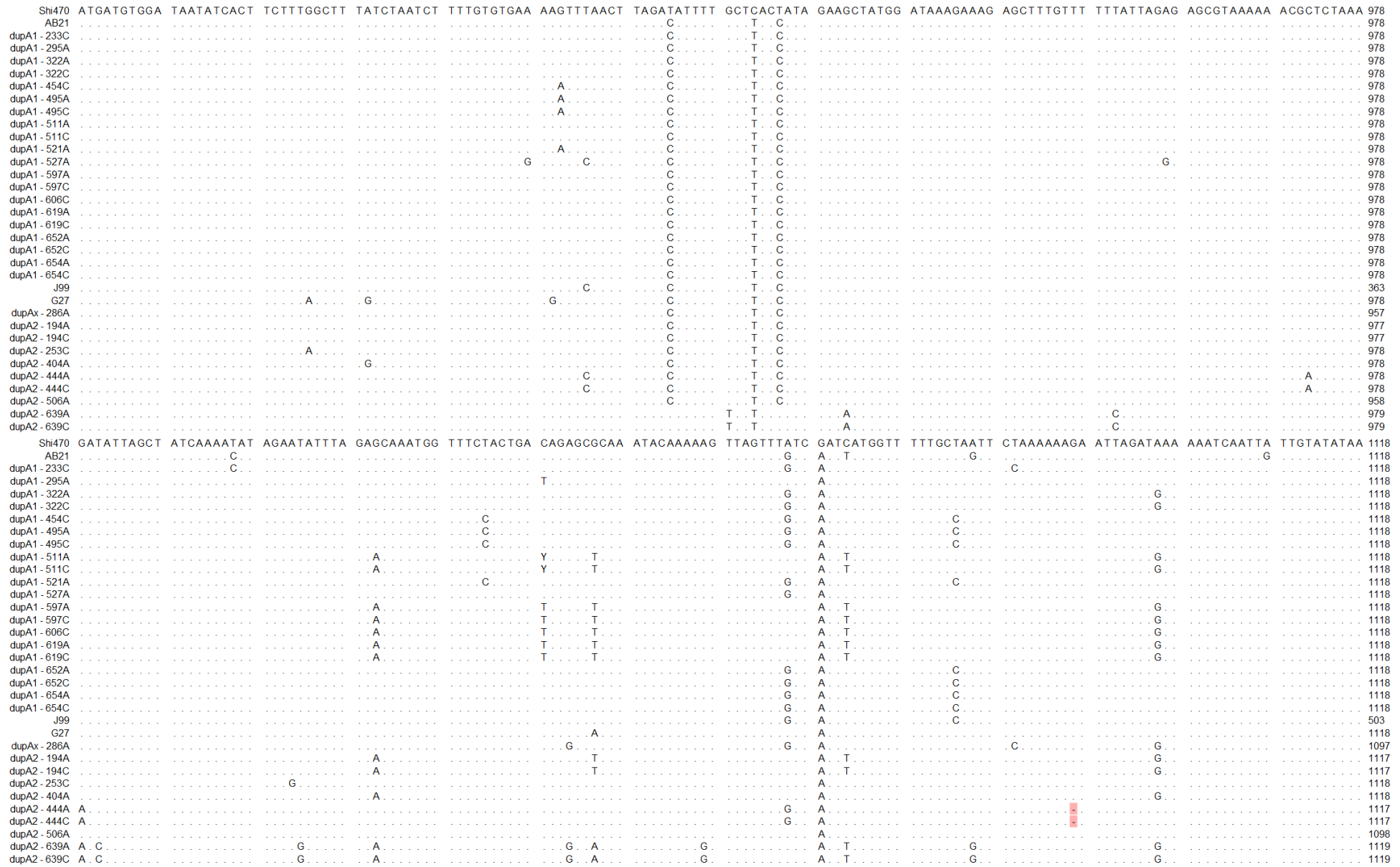

Figure 7.3 – alignment of representative *dupA* sequences (cont.)

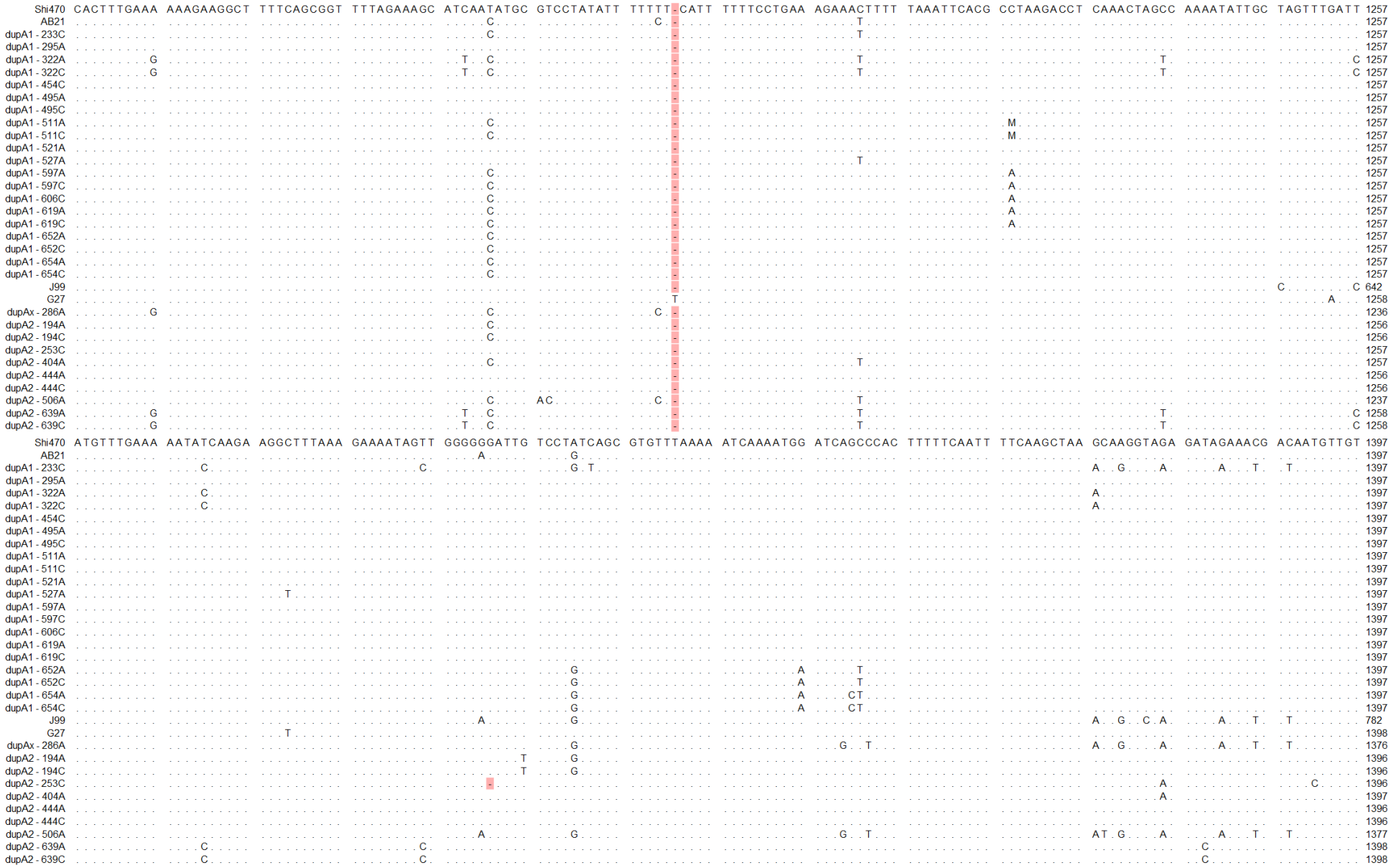

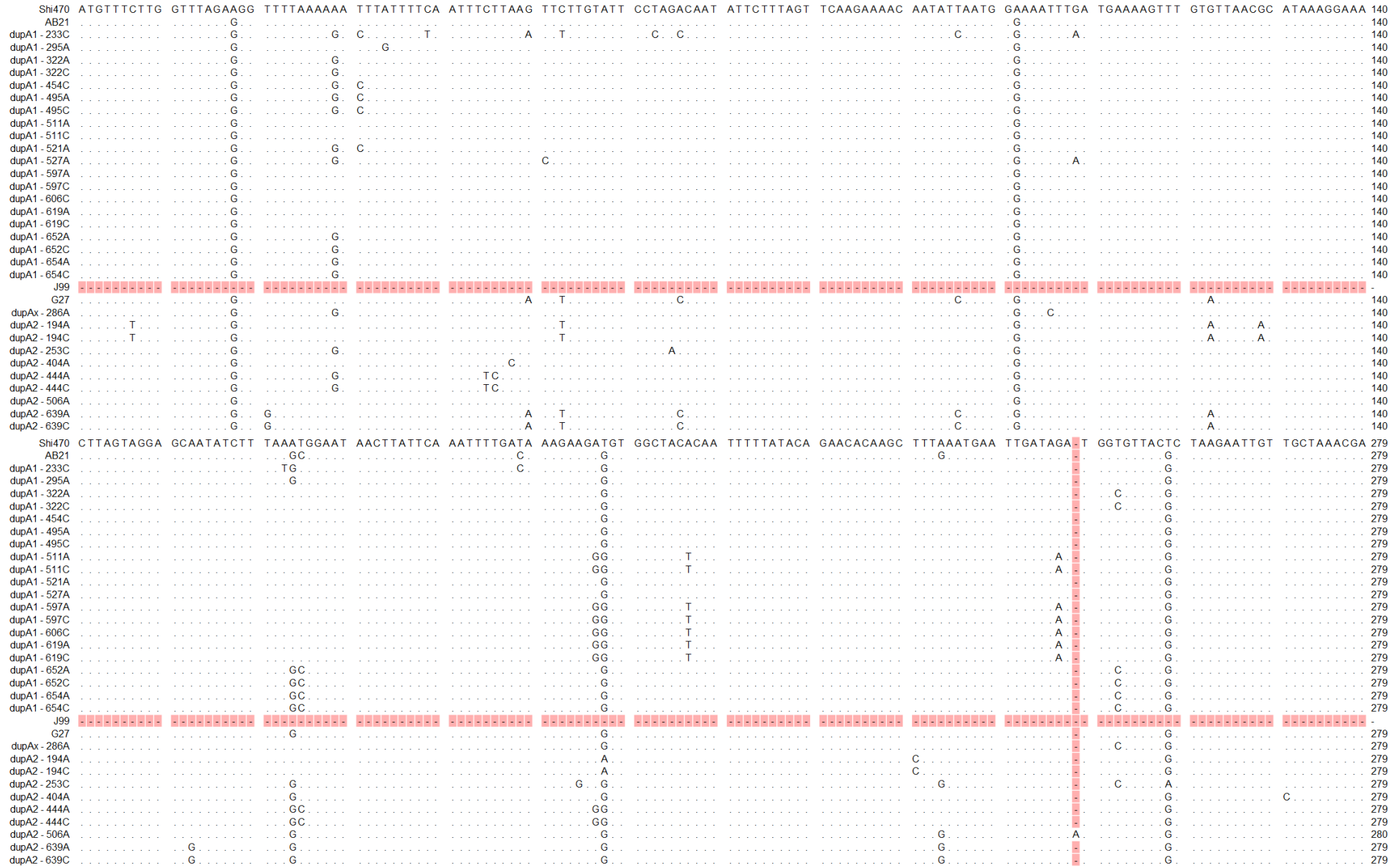

Figure 7.3 – alignment of representative *dupA* sequences (cont.)

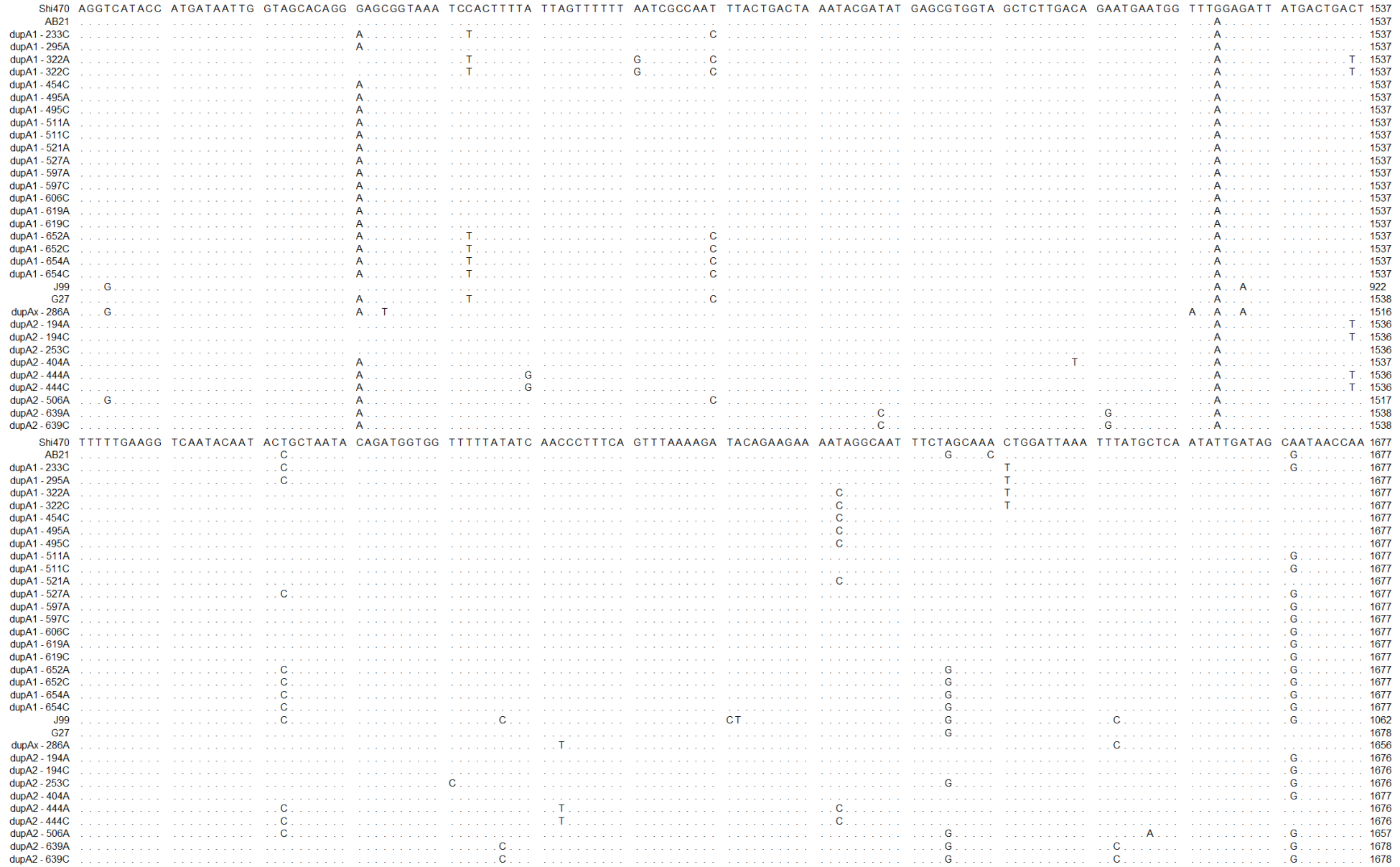

Figure 7.3 – alignment of representative *dupA* sequences (cont.)

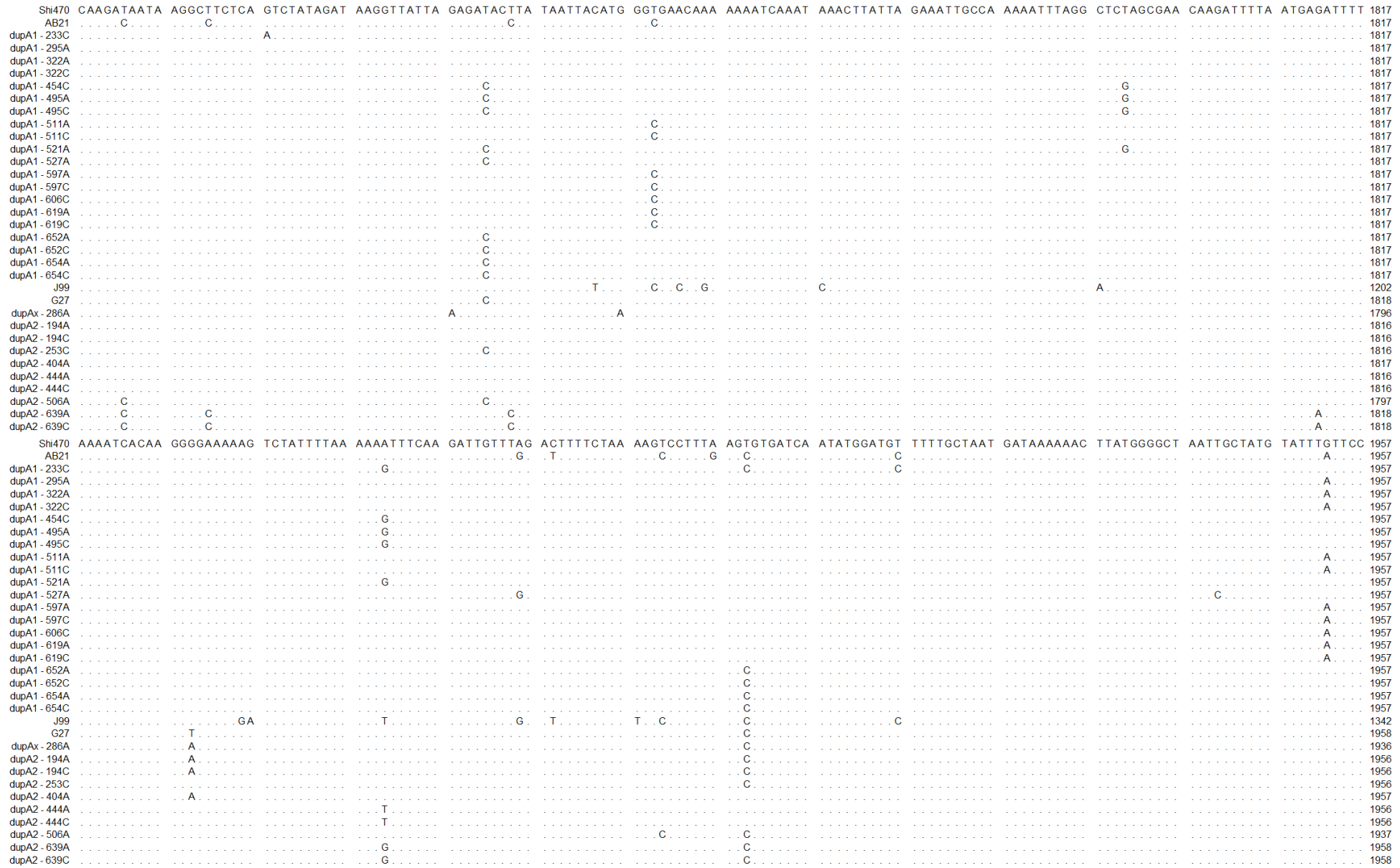

Figure 7.3 – alignment of representative *dupA* sequences (cont.)

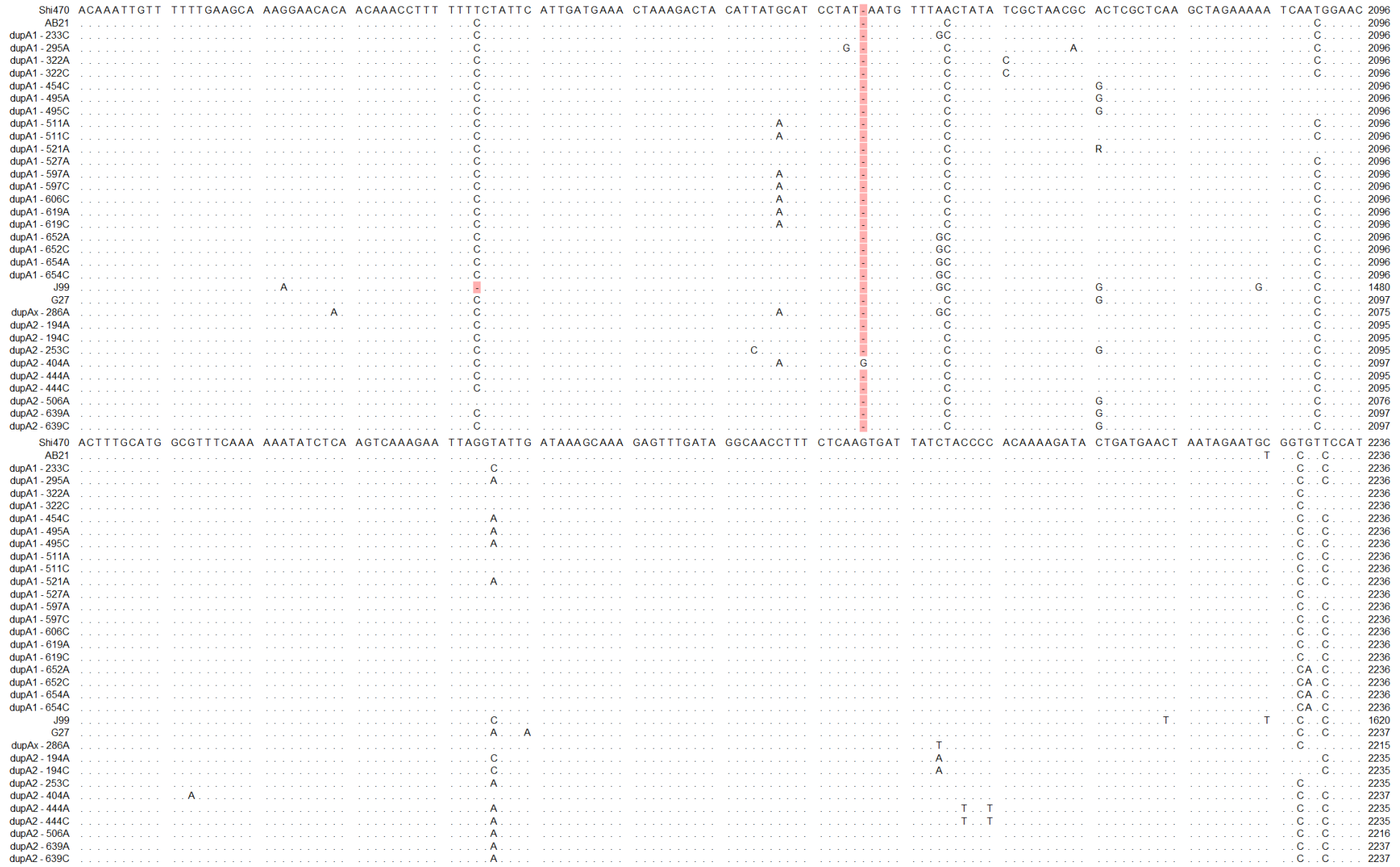

Figure 7.3 – alignment of representative *dupA* sequences (cont.)

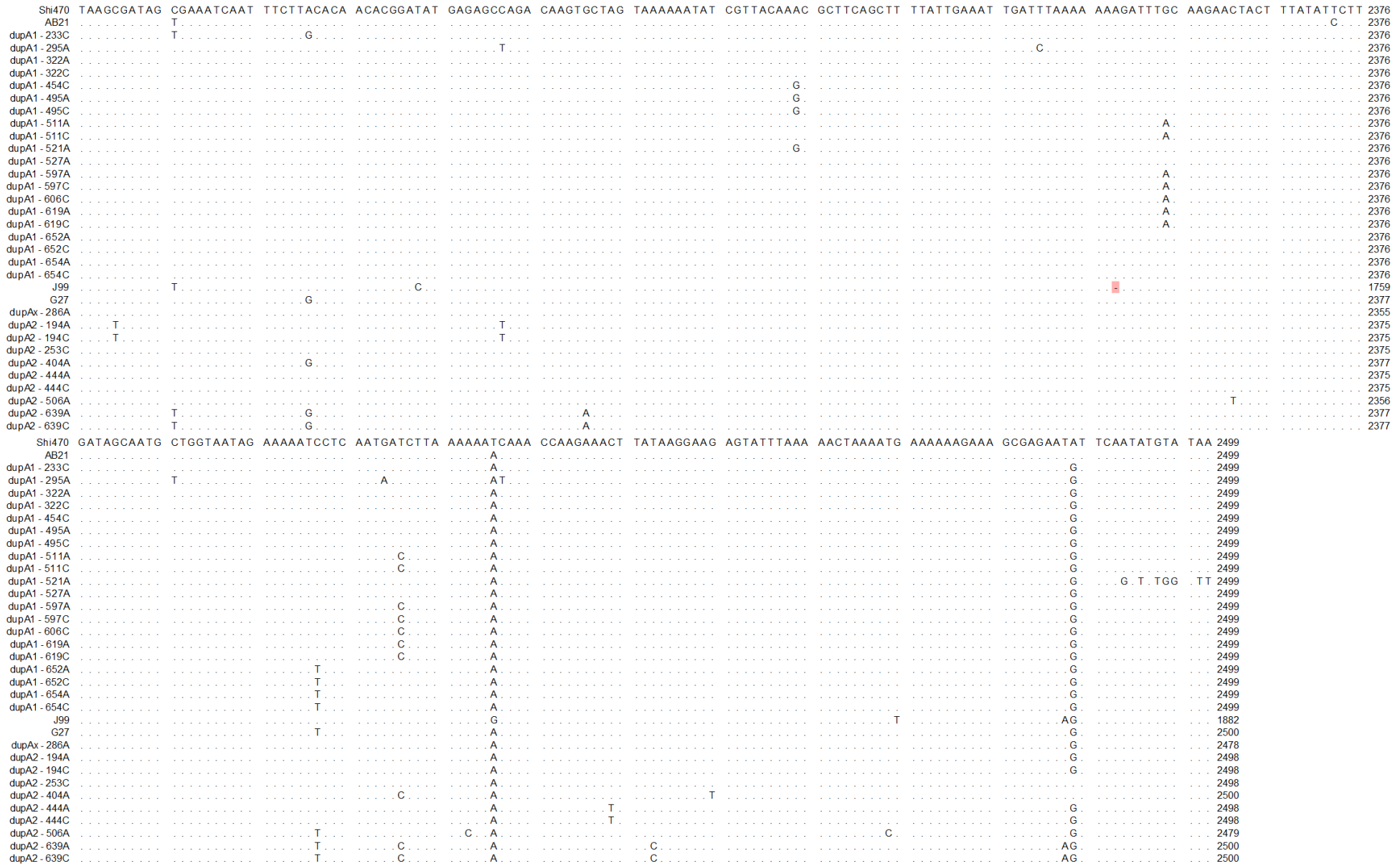

Figure 7.3 – alignment of representative *dupA* sequences (cont.)

7.3.2 Example Forest plot for initial meta-analysis

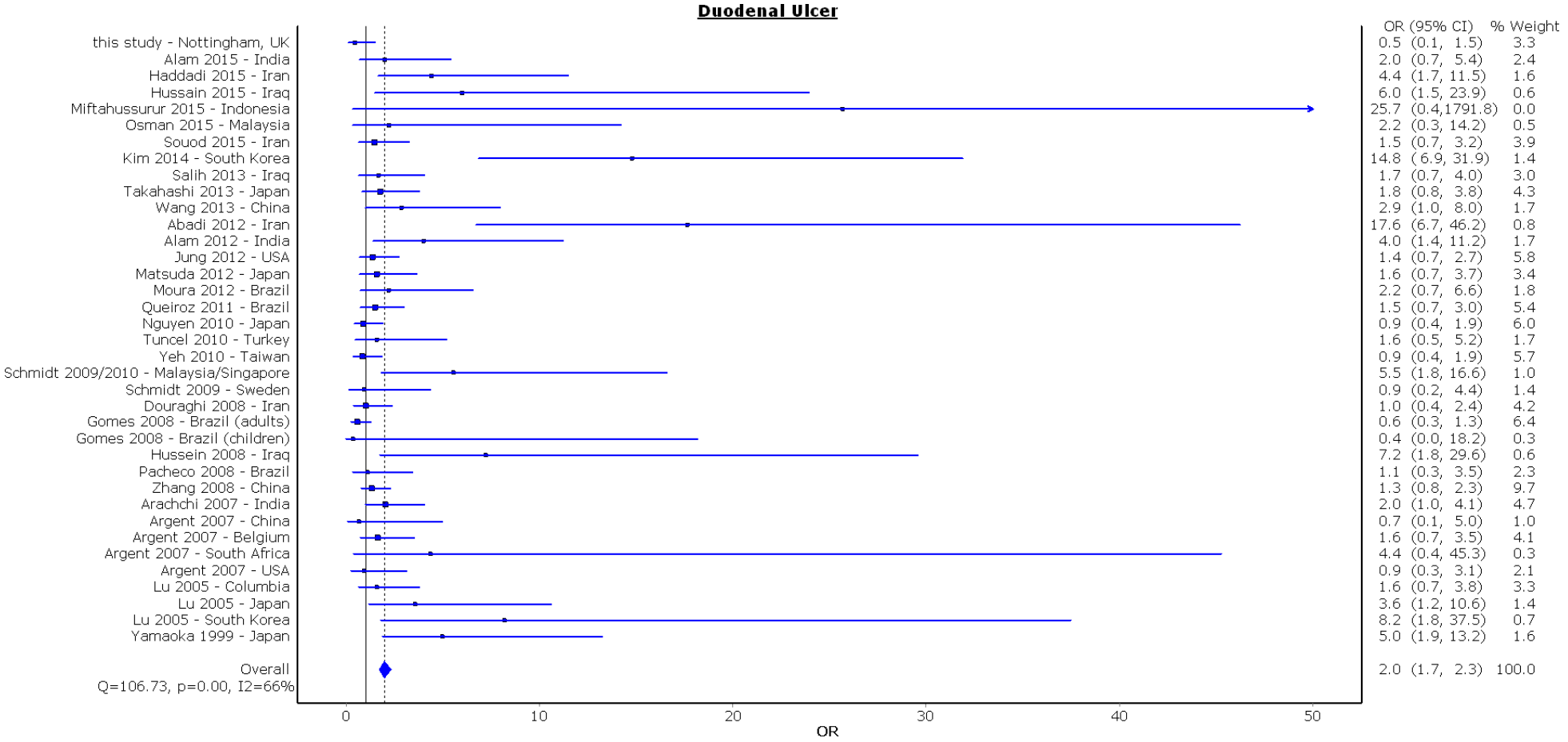

Figure 7.4 – results of initial meta-analysis for the risk DU in *dupA+ H. pylori* infection, before heterogeneity was identified and addressed

This meta-analysis included 776 cases and 1674 controls from 37 study populations. There was strong evidence of substantial heterogeneity between study populations, such that the summary effect measure should be interpreted with caution.

7.4 Appendix for chapter 4 – Results Two

7.4.1 Interferon-gamma protein-level expression was associated with *H. pylori* infection using a different assay

We did not demonstrate an association with *H. pylori* infection for IFN-γ using Luminex assays, though this was shown for *IFNG*. Protein-level analysis was repeated for a proportion of samples using MSD assays, which have greater resolution at the limits of detection (0.28 pg/mL). A significant difference was identified (1.7-fold, $P = 0.008$).

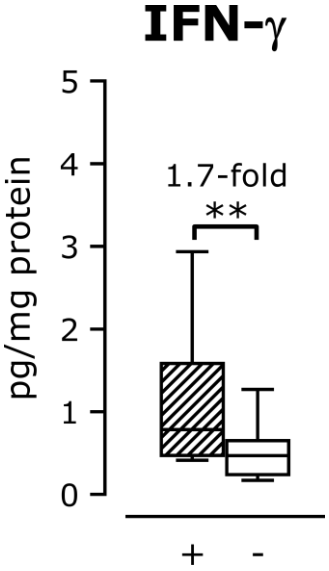

Figure 7.5 – antral gastric mucosal concentrations of IFN-γ using MSD assays

IFN-γ mucosal concentrations were determined in homogenised snap frozen human gastric biopsies in duplicate using Meso Scale Discovery V-PLEX assays and adjusted for total protein concentration.

H. pylori-infected participants (+, n=28) are shown by a hatched box and uninfected participants (–, n=19) by a white box. The horizontal and error bars show median values and inter-quartile ranges (IQRs) respectively. The box-and-whisker plots show median values, IQRs and 10-90th centiles.

Data for *H. pylori*-infected vs. uninfected participants were compared by a Mann-Whitney U test. Statistically significant differences are shown above the plotted data with the fold-difference in group medians (* $P < 0.05$, ** $P < 0.01$, *** $P < 0.001$).

7.5 Appendix for chapter 5 – Results Three

7.5.1 Co-culture of mutant strains with PBMCs – adjusted cytokine and chemokine concentrations

Results are shown in Figure 7.6. No inferential statistical analysis was planned. Cells and bacteria were co-cultured at an expected MOI of 10. An observed MOI was calculated from colony forming unit counts for each donor/strain combination. Measured cytokine concentrations were adjusted by multiplication by a correction factor calculated as $\log_{10}$(expected MOI) / $\log_{10}$(observed MOI). Unadjusted concentrations were used for controls. Media only negative controls performed as expected. Positive controls with LPS and lysate did demonstrate higher concentrations for all analytes, though live bacteria more effectively stimulated cytokine production such that this is not graphically demonstrated on a linear scale for some analytes.

Absolute cytokine concentrations, from highest to lowest, were observed for IL-8, IFN-γ, IL-12/23p40, TNF-α, IL-6 and IL-1β. Concentrations were lower for IL-12p70, IL-10 and IL-17A, which should be considered when interpreting the percentage differences from wild-type reported in the next section.

There was variability in relative concentrations of different cytokines between donors, which we had anticipated. Therefore, these experiments were designed and analysed to mitigate this, with multiple biological (and technical) replicates of both human donors and bacterial strains, including two independent sets of mutants.

Figure 7.6 – adjusted cytokine concentrations for 48 h PBMC co-culture

Peripheral blood mononuclear cells (PBMCs) were purified from 10 donors and co-cultured with media only, with lipopolysaccharide (LPS) or sonicated *H. pylori* (lysate), or with sets of wild-type and isogenic/double mutants of strain AB21 that had been constructed and stored separately (denoted by O and X). Cytokine/chemokine concentrations in 48 h co-culture supernatants were measured for 9 analytes in at least duplicate using Meso Scale Discovery V-PLEX assays (panels A to I).

Data points represent the mean concentration for each donor/strain combination adjusted for multiplicity of infection (MOI) by a correction factor calculated as $\log_{10}$(expected MOI) / $\log_{10}$(observed MOI) and unadjusted concentrations were used for controls (media n=10, LPS n=10, lysate n=5, wild-type n=19, Δ*dupA* n=16, Δ*tfs4* n=7, Δ*cagE* n=16, Δ*dupA*Δ*cagE* n=14, Δ*virB2* n=6, Δ*virB8* n=8, Δ*virB9* n=6, Δ*virB8*Δ*dupA* n=3; not every data point is plotted – see note). The horizontal bars show overall mean values.

Note that for clarity some data points are not shown but were included in summary statistics – donor A wild-type O, wild-type X and Δ*cagE* X for panel D: IL-8 (7.76×10^7, 5.12×10^7 and 7.21×10^7 pg/mL respectively).

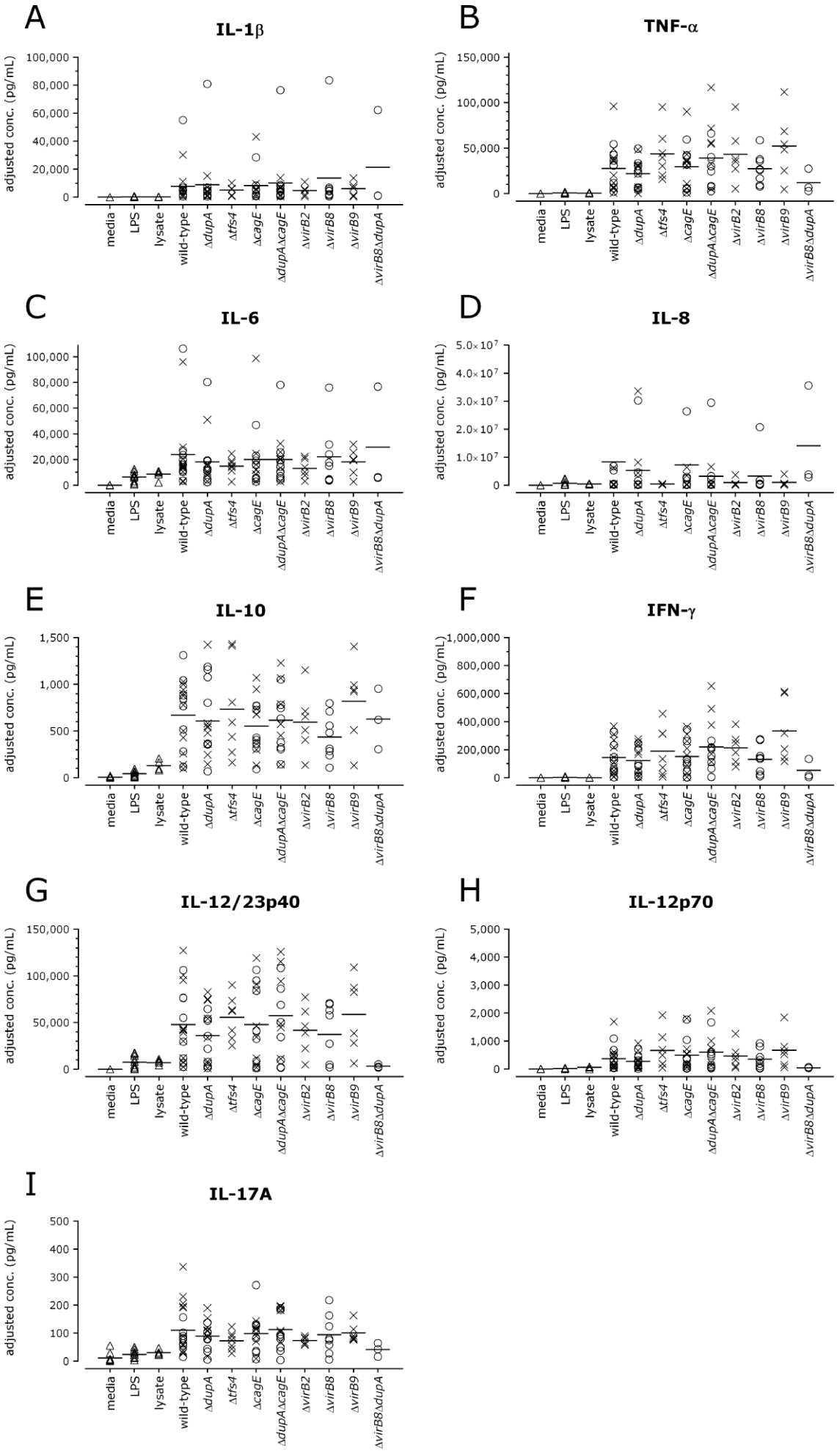

Figure 7.6 – adjusted cytokine concentrations for 48 h PBMC co-culture

7.5.2 Co-culture of mutant strains with CD14$^+$ monocytes – adjusted cytokine and chemokine concentrations

Results are shown in Figure 7.7. No inferential statistical analysis was planned. Each donor/strain combination was adjusted for observed MOI as described in Appendix Section 7.5.1. Controls performed as expected.

Absolute cytokine concentrations, from highest to lowest, were similarly observed for IL-8, IL-12/23p40, TNF-α, IL-6 and IL-1β. This order is the same as that noted in Appendix Section 7.5.1 for PBMCs, although IFN-γ production by monocytes was much less (around 200-fold lower), as one would expect. The lowest concentrations were observed for IL-10 (3- to 4-fold higher vs. PBMCs), IFN-γ and IL-12p70 (5-fold lower vs. PBMCs).

There was similar variability in cytokine abundance between particular donor/strain pairs as seen with PBMC co-culture (Appendix Figure 7.6). These appeared largely to be internally consistent between strains, though with higher concentrations across all strains for some donors. For example, the highest data points in panel G in Appendix Figure 7.7 were for cells from donor J (denoted by X, same for panel E).

7.5.3 Co-culture of clinical strains with CD14$^+$ monocytes

The median adjusted concentration of IL-6 was significantly higher for *dupA1* isolates co-cultured with CD14$^+$ cells (26.2 vs. 16.0 ng/mL, $P = 0.008$), as had previously been observed with PBMCs (29.5 vs. 23.1 ng/mL, $P = 0.003$) in Section 5.2. There were no other significant differences between *dupA1* and non-*dupA1* clinical strains. These are non-isogenic strains, so the data may reflect other important factors than *dupA* status.

Figure 7.7 – adjusted cytokine concentrations for 48 h monocyte co-culture

$CD14^+$ monocytes were purified from 10 donors and co-cultured with media only, with lipopolysaccharide (LPS) or sonicated *H. pylori* (lysate), or with sets of wild-type and isogenic/double mutants of strain AB21 that had been constructed and stored separately (denoted by O and X). Cytokine/chemokine concentrations in 48 h co-culture supernatants were measured for 8 analytes using Meso Scale Discovery V-PLEX assays in at least duplicate (panels A to H).

Data points represent the mean concentration for each donor/strain combination. These were adjusted for multiplicity of infection (MOI) by a correction factor, calculated as $\log_{10}$(expected MOI) / $\log_{10}$(observed MOI), and unadjusted concentrations were used for controls (media n=10, LPS n=10, lysate n=5, wild-type n=19, Δ*dupA* n=15, Δ*tfs4* n=7, Δ*cagE* n=15, Δ*dupA*Δ*cagE* n=13, Δ*virB2* n=6, Δ*virB8* n=7, Δ*virB9* n=6, Δ*virB8*Δ*dupA* n=2; not every data point is plotted – see note). The horizontal bars show overall mean values.

Note that for clarity some data points are not shown but were included in summary statistics – donor A wild-type O for panel C: IL-6 (1.23×10^5 pg/mL); donor B wild-type X for panel D: IL-8 (1.06×10^8 pg/mL); donor F Δ*tfs4* X for panel G: IL-12/23p40 (2.98×10^5 pg/mL); donor J wild-type X and Δ*cagE* X for panels B: TNF-α (2.34×10^5 and 2.42×10^5 pg/mL respectively) and G: IL-12/23p40 (1.87×10^5 and 1.82×10^5 pg/mL respectively).

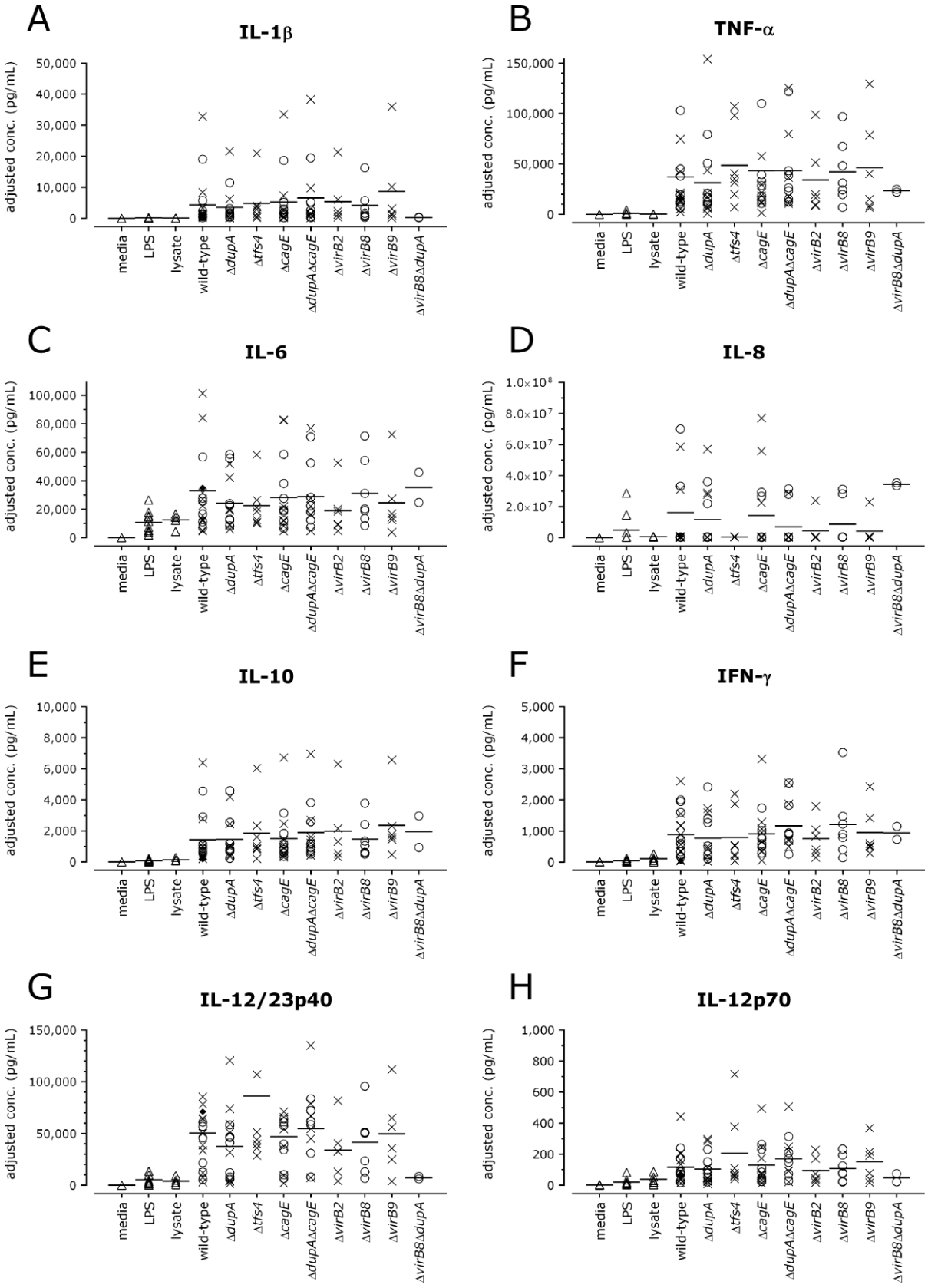

Figure 7.7 – adjusted cytokine concentrations for 48 h monocyte co-culture

Figure 7.8 – cytokine expression in monocyte co-cultures with clinical strains

$CD14^+$ monocytes were purified from 4 donors (G-J). Cells were co-cultured with clinical isolates of *H. pylori* characterised by sequencing as *dupA1* (n=6) or non-*dupA1* (n=6). Cytokine/chemokine concentrations in 48 h co-culture supernatants were measured for 8 analytes in at least duplicate using Meso Scale Discovery V-PLEX assays (panels A to H).

The *dupA1* strains were 454, 521, 527, 597, 606 and 619, and the non-*dupA1* strains, which lack a complete full-length *dupA1* gene, were 461, 529, 536, 547, 563 and 565. The non-*dupA1* strains were all typed as *dupA* negative.

Data points represent the measured concentration adjusted for observed multiplicity of infection after determination of colony forming units and cell counts for each donor/strain combination. The overlaid red horizontal bars show overall mean values. The separate black horizontal and error bars show overall median values and inter-quartile ranges (IQRs) respectively.

Data from *dupA1* and non-*dupA1* groups for each analyte were compared by Mann-Whitney tests. Statistically significant differences are shown (* $P < 0.05$, ** $P < 0.01$, *** $P < 0.001$).

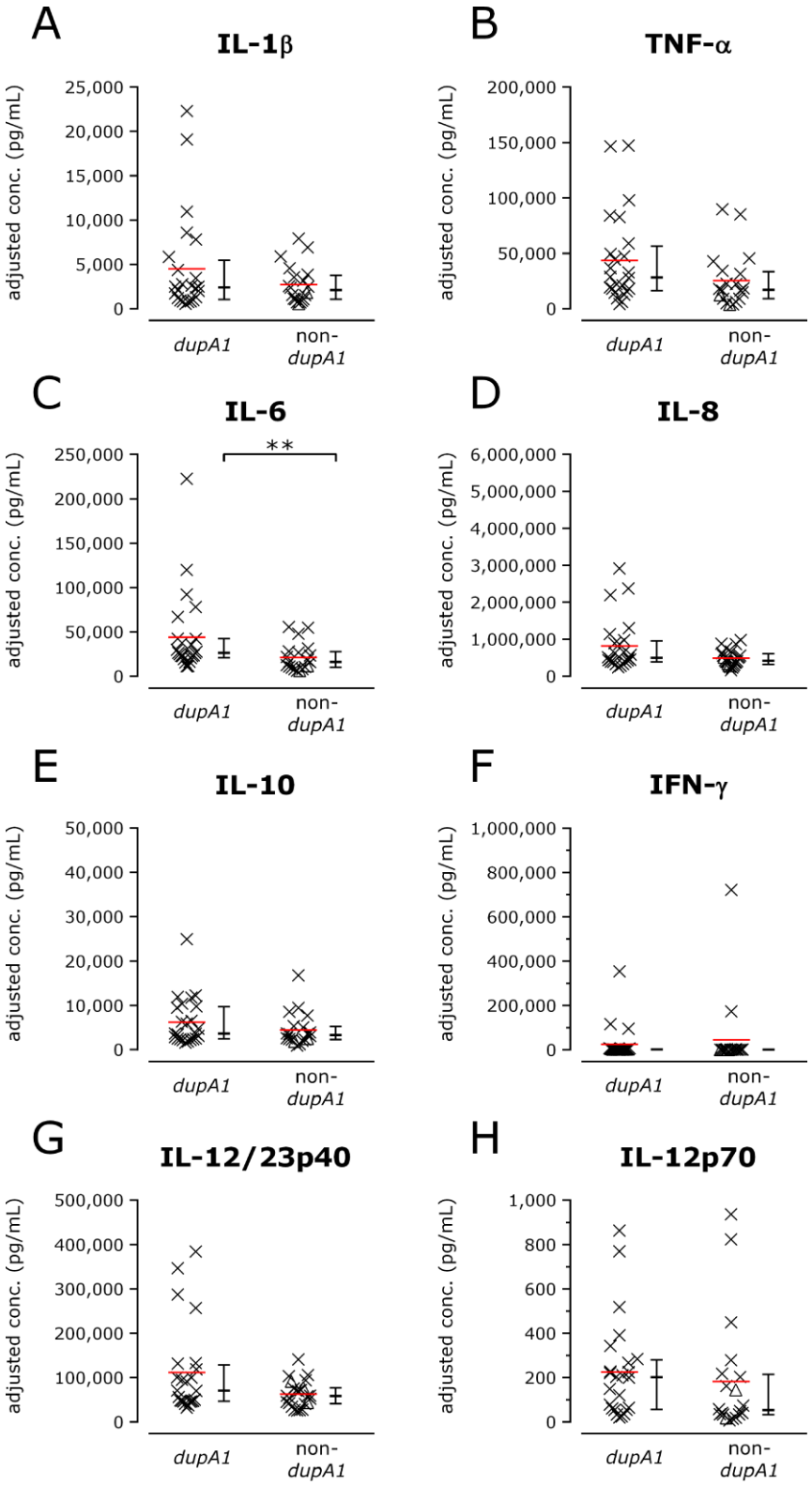

Figure 7.8 – cytokine expression in monocyte co-cultures with clinical strains

7.5.4 Co-culture of mutant strains with CD14$^+$ monocytes – IL-12/23p40 expression by flow cytometry

Results are shown in Figure 7.9. CD14$^+$ monocytes were enriched from 5 donors (F-J) and co-cultured for 16 h, with media only, with lipopolysaccharide (LPS) or sonicated *H. pylori* (lysate), or with sets of wild-type and isogenic mutants of strain AB21.

The percentage of IL-12/23p40$^+$ events (panels A and B) and the fluorescence intensity of IL-12/23p40 (panels C and D) were determined by flow cytometry. We also gated for CD14$^+$ and CD14$^-$ events. Panels A and C show all events gated for relevant cells, and panels B and D show CD14$^+$ events. Data points on the right side of each panel represent the percentage difference from wild-type for each donor/strain combination for Δ*dupA* and Δ*tfs4* mutants.

Flow cytometric analysis of CD14$^+$ monocytes co-cultured with wild-type and mutant bacteria also showed no consistent differences in IL-12/23p40 expression between strains.

The only statistically significant differences after adjustment for multiple comparisons were between media only controls and samples where monocytes were co-cultured with wild-type or Δ*dupA* mutant bacterial strains (asterisked in Figure 7.9).

Overall there were no statistically significant differences between groups for CD14 enriched cell co-culture. No consistent differences were observed between wild-type and Δ*dupA* strains in the percentage of IL-12/23p40$^+$ events or in IL-12/23p40 fluorescence intensity, and again there was considerable variation between donor/strain combinations. These data at first appeared consistently lower for Δ*tfs4* strains compared with wild-type, but when expressed as a percentage difference from wild-type (right side of each panel) this trend was lost.

Figure 7.9 – IL-12/23p40 events and fluorescence intensity by flow cytometry for 16 h co-culture with monocytes

Peripheral blood mononuclear cells (PBMCs) were purified from 5 donors (F-J) using the optimised protocol. Cells expressing CD14 were enriched from these PBMCs by positive (+) selection. Cells were co-cultured with sets of wild-type and isogenic mutants of strain AB21 that had been constructed and stored separately (denoted by O and X) and incubated for 16 h with brefeldin A added after 1 h. There were 10 biological replicates for wild-type and Δ*dupA* strains (O and X) and 4 biological replicates for Δ*tfs4* strains (X only, not studied for donor F). Control cells (denoted by Δ) were co-cultured with media only, lipopolysaccharide (LPS) or sonicated *H. pylori* (lysate). Cells were stained with mouse IgG2a anti-human CD14–FITC and mouse IgG1κ anti-human IL-12/23p40–PE. Unstained, fluorescence minus one and isotype controls were included (data not shown). Fifty-thousand events were acquired with a Beckman Coulter FC500 flow cytometer. Events were gated for relevant cells on forward-scatter/side-scatter plots, and as $CD14^+$ and IL-12/23p40$^+$ on FL1–FITC/FL2–PE plots.

Data points in the upper panels represent the percentage of IL-12/23p40+ events for all gated (panel A) and for $CD14^+$ events (panel B). The horizontal and error bars show overall median values and inter-quartile ranges (IQRs) respectively. Data across all groups were compared by Kruskal-Wallis tests with Dunn's correction for multiple comparisons (* $P < 0.05$, ** $P < 0.01$, *** $P < 0.001$).

Data points in the lower panels represent the mean fluorescence intensity of IL-12/23p40 (arbitrary units) for all gated (panel C) and $CD14^+$ events (panel D). The horizontal and error bars show overall mean values and 95% confidence intervals of the mean respectively. Data for all groups were compared by one-way ANOVAs with Tukey's correction for multiple comparisons (no significant differences).

Data points on the right side of each panel represent the percentage difference from wild-type for each donor/strain combination. The horizontal and error bars show overall median values and inter-quartile ranges (IQRs) respectively. Data for each group were separately compared against a median of 100% (dotted red line) by Wilcoxon signed-rank tests (no significant differences).

Over 90% of IL-12/23p40$^+$ events were $CD14^+$ (median [IQR, n], 92.7% [90.3-99.1, 39]). IL-12/23p40 mean fluorescence for $CD14^-$ events was similar across all samples (mean ± standard deviation [n], 42.7 ± 15.4 arbitrary units [39]). Overall, less than 1% of $CD14^-$ events were IL-12/23p40$^+$ (median [IQR, n], 0.7% [0.2-3.3, 39]).

Note that for clarity one data point is not shown but is included in summary statistics and analysis – donor I for panel A: percentage difference of Δ*dupA* X from wild-type (244%).

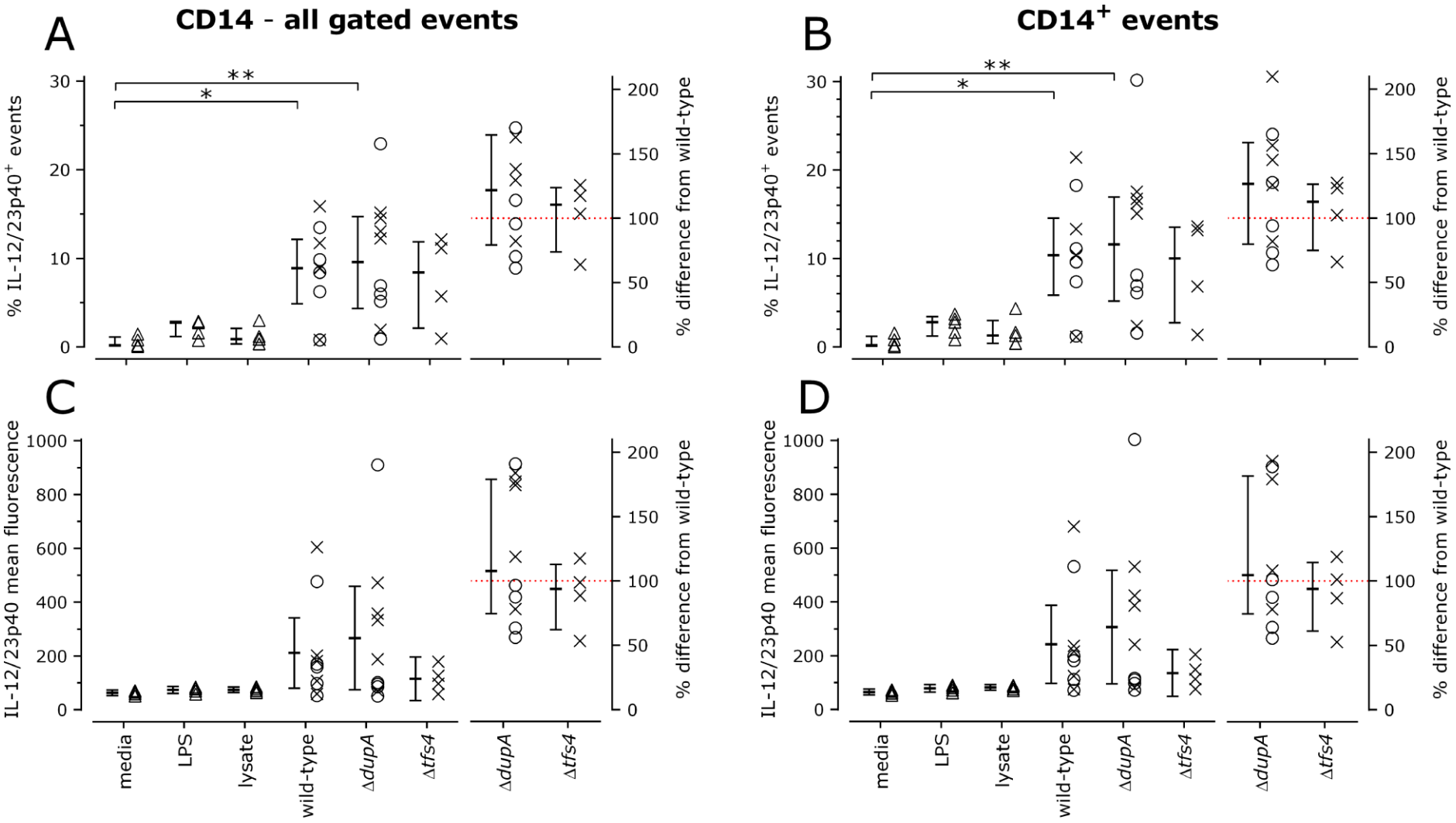

Figure 7.9 – IL-12/23p40 events and fluorescence intensity by flow cytometry for 16 h co-culture with monocytes

7.5.5 Co-culture of treated bacteria with PBMCs

7.5.5.1 Heat-inactivation (HI)

Results for PBMCs are shown in Appendix Figure 7.10.

Median expression was variably reduced between different cell types for some cytokines (IL-10 and IL-12/23p40, IFN-γ and IL-12p70) but was relatively preserved for IL-6 and IL-17A.

Relative expression for HI strains vs. untreated strains for IL-10 was 24.9% (15.3-47.2%) and IL-12/23p40 was 10.7% (4.5-17.2%), which were both higher from PBMCs than from $CD14^+$ cells, and for IL-12p70 was 3.3% (1.9-10.3%) and IFN-γ was 0.6% (0.5-2.3%), which were both lower from PBMCs than from $CD14^+$ cells. Relative expression was less than 4 percent and similar between cell types IL-1β, TNF-α and IL-8. For IL-6, median cytokine expression was less markedly reduced by heat inactivation (35.8% [24.4-45.3%]). Median IL-17A expression in PBMC co-culture was 47.9% (17.4-91.9%) for HI strains relative to untreated strains. However, absolute concentrations were low from both HI strains and untreated strains (53.4 pg/mL [range, 5.9-139.7 pg/mL] and 82.3 pg/mL [5.1-336.9 pg/mL] respectively) so relative expression is less meaningful.

7.5.5.2 Paraformaldehyde (PFA) treatment

Results for PBMCs are shown in Appendix Figure 7.10.

Wilcoxon signed-rank tests were not used given that only the minority of conditions had sufficient data to be able to demonstrate statistical significance.

First, Kruskal-Wallis tests were used across all 5 PFA-treated strain types for each analyte. These provided evidence to reject the null hypothesis that strain groups in PBMC co-culture were sampled from populations with identical distributions for TNF-α, IL-8 and IL-10 ($P = 0.016$, $P = 0.041$ and $P = 0.025$ respectively; Chi-square values and mean ranks are not shown) but not for other analytes ($P > 0.05$). Post-test Dunn's correction was then used when applicable for 6 planned comparisons (each PFA-treated mutant vs. PFA-treated wild-type, PFA-treated Δ*dupA* vs. PFA-treated Δ*virB2*, PFA-treated Δ*virB9* vs. PFA-treated Δ*dupA*). Significant results after correction are shown above the plotted data in Figure 7.10 (see legend).

Second, to assess the impact of PFA treatment on the expression of different cytokines for each mutant strain, treated and untreated mutant strains were compared referenced against the equivalent treated and untreated wild-types. Kruskal-Wallis tests were used across 4 PFA-treated mutant and 4 untreated mutant datasets for each analyte. These provided evidence to reject the null hypothesis that strain groups were sampled from populations with identical distributions for all analytes ($P = 0.020$ for IL-10, $P = 0.037$ for IL-17A, $P \leq 0.010$ for all other analytes; Chi-square values, mean ranks and individual P values are not shown). Post-test Dunn's correction was then used for 4 planned data pairs (PFA-treated mutant strain as percentage of PFA-treated wild-type vs. untreated mutant strain as percentage of untreated wild-type). Significant results are indicated by asterisks below the plotted data in Figure 7.10.

IL-17A expression by PBMCs was increased in co-culture with PFA-treated *tfs4* null mutant relative to untreated AB21Δ*tfs4*. However, this was limited to one analysis and IL-17A was expressed at very low concentrations.

Relative IL-17A expression was also increased for PFA-treated AB21Δ*tfs4* in PBMC co-culture only ($P < 0.05$, 41.4% [36.3-118.4%] vs. 141.9% [110.2-165.3%]). However, median IL-17A expression by PBMCs across all PFA-treated strains was only 106.0 pg/mL (range, 34.1-278.0 pg/mL). In contrast, median IL-12/23p40 expression was 2-3 orders of magnitude greater at 71.9 ng/mL (24.0-98.2 ng/mL) and median IL-10 expression was 3-4 times higher at 361.7 pg/mL (167.7-870.1 pg/mL).

The results for IL-12/23p40 and IL-10 for PFA-treated strains in PBMC co-culture are reported together with those results from $CD14^+$ cell coculture in Section 5.6.2.

Figure 7.10 – cytokine concentrations from PBMCs co-cultured with heat inactivated and paraformaldehyde-treated bacteria, relative to live untreated bacteria

Peripheral blood mononuclear cells (PBMCs) were purified from up to 6 donors (E-J). Cells were co-cultured with wild-type and isogenic mutants of strain AB21 (denoted by X). Strains were untreated, heat inactivated (HI) or treated with paraformaldehyde (PFA). Cytokine/chemokine concentrations in 48 h co-culture supernatants were measured for 9 analytes using Meso Scale Discovery V-PLEX assays in at least duplicate (panels A to I).

Data points show each treated strain as a percentage of the equivalent untreated strain for each donor/treatment/strain combination (HI wild-type and Δ*tfs4* n=6, PFA treated wild-type and Δ*tfs4* n=5, all others n=4; every data point is plotted but note different Y-axis scales for panels D: IL-8 and I: IL-17A). The horizontal and error bars show overall median values and inter-quartile ranges respectively.

Data for HI strains were not analysed using inferential statistics.

Analysis of PFA-treated strains followed two separate approaches, rather than the previous two step approach. Note that Wilcoxon signed-rank tests were not used.

First, in order to assess for differences between treated strains, data across all PFA-treated groups for each analyte were compared by Kruskal-Wallis tests with Dunn's correction for multiple comparisons with 6 planned data pairs (each PFA-treated mutant vs. PFA-treated wild-type, PFA-treated Δ*dupA* vs. PFA-treated Δ*virB2,* PFA-treated Δ*virB9* vs. PFA-treated Δ*dupA*). Statistically significant differences after these corrections are shown above the plotted data (**P* < 0.05, ** *P* < 0.01, *** *P* < 0.001).

Second, to assess the impact of PFA treatment on the expression of different cytokines for each mutant strain, it was necessary to compare treated and untreated mutant strains referenced against the equivalent treated and untreated wild-types. Across these 8 datasets per analyte/cell type, Kruskal-Wallis tests and Dunn's correction for multiple comparisons were used with 4 planned data pairs (PFA-treated mutant strain as percentage of PFA-treated wild-type vs. untreated mutant strain as percentage of untreated wild-type). Statistically significant differences after these corrections are shown below the plotted data (*/*P* value combinations as before).

PFA-treated strain Δ*virB9* is highlighted in bold as there were statistically significant differences in multiple analyses.

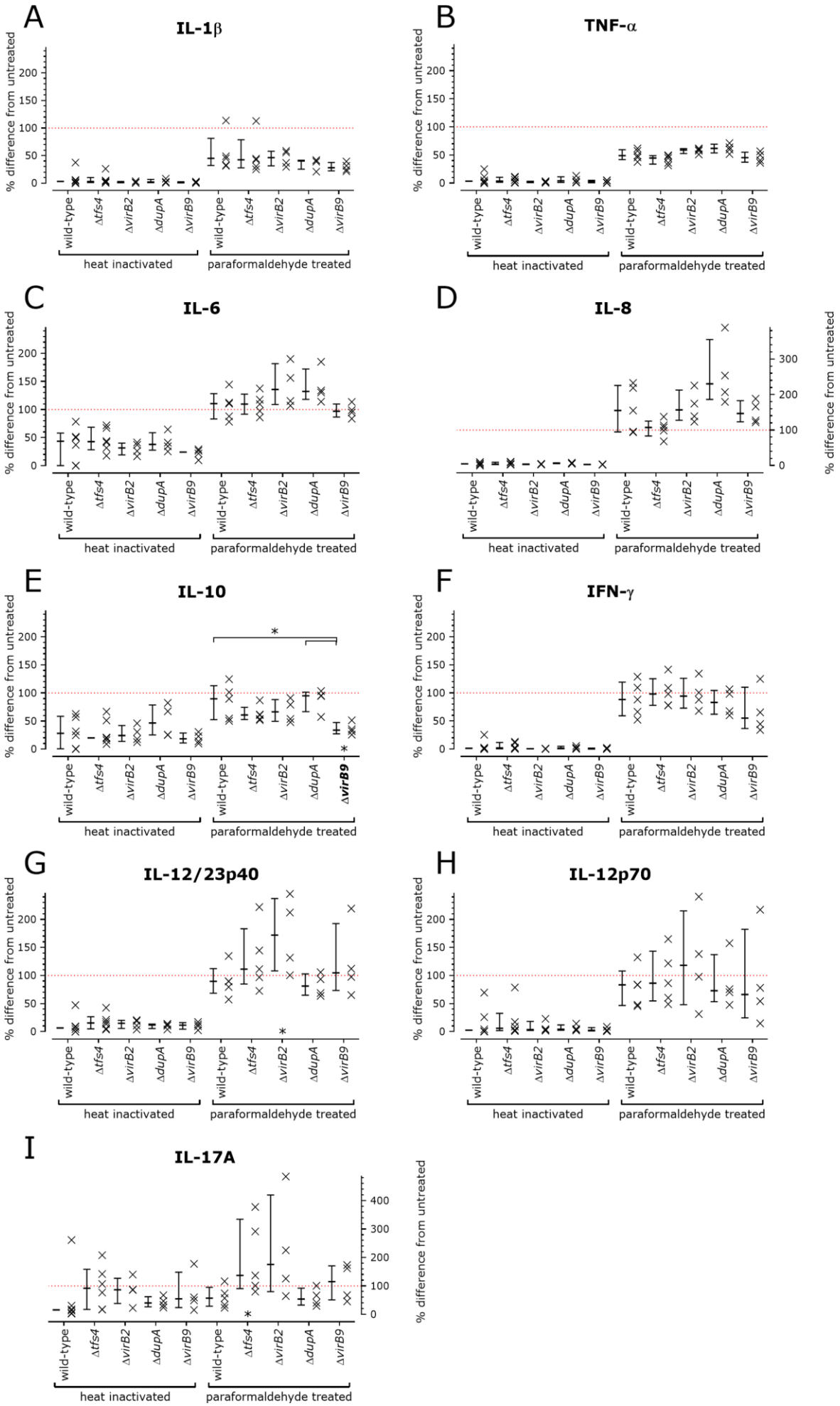

Figure 7.10 – cytokine concentrations from PBMCs co-cultured with heat inactivated and paraformaldehyde-treated bacteria, relative to live untreated bacteria

8 References

Abadi, A.T.B., Loffeld, R.J.L.F., Constancia, A.C., … Kusters, J.G. (2014). Detection of the *Helicobacter pylori dupA* gene is strongly affected by the PCR design. *Journal of Microbiological Methods*, **106**:55–66.

Abadi, A.T.B., Taghvaei, T., Wolfram, L. and Kusters, J.G. (2012). Infection with *Helicobacter pylori* strains lacking *dupA* is associated with an increased risk of gastric ulcer and gastric cancer development. *Journal of Medical Microbiology*, **61**(1):23–30.

Abuzakouk, M., Feighery, C. and O'Farrelly, C. (1996). Collagenase and dispase enzymes disrupt lymphocyte surface molecules. *Journal of Immunological Methods*, **194**(2):211–216.

Akashi-Takamura, S. and Miyake, K. (2008). TLR accessory molecules. *Current Opinion in Immunology*, **20**(4):420–425.

Akopyants, N.S., Clifton, S.W., Kersulyte, D., … Berg, D.E. (1998). Analyses of the *cag* pathogenicity island of *Helicobacter pylori*. *Molecular Microbiology*, **28**(1):37–53.

Alam, J., Ghosh, P., Ganguly, M., … Mukhopadhyay, A.K. (2015). Association of Intact *dupA* (*dupA1*) rather than *dupA1* cluster with duodenal ulcer in Indian population. *Gut Pathogens*, **7**(1):9.

Alam, J., Maiti, S., Ghosh, P., … Mukhopadhyay, A.K. (2012). Significant association of the *dupA* gene of *Helicobacter pylori* with duodenal ulcer development in a South-east Indian population. *Journal of Medical Microbiology*, **61**(PART 9):1295–1302.

Algood, H.M.S. and Cover, T.L. (2006). *Helicobacter pylori* persistence: an overview of interactions between *H. pylori* and host immune defenses. *Clinical Microbiology Reviews*, **19**(4):597–613.

Alm, R., Ling, L., Moir, D., … Trust, T. (1999). Genomic-sequence comparison of two unrelated isolates of the human gastric pathogen *Helicobacter pylori*. *Nature*, **397**(6715):176–180.

de Almeida, M.C., Silva, A.C., Barral, A. and Barral Netto, M. (2000). A simple method for human peripheral blood monocyte isolation. *Memorias do Instituto Oswaldo Cruz*, **95**(2):221–223.

de Almeida, S.F., Carvalho, I.F., Cardoso, C.S., … de Sousa, M. (2005). Hfe cross-talks with the MHC class I antigen presentation pathway. *Blood*, **106**(3):971–7.

de Almeida, S.F. and de Sousa, M. (2008). The unfolded protein response in hereditary haemochromatosis. *Journal of Cellular and Molecular Medicine*, **12**(2):421–34.

Amedei, A., Cappon, A., Codolo, G., … De Bernard, M. (2006). The neutrophil-activating protein of *Helicobacter pylori* promotes Th1 immune responses. *Journal of Clinical Investigation*, **116**(4):1092–1101.

Amieva, M.R. and El-Omar, E.M. (2008). Host-bacterial interactions in *Helicobacter pylori* infection. *Gastroenterology*, **134**(1):306–323.

Arachchi, H.S.J., Kalra, V., Lal, B., … Ahuja, V. (2007). Prevalence of duodenal ulcer-promoting gene (*dupA*) of *Helicobacter pylori* in patients with duodenal ulcer in North Indian population. *Helicobacter*, **12**(6):591–597.

Argent, R.H., Burette, A., Deyi, V.Y.M. and Atherton, J.C. (2007). The presence of *dupA* in *Helicobacter pylori* is not significantly associated with duodenal ulceration in Belgium, South Africa, China, or North America. *Clinical Infectious Diseases*, **45**(9):1204–1206.

Argent, R.H., Thomas, R.J., Aviles-Jimenez, F., … Atherton, J.C. (2008). Toxigenic *Helicobacter pylori* infection precedes gastric hypochlorhydria in cancer relatives, and *H . pylori* virulence evolves in these families. *Clinical Cancer Research*, **14**(7):2227–2235.

Ashrafian, H. (2003). Hepcidin: the missing link between hemochromatosis and infections. *Infection and Immunity*, **71**(12):6693–700.

Atherton, J.C. (2006). The pathogenesis of *Helicobacter pylori*-induced gastro-duodenal diseases. *Annual Review of Pathology: Mechanisms of Disease*, **1**(1):63–96.

Atherton, J.C. and Blaser, M.J. (2009). Coadaptation of *Helicobacter pylori* and humans: ancient history, modern implications. *Journal of Clinical Investigation*, **119**(9):2475–2487.

Atherton, J.C., Cao, P., Peek Jr., R.M., … Cover, T.L. (1995). Mosaicism in vacuolating cytotoxin alleles of *Helicobacter pylori*. Association of specific *vacA* types with cytotoxin production and peptic ulceration. *The Journal of Biological Chemistry*, **270**(30):17771–17777.

Autengruber, A., Gereke, M., Hansen, G., … Bruder, D. (2012). Impact of enzymatic tissue disintegration on the level of surface molecule expression and immune cell function. *European Journal of Microbiology and Immunology*, **2**(2):112–120.

Backert, S. and Selbach, M. (2008). Role of type IV secretion in *Helicobacter pylori* pathogenesis. *Cellular Microbiology*, **10**(8):1573–1581.

Bain, C.C. and Mowat, A.M.I. (2014). The monocyte-macrophage axis in the intestine. *Cellular Immunology*, **291**(1–2):41–48.

Barker, B.R., Taxman, D.J. and Ting, J.P.Y. (2011). Cross-regulation between the IL-1β/IL-18 processing inflammasome and other inflammatory cytokines. *Current Opinion in Immunology*, **23**(5):591–597.

Basso, D., Zambon, C.F.F., Letley, D.P., … Atherton, J.C. (2008). Clinical relevance of *Helicobacter pylori cagA* and *vacA* gene polymorphisms. *Gastroenterology*, **135**(1):91–99.

Beadling, C. and Slifka, M.K. (2006). Regulation of innate and adaptive immune responses by the related cytokines IL-12, IL-23, and IL-27. *Archivum Immunologiae et Therapiae Experimentalis*, **54**(1):15–24.

Bebb, J.R., Letley, D.P., Thomas, R.J., … Atherton, J.C. (2003). *Helicobacter pylori* upregulates matrilysin (MMP-7) in epithelial cells *in vivo* and *in vitro* in a Cag dependent manner. *Gut*, **52**(10):1408–13.

Beliakova-Bethell, N., Massanella, M., White, C., … Woelk, C.H. (2014). The effect of cell subset isolation method on gene expression in leukocytes. *Cytometry Part A*, **85**(1):94–104.

Ben-Arieh, S. V, Zimerman, B., Smorodinsky, N.I., … Ehrlich, R. (2001). Human cytomegalovirus protein US2 interferes with the expression of human *HFE*, a nonclassical class I major histocompatibility complex molecule that regulates iron homeostasis. *Journal of Virology*, **75**(21):10557–62.

Betten, A.̊, Bylund, J., Cristophe, T., … Dahlgren, C. (2001). A proinflammatory peptide from *Helicobacter pylori* activates monocytes to induce lymphocyte dysfunction and apoptosis. *Journal of Clinical Investigation*, **108**(8):1221–1228.

Bhattacharyya, A., Pathak, S., Datta, S., … Kundu, M. (2002). Mitogen-activated protein kinases and nuclear factor-kappaB regulate *Helicobacter pylori*-mediated interleukin-8 release from macrophages. *The Biochemical Journal*, **368**(Pt 1):121–9.

Bimczok, D., Clements, R.H., Waites, K.B., … Smythies, L.E. (2010). Human primary gastric dendritic cells induce a Th1 response to *H. pylori*. *Mucosal Immunology*, **3**(3):260–9.

Bimczok, D., Grams, J.M., Stahl, R.D., … Smith, P.D. (2011). Stromal regulation of human gastric dendritic cells restricts the Th1 response to *Helicobacter pylori*. *Gastroenterology*, **141**(3):929–938.

Blaser, M.J., Chen, Y. and Reibmann, J. (2008). Does *Helicobacter pylori* protect against asthma and allergy? *Gut*, **57**(8):1178–1179; author reply 1179.

Bliss, C.M., Golenbock, D.T., Keates, S., … Kelly, C.P. (1998). *Helicobacter priori* lipopolysaccharide binds to CD14 and stimulates release of interleukin-8, epithelial neutrophil-activating peptide 78, and monocyte chemotactic protein 1 by human monocytes. *Infection and Immunity*, **66**(11):5357–5363.

Bokhoven, M.A., Deursen, C.T.B.M. and Swinkels, D.W. (2011). Diagnosis and management of hereditary haemochromatosis. *British Medical Journal*, **342**(2):c7251–c7251.

Booth, J.S., Toapanta, F.R., Salerno-Goncalves, R., … Sztein, M.B. (2014). Characterization and functional properties of gastric tissue-resident memory T cells from children, adults, and the elderly. *Frontiers in Immunology*, **5**:294.

Borlace, G.N., Butler, R.N. and Brooks, D.A. (2008). Monocyte and macrophage killing of *Helicobacter pylori*: relationship to bacterial virulence factors. *Helicobacter*, **13**(5):380–387.

Bossuyt, P.M., Reitsma, J.B., Bruns, D.E., … Lijmer, J.G. (2003). The STARD statement for reporting studies of diagnostic accuracy: explanation and elaboration. *Clinical Chemistry*, **49**(1):7–18.

Bowcutt, R., Malter, L.B., Chen, L.A., … Loke, P. (2015). Isolation and cytokine analysis of lamina propria lymphocytes from mucosal biopsies of the human colon. *Journal of Immunological Methods*, **421**:27–35.

Brandtzaeg, P., Kiyono, H., Pabst, R. and Russell, M.W. (2008). Terminology: nomenclature of mucosa-associated lymphoid tissue. *Mucosal Immunology*, **1**(1):31–37.

Bridle, K.R., Frazer, D.M., Wilkins, S.J., … Ramm, G.A. (2003). Disrupted hepcidin regulation in *HFE*-associated haemochromatosis and the liver as a regulator of body iron homoeostasis. *Lancet*, **361**(9358):669–73.

Bustin, S.A., Benes, V., Garson, J.A., … Wittwer, C.T. (2009). The MIQE guidelines: minimum information for publication of quantitative real-time PCR experiments. *Clinical Chemistry*, **55**(4):611–622.

Camargo, M.C., Mera, R., Correa, P., … Schneider, B.G. (2006). Interleukin-1β and Interleukin-1 receptor antagonist gene polymorphisms and gastric cancer: a meta-analysis. *Cancer Epidemiology Biomarkers & Prevention*, **15**(9):1674–1687.

Cancer Research UK (2014). Cancer Stats - Stomach Cancer. Available at: http://www.cancerresearchuk.org/health-professional/cancer-statistics/statistics-by-cancer-type/stomach-cancer/ [Accessed December 31, 2014].

Capelle, L.G., Vries, A.C. De, Haringsma, J. and Borg, F. Ter (2010). The staging of gastritis with the OLGA system by using intestinal metaplasia as an accurate alternative for atrophic gastritis. *Gastrointestinal Endoscopy*, **71**(7):1150–1158.

Cascales, E. (2004). Definition of a bacterial type IV secretion pathway for a DNA substrate. *Science*, **304**(5674):1170–1173.

Castaño-Rodríguez, N., Kaakoush, N.O. and Mitchell, H.M. (2014). Pattern-recognition receptors and gastric cancer. *Frontiers in Immunology*, **5**(JUL):336.

Centre Physiopathologie de Toulouse-Purpan INSERM UMR 1043 France (2015). PBMC isolation from buffy coats or whole blood (version 2015 03 05). Available at: http://www.cptp.inserm.fr/the-cptp-human-immune-monitoring-platform-578092.kjsp [Accessed August 1, 2015].

Chakrabarty, S., Snyder, J.T., Shen, J., … Ragheb, J.A. (2011). Human CD14hi monocytes and myeloid dendritic cells provide a cell contact–dependent costimulatory signal for early CD40 ligand expression. *Blood*, **117**(5):1585–1594.

Chanput, W., Mes, J.J. and Wichers, H.J. (2014). THP-1 cell line: an *in vitro* cell model for immune modulation approach. *International Immunopharmacology*, **23**(1):37–45.

Cho, Y.S., Chae, H.S., Jang, S.N., … Chang, E.D. (2008). Comparison of the 13C-urea breath test and the endoscopic phenol red mucosal pH test in the quantification of *Helicobacter pylori* infection loading. *The Korean Journal of Internal Medicine*, **23**(3):134–139.

Christenson, R.H. (2007). Evidence-based laboratory medicine - a guide for critical evaluation of *in vitro* laboratory testing. *Annals of Clinical Biochemistry*, **44**(Pt 2):111–30.

Christie, P.J., Whitaker, N. and González-Rivera, C. (2014). Mechanism and structure of the bacterial type IV secretion systems. *Biochimica et Biophysica Acta*, **1843**(8):1578–1591.

Cipriani, G., Gibbons, S.J., Kashyap, P.C. and Farrugia, G. (2016). Intrinsic gastrointestinal macrophages: their phenotype and role in gastrointestinal motility. *Cellular and Molecular Gastroenterology and Hepatology*, **2**(2):120–130.e1.

Cooper, M.A., Fehniger, T.A., Ponnappan, A., … Caligiuri, M.A. (2001). Interleukin-1beta costimulates interferon-gamma production by human natural killer cells. *European Journal of Immunology*, **31**(3):792–801.

Correa, P. (1992). Human gastric carcinogenesis: a multistep and multifactorial process. *Cancer Research*, **52**(24):6735–6740.

Cover, T.L. and Blanke, S.R. (2005). *Helicobacter pylori* VacA, a paradigm for toxin multifunctionality. *Nature Reviews Microbiology*, **3**(4):320–332.

Crabtree, J.E. (1996). Gastric mucosal inflammatory responses to *Helicobacter pylori*. *Alimentary Pharmacology and Therapeutics*, **10**(s1):29–37.

Cros, J., Cagnard, N., Woollard, K., … Geissmann, F. (2010). Human CD14dim monocytes patrol and sense nucleic acids and viruses via TLR7 and TLR8 receptors. *Immunity*, **33**(3):375–86.

Cunliffe, J., Derbyshire, N., Keeler, S. and Coldwell, R. (2009). An approach to the validation of flow cytometry methods. *Pharmaceutical Research*, **26**(12):2551–7.

D'Elios, M.M., Amedei, A., Benagiano, M., … Del Prete, G. (2005). *Helicobacter pylori*, T cells and cytokines: the "dangerous liaisons." In *FEMS Immunology and Medical Microbiology*. pp. 113–119.

D'Elios, M.M., Manghetti, M., De Carli, M., … Del Prete, G. (1997). T helper 1 effector cells specific for *Helicobacter pylori* in the gastric antrum of patients with peptic ulcer disease. *J. Immunol.*, **158**(2):962.

Dailidiene, D., Dailide, G., Kersulyte, D. and Berg, D.E. (2006). Contraselectable streptomycin susceptibility determinant for genetic manipulation and analysis of *Helicobacter pylori*. *Applied and Environmental Microbiology*, **72**(9):5908–5914.

van Damme, N., Baeten, D., De Vos, M., … De Keyser, F. (2000). Chemical agents and enzymes used for the extraction of gut lymphocytes influence flow cytometric detection of T cell surface markers. *Journal of Immunological Methods*, **236**(1–2):27–35.

Datta De, D. and Roychoudhury, S. (2015). To be or not to be: the host genetic factor and beyond in *Helicobacter pylori* mediated gastro-duodenal diseases. *World Journal of Gastroenterology*, **21**(10):2883–2895.

Derveaux, S., Vandesompele, J. and Hellemans, J. (2010). How to do successful gene expression analysis using real-time PCR. *Methods*, **50**(4):227–230.

Dinarello, C.A. (2009). Immunological and inflammatory functions of the interleukin-1 family. *Annual Review of Immunology*, **27**(1):519–50.

Dixon, M.F., Genta, R.M., Yardley, J.H. and Correa, P. (1996). Classification and grading of gastritis: the updated Sydney system. *The American Journal of Surgical Pathology*, **20**(10):1161–1181.

Douraghi, M., Mohammadi, M., Oghalaie, A., … Mohajerani, N. (2008). *dupA* as a risk determinant in *Helicobacter pylori* infection. *Journal of Medical Microbiology*, **57**(5):554–562.

Du, X., Tang, Y., Xu, H., … Sharp, F.R. (2006). Genomic profiles for human peripheral blood T cells, B cells, natural killer cells, monocytes, and polymorphonuclear cells: comparisons to ischemic stroke, migraine, and Tourette syndrome. *Genomics*, **87**(6):693–703.

Du, Y., Agnew, A., Ye, X.P., … Crabtree, J.E. (2006). *Helicobacter pylori* and *Schistosoma japonicum* co-infection in a Chinese population: helminth infection alters humoral responses to *H. pylori* and serum pepsinogen I/II ratio. *Microbes and Infection*, **8**(1):52–60.

Dubois, A. and Borén, T. (2007). *Helicobacter pylori* is invasive and it may be a facultative intracellular organism. *Cellular Microbiology*, **9**(5):1108–1116.

Duchmann, R., Scherer, H., Neurath, M., … ZumBuschenfelde, K.H.M. (1997). Normal interleukin-12 production in individuals with antibodies to *Helicobacter pylori*. *Acta Pathologica Microbiologica et Immunologica Scandinavica*, **105**(11):824–830.

Durand, M. and Segura, E. (2015). The known unknowns of the human dendritic cell network. *Frontiers in Immunology*, **6**(MAR):129.

El-Omar, E.M. (2001). The importance of Interleukin 1beta in *Helicobacter pylori* associated disease. *Gut*, **48**(6):743–747.

El-Omar, E.M., Carrington, M., Chow, W.H., … Rabkin, C.S. (2000). Interleukin-1 polymorphisms associated with increased risk of gastric cancer. *Nature*, **404**(6776):398–402.

El-Omar, E.M., Penman, I.D., Ardill, J.E., … McColl, K.E.L. (1995). *Helicobacter pylori* infection and abnormalities of acid secretion in patients with duodenal ulcer disease. *Gastroenterology*, **109**(3):681–691.

von Elm, E., Altman, D.G., Egger, M., … Vandenbroucke, J.P. (2008). The Strengthening the Reporting of Observational Studies in Epidemiology (STROBE) statement: guidelines for reporting observational studies. *Journal of Clinical Epidemiology*, **61**(4):344–349.

Enroth, H. and Engstrand, L. (1995). Immunomagnetic separation and PCR for detection of *Helicobacter pylori* in water and stool specimens. *Journal of Clinical Microbiology*, **33**(8):2162–2165.

Ernst, P.B. and Gold, B.D. (2000). The disease spectrum of *Helicobacter pylori*: the immunopathogenesis of gastroduodenal ulcer and gastric cancer. *Annual Review of Microbiology*, **54**(1):615–640.

Ethuin, F., Delarche, C., Benslama, S., … Chollet-Martin, S. (2001). Interleukin-12 increases Interleukin-8 production and release by human polymorphonuclear neutrophils. *Journal of Leukocyte Biology*, **70**(3):439–446.

Faber, K. (1927). Srhorstein Lecture - on chronic gastritis: its relation to achylia and ulcer. *Lancet*, **210**(5435):901–907.

Fan, X.J., Chua, A., O'Connell, M.A., … Keeling, P.W.N. (1993). Interferon-gamma and tumour necrosis factor production in patients with *Helicobacter pylori* infection. *Irish Journal of Medical Science*, **162**(10):408–411.

Feder, J.N., Gnirke, A., Thomas, W., … Wolff, R.K. (1996). A novel MHC class I-like gene is mutated in patients with hereditary haemochromatosis. *Nature Genetics*, **13**(4):399–408.

Fehlings, M., Drobbe, L., Moos, V., … Ignatius, R. (2012). Comparative analysis of the interaction of *Helicobacter pylori* with human dendritic cells, macrophages, and monocytes. *Infection and Immunity*, **80**(8):2724–2734.

Fernandez-Gonzalez, E. and Backert, S. (2014). DNA transfer in the gastric pathogen *Helicobacter pylori*. *Journal of Gastroenterology*, **49**(4):594–604.

Ferraz, M.A., Zabaglia, L.M., Pereira, W.N., … Rasmussen, L.T. (2016). Downregulated expression of E-cadherin and TP53 in patients with gastric diseases: the involvement of *H. pylori* infection and its virulence markers. *Journal of Gastrointestinal Cancer*, **47**(1):20–26.

Figdor, C.G., Bont, W.S., Touw, I., … de Vries, J.E. (1982). Isolation of functionally different human monocytes by counterflow centrifugation elutriation. *Blood*, **60**(1):46–53.

Fiorentino, M., Ding, H., Blanchard, T.G., … Fasanoa, A. (2013). *Helicobacter pylori*-induced disruption of monolayer permeability and proinflammatory cytokine secretion in polarized human gastric epithelial cells. *Infection and Immunity*, **81**(3):876–883.

Fischer, W., Breithaupt, U., Kern, B., … Haas, R. (2014). A comprehensive analysis of *Helicobacter pylori* plasticity zones reveals that they are integrating conjugative elements with intermediate integration specificity. *BMC Genomics*, **15**(1):310.

Fischer, W., Püls, J., Buhrdorf, R., … Haas, R. (2001). Systematic mutagenesis of the *Helicobacter pylori cag* pathogenicity island: essential genes for CagA translocation in host cells and induction of interleukin-8. *Molecular Microbiology*, **42**(5):1337–1348.

Fischer, W., Windhager, L., Rohrer, S., … Haas, R. (2010). Strain-specific genes of *Helicobacter pylori*: genome evolution driven by a novel type IV secretion system and genomic island transfer. *Nucleic Acids Research*, **38**(18):6089–6101.

Ford, A.C., Delaney, B.C., Forman, D. and Moayyedi, P. (2011). Eradication therapy for peptic ulcer disease in *Helicobacter pylori* positive patients. *Cochrane Database of Systematic Reviews*, **1**(2):CD003840.

Ford, A.L., Foulcher, E., Goodsall, A.L. and Sedgwick, J.D. (1996). Tissue digestion with dispase substantially reduces lymphocyte and macrophage cell-surface antigen expression. *Journal of Immunological Methods*, **194**(1):71–75.

Fox, J.G., Beck, P., Dangler, C.A., … Nagler-Anderson, C. (2000). Concurrent enteric helminth infection modulates inflammation and gastric immune responses and reduces *Helicobacter*-induced gastric atrophy. *Nature Medicine*, **6**(5):536–542.

Freundlich, B. and Avdalovic, N. (1983). Use of gelatin/plasma coated flasks for isolating human peripheral blood monocytes. *Journal of Immunological Methods*, **62**(1):31–37.

Fronzes, R., Christie, P.J. and Waksman, G. (2009). The structural biology of type IV secretion systems. *Nature Reviews Microbiology*, **7**(10):703–714.

Fuccio, L., Zagari, R., Eusebi, L., … Bazzoli, F. (2009). Meta-analysis: can *Helicobacter pylori* eradication treatment reduce the risk for gastric cancer? *Annals of Internal Medicine*, **151**(2):121–128.

Geissmann, F., Gordon, S., Hume, D.A., … Randolph, G.J. (2010). Unravelling mononuclear phagocyte heterogeneity. *Nature Reviews Immunology*, **10**(6):453–460.

Geraghty, R.J., Capes-Davis, A., Davis, J.M., … Vias, M. (2014). Guidelines for the use of cell lines in biomedical research. *British Journal of Cancer*, **111**(6):1021–1046.

Ghalehnoei, H., Ahmadzadeh, A. and Farzi, N. (2016). Relationship between *ureB* sequence diversity, urease activity and genotypic variations of different *Helicobacter pylori* strains in patients with gastric disorders. *Polish Journal of Microbiology*, **65**(2):153–159.

Ghosh, T., Lewis, D.I., Axon, A.T.R. and Everett, S.M. (2011). Review article: methods of measuring gastric acid secretion. *Alimentary Pharmacology and Therapeutics*, **33**(7):768–781.

Ghoshal, U.C. and Chourasia, D. (2010). Gastroesophageal reflux disease and *Helicobacter pylori*: what may be the relationship? *Journal of Neurogastroenterology and Motility*, **16**(3):243–50.

Giefing-Kröll, C., Berger, P., Lepperdinger, G. and Grubeck-Loebenstein, B. (2015). How sex and age affect immune responses, susceptibility to infections, and response to vaccination. *Aging Cell*, **14**(3):309–21.

Gieseler, S., König, B., König, W. and Backert, S. (2005). Strain-specific expression profiles of virulence genes in *Helicobacter pylori* during infection of gastric epithelial cells and granulocytes. *Microbes and Infection*, **7**(3):437–447.

Gmelig-Meyling, F. and Waldmann, T.A. (1980). Separation of human blood monocytes and lymphocytes on a continuous percoll gradient. *Journal of Immunological Methods*, **33**(1):1–9.

Gomes, L.I., Rocha, G.A., Rocha, A.M.C., … Queiroz, D.M.M. (2008). Lack of association between *Helicobacter pylori* infection with *dupA*-positive strains and gastroduodenal diseases in Brazilian patients. *International Journal of Medical Microbiology*, **298**(3–4):223–230.

Gomez Perdiguero, E., Klapproth, K., Schulz, C., … Rodewald, H.R. (2014). Tissue-resident macrophages originate from yolk-sac-derived erythro-myeloid progenitors. *Nature*, **518**(7540):547–551.

Grage-Griebenow, E., Flad, H.D. and Ernst, M. (2001). Heterogeneity of human peripheral blood monocyte subsets. *Journal of Leukocyte Biology*, **69**(1):11–20.

Graham, D.Y., Opekun, A.R., Osato, M.S., … Monath, T.P. (2004). Challenge model for *Helicobacter pylori* infection in human volunteers. *Gut*, **53**(9):1235–43.

Graham, D.Y. and Yamaoka, Y. (2000). Disease-specific *Helicobacter pylori* virulence factors: the unfulfilled promise. *Helicobacter*, **5 Suppl 1**:S3-9-31.

Griffiths, A.E. and Walker, M.M. (1997). *Helicobacter pylori* and its role in peptic ulcer disease. *Nutrition and Food Science*, **97**(4):141–145.

Grimm, M., Pullman, W., Bennett, G., … Doe, W. (1995). Direct evidence of monocyte recruitment to inflammatory bowel disease mucosa. *Journal of Gastroenterology and Hepatology*, **10**(4):387–395.

Grove, J.I., Alandiyjany, M.N. and Delahay, R.M. (2013). Site-specific relaxase activity of a VirD2-like protein encoded within the *tfs4* genomic island of *Helicobacter pylori*. *Journal of Biological Chemistry*, **288**(37):26385–26396.

Guillemin, K., Salama, N.R., Tompkins, L.S. and Falkow, S. (2002). Cag pathogenicity island-specific responses of gastric epithelial cells to *Helicobacter pylori* infection. *Proceedings of the National Academy of Sciences*, **99**(23):15136–15141.

Guilliams, M., Ginhoux, F., Jakubzick, C., … Yona, S. (2014). Dendritic cells, monocytes and macrophages: a unified nomenclature based on ontogeny. *Nature Reviews Immunology*, **14**(8):571–578.

Guiney, D.G., Hasegawa, P. and Cole, S.P. (2003). *Helicobacter pylori* preferentially induces Interleukin 12 (IL-12) rather than IL-6 or IL-10 in human dendritic cells. *Infection and Immunity*, **71**(7):4163–4166.

Guo, H., Callaway, J.B. and Ting, J.P.Y. (2015). Inflammasomes: mechanism of action, role in disease, and therapeutics. *Nature Medicine*, **21**(7):677–687.

Haddadi, M.H., Bazargani, A., Khashei, R. and Fattahi, M.R. (2015). Different distribution of *Helicobacter pylori* EPIYA-*cagA* motifs and *dupA* genes in the upper gastrointestinal diseases and correlation with clinical outcomes in Iranian patients. *Gastroenterology and Hepatology from Bed to Bench*, **8**(1):37–46.

Haniffa, M., Bigley, V. and Collin, M. (2015). Human mononuclear phagocyte system reunited. *Seminars in Cell and Developmental Biology*, **41**:59–69.

Hansen, P.S., Go, M.F., Varming, K., … Nielsen, H. (1999). Proinflammatory activation of neutrophils and monocytes by *Helicobacter pylori* in patients with different clinical presentations. *Infection and Immunity*, **67**(6):3171–4.

Harris, P.R., Mobley, H.L.T., Perez-Perez, G.I., … Smith, P.D. (1996). *Helicobacter pylori* urease is a potent stimulus of mononuclear phagocyte activation and inflammatory cytokine production. *Gastroenterology*, **111**(2):419–425.

Hart, A.L., Lammers, K., Brigidi, P., … Stagg, A.J. (2004). Modulation of human dendritic cell phenotype and function by probiotic bacteria. *Gut*, **53**(11):1602–9.

Helmin-Basa, A., Czerwionka-Szaflarska, M., Bala, G., … Michalkiewicz, J. (2012). Expression of adhesion and activation molecules on circulating monocytes in children with *Helicobacter pylori* infection. *Helicobacter*, **17**(3):181–186.

Hennig, C., Adams, N. and Hansen, G. (2009). A versatile platform for comprehensive chip-based explorative cytometry. *Cytometry Part A: The Journal of the International Society for Analytical Cytology*, **75**(4):362–70.

Higgins, J.P.T. and Green, S. (2011). Cochrane Handbook for Systematic Reviews of Interventions, Version 5.1.0 [updated March 2011]. *The Cochrane Collaboration*:Chapter 9. Available at: www.handbook.cochrane.org.

Hilgendorf, I. and Swirski, F.K. (2012). Making a difference: monocyte heterogeneity in cardiovascular disease. *Current Atherosclerosis Reports*, **14**(5):450–459.

Hitzler, I., Kohler, E., Engler, D.B., … Müller, A. (2012). The role of Th cell subsets in the control of *Helicobacter* infections and in T cell-driven gastric immunopathology. *Frontiers in Immunology*, **3**:142.

Hold, G.L. and El-Omar, E.M. (2008). Genetic aspects of inflammation and cancer. *The Biochemical Journal*, **410**(2):225–235.

Hold, G.L., Mukhopadhya, I. and Monie, T.P. (2011). Innate immune sensors and gastrointestinal bacterial infections. *Clinical and Developmental Immunology*, **2011**:579650.

Hold, G.L., Rabkin, C.S., Chow, W.H., … El-Omar, E.M. (2007). A functional polymorphism of Toll-like receptor 4 gene increases risk of gastric carcinoma and its precursors. *Gastroenterology*, **132**(3):905–912.

Horemans, T., Deschacht, M., Clais, S., … Cos, P. (2011). An alternative, sensitive method to detect *Helicobacter pylori* DNA in feces. *Helicobacter*, **16**(2):113–118.

Hulstaert, F., Hannet, I., Deneys, V., … Strauss, K. (1994). Age-related changes in human blood lymphocyte subpopulations. II. Varying kinetics of percentage and absolute count measurements. *Clinical Immunology and Immunopathology*, **70**(2):152–8.

Hunt, R.H., Xiao, S.D., Mégraud, F., … Le Mair, A. (2011). *Helicobacter pylori* in developing countries. World Gastroenterology Organisation global guideline. *Journal of Gastrointestinal and Liver Dieases*, **20**(3):299–304.

Hussein, N.R. (2010). The association of *dupA* and *Helicobacter pylori*-related gastroduodenal diseases. *European Journal of Clinical Microbiology and Infectious Diseases*, **29**(7):817–821.

Hussein, N.R., Abdullah, S.M., Salih, A.M. and Assafi, M.A. (2012). *dupA1* is associated with duodenal ulcer and high Interleukin-8 secretion from the gastric mucosa. *Infection and Immunity*, **80**(8):2971–2972.

Hussein, N.R., Argent, R.H., Marx, C.K., … Atherton, J.C. (2010). *Helicobacter pylori dupA* is polymorphic, and its active form induces proinflammatory cytokine secretion by mononuclear cells. *Journal of Infectious Diseases*, **202**(2):261–269.

Hussein, N.R., Mohammadi, M., Talebkhan, Y., … Atherton, J.C. (2008). Differences in virulence markers between *Helicobacter pylori* strains from Iraq and those from Iran: Potential importance of regional differences in *H. pylori*-associated disease. *Journal of Clinical Microbiology*, **46**(5):1774–1779.

Hussein, N.R. and Tuncel, I.E. (2015). *Helicobacter pylori dupA* and smoking are associated with increased levels of IL-8 in gastric mucosa in Iraq. *Human Pathology*, **46**(6):929–30.

Hussein, N.R., Tunjel, I., Majed, H.S., … Assafi, M.S. (2015). Duodenal ulcer promoting gene 1 (*dupA1*) is associated with A2147G clarithromycin-resistance mutation but not interleukin-8 secretion from gastric mucosa in Iraqi patients. *New Microbes and New Infections*, **6**:5–10.

Ianiro, G., Molina-Infante, J. and Gasbarrini, A. (2015). Gastric microbiota. *Helicobacter*, **20**:68–71.

IARC Working Group on the Evaluation of Carcinogenic Risks to Humans (1994). Schistosomes, liver flukes and *Helicobacter pylori*. *IARC Monographs on the Evaluation of Carcinogenic Risks to Humans*, **61**:1–241.

Ieni, A., Barresi, V., Rigoli, L., … Caruso, R.A. (2016). Morphological and cellular features of innate immune reaction in *Helicobacter pylori* gastritis: a brief review. *International Journal of Molecular Sciences*, **17**(1):109.

Imagawa, S., Ito, M., Yoshihara, M., … Chayama, K. (2010). *Helicobacter pylori dupA* and gastric acid secretion are negatively associated with gastric cancer development. *Journal of Medical Microbiology*, **59**(12):1484–1489.

Ingram, R.J.M., Ragunath, K. and Atherton, J.C. (2015). Peptic ulcer disease. In D. K. Podolsky, ed. *Yamada's Textbook of Gastroenterology, sixth edition*. New Jersey: Wiley-Blackwell.

Innocenti, M., Svennerholm, A.M. and Quiding-Jarbrink, M. (2001). *Helicobacter pylori* lipopolysaccharides preferentially induce CXC chemokine production in human monocytes. *Infection and Immunity*, **69**(6):3800–3808.

Ioannou, G.N. and Kowdley, K. V (2004). Hepcidin in *HFE*-associated hemochromatosis: another piece of the "iron" puzzle. *Gastroenterology*, **126**(2):615–6; discussion 616.

Israel, D.A., Salama, N., Krishna, U., … Peek, R.M. (2001). *Helicobacter pylori* genetic diversity within the gastric niche of a single human host. *Proceedings of the National Academy of Sciences of the United States of America*, **98**(25):14625–14630.

Janeway, C.A., Travers, P., Walport, M. and Sclomchik, M.J. (2001). *Immunobiology: the immune system in health and disease, fifth edition*, New York: Garland Science.

Janssens, A.S., Pavel, S., Tensen, C.P., … de Gruijl, F.R. (2009). Reduced IL-1Ra/IL-1 ratio in ultraviolet B-exposed skin of patients with polymorphic light eruption. *Experimental Dermatology*, **18**(3):212–217.

Jersmann, H.P. (2005). Time to abandon dogma: CD14 is expressed by non-myeloid lineage cells. *Immunology and Cell Biology*, **83**(5):462–467.

Jiménez-Soto, L.F., Kutter, S., Sewald, X., … Haas, R. (2009). *Helicobacter pylori* type IV secretion apparatus exploits beta1 integrin in a novel RGD-independent manner G. T. Van Nhieu, ed. *PLoS Pathogens*, **5**(12):e1000684.

Johnson, E.E. and Wessling-Resnick, M. (2012). Iron metabolism and the innate immune response to infection. *Microbes and Infection*, **14**(3):207–16.

Jones, A.R., Twedt, D., Swaim, W. and Gottfried, E. (1996). Diurnal change of blood count analytes in normal subjects. *American Journal of Clinical Pathology*, **106**(6):723–7.

Jones, K.R., Joo, Y.M., Jang, S., … Cha, J.H. (2009). Polymorphism in the CagA EPIYA motif impacts development of gastric cancer. *Journal of Clinical Microbiology*, **47**(4):959–968.

de Jonge, R., Kuipers, E.J., Langeveld, S.C.L., … Kusters, J.G. (2004). The *Helicobacter pylori* plasticity region locus *jhp0947-jhp0949* is associated with duodenal ulcer disease and interleukin-12 production in monocyte cells. *FEMS Immunology and Medical Microbiology*, **41**(2):161–167.

de Jonge, R., Kusters, J.G., Timmer, M.S., … Kuipers, E.J. (2001). The role of *Helicobacter pylori* virulence factors in interleukin production by monocytic cells. *FEMS Microbiology Letters*, **196**(2):235–238.

Jung, S.W., Sugimoto, M., Graham, D.Y. and Yamaoka, Y. (2010). New type IV secretion system homologue: *dupA* gene cluster of *Helicobacter pylori*. *Gastroenterology*, **138**(5.s1):S-249.

Jung, S.W., Sugimoto, M., Toracchio, S., … Lotzing, N. (2009). Is the *dupA* gene one of the gene cluster for new type IV secretion system? *Gastroenterology*, **136**(5.s1):A-549.

Jung, S.W.W., Sugimoto, M., Shiota, S., … Yamaoka, Y. (2012). The intact *dupA* cluster is a more reliable *Helicobacter pylori* virulence marker than *dupA* alone. *Infection and Immunity*, **80**(1):381–387.

Kadowaki, N., Ho, S., Antonenko, S., … Liu, Y.J. (2001). Subsets of human dendritic cell precursors express different toll-like receptors and respond to different microbial antigens. *The Journal of Experimental Medicine*, **194**(6):863–9.

Kadowaki, T., Shimada, M., Inagawa, H., … Soma, G.I. (2012). Reconsideration of macrophage and dendritic cell classification. *Anticancer Research*, **32**(6):2257–2261.

Kerkar, S.P., Chinnasamy, D., Hadi, N., … Barrett, A.J. (2014). Timing and intensity of exposure to interferon-gamma critically determines the function of monocyte-derived dendritic cells. *Immunology*, **143**(1):96–108.

Kersulyte, D., Lee, W., Subramaniam, D., … Berg, D.E. (2009). *Helicobacter Pylori*'s Plasticity Zones Are Novel Transposable Elements. *PLoS One*, **4**(9):e6859.

Kersulyte, D., Velapatin, B., Asish, K., … Mukhopadhyay, A.K. (2003). Cluster of type IV secretion genes in *Helicobacter pylori*'s plasticity zone. *Journal of Bacteriology*, **185**(13):3764–72.

Khan, F.A., Fisher, M.A. and Khakoo, R.A. (2007). Association of hemochromatosis with infectious diseases: expanding spectrum. *International Journal of Infectious Diseases*, **11**(6):482–7.

Kidd, M. and Modlin, I.M. (1998). A century of *Helicobacter pylori*: paradigms lost-paradigms regained. *Digestion*, **59**(1):1–15.

Kim, J.Y., Kim, N., Nam, R.H., … Jung, H.C. (2014). Association of polymorphisms in virulence factor of *Helicobacter pylori* and gastroduodenal diseases in South Korea. *Journal of Gastroenterology and Hepatology (Australia)*, **29**(5):984–991.

Kitchens, R.L. (2000). Role of CD14 in cellular recognition of bacterial lipopolysaccharides. *Chemical Immunology*, **74**:61–82.

Kiyohira, K., Yoshihara, M., Ito, M., … Chayama, K. (2003). Serum pepsinogen concentration as a marker of *Helicobacter pylori* infection and the histologic grade of gastritis; evaluation of gastric mucosa by serum pepsinogen levels. *Journal of Gastroenterology*, **38**(4):332–338.

Kraaij, M.D., Vereyken, E.J.F., Leenen, P.J.M., … Rowshani, A.T. (2014). Human monocytes produce interferon-gamma upon stimulation with LPS. *Cytokine*, **67**(1):7–12.

Kruczkiewicz, P., Mutschall, S., Barker, D., … Taboada, E.N. (2013). MIST: a tool for rapid *in silico* generation of molecular data from bacterial genome sequences. *International Conference on Bioinformatics Models, Methods and Algorithms (BIOINFORMATICS 2013)*:316–323.

Krulwich, T.A., Sachs, G. and Padan, E. (2011). Molecular aspects of bacterial pH sensing and homeostasis. *Nature Reviews Microbiology*, **9**(5):330–343.

Kuipers, E.J., Uyterlinde, A.M., Peña, A.S., … Meuwissen, S.G. (1995). Increase of *Helicobacter pylori*-associated corpus gastritis during acid suppressive therapy: implications for long-term safety. *American Journal of Gastroenterology*, **90**(9):1401–1406.

Kusters, J.G., van Vliet, A.H.M. and Kuipers, E.J. (2006). Pathogenesis of *Helicobacter pylori* infection. *Clinical Microbiology Reviews*, **19**(3):449–490.

Kwok, T., Zabler, D., Urman, S., … Backert, S. (2007). *Helicobacter* exploits integrin for type IV secretion and kinase activation. *Nature*, **449**(7164):862–866.

Landmann, R., Knopf, H.P., Link, S., … Zimmerli, W. (1996). Human monocyte CD14 is upregulated by lipopolysaccharide. *Infection and Immunity*, **64**(5):1762–1769.

Lanier, L.L., Yu, G. and Phillips, J.H. (1991). Analysis of Fc gamma RIII (CD16) membrane expression and association with CD3 zeta and Fc epsilon RI-gamma by site-directed mutation. *Journal of Immunology*, **146**(5):1571–6.

Liberati, A., Altman, D.G., Tetzlaff, J., … Moher, D. (2009). The PRISMA statement for reporting systematic reviews and meta-analyses of studies that evaluate health care interventions: explanation and elaboration. *Journal of Cinical Epidemiology*, **62**(10):e1-34.

Lin, S.N., K, A., Y, Z., … K, O. (2005). *Helicobacter pylori* heat-shock protein 60 induces production of the pro-inflammatory cytokine IL-8 in monocytic cells. *Journal of Medical Microbiology*, **54**(3):225–233.

Little, J., Higgins, J.P.T., Ioannidis, J.P.A., … Birkett, N. (2009). STrengthening the REporting of genetic association studies (STREGA) - an extension of the STROBE statement. *Genetic Epidemiology*, **33**(7):581–598.

Liu, C., Zhang, Z. and Zhu, M. (2016). Immune responses mediated by Th17 cells in *Helicobacter pylori* infection. *Integrative Medicine International*, **3**(1–2):57–63.

Liu, Q. and Ding, J.L. (2016). The molecular mechanisms of TLR-signaling cooperation in cytokine regulation. *Immunology and Cell Biology*, **94**(November 2015):1–5.

Liu, X., He, B., Cho, W.C., … Wang, S. (2016). A systematic review on the association between the *Helicobacter pylori vacA* i genotype and gastric disease. *FEBS Open Bio*, **6**(5):409–417.

Logan, R.P., Walker, M.M., Misiewicz, J.J., … Baron, J.H. (1995). Changes in the intragastric distribution of *Helicobacter pylori* during treatment with omeprazole. *Gut*, **36**(1):12–6.

Loos, H., Blok-Schut, B., van Doorn, R., … Meerhof, L. (1976). A method for the recognition and separation of human blood monocytes on density gradients. *Blood*, **48**(5):731–42.

Lu, H., Hsu, P.I., Graham, D.Y. and Yamaoka, Y. (2005). Duodenal ulcer promoting gene of *Helicobacter pylori*. *Gastroenterology*, **128**(4):833–848.

Lu, H., Yamaoka, Y. and Graham, D.Y. (2005). *Helicobacter pylori* virulence factors: facts and fantasies. *Current Opinion in Gastroenterology*, **21**(6):653–659.

Lu, W., Wise, M.J., Tay, C.Y., … Perkins, T. (2014). Comparative analysis of the full genome of *Helicobacter pylori* isolate Sahul64 identifies genes of high divergence. *Journal of Bacteriology*, **196**(5):1073–1083.

Lynch, S. V. and Pedersen, O. (2016). The human intestinal microbiome in health and disease E. G. Phimister, ed. *New England Journal of Medicine*, **375**(24):2369–2379.

Lyons, P.A., Koukoulaki, M., Hatton, A., … Smith, K.G.C. (2007). Microarray analysis of human leucocyte subsets: the advantages of positive selection and rapid purification. *BMC Genomics*, **8**(1):64.

Macarthur, M., Hold, G.L. and El-Omar, E.M. (2004). Inflammation and Cancer II. Role of chronic inflammation and cytokine gene polymorphisms in the pathogenesis of gastrointestinal malignancy. *American Journal of Physiology. Gastrointestinal and Liver Physiology*, **286**(4):G515-20.

Maeda, S., Akanuma, M., Mitsuno, Y., … Omata, M. (2001). Distinct mechanism of *Helicobacter pylori*-mediated NF-kappaB activation between gastric cancer cells and monocytic cells. *Journal of Biological Chemistry*, **276**(48):44856–44864.

Mai, U.E.H., Perez-Perez, G.I., Wahl, L.M., … Smith, P.D. (1991). Soluble surface proteins from *Helicobacter pylori* activate monocytes/macrophages by lipopolysaccharide-independent mechanism. *Journal of Clinical Investigation*, **87**(3):894–900.

Malfertheiner, P., Chan, F.K.L. and McColl, K.E.L. (2009). Peptic ulcer disease. *Lancet*, **374**(9699):1449–1461.

Malfertheiner, P., Megraud, F., O'Morain, C., … Vakil, N. (2007). Current concepts in the management of *Helicobacter pylori* infection: the Maastricht III Consensus Report. *Gut*, **56**(6):772–781.

Malfertheiner, P., O'Morain, C., Megraud, F. and Axon, A.T.R. (2011). Management of *Helicobacter pylori* infection: the Maastricht IV/Florence Consensus. In Stockholm: United European Gastroenterology Week (UEGW) 2011.

Malone, J.L., Simms, T.E., Gray, G.C., … Burke, D.S. (1990). Sources of variability in repeated T-helper lymphocyte counts from human immunodeficiency virus type 1-infected patients: total lymphocyte count fluctuations and diurnal cycle are important. *Journal of Acquired Immune Deficiency Syndromes*, **3**(2):144–51.

Marshall, B. and Schoep, T. (2007). *Helicobacter pylori* as a vaccine delivery system. *Helicobacter*, **12**(s2):75–79.

Marshall, B.J. and Warren, J.R. (1984). Unidentified curved bacilli in the stomach of patients with gastritis and peptic ulceration. *Lancet*, **1**(8390):1311–1315.

Martínez-Carrillo, D.N., Atrisco-Morales, J., Hernández-Pando, R., … Fernández-Tilapa, G. (2014). *Helicobacter pylori vacA* and *cagA* genotype diversity and interferon gamma expression in patients with chronic gastritis and patients with gastric cancer. *Revista de Gastroenterología de México*, **79**(4):220–228.

Matsuda, H., Ito, Y., Suto, H., … Nakamoto, Y. (2012). Clinical relevance and sequence analysis of the *Helicobacter pylori dupA* region from two areas in Japan with different gastric cancer risks. *ImmunoGastroenterology*, **1**(2):127.

Matteo, M.J., Armitano, R.I., Granados, G., … Catalano, M. (2010). *Helicobacter pylori oipA*, *vacA* and *dupA* genetic diversity in individual hosts. *Journal of Medical Microbiology*, **59**(1):89–95.

Mattsson, A., Quiding-Järbrink, M., Lönroth, H., … Svennerholm, A.M. (1998). Antibody-secreting cells in the stomachs of symptomatic and asymptomatic *Helicobacter pylori*-infected subjects. *Infection and Immunity*, **66**(6):2705–2712.

Mégraud, F. and Lehours, P. (2007). *Helicobacter pylori* detection and antimicrobial susceptibility testing. *Clinical Microbiology Reviews*, **20**(2):280–322.

Merrell, D.S., Goodrich, M.L., Otto, G., … Tompkins, L.S. (2003). pH-regulated gene expression of the gastric pathogen *Helicobacter pylori*. *Infection and Immunity*, **71**(6):3529–3539.

Metharom, P., Velten, F.W. and Goerdt, S. (2006). Highly phagocytic, CD4hi, CD14hi and CD16hi antigen-presenting cells modulated by tumour-conditioned media retain the capacity to mature and induce TH1 T-cell proliferation. *Molecular Immunology*, **43**(13):2070–2082.

Miftahussurur, M., Syam, A.F., Makmun, D., … Yamaoka, Y. (2015). *Helicobacter pylori* virulence genes in the five largest islands of Indonesia. *Gut Pathogens*, **7**(11):26.

Miftahussurur, M. and Yamaoka, Y. (2015). *Helicobacter pylori* virulence genes and host genetic polymorphisms as risk factors for peptic ulcer disease. *Expert Review of Gastroenterology and Hepatology*, **9**(12):1535–1547.

Miles, A.A., Misra, S.S. and Irwin, J.O. (1938). The estimation of the bactericidal power of the blood. *The Journal of Hygiene*, **38**(6):732–49.

Mills, C.D. (2015). Anatomy of a discovery: M1 and M2 macrophages. *Frontiers in Immunology*, **6**.

Minelli, C., Thompson, J.R., Abrams, K.R., … Attia, J. (2009). The quality of meta-analyses of genetic association studies: a review with recommendations. *American Journal of Epidemiology*, **170**(11):1333–1343.

Mogensen, T.H. (2009). Pathogen recognition and inflammatory signaling in innate immune defenses. *Clinical Microbiology Reviews*, **22**(2):240–273.

Monteiro, L., Gras, N. and Megraud, F. (2001). Magnetic immuno-PCR assay with inhibitor removal for direct detection of *Helicobacter pylori* in human feces. *Journal of Clinical Microbiology*, **39**(10):3778–3780.

Moura, S.B., Costa, R.F.A., Anacleto, C., … Queiroz, D.M.M. (2012). Single nucleotide polymorphisms of *Helicobacter pylori dupA* that lead to premature stop codons. *Helicobacter*, **17**(3):176–180.

Mukhopadhyay, A.K., Kersulyte, D., Jeong, J.Y., … Berg, D.E. (2000). Distinctiveness of genotypes of *Helicobacter pylori* in Calcutta, India. *Journal of Bacteriology*, **182**(11):3219–3227.

Mulder, W.M.C., Koenen, H., van de Muysenberg, A.J.C., … Scheper, R.J. (1994). Reduced expression of distinct T-cell CD molecules by collagenase/DNase treatment. *Cancer Immunology Immunotherapy*, **38**(4):253–258.

Müller, A., Oertli, M. and Arnold, I.C. (2011). *H. pylori* exploits and manipulates innate and adaptive immune cell signaling pathways to establish persistent infection. *Cell Communication and Signaling*, **9**(1):25.

Nagai, S., Mimuro, H., Yamada, T., … Koyasu, S. (2007). Role of Peyer's patches in the induction of *Helicobacter pylori*-induced gastritis. *Proceedings of the National Academy of Sciences*, **104**(21):8971–8976.

Nagashima, H. and Yamaoka, Y. (2015). *Helicobacter pylori dupA* and smoking are associated with increased levels of interleukin-8 in gastric mucosa in Iraq-reply. *Human Pathology*, **46**(6):931.

Naito, M., Yamazaki, T., Tsutsumi, R., … Hatakeyama, M. (2006). Influence of EPIYA-repeat polymorphism on the phosphorylation-dependent biological activity of *Helicobacter pylori* CagA. *Gastroenterology*, **130**(4):1181–1190.

Narayanan, G.L. (2005). *Determinants of vacuolating cytotoxin production in the gastric pathogen Helicobacter pylori.* Thesis (PhD). University of Nottingham.

Nathanson, S.D., Zamfirescu, P.L., Drew, S.I. and Wilbur, S. (1977). Two-step separation of human peripheral blood monocytes on discontinuous density gradients of colloidal silica-polyvinylpyrrolidinone. *Journal of Immunological Methods*, **18**(3–4):225–234.

Necchi, V., Manca, R., Ricci, V. and Solcia, E. (2009). Evidence for transepithelial dendritic cells in human *H. pylori* active gastritis. *Helicobacter*, **14**(3):208–222.

Nguyen, L.T., Uchida, T., Tsukamoto, Y., … Moriyama, M. (2010). *Helicobacter pylori dupA* gene is not associated with clinical outcomes in the Japanese population. *Clinical Microbiology and Infection*, **16**(8):1264–1269.

Nieto, J.C., Cantó, E., Zamora, C., … Vidal, S. (2012). Selective loss of chemokine receptor expression on leukocytes after cell isolation. *PLoS ONE*, **7**(3).

Nilsson, C., Aboud, S., Karlén, K., … Biberfeld, G. (2008). Optimal blood mononuclear cell isolation procedures for gamma interferon enzyme-linked immunospot testing of healthy Swedish and Tanzanian subjects. *Clinical and Vaccine Immunology*, **15**(4):585–589.

O'Mahony, D.S., Pham, U., Iyer, R., … Liles, W.C. (2008). Differential constitutive and cytokine-modulated expression of human Toll-like receptors in primary neutrophils, monocytes, and macrophages. *International Journal of Medical Sciences*, **5**(1):1–8.

Occhialini, A., Marais, A., Alm, R., … Mégraud, F. (2000). Distribution of open reading frames of plasticity region of strain J99 in *Helicobacter pylori* strains isolated from gastric carcinoma and gastritis patients in Costa Rica. *Infection and Immunity*, **68**(11):6240–6249.

Odenbreit, S., Linder, S., Gebert-Vogl, B., … Haas, R. (2006). Interleukin-6 induction by *Helicobacter pylori* in human macrophages is dependent on phagocytosis. *Helicobacter*, **11**(3):196–207.

Oertelt-Prigione, S. (2012). The influence of sex and gender on the immune response. *Autoimmunity Reviews*, **11**(6–7):A479-85.

Oertli, M. and Müller, A. (2012). *Helicobacter pylori* targets dendritic cells to induce immune tolerance, promote persistence and confer protection against allergic asthma. *Gut Microbes*, **3**(6):566–571.

Oktem-Okullu, S., Tiftikci, A., Saruc, M., … Sayi-Yazgan, A. (2015). Multiplex-PCR-based screening and computational modeling of virulence factors and T-cell mediated immunity in *Helicobacter pylori* infections for accurate clinical diagnosis. *PLoS ONE*, **10**(8):1–13.

Osborne, N.J., Gurrin, L.C., Allen, K.J., … English, D.R. (2010). *HFE* C282Y homozygotes are at increased risk of breast and colorectal cancer. *Hepatology*, **51**(4):1311–8.

Osman, H.A., Hasan, H., Suppian, R., … Zilfalil, B.A. (2015). Prevalence of *Helicobacter pylori cagA, babA2,* and *dupA* genotypes and correlation with clinical outcome in Malaysian patients with dyspepsia. *Turkish Journal of Medical Sciences*, **45**(4):940–946.

Pacheco, A.R., Proença-Módena, J.L., Sales, A.I.L., … Brocchi, M. (2008). Involvement of the *Helicobacter pylori* plasticity region and *cag* pathogenicity island genes in the development of gastroduodenal diseases. *European Journal of Clinical Microbiology and Infectious Diseases*, **27**(11):1053–1059.

Papamichael, K., Konstantopoulos, P. and Mantzaris, G.J. (2014). *Helicobacter pylori* infection and inflammatory bowel disease: is there a link? *World Journal of Gastroenterology*, **20**(21):6374–6385.

Patel, S.K., Pratap, C.B., Jain, A.K., … Nath, G. (2014). Diagnosis of *Helicobacter pylori*: what should be the gold standard? *World Journal of Gastroenterology*, **20**(36):12847–12859.

Patel, S.R. (2010). *Determinants of* Helicobacter pylori *density in the human stomach and implications in disease.* Thesis (PhD). University of Nottingham.

Patel, S.R., Letley, D.P., Hussein, N.R. and Atherton, J.C. (2009). Determinants of *H. pylori* localization and *IL8* expression in the human gastric mucosa. *Helicobacter*, **14**(4):411.

Patel, S.R., Smith, K., Letley, D.P., … Robinson, K. (2013). *Helicobacter pylori* downregulates expression of human beta-defensin 1 in the gastric mucosa in a type IV secretion-dependent fashion. *Cellular Microbiology*, **15**(12):2080–2092.

Pellicanò, A., Sebkova, L., Monteleone, G., … Luzza, F. (2007). Interleukin-12 drives the Th1 signaling pathway in *Helicobacter pylori*-infected human gastric mucosa. *Infection and Immunity*, **75**(4):1738–1744.

Pereira, W.N., Ferraz, M.A., Zabaglia, L.M., … Rasmussen, L.T. (2014). Association among *H. pylori* virulence markers *dupA, cagA* and *vacA* in Brazilian patients. *The Journal of Venomous Animals and Toxins Including Tropical Diseases*, **20**(1):1.

Perri, F., Clemente, R., Pastore, M., … Andriulli, A. (1998). The 13C-urea breath test as a predictor of intragastric bacterial load and severity of *Helicobacter pylori* gastritis. *Scandinavian Journal of Clinical and Laboratory Investigation*, **58**(1):19–27.

Persoskie, A. and Ferrer, R.A. (2017). A most odd ratio: interpreting and describing odds ratios. *American Journal of Preventive Medicine*, **52**(2):224–228.

Persson, C., Canedo, P., MacHado, J.C., … Forman, D. (2011). Polymorphisms in inflammatory response genes and their association with gastric cancer: a HuGE systematic review and meta-analyses. *American Journal of Epidemiology*, **173**(3):259–270.

Pfaffl, M.W. (2001). A new mathematical model for relative quantification in real-time RT-PCR. *Nucleic Acids Research*, **29**(9):e45.

Philpott, D.J., Sorbara, M.T., Robertson, S.J., … Girardin, S.E. (2014). NOD proteins: regulators of inflammation in health and disease. *Nature Reviews Immunology*, **14**(1):9–23.

Pietrangelo, A. (2015). Genetics, genetic testing, and management of hemochromatosis: 15 years since hepcidin. *Gastroenterology*, **149**(5):1240–1251.e4.

Pimentel-Nunes, P., Afonso, L., Lopes, P., … Dinis-Ribeiro, M. (2011). Increased expression of Toll-like receptors (TLR) 2, 4 and 5 in gastric dysplasia. *Pathology Oncology Research*, **17**(3):677–83.

Porto, G. and De Sousa, M. (2007). Iron overload and immunity. *World Journal of Gastroenterology*, **13**(35):4707–15.

Posselt, G., Backert, S. and Wessler, S. (2013). The functional interplay of *Helicobacter pylori* factors with gastric epithelial cells induces a multi-step process in pathogenesis. *Cell Communication and Signaling*, **11**(1):77.

Queiroz, D.M.M., Moura, S.B., Rocha, A.M.C., … Rocha, G.A. (2011). The genotype of the Brazilian *dupA*-positive *Helicobacter pylori* strains is *dupA1*. *Journal of Infectious Diseases*, **203**(7):1033–1034.

Queiroz, D.M.M., Rocha, G.A.A., Rocha, A.M.C., … Oliveira, C.A.A. (2011). *dupA* polymorphisms and risk of *Helicobacter pylori*-associated diseases. *International Journal of Medical Microbiology*, **301**(3):225–228.

Queiroz, D.M.M., Rocha, G.A., Gomes, L.I., … Oliveira, C.A. (2008). *dupA* polymorphisms and risk of distal gastric carcinoma. *Gastroenterology*, **134**(4.s1):A-85.

Rabinowitz, Y. (1964). Separation of lymphocytes, polymorphonuclear leukocytes and monocytes on glass columns, including tissue culture observations. *Blood*, **23**:811–828.

Rad, R., Ballhorn, W., Voland, P., … Krug, A. (2009). Extracellular and intracellular pattern recognition receptors cooperate in the recognition of *Helicobacter pylori*. *Gastroenterology*, **136**(7):2247–2257.

Rad, R., Brenner, L., Krug, A., … Prinz, C. (2007). Toll-like receptor-dependent activation of antigen-presenting cells affects adaptive immunity to *Helicobacter pylori*. *Gastroenterology*, **133**(1):150–163.e3.

Randolph, G.J., Jakubzick, C. and Qu, C. (2008). Antigen presentation by monocytes and monocyte-derived cells. *Current Opinion in Immunology*, **20**(1):52–60.

Rappl, C., Deiwick, J. and Hensel, M. (2003). Acidic pH is required for the functional assembly of the type III secretion system encoded by *Salmonella* pathogenicity island 2. *FEMS Microbiology Letters*, **226**(2):363–372.

Rasheed, F., Campbell, B.J., Alfizah, H., … Pritchard, D.M. (2014). Analysis of clinical isolates of *Helicobacter pylori* in Pakistan reveals high degrees of pathogenicity and high frequencies of antibiotic resistance. *Helicobacter*, **19**(5):387–399.

Rescigno, M., Urbano, M., Valzasina, B., … Ricciardi-Castagnoli, P. (2001). Dendritic cells express tight junction proteins and penetrate gut epithelial monolayers to sample bacteria. *Nature Immunology*, **2**(4):361–367.

Rhead, J.L., Letley, D.P., Mohammadi, M., … Atherton, J.C. (2007). A new *Helicobacter pylori* vacuolating cytotoxin determinant, the intermediate region, is associated with gastric cancer. *Gastroenterology*, **133**(3):926–936.

Ritter, B., Kilian, P., Reboll, M.R., … Nourbakhsh, M. (2011). Differential effects of multiplicity of infection on *Helicobacter pylori*-induced signaling pathways and interleukin-8 gene transcription. *Journal of Clinical Immunology*, **31**(1):60–68.

Robinson, K. (2015). *Helicobacter pylori*-mediated protection against extra-gastric immune and inflammatory disorders: the evidence and controversies. *Diseases*, **3**(2):34–55.

Robinson, K., Argent, R.H. and Atherton, J.C. (2007). The inflammatory and immune response to *Helicobacter pylori* infection. *Best Practice and Research Clinical Gastroenterology*, **21**(2):237–259.

Robinson, K., Kenefeck, R., Pidgeon, E.L., … Atherton, J.C. (2008). *Helicobacter pylori*-induced peptic ulcer disease is associated with inadequate regulatory T cell responses. *Gut*, **57**(10):1375.

Roderick, P., Davies, R., Raftery, J., … Bhandari, P. (2003). Cost-effectiveness of population screening for *Helicobacter pylori* in preventing gastric cancer and peptic ulcer disease, using simulation. *Journal of Medical Screening*, **10**(3):148–156.

Rogers, A.B. (2012). Gastric *Helicobacter* spp. in animal models: pathogenesis and modulation by extragastric coinfections. *Methods in Molecular Biology*, **921**:175–188.

Rogler, G., Hausmann, M., Vogl, D., … Gross, V. (1998). Isolation and phenotypic characterization of colonic macrophages. *Clinical and Experimental Immunology*, **112**(2):205–215.

Rohrer, S., Holsten, L., Weiss, E., … Haas, R. (2012). Multiple pathways of plasmid DNA transfer in *Helicobacter pylori* E. Cascales, ed. *PLoS ONE*, **7**(9):e45623.

Rohrlich, P.S., Fazilleau, N., Ginhoux, F., … Lemonnier, F.A. (2005). Direct recognition by alphabeta cytolytic T cells of Hfe, a MHC class Ib molecule without antigen-presenting function. *Proceedings of the National Academy of Sciences of the United States of America*, **102**(36):12855–60.

Rokbi, B., Seguin, D., Guy, B., … Quentin-Millet, M.J. (2001). Assessment of *Helicobacter pylori* gene expression within mouse and human gastric mucosae by real-time reverse transcriptase PCR. *Infection and Immunity*, **69**(8):4759–4766.

Romo-Gonzalez, C., Consuelo-Sanchez, A., Camorlinga-Ponce, M., … Coria-Jimenez, R. (2015). Plasticity region genes *jhp0940*, *jhp0945*, *jhp0947*, and *jhp0949* of *Helicobacter pylori* in isolates from mexican children. *Helicobacter*, **20**(3):231–237.

Rugge, M., Correa, P., Di Mario, F., … Vieth, M. (2008). OLGA staging for gastritis: a tutorial. *Digestive and Liver Disease*, **40**(8):650–658.

Ruschen, S., Stellberg, W. and Warnatz, H. (1992). Kinetics of cytokine secretion by mononuclear cells of the blood from rheumatoid arthritis patients are different from those of healthy controls. *Clinical and Experimental Immunology*, **89**(1):32–7.

Salih, A.M., Goreal, A., Hussein, N.R., … Assafi, M. (2013). The distribution of *cagA* and *dupA* genes in *Helicobacter pylori* strains in Kurdistan region, northern Iraq. *Annals of Saudi Medicine*, **33**(3):290–293.

Santos, A., Queiroz, D.M.M., Ménard, A., … Mégraud, F. (2003). New pathogenicity marker found in the plasticity region of the *Helicobacter pylori* genome. *Journal of Clinical Microbiology*, **41**(4):1651–1655.

Sanui, T., Takeshita, M., Fukuda, T., … Nishimura, F. (2017). Anti-CD14 antibody-treated neutrophils respond to LPS: possible involvement of CD14 upregulated by anti-CD14 antibody binding. *Immunological Investigations*, **46**(2):190–200.

Saribasak, H., Salih, B.A., Yamaoka, Y. and Sander, E. (2004). Analysis of *Helicobacter pylori* genotypes and correlation with clinical outcome in Turkey. *Journal of Clinical Microbiology*, **42**(4):1648–1651.

Satpathy, A.T., Wu, X., Albring, J.C. and Murphy, K.M. (2012). Re(de)fining the dendritic cell lineage. *Nature Immunology*, **13**(12):1145–54.

Sawai, N., Kita, M., Kodama, T., … Imanishi, J. (1999). Role of gamma interferon in *Helicobacter pylori*-induced gastric inflammatory responses in a mouse model. *Infection and Immunity*, **67**(1):279–85.

Schildberger, A., Rossmanith, E., Eichhorn, T., … Weber, V. (2013). Monocytes, peripheral blood mononuclear cells, and THP-1 cells exhibit different cytokine expression patterns following stimulation with lipopolysaccharide. *Mediators of Inflammation*, **2013**:697972.

Schlaermann, P., Toelle, B., Berger, H., … Meyer, T.F. (2016). A novel human gastric primary cell culture system for modelling *Helicobacter pylori* infection *in vitro*. *Gut*, **65**(2):202–13.

Schmaußer, B., Andrulis, M., Endrich, S., … Eck, M. (2004). Expression and subcellular distribution of toll-like receptors TLR4, TLR5 and TLR9 on the gastric epithelium in *Helicobacter pylori* infection. *Clinical and Experimental Immunology*, **136**(3):521–526.

Schmidt, H.M.A., Andres, S., Kaakoush, N.O., … Mitchell, H. (2009). The prevalence of the duodenal ulcer promoting gene (*dupA*) in *Helicobacter pylori* isolates varies by ethnic group and is not universally associated with disease development: a case-control study. *Gut Pathogens*, **1**(1):5.

Schmidt, H.M.A., Andres, S., Nilsson, C., … Mitchell, H. (2010). The cag PAI is intact and functional but HP0521 varies significantly in *Helicobacter pylori* isolates from Malaysia and Singapore. *European Journal of Clinical Microbiology and Infectious Diseases*, **29**(4):439–451.

Schoeb, T.R. and Bullard, D.C. (2012). Microbial and histopathologic considerations in the use of mouse models of inflammatory bowel diseases. *Inflammatory Bowel Diseases*, **18**(8):1558–1565.

Schroder, K., Hertzog, P.J., Ravasi, T. and Hume, D.A. (2004). Interferon-gamma: an overview of signals, mechanisms and functions. *Journal of Leukocyte Biology*, **75**(2):163–89.

Schultze, V., Hackelsberger, A., Günther, T., … Malfertheiner, P. (1998). Differing patterns of *Helicobacter pylori* gastritis in patients with duodenal, prepyloric, and gastric ulcer disease. *Scandinavian Journal of Gastroenterology*, **33**(2):137–142.

Semper, R.P., Mejías-Luque, R., Groß, C., … Gerhard, M. (2014). *Helicobacter pylori*-induced IL-1β secretion in innate immune cells is regulated by the NLRP3 inflammasome and requires the *cag* pathogenicity island. *Journal of Immunology*, **193**(7):3566–76.

Serelli-Lee, V., Ling, K.L., Ho, C., … Wong, S.B.J. (2012). Persistent *Helicobacter pylori* specific Th17 responses in patients with past *H. pylori* infection are associated with elevated gastric mucosal IL-1β. *PLoS One*, **7**(6):e39199.

Shaffer, C.L., Gaddy, J.A., Loh, J.T., … Cover, T.L. (2011). *Helicobacter pylori* exploits a unique repertoire of type IV secretion system components for pilus assembly at the bacteria-host cell interface N. Salama, ed. *PLoS Pathogens*, **7**(9):e1002237.

Shah, A., Talley, N.J., Walker, M., … Holtmann, G. (2017). Is there a link between *H. pylori* and the epidemiology of Crohn's disease? *Digestive Diseases and Sciences*:1–9.

Shamliyan, T.A., Kane, R.L., Ansari, M.T., … Tsouros, S. (2011). Development quality criteria to evaluate nontherapeutic studies of incidence, prevalence, or risk factors of chronic diseases: pilot study of new checklists. *Journal of Clinical Epidemiology*, **64**(6):637–657.

Shamliyan, T.A., Kane, R.L. and Dickinson, S. (2010). A systematic review of tools used to assess the quality of observational studies that examine incidence or prevalence and risk factors for diseases. *Journal of Clinical Epidemiology*, **63**(10):1061–1070.

Shamliyan, T.A., Kane, R.L. and Jansen, S. (2012). Systematic reviews synthesized evidence without consistent quality assessment of primary studies examining epidemiology of chronic diseases. *Journal of Clinical Epidemiology*, **65**(6):610–618.

Shiota, S., Matsunari, O., Watada, M., … Yamaoka, Y. (2010). Systematic review and meta-analysis: the relationship between the *Helicobacter pylori dupA* gene and clinical outcomes. *Gut Pathogens*, **2**(1):13.

Shiota, S., Nguyen, L.T., Murakami, K., … Yamaoka, Y. (2012). Association of *Helicobacter pylori dupA* with the failure of primary eradication. *Journal of Clinical Gastroenterology*, **46**(4):297–301.

Silva, B., Nunes, A., Rocha, R., … Oleastro, M. (2015). The expression of *Helicobacter pylori dupA* cluster is regulated by adherence and pH, and its genetic organization is associated with differential gastric IL-8 secretion. *Helicobacter*, **20**(s1):110 (P05.03).

Sims, G.E., Jun, S.R., Wu, G.A. and Kim, S.H. (2009). Alignment-free genome comparison with feature frequency profiles (FFP) and optimal resolutions. *Proceedings of the National Academy of Sciences of the United States of America*, **106**(8):2677–2682.

Smith, M.F., Mitchell, A., Li, G., … Goldberg, J.B. (2003). Toll-like receptor (TLR) 2 and TLR5, but not TLR4, are required for *Helicobacter pylori*-induced NF-κB activation and chemokine expression by epithelial cells. *Journal of Biological Chemistry*, **278**(35):32552–32560.

Smith, P.D., MacDonald, T.T. and Blumberg, R.S. (2013). *Principles of mucosal immunology*. P. D. Smith, T. T. MacDonald, & R. S. Blumberg, eds., London: Garland Science.

Smith, P.D., Smythies, L.E., Shen, R., … Wahl, S.M. (2011). Intestinal macrophages and response to microbial encroachment. *Mucosal Immunology*, **4**(1):31–42.

Snaith, A. and El-Omar, E.M. (2008). *Helicobacter pylori*: host genetics and disease outcomes. *Expert Review of Gastroenterology and Hepatology*, **2**(4):577–585.

So, E.C., Sallin, M.A., Zhang, X., … Jain, A. (2013). A high throughput method for enrichment of natural killer cells and lymphocytes and assessment of in vitro cytotoxicity. *Journal of Immunological Methods*, **394**(1–2):40–48.

Sobala, G.M., Crabtree, J.E., Dixon, M.F., … Axon, A.T. (1991). Acute *Helicobacter pylori* infection: clinical features, local and systemic immune response, gastric mucosal histology, and gastric juice ascorbic acid concentrations. *Gut*, **32**(11):1415–1418.

Souod, N., Sarshar, M., Dabiri, H., … Abdi, S. (2015). The study of the *oipA* and *dupA* genes in *Helicobacter pylori* strains and their relationship with different gastroduodenal diseases. *Gastroenterology and Hepatology from Bed to Bench*, **8**(Suppl 1):S47-53.

Stanciu, L.A., Shute, J., Holgate, S.T. and Djukanović, R. (1996). Production of IL-8 and IL-4 by positively and negatively selected CD4+ and CD8+ human T cells following a four-step cell separation method including magnetic cell sorting (MACS). *Journal of Immunological Methods*, **189**(1):107–115.

Stanley, A.C. and Lacy, P. (2010). Pathways for cytokine secretion. *Physiology*, **25**(4):218–29.

Staples, E., Ingram, R.J.M., Atherton, J.C. and Robinson, K. (2013). Optimising the quantification of cytokines present at low concentrations in small human mucosal tissue samples using Luminex assays. *Journal of Immunological Methods*, **394**(1–2):1–9.

Steinman, R.M. and Banchereau, J. (2007). Taking dendritic cells into medicine. *Nature*, **449**(7161):419–26.

Stevens, A. and Lowe, J.S. (1997). Blood cells. In *Human Histology, second edition*. London: Mosby, pp. 99–116.

Stroup, D.F., Berlin, J. a, Morton, S.C., … Thacker, S.B. (2000). Meta-analysis of observational studies. *Methods*, **283**:2008–12.

Sýkora, J. and Rowland, M. (2011). *Helicobacter pylori* in Pediatrics. *Helicobacter*, **16**(s.1):59–64.

Tacke, F. and Randolph, G.J. (2006). Migratory fate and differentiation of blood monocyte subsets. *Immunobiology*, **211**(6–8):609–618.

Takahashi, A., Shiota, S., Matsunari, O., … Yamaoka, Y. (2013). Intact long-type *dupA* as a marker for gastroduodenal diseases in Okinawan subpopulation, Japan. *Helicobacter*, **18**(1):66–72.

Taylor, S., Wakem, M., Dijkman, G., … Nguyen, M. (2010). A practical approach to RT-qPCR. Publishing data that conform to the MIQE guidelines. *Methods*, **50**(4):S1–S5.

Tomasini, M.L., Zanussi, S., Sozzi, M., … De Paoli, P. (2003). Heterogeneity of *cag* genotypes in *Helicobacter pylori* isolates from human biopsy specimens. *Journal of Clinical Microbiology*, **41**(3):976–980.

Tomb, J.F., White, O., Kerlavage, A.R., … Venter, J.C. (1997). The complete genome sequence of the gastric pathogen *Helicobacter pylori*. *Nature*, **388**(6642):539–547.

Tominaga, K., Yoshimoto, T., Torigoe, K., … Nakanishi, K. (2000). IL-12 synergizes with IL-18 or IL-1beta for IFN-gamma production from human T cells. *International Immunology*, **12**(2):151–60.

Tuncel, I.E., Hussein, N.R., Bolek, B.K., … Salih, B.A. (2010). *Helicobacter pylori* virulence factors and their role in peptic ulcer diseases in Turkey. *Acta Gastro-Enterologica Belgica*, **73**(2):235–238.

Turner, M.D., Nedjai, B., Hurst, T. and Pennington, D.J. (2014). Cytokines and chemokines: at the crossroads of cell signalling and inflammatory disease. *Biochimica et Biophysica Acta - Molecular Cell Research*, **1843**(11):2563–2582.

Uemura, N., Okamoto, S., Yamamoto, S., … Schlemper, R.J. (2001). *Helicobacter pylori* infection and the development of gastric cancer. *New England Journal of Medicine*, **345**(11):784–789.

Varbanova, M. and Malfertheiner, P. (2011). Bacterial load and degree of gastric mucosal inflammation in *Helicobacter pylori* infection. *Digestive Diseases*, **29**(6):592–599.

Viala, J., Chaput, C., Boneca, I.G., … Ferrero, R.L. (2004). Nod1 responds to peptidoglycan delivered by the *Helicobacter pylori cag* pathogenicity island. *Nature Immunology*, **5**(11):1166–1174.

Vicari, J.J., Peek, R.M., Falk, G.W., … Richter, J.E. (1998). The seroprevalence of *cagA*-positive *Helicobacter pylori* strains in the spectrum of gastroesophageal reflux disease. *Gastroenterology*, **115**(1):50–57.

Vissers, M.C.M., Jester, S.A. and Fantone, J.C. (1988). Rapid purification of human peripheral blood monocytes by centrifugation through Ficoll-Hypaque and Sepracell-M. *Journal of Immunological Methods*, **110**(2):203–207.

Wahl, L.M., Wahl, S.M., Smythies, L.E. and Smith, P.D. (2006). Isolation of human monocyte populations. In J. E. Coligan et al., eds. *Current Protocols in Immunology*. Hoboken, NJ: John Wiley and Sons, p. Unit 7.6A.

Walker, E.M. and Walker, S.M. (2000). Effects of iron overload on the immune system. *Annals of Clinical and Laboratory Science*, **30**(4):354–65.

Walker, M.R., Kasprowicz, D.J., Gersuk, V.H., … Ziegler, S.F. (2003). Induction of FoxP3 and acquisition of T regulatory activity by stimulated human CD4+CD25- T cells. *Journal of Clinical Investigation*, **112**(9):1437–1443.

Wang, L., Johnson, E.E., Shi, H.N., … Cherayil, B.J. (2008). Attenuated inflammatory responses in hemochromatosis reveal a role for iron in the regulation of macrophage cytokine translation. *Journal of Immunology*, **181**(4):2723–31.

Wang, M.Y., Chen, C., Gao, X.Z., … Shao, S.H. (2013). Distribution of *Helicobacter pylori* virulence markers in patients with gastroduodenal diseases in a region at high risk of gastric cancer. *Microbial Pathogenesis*, **59**–**60**:13–18.

Wang, M.Y., Chen, C., Shao, C., … Shao, S.H. (2015). Intact long-type DupA protein in *Helicobacter pylori* is an ATPase involved in multifunctional biological activities. *Microbial Pathogenesis*, **81**:53–59.

Wang, M.Y., Shao, C., Li, J., … Shao, S.H. (2015). *Helicobacter pylori* with the intact *dupA* cluster is more virulent than the strains with the incomplete *dupA* cluster. *Current Microbiology*, **71**(1):16–23.

Wang, Y., Bi, Y., Zhang, L. and Wang, C. (2012). Is *Helicobacter pylori* infection associated with asthma risk? A meta-analysis based on 770 cases and 785 controls. *International Journal of Medical Sciences*, **9**(7):603–610.

Watanabe, T., Higuchi, K., Tominaga, K., … Arakawa, T. (2001). Acid regulates inflammatory response in a rat model of induction of gastric ulcer recurrence by interleukin 1. *Gut*, **48**(6):774–781.

Wells, G.A., Shea, B., O'Connell, D., … Tugwell, P. (2011). The Newcastle–Ottawa Scale (NOS) for assessing the quality of nonrandomised studies in meta-analyses. *Ottawa Health Research Institute*.

Weston, C. and Connor, J. (2014). Evidence for the influence of the iron regulatory MHC class I molecule Hfe on tumor progression in experimental models and clinical populations. *Translational Oncogenomics*, **6**:1–12.

White, J.R., Winter, J.A. and Robinson, K. (2015). Differential inflammatory response to *Helicobacter pylori* infection: etiology and clinical outcomes. *Journal of Inflammation Research*, **8**:137–147.

Whiting, P., Rutjes, A.W.S., Dinnes, J., … Kleijnen, J. (2005). A systematic review finds that diagnostic reviews fail to incorporate quality despite available tools. *Journal of Clinical Epidemiology*, **58**(1):1–12.

Whiting, P., Rutjes, A.W.S., Reitsma, J.B., … Kleijnen, J. (2003). The development of QUADAS: a tool for the quality assessment of studies of diagnostic accuracy included in systematic reviews. *BMC Medical Research Methodology*, **3**:25.

Whiting, P.F., Rutjes, A.W.S., Westwood, M.E., … Bossuyt, P.M.M. (2011). QUADAS-2: a revised tool for the quality assessment of diagnostic accuracy studies. *Annals of Internal Medicine*, **155**(8):529–536.

Williams, J.G., Roberts, S.E., Ali, M.F., … Williams, J.C. (2007). Gastroenterology services in the UK. The burden of disease, and the organisation and delivery of services for gastrointestinal and liver disorders: a review of the evidence. *Gut*, **56**(s1):1–113.

Winter, J.A., Letley, D.P., Cook, K.W., … Atherton, J.C. (2014). A role for the vacuolating cytotoxin, VacA, in colonization and *Helicobacter pylori*-induced metaplasia in the stomach. *Journal of Infectious Diseases*, **210**(6):954–963.

Winter, J.A., Letley, D.P., Rhead, J.L., … Robinson, K. (2014). *Helicobacter pylori* membrane vesicles stimulate innate pro- and anti-inflammatory responses and induce apoptosis in Jurkat T cells. *Infection and Immunity*, **82**(4):1372–1381.

Wolfe, M.M. and Nompleggi, D.J. (1992). Cytokine inhibition of gastric acid secretion - a little goes a long way. *Gastroenterology*, **102**(6):2177–8.

Wong, B.C.Y., Lam, S.K., Wong, W.M., … Chen, J.S. (2004). *Helicobacter pylori* eradication to prevent gastric cancer in a high-risk region of China. *Journal of the American Medical Association*, **291**(2):187–194.

Wu, C.Y., Kuo, K.N., Wu, M.S., … Lin, J.T. (2009). Early *Helicobacter pylori* eradication decreases risk of gastric cancer in patients with peptic ulcer disease. *Gastroenterology*, **137**(5):1641-1648–2.

Yamaoka, Y. (2010). Mechanisms of disease: *Helicobacter pylori* virulence factors. *Nature Reviews Gastroenterology and Hepatology*, **7**(11):629–641.

Yamaoka, Y. (2008). Roles of the plasticity regions of *Helicobacter pylori* in gastroduodenal pathogenesis. *Journal of Medical Microbiology*, **57**(5):545–553.

Yamaoka, Y. and Graham, D.Y. (2014). *Helicobacter pylori* virulence and cancer pathogenesis. *Future Oncology*, **10**(8):1487–1500.

Yamaoka, Y., Kodama, T., Kita, M., … Graham, D.Y. (1999). Relation between clinical presentation, *Helicobacter pylori* density, interleukin 1 and 8 production, and *cagA* status. *Helicobacter*, **45**(6):804–811.

Yeh, Y.C., Cheng, H.C., Chang, W.L., … Sheu, B.S. (2010). Matrix metalloproteinase-3 promoter polymorphisms but not *dupA*-*H. pylori* correlate to duodenal ulcers in *H. pylori*-infected females. *BMC Microbiology*, **10**:218.

Yewdell, J.W. and Hickman-Miller, H.D. (2005). Back to the fold: T cell recognition of Hfe, a MHC class Ib molecule that regulates iron metabolism. *Proceedings of the National Academy of Sciences of the United States of America*, **102**(36):12649–50.

Yona, S. and Jung, S. (2010). Monocytes: subsets, origins, fates and functions. *Current Opinion in Hematology*, **17**:53–59.

Yoshii, A., Plaut, D.A., McGraw, K.A., … Wellik, K.E. (2009). Analysis of the reporting of search strategies in Cochrane systematic reviews. *Journal of the Medical Library Association : JMLA*, **97**(1):21–9.

Yu, S., Yang, M. and Nam, K.T. (2014). Mouse models of gastric carcinogenesis. *Journal of Gastric Cancer*, **14**(2):67–86.

Zentilin, P., Iiritano, E., Vignale, C., … Savarino, V. (2003). *Helicobacter pylori* infection is not involved in the pathogenesis of either erosive or non-erosive gastro-oesophageal reflux disease. *Alimentary Pharmacology and Therapeutics*, **17**(8):1057–64.

Zhang, B.B., Yin, Y.W. and Sun, Q.Q. (2012). No association between IL-1β-511 C/T polymorphism and the risk of duodenal ulcer: a meta-analysis of 4667 subjects. *Gene*, **506**(1):188–194.

Zhang, J. and Yu, K.F. (1998). What's the relative risk?: a method of correcting the odds ratio in cohort studies of common outcomes. *Journal of the American Medical Association*, **280**(19):1690–1691.

Zhang, Z., Zheng, Q., Chen, X., … Lu, H. (2008). The *Helicobacter pylori* duodenal ulcer promoting gene, *dupA* in China. *BMC Gastroenterology*, **8**:49.

Zhao, Y., Yokota, K., Ayada, K., … Oguma, K. (2007). *Helicobacter pylori* heat-shock protein 60 induces interleukin-8 via a Toll-like receptor (TLR)2 and mitogen-activated protein (MAP) kinase pathway in human monocytes. *Journal of Medical Microbiology*, **56**(PART 2):154–164.

Zhao, Y., Zhou, Y., Sun, Y., … Jia, J. (2011). Virulence factor cytotoxin-associated gene A in *Helicobacter pylori* is downregulated by interferon-γ *in vitro*. *FEMS Immunology and Medical Microbiology*, **61**(1):76–83.

Zhou, L., Somasundaram, R., Nederhof, R.F., … Fuhler, G.M. (2012). Impact of human granulocyte and monocyte isolation procedures on functional studies. *Clinical and Vaccine Immunology*, **19**(7):1065–1074.

Ziegler-Heitbrock, H.W.L. and Ulevitch, R.J. (1993). CD14: cell surface receptor and differentiation marker. *Immunology Today*, **14**(3):121–125.

Ziegler-Heitbrock, L. (2015). Blood monocytes and their subsets: established features and open questions. *Frontiers in Immunology*, **6**(AUG):423.

Ziegler-Heitbrock, L., Ancuta, P., Crowe, S., … Lutz, M.B. (2010). Nomenclature of monocytes and dendritic cells in blood. *Blood*, **116**(16).